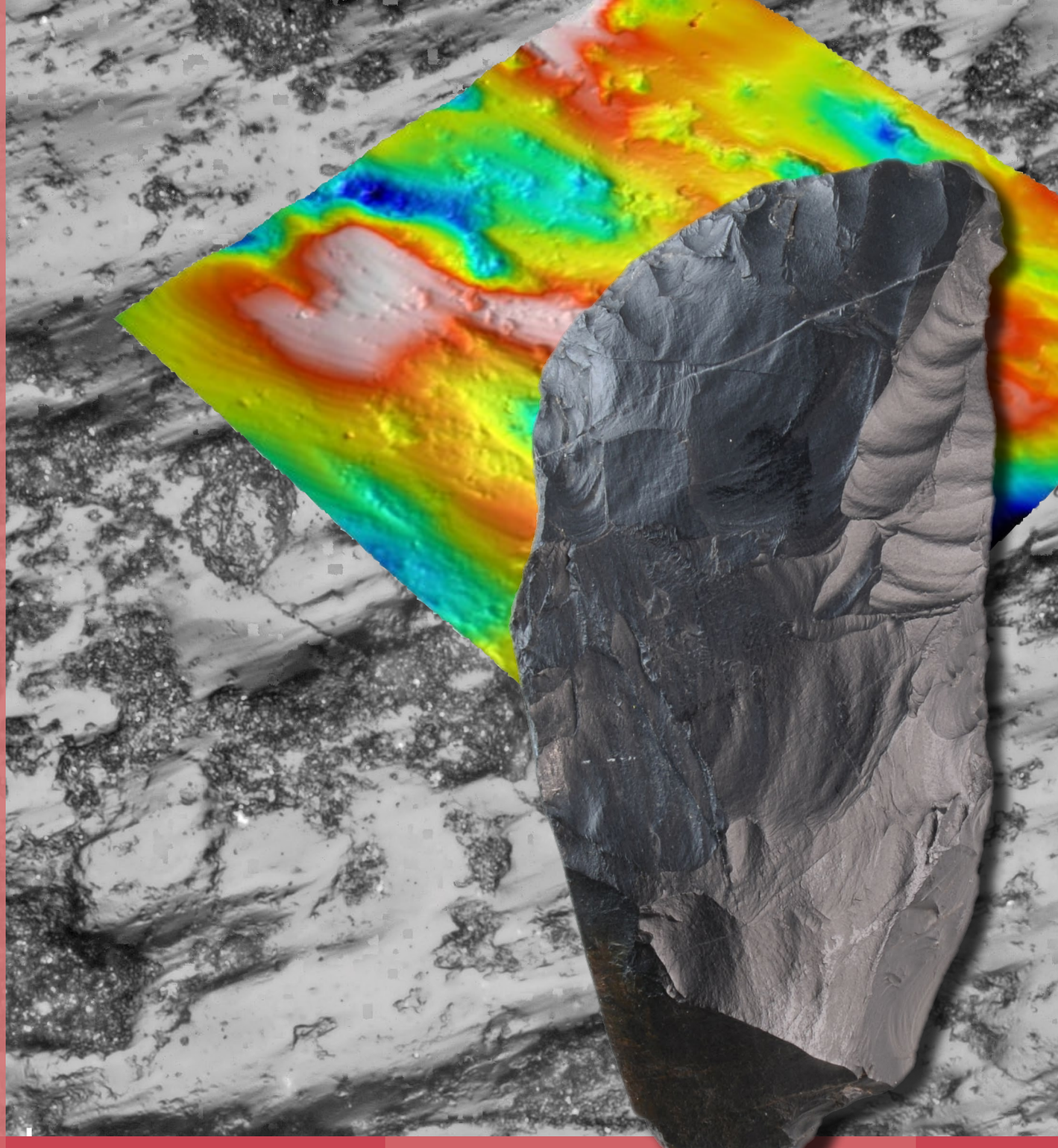

Lisa Schunk

Understanding Middle Palaeolithic asymmetric stone tool design and use

Functional analysis and controlled experiments to assess Neanderthal technology

Propylaeum
FACHINFORMATIONSDIENST ALTERTUMSWISSENSCHAFTEN

Römisch-Germanisches Zentralmuseum
Leibniz-Forschungsinstitut für Archäologie
R G Z M

Lisa Schunk

Understanding Middle Palaeolithic asymmetric stone tool design and use
Functional analysis and controlled experiments to assess Neanderthal technology

MONOGRAPHIEN

des Römisch-Germanischen Zentralmuseums

Band 159

Römisch-Germanisches Zentralmuseum
Leibniz-Forschungsinstitut für Archäologie

R G Z M

Römisch-Germanisches Zentralmuseum
Leibniz-Forschungsinstitut für Archäologie

Lisa Schunk

UNDERSTANDING MIDDLE PALAEOLITHIC ASYMMETRIC STONE TOOL DESIGN AND USE

FUNCTIONAL ANALYSIS AND CONTROLLED EXPERIMENTS TO ASSESS NEANDERTHAL TECHNOLOGY

Verlag des Römisch-Germanischen Zentralmuseums Mainz 2022

Die vorliegende Arbeit wurde vom Fachbereich 07 – Geschichts- und Kulturwissenschaften der Johannes Gutenberg-Universität Mainz im Jahr 2021 als Dissertation zur Erlangung des Grades eines Doktors der Philosophie (Dr. phil.) angenommen.

The present work was accepted in 2021 by the department 07 – Historical and Cultural Sciences of the Johannes Gutenberg University Mainz as dissertation to attain the academic degree of a Doctor of Philosophy (Dr. phil.).

Römisch-Germanisches Zentralmuseum
Leibniz-Forschungsinstitut für Archäologie
R G Z M

Bibliografische Information der Deutschen Nationalbibliothek

Die Deutsche Nationalbibliothek verzeichnet diese Publikation in der Deutschen Nationalbibliografie; detaillierte bibliografische Daten sind im Internet über http://dnb.d-nb.de abrufbar.



Dieses Werk ist unter der Creative Commons-Lizenz 4.0 (CC BY-SA 4.0) veröffentlicht. Die Umschlaggestaltung unterliegt der Creative-Commons-Lizenz CC BY-ND 4.0

Propylaeum
FACHINFORMATIONSDIENST ALTERTUMSWISSENSCHAFTEN

Diese Publikation ist auf http://www.propylaeum.de dauerhaft frei verfügbar (Open Access).
urn: urn:nbn:de:bsz:16-propylaeum-ebook-1076-2
doi: https://doi.org/10.11588/propylaeum.1076

Publiziert im Auftrag des RGZM bei der
Universität Heidelberg / Universitätsbibliothek
Propylaeum – Fachinformationsdienst Altertumswissenschaften
Grabengasse 1, 69117 Heidelberg
https://www.uni-heidelberg.de/de/impressum

Inhalt und Layout © 2022 Verlag des Römisch-Germanischen Zentralmuseums, Ernst-Ludwig-Platz 2, 55116 Mainz

ISSN 0171-1474
eISSN 2629-673X

ISBN 978-3-96929-194-8 (Hardcover)
ISBN 978-3-96929-170-2 (PDF)

CONTENTS

Acknowledgements IX

Introduction 1

State-of-the-art 5
Middle Palaeolithic asymmetric tools 5
Keilmesser 6
Prądnik scraper 7
Prądnik method 7
Tool design 8
Technology 9
Tool function and use 14
Summary 16
Aims 17

Materials 19
Selection of the sites 20
Buhlen 21
Site location and excavations 21
Buhlen lithic assemblage 22
Balver Höhle 23
Site location and excavations 23
Balver Höhle lithic assemblage 24
Ramioul 25
Site location and excavations 25
Ramioul lithic assemblage 26

Methods 27
Raw material characterisation 27
Techno-typological analysis 29
Blanks and cortex 29
Morphometric quantitative analysis 30
Tool back 30
Active edge retouch 30
Lateralisation 30
Morphological shape variability 31
Application of the *Prądnik method* 32
Prądnik spalls 32
Data analysis 32
Sampling strategy 32

Quantification of edge design . . . 34
Edge angle variability and morpho-functional design . . . 35
3D data preparation and acquisition . . . 36
»3-point« procedure . . . 37
»2-lines« procedure . . . 37
»best-fit« procedure . . . 38
Parameters . . . 38
Edge angle data analysis . . . 39
Use-wear analysis . . . 39
Traceology, use-wear analysis & functional analysis . . . 40
Artefact cleaning procedure . . . 42
Qualitative use-wear analysis . . . 42
Quantitative use-wear analysis . . . 46
Controlled experiments . . . 58
First generation experiments . . . 58
Second generation experiments . . . 58
Third generation experiments . . . 59
Experimental setup – initial experiment . . . 61
Experimental setup – »artificial VS. natural« experiment . . . 62
Experimental setup – tool function experiment . . . 64
Analysis of the experiments . . . 66

Results . . . 71
Raw material characterisation . . . 71
Techno-typological analysis . . . 75
Blanks and cortex . . . 75
Morphometric quantitative analysis . . . 78
Tool back . . . 87
Active edge retouch . . . 92
Lateralisation . . . 96
Morphological shape variability . . . 98
Application of the *Prądnik method* . . . 104
Prądnik spalls . . . 105
Quantification of edge design . . . 112
Edge angle variability . . . 112
»3-point« procedure . . . 113
»2-lines« procedure . . . 115
»best-fit« procedure . . . 119
Edge angle analysis . . . 121
Use-wear analysis . . . 125
Qualitative use-wear analysis . . . 125
Quantitative use-wear analysis . . . 135
Controlled experiments . . . 152
Data analysis – initial experiment . . . 152
Data analysis – »artificial VS. natural« experiment . . . 157

Data analysis – tool function experiment . . . 169
Combined data of the experiments . . . 179

Discussion . . . 181
Tool standardisation . . . 181
Tool dimensions and the effect of reduction . . . 181
Shape variability in *Keilmesser* . . . 184
Transmission of skills and knowledge . . . 184
Tool design: technological choices and edge design . . . 185
The *Keilmesser* concept . . . 185
Keilmesser edge design . . . 186
Tool handling . . . 187
Prądnik scrapers and the *Keilmesser* concept . . . 188
Tool lateralisation and the implications for human hand preferences . . . 190
Technology and use-wear to infer tool laterality . . . 190
Resharpening and recycling behaviour . . . 192
Resharpening addressed by a functional analysis . . . 192
Raw material and their implications for tool performance . . . 195
Material loss, tool damage and blunting . . . 195
Tool use and functionality . . . 197
The multifunctional aspect of *Keilmesser* . . . 197
Tool use in site context . . . 202
Tool performance and variables affecting it . . . 202
Surface texture roughness and the formation of use-wear traces . . . 203
Contact material and use intensity . . . 204

Conclusion . . . 207

References . . . 213

Appendix I: Results of the qualitative and quantitative use-wear analyses performed on samples from the archaeological sites Buhlen, Balver Höhle and Ramioul – Plates A1-156

Appendix II: Results of the qualitative and quantitative use-wear analyses performed on standard samples used during the »artificial VS. natural« experiment and the tool function experiment – Plates B1-16

ACKNOWLEDGEMENTS

The submission of this dissertation marks the end of a long and not always straightforward, often curvy road. Following this road was challenging, yet equally rewarding. I would like to express my gratitude to everyone who joined me on this path and helped me keeping on track. Moreover, thank you also for reading the results of those years of effort. I hope all of you find your effort in some parts reflected in this thesis.

My sincerest thanks I offer to Prof. Dr. Sabine Gaudzinski-Windheuser who advised this PhD project and supported me with insightful comments and suggestions. I am also grateful for the support of Dr. Olaf Jöris, who has accompanied me since my first year at university. I particularly appreciate your critical view that made me reconsider and scrutinize many of my thoughts. Thank you both for dedicating your time through all these years to me and for providing me with the tools necessary to find my path in the research landscape. Many thanks also to Prof. Dr. Christopher Pare and Dr. habil. Peter Haupt for their immediate agreement on being part of the PhD committee.

I further extend my gratitude to those who provided me access to the archeological material. Without this opportunity, this research would not have been possible. I wish to thank Dr. Irina Görner (Hessisches Landesmusem Kassel, Germany), Dr. Birgit Mecke (Landschaftverband Westfalen-Lippe – Archäologie für Westfalen, Münster, Germany) and Dr. Cécile Jungels (Préhistomuseum, Belgium) for providing access to the assemblages from Buhlen, Balver Höhle and Ramioul. Many thanks for the good and helpful cooperation. At the same time, I am thankful for the funding of my research by the Leibniz-Association's extraordinary item of expenditure (Sondertatbestand).

To my colleagues at MONREPOS and at the RGZM in Mainz I am also much indebted. I am thankful for everything I have learned from you and for all the knowledge you shared with me and your patience during the process. I am especially glad about getting the chance to join TraCEr. Special thanks go to Dr. Martin Street, Geoff Carver, M.A., Dipl.-Ing. Guido Heinz, Dipl.-Ing. Anja Cramer, Walter Gneisinger, B.Sc., and Dr. Ivan Calandra. I highly appreciate the immense effort you all invested in this project. Thank you for helping to produce and in turn to process the data. Without the data and your input, this dissertation would not exist.

I further extend my appreciation to my family and friends. I value your moral support, your motivation and your kindness. Thank you for believing in me. I would also like to thank you, João. I am truly grateful for your continuous support and optimism. Thank you for joining me on this journey and for showing me the way forward whenever I lost my track.

INTRODUCTION

Lithic artefacts represent a crucial source of information in the archaeological record, serving as a window into the study of the evolution of human technological and ecological adaptations (Bar-Yosef/Kuhn 1999; Klein 2000; Ambrose 2001; Eerkens/Lipo 2007; Whiten/Schick/Toth 2009; Iovita 2010; Goodale/Andrefsky 2015; Lycett 2015). In the Middle Palaeolithic record, samples for lithic analyses are provided by categories such as blank production, retouched tools or debris presented within archaeological lithic assemblages. In this context, Middle Palaeolithic retouched tools are found intentionally worked unifacially as well as bifacially. Both cases commonly result in characteristic sharp active edges (Iovita 2010; Iovita/McPherron 2011; Retzek et al. 2019). Asymmetric tools as bifacial backed knives (hereafter *Keilmesser*) or »*Prądnik scrapers*« (hereafter *Prądnik scraper*) illustrate no exception in this technological characterisation. These asymmetric tools characterise the so-called »*Keilmessergruppen*« (KMG) (Mania 1990; Veil et al. 1994; Jöris 2004; 2006; 2012) and are known from Central and Eastern European archaeological sites dating from late OIS 5 until mid OIS 3 (Jöris 2004; 2006). In KMG assemblages, *Keilmesser* usually occur together with a spectrum of tools, for example hand axes, foliate pieces, scrapers and points of different shapes (Bosinski 1967; Jöris 2004). Within this spectrum, *Keilmesser* as well as *Prądnik scrapers* offer a unique opportunity to study several aspects, for instance tool standardisation and design, tool function and curation. Furthermore, *Keilmesser* represent an archive for tracing certain behavioural phenomena of Neanderthals such as learning strategies, the formation of tool making tradition and knowledge transfer across generations. One reason for that is their morphology.

Keilmesser can be described as tools with a sophisticated morphology and design, which is reflected by a combination of a single active edge opposed by a natural or roughly worked back (Krukowski 1939; Bosinski 1967; Jöris 2001; 2012). Numerous technological studies demonstrate that the manufacturing of the tools seems to follow an underlying concept, highlighting a high degree of tool standardisation (Jöris 1994; Veil et al. 1994; Richter 1997; Jöris 2001; 2012). Long reduction sequences have repeatedly been documented, allowing for detailed morpho-technological reconstructions of their use-life histories, including repeated phases of production, resharpening and reworking (in the sense of shape transformation) (Jöris 1994; Richter 1997; Pastoors 2001; Migal/Urbanowski 2006; Iovita 2014; Jöris 2001; 2006; Jöris/Uomini 2019). This has been argued as a technological strategy requiring the application of comparable production concepts and elaborated resharpening strategies. While these aspects concern tool standardisation, they also account for tool design. Tool design includes a multitude of aspects and goes beyond the overall tool shape. Design also involves the producer's anticipation of the envisaged tool function and its interaction with the user. Thereby, design can be reflected by more obvious aspects such as tool morphology and handling but also includes details like a specific edge retouch.

Within asymmetric tools, such as *Keilmesser* and *Prądnik scraper*, the active edge is seen as being the most characteristic part of the tool. *Keilmesser* mostly display a bifacially worked, acute active edge. Frequently, this edge is altered by the application of the so-called »*Prądnik method*« (hereafter *Prądnik method*) (Jöris 1992; 2006; Frick et al. 2017; Frick/Herkert 2019; Frick 2020a). Here, the *Prądnik method* describes a special type of lateral edge removal from the distal part of the tool (Bosinski 1969; Jöris 2001; Jöris/Uomini 2019). This modification detaches an elongated spall running from the tool's tip along the active lateral edge. This method is used to produce a stable and straight active edge (Jöris 2006; Frick et al. 2017; Frick/Herkert 2019). At the same time, it divides the active edge into two parts. Compared to the proximal part of the tool, the distal part seems frequently sharper due to a more acute edge angle. Given this observation, the

interpretation of *Keilmesser* as a tool with a multifunctional morphology arose (Jöris 2001; Rots 2009; Jöris 2006; 2012; Golovanova et al. 2017). However, this assumption has not been experimentally tested yet. Some tools testify a sequential application of the *Prądnik method*, leading researchers to the conclusion that this strategy is embedded within »resharpening cycles« on tool production, use and maintenance (Jöris 2001; Frick/Herkert 2019; Jöris/Uomini 2019). The implications of the *Prądnik method* are not conclusively clear. For instance, improvement of the edge angle in the sense of increasing sharpness has not been investigated in detail. A further question is also, which influence(s) the modification of the active edge has on tool efficiency and durability during a performed task.

Moreover, the possible influence(s) of the raw material has rarely been discussed. Although *Keilmesser* seem to be standardised in several aspects, the raw material used for the production of these tools has not always been the same (e. g. flint, silicified schist). This variability likely reflects intentional choices based on the availability and the characteristics of the individual raw materials. Raw material properties are known to have a significant impact on tool production and use (Odell 1981; Eren et al. 2016; Dogandžić et al. 2020; Key/Proffitt/de la Torre 2020). The effects of the raw material properties on the *Keilmesser* production, use and maintenance still need to be tested experimentally.

As previously mentioned, tool design also includes aspects such as tool handling and function. Since the back of a *Keilmesser* normally forms the thickest part of the tool and the lower surface is usually flatter compared to the more strongly curved upper surface (Jöris 2012; Weiss 2018; Wiśniewski et al. 2020), the morphological design supports the idea of a *Keilmesser* as a handheld tool (Jöris 2001; Frick et al. 2017; Jöris/Uomini 2019). Moreover, the tools can be distinguished into left-lateral and right-lateral specimens (Jöris/Uomini 2019). This distinction is based on the length-axial tool asymmetry. It has been argued that tool lateralisation reflects hand preferences and thus can serve as a proxy for human handedness. While techno-typological analyses have been conducted extensively (e. g. Krukowski 1939; Richter 1997; Jöris 2001; Pastoors 2001; Frick 2016a; 2016b; Weiss 2015; Weiss/Otcherednoy/Wiśniewski 2017), the same does not apply to other types of analysis, for instance use-wear studies (Rots 2009) or experimental approaches (Migal/Urbanowski 2006). This PhD thesis targets at filling this gap. Asymmetric tools such as *Keilmesser* and *Prądnik scraper* are highly suitable for this endeavour due to their special morphology. Already the fact that *Keilmesser* as well as *Prądnik scrapers* have only one active edge compared to other tools, such as hand axes, simplifies the analysis. It does not reduce the work, but leads instead to less complex and more reliable results when the spacial assignment (active edge VS back etc.) of the use-wear traces is given.

The aim of this study is to obtain a more precise picture about Late Middle Palaeolithic *Keilmesser* and *Prądnik scrapers*. Thus, the overarching research question is to gain a better understanding of the tools by combining data concerning the techno-typology as well as data regarding functionality and tool use. To test generally accepted models about *Keilmesser*, the approach chosen for this research moves beyond conventional technological and typological studies. The multidisciplinary approach also includes the analysis of 3D data, qualitative and quantitative use-wear analysis and controlled experiments. To capture tool design in more detail, high resolution 3D data, next to quantitative metric measurements and qualitative attributes, offer the possibility for testing these models. Within these analyses, a special focus lies on the detailed morphology of the tool's edge. To address tool use directly, use-wear analysis aims to combine qualitative and quantitative data. Additionally, controlled experiments add data to aspects such as tool use, performance, efficiency and durability. At the same time, the experiments are designed to test the possible functionality of *Keilmesser* by executing different movements such as cutting and carving. The influencing factor of the different raw materials involved – silicified schist and flint – and their properties, will be tested throughout the experiments.

Taken together, the proposed approach has two main goals. The first goal is to gain new data about *Keilmesser* focussing on tool design, function and use. This data aims to be predominantly quantitative over qualitative and thus, also statistically evaluable. The second goal of this study is to test given interpretations or accepted models about *Keilmesser*. The only way to do so is by applying a multidisciplinary approach. The combination of the different scales of analysis and methods as techno-typological and material properties studies, use-wear analysis and controlled experiments can lead to a more holistic view on *Keilmesser*. Investigating and understanding aspects as the underlying tool concept and design, as well as tool function and use is conditional upon tracing certain behavioural phenomena of Neanderthals such as learning strategies, knowledge transmission and the formation of rules and regulations that can be approached from such a perspective. The study of these asymmetric tools may contribute to answering such questions and may allow us to gain new insights into Late Middle Palaeolithic technological choices.

Three selected Middle Palaeolithic assemblages from Central Europe, namely Buhlen (Bosinski 1969; Bosinski/Kulick 1973; Jöris 2001), Balver Höhle (Andree 1928; Bahnschulte 1940; Günther 1964; 1988) and Ramioul (Vandebosch 1921; 1929; Ulrix-Closset 1975) serve as a case study. The Upper Site of Buhlen is a collapsed rock-shelter in northern Hesse, while Balver Höhle is a large cave in North Rhine-Westphalia, both are in Germany. Ramioul represents a cave located in Belgium. All three sites have been excavated mainly in the beginning of the twentieth century or in the case of Buhlen in the beginning of the second half of the twentieth century.

To address the research question, this study is structured as follows: »State-of-the-art« for the topics: 1) Middle Palaeolithic asymmetric tools and 2) Tool design. These are the topics building the foundation for this research. Based on this, a discussion of the research questions including all objectives and aim will follow. The chapter »Materials« refers to the archaeological sites, which serve as case studies. The chapter provides basic information about the archaeological sites selected for this research, including short excavation histories and the samples used in this study. The applied methods are outlined in the chapter »Methods«. Here, the methodological workflow of this study can be summarised in its main approaches: 1) Raw material characterisation, 2) Techno-typological analysis 3) Quantification of edge design, 4) Qualitative and quantitative use-wear analysis and lastly 6) Controlled experiments. The results of all these methods are presented in the subsequent chapter. The »Discussion« chapter refers to the major interpretations and implications resulting from the newly presented data. Aspects such as tool standardisation and design, the influence of the raw material properties in terms of tool modification, performance and efficiency and the edge design are part of the discussion. Also addressed are topics such as the tool lateralisation and the lateralisation as a proxy for human handedness, tool function and use. The following chapter »Conclusion« combines the aforementioned topics and aims to provide a more distinct and holistic view on *Keilmesser*. The chapter also addresses the role of *Keilmesser* in Late Middle Palaeolithic assemblages and the interpretations and inferences on Neanderthal behaviour, which can be made. Additionally, it also points out the limitations experienced within this research and elaborates further on existing unclear aspects. Finally, this PhD project highlights the necessary work, which could enhance specific future research.

Furthermore, images of all the use-wear traces documented on the archaeological artefacts as well as on the experimental samples can be found in the **appendix** (**I-II**).

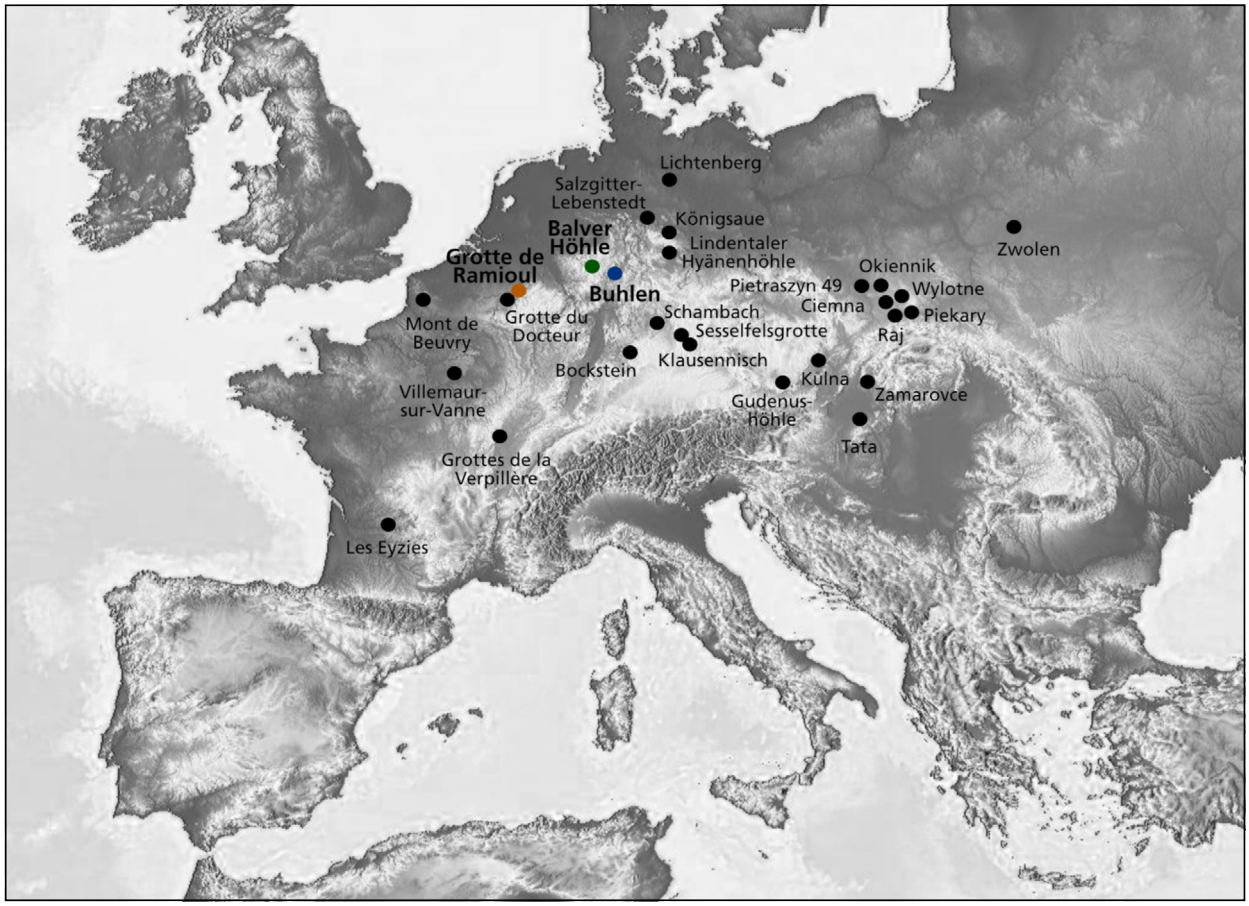

Fig. 1 Distribution of the major *Keilmessergruppen* sites in Central Europe. The sites of Buhlen (blue point), Balver Höhle (green dot), both in Germany and La Grotte de Ramioul, in Belgium (orange dot) are highlighted. – (The map is adapted from Jöris/Uomini 2019).

STATE-OF-THE-ART

MIDDLE PALAEOLITHIC ASYMMETRIC TOOLS

Archaeologists attempt to answer questions regarding the evolution of human behaviour through the study of material culture. In the Pleistocene, stone tools were essential to the survival of hominins. Hence, lithic artefacts provide insights into early hominin behaviour, through their technological adaptations and innovations (Klein 2000; Odell 2000; Ambrose 2001; Lycett 2015; Dibble 2017; Key/Proffitt/de la Torre 2020). This is conditional upon understanding the production, design, function and use of the huge variety of artefact categories in the archaeological record. In the case of Middle Palaeolithic Neanderthal's assemblages, the tool variety can be described by an occurrence of mainly hand axes, foliated pieces and several types of scrapers and points. Throughout the Middle Palaeolithic, this pattern seems consistent, leading to the impression of a certain stasis and little alteration concerning the composition of lithic assemblages (Gamble/Roebroeks 1999; Hovers/Belfer-Cohen 2006). Besides the aforementioned tools, the presence of some asymmetric tools in the Late Middle Palaeolithic became prominent in Central and Eastern European sites (Bosinski 1967, Mania/Toepfer 1973; Veil et al. 1994).

The asymmetry of these tools is due to the presence of only one single active edge opposed to a back, contrary to tools with two similar lateral edges as for instance hand axes. Tools with such an outstanding characteristic are namely *Keilmesser* – bifacial backed knives – and *Prądnik scrapers* (Krukowski 1939; Bosinski 1967; Jöris 2001; 2012). Although *Keilmesser* are occasionally found in older site contexts (e. g. Marks 2002; Solecki/Solecki 2001), the vast majority of these tools as a morphological type is associated with the Late Middle Palaeolithic of Central and Eastern Europe (Jöris 2004; 2006).

The geographical distribution of these assemblages can be roughly defined by Central and Eastern Europe (fig. 1). Recently, also sites in the Altay Mountains (Okladnikow Cave, Chagyrskaya Cave) (Kolobova 2020) were described as *Keilmesser* yielding assemblages, expanding the geographical distribution further east to Asia. The majority of sites are located in Central Europe. Eastern sites are located in Poland (e. g. Ciemna, Zwolén, Wylotne, Bisnik Cave) (e. g. Krukowski 1939; Burdukiewicz 2000; Urbanowski 2003; Serwatka 2014; Valde-Nowak et al. 2016) and Czech Republic (e. g. Kůlna Cave) (Neruda 2017). Well-studied German sites include for example Sesselfelsgrotte (Richter 1997; 2016; Delpiano/Uthmeier 2020), Klausennische (Mania/Toepfer 1973; Picin 2016) and Bockstein (Wetzel 1958; Bosinski 1969) in the South, Lichtenberg (Veil et al. 1994; Weiss 2020) in the North and Balver Höhle (Andree 1928; Bahnschulte 1940; Günther 1964; Wetzel/Bosinski 1969; Günther 1988) and Buhlen (Bosinski/Kulick 1973; Bosinski 1969; Jöris 2001) in Central Germany. The site of Grotte de la Verpilliere (Frick 2016a; 2016b; Frick/Floss 2017) is to mention as an example for the French region. La Grotte du Docteur (Ulrix-Closset 1975) and Ramioul (Vandebosch 1921; Ulrix-Closset 1975) in Belgium are further examples for Central European sites. The frequency of *Keilmesser* within a chronological comparably narrow time interval (late OIS 5 until mid OIS 3 (Jöris 2004; 2006) led to the introduction of the term »*Keilmessergruppen*« for such lithic assemblages (Mania 1990; Veil et al. 1994; Jöris 2004; 2006; 2012). The term was first introduced by Mania in 1990.

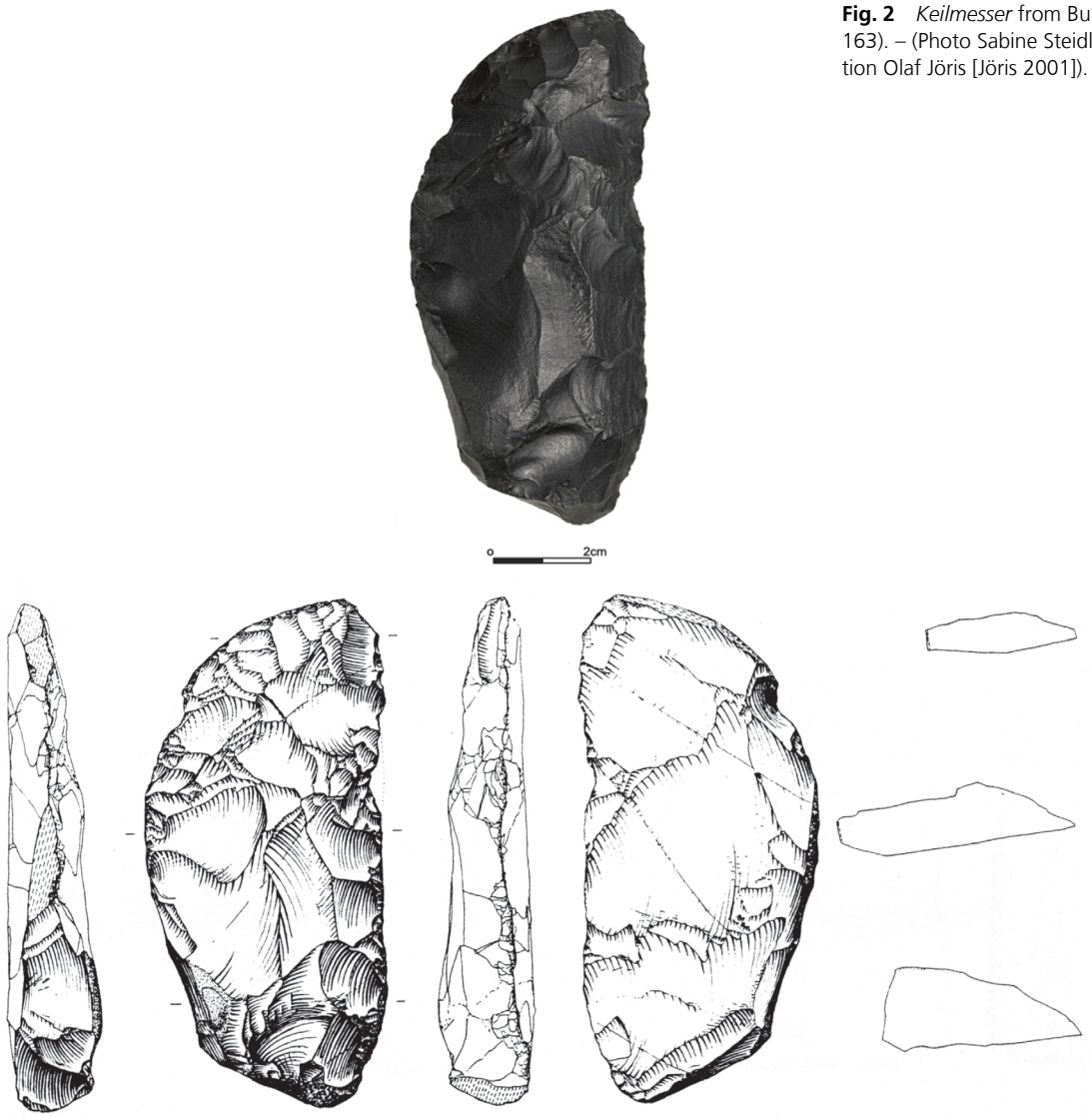

Fig. 2 *Keilmesser* from Buhlen (ID BU-163). – (Photo Sabine Steidl, RGZM; Illustration Olaf Jöris [Jöris 2001]). – Scale 2:3.

Keilmesser

Based on their morphology, *Keilmesser* display a clear asymmetric shape with a triangular or wedge-shaped cross section (Jöris 2006; 2012) (**fig. 2**). The German tool's name, *Keilmesser*, originates from this wedge-shaped section. *Keilmesser* are mainly produced as core tools and, more rarely, from flakes (Jöris 2001; Jöris/Uomini 2019). The shape characteristics of the blank chosen for the manufacture of the *Keilmesser* appear integrated into the overall tool concept (Jöris 2006; 2012; Frick/Floss 2017; Frick/Herkert 2019, Wiśniewski et al. 2020). Resulting from this specific selection, the back of a *Keilmesser* normally forms the thickest part of the tool. While the back is commonly natural or roughly worked, the active edge is mostly bifacially retouched. Additionally, *Keilmesser* usually have a flatter lower surface compared to the more strongly curved upper surface. The morphological design supports the idea of *Keilmesser* as a handheld tool (Jöris 2001; Jöris/Uomini 2019). Evidence for hafting is rare, if not absent (Rots 2009).

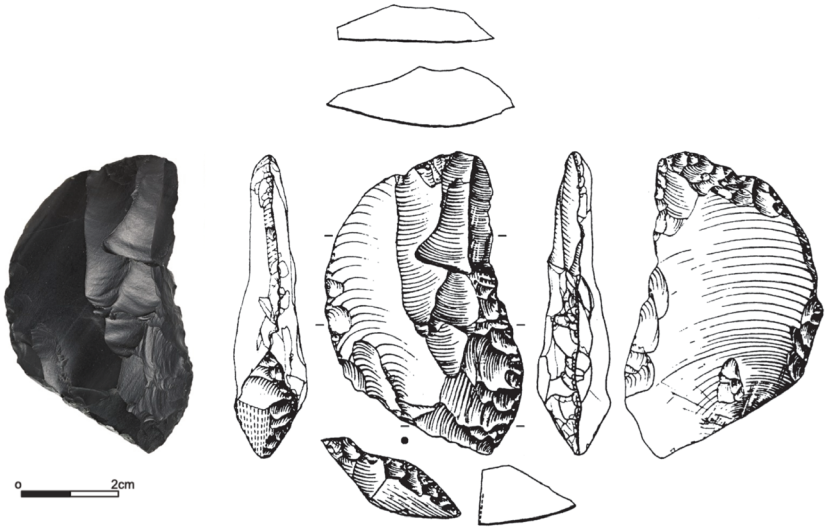

Fig. 3 *Prądnik scraper* from Buhlen (ID BU-194). – (Photo Sabine Steidl, RGZM; Illustration Olaf Jöris [Jöris 2001]). – Scale 2:3.

Prądnik scrapers

Alongside *Keilmesser*, KMG assemblages sometimes yield scrapers, the so-called *Prądnik scraper,* displaying many similarities with the previous described *Keilmesser* (Jöris 2001; 2004; Jöris/Uomini 2019) (**fig. 3**). Even though the distinction between the two artefact categories is not clear cut, a terminological differentiation is required. The scrapers are usually made from flakes, not from cores. Similar to *Keilmesser,* they have natural back, asymmetric sections and/ or clear, intentional blunting opposite the active edge. In comparison, the production of this artefact category seems to follow the same underlying tool design as for *Keilmesser*, but the entire processing sequence appears to be simplified and less complex (Jöris/Uomini 2019). This assumption might be associated with rather short tool biographies and the usual absence of indications for re-working and re-use in contrast to *Keilmesser*.

So far, *Prądnik scrapers* have rarely been an intensive focus of lithic studies. A reason for this can be found in their occurrence. *Prądnik scrapers* are not always part of *Keilmesser* assemblages. Although they can be found together with *Keilmesser,* they exist always in smaller numbers. Nevertheless, further analyses focusing more on the similarities and /or on the distinctions might provide new information about this artefact category, inevitably raising the question of how *Keilmesser* and these scrapers are related.

Prądnik method

Prądnik scrapers are always, *and Keilmesser* frequently, characterised by a special lateral tranchet blow modification on the active edge (Jöris 1992 2001; Frick et al. 2017; Frick/Herkert 2019; Frick 2020a) (**fig. 4**). This modification detaches an elongated spall running from the tool's tip along the lateral edge. Various names are known to describe the modification as for instance »*Prądnik technique*«, »*Prądnik method*« or tranchet blow (Frick et al 2017; Frick/Herkert 2019; Frick 2020a). Since the modification on *Keilmesser* and *Prądnik scrapers* is not identical to tranchet blows on other artefact categories (e. g. scraper) (Cornford 1986; Douze 2014; Zaidner/Grosman 2015; Frick et al. 2017; Frick 2020a; Prévost/Centi/Zaidner 2020), the term *Prądnik method* is given preference here. The method can be applied by one or more blows to the distal part of the tool. Depending on the state of the active edge, a certain preparation was required (e. g. previous blunting). The repeated application can be either seen on the tool itself by superimposed negatives



Fig. 4 *Keilmesser* from Balver Höhle (ID SM-003) modified by the application of the *Prądnik method*. Blue coloured area indicates the scar resulting from the *Prądnik spall* removal. – (Photo Michael Baales; Illustration Olaf Jöris [Jöris 1992]). – Scale 2:3.

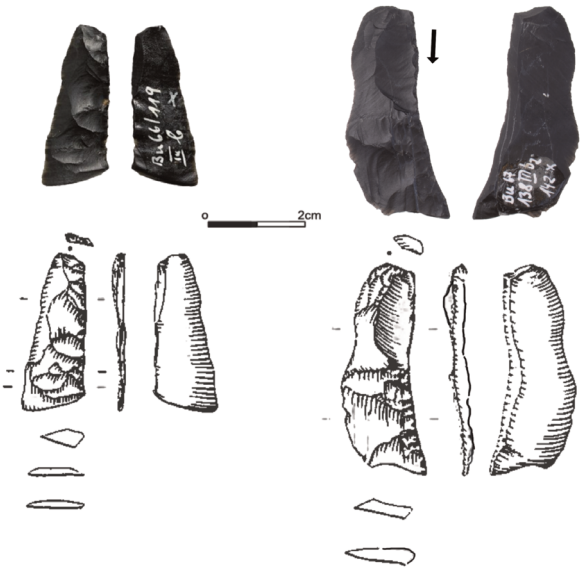

Fig. 5 *Prądnik spalls* from Buhlen (left ID BU-155, right ID BU-136). The artefact on the left side illustrates a primary, the on the right side a secondary *Prądnik spall*. The black arrow indicates the direction of the applied *Prądnik method*. – (Photo left Sabine Steidl, RGZM; Illustration Olaf Jöris [Jöris 2001]). – Scale 2:3.

or on the resulting »*Prądnik spalls*« (hereafter *Prądnik spall*) (**fig. 5**). Based on the pattern of scars on the dorsal face of the *Prądnik spalls* it is possible to distinguish primary from secondary removals (Jöris 2001). The application of the *Prądnik method* results in a tool with a stable and straight active edge. At the same time, the lateral removal (re-)sharpens the tool by reducing the edge angle (Jöris 2006; Frick et al. 2017; Frick/Herkert 2019; Jöris/Uomini 2019; Frick 2020a). Reconstructions of the *chaînes opératoires* of *Keilmesser* placed the *Prądnick method* as a technological modification at the end of the manufacturing sequences (Jöris 2001; 2006; Frick et al. 2017; Frick/Herkert 2019). Hence, the removal of a *Prądnik spalls* can also been seen as tool finishing (Frick/Herkert 2019; Jöris/Uomini 2019). In this sense, another aspect should also be discussed: *Keilmesser*, in particular such pieces with a *Prądnik method* modification, display a two-parted active edge (double morphology). This horizontal separation in two parts becomes visible by the changing quality (in the sense of different retouch, different edge angle etc.) of the active edge, which puts a special emphasis on the distal part of the tool. Therefore, these tools seem to have been created as at least bi-functional tools (Jöris/Uomini 2019). The lower part with the larger edge angle is assumed to function thereby as a scraper or the like and the distal part with the smaller edge angle as a knife for cutting (Frick/Herkert 2019).

TOOL DESIGN

Artefacts, especially stone tools, do provide insights into human behaviour (Klein 2000; Odell 2000; Ambrose 2001; Lycett 2015; Dibble et al. 2017; Key/Proffitt/de la Torre 2020). Understanding the tool design can thereby provide information about early human technological and ecological adaptations. More importantly, it always reflects human behaviour in the sense of conscious or unconscious decision-making. One of these behaviour-related attributes reflected by the tools is the choice of raw material. This decision can be based on the availability, the size, the shape or even by the knappability. Also, the shape of a tool is

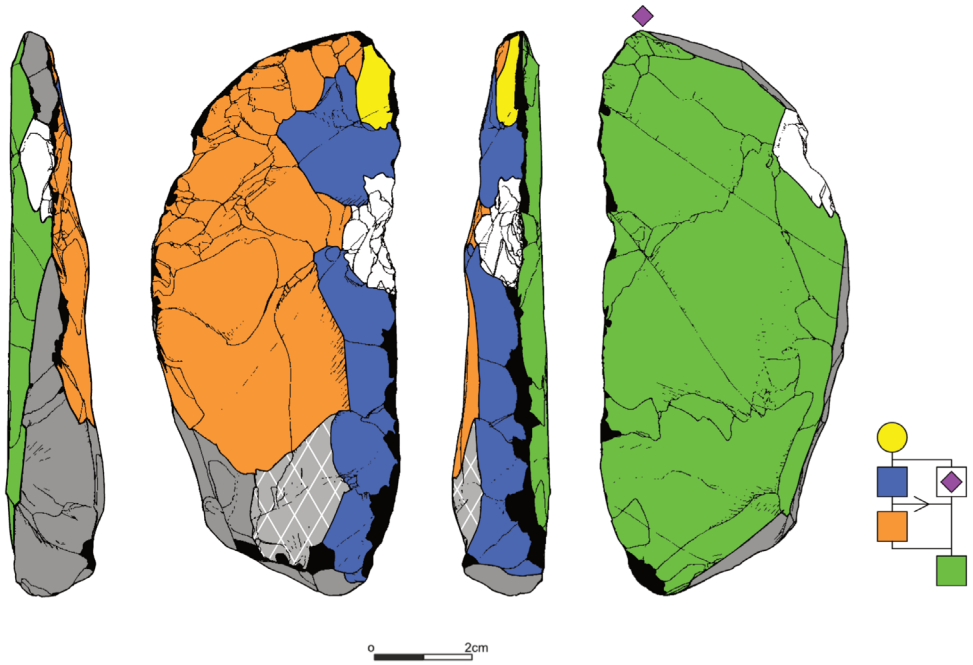

Fig. 6 *Keilmesser* from Buhlen (ID BU-163). The colours correlate with the Harris diagram on the right, indicating the order of individual retouch sequences from bottom to top. The yellow circle indicates the removal of a *Prądnik spall*, the purple diamond indicates the preparation of a striking platform. – (After Jöris/Uomini 2019). – Scale 2:3.

undeniably (and maybe even to a great extent) the result of human decision-making. While the choice of the raw material can probably be seen as the most obvious aspects concerning human behaviour (Dibble et al. 2017), there are other details in the tool design, for instance edge retouch or hafting, which can provide information (Kuhn 1994; Carr 1995).

Technology

Many *Keilmesser* assemblages are well studied from a technological and typological point of view. Considerable research on the tool production, curation and function has been done, resulting in assumptions, which are for the most part considered as valid **tab. 1**). It has been argued that *Keilmesser* are highly standardised tools (Jöris 1994; Richter 1997, Jöris 2001; 2012). The overall tool concept seems to be present from the first step of the tool production onwards (Jöris 2001; Migal/Urbaowski 2006; Jöris 2012). The earliest step thereby is the selection of the raw material based on the shape. Depending on the morphology of the raw material, the back of the tool often stays unworked or only slightly retouched. Therefore, it seems certain that the raw material shape was integrated in the desired tool morphology. Due to the well-understood *chaînes opératoire,* it is possible to reconstruct the sequences of surface flake removals, giving the impression of a pattern that was mostly followed (Jöris 1992; Richter 1997; Jöris 2001; Pastoors 2001; Jöris 2006; Migal/Urbanowski 2006; Jöris/Uomini 2019; **fig. 6**). Technological studies also suggest an intended long usage for *Keilmesser* with a great potential for repeated reduction and re-use (Jöris 2001; Pastoors 2001; Jöris 2006). Analyses highlight the presence of different phases of retouch by overlaying negatives, which could be seen as a resharpening process. The tool size is known to vary between approximately 3 cm and 14 cm maximum length. It has been argued that this difference in size is the result of long-term use (Richter 1997; Pastoors/Schäfer 1999; Jöris 2001; Pastoors 2001; Jöris 2006). At the same time, the tool shape in relation seems to change isometrically (Iovita 2010). This required the application of consistent produc-

techno-functional aspects	interpretation	evidence	references (examples)	test method
technological choices and strategies	raw-material piece as integrated into the overall tool concept	mostly made from consciously shape-selected blocks / pebbles	Jöris 2001; 2006; 2012; Frick/Floss 2017; Wiśniewski et al. 2020	**lithic analysis**: characterisation of the back
		natural or roughly worked back	Krukowski 1939; Wetzel 1958; Bosinski 1967; Jöris 2001; 2012	
	preferential use of the local raw-material	mostly made from one type of raw-material	Veil et al. 1994; Jöris 2001; 2006; 2012	**raw material properties characterisation**
	raw material and blank selection as a conscious choice due to shape	mainly core-tools		**lithic analysis**: blank selection
	standardised manufacturing	similar manufacturing stages	Richter 1997; Jöris 1994; 2001; 2006; 2012; Migal/Urbaowski 2006; Frick/Herkert 2019, Wiśniewski et al. 2020	**lithic analysis**: documentation of the *chaîne opératoire*
	underlying tool concept			**lithic analysis**: comparison between samples + inter-site comparison
general morphology	tool with only one active edge	tool asymmetry	Bosinski 1967; Veil et al. 1994; Jöris 2006; 2012	**quantification edge design**: comparison between back and active edge values
				use-wear analysis: do traces on the back exist?
	conscious tool design (e.g. designed for handling)	triangular or wedge-shaped cross section	Jöris 2001; Jöris/Uomini 2019; Frick/Herkert 2019	**use-wear analysis**: distribution of use-wear traces
		flatter lower and more curved upper surface	Bosinski 1967; Veil et al. 1994; Jöris 2006	**use-wear analysis**: do hafting traces exist? geometric morphometrics
active edge design	focus on active edge	mostly bifacially retouched	Bosinski 1969; Jöris 2001; 2012; Weiss et al. 2018; Weiss 2020	**lithic analysis**: documentation of edge retouch
				quantification edge design: comparison back and active edge values
	bipartite / bi-functional edge	changing morphology/ retouch along the edge	Jöris 2001; Frick et al. 2017; Frick/Herkert 2019; Jöris/Uomini 2019; Weiss 2020	**quantification edge design**: edge angle along the edge
				use-wear analysis: do the traces differ in the distal and proximal part of the active edge?
				controlled experiments: edge angle functionality

techno-functional aspects	interpretation	evidence	references (examples)	test method
shape diversity	different *Keilmesser* shapes exist as chronological sequence	variety of Keilmesser shapes	Bosinski 1967; 1969	**lithic analysis**: size independent comparison
	shape of initial raw material pieces and resharpening lead to different *Keilmesser* shapes		Jöris 2001; 2004; 2006	
lateralisation	proxy for handedness	left- or right-lateral retouch	Jöris/Uomini 2019	**use-wear analysis**: orientation use-wear traces
				quantitative use-wear analysis: parameters texture directionality
Prądnik method	tool finishing / tool (re-)sharpening	frequent application (with intensive preparation)	Jöris 1992; 1994; 2001; Frick et al. 2017; Frick/Herkert 2019	**use-wear analysis**: are the spalls free from use-wear traces?
				lithic analysis: documentation of the *chaîne opératoire*
	attempt to gain an elongated spall for further usage			**use-wear analysis**: are there any use-wear traces on the spalls apart from the former active edge?
resharpening and reworking	resharpening in respect to perimeter sections to retain their functions	isometrical size changes	Iovita 2010; Weiss et al. 2018	**lithic analysis**: measurements perimeter section
				lithic analysis: length-width ratio of the tools
	extended tool use	(multiple) application of *Prądnik method*	Jöris 2001, Frick et al. 2017; Frick/Herkert 2019; Jöris/Uomini 20019	**lithic analysis**: recording of the *Prądnik spall* removals and *Prądnik spalls*
				use-wear analysis: do traces indicate a fresh resharpening?
		secondary *Prądnik spalls*		**lithic analysis**: recording of *Prądnik spall* type
				use-wear analysis: are there use-wear traces on the *Prądnik spall*s?
		removal of the distal tip	Jöris 2001	**lithic analysis**: recording *Keilmesser* tips

Table 1 Summary of the main morpho- and techno-functional aspects concerning *Keilmesser*. The table also includes common interpretations and ideas how to address and test them. Methods highlighted in green have been applied in this project.

techno-functional aspects	interpretation	evidence	references (examples)	test method
tool biographies	long life-histories	negatives / scars on tools	Richter 1997; Pastoors/Schäfer 1999; Pastoors 2001; Jöris 2001; 2006	**controlled experiments**: when is re-sharpening needed? (tool durability)
				use-wear analysis: are there traces corresponding to long-term / intensive use?
				quantitative use-wear analysis: parameters areal surface texture
		numerous *Prądnik spalls*	Jöris 2001; Frick et al. 2017; Frick/Herkert 2019	**use-wear analysis**: are there use-wear traces on the *Prądnik spalls*?
function	tool suitable for cutting tasks	sharp tool edges	Jöris 2001; Frick et al. 2017; Frick/Herkert 2019; Jöris/Uomini 2019; Weiss 2020	**quantification edge design**
	multifunctional tool	changing morphology / retouch along the edge	Jöris 2001; 2006; 2012; 2014; Rots 2009; Golovanova et al. 2017; Frick/Herkert 2019	**quantification edge design**
				controlled experiments: testing tool performance based on edge angle

Table 1 (continued)

tion concepts and elaborated resharpening strategies. Changes in morphology due to modification (e. g. resharpening in the case of bifacial retouched tools) or recycling is widely accepted and has been argued repeatedly (Dibble 1995; Iovita 2009; 2010; 2014; Vaquero et al. 2015). Analysis of different Middle Palaeolithic assemblages such as Buhlen, Germany (Jöris 2001), Grotte de la Verpillière I and II, France (Frick 2016a; 2016b), and Ciemna Cave, Poland (Valde-Nowak et al. 2014; 2016) were able to demonstrate the entire *chaînes opératoire* of *Keilmesser* production, including rejuvenation processes.

Although the manufacture of *Keilmesser* follows an underlying tool concept and a high degree of standardisation, they often display a morphological diversity (**fig. 7**). In general, the outline shape of a *Keilmesser* can be separated in three distinct parts (perimeter characteristics). The first part defines the unworked or roughly thinned base, which merges into the back. The distal posterior part of the tool often forms an arch or a bow. The active edge is the third of these tool parts. The size and shape of these outline parts can vary, resulting in the morphological differentiation of different *Keilmesser* shapes. In literature, the *Keilmesser* shapes are named after well-known sites like »Königsaue-type *Keilmesser*« (Mania/Toepfer 1973), »Lichtenberger *Keilmesser*« (Veil et al. 1994), »Bockstein-« (Wetzel/Bosinski 1969), »*Prądnik*-« (Wetzel/Bosinski 1969) or »*Klausennische-Messer*« (Wetzel/Bosinski 1969) and »*Balver*« (Jöris 2001) or »*Buhlener Keilmesser*« (Jöris 2001). It is most likely that these various *Keilmesser* shapes reflect distinct stages in the reduction of a tool during its use and subsequent modification (Jöris 2001; Pastoors 2001; Jöris 2004; Migal/Urbanowski 2006). The reasons for this outline shape variability, is most likely due to reduction and reworking processes (Jöris 2001; Pastoors 2001; Jöris 2004; Migal/Urbanowski 2006; Weiss 2020).

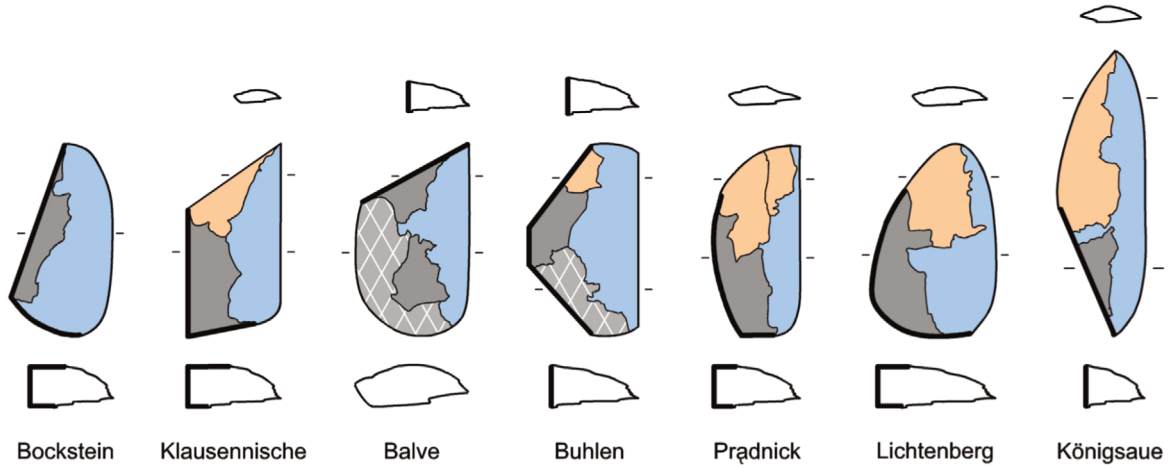

Fig. 7 Half-schematic illustration of the range of different shapes of *Keilmesser*. The thick black line indicates the back and the base as one perimeter section. The colours relate to unworked parts or thinning retouch orientated from the back and the base (grey), thinning of the distal posterior part (orange) and flat surface retouch of the active edge (light blue). – (After Jöris/Uomini 2019). – Not to scale.

An interesting aspect concerning long tool usage and reworking processes are distal *Keilmesser* fragments – here referred to as *Keilmesser* tips (**fig. 8**). The *Keilmesser* tips are sometimes part of *Keilmesser* inventories. An intentional removal of the distal part of the *Keilmesser* has been documented (Jöris 2001). This has been seen as a likely possibility to facilitate a longer tool use. Consequently, the tool's length is notably shorter, but the created fracture surface could serve as a new striking platform for a further thinning of the distal end. It is therefore probable that *Keilmesser* tips represent the reworking of one (worn out) *Keilmesser* shape into another.

The design of a tool is not only determined by the raw material used or the technology applied, but also directly influenced by the producer. Conversely, a tool can tell a lot about the individual who created it. This can be the handedness for instance. Some tools, as *Keilmesser* and *Prądnik scraper* can likely provide information about the handedness of the producer.

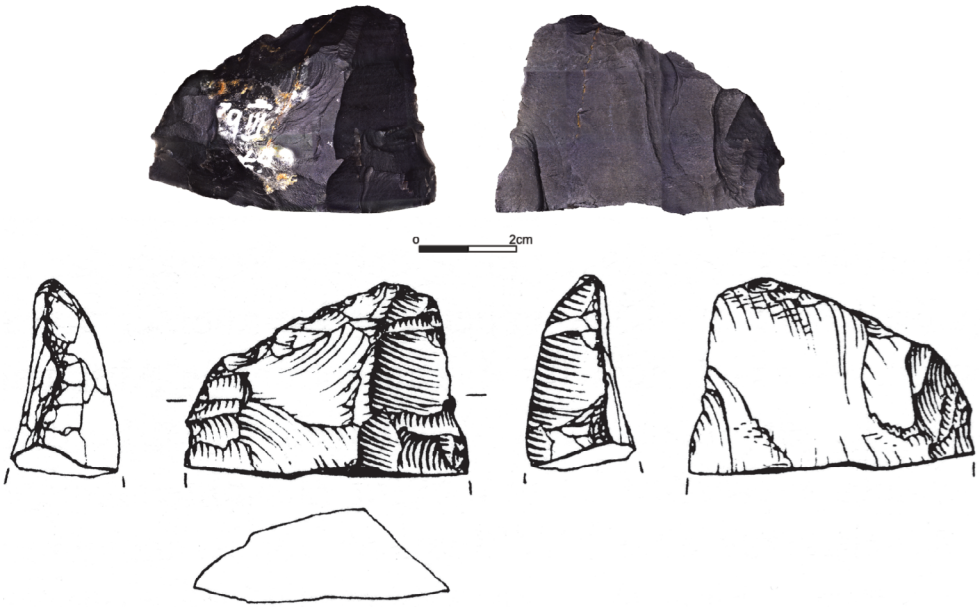

Fig. 8 *Keilmesser* tip from Buhlen (ID BU-086). – (Illustration Olaf Jöris [Jöris 2001]). – Scale 2:3.

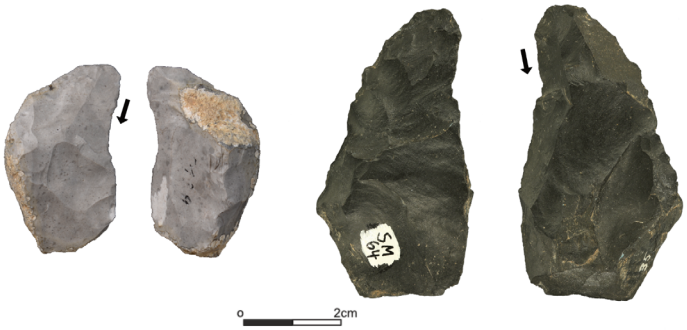

Fig. 9 Left-lateral *Keilmesser* (left) from Ramioul (ID R-002) and right-lateral *Keilmesser* (right) from Balver Höhle (ID MU-280). The black arrows indicate the direction of the applied *Prądnik method* visible as negative of the removal. – Scale 2:3.



Fig. 10 Top row: Primary left-lateral *Prądnik spall* (left) from Balver Höhle (ID MU-116) and primary right-lateral *Prądnik spall* (right) from Buhlen (ID BU-157). Bottom row: Secondary left-lateral *Prądnik spall* (left) from Balver Höhle (ID MU-307) and secondary right-lateral *Prądnik spall* (right) from Buhlen (ID BU-121). The black arrows indicate the direction of the applied *Prądnik method* visible as the negative of the removal. – (Photo Buhlen artefacts Sabine Steidl, RGZM). – Scale 1:1.

Based on the overall tool asymmetry, it is possible to distinguish left-lateral from right-lateral tools (Jöris/Uomini 2019; **fig. 9**). Moreover, this lateralisation can also be noticed regarding the *Prądnik spalls* (**fig. 10**). The implications resulting from the documented tool lateralisation are uncertain though. Arguments have been put forward which see the tool lateralisation as a proxy for human handedness (Cashmore/Uomini/Chapelain 2008; Uomini 2009). Since the production of a *Keilmesser* is rather complicated due to complex morphology and the asymmetry, each tool was probably produced by the intended user (Jöris/Uomini 2019). Unlike apes, humans have a species-level bias towards one hand preference (McGrew/Marchant 1997; Cashmore/Uomini/Chapelain 2008; Uomini 2009). Handedness, which, is closely related to brain lateralisation, has to be seen as a key feature of the motor-cognitive development from early human ancestors onwards (Uomini/Ruck 2018). It has been argued that the bias towards the preference of one hand is likely to increase in hominins when coupled with social learning (Morgan et al. 2015; Uomini/Lawson 2017; Uomini/Ruck 2018). Thus, together with the standards in tool design, the link between Middle Palaeolithic evidence for handedness and knowledge transfer in Neanderthals could likely be made.

Tool function and use

Tools are produced in a way to function. Some tools are manufactured for one function, some for multiple. Moreover, the function can change within the use-life of a tool. Design is thereby the key to function. In *Keilmesser*, the tool's morphology suggests that they could have been used for different activities, for example cutting, scraping and carving. Interpretations see *Keilmesser* as multifunctional or at least bi-functional tools (Jöris 2001; Rots 2009; Jöris 2006; 2012; Golovanova et al. 2017; Frick/Herkert 2019; **fig. 11**). This argumentation is based on tool morphology only and has not been verified through further analysis. The same counts for the tool handling. The morphology suggests a tool handling without additional hafting (Jöris 2001; Jöris/Uomini 2019).

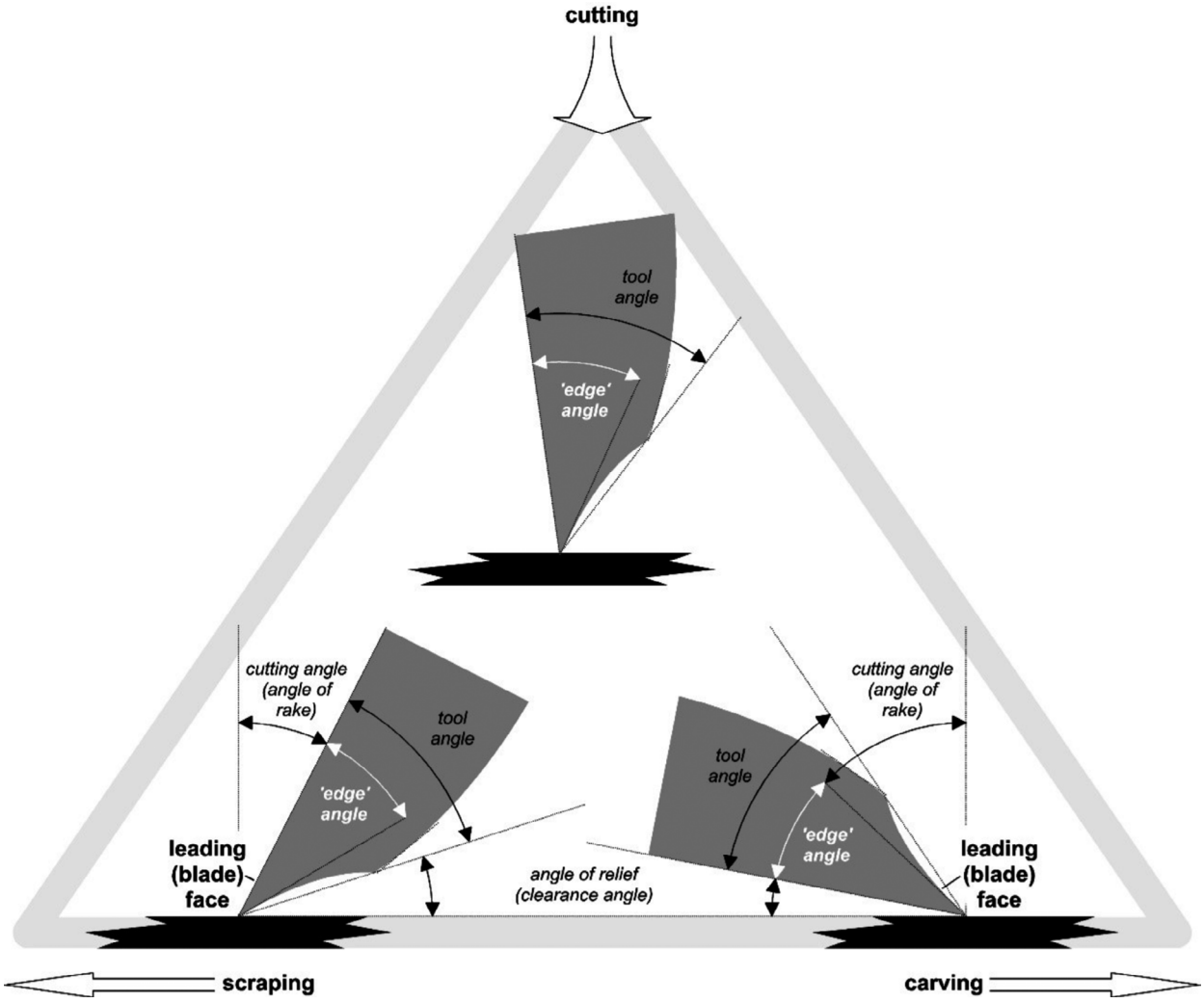

Fig. 11 Cross section of an idealised right-sided *Keilmesser* performing cutting, carving and scraping. Depending of the performed movement, the angle of relief has to be adapted. – (After Jöris/Uomini 2019).

Except from the morphological point of view, the function of *Keilmesser* and *Prądnik scrapers* has only been rarely addressed. Reports about use-wear analysis performed on *Keilmesser*, *Prądnik scrapers* or *Prądnik spalls* are almost absent. In one study, a large variety of tool uses was identified for *Keilmesser* (Rots 2009). Whether *Keilmesser* and *Prądnik* scrapers share not only technological attributes (Jöris 2001; 2004; Jöris/Uomini 2019) but also the function, has not been addressed yet. The aspect of tool function is also related to the observed long use-life histories of *Keilmesser*. Especially the interpretation of the *Prądnik method* for tool resharpening can be tested with use-wear analysis.

Although use-wear analysis provides the only way of finding direct evidence for tool use, not every aspect of tool use can be addressed with use-wear analysis solely. Also, aspects such as tool performance, durability and efficiency are relevant concerning tool function and use (Key/Lycett 2014; Key/Fisch/Eren 2018; Key/Lycett 2018). Thus, use-wear analysis ideally needs to be combined with controlled experiments. Since the aforementioned terms are critical for the understanding and the interpretation of results, their definition in the sense of tool use should be given:

Performance as a term implicates action in some kind. Performance describes how well a process or task was accomplished. While performance can be basically defined by the combination of the two aspects ef-

fectiveness and efficiency, effectiveness itself does not imply efficiency. Effectiveness (synonym to efficacy) is a measure that describes the relationship between a goal achievement and a defined goal. It therefore can also be described as a measure of effect. Efficiency defines the ratio between costs and benefits. In other words, it can be seen as an indicator of the consumed resources (e. g. energy, time) to achieve a goal. Durability is a measure of functionality over use. The term describes the ability of something (e. g. a physical product) to retain function. Loss of durability could be due to attrition from use or other factors that are not related to use such as age, natural decay etc. Durability excludes processes of maintenance or repair.
In the case of a controlled experiment with lithic samples the definitions could be transferred in the following sense: Performance would describe how the sample was able to conduct a task, e. g. cutting. This could be for instance reviewed by the cut (depth, quality etc.) the sample produced compared with the material loss on the sample itself (e. g. breakage). Effectiveness again could be assessed by the cut and its penetration depth etc. Efficiency can be addressed by aspects such as the applied force needed to perform the task or material loss on the sample itself and the ratio between these aspects and the achieved goal, in this instance the cut. Durability describes how often a task could be performed under the same condition before the sample was altered in a way that it could not function anymore as initially intended. For instance, the sample could be blunt or fractured. Durability in this sense excludes an adjustment of the given parameters (e. g. increasing the force) and tool maintenance.

SUMMARY

Due to the aforementioned characteristics, *Keilmesser* and *Prądnik scraper* provide a unique archive for tracing certain aspects of late Neanderthal behaviour. These may range from understanding tool function and its underlying design and production concept, technical innovations, learning strategies, the transmission of ideas and knowledge to the formation of late Neanderthal regional studies. Although these concepts are most often difficult to recognise over much of the Palaeolithic archaeological record, they gain visibility in the Late Middle Palaeolithic. In *Keilmesser*, long reduction sequences have repeatedly been documented. This allows for detailed morpho-technological reconstructions of the tool's use-life histories, including repetitive phases of production and tool maintenance, re-sharpening and re-use. Another focus has often been on the degree of tool standardisation. Technological studies could demonstrate the existence of similar working steps within the manufacture of *Keilmesser*. This implies an underlying tool concept with several production as well as reworking sequences. Which processes provoked Neanderthals to follow this level of tool standardisation remains speculative. Nevertheless, it raises the question of culturally transmitted tool-concepts. Related to this aspect are the implications that could be made from tool lateralisation. Tool lateralisation is likely to be interpreted as a proxy for handedness and would thus provide early evidence for human hand preference, social learning and knowledge transfer (Uomini/Ruck 2018; Jöris/Uomini 2019). The majority of *Keilmesser* assemblages are well studied from a technological and typological point of view. By contrast, use-wear analysis has rarely been done yet (Rots 2009). So far, only a small sample has been analysed, resulting in the identification of a large variety of tool uses. Many functional assumptions concerning the use of *Keilmesser* have been based on tool design and morphology according to archaeologists' interpretations and ethnographic observations. These interpretations ascribe *Keilmesser* a multifunctional purpose (Jöris 2001; 2006; Rots 2009; Jöris 2012; Golovanova et al. 2017, Frick/Herkert 2019). Other observations address the design and the modification of the active edge of *Keilmesser*. The mostly bifacially worked, acute active edge is frequently altered by an application of the *Prądnik method*. The implications of

this modification can be assumed (Jöris 2001; Frick et al. 2017; Frick/Herkert 2019), but they have not been tested experimentally. In order to use such interpretations as baselines when inferring human behaviour, the interpretations have to be tested and validated.
To summarise, asymmetric tools such as *Keilmesser* and *Prądnik scrapers* from the Late Middle Palaeolithic serve as a perfect case study to investigate tool design as a bridge between technology, typology, tool function and individual impact from the producer.

AIMS

The aim behind this PhD project can be summarised in the following way: to test known interpretations and gain new information about asymmetric tools from the Late Middle Palaeolithic. *Keilmesser* as well as *Prądnik scrapers* thereby serve as a case study. The only way to do so is by applying and combining different methods in order to focus on these tools from all possible angles. Therefore, this project consequently addresses aspects such as technology, typology, tool use and tool function in combination.
To start with, a techno-typological analysis has to be carried out. As mentioned before, techno-typological analyses on *Keilmesser* have already been extensively conducted. These analyses resulted in numerous information about the lithics, providing a detailed picture. However, since techno-typological studies do have their limitations, as all studies do, some observations will not pass the stage of a hypothesis. Other methods or types of analysis are unavoidable in order to test these observations. Thus, a multidisciplinary approach has been chosen. This approach moves beyond conventional technological and typological lithic studies by also involving a study of material properties, use-wear analysis and controlled experiments. This way, generally accepted models regarding *Keilmesser* can be tested (**tab. 1**). In the following, central aspects concerning the tools will be listed. Likewise, the selected methods, which can help testing these aspects, will be addressed and explained.
The general aim is to capture information about the tool design. Next to the technological and typological analysis, 3D data turns out to beneficial in addition to this. High-resolution 3D data facilitate the possibility for further and precise measurements. Moreover, a more distinct, high resolution picture of the active edge of the *Keilmesser* and *Prądnik scrapers* can be obtained. This aspect is relevant, because it allows addressing several questions regarding *Keilmesser.* For example, the edge angle can be calculated in detail. In this way, the idea that a lower edge angle is more efficient than a higher one (especially for tasks such as cutting) can be taken up. Through a comparison, the angles calculated along all entire tool edges can be put in proportions. This will lead to a better understanding of the edge design. Furthermore, the effect of an edge modification through the *Prądnik method* can be analysed quantitatively.
A second aspect is the raw material. The tool design is usually influenced to a certain extent by the selected raw material. Measuring the raw material properties is thus an important component of the methodological approach. Next to the possible influence of the raw material on tool morphology, also the potential efficiency during the use-life of the tool can be evaluated. The two raw materials, mainly encountered in the studied assemblages, silicified schist and flint, serve as a comparison.
To interpret the meaning of *Keilmesser* in the variability of Middle Palaeolithic lithics, one of the most important questions concerns their usage. The only way of gaining direct evidence for tool use is by the performance of use-wear analysis, or more precisely qualitative and quantitative use-wear analysis. With this project, this method will be applied for the first time to a large series of artefacts related to asymmetric tool production and use. This approach is relevant for several reasons. The first and most obvious one is

the identification of tool use. The given interpretation of *Keilmesser* as multifunctional tools can be tested. The documentation of the location and the orientation of the use-wear traces is a second objective of the use-wear analysis. The location is important to address aspects such as tool handling, also in the sense of potential tool hafting, and again, to understand overall tool design. The distribution in combination with the orientation of the traces can offer new information about the potential left- or right-handedness of the tool user. Furthermore, use-wear analysis of the *Prądnik spalls* can reveal the answer to the questions if the *Prądnik method* was applied to sharpen the tool edge or as a last finishing step within the tool manufacturing process. The latter would be disproven by the presence of use-wear traces on the dorsal surface of primary *Prądnik spalls*. Use-wear analyses are also likely to contribute on revealing the relationship between *Keilmesser* and *Prądnik scraper*. The tools share technological attributes, but it is unclear if the same counts for their function.

Another methodological approach with the purpose of gaining new data and testing interpretations is given by the conduction of controlled experiments. With the so-called *second generation experiments* (Eren et al. 2016; Lin/Režek/Dibble 2018; *sensu* Marreiros et al. 2020), different aspects regarding tool use and tool performance can be addressed by the use of a mechanical devise. Samples prepared with edge angles derived from the measurements taken from the *Keilmesser* assemblages will be used for the experiments. In this way, their ability to perform different tasks – cutting, carving and scraping – can be tested. The suitability for certain edge angles during these movements can be examined. The approach is meant to test the possible (multi-) functionality of the tool. At the same time, using controlled experiments allow to assess tool performance, efficiency and durability. Questions regarding the behaviour of the two involved raw materials as well as an alteration of the edge angle during the tool use can be raised. In general, *second generation experiments* offer the possibility to test and understand the cause-effect relations of the involved variables (e. g. edge angle, raw material). The results of the experiments can lead to an understanding of when for example re-sharpening is necessary to keep the tool efficient. This approach brings the functional inferences from the experimental setup together with independent data obtained from the archaeological artefacts. Simultaneously, the conduction of the experiments is beneficial in terms of contributing to a use-wear traces reference collection.

To summarise, the employment of several approaches aims at gaining new information about the techno-typological and the morpho-functional tool use of *Keilmesser*. This multidisciplinary approach can be condensed under the umbrella term of a functional analysis (*sensu* Marreiros et al. 2020). Functional analysis consists of technological, typological and use-wear studies. At the same time, and especially in the case of this project, experiments are a significant part of it. While use-wear analysis will contribute to an understanding of the actual tool use, experiments are indispensable to address the relationship between the morphological design of *Keilmesser* and their functionality. This proposed approach aims at providing new data to test the given interpretations of *Keilmesser*. Taken together, the only way to gain a more holistic view on *Keilmesser* is a multidisciplinary approach. The combination of the different scales of analysis and methods as techno-typological and material properties studies, use-wear analysis and controlled experiments is conditional upon understanding the concepts underlying tool design, function and its realisation. Linked in coherence with these topics are aspects such as learning strategies, the transmission of ideas and knowledge about the formation of late Neanderthal rules and regulations. Thus, this case study will lead to an improved understanding of Late Middle Palaeolithic technological adaptability and in context, will throw light on Neanderthal behavioural choices. Although human behaviour is multifaceted and complex, every piece of a puzzle should be a desirable contribution.

MATERIALS

The research within this PhD project is built on the study of the lithic assemblages from three Late Middle Palaeolithic sites, namely the Upper site of Buhlen, Balver Höhle, both in Germany, and the Belgian site of Ramioul (**fig. 12**). The data will be obtained from selected samples of the associated lithic assemblages. The selection of asymmetric tools – more precisely *Keilmesser* and *Prądnik scrapers* – and *Prądnik spalls* as candidates for specific artefact categories and elements from the reduction sequence are a result of the topic itself and the formulated research questions.

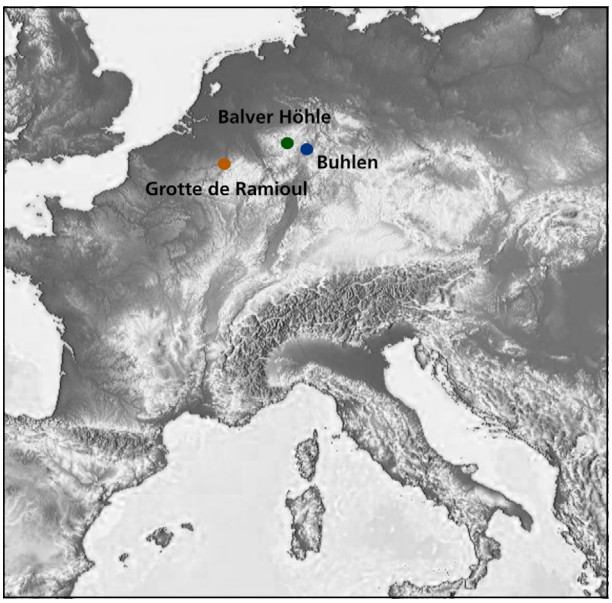

Fig. 12 Location of the three Middle Palaeolithic sites Buhlen (●), Balver Höhle (●) and Ramioul (●).

As explained in the »State-of-the-art«, *Prądnik scrapers* share certain technological and typological similarities with *Keilmesser* (Jöris 2001; 2004; **fig. 13**). The main discriminating feature is thereby the application of the *Prądnik method*, which also differentiates these *Prądnik scrapers* from other scrapers. The typological categorisation is based on an attribute analysis, explained hereafter.

Keilmesser are usually made from cores, rarely from flakes. They display in general a bifacially worked active edge. The retouch is applied sequentially, surface after surface (alternating unifacial edge regularization; see Bosinski 1967). The opposing back is natural (often with the presence of cortex) or roughly worked and builds mostly the thickest part of the tool. *Keilmesser* are in their morphology clearly asymmetric with a wedge-shaped cross section. Their lower surface is commonly flatter compared to the more strongly curved upper surface. *Keilmesser* are usually characterised by sequences of flat, standardised surface retouch, leading to the aforementioned typical shape. The complex pattern of scars on the surface often indicates numerous stages and phases of resharpening or modification. The application of the *Prądnik method* appears frequently not as a single event, judged by the overlying negatives of the removed *Prądnik spalls*.



Fig. 13 *Keilmesser* from Buhlen (ID BU-172) and *Prądnik scraper* from Balver Höhle (ID MU-290) in comparison. – (Photo Buhlen João Marreiros, RGZM). – Scale 2:3.

site		raw material			
		silicified schist	flint	other	total
Buhlen	n	195	2	1	**198**
	%	98.5	1.0	0.5	100.0
Balve	n	337	10	0	**347**
	%	97.1	2.9	0.0	100.0
Ramioul	n	2	18	0	**20**
	%	10.0	90.0	0.0	100.0
total	n	**534**	**30**	**1**	**565**
	%	94.5	5.3	0.2	100.0

Table 2 Distribution of the raw materials used for the production of the studied artefacts from Buhlen, Balver Höhle and Ramioul. For Buhlen, other refers to carnelian.

Prądnik scrapers, on the contrary, are commonly made from flakes, not from cores. They display one unifacial or semi-bifacial retouched active edge. The back, opposed to the active edge, is either natural or modified with a clear, intentional blunting. Thus, also *Prądnik scrapers* show a distinct asymmetry. Usually, retouch extension over the surface is far scarcer, which leads to a less obvious surface curvature. *Prądnik scrapers* are characterised by at least one negative scar, resulting from the application of the *Prądnik method*. Although *Keilmesser* and *Prądnik scrapers* share morphological attributes, *Prądnik scrapers* appear technologically less complex.

Sometimes, a distinction between the two artefact categories is not clear cut. However, based on these attributes, the artefacts can be analysed and categorised as either *Keilmesser* or *Prądnik scrapers.*

In general, all available artefacts belonging to one of these three categories – *Keilmesser*, *Prądnik scrapers* and *Prądnik spalls* – have been chosen for the study. The *Prądnik spalls* from the site Buhlen form a sole exception. In this case, only some representative pieces have been sampled out. Additionally, a small number of scrapers and flakes are part of the study. Within the analysis they form an outgroup. With the outgroup the possibility will be given to put the results of the other studied artefact categories in relation.

Brief information about the sites, their research history and the number of selected artefacts from the lithic assemblages will follow in this chapter. An extended version and a detailed description can be found in earlier published literature concerning the sites Buhlen (Bosinski 1969; Bosinski/Kulick 1973; Jöris 2001), Balver Höhle (Günther 1964; Kindler 2012) and Ramioul (Vandebosch 1921).

SELECTION OF THE SITES

Although the three sites, Buhlen, Balver Höhle and Ramioul are not dated radiometrically and not all finds are stratified, the classification of the material as Late Middle Palaeolithic assemblages is unquestioned. In fact, according to the research question, a refined chronological dating is not of major relevance for this study. Buhlen represents one of the richest *Keilmesser* assemblages and especially the huge quantity of lateral sharpening spalls is unique. In fact, the inventories of the Balver Höhle can be described as forming one of the largest *Keilmesser* assemblages in central Europe and are therefore especially suitable for the analysis of the artefact category itself, the main goal of the presented project. The assemblages from Buhlen and



Fig. 14 The site Buhlen seen from the East. The loess quarry is visible between the trees on the right of the picture. – (Photo Gerhard Bosinski).

Balver Höhle thus allow an in-depth study of the selected artefact categories concerning metric as well as qualitative aspects. Based on the numerous samples a statistic evaluation of the analysis is possible. Ramioul displays, in contrast to Buhlen and Balver Höhle, a small *Keilmesser* assemblage only. The reason to include the site is based on the technology concerning the tool manufacturing. All three sites attest similar technological sequences including the application of the *Prądnik method*. From a technological point of view, the sites are much alike and display a high inter-comparability. Additionally, the artefacts are so similar that an analogous function can be assumed. Also important to mention is that the raw materials used to produce the tools is the same in the three sites, silicified schist and flint (**tab. 2**). Buhlen, Balver Höhle and Ramioul are perfectly suitable for an inter-site comparison.

BUHLEN

Site location and excavations

The archaeological site of Buhlen is located in northern Hesse, Germany, roughly 200 m north-northeast of the village Buhlen in the district Waldeck-Fankenberg/ Nordhessen. The site consists of two units – the Lower Site of Buhlen at the banks of the Netze river and the Buhlen Upper Site, a small collapsed rock-shelter (Bosinski 1969; Bosinski/Kulick 1973; Jöris 2001; **fig. 14**). In this PhD project, only the material from the Upper site is addressed.

Buhlen has been known as a paleontological site in a loess quarry since 1840. At the beginning of the 1960s, a small Dolomitic limestone ridge was partly removed by road construction, during which Pleistocene animal bones became exposed. In the context of geological mapping work, two geologists, M. Horn and J. Kulick revisited the outcrop in 1963. Within the Upper Pleistocene loess sequence of the site, they found animal bones and the first lithic artefacts. As a consequence, Kulick started the first test trenches. After contacting Gerhard Bosinski at Cologne University, the site was excavated in 1966 to 1967 and in 1969, starting with the Lower Site and finally uncovering the Upper Site with the collapsed rock-shelter and its small terrace. Excavation standards also included wet-screening of the entire sediment. Thus, a high amount of artefacts belonging to smallest fraction is part of the excavated material. In cooperation with the Hessische

artefacts	n
Keilmesser	115
Keilmesser tip	15
Prądnik scraper	24
Prądnik spall	42
scraper	2
total	198

Table 3 Categories of the selected and studied artefacts from Buhlen.

layer	artefacts [n]					
	Keilmesser	*Keilmesser* tip	*Prądnik scraper*	*Prądnik spall*	scraper	total
I	3	2	2	1	1	**9**
II	15	0	2	2	0	**19**
II b	2	0	0	1	0	**3**
III a	3	0	0	3	0	**6**
III b	77	9	17	26	1	**130**
III c	6	3	2	5	0	**16**
III d	1	0	1	1	0	**3**
unknown	8	1	0	3	0	**12**
total	**115**	**15**	**24**	**42**	**2**	**198**

Table 4 Stratigraphic attribution of the artefacts from Buhlen. A small amount of n = 13 artefacts could not be ascribed to a layer.

Landesamt für Bodenforschung in Wiesbaden and the Institute for Palaeontology at the University of Mainz, Bosinski's excavation covered almost the entire spatial extent of the Upper Site (Bosinski/Kulick 1973; Jöris 2001). In total, the site yielded over a surface of less than 80 m² an extremely rich assemblage of around 200,000 lithic artefacts and 150,000 animal bones (Jöris 2001). The material is stored and also partly on display in the Hessisches Landesmuseum in Kassel. The majority of the artefacts relevant for this PhD project derive from one find complex: Bu-III. Based on sedimentological and biostratigraphical arguments, this find complex most likely dates to the transition from late OIS 5 into early OIS 4 (Jöris 2001; 2004).

Buhlen lithic assemblage

The lithics selected for this project are almost all associated with the basal find complex of the Upper Site of Buhlen, BU-III (**tabs 3-4**). However, in the periphery of the rock shelter, the material seems to have been mixed up with the succeeding complex, BU-II (Jöris 2001). Thus, single artefacts have to be ascribed to BU-II instead of BU-III. In the case of the selected lithics here n = 9 artefacts originate from BU-I, n = 22 artefacts from BU-II, while n = 155 artefacts are associated with BU-III. N = 13 artefacts cannot be ascribed to a specific find complex due to missing labels.

The artefacts from the Upper Site of Buhlen are with a few exceptions made of local silicified schist. On a rare occasion Baltic flint or carnelian have been used as raw material. Although the *Keilmesser* assemblage, as demonstrated by Jöris (2001) is known to be bigger than selected for this project, the accessibility of the material was a limiting factor. The present study refers therefore to n = 130 *Keilmesser* and n = 24 *Prądnik scrapers*. N = 42 *Prądnik spalls* were selected next to n = 2 scrapers as outgroup.

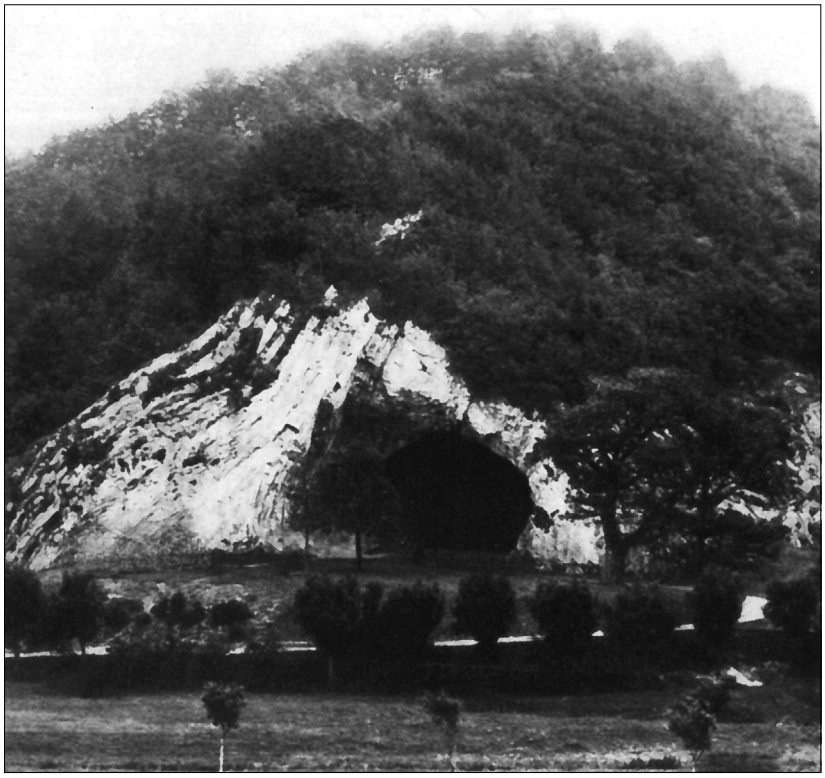

Fig. 15 Balver Höhle in North Rhine-Westphalia, Germany. – (After Günther 1964).

BALVER HÖHLE

Site location and excavations

The Balver Höhle describes a karst cave within the Rhenish Slate Massif in North Rhine-Westphalia, Germany (fig. 15). The cave is situated in the Hönne valley, one of the most important karst areas in the region, north of the city Balve in the district Märkischer Kreis. The Balver Höhle represents the largest archaeological cave in Germany (Andree 1939) and is used nowadays as a cultural venue. The cave system is composed of a main cave of circa 54 m length, the major distributary and two lateral distributaries, each about 20 m long (fig. 16). These latter are named after Heinrich von Dechen and Rudolf Virchow, scientists who were both responsible for early excavations at the site (Günther 1964).

Research history started early in the middle of the nineteenth century with the exploitation of phosphate-rich cave sediments, which were used as a fertilizer for the surrounding fields. The majority of the excavations took place at the end of the nineteenth century and the beginning of the twentieth century (Bahnschulte 1940; Günther 1964). The excavations opened an up to 7 m long stratigraphic sequence, covering large parts of the Upper Pleistocene and Holocene.

With the first reported findings of lithic artefacts in 1843 archaeologists became aware of the site. During the succeeding decades archaeological interest into the cave sequence intensified, resulting in a se-

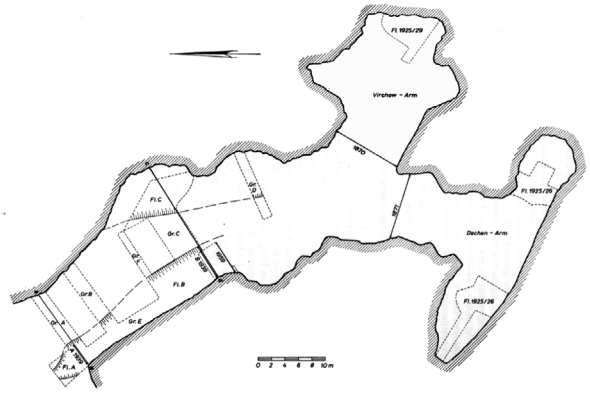

Fig. 16 Cave plan of the Balver Höhle in North Rhine-Westphalia, Germany. – (After Günther 1964).

ries of field campaigns that emptied large parts of the cave's interior and also examined the terrace in front of the cave's entrance (Andree 1928; Bahnschulte 1940; Günther 1988; 1964). Nevertheless, it was not until 1939 that major systematic excavations at different localities near the entrance and within the cave were conducted by Bernhard Bahnschulte (1940). Since the topmost layers, including Upper Palaeolithic sediments, had already been removed during earlier years, Bahnschulte's work concentrated on remnant sediments in lower fissures of the cave floor. Thereby, he excavated thousands of artefacts from a surface of several m² and from almost all sedimentary layers (I-V from bottom to top). The vast majority of these finds as well as the associated fauna are ascribed to the Late Middle Palaeolithic. In 1959, to gain new geoscientific data for an improved understanding of the site's stratigraphy, geochronology and site formation, Klaus Günther added small trenches immediately near to those of Bahnschulte. Most recently, in 2009, Michael Baales aimed at re-opening the site to obtain samples for OSL-dating, but unfortunately did not succeed in finding undisturbed horizons (Baales 2013). Due to the long and intensive research history at the site and later constructions to use the cave as a public cultural venue, no remaining *in situ* deposits could be detected. The majority of the material attributed to the Balver Höhle is today stored in the Amt für Archäologie und Denkmalpflege in Münster, the Landesmuseum für Archäologie in Herne and – until recently – in the Sauerlandmuseum in Arnsberg. The material derives mainly from Bahnschulte's excavations, to lesser degree from other archaeological fieldwork at the site, but also from several private collections. In total, the entire lithic inventory adds up to 40,600 artefacts, although only 9,100 artefacts are stratified and a substantial loss of material over time can be assumed (Günther 1964). This includes for example small chips, which have not been kept in the course of the excavations, except for those from Günther's 1959 sondages. The sediment removal to fertilize the surrounding fields has not spared the artefacts from being removed, either. As a result, artefacts can be found on the surrounding fields, which originate from the cave deposits. As mentioned before, the inventory represents a broad range of different Middle Palaeolithic artefact types, characterised by a particularly high amount of bifacial tools.
In particular, the material from archaeological horizon (AH) II up to AH V has been attributed to the Micoquian (Günther 1964; Bosinski 1967) and later referred to as KMG (Jöris 2004). Based on the results from Olaf Jöris (1992; 2004; 2006) and Lutz Kindler (2007), the sequence of Middle Palaeolithic layers in the Balver Höhle spans from late OIS 5 to early OIS 3 (Jöris 2004; 2006). The settlement in the Balver Höhle is characterised by recurrent Neanderthal presence (Kindler 2012).

Balver Höhle lithic assemblage

The selected assemblage from the Balver Höhle represents artefacts from the entire stratigraphic sequence (tabs 5-6). The stratigraphic correlation of the results from the various excavations is complicated and leads sometimes to an ambiguous attribution of the artefacts (Pastoors/Tafelmaier 2010). In total, the sequence extends from the lowest layer AH I to the uppermost layer with archaeological artefacts, layer AH VI (Günther 1964). For the production of the tools the local silicified schist served as a raw material. Although the entire lithic assemblage from the Balve cave is characterised by the use of this specific raw material, Baltic flint was also used in a few exceptional cases.
The material consists of n = 189 *Keilmesser* and n = 27 *Prądnik scrapers*. The amount of corresponding *Prądnik spalls* is n = 117. Additionally, n = 12 scrapers were selected for an outgroup comparison. From these 347 artefacts, only 94 samples can be attributed to a stratigraphic horizon. The majority originates thereby from layer AH II, followed by layer AH III. Due to missing labels the other three-quarters of the selected assemblages cannot be associated with a specific layer.

Table 5 Categories of the selected and studied artefacts from Balver Höhle.

artefacts	n
Keilmesser	170
Keilmesser tip	21
Prądnik scraper	27
Prądnik spall	117
scraper	12
total	347

layer (AH)	artefacts [n]					
	Keilmesser	*Keilmesser* tip	*Prądnik scraper*	*Prądnik spall*	scraper	total
IV	4	2	2	7	0	**15**
sterile	2	0	0	0	0	**2**
III	10	1	3	4	5	**23**
II + III	2	0	0	14	0	**16**
II	27	5	0	4	0	**36**
I	2	0	0	0	0	**2**
unknown	123	13	22	88	7	**253**
total	**170**	**21**	**27**	**117**	**12**	**347**

Table 6 Stratigraphic attribution of the artefacts from Balver Höhle. Out of the n = 347 studied artefacts, only n = 94 artefacts can be ascribed to one of the archaeological layers (AH = archaeological horizon).

RAMIOUL

Site location and excavations

La Grotte de Ramioul, short Ramioul (sometimes also Ramioulle) belongs to a karstic system on the right riverside of the Meuse, near Liege, in the municipal Flémalle, Belgium (Vandebosch 1921; Ulrix-Closset 1975; **fig. 17**). It is located between two quarries, Abime Martel to the West and Caverne à végétations to the East. The cave is separated in three vertical levels (**fig. 18**): the upper section (»*superieure*«), the mid section (»*moyenne*«) and the lower section (»*inférieur*« or »*réseau actif*«). The levels are connected through a shaft and linked to a main chamber (»*salle*«). Additionally, there is an open air area with a small rock shelter associated with the cave (»*terrasse*«) (Vandebosch 1921; Quinif et al. 2011).
In 1908, a group called »*Les Chercheurs de la Wallonie*« discovered two prehistoric burials (Vandebosch 1921; 1929; Ulrix-Closset 1975). The burials contained bones, but no further artefacts, which would have allowed for a more precise age estimation. By



Fig. 17 Entrance portal of the Grotte de Ramioul, Belgium. – (After Ulrix-Closset 1975).

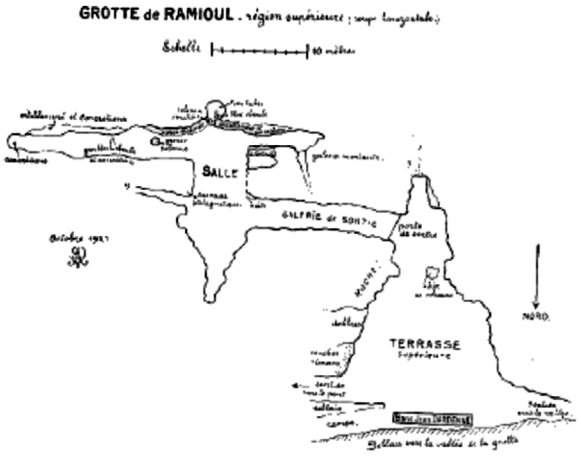

Fig. 18 Cave plan of the Grotte de Ramioul, Belgium. – (After Vandebosch 1921).

continuing the research within the cave, a total of seven child burials have been found. Additionally, lithic tools, ceramics and fauna have been unveiled. Together, these finds could be attributed to the Neolithic. This marks the beginning of the research in Ramioul. Back then, sediment layers reached a depth of 5.5 m. In total five different layers could be distinguished (layer one to five, from top to bottom, whereas layer five is connected to the bedrock). Based on the initial finds, a second excavation was initiated in 1911. During this excavation, Palaeolithic artefacts of undetermined age were found. Among them, numerous lithics (circa 200 pieces) mainly made of flint and glacial fauna. Most of these finds have been found in front of the cave (»terrasse«), rather than inside. However, the excavated layers of the terrace could be correlated with the cave's stratigraphy from the cave. In general, not all finds are stratified, since parts of the layers seemed somewhat disturbed. In the years 1914 and 1915, research has been continued further, unearthing the lowest level (»*inférieur*« or »*réseau actif*«) that contains no archaeological finds (Vandebosch 1921; 1957; Quinif et al. 2011).

Based on the finds and especially the lithic assemblage form the fourth layer, which contains a high percentage of bifaces, Levallois tools, scrapers and leaf-points (or leaf-point-like artefacts), the Ramioul assemblage has been associated with the »Mousterian« (Ulrix-Closset 1975). The entire occupation of the cave starts at the Late Middle Palaeolithic and spans into the Holocene.

Since 1994, the Préhistomuseum (before Préhistosite de Ramioul), is located near *La Grotte de Ramioul.* The finds from Ramioul are stored and partly displayed in the very same museum.

Ramioul assemblage

The material consists of n = 9 *Keilmesser* and n = 3 *Prądnik scrapers* (**tab. 7**). Unfortunately, *Prądnik spalls* could not be sampled, due to the fact, that all artefacts which have not been categorised as tools were stored together with material from a nearby located site. An identification of material clearly belonging to the site Ramioul is therefore impossible. N = 6 scrapers and n = 2 flakes were selected additionally. The stratigraphic or spatial assignment for these 20 samples is undetermined. Unfortunately, the assemblage is poorly published (Ulrix-Closset 1975; cf. Jöris 1992).

Concerning the raw material, the situation in Ramioul is different than in Buhlen or Balver Höhle. The predominantly used raw material is flint. In a few exceptions, silicified schist served as a raw material too.

artefacts	n
Keilmesser	9
Prądnik scraper	3
scraper	6
flake	2
total	20

Table 7 Categories of the selected and studied artefacts from Ramioul. For none of these artefacts a stratigraphic attribution is possible.

METHODS

This chapter focuses on the methods and techniques applied within this project. It is organised according to the different steps of the research and types of analysis. The project is trying to follow an integrative and multidisciplinary approach to gain a more holistic view on asymmetric tools from the Late Middle Palaeolithic. At the same time, a standardised analytical workflow is aimed for. Irrespective of the applied method or pieces of equipment used, following standards and protocols were sought. Used settings, programs and software were reported as transparently as possible. The scripts and templates used to analyse the data are saved and stored on GitHub, a distributed version-control system for tracking changes [https://github.com/lschunk]. The same applies to all involved data, including the raw data.
The first subchapter describes the raw material characterisation, followed by the techno-typological analysis, and a subchapter on the quantification of the edge design. The next two subchapters addressing the use-wear analysis are separated into a qualitative and a quantitative analysis. The last part of this chapter is dedicated to the controlled experiments. All methods are targeted at gaining information about the archaeological assemblages and producing data, which in most cases is statistically evaluable. Although it goes beyond the scope of a method chapter, an introduction to some of the methods are given. This is the case for the chapters addressing raw material characterisation, use-wear analysis, edge design and experiments. Thereby, the introductions focus on the perspective of lithic analysis. Additionally, the advantages, disadvantages and limitations of these methods are discussed.

RAW MATERIAL CHARACTERISATION

Early humans had to select suitable raw material for the production of tools. Whether this process was a conscious decision or not was also presumably dependent on the raw material availability and variability. Research on the raw material variability present in archaeological assemblages has already been established for many decades (Dibble 1985; Féblot-Augustins 1993; Floss 1994; Féblot-Augustins 1997; 2008; Andrefsky 2009; Meignen/Delagnes/Bourguignon 2009). The reasons for studying the raw material can differ. The most obvious one is the classification of the raw material and identification of the possible source, which can provide information about movement patterns of early hominids (Andrefsky 1994; Féblot-Augustins 1997; Brantingham 2003; Féblot-Augustins 2008). Alongside raw material procurement, the raw material properties themselves are another aspect which can be analysed. The properties of raw material, for instance the size and shape of the original blocks or nodules as well as density and hardness, have a critical influence on the ability to knap a tool (Kuhn 1992; Braun et al. 2009; Dogandžić et al. 2020). Moreover, the tool design correlated with the used raw material can provide information about intentional selection. Therefore, raw material properties are assumed to affect not only tool production, but also technical choices in general and tool use specifically (Odell 1981; Delgado-Raack/Gómez-Gras/Risch 2009; Nonaka/Bril/Rein 2010; Key/Proffitt/de la Torre 2020). By the analysis of their characteristics, it is possible to say whether, for example, physical properties have been manipulated through heat treatment (Brown et al. 2009; Schmidt/Mackay 2016; Key/Pargeter/Schmidt 2020). Features such as surface roughness are also recognised as a determining factor in the development and the characteristics of use-wear traces (Lerner 2014). As demonstrated by several studies, the nature and the properties of the contact material can be associated with specific

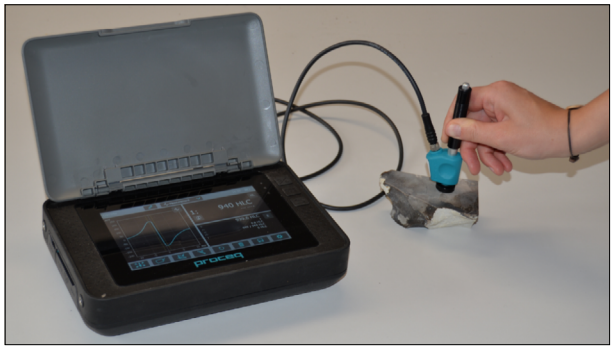

Fig. 19 Hardness measurements taken on a flint sample using the Leeb rebound hardness tester with the Leeb C probe (Proceq Equotip 550).

use-wear traces (Stemp/Stemp 2003; Lerner 2007; 2014). The rate at which use-wear forms on a given tool surface, is dependent on the surface hardness and roughness of both the tool and the contact material. This means that raw material properties are known to affect the development and the characteristics of use-wear traces, for instance polish (Lerner 2007; 2014; Lerner et al. 2014). Analysing the material properties of a given raw material is therefore a prerequisite to understand the formation of use-wear traces and their interpretation, respectively. To go into more detail, raw material properties are an influencing factor not only for tool morphology, but also for tool efficiency and durability. As demonstrated recently, early hominins might have actively chosen certain raw materials for specific functional performances (Agam/Zupancich 2020; Key/Proffitt/de la Torre 2020). Consequently, analysing raw material properties should be part of each lithic study.

Thus, the first aspect of this study addresses the raw material used to produce the tools. In the case of the three examined sites, only two types of raw material are involved in the analysis: silicified schist and cretaceous (»Baltic«) flint (Vandebosch 1921; Günther 1964; Bosinski 1969; Jöris 2001). For the petrographic analysis, only optical factors such as the colour, the nature of the cortex and the translucency of the raw material were of relevance. The raw material from the archaeological sites was compared with the lithic raw material collection at MONREPOS Archaeological Research Centre and Museum for Human Behavioural Evolution, RGZM as a reference (https://monrepos.rgzm.de/en/ausstattung/#Sml). This collection contains siliceous rock samples from different sources used to manufacture tools in western Central Europe during the Palaeolithic and Mesolithic (Floss 1994).

The properties of the raw materials, for instance hardness, can be measured to evaluate the possible influence of the raw material itself on tool morphology and also to predict potential efficiency and durability during the use-life of the tool (Key/Lycett 2017; Key/Pargeter/Schmidt 2020; Key/Proffitt/de la Torre 2020). Relatively common is the use of a Schmidt hammer to estimate mechanical properties of rock material (Yilmaz/Sendir 2002; Yaşar/Erdoğan 2004; Braun et al. 2009). The Schmidt hammer is a device that works with a rebound hammer to test surface hardness and penetration resistance based on elastic properties and the strength of rock. An alternative method has been provided recently using a Leeb rebound hardness tester. The hardness test was originally developed for metals but has been correlated for rocks (Braun et al. 2009; Rodríguez-Rellán 2016; Corkum et al. 2018; Kovler/Wang/Muravin 2018). The measurements can be carried out rapidly and non-destructively. Micro surface roughness of knapped surfaces as another parameter, can be measured for example with a 3D confocal laser scanning microscope. Even though important, the material properties of the raw materials present in archaeological assemblages have been rarely tested. Although highly relevant in experimental design, they are often neglected (Evans et al. 2014). The reason for this might be the costly equipment needed to calculate some of the properties or maybe an underestimation of their relevance.

Here, the material properties of the raw material were tested using the Leeb rebound hardness tester (Proceq Equotip 550, Leeb C probe; **fig. 19**). Two types of raw material were involved in the analysis: silicified schist and Baltic flint. The advantage of the hardness test conducted with the Leeb rebound is that the measurements can be carried out rapidly and are non-destructive. The disadvantages are the required flat surface and mandatory maximum size of the object. For the knapped archaeological tools, it was not possible to measure the hardness with the Leeb rebound. Based on their morphology it is impossible to position

the tools entirely flat, so that one face is in contact over its total surface with the stable supporting base (here a flat rock slab of about 20 kg). Additionally, the other tool surface must be flat as well in order to conduct the measurements. However, one semi-finished tool from Balve (ID MU-278) fulfilled these requirements. While this approach was used only once for the archaeological samples, it was always applied for the experimental samples (see chapter Controlled experiments). With the hardness tester, to insure and test intra-variability in each sample, ten measurements per sample were taken. The number of measurements not only ensures the inclusion of the raw material variability within the result but also identifies potential outliers. When the samples did not fulfil minimum sample size requirements, an additional coupling paste was used to connect the sample with a massive support plate.

TECHNO-TYPOLOGICAL ANALYSIS

Initial information for all assemblages from the three different archaeological sites was acquired through traditional lithic analysis methods (Hahn 1993; Debénath/Dibble 1994; Andrefsky 1998; Odell/Vergès 2014). This technological and typological analysis was based on two different but complementary methods. While one approach produced qualitative data related to several descriptive attributes, e. g. tool morphology, the shape and character of the back or the application of the *Prądnik method*, the second method generated quantitative results obtained by standard calliper-based morphometric data (e. g. length, width and thickness). *Keilmesser* as well as *Prądnik scrapers* were analysed in the exact same way. The approach described here is therefore identical for both artefact categories respectively. Mentionable exceptions are the *Prądnik spalls*, the *Keilmesser tips*, scrapers and simple flakes, which are treated differently in some respects. These artefact categories were analysed in the same way but certain steps of the analysis (e. g. definition *Keilmesser* shapes, perimeter sections) were not of relevance and have therefore been omitted. Concerning the »*Keilmesser tips*«, it needs to be noted that these tools are notably shorter than a complete *Keilmesser*. Thus, their metric values are not directly comparable with those of the remaining artefacts.
The database for the techno-typological analysis was done by using E4 for Microsoft Windows 10 (Old Stone Age, S. McPherron), as a data entry program. To use E4, a script with all variables was entered and their type (e. g. text, numeric) was configured. Since E4 offers the possibility, to create conditional statements, variables can be skipped based on values entered for previous variables. The script was written in the open-source software R (version 4.0.2 through RStudio version 1.3.1073, RStudio Inc., Boston, USA) for Microsoft Windows 10. The data was saved in MDB format.

Blanks and cortex

To begin with, a qualitative attribute is addressed with the determination of the blank used for the tool production. The tools can be manufactured on different blanks (Jöris 2001). If a distinction is possible, it should be determined in this part of the analysis, whether a core or a flake was used as a blank to produce the tool. In some cases, it is not possible to identify the type of blank. Thus, the term »undeterminable« was selected. Another feature that can provide valuable information, for instance on manufacturing sequences or methods, is the amount of cortex left on the tool surface (Dibble et al. 2005). The first question is whether there is cortex on the artefact. If yes, the amount of cortex in percent (>25 %, 25-50 %, 50-75 %, <75 %, total) was indicated as well as the location.

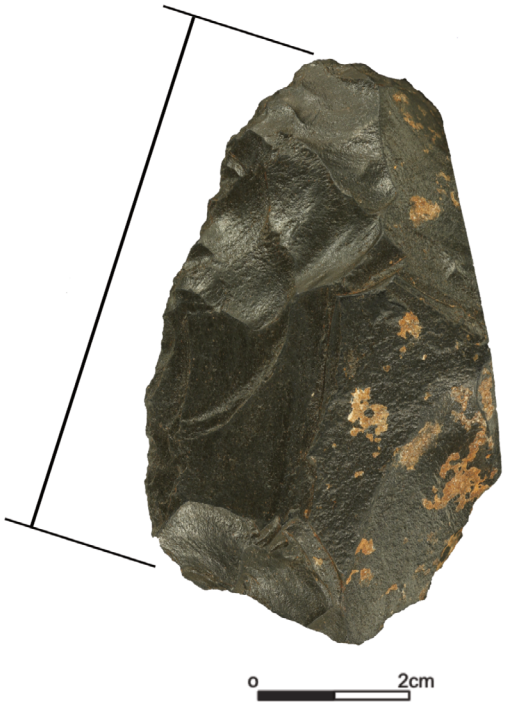

Fig. 20 *Keilmesser* from Balver Höhle (ID MU-021). The black lines indicate the length measurement of the active edge. – Scale 1:1.

Morphometric quantitative analyses

All metric data were recorded using a digital calliper of the brand Mitutoyo with a direct data output. The used model achieves a precision of 0.01 mm with an error margin of 0.03 mm. Dimensions were taken for complete and incomplete artefacts, the latter being recoded as such. The length measurement was determined using the active edge and not necessarily the maximal dimension of the tool (fig. 20). However, the maximum dimensions were applied for the measurements of width and thickness (Debénath/Dibble 1994).

Tool back

The design of the back forms another of the criteria of the attribute analysis. Here, the relevant trait is the state of the back (Bosinski 1967; Jöris 2001). The design of the artefact back can inform about the extent to which the back already formed a conceptual part of the tool manufacture and influence of the morphology of the raw material blank used. For instance, the back can be characterised by unworked cortex surfaces or natural fragmentation. Moreover, clear traces of intentional retouch or minor working traces can be observed.
The thickness of the tool back was recorded identically to the dimensions described above, at its maximum extent, meaning the most pronounced section of the back.

Active edge retouch

In addition to the back, the design of the active edge was analysed. The interesting technological aspect was the type of retouch along the edge. The retouch was classified into either bifacial retouch, semi-bifacial retouch or unifacial retouch.

Lateralisation

Another feature documented as a qualitative attribute is the laterality of the artefacts. The lateralisation results from tool asymmetry (Jöris/Uomini 2019; fig. 9). Tool lateralisation can be determined when the artefact is aligned with the proximal part of the tool towards the observer and the flat surface (of *Keilmesser*) or the ventral surface (of *Prądnik scrapers*). If the back is then on the left side and the active edge on the right side, the artefact counts as *dextrolateral* (dex.). If the back is to the right and the active edge at the left, the tool is recorded as *sinistrolateral* (sin.).

Morphological shape variability

The artefacts were assigned to one of the seven distinct *Keilmesser* shapes respectively (**fig. 7**). However, the division was made baes only on a visual impression. The fundamental question to be asked is whether these *Keilmesser* shapes indeed exist as strictly distinguishable types or if the types merge into each other and show the result of reworking and resharpening processes. In the following, the seven *Keilmesser* shapes are described in more detail (e. g. Jöris 2001).

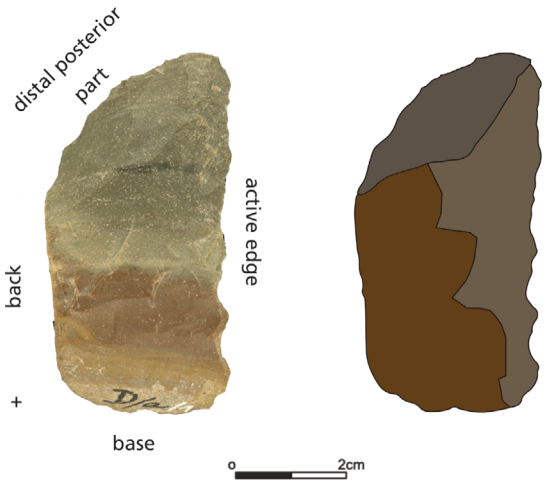

Fig. 21 Dorsal surface of a *Keilmesser* from Balver Höhle (ID MU-114) (left), indicating the different perimeter sections base and back, distal posterior part as well as active edge. The half-schematic illustration (right) displays the identical *Keilmesser*. The three perimeter sections are highlighted in colours. – Not to scale.

The »*Bockstein knife*« is characterized by the absence of a transition between the back and the active edge. Both these tool areas, the back and the active edge, meet at an acute-angle (Wetzel/Bosinski 1969).

The back and the active edge of the »*Klausennische Messer*« run almost parallel to each other. A bifacially worked, mostly obliquely running distal posterior part connects the back with the active edge. This distal posterior part and the active edge display an acute angle (Wetzel/Bosinski 1969).

The »*Prądnik Messer*« is morphologically closest to given definition of a »*Klausennischen Messer*«. The back of this *Keilmesser* shape changes into a retouched, bow-shaped distal posterior part, which is more rounded and connects with the active edge at approximately right angles (Wetzel/Bosinski 1969).

The outline of the »*Buhlener Keilmesser*« resembles a right-angled, equilateral triangle. The two catheti are formed by the back and the distal posterior part, whereas the active edge corresponds to the hypotenuse (Jöris 2001).

Characteristic for the »*Lichtenberger Keilmesser*« is a clear convexity of the active edge. Both the base and the distal posterior part are rounded and thus the active edge is slightly elongated. The description of this *Keilmesser* shape is not narrowly defined and can vary (Veil et al. 1994).

Artefacts of the type »*Königsaue-type Keilmesser*« are also characterized by a convex active edge. The back is located at the proximal part of the tool. The biconvex distal end of the artefact resembles the morphology of a leaf point (Mania/Toepfer 1973).

The »*Balver Keilmesser*« is defined by a crudely worked base. From the top view, the base seems rounded. The distal posterior part runs obliquely, comparable to the »*Klausennische*« *Keilmesser* shape (Jöris 2001).

Following this descriptive morphology of *Keilmesser*, the outline of the artefacts can be separated into three distinct components, resulting together in the artefact's perimeter (Jöris 2001; Frick/Herkert 2019; **fig. 21**). Firstly, one segment is defined by the tool base and the back. The second section is described by the distal posterior part, connected directly to the back. The overall perimeter is completed by the third region made up of the active edge of the tool. The respective lengths of the different sections of the artefact's perimeter were measured. Only complete tools were suitable for this measurement.

The morphological distinction, of the *Keilmesser* shapes defined above is largely a reflection of the different length ratios of the individual perimeter sections (Jöris 2001; Pastoors 2001; Jöris 2004; Migal/Urbanowski 2006). The metrical measurements can therefore as an objective control whether the different subjectively defined *Keilmesser* shapes exist as valid entities or not. If they are confirmed as valid the different *Keilmesser* shapes should cluster as such when the metrical results are plotted.

Application of the *Prądnik method*

Use of the *Prądnik method* leaves a characteristic negative on the surface of the artefact (Jöris 1992; 2001; Frick at al. 2017; Frick/Herkert 2019; Frick 2020a; fig. 4). The purpose of this part of the analysis is to document whether the method has been applied or not. In some cases more recent negatives overlap with negatives resulting from a previous application of the *Prądnik method.* In this case, the information was labelled as »multiple« applications. Artefacts for which the presence of a negative is debatable are classified as »undetermined«.

Prądnik spalls

Lateral *Prądnik spalls* emerge during the artefact modification by one or more blows to the distal part of the active edge. It is possible to distinguish primary from secondary sharpening spalls based on the pattern of scars on the dorsal face of the flake (Jöris 1992; 2001; Frick/Herkert 2019; fig. 5). The lateralisation, as described before, can also be determined for the *Prądnik spalls*. Based on the orientation of the retouch it can be defined if the spall has been removed from a left-sided or right-sided tool (Cornford 1986; Jöris/Uomini 2019).

Data analysis

All descriptive analyses (summary statistics, scatter plots and bar plots) were performed in the open-source software R version 4.0.2 through RStudio version 1.3.1073 (RStudio Inc., Boston, USA) for Microsoft Windows 10. The following packages were used openxlsx v. 4.1.5, R.utils v. 2.9.2, doBy v. 4.6.7, ggsci v. 2.9, dplyr v. 1.0.2, patchwork v. 1.0.1, ggplot2 v. 3.3.2, tidyverse v. 1.3.0, wesanderson v. 0.3.6. The analysis was done for each archaeological site individually and once for the three sites together. Reports of the analysis in HTLM format, created with knitr v. 1.29 and rmarkdown v. 2.3 are available on GitHub [https://github.com/lschunk/Lithic_analysis_archaeology]. Moreover, the raw data, the scripts and the RStudio project are saved in the same repository.

Sampling strategy

During the techno-typological analysis, samples of the three assemblages were selected for further examination. Artefacts were chosen for edge angle measurements as well as for the use-wear analysis.
Use-wear analysis is a time-consuming methodology, in most cases necessitating sub-sampling of the assemblage. Depending on the research question, the sampling can follow different strategies (Marreiros et al. 2020; fig. 22). What often happens though, is that the supposedly more important artefacts, for instance *fossiles directeurs* or retouched tools will form most of the subset. While this sampling approach would be still debatable, the following interpretation is mostly not. The results obtained for this chosen subset are then applied to the entire assemblage. Sampling based on this rather problematic strategy is frequently criticised as biased. To avoid this bias, sampling strategies should be defined by the research question and not be influenced by preconceived interpretations. The intention is to transfer the analytical results for a subsample to the total assemblage. Elements of all represented technological categories should be integrated

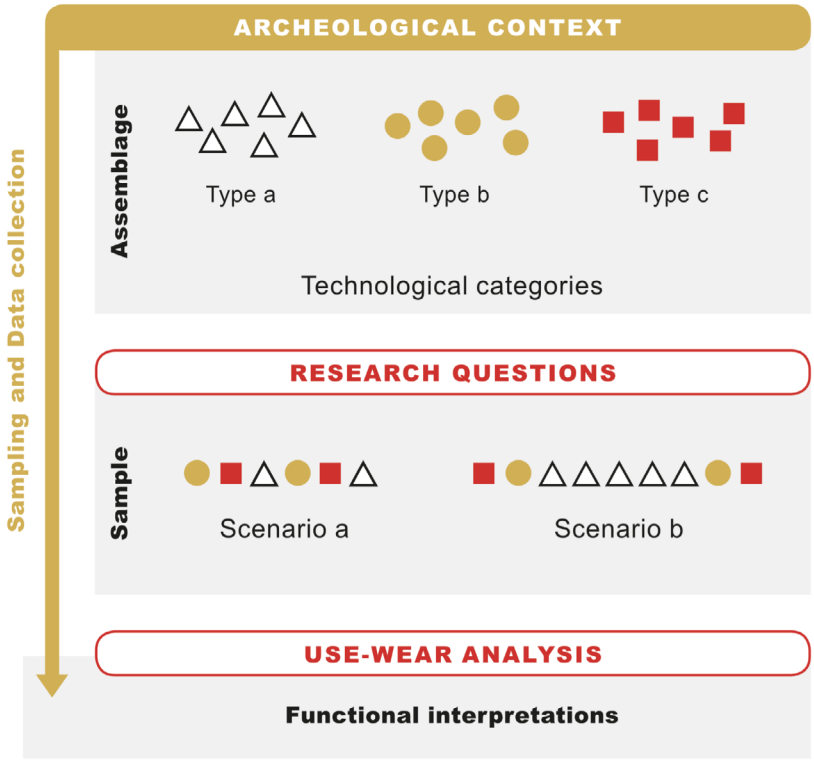

Fig. 22 Schematic representation of the different sampling and data collection strategies commonly used in functional studies. Scenario b was chosen as a sampling strategy for the presented project. – (After Marreiros et al. 2020).

in the analysis. This includes retouched artefacts as well as unretouched specimens often ignored because believed to be unused. If the research question focusses on the use of a certain artefact type, this specific artefact type should represent the most numerous group in the analysis, but outgroups should also be selected to form part of it. Otherwise, the data do not allow for any comparison. Following this idea, lithics were sampled comprehensively to represent all the existing categories present (*Keilmesser*, *Keilmesser tips*, *Prądnik scrapers* and *Prądnik spalls*) as well as *Keilmesser* shapes from the two different raw materials. Additionally, scrapers and flakes were selected as outgroups. Crucial for the sampling was also the preservation of the artefacts.

With this sampling strategy as a prerequisite, artefacts have been selected for two purposes: firstly, for the quantification of their edge design and secondly, for the qualitative use-wear analysis. The sub-sample for calculating the edge angle consists of n = 226 artefacts (**tab. 8**). Only complete artefacts were selected.

site		artefact category						
		Keilmesser	*Keilmesser* tip	*Prądnik scraper*	*Prądnik spall*	scraper	flake	total
Buhlen	n	83 [115]	8 [15]	16 [24]	21 [42]	2 [2]	0 [0]	130 [198]
	%	63.9	6.2	12.3	16.2	1.5	0.0	100.0
Balve	n	65 [170]	10 [21]	3 [27]	0 [117]	0 [12]	0 [0]	78 [347]
	%	83.3	12.8	3.9	0.0	0.0	0.0	100.0
Ramioul	n	9 [9]	0 [0]	1 [3]	0 [0]	6 [6]	2 [2]	18 [20]
	%	50.0	0.0	5.6	0.0	33.3	11.1	100.0
total	n	157 [294]	18 [36]	20 [54]	21 [159]	8 [20]	2 [2]	226 [565]
	%	69.2	7.9	8.8	9.3	3.9	0.90	100.0

Table 8 Number of artefacts from Buhlen, Balver Höhle and Ramioul selected for the quantification of the edge design. The numbers in the square brackets sow the total number of assemblage, respectively.

site		artefact category						
		Keilmesser	*Keilmesser* tip	*Prądnik scraper*	*Prądnik spall*	scraper	flake	total
Buhlen	n	58 [115]	8 [15]	15 [24]	18 [42]	2 [2]	0 [0]	**101** [198]
	%	57.4	7.9	14.9	17.8	2.0	0.0	100.0
Balve	n	42 [170]	2 [21]	5 [27]	21 [117]	9 [12]	0 [0]	**79** [347]
	%	53.2	2.5	6.3	26.6	11.4	0.0	100.0
Ramioul	n	9 [9]	0 [0]	3 [3]	0 [0]	6 [6]	2 [2]	**20** [20]
	%	45.0	0.0	15.0	0.0	30.0	10.0	100.0
total	n	**109** [294]	**10** [36]	**23** [54]	**39** [159]	**17** [20]	**2** [2]	**200** [565]
	%	54.5	5.0	11.5	19.5	8.5	1.00	100.0

Table 9 Number of artefacts from Buhlen, Balver Höhle and Ramioul selected for the qualitative use-wear analysis. The numbers in the square brackets sow the total number of assemblage, respectively.

These artefacts can be divided into n = 157 *Keilmesser*, n = 18 *Keilmesser* tips, n = 20 *Prądnik scraper* and n = 21 *Prądnik spalls*. Additionally, artefacts not belonging to the selected artefact categories were samples for references as a relevant outgroup. Thus, n = 8 scrapers as well as n = 2 flakes.
For the use-wear analysis, more than one third of the total assemblage has been sampled (**tab. 9**). Concretely, n = 200 artefacts from the three archaeological sites have been selected. With n = 129 artefacts, mainly *Keilmesser* (including n = 10 *Keilmesser* tips) have been sampled. Additionally, n = 23 *Prądnik scraper* as well as n = 39 *Prądnik spalls* have been chosen for the qualitative use-wear analysis. Also here, n = 17 scraper and n = 2 flakes build a typological outgroup within the analysis.

QUANTIFICATION OF EDGE DESIGN

Tool design incorporates several attributes, from the overall morphology through to a specific edge retouch. Thus, design builds the bridge between tool shape on the one hand and function and handling on the other. Several methods exist to analyse different aspects of lithic tool design. Recording metric variables, for instance the tool dimensions and mass, presents the most standard of these (Kuhn 1990; Hahn 1993; Andrefsky 1998; Dibble et al. 2017). Although useful, orthogonal dimensions do not capture the geometric configuration of the artefact since artefacts can in fact have similar linear measurements but possess have different morphologies (Borel/Dobosi/Mocel 2017). More detail can be gained through methods such as a geometric morphometrics (e. g. Lycett/Chauhan 2010; Shott/Trail 2010; Serwatka 2015; Weiss et al. 2018) or elliptical Fourier analysis (e. g. Iovita 2009; 2010; Archer et al. 2018; Wiśniewski et al. 2020). Geometric morphometrics focuses on the shape of the tool. Based on defined landmarks and semi-landmarks as well as the spatial and geometric relation between them, this approach captures morphologically distinct shape variables. Elliptical Fourier analysis follows the same main idea to capture the relation between size and shape. It was designed to describe shape by a closed outline, independent of the object's orientation. The method does not depend on landmarks, but on the elliptical Fourier coefficients. The so-called *techno-functional analysis* (Lepot 1993; Boëda 2001; Boëda/Auduze 2013) tries to combine information about the tool morphology and the location of modified and unmodified tool areas. This approach aims to understand tool design including tool function.

Other analyses go further into detail and focus directly on specific areas of the artefact, for example retouched edges. Important therefore is the recognition of an artefact not as a morphological end product (Dibble 1987; Rolland/Dibble 1990; Dibble 1995; Iovita 2014). Tool use as well as maintaining processes can change a tool's shape. Based on retouch intensity, assumptions about the length of the tool-life history are possible (Lin/Marreiros 2020). Identifying these reduction dynamics (Kuhn 1990; Morales/Lorenzo/Vergès 2015) is important to make behavioural inferences based on tool design. As an integrated part of the overall tool design, the tool edge, whether modified or unmodified, can be analysed by a qualitative description (e. g. »stepped scaler retouch«, »trapezoidal retouch«) or quantified by calculating the edge angle. The performance of a given task with a tool is linked with its edge angle (Collins 2008; Key/Lycett 2015; Key/Lycett 2020; Key/Proffitt/de la Torre 2020). This is based on the assumption that the presence of sharp active edges determines a stone tool's utility, whereas the form of a tool's edge determines its functional efficiency, effectiveness, reliability and durability (Key/Lycett 2014; Key/Proffitt/de la Torre 2020). Therefore, the acuteness of an edge angle often plays a role in the interpretation of a tool's function. Several techniques for the recording of measurements have been devised. Among them are manual techniques (e. g. Dibble/Bernard 1980; Pop 2013) or technically more advanced methods, using 3D models (Zaidner/Grosman 2015; Archer et al. 2018; Weiss et al. 2018; Stemp/Macdonald/Gleason 2019; Porter/Roussel/Soressi 2019; Valletta et al. 2020; Weiss 2020; see also ISO 8442-5), all of which being afflicted with their own levels of imprecision inherent to the applied techniques. The recent developments with the integration of script-, algorithm-based and automated analysis of 3D models are clear improvements. On the one hand, it increases the possibility to gain considerable information, and leads to reproducible results and on the other hand decreases random errors. Nevertheless, such methods often result in an overall numeric value per artefact, ignoring possible variability along the edge. To address and understand tool design, a mean value of the edge angle is not sufficient. With more detail, it is possible to address technical choices as well as the effects of retouch on the tool. Thus far, the recording methods are limited by the resolution and accuracy.

Edge angle variability and morpho-functional design

One integrated part of the overall tool design is the tool's active edge. It is common to describe the active edge in a qualitative way (e. g. sharpness, retouch) or quantified by calculating the edge angle (Dibble/Bernard 1980; Pop 2013; Zaidner/Grosman 2015; Archer et al. 2018; Stemp/Macdonald/Gleason 2019; Porter/Roussel/Soressi 2019; Valletta et al. 2020; Weiss 2020). The edge angle describes the angle between two intersecting planes. In the case of lithics, it means the intersection between the dorsal and the ventral surface. To address and understand tool design, it is a prerequisite to know the edge angle values whereby a mean value is not sufficient. With more detail, it is possible to address technological choices as well as the implications of retouch on the tool (Dibble 1995). To acquire the data, an objective method to measure the edge angle at cross sections along the entire tool edge in defined steps as well as measurements at different distances perpendicular to the edge, was chosen. The method is applicable with a 3D model, script based and semi-automated. It provides a systematically error avoiding and reproducible approach, resulting in quantitative and statistically evaluable data.

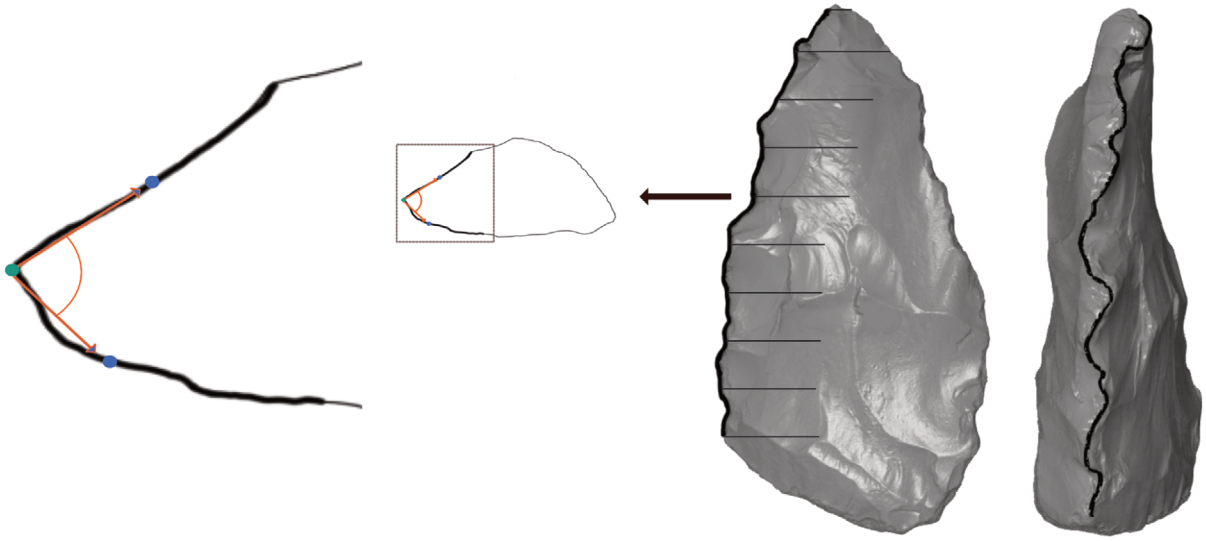

Fig. 23 3D scan of a *Keilmesser* from Ramioul (ID R-007). The scan displays the ventral surface (left) and the active edge (right). The vertical irregular black line represents the »surface curve«, the ten horizontal black lines the sections. The left part of the illustration shows the »3-point« measurement procedure explained on the cross-section of the *Keilmesser* at the position of the fifth section. The green point indicates the intersection between the vertical »surface curve« and the horizontal section. The two blue points are placed on the section in a defined distance. The edge angle measurement (orange lines) is taken based on these three points.

3D data preparation and acquisition

The application of the method is based on the use of a 3D model. Thus, the selected samples were scanned with an AICON smartScan-HE R8 from the manufacturer Hexagon, Germany (software version OptoCat 2018R1). The S-150 FOV used has a resolution of 33µm. Identical settings were used for all scans. Approximately 20 to 27 scans per tool were needed to create a closed model – a prerequisite for the application of the method. Afterwards, the scans were exported in an STL-format.

With a complete model as a basis, some preparatory steps were necessary before calculating the edge angle. The following steps were manually done in GOM Inspect, an open source software for 3D measurement data (GOM Software 2018, Hotfix 1, Rev. 111729, build 2018-08-22). The edge of interest for calculating the edge angle needed to be defined. Since archaeological tools are variable in themselves and display a complex geometry, this is a step that has to be done manually to reach the intended accuracy. Therefore, a »surface curve« was added to each 3D model (**figs 23-25**). This means, a polyline was defined, tracking the edge of the object as precisely as possible and exported in an IGES-format. This step was repeated for all tool edges. In case of *Keilmesser*, most of the time, three polylines (one for the active edge and two for the back) had to be digitalised. With this procedure, the interpretation should be kept apart from the analysis.

The next steps are script-based and also done in GOM Inspect. Based on the defined polyline the software replaces this line with a »reference curve«, which is slightly straightened by filtering the changes in direction out. It is a smoothing function, reducing the point distance to one mm. This parameter was chosen according to the resolution of the 3D model and therefore not a universal parameter. The »reference curve« was used for only one purpose, which is the definition of the sections. The sections are the horizontal lines originating rectangular from the »reference curve« and following the artefact surface in a defined length. These sections are horizontal polylines compared to the vertical polylines along the edge. In case of using the »surface curve« instead of the »reference curve« polyline, the sections would not always be rectangular orientated because of the small changes in direction as a result of the detailed and complex artefact surface.

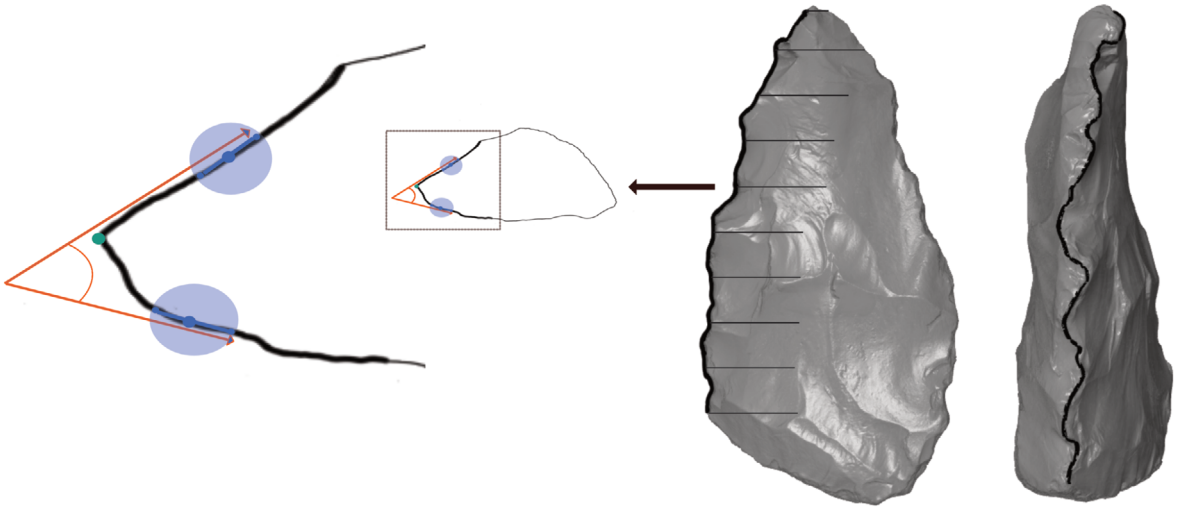

Fig. 24 3D scan of a *Keilmesser* from Ramioul (ID R-007). The scan displays the ventral surface (left) and the active edge (right). The vertical irregular black line represents the »surface curve«, the ten horizontal black lines the sections. The left part of the illustration shows the »2-lines« measurement procedure explained on the cross-section of the *Keilmesser* at the position of the fifth section. The green point indicates the intersection between the vertical »surface curve« and the horizontal section. The two blue points are placed on the section in a defined distance. They build the centre for the two lines. The edge angle measurement (orange lines) is taken based on intersection and the constructed lines.

After generating the »sections«, the »reference curve« was no longer needed. All further steps used the previously created »surface curve«.

»3-point« procedure

For calculating the edge angle in a final step, three different measuring procedures are possible (**fig. 23**). The first one, the so-called 3-point measurement, is modelled on the previously mentioned »*caliper method*« described by H. Dibble and M. Bernard in 1980. Whereas the result of the »*caliper method*« is based on a measurement taken by a special modified calliper at a known distance from the edge of the artefact by using a formula (Dibble/Bernard 1980), the 3-point measurement is using the same topographical indexes represented by 3 points. One of the points is the intersection between the vertical polyline, the »surface curve«, and the horizontal polyline, the section. The two other points are placed on the section, each on one surface, in a defined distance away from the intersection. The edge angle can be calculated between these three points.

»2-lines« procedure

The second measuring procedure is the so-called 2-lines measurement (**fig. 24**). This approach takes the intersection between the two polylines, as described in the first method, as one point. Beginning with this point, it follows the section on both surfaces in a given distance. Until this step, the two procedures are identical. These points on the section are used as a reference for two constructed lines. The lines have a defined length and take the points as a centre from where they spread in both directions. The calculation of the edge angle takes the two lines and the intersection into account.

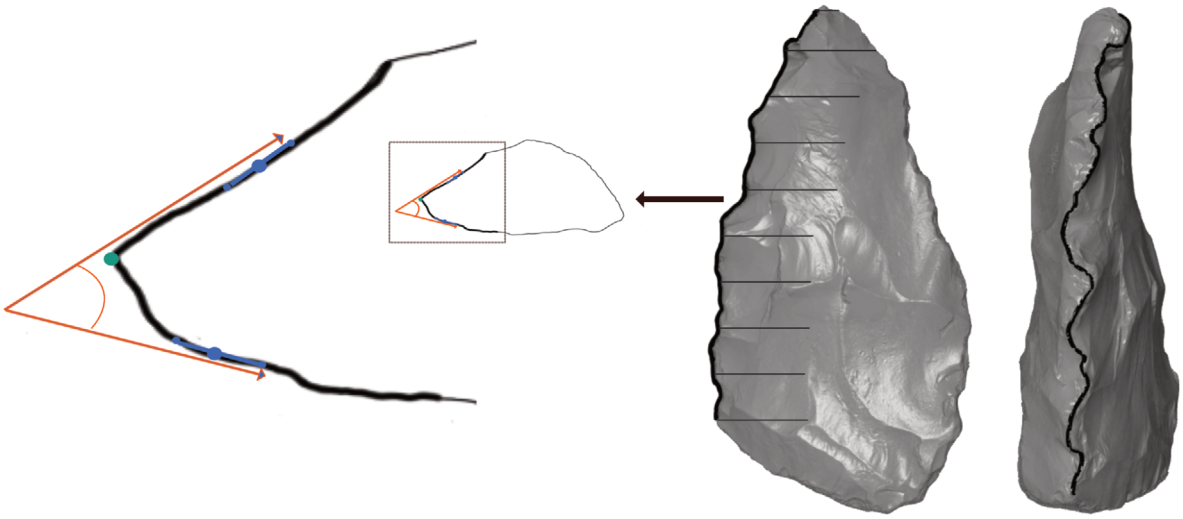

Fig. 25 3D scan of a *Keilmesser* from Ramioul (ID R-007). The scan displays the ventral surface (left) and the active edge (right). The vertical irregular black line represents the »surface curve«, the ten horizontal black lines the sections. The left part of the illustration shows the »best-fit« measurement procedure explained on the cross-section of the *Keilmesser* at the position of the fifth section. The green point indicates the intersection between the vertical »surface curve« and the horizontal section. The two blue points are placed on the section in a defined distance. They build the centre for the two lines. All mesh points of the 3D model in between the two lines are interpolated (indicated by the light-blue circles). The edge angle measurement (orange lines) is taken based on intersection and the constructed lines.

»best-fit« procedure

This approach – the so-called »best-fit« – takes the intersection between the two polylines, the vertical (surface curve) and the horizontal (section) polyline, as one point (**fig. 25**). Beginning with this point, it follows the section on both surfaces in a given distance. These points on the section are used as a reference for two constructed lines. The lines have a defined length and take the points as a centre from where they spread in both directions. The mesh points between the constructed lines were interpolated. The calculation of the edge angle takes the two lines and the intersection into account.
Since it seems like the »best-fit« procedure is more precise and accurate for complex archaeological artefacts, a bit more emphasis was put on these results in the following data analysis.

Parameters

There are several parameters or variables, which need to be chosen in order to apply the method. One of these variables is the number of horizontal sections, represented here by ten sections per tool. The length of the lines, starting at the intersection, was defined with 12 mm. Another parameter is the distance from the edge along the sections. In the described procedures, the intersection between the vertical polyline and the horizontal section determine one crucial point, but the other two (always identical) points per measurement have to be defined numerically. Here the points were defined in 1 mm steps. The last variable is the lengths of the lines used in the »2-lines« and »best fit« measuring procedure, which were always 2 mm.

Edge angle data analysis

The obtained, calculated edge angle values, were analysed. This enabled a comparison between artefacts. To do so, a statistical analysis was performed with R (version 4.0.2 through RStudio version 1.3.1073, RStudio Inc., Boston, USA). The following packages were used: writexl v. 1.3, tidyverse v. 1.3.0, openxlsx v. 4.1.5, ggrepel v. 2.3, doBy v. 4.6.7, patchwork, v. 1.0.1, ggplot2 v. 3.3.2 and R.utils v. 2.9.2. Reports of the analysis in HTLM format, created with knitr v. 1.29 and rmarkdown v. 2.3 are available on GitHub as well as the raw data, the scripts and the RStudio project [https://github.com/lschunk/edge_angle_analysis]. The analysis of the data aims at illustrating possible changes for instance along the tool edges and towards the surfaces.

USE-WEAR ANALYSIS

Stone tools enabled past humans to access food resources like animals and plants (Lombard 2005; McPherron et al. 2010; Wilkins et al. 2012). At the same time, they are the most commonly found physical evidence and the only continuous record to study the evolution of human behaviour (Key Proffitt/de la Torre 2020). Stone tools witness technological developments and innovations. Investigation how early hominins produced, used and curated their tools is thus a prerequisite for understanding the Pleistocene record. Stone tools can be observed in a great variety concerning their morphology. Nevertheless, in principle they all have something in common: they all have a certain function or combine several functions. All stone tools display the capacity to be used for a function, for instance modifying material, for movements e. g. scraping and cutting or for displaying a symbolic reason. Additionally, a tool's function can change over time or as a consequence of its use. Investigating the function of an artefact has long been part of archaeological research, either through the study of lithic typology and technology or directly through use-wear analysis. Use-wear analysis originates from the late nineteenth century, early twentieth century (Grace 1996). It includes the study of characteristic patterns of macroscopic and microscopic traces left on a tool, resulting from its use. Use-wear analysis is therefore the only approach providing a direct proof of a tool's utilisation (Shea 2011). Although the existence of retouch on a tool might imply tool use, solely use-wear analysis can confirm the actual use. The processes as to how use-wear forms are dependent on several aspects. For instance, the different types of use-wear traces respond to the raw material of the tool itself and the contact material, the tool morphology as well as the performed action and its duration (Kamminga 1979; Astruc/Vargiolu/Zahouani 2003; Lerner et al. 2007).

During the last couple of decades, use-wear analysis as a sub-discipline of archaeology passed through several changes, including methodological developments, theoretical and conceptual shifts. This process is also reflected by the given terminology. Discussions about the interchangeable character of these names and the definition of the discipline are thus the result (Marreiros et al. 2015).

Following Marreiros et al. (2020), the respective terminology – traceology, use-wear analysis and functional analysis – implies different levels of analysis and different objectives. To start with use-wear analysis, it defines the study of physical traces (microscopically and macroscopically) visible on an artefact's surface (Thomas et al. 2001; Marreiros et al. 2015). These traces are caused by human use. Traceology thereby goes a bit further. While it refers to the study of use-wear traces, it also includes traces resulting from production, non-utilitarian wear, and post-depositional traces. Ideally, use-wear analysis as well as traceology can and should be complemented with residue analysis. Functional analysis, however, combines methods such as technology, typology and use-wear analysis. Also, residue analysis can be part of functional analysis (Pe-

dergnana 2000). The aim of it has to be defined in a broader sense than only to identify the use of a tool. Functional studies target the evaluation of tool design, function and utilisation.

Traceology, use-wear analysis & functional analysis

In the following part, the history of this sub-discipline is summarised. Giving this context is of relevance, because it illustrates and justifies the steps and methods chosen and applied within this project. It also puts some emphasis on the circumstances as to why only a combination of different scales of analysis and methods can add more – and also new – information about *Keilmesser* and *Prądnik scrapers* to our current point of view.

The beginning of traceology/use-wear analysis can be traced back until the end of the nineteenth century. John Evans was presumably one of the first scientists stating the fact that the use of a tool can leave corresponding traces on its surface (Tringham et al. 1974). Equally early is the work of William Greenwill (Hayden 1979; Kamminga 1979). He identified use-wear traces on Palaeolithic tools and recognized the potential of the discipline. Nevertheless, it would take decades until traceology/use-wear analysis found a broader attention. This was thanks to Sergei Semenov (Semenov 1957; 1964), who created a methodological and systematic framework for the study of use-wear traces. For his work, Semenov is valued as the pioneer of the discipline. His publication *Prehistoric Technology* provides functional interpretations and experimental comparisons based on microscopic analysis. With his work, for the first time, experimental data has been applied as proxy for the identification of use-wear traces on archaeological samples. For his analysis, Semenov used a low magnification stereomicroscope (low-power approach) which led to a promotion of a systematic use of microscopic observations mainly on bones and lithics.

At the end of the 1960s, Semenov's work was translated and hence accessible to Western European scholars. Together with the rise of the *New Archaeology* (Binford 1962; Longacre 2010), it marked the beginning of a new period. The *New Archaeology* put the emphasis on developing scientific, hypothetic-deductive methods for the understanding of past human behaviour. The interest in for example ethnoarchaeology and the use of analogies grew. Traceology/use-wear analysis with its focus on tool function and utilisation and the microscopic approach fit the zeitgeist of the 1960s. Several researchers, for example Ruth Tringham (1974), George Odell (1975), Brian Hayden (1979) and Lawrence Keeley (1974; 1980), to mention only a few, concentrated on the new approach and tested its limitations. Consequently, the applied methods have been developed and improved, mainly by employing different microscopic magnifications. The end of the 1970s and the beginning of the 1980s are to mention as the timeframe for the introduction of the high-power approach (Keeley/Newcomer 1977). Compared to the low-power approach, the high-power approach is based on the use of high magnification microscopes, mostly upright metallographic microscopes. Since then, both approaches are used complementary, in the awareness of their limitations respectively. Additionally, the focus on experimental replications grew, achieving fundamental insights into the categorisation of diagnostic wear traces (Hardy/Garufi 1998; Vaughan 1985). With the aid of experimental samples, it could be demonstrated that the tool's raw material influences the nature of the resulting wear pattern. A comparison between archaeological and experimental assemblages requires therefore an inclusion of the corresponding raw material (Burroni et al. 2002; Evans/Donahue 2005).

The following years were characterised by improvements such as the development of more reliable and accurate methodologies by implementing more experiments and blind tests. At the same time, the limitations of a qualitative use-wear analysis became evident (Keeley 1974; Schiffer 1979; Grace/Graham/Newcomer 1985; Newcomer/Grace/Unger-Hamilton 1986; 1988; Moss 1987; Bamforth 1988; Hurcombe 1988).

These can be mainly summarised by the complexity of understanding use-wear traces, solely by the use of a stereomicroscope.
A new era was marked with the introduction of quantitative use-wear analysis. This significant step in the history of use-wear analysis was mainly possible due to the integration of a range of imaging equipment. The introduction of the following equipment and software is to name (Marreiros et al. 2020): the tactile profilometer (Beyries/Delamare/Quantin 1988), the atomic force microscopy (Kimball/Kimball/Allen 1995; Faulks et al. 2011; Kimball et al. 2017), the interferometry (Dumont 1982; d'Errico/Backwell 2009), the laser profilometry (Stemp/Stemp 2001; 2003), the confocal microscopy (Evans/Donahue 2008; Stemp/Chung 2011; Stemp/Lerner/Kristant 2013; Evans 2014; Macdonald/Harman/Evans 2018), and the image analysis and surface metrology software (d'Errico/Backwell 2009; Sahle et al. 2013; Ibáñez/Lazuen/González-Urquijo 2018; Martisius et al. 2018; 2020; Calandra et al. 2019a, b). The aim of quantitative use-wear analysis is the identification of different use-wear traces following standardised, quantitative criteria based on 2D and 3D images and surface roughness measurements. More recently, new attempts to quantify surface textures have been made (Evans/Macdonald 2011; Stemp et al. 2015; Martisius et al. 2018; Ibáñez/Lazuen/González-Urquijo 2018; Pedergnana et al. 2020b; Pedergnana/Ollé/Evans 2020). Still, criticism has been raised against a lack of reproducibility regarding the acquired data (Evans et al. 2014; Calandra et al. 2019c; Marreiros et al. 2020). While traceology/use wear analysis as a sub-discipline of archaeology is still continuously improving, scientists are aware of the current limitations of the approach. The integration of established methods from related disciplines (e. g. dental microwear) could offer great potential for further improvements (Calandra et al. 2019b).

Methods and techniques in use-wear analysis

Initial use-wear studies were characterised by the use of the low-power approach. Since the introduction of a systematic use of low magnification stereomicroscopy by Semenov, this was the state-of-the-art for use-wear analysis. This changed in the 1970s, when Keeley introduced the high-power approach. He used a reflected light microscope for his work. After years of discussion and debates about the advantages and disadvantages of both approaches, a broad agreement has been reached. Only a complementary method by the combination of low- and high-power approach can lead to a profound analysis and a reliable result (Odell 2001). The use of the low-power approach should thereby allow the identification of macro-wear traces as for example edge damage and impact fractures. Moreover, this approach should help with identifying the areas of interest for the subsequent high-power approach. The observation under higher magnifications should allow for a detailed analysis of micro-wear traces as for instance striations and polish formations (Marreiros et al. 2015).
In general, the methods applied in use-wear analysis nowadays can be distinguished in digital microscopy, II) optical microscopy (stereomicroscopes, upright metallographic microscopes), III) scanning electron microscopy (SEM), and IV) laser scanning confocal microscopy (LSM).
When referring to the low-power approach, a stereomicroscopic analysis in the range of four to ten × magnification is common. Enabled by a movable light source, reflected light, the artefact can be illuminated from different angles, allowing for a shadow effect and thus an easier detection of possible traces. The implementation of the high-power approach is usually characterised by a metallographic microscope and magnifications between 50 and 400×. An incident light serves as a light source perpendicular (90°) to the material surface.

Another high magnification observation method offers the scanning electron microscopy (SEM). An SEM uses instead of a light illumination a focused beam of electrons controlled by magnetic or electric fields. The advantages of an SEM are the higher possible magnifications, resolutions, and depth of field compared to a metallographic microscope (Hay 1977; Del Bene 1979). The use of an SEM has also proven to lead to better results with certain raw materials, for example quartzite (Ollé et al. 2016; Pedergnana 2017). However, the use of an SEM is also accompanied with disadvantages. Commonly, an SEM provides only a small chamber for the sample, meaning the object volume is limited. A sample preparation is typically needed, sometimes including a sample coating. Furthermore, an SEM is a costly piece of equipment and the analysis is relatively time-consuming. These aspects taken together usually lead to an analysis of a comparable small sample size. Studies have demonstrated the effectiveness of a complementary approach, the combination of optical and electron microscopy (Monnier/Ladwig/Porter 2012; Borel et al. 2014; Ollé et al. 2016).
A quantitative use-wear analysis can be done by the means of laser scanning microscopy. The laser scanning microscopy (LSM) is an optical imaging technique. The illumination of the sample happens through a spatial pinhole system, which blocks out-of-focus light. This means, only one point on the sample at a time is illuminated. In order to acquire 2D or 3D images, the sample has to be scanned over a raster. An LSM allows observations ranging between 25-800× magnification (e. g. Mansur-Franchomme 1983; Derndarsky/Ocklind 2001; Shanks et al. 2001; Scott et al. 2005; 2006; Debert/Sherriff 2007; Evans/Donahue 2008). Laser confocal microscopy has been used mainly in archaeology for the illustration and the modelling of surface topography. Several parameters, also in accordance with ISO Norms, can be calculated on the tool's surface (e. g. amplitude parameters, spatial parameters, roughness parameters) (Calandra et al. 2019c). Based on basic roughness parameters it is possible to distinguish diagnostic use-wear traces (Giusca et al. 2012). During the last years, the LSM as well as the SEM have been used more frequently in use-wear analysis (Stemp/Stemp 2001; 2003; Lerner et al. 2007; Evans/Donahue 2008; Evans/Macdonald 2011; Stemp/Chung 2011; Giusca et al. 2012; Pedergnana et al. 2020b; Pedergnana/Ollé/Evans 2020). The likely explanation for this is the possibility to quantify micro-wear traces with both types of equipment. Unfortunately, the LSM is an expensive purchase, but the running costs are smaller and the limitations regarding the sample size are less restricting.

Artefact cleaning procedure

Before doing the use-wear analysis, the sampled artefacts had to be cleaned (Pedergnana et al. 2016; Pedergnana et al. 2020a). To do so, each sample was individually packed in a plastic bag filled with ~ 100 ml of demineralised water and a non-ionic detergent (BASF Plurfac LF901, 1 g/l = 1 % w/v; BASF SE, Ludwigshafen, Germany). The closed bags were put into a preheated ultrasonic bath (EMAG Emmi 20HC). The samples were left in the bath for 15 min at 40°C and 100 KHz.
Thereafter, the samples, still placed in the bags, were rinsed three times with tap water. This step is meant to remove the surfactant residues. The bags were then filled once with ~100 ml purified water and emptied after rinsing. After that, the samples were air-dried. Immediately before and during the data acquisition, the measured surface was cleaned with 2-propanol 70 % v/v.

Qualitative use-wear analysis

The methodological approach of use-wear analysis can be divided in a low-power and high-power approach (Keeley 1974; 1980; Marreiros et al. 2015). While the low-power approach is equal to a macroscopic meth-

odology, the high-power approach involves the use of optical microscopy magnification. The sampling for the use-wear analysis was done on a macroscopic observation level. When necessary, the artefacts were observed regarding their preservation with a stereomicroscope (ZEISS SteREO Discovery.V8). Only complete lithics representing all existing categories as well as *Keilmesser* shapes from the two different raw materials were sampled.

The qualitative use-wear analysis was done in a high-power approach by means of an upright light microscope (ZEISS Axio Scope.A1 MAT; **tab. 10**). The samples were studied with a 5×, 10× and 20× magnification. Traces were documented as an EDF image in black and white settings.

Tool areas displaying use-wear traces were afterwards documented with a digital microscope (ZEISS Smartzoom 5) by the use of a 1.6× objective and 34-× zoom. The combination of stitching and EDF makes a documentation of an entire tool edge in focus possible.

		LSM	upright light microscope	digital microscope	3D scanner
Microscope	Manufacturer	Carl Zeiss Microscopy GmbH	Carl Zeiss Microscopy GmbH	Carl Zeiss Microscopy GmbH	AICON, now part of Hexagon AB
	Model	Axio Imager.Z2 Vario + LSM 800 MAT	Axio Scope.A1 MAT	Smartzoom 5	smartScan-HE R8
Location	Laboratory	TraCEr, MONREPOS, Germany	TraCEr, MONREPOS, Germany	TraCEr, MONREPOS, Germany	TraCEr, MONREPOS, Germany
	Floor	basement (-1)	basement (-1)	basement (-1)	basement (-1)
	Setup	Passive anti-vibration table on solid concrete base	Standard office desk	Stable table on solid concrete base	column stand
Acquisition	Software	ZEN blue 2.3 with Shuttle&Find module	Zen core 2.7	Smartzoom software with Shuttle&Find module	OptoCat 2018R1
	Mode	LSM (laser scanning confocal microscopy)	Bright field	Bright field	Structured light
Objective	Manufacturer	Carl Zeiss Microscopy GmbH	Carl Zeiss Microscopy GmbH	Carl Zeiss Microscopy GmbH	Hexagon
	Objective	C Epiplan-Apochromat 10× / NA = 0.40 / WD = 5.4 mm	EC Epiplan 5× / NA = 0.13 / WD = 11.8 mm	PlanApo D 1.6× / NA = 0.1 / WD =36 mm	M-450, 108 µm point-to-point distance
		C Epiplan-Apochromat 20× / NA = 0.70 / WD = 1.30 mm	EC Epiplan 10× / NA = 0.25 / WD = 11.0 mm	-	S-150, 33 µm point-to-point distance
		C Epiplan-Apochromat 50× / NA = 0.95 / WD = 0.22 mm	EC Epiplan 20× / NA = 0.40 / WD = 3.2 mm	-	-

Table 10 Acquisition settings for the involved pieces of equipment including the objective specifications and the resulting magnifications and resolutions. NA = numerical aperture, WD = working distance, FOV = field of view. The total on-screen magnification can be calculated as follows: objective magnification × optical zoom × camera adaptor × screen diagonal × digital zoom camera/camera sensor diagonal.

		LSM	upright light microscope	digital microscope	3D scanner
Illumination	Source	Laser	White LED, reflected co-axial light **	White LED, reflected ring-light	Blue LED
	Wavelength	405 nm	550 nm	550 nm	-
Settings	Master Gain	245 V	-	-	-
	Scanning direction	Both ways (no correction, line step = 1)	-	-	-
	Scanning speed	8 (max)	-	-	-
	Bit depth	16 bits	-	-	-
	Pinhole diameter	54 µm (50× obj.) / 34 µm (20× obj.) (1 AU lateral optical resolution)	-	-	-
Size and resolution	Zoom	0.5× (50× obj.) / 0.2× (20× obj.)	-	-	-
	Step size	0.25 µm	-	-	-
	Data quality	No noise cut (0-65335 levels, post-processing)	-	-	-
	FOV	255.56 × 255.56 µm (50× obj.) / 638.9 × 638.9 µm (20× obj.)	1.70 × 1.42 mm (5× obj.) / 850.08 × 709.32 µm (10× obj.) / 425.04 × 354.66 µm (20× obj.)	10.475 7.856 mm	355 × 265 × 220 mm measuring volume (M-450) / 110 × 80 × 70 mm measuring volume (S-150)
	Frame size	1198 × 1198 pi×els (50× obj.) / 3000 × 3000 pi×els (20× obj.)	2464 × 2056 pi×els	15875 × 3301 pixels	-
	Total on-screen magnification	1318× (50× obj.) / 527× (20× obj.)	187× (5× obj.) / 375× (10× obj.) / 750× (20× obj.)	34×	-

Table 10 (continued)

Spatial pattern recognition

A scheme was developed to locate and map use-wear traces (for similar scheme see Plisson 1985; Van Gijn 1990; Lombard 2008; Mazzucco 2018). The outline of the artefact was used as a grid (**fig. 26**). *Keilmesser*, *Prądnik scrapers*, scraper and flakes were separated in a grid of six areas, *Prądnik spalls* in four areas. This was done for the dorsal (A and B) as well as for the ventral (D and C) surface. The areas are numbered from one, distal part of the tool, to two, the medial part, and three, the proximal part of the tool. Following this scheme, use-wear traces can easily be located and a map for all use-wear traces can be generated, allowing for statements regarding the frequency and distribution of the use-wear traces. Thus, this qualitative use-wear approach aims for pattern recognition (e. g. location of the use-wear traces on tool's surface). Included in the scheme is the type of use-wear and the orientation. Possible predefined use-wear types are polish, striations and impact marks. Here, polish refers to a modification of the tool surface caused by contact between the tool and the worked material. Polish appears as a dull, brighter or smoothed area on the surface (Keeley 1980; Haslam 2009; Rots 2013; Evans 2014). The term striation refers to linear scratches, furrows or grooves

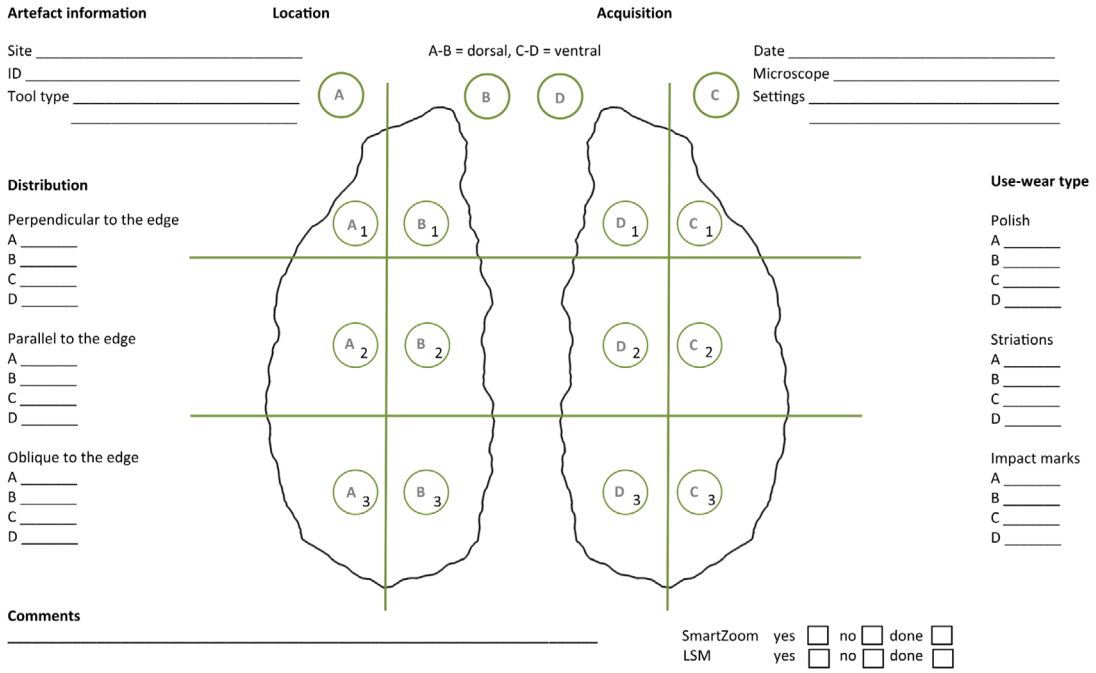

Fig. 26 Scheme used during the qualitative use-wear analysis for the documentation of the analysed tools. Here, the outline represents a *Keilmesser*. The dorsal (A and B) and ventral surfaces (D and C) are exemplarily labelled as if the tool would be a right-sided *Keilmesser*. However, the outline is different for the other artefact categories. Additionally, the scheme includes information about the analysed artefact itself, the acquisition date and settings, as well as information about the use-wear traces (location, distribution and type). The scheme also contains information, whether further acquisition or analysis are needed (SmartZoom = digital microscope images, LSM = quantitative use-wear analysis).

reflecting an abrasive action between the tool and the worked material (Keeley 1980). Moreover, the orientation for the use-wear traces can be specified with the options perpendicular, parallel or oblique to the edge.

Description use-wear traces

The aim of use-wear analysis is to identify traces left on the tool's surface. The first step is the recognition and the characterisation of different types of traces, for example polish, impact fractures or striations. It is known that wear patterns correlate with the worked material (Keeley 1980; Haslam 2009; Rots 2013). A further step usually seeks, especially concerning polish, a more detailed description and identification of the observed traces. In the qualitative approach, this is exclusively based on visual identification of the traces. Polish is a modified area on the tool, recognisable with an optical microscope by a brighter or smoother appearance (Keeley 1980). It is caused by a gradual removal or deformation of the natural surface. Various names for different types of polish can be found in literature for example wavy polish, and also their functional interpretation as wood polish, bone polish, hide polish etc. Although the classification of polish and its formation is one of the fundamental questions addressed in use-wear analysis (Marreiros et al. 2015), a consensus and an agreement on the various terms and identifications is still missing (Grace/Graham/Newcomer 1985; Grace 1989; Evans 2014; Van Gijn 2014; Marreiros et al. 2020). The different types of polish are likely related to several other aspects such as the raw material, the use intensity, the performed task and not only the worked material (Buc 2011). This means, even the same combination of tool and worked material can lead to varying traces by performing the same movement when only the duration differs. This makes it extremely difficult to assess the exact use of a tool confidentially by visual means only.

Here, documented traces were visually inspected and categorised. A subjective description of these categorised wear traces was done. With respect to the various existing definitions, nine types of use-wear traces were defined for the samples from the three analysed assemblages. Sometimes, the distinction between two types of use-wear traces was ambiguous. In these cases, the combination of two of the defined types was chosen.

Analysis use-wear data

After documenting and defining the use-wear traces on all analysed artefacts, the manually filled scheme for the use-wear pattern recognition (see section 4.4.3.1) had to be digitalised. Therefore, the initially used artefact outline templates (SVG files) were converted into DXF format using the open-source software Potrace tracing program (version 1.1.6), producing internal and external outlines as well as the grid. The DXF were modified using CAD. The resulting DXF files were then imported into QGIS (version 3.14.16) templates as vectors. QGIS is a free and open source geographic information system, which was used here to map the documented traces. Next to the described vector layers, additional point layers for each individual type of use-wear trace were created. The point layers were given a suitable colour scheme. This method allows a simple and visual presentation of all use-wear traces separated per artefact type.

Quantitative use-wear analysis

Based on the results from the previously described qualitative use-wear analysis, samples were selected for a quantitative use-wear analysis. Thus, the quantitative use-wear analysis was done on samples displaying different types of use-wear and use-wear on the different locations. The minimum number of measurements per use-wear type was three. The 3D surface topography data was acquired with a confocal microscope. The confocal microscope is an upright light microscope coupled with a laser-scanning confocal microscope (ZEISS Axio Imager.Z2 Vario + ZEISS LSM 800 MAT; **tab. 10**).
When time played a limiting factor, for example during a short time loan from a museum or during the execution of an experiment, moulds of the region of interest were taken. The moulds assure a possibility of a quantitative use-wear analysis at a later time, since they serve as an identical copy of the real surface. The moulds were made of Provil novo Light regular (Kulzer GmbH, Hanau, Germany), a two-component silicone impression material applied with a dispensing gun. Under regular room conditions, the moulds are fully hardened after 5-8 minutes.
In total 50 different use-wear spots were measured with the LSM. Six of these use-wear traces are on artefacts from Buhlen, 33 from Balver Höhle and eleven from Ramioul. Four of these 50 measurements were taken on moulds instead of the original artefact surface.
Before using the LSM, the system always had to be turned on one hour in advance in order to warm up all components and to limit thermic drift. In order to assure that the artefacts cannot move and stay stable during the acquisition, a mould with a flat lower surface in the sense of a sample holder was made. The mould was made of Provil novo Putty regular set (Kulzer GmbH, Hanau, Germany). This set is a two-component silicone impression material consisting of a base paste and a matching catalyst paste. After combining these two components in a ratio 50:50, the curing time is roughly three to five minutes in room conditions. Additionally, a goniometer stage was used to position the sample with the area to measure as horizontal as possible. The LSM is equipped with a motorized revolver allowing an easy change of objectives. For the

acquisition with the LSM the aim was to scan the surface under the highest magnification, respectively. Therefore, the objective C Epiplan-Apochromat 50× with the numerical apertures 0.95 was used. The field of view (FOV) was 255.6 × 255.6 µm. Sometimes the artefact surfaces were not straight enough or the artefacts could not be positioned in a way needed in order to measure the surfaces with the 50× /0.95 objective, so that the C Epiplan 50× /0.75 (for nine samples) or the C Epiplan-Apochromat 20× /0.70 (for one sample) had to be used. While the 50× /0.75 has the same FOV than the other 50× objective, the 20× /0.70 objective has a FOV of 638.9 × 638.9 µm. Each use-wear trace was measured three times at nearby but non-identical spots. These scans are treated as replicas and verify (or not) the homogeneity within each trace.
Wide field images as an overview were not acquired with the LSM since EDF pictures were already taken with the upright light microscope.

Data processing

The acquired data was processed in batch for each archaeological site respectively with templates in ConfoMap (a derivative of MountainsMap Imaging Topography developed by Digital Surf, Besançon, France; version ST 8.1.9286; for details see https://guide.digitalsurf.com/en/guide.html). In total four different templates had to be applied. The first template – the »extracting template« – was only used for the 3D surfaces acquired with the 20× /0.70 objective (**figs 27-34**). After applying this template, all surfaces had the same size of 254.9 × 254.9 µm. The following second template, »resampling template« was by contrast used to perform a resampling in x and y on all 150 surfaces, leading to an identical spacing. For the scans acquired on moulds, an additional third template was needed, the »mirroring template«. Moulds always just display a mirrored version of the original surfaces. Therefore, the acquired surface needed to be mirrored in order to match the original surface again. In a final step, the data was processed with a »processing template«. The following procedure was performed: I.) Levelling (least squares method by subtraction), II.) From removal (polynomial of degree 3), III.) Outliers removal (maximum slope of 80°), IV.) Thresholding the surface between 0.1 and 99.9 % material ratio to remove the aberrant positive and negative spikes, V.) Applying a robust Gaussian low-pass S-filter (S_1 nesting index = 0.425 µm, corresponding to about five pixels, end effects managed) to remove noise, VI.) Filling-in the non-measured points (NMP), VII.) Analysis: Calculation of 21 ISO 25178-2 parameters, 3 furrow parameters, 3 texture direction parameters, one texture isotropy parameter and the scale-sensitive fractal analysis (SSFA) parameters *epLsar, NewEplsar, Asfc, Smfc, HAsfc9 and HAsfc81* (**tab. 11**).
The ConfoMap templates for each site and surface in MNT and PDF formats are available on GitHub [https://github.com/lschunk/Archaeology_use-wear]. This also includes all original and processed surfaces, as well as the results.

Statistical procedure

All descriptive analyses (summary statistics, scatter plots, box plots, histogram plots and principal component analysis, PCA) were performed in the open-source software R version 4.0.2 through RStudio version 1.3.1073 (RStudio Inc., Boston, USA) for Microsoft Windows 10. The following packages were used openxlsx v. 4.1.5, R.utils v. 2.9.2, doBy v. 4.6.7, ggrepel v. 0.8.2, patchwork v. 1.0.1, ggplot2 v. 3.3.2, tidyverse v. 1.3.0, wesanderson v. 0.3.6. Reports of the analysis in HTLM format, created with knitr v. 1.29 and rmarkdown v. 2.3 are available on GitHub [https://github.com/lschunk/Archaeology_use-wear]. Also the raw data, the scripts and the RStudio project are saved in the same repository.

Quantitative use-wear analysis: Balver Höhle
Template to extract a 255 x 255 µm surface acquired with the LSM800 with the 20x/0.7 objective in order to match the FOV of the 50x0.95 and 50x0.7 objectives

This template is used for one sample with three measurements (surfaces).

A. Extracting

1. Original surface; frame indicates the area to extract

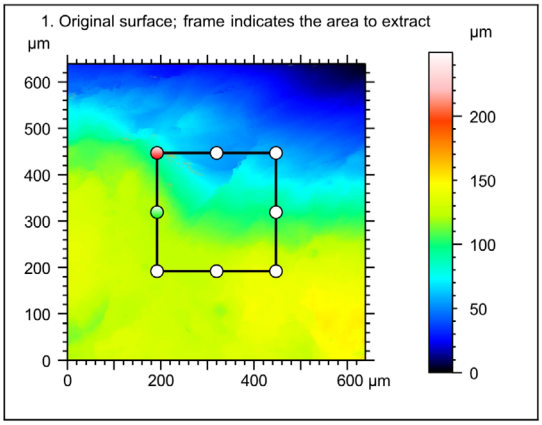

Identity card		
Name:	MU-232-B2-01-a_20x07_LSM_Topo	
Created on:	7/7/2020 4:58:00 PM	
Studiable type:	Surface	
Axis:	X	
Length:	638.7	µm
Size:	3000	points
Spacing:	0.2130	µm
Axis:	Y	
Length:	638.7	µm
Size:	3000	points
Spacing:	0.2130	µm
Axis:	Z	
Layer type:	Topography	
Length:	249.7	µm
Size:	65531	digits
Spacing:	3.810	nm
NM-points ratio:	0.000 % (0 Pts)	

2. Extracted area

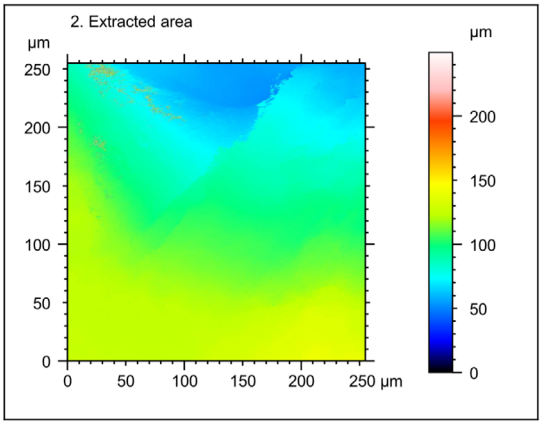

Identity card		
Name:	MU-232-B2-01-a_20x07…_Topo > Extracted area	
Created on:	7/7/2020 4:58:00 PM	
Studiable type:	Surface	
Axis:	X	
Length:	254.9	µm
Size:	1198	points
Spacing:	0.2130	µm
Axis:	Y	
Length:	254.9	µm
Size:	1198	points
Spacing:	0.2130	µm
Axis:	Z	
Layer type:	Topography	
Length:	249.6	µm
Size:	65505	digits
Spacing:	3.810	nm
NM-points ratio:	0.000 % (0 Pts)	

ConfoMap ST 8.1.9286 23-Jul-20 - 1 / 1 -

Fig. 27 »Extracting template« created in ConfoMap (a derivative of MountainsMap Imaging Topography developed by Digital Surf, Besançon, France; version ST 8.1.9286) to process the data acquired from the quantitative use-wear analysis. Here, the template was applied to a *Keilmesser* from Balver Höhle (MU-232). The template was only used for samples analysed with the 20×/0.7 objective.

Quantitative use-wear analysis: Balver Höhle
Template to resample in x and y in order to reach an identical spacing in all with the LSM800 acquired surfaces (50x/0.7 and 50x/0.95 objectives).

This template is used for thirty-three samples with three measurements (surfaces) respectively.

B. Resampling

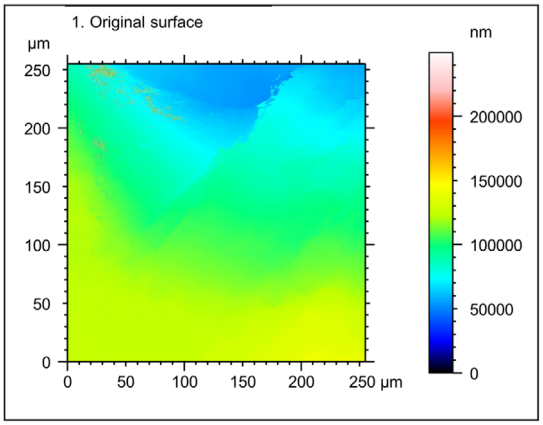

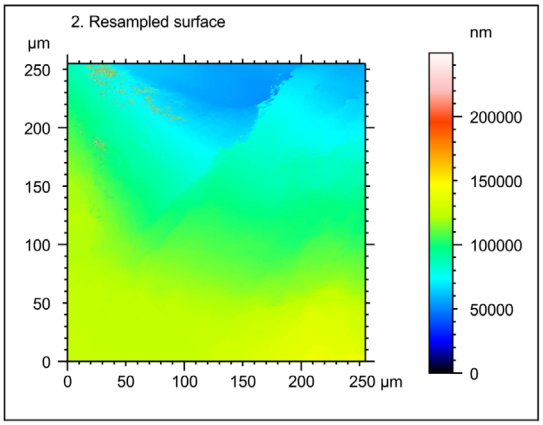

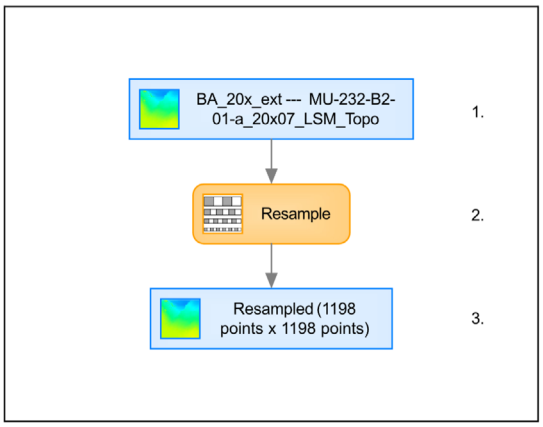

Identity card		
Name:	BA_20x_ext --- MU-232…01-a_20x07_LSM_Topo	
Created on:	7/7/2020 4:58:00 PM	
Studiable type:	Surface	
Axis:	X	
Length:	254.9	µm
Size:	1198	points
Spacing:	0.2130	µm
Axis:	Y	
Length:	254.9	µm
Size:	1198	points
Spacing:	0.2130	µm
Axis:	Z	
Layer type:	Topography	
Length:	249564	nm
Size:	65505	digits
Spacing:	3.810	nm
NM-points ratio:	0.000 % (0 Pts)	

Identity card		
Name:	BA_20x_ext --- MU-232…8points x 1198 points)	
Created on:	7/7/2020 4:58:00 PM	
Studiable type:	Surface	
Axis:	X	
Length:	254.9	µm
Size:	1198	points
Spacing:	0.2130	µm
Axis:	Y	
Length:	254.9	µm
Size:	1198	points
Spacing:	0.2130	µm
Axis:	Z	
Layer type:	Topography	
Length:	249564	nm
Size:	65505	digits
Spacing:	3.810	nm
NM-points ratio:	0.000 % (0 Pts)	

ConfoMap ST 8.1.9286

25-Aug-20

- 1 / 1 -

Fig. 28 »Resampling template« created in ConfoMap (a derivative of MountainsMap Imaging Topography developed by Digital Surf, Besançon, France; version ST 8.1.9286) to process the data acquired from the quantitative use-wear analysis. Here, the template was applied to a *Keilmesser* from Balver Höhle (MU-232).

Quantitative use-wear analysis: Balver Höhle
Template to mirror the surfaces in x and z that have been acquired with the LSM800 based on moulds instead of the original artefact surface.

This template is used for three samples with three measurements (surfaces) respectively.

C. Mirroring

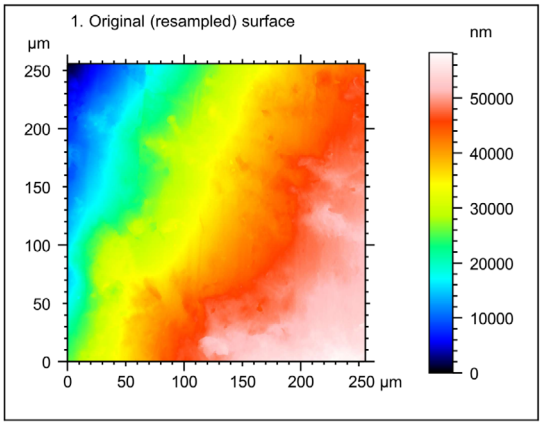

Identity card		
Name:	BA_50x_res --- MU-020 …01-a_50x09_LSM_Topo	
Created on:	7/8/2020 4:41:00 PM	
Studiable type:	Surface	
Axis:	X	
Length:	255.5	µm
Size:	1198	points
Spacing:	0.2134	µm
Axis:	Y	
Length:	255.5	µm
Size:	1198	points
Spacing:	0.2134	µm
Axis:	Z	
Layer type:	Topography	
Length:	58262	nm
Size:	65509	digits
Spacing:	0.8894	nm
NM-points ratio:	0.000 % (0 Pts)	

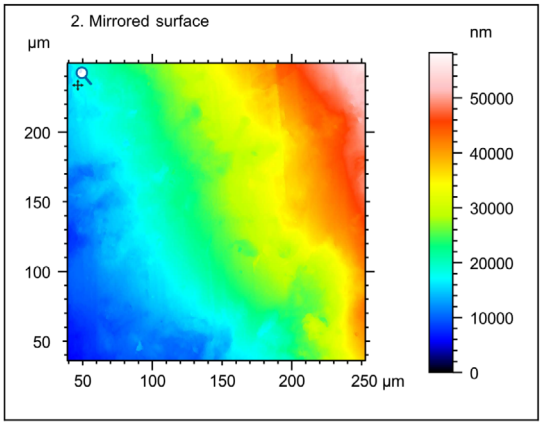

Identity card		
Name:	BA_50x_res --- MU-020 …> Mirrored (in X and Z)	
Created on:	7/8/2020 4:41:00 PM	
Studiable type:	Surface	
Axis:	X	
Length:	255.5	µm
Size:	1198	points
Spacing:	0.2134	µm
Axis:	Y	
Length:	255.5	µm
Size:	1198	points
Spacing:	0.2134	µm
Axis:	Z	
Layer type:	Topography	
Length:	58262	nm
Size:	65509	digits
Spacing:	0.8894	nm
NM-points ratio:	0.000 % (0 Pts)	

ConfoMap ST 8.1.9286 25-Aug-20 - 1 / 1 -

Fig. 29 »Mirroring template« created in ConfoMap (a derivative of MountainsMap Imaging Topography developed by Digital Surf, Besançon, France; version ST 8.1.9286) to process the data acquired from the quantitative use-wear analysis. Here, the template was applied to a *Keilmesser* from Balver Höhle (MU-020). This template was only used when a mould instead of the original artefact surface was analysed.

Quantitative use-wear analysis: Balver Höhle
Template to process all surfaces aquired with the LSM with the 20x/0.7, 50x/0.75 and 50x/0.95 objectives.

This template is used for thirty-three sampleswith three measurements(surfaces) respectively.

D. Processing

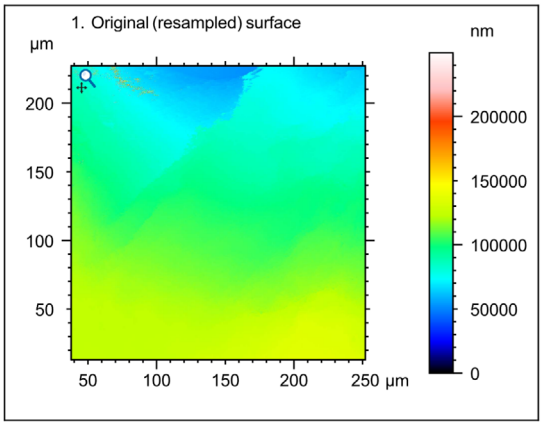

Identity card		
Name:	BA_50x_res --- BA_20x...01-a_20x07_LSM_Topo	
Created on:	7/7/2020 4:58:00 PM	
Studiable type:	Surface	
Axis:	X	
Length:	254.9	µm
Size:	1198	points
Spacing:	0.2130	µm
Axis:	Y	
Length:	254.9	µm
Size:	1198	points
Spacing:	0.2130	µm
Axis:	Z	
Layer type:	Topography	
Length:	249564	nm
Size:	65505	digits
Spacing:	3.810	nm
NM-points ratio:	0.000 % (0 Pts)	

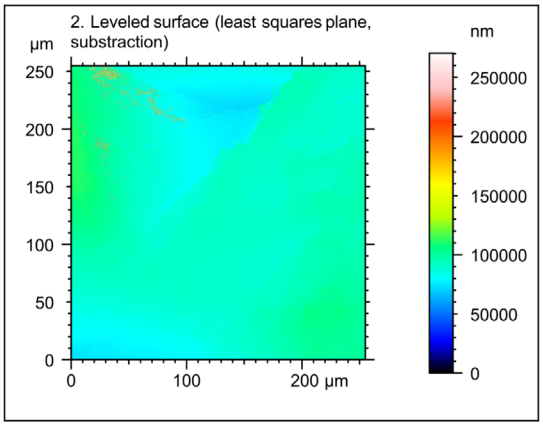

Identity card		
Name:	BA_50x_res --- BA_20x...po> Leveled (LS-plane)	
Created on:	7/7/2020 4:58:00 PM	
Studiable type:	Surface	
Axis:	X	
Length:	254.9	µm
Size:	1198	points
Spacing:	0.2130	µm
Axis:	Y	
Length:	254.9	µm
Size:	1198	points
Spacing:	0.2130	µm
Axis:	Z	
Layer type:	Topography	
Length:	270491	nm
Size:	70998	digits
Spacing:	3.810	nm
NM-points ratio:	0.000 % (0 Pts)	

ConfoMap ST 8.1.9369 07-Sep-20 - 1 / 5 -

Fig. 30 »Processing template« created in ConfoMap (a derivative of MountainsMap Imaging Topography developed by Digital Surf, Besançon, France; version ST 8.1.9286) to process the data acquired from the quantitative use-wear analysis. Here, the template was applied to a *Keilmesser* from Balver Höhle (MU-232). This is page 1 of 5.

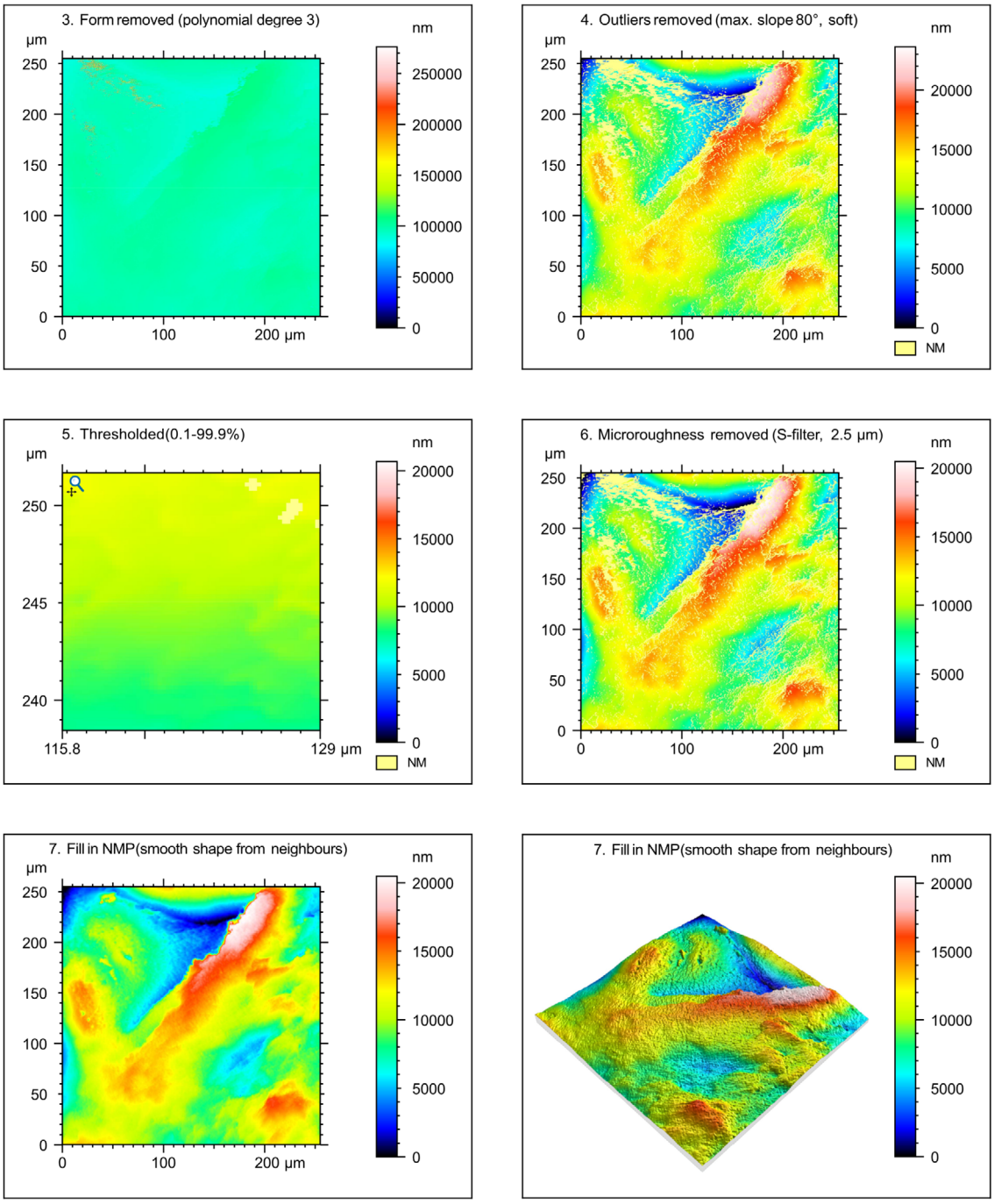

Fig. 31 »Processing template« created in ConfoMap (a derivative of MountainsMap Imaging Topography developed by Digital Surf, Besançon, France; version ST 8.1.9286) to process the data acquired from the quantitative use-wear analysis. Here, the template was applied to a *Keilmesser* from Balver Höhle (MU-232). This is page 2 of 5.

Identity card			
Name:	BA_50x_res --- BA_20x...innon-measured points		
Created on:	7/7/2020 4:58:00 PM		
Studiable type:	Surface		
Axis:	X		
Length:	254.9	µm	
Size:	1198	points	
Spacing:	0.2130	µm	
Axis:	Y		
Length:	254.9	µm	
Size:	1198	points	
Spacing:	0.2130	µm	
Axis:	Z		
Layer type:	Topography		
Length:	20482	nm	
Size:	53762	digits	
Spacing:	0.3810	nm	
NM-points ratio:	0.000 % (0 Pts)		

C. Analyses

8. ISO 25178-2 parameters on surface #7

ISO 25178 - Primary surface		
F: [Workflow] Form removed (LS-poly 3)		
S-filter (λs): [Workflow] S-filtered (λs 2.500 µm)		
Height parameters		
Sq	3243	nm
Ssk	0.06336	
Sku	3.457	
Sp	10477	nm
Sv	10005	nm
Sz	20482	nm
Sa	2506	nm
Functional parameters		
Smr	0.5510	%
Smc	3754	nm
Sxp	6582	nm
Spatial parameters		
Sal	25.95	µm
Str	0.3211	
Std	42.50	°
Hybrid parameters		
Sdq	0.6025	
Sdr	9.994	%
Functional parameters (Volume)		
Vm	0.2094	µm³/µm²
Vv	3.963	µm³/µm²
Vmp	0.2094	µm³/µm²
Vmc	2.775	µm³/µm²
Vvc	3.559	µm³/µm²
Vvv	0.4034	µm³/µm²

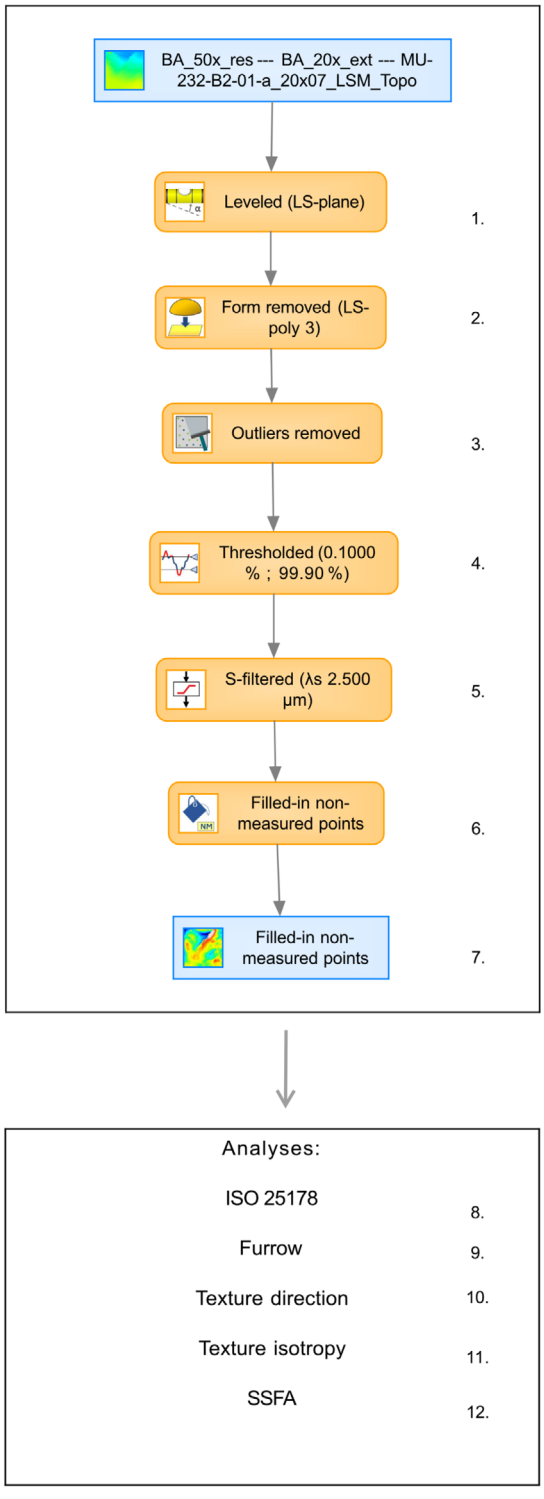

ConfoMap ST 8.1.9369

07-Sep-20

- 3 / 5 -

Fig. 32 »Processing template« created in ConfoMap (a derivative of MountainsMap Imaging Topography developed by Digital Surf, Besançon, France; version ST 8.1.9286) to process the data acquired from the quantitative use-wear analysis. Here, the template was applied to a *Keilmesser* from Balver Höhle (MU-232). This is page 3 of 5.

9. Furrow analysis on surface #7

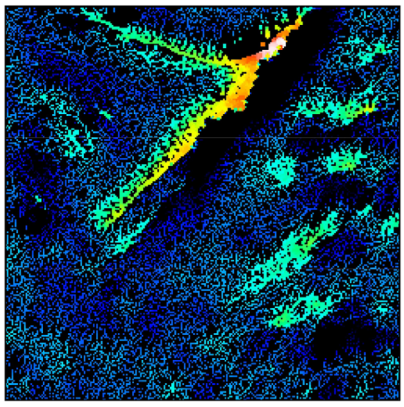

All furrows are shown.

Parameters	Value	Unit
Maximum depth of furrows	12698	nm
Mean depth of furrows	2586	nm
Mean density of furrows	2987	cm/cm2

10. Texture direction on surface #7

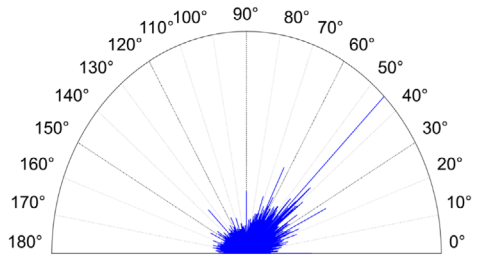

Parameters	Value	Unit
First direction	44.98	°
Second direction	26.45	°
Third direction	63.53	°

11. Texture isotropy on surface #7

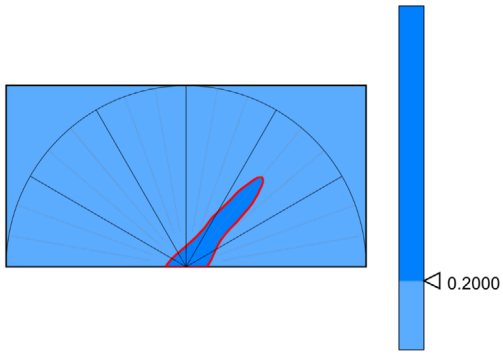

Parameters	Value	Unit
Isotropy	13.50	%

Fig. 33 »Processing template« created in ConfoMap (a derivative of MountainsMap Imaging Topography developed by Digital Surf, Besançon, France; version ST 8.1.9286) to process the data acquired from the quantitative use-wear analysis. Here, the template was applied to a *Keilmesser* from Balver Höhle (MU-232). This is page 4 of 5.

12. SSFAon surface #7

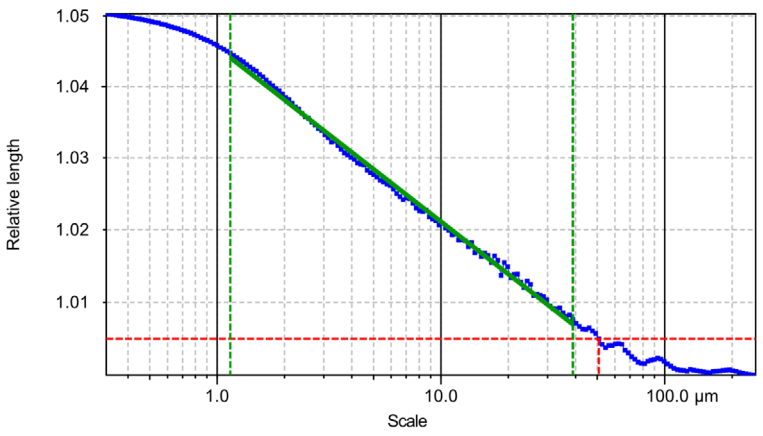

Information	
Method	Length-scale (rows)

Parameters	Value	Unit	Comment
epLsar	0.003683		*Length-scale anisotropy (Sfrax) (1.8 µm, 5°)*
NewEplsar	0.0181		*Length-scale anisotropy (1.8 µm, 5°)*

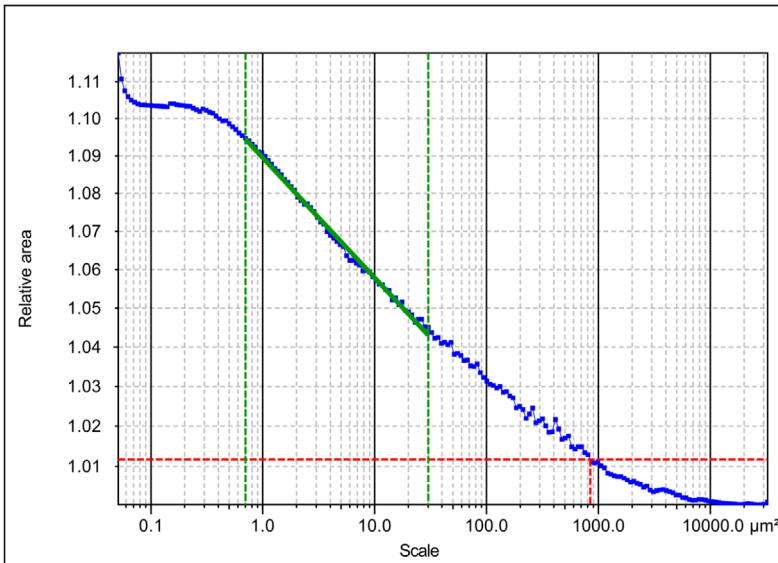

Information	
Method	Area-scale (four corners)

Parameters	Value	Unit	Comment
Asfc	12.80		*Fractal complexity*
Smfc	2.508	µm²	*Scale of max complexity*
HAsfc9	0.6292		*Heterogeneity of Asfc (3x3)*
HAsfc81	0.8102		*Heterogeneity of Asfc (9x9)*

ConfoMap ST 8.1.9369

07-Sep-20

- 5 / 5 -

Fig. 34 »Processing template« created in ConfoMap (a derivative of MountainsMap Imaging Topography developed by Digital Surf, Besançon, France; version ST 8.1.9286) to process the data acquired from the quantitative use-wear analysis. Here, the template was applied to a *Keilmesser* from Balver Höhle (MU-232). This is page 5 of 5.

parameter	unit	category	subcategory	name	description
Smc (mr = 10 %)	µm	Field	Functional	inverse areal material ratio of the scale-limited surface	height *c* at which a given areal material ratio (*mr*, or *p* in MountainsMap) is satisfied
Smr (c = 1 µm under the highest peak)	%	Field	Functional	areal material ratio of the scale-limited surface	ratio of the area of the material at a specified height *c* to the evaluation area
Sxp (p = 50 %, q = 97.5 %)	µm	Field	Functional	peak extreme height	difference in height between the p and q material ratios
Sa	µm	Field	Height	arithmetical mean height of the scale limited surface	arithmetic mean of the absolute of the ordinate values within a definition area (*A*)
Sku	<no unit>	Field	Height	kurtosis of the scale-limited surface	quotient of the mean quartic value of the ordinate values and the fourth power of Sq within a definition area (*A*)
Sp	µm	Field	Height	maximum peak height of the scale limited surface	largest peak height value within a definition area
Sq	µm	Field	Height	root mean square height of the scale-limited surface	root mean square value of the ordinate values within a definition area (*A*)
Ssk	<no unit>	Field	Height	skewness of the scale-limited surface	quotient of the mean cube value of the ordinate values and the cube of Sq within a definition area (*A*)
Sv	µm	Field	Height	maximum pit height of the scale limited surface	minus the smallest pit height value within a definition area
Sz	µm	Field	Height	maximum height of the scale-limited surface	sum of the maximum peak height value and the maximum pit height value within a definition area
Sdq	<no unit>	Field	Hybrid	root mean square gradient of the scale-limited surface	root mean square of the surface gradient within the definition area (*A*) of a scale-limited surface
Sdr	%	Field	Hybrid	developed interfacial area ratio of the scale-limited surface	ratio of the increment of the interfacial area of the scale-limited surface within the definition area (*A*) over the definition area
Sal (s = 0.2)	µm	Field	Spatial	autocorrelation length	horizontal distance of the $f_{ACF}(t_x,t_y)$ which has the fastest decay to a specified value *s*, with $0 \leq s < 1$
Std (Reference angle = 0°)	°	Field	Spatial	texture direction of the scale-limited surface	angle, with respect to a specified direction θ, of the absolute maximum value of the angular spectrum
Str (s = 0.2)	<no unit>	Field	Spatial	texture aspect ratio	ratio of the horizontal distance of the $f_{ACF}(t_x,t_y)$ which has the fastest decay to a specified value *s* to the horizontal distance of the $f_{ACF}(t_x,t_y)$ which has the slowest decay to *s*, with $0 \leq s < 1$
Vm *(p = 10 %)*	µm³/ µm²	Field	Volume	material volume	volume of the material per unit area at a given material ratio calculated from the areal material ratio curve
Vmc (p = 10 %, q = 80 %)	µm³/ µm²	Field	Volume	core material volume of the scale-limited surface	difference in material volume between the *p* and *q* material ratios

parameter	unit	category	subcategory	name	description
Vmp (p = 10 %)	µm³/ µm²	Field	Volume	peak material volume of the scale-limited surface	material volume at *p* material ratio
Vv (p = 10 %)	µm³/ µm²	Field	Volume	void volume	volume of the voids per unit area at a given material ratio calculated from the areal material ratio curve
Vvc (p = 10 %, q = 80 %)	µm³/ µm²	Field	Volume	core void volume of the scale-limited surface	difference in void volume between *p* and *q* material ratios
Vvv (p = 80 %)	µm³/ µm²	Field	Volume	dale void volume of the scale-limited surface	dale volume at *p* material ratio
Asfc	<no unit>	SSFA		Area-scale fractal complexity	The slope of the steepest part of the curve, fit to a log-log plot of relative area over the range of scales multiplied by -1000
epLsar	<no unit>	SSFA		Exact proportion Length-scale anisotropy of relief	Radial profiles are extracted from the centre of the surface, by default every 5°, and the value of relative-length is calculated at a scale of 1.8 µm
HAsfc	<no unit>	SSFA		Heterogeneity of Area-scale fractal complexity	Calculated in a scale-sensitive manner by splitting individual scanned areas into successively smaller subregions given equal numbers of rows and columns
NewEpLsar	<no unit>	SSFA		Exact proportion Length-scale anisotropy of relief	Radial profiles are extracted from the centre of the surface, by default every 5°, and the value of relative-length is calculated at a scale of 1.8 µm
Smfc	µm²	SSFA		Scale of maximum complexity	The scale range over which *Asfc* is calculated (the steepest part of the relative area versus scale curve)
Isotropy	%	Texture direction		Isotropy	Identical to ISO 25178 *Str*
Tr1R	°	Texture direction		First direction	Only relevant if Isotropy ≤ 30 %. Identical to ISO 25178 *Std*
Tr2R	°	Texture direction		Second direction	Only relevant if *Isotropy* ≤ 30 %
Tr3R	°	Texture direction		Third direction	Only relevant if *Isotropy* ≤ 30 %
madf	µm	Furrow		Maximum depth of furrows	Furrows are micro-valleys. The furrow analysis identifies the areas where points are lower than the neighbouring points on a given surface
metf	µm	Furrow		Mean depth of furrows	Furrows are micro-valleys. The furrow analysis identifies the areas where points are lower than the neighbouring points on a given surface
medf	cm/cm²	Furrow		Mean density of furrows	Furrows are micro-valleys. The furrow analysis identifies the areas where points are lower than the neighbouring points on a given surface

Table 11 3D parameters calculated within the qualitative use-wear analysis. These 3D parameters include 21 ISO 25178-2 parameters, 3 furrow parameters, 3 texture direction parameters, 1 texture isotropy parameter and 6 SSFA parameters.

CONTROLLED EXPERIMENTS

Assigning a function to Palaeolithic artefacts requires profound technological and morphological knowledge as well as suitable analogies and comparisons. While ethnographic comparisons are most likely revealing, they do not provide a one-to-one interpretation (Binford 1968). Determining a tool's function has proven to be especially complicated in time periods, when toolkits were not highly specialised and tools used for multifunctional purposes as for example in the Middle Palaeolithic (Plisson et al. 1998). In order to address tool function, experiments provide an alternative possibility to test assumptions and gather new information. Experiments have played an important role in archaeology since the 1970s (Tringham et al. 1974; Coles 1979; Odell/Odell-Vereecken 1980; Outram 2008). The general idea behind the conduction of experiments is to reconstruct past processes and to replicate potential past human activities. Experiments also frequently serve the purpose to produce reference collections for comparison with archaeological samples. Although different experiments follow different research questions, they all have something in common: they all test hypothesis. Hypothesis testing is used to assess the plausibility of a hypothesis (null hypothesis) by using sample data. A test can thereby only provide evidence concerning the plausibility of the hypothesis and the conclusion cannot be proven as true. A tested assumption can only be accepted as temporarily valid.
Depending on the question addressed by an experiment, different levels or types of experiments can be conducted. The distinction between »*Actualistic*«, »*Pilot*« or »*Exploratory*« on the one hand and »*Controlled*«, »*Second generation*« or »*Laboratory*« experiments on the other hand can be made (Eren et al. 2016; Marreiros/Pereira/Iovita 2020). The first type of experiments (»*Actualistic*«*,* »*Pilot*« or »*Exploratory*«) aims mainly at replicating human actions in realistic contexts, whereas the second type focuses on testing individual variables *(*»*Controlled*«*,* »*Second generation*« or »*Laboratory*«). These experiments often involve mechanical devices in order to limit the human bias. By isolating certain variables, their effect on the final result can be comprehended. Recently, an attempt has been made to refine this terminology (Marreiros et al. 2020). Based on this, a distinction of three generations of experiments is reasonable.

First generation experiments

First generation experiments are comparable with the prior described »*Actualistic*«, »*Pilot*« or »*Exploratory*« experiments. These experiments build the foundation for new hypothesis. *First generation experiments* often test the possibility to perform a certain action with a tool. With this, they provide information in order to help understanding past technologies. *First generation experiments* are a crucial step for making preliminary observations and the identification of major variables. Nevertheless, these experiments cannot go further than delivering insights into certain aspects concerning for instance, tool performance.

Second generation experiments

Second generation experiments do not seek to answer overarching research questions, instead they are focused on basic fundamental aspects. This often concerns uniform principles for instance physical principles, operating uniformly across space and time. The identification of patterns, processes and the test of key properties should be the focus of the experiments. Therefore, the archaeological interpretations should be detached from the data interpretation. Performing a *second generation experiment* means testing individual variables. With this approach, the effect of the individual variables in the setup can be evaluated

respectively. Furthermore, the aim of *second generation experiments* is to control and manipulate actions. The design of these experiments is thus more complex and involves mechanical devices. Human variability should be reduced to a minimum. By following this approach, not only the performed action is standardised through a mechanical apparatus, but also the samples and the contact material. Ideally, the samples imitating archaeological artefacts or at least certain features are standardised in order to guarantee variable control and comparability. The same applies to the contact material. *Second generation experiments* reduce subjectivity and result in information about the cause and effect of the tested variables, but at the same time, they are further away from replicating human actions and thus the results cannot directly be transferred to the archaeological record. Since *second generation experiments* are controlled and standardised, they also seek to produce repeatable and reproducible results.

Third generation experiments

Experiments from the *third generation* build on the results gained through *second generation experiments*. In this step, the human variability should again be incorporated. The recognised patterns and the generated models from the *second generation experiments* should be tested in a more naturalistic way. Mechanical devices are not needed in this type of experiment. Instead, the use of so-called multi-sensor systems for gesture recognition (Pfleging et al. 2015; Key 2016; Williams-Hatala et al. 2018) is recommended. Standard samples and replicas of archaeological tools should be employed in an identical way. This approach makes it possible to correlate the results. The *third generation experiments* allow evaluating the results from the *second generation experiment* by adding the human variability and bias. Doing so, the results can have implications on the interpretation of archaeological assemblages and can address overriding research questions. Archaeologists have conducted experiments for decades. Since then, criticism has also accumulated. In particular *controlled* or *second generation experiments* are exposed to scepticism. As a major point of criticism, the artificial nature of these experiments has to be highlighted. The division in the three generations of experiments is trying to overcome this problem. It needs to be stressed that the different generations do not exclude each other, on the contrary; they should be seen as complementary. To go further, for designing a *second generation experiment*, several researchers require keeping the following conditions: the research question should be defined clearly, including a hypothesis as well as an alternative hypothesis which can be tested. The number of trials and samples has to be high enough in order to be statistically evaluable. This should also lead to a dominant use of quantitative over qualitative methods. The involved variables need to be identified and assigned as independent, dependent and random variables. The experimental setup has to be detailed in the explanations in corresponding publications. Together, *second generation experiments* should target at repeatability and reproducibility.

Although discussions concerning experiments, especially *second generation experiments* are becoming numerous and first improvements are visible, there are limitations. In general, sequential experiments are time consuming. Moreover, mechanical devices are expensive and their incorporation in an experimental design is most commonly unrealistic. Even if the use of a mechanical device is possible, testing, manipulating and controlling each variable related to an archaeological assemblage is extremely elaborated. The use of quantitative methods and open data in archaeological research is unfortunately not yet common practice. Thus, cooperation and data exchange in order to minimise the costs and the time investment are difficult to implement.

The controlled experiments conducted within this project belong to the so-called *second generation experiments*. These experiments aim to address basic questions and to understand the influence of specific

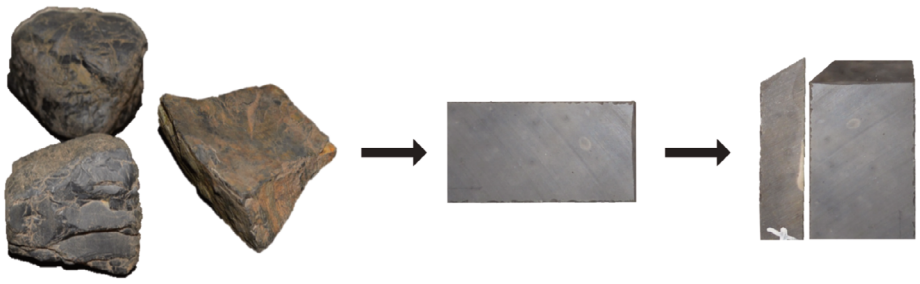

Fig. 35 Standard sample production. The raw pieces (left; here silicified schist) are cut into blanks (middle) with a rock-saw. A diamond band-saw was used to cut the blank in order to create a typical standard deign sample with a defined edge angle (right).

variables within a complex system. Thus, variables need to be tested individually in order to test their effect-causation with other variables in the experiment. In *second generation experiments*, the human factor as well as subjectivity are reduced to a minimum. To do so, a mechanical device was used to perform defined actions. This mechanical device involved in the controlled experiments here is a modular material tester (SMARTTESTER®, Inotec AP GmbH, Germany). The SMARTTESTER® allows for precise movements and is sensor-controlled (Calandra/Gneisinger/Marreiros 2020). Using the mechanical device makes the experiment itself repeatable. To further improve this aspect and to actually isolate certain variables, standard samples were used during the experiments. Raw-material intra-variability was limited by the use of as few as possible raw material nodules. The standard samples are machine cut samples with a predefined shape (**fig. 35**). Baltic flint as well as silicified schist served as raw material. The raw material, in case of the silicified schist, was collected next to the small streams in the surrounding areas of the two sites Buhlen and Balver Höhle. The silicified schist and flint nodules were cut with a rock-saw into cubes, and further cut into size-defined blanks. While the sample length could vary, the standard width (length edge) of the samples was always 3 cm. The cubes were separated into as many blanks as possible to reduce raw material variation. In the next step, one end of the blanks was cut with a diamond band-saw (EXAKT 310 CP) in a given angle. One side of the active edge was in addition modified by a 45° chamfered edge (exception: initial experiment). The chamfered edge was meant to reduce the force applied on only one point of the sample when the contact with the worked material was initialised. The idea was, that this modification would spread the applied force on a bigger area and would therefore minimise the risk of immediate fracture. This cut was also done with the diamond band saw. Usually, the cut with the band saw left a small burr between the two adjacent surfaces – the surface of the active edge and the chamfered edge. This burr was manually removed with a mini diamond drill bit. The samples were cleaned after cutting. First the samples were rinsed with tap water and then with a preheated ultrasonic bath (EMAG Emmi 20HC). For that reason, the samples were individually packed in a plastic bag filled with ~ 100 ml of demineralised water and a non-ionic detergent (BASF Plurfac LF901, 1 g/l = 1 % w/v; BASF SE, Ludwigshafen, Germany). The samples were left in the bath for 10 min at 45°C and 100 KHz. Subsequently, the demineralised water was exchanged with tap water. This was repeated two more times. In a final step, the bags were filled with ~100 ml purified water and emptied after rinsing. Since it was crucial for the later use-wear analysis to enable the analysis of the exact same surface, a coordinate system was created directly on the sample (Calandra et al. 2019a). For this, three 100-200 µm diameter ceramic beads were adhered with epoxy resin (Epoxydharz L mixed with Härter S in a ratio 10:4 by weight) on the dorsal and ventral site of the tool.

The experiments were described with the aim to address the same overall research question. The goal is to bring the relation between tool morphology and tool function into question.

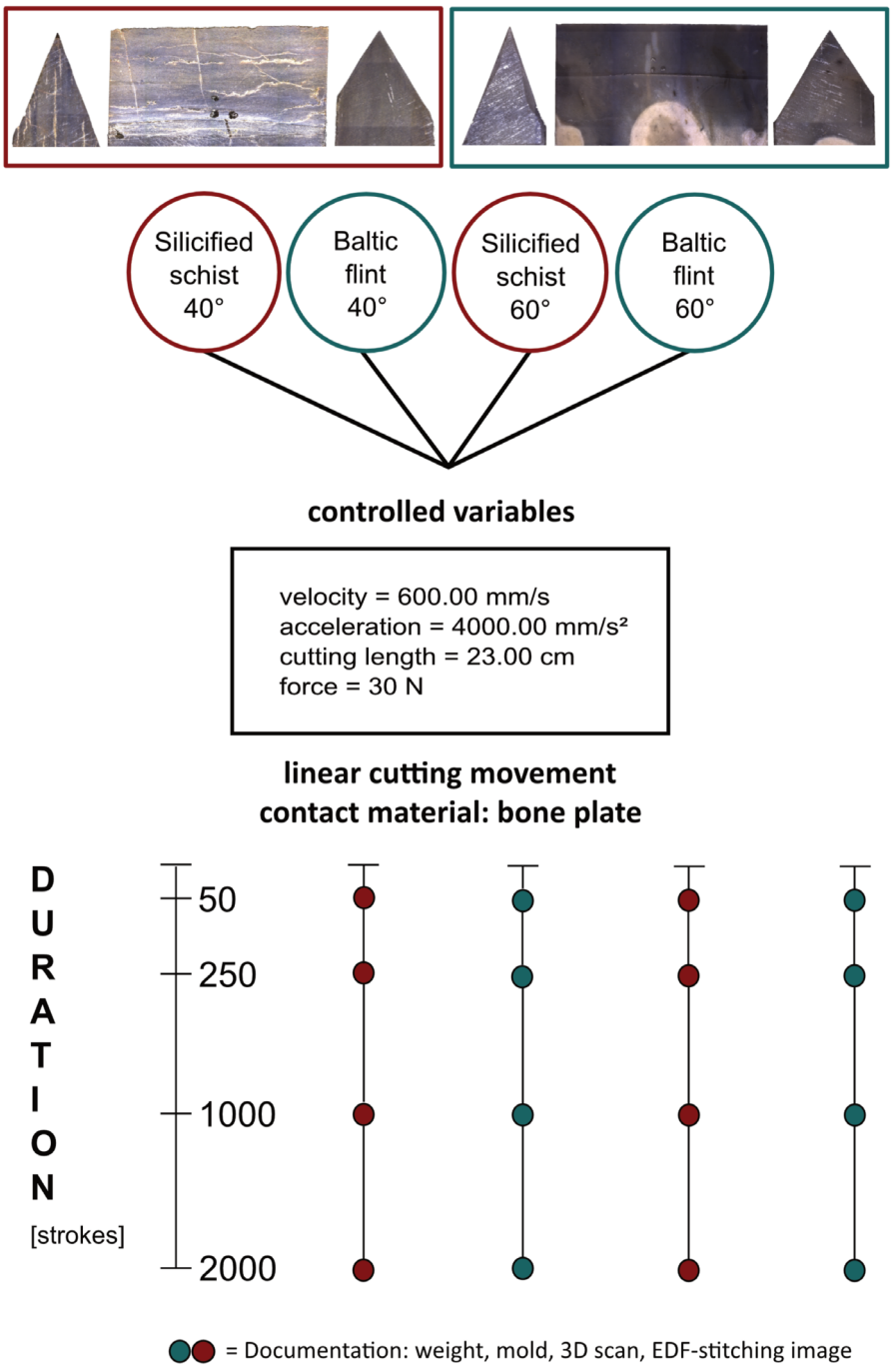

Fig. 36 Experimental design for the initial experiment.

Experimental setup – initial experiment

The initial experiment was designed to evaluate the experimental setup and to test two variables, raw material and edge angle (**fig. 36**). Silicified schist as well as Baltic flint served as raw material. The standard samples were bifacially cut as 40° and 60° degree edge angles respectively. The experiment had no demand on statistical validity. With a sample size of n = 7 (3× silicified schist 40°, 2× silicified schist 60°, 1× flint 40°, 1× flint 60°) not enough replicas were included in order to lead to statistically significant results. The electric, linear drive (z-direction) of the mechanical devise, the SMARTTESTER®, was used in order to perform a unidirectional cutting movement. As a prerequisite in order to standardise the experiment as much

as possible and to test the effects of the two mentioned variables individually, the contact material was also standardised. Therefore, an artificial bone plate (PR0114) from the Swiss company SYNBONE® was used. This generic plate is a modified bone-like polyurethane with the dimensions 250 mm × 250 mm × 6 mm and a shore hardness (D) of 78 5/- 5 %.
The experiment was built up as a sequential experiment. Four cycles defined by a number of cutting strokes were executed. The first cycle started from zero to 50 strokes, the second from 51-250 strokes, the third 251-1000 strokes and the final cycle from 1001-2000 strokes. The cutting length was thereby 23 cm. Each sample had to perform the four cycles with 2000 strokes in total by always using the same cutting track. Certain factors were set up during the experiment, others were measured by sensors only. The velocity with 600.00 mm/s and the acceleration 4000.00 mm/s belong to the predetermined factors. The force of 30 N was also defined by the weight of the sample holder (~ 1 kg) and two manually added kg. In total five sensors were activated during the entire duration of the experiment. Three sensors recorded the predetermined factors velocity, acceleration and force. The other two sensors recorded the penetration depth in mm and the friction in N. The sampling rate was in a frequency of ten Hz. The samples were clamped straight into the sample holder in a 90° angle between sample and contact material. A template per sample was created to assure the constancy of the programmed settings as for instance the position of the sample on the x-, y- and z-axis.
To test aspects such as efficiency, performance and durability by comparing the two raw materials and the two edge angle values, the documentation of the samples needed to follow a protocol. Initially, the samples were photographed with a Nikon D610. The weight was recorded with a weighing scale, Kern PCB 3500.2, with an accuracy of 0.1 g. To avoid inaccuracies, each sample was measured three times. The material properties of the raw material were tested using the Leeb rebound hardness tester (Proceq Equotip 550, Leeb C probe) by means of a coupling paste. The samples were scanned with an AICON smartScan-HE R8 from the manufacturer Hexagon. The system was always turned on one hour in advance in order to warm up all components. The S-150 FOV used has a resolution of 33µm. Identical settings were used for all scans; scans were exported afterwards in an STL-format. Three of the four surfaces per sample (one lateral and the two main surfaces) were documented with the ZEISS Smartzoom 5, a digital microscope. The 1.6× objective was used to create EDF-stitching images. Moulds were taken from the two cutting surfaces covering the edge. This protocol was not only followed before the experiment, but also after each cycle. Frequently, single cycles were video recorded.

Experimental setup – »artificial VS. natural« experiment

In the sequence of experiments was the so-called »artificial VS. natural experiment« the second one (**fig. 37**). This experiment aimed to validate the comparability of artificial with natural contact material. Tool performance and durability as well as the produced use-wear traces served as a measure of criteria. In order to standardise the contact material during an experiment, these artificial materials are a convenient solution, but their use needs to be justified. In addition, the experiment aimed at understanding the development of use-wear traces and testing the mechanical trends behind the formations.
Within this experiment, the independent variables were the raw material – silicified schist and Baltic flint – and the contact material. Four different contact materials were tested. Two belonging to the category artificial material and the other two were natural, fresh materials. An artificial bone plate coated with a rubber skin (PR0114.G) from the Swiss company SYNBONE® was used. This generic plate is a modified bone-like polyurethane with the dimensions 250 mm × 250 mm × 6 mm and a shore hardness (D) of 78 5/- 5 %. The

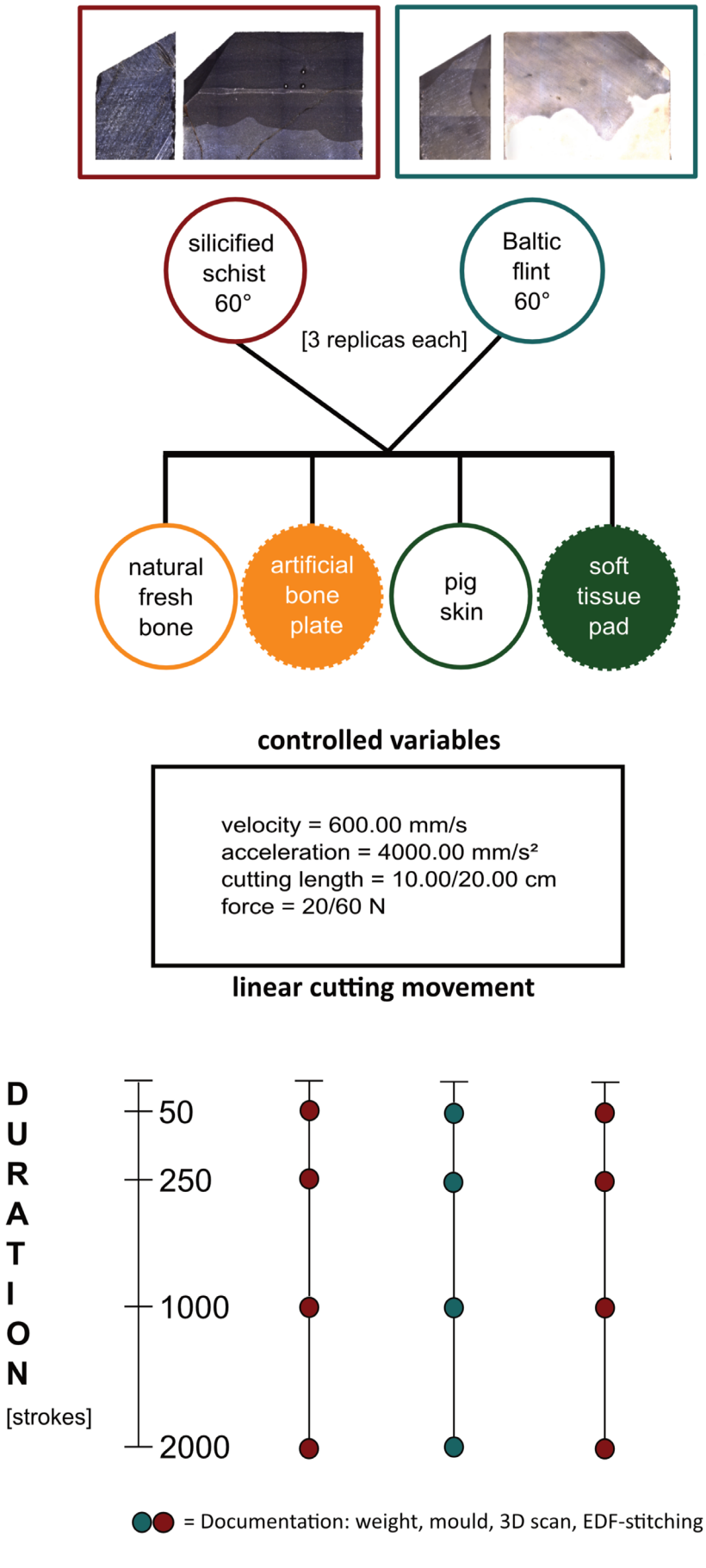

Fig. 37 Experimental design for the »artificial VS. natural« experiment.

bone plate with the rubber skin layer, imitating the periosteum, was therefore an artificial equivalent to a fresh and defleshed bone. The bone in this experiment was a cow scapula (*Bos primigenius Tarurus, Angus*) provided in a fresh state by a butcher. The periosteum and small pieces of flesh were still attached. The experiment was carried out in a laboratory under ambient room temperature conditions. During the course of the experiment, the bone started to dry out but apart from desiccation no other degradation were visible. The reason to choose a cow scapula can be explained by the size and shape. The morphology of the bone offers the possibility to perform long cutting strokes on a considerably straight surface, providing better conditions for a comparison of the results between the bone plate and the bone. The second set of contact material was skin. As artificial skin a soft tissue pad with a matrix (PR1043.10) SYNBONE® was used. This skin pad is made of silicone ecoflex and has the dimensions 140 mm × 130 mm × 4.2 mm and a shore hardness 0-3A. A piece of natural pork skin was provided by a butcher by separating the skin from the flesh below. The skin was kept outside under room temperature and overnight it was kept cold in a fridge. Two pieces of skin were needed during the course of the experiment. The n = 24 samples were cut unifacailly with an edge angle of 60° and equally distributed between the four contact materials. Thus always three replicas per raw material were tested on one contact material.
The setup for this experiment was identical with the setup from the initial experiment. The same linear drive was used in order to perform unidirectional cutting strokes, the same number of strokes separated in four cycles was executed and the same sensors with identical settings were used. A few changes however, are noteworthy. For the bone plate and the natural bone a force of 60 N was applied, while the force for the artificial and natural skin was only 20 N. The cuts on the bone plate had a length of 20 cm and half of the cuts on the fresh bone, too. The other cutting strokes were ten cm long, but the amount of strokes was doubled in these cases. The documentation followed the same protocol mentioned for the initial experiment.

Experimental setup – tool function experiment

The third and main experiment built up on the results carried out during the other two experimental setups (**fig. 38**). The goal was again to test efficiency, durability and performance by comparing two raw materials and different edge angles on standardised contact material. To further investigate the relation between tool morphology and function, the edge angle values for the standard samples were extrapolated from the edge angle measurements (see chapter Quantification of edge design) from the sampled *Keilmesser*. These measurements are based on 3D scans of in total 157 *Keilmesser*. The selected tools were separated in *Keilmesser* (n = 57) and *Keilmesser* with a modification through the application of the *Prądnik method* (n = 100). From all the calculated edge angle data only the results from the »2-lines« procedure with measurements at 5 mm distance to the intersection were selected. The statistical analysis was performed with the open-source software R version 4.0.2 through RStudio version 1.3.1073 (RStudio Inc., Boston, USA) for Microsoft Windows 10. The following packages were used: writexl v. 1.3, tidyverse v. 1.3.0, openxlsx v. 4.1.5. and R.utils v. 2.9.2. Reports of the analysis in HTLM format, created with knitr v. 1.29 and rmarkdown v. 2.3 are available on GitHub [https://github.com/lschunk/edge_angle_analysis] as well as the raw data, the scripts and the RStudio project. For calculating the average edge angle on the selected tools, the first and the last horizontal section (always ten sections per tool) were excluded (**fig. 39**). This is reasoned by the fact that these sections usually display edge angle values distinct from the values of the other eight sections. These two sections are likely not representing the active edge anymore. It is possible that they are already part of the base and the arch of the tool. Based on the eight horizontal sections and the measurements at 5 mm the average per tool could be calculated. Since there was a notable change in the edge angle values in the distal

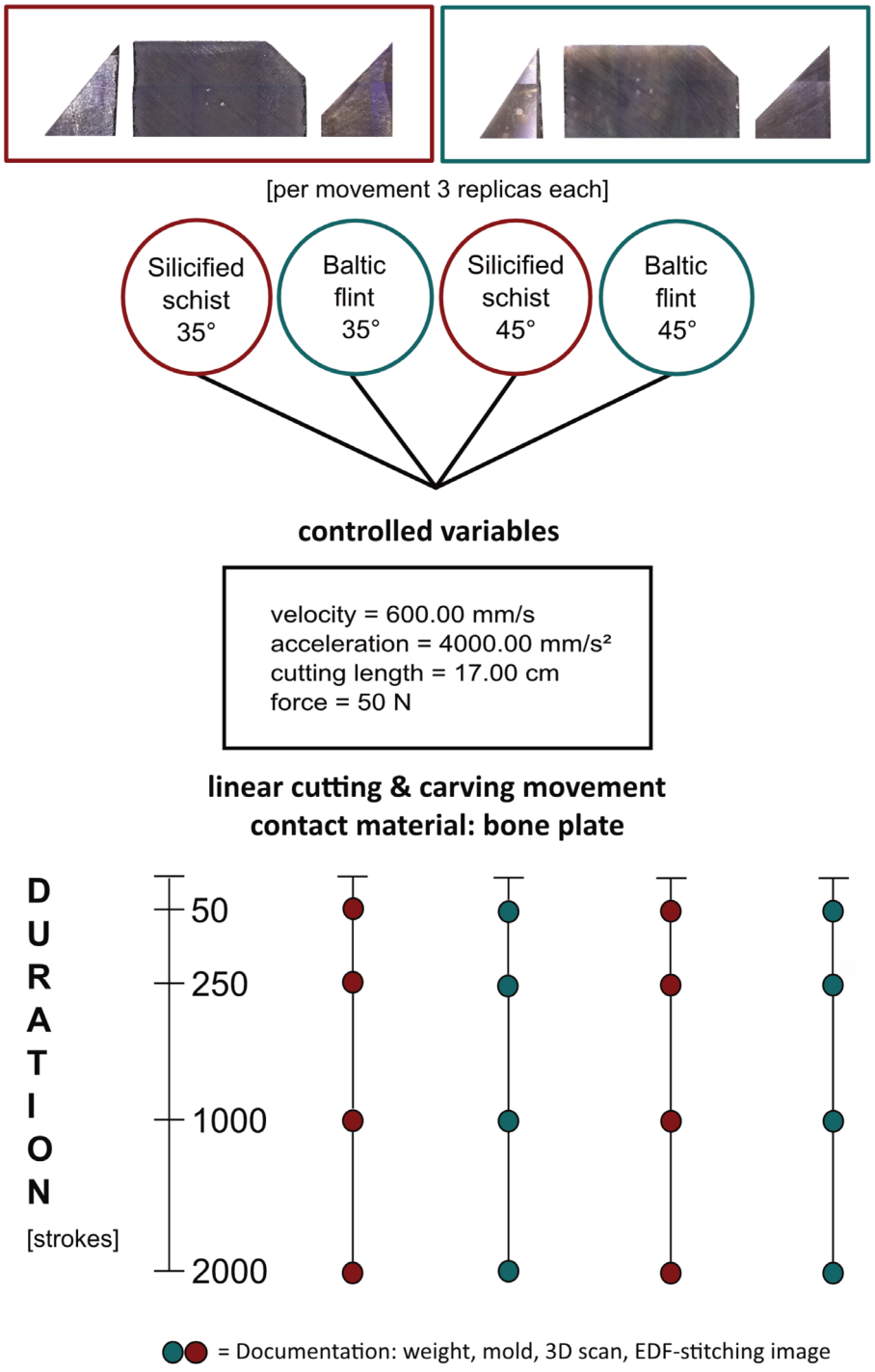

Fig. 38 Experimental design for the tool function experiment.

and the proximal part of the tool, two instead of one average value were calculated. The first built on the results of the section two to four and the second on the results of the section five to nine. The average was calculated per classification (*Keilmesser* and *Keilmesser* with *Prądnik method*). The results for the proximal tool part were nearly identical in the two classifications (44.75° and 44.48° respectively). For the distal part of the tool the results varied slightly. While *Keilmesser* reach an average of 36.06°, *Keilmesser* modified by the *Prądnik method* show an average of about 33.50°. Therefore, the decision was made to test two different edge angle values – 45° and 35° – as a proxy for the proximal and the distal part of the tool, respectively.

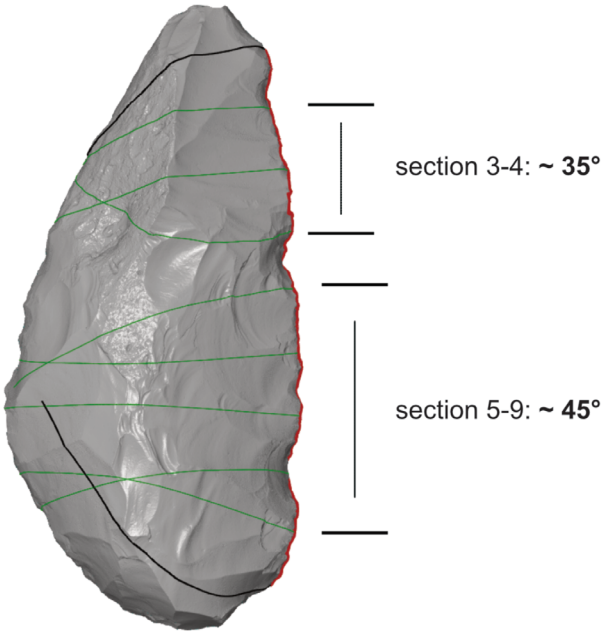

Fig. 39 Calculation of the edge angles, illustrated here on a 3D model of a *Keilmesser* from Ramioul (ID R-019). The horizontal lines are the section. The sections used to calculate the edge angels in green, in black the ones excluded for the calculation. The edge angle values have been calculated with the »2-lines«.

In total 24 standardised samples were unifacially cut. Twelve of these 24 samples were produced out of Baltic flint nodules, the other twelve from silicified schist blocks. The linear drive was used to perform two different movements: unidirectional cutting and carving. Artificial bone plates served as contact material (PR0114), the same modified bone-like polyurethane plates as used during the initial experiment. The cutting and carving length was 17 cm each. Three samples per raw material and edge angle were tested for cutting and carving respectively. The experimental setup was identical to the ones during the first and second experiment. Thus, the tool function experiment was also designed as a sequential experiment with the same four cycles and 2000 strokes in total per sample. A force of 50 N was applied for both movements. While the samples for the cutting movement were clamped again straight into the sample holder in a 90° angle between sample and contact material, the sample was adjusted differently for the carving movement. With the flat, not angled tool surface, the samples were clamped into the sample holder in a 20° angle towards the contact material. Consequently, the carving movement was performed in a flat and unidirectional motion. The documentation followed the same protocol as mentioned for the initial and the »artificial VS. natural« experiment.

Analysis of the experiments

Since the three experiments were following an identical experimental setup and protocol for the documentation, the acquired date could be evaluated similarly. Furthermore, the data could be combined. To answer questions related to tool efficiency, durability and performance, the samples were review in terms of their morphological changes. Material loss, fractures, retouch and changes in the edge angle were documented. The contact material was evaluated on the one hand concerning material loss, on the other hand the penetration depth was a valid indicator. Use-wear traces resulting from different actions and contact materials on the two different raw materials can be compared as well. Due to the sequential aspect of the experiments, also statements regarding the temporal formation and the development of the use-wear traces can be addressed.

Analysis 3D data

Part of the documentation before and after each cycle of the experiments was the 3D scanning of the samples. In order to further analyse the 3D models, a few preparatory steps were necessary. After scanning, the resulting STL file was imported in GOM Inspect, an open source software for 3D measurement data (GOM

Software 2018, Hotfix 1, Rev. 111729, build 2018-08-22). With GOM inspect, the 3D models were checked for holes in the mesh. Existing holes were closed automatically with a maximum hole size of 10.000 mm and 1000 as maximum number of edges. Mesh errors were eliminated. Depending on the number or the size of the holes, these two steps were repeatedly applied. The holes were not closed directly in one step with a higher maximum hole size value in order to avoid a change in the original morphology of the scanned sample.
Based on the closed models, the volume per sample could be computed. In this way, material loss of the samples due to the use within the experiment can be detected. At the same time, the 3D models can be inspected visually. GOM inspect allows for a comparison of 3D meshes. For this step, one of the meshes needs to be defined as CAD body (computer-aided design), while the other one can be imported as a mesh. The two models can be optically combined with a local best-fit alignment. Afterwards, a surface comparison on the CAD can be initialised. Based on a colour scale, the differences between the two 3D meshes can be optically seen and also numerically read.

Analysis edge angle

The closed 3D models also serve for the edge angle calculation (see method section 4.3). A surface curve defining the edge of each sample was added in GOM inspect. This polyline was exported in an IGES-format. All further steps were identical as described in the section »Quantification of edge angle design« earlier in this chapter. The following parameters were chosen: The number of horizontal sections is represented by ten sections per tool. The measurements were taken in one mm steps starting with the intersection between the vertical and the horizontal polylines. The lengths of the lines used in the »2-lines« and »best fit« measuring procedure, was always 2 mm. Calculating the edge angle of the experimental samples allows for a quantification of a change in the edge angle.
The statistical analysis was performed with R (version 4.0.2 through RStudio version 1.3.1073, RStudio Inc., Boston, USA). The following packages were used: writexl v. 1.3, tidyverse v. 1.3.0, openxlsx v. 4.1.5, ggrepel v. 2.3, doBy v. 4.6.7, patchwork, v. 1.0.1, ggplot2 v. 3.3.2 and R.utils v. 2.9.2. Reports of the analysis in HTLM format, created with knitr v. 1.29 and rmarkdown v. 2.3 are available on GitHub as well as the raw data, the scripts and the RStudio project [https://github.com/lschunk/edge_angle_experiments].

Use-wear analysis

Use-wear analysis was not done for all experimental samples. Instead, the pieces were systematically sampled. None of the samples from the initial experiment were part of the use-wear analysis. In the case of the second experiment, the »artificial VS. natural' experiment, eight samples were selected. These samples consist of four silicified schist and four flint samples. Each of the four samples was tested on a different contact material: bone plate, scapula, skin pad and pork skin. A further eight samples belonging to the tool function experiment were analysed. The selection was based on the raw material of the sample, the edge angle and the movement. Thus, one tool per cutting with 35° and 45° edge angle and one tool per carving with 35° and 45° edge angle made of silicified schist and flint were sampled.
As for the archaeological material, a scheme was designed for the quantitative use-wear analysis as well (**fig. 40**). The scheme fulfilled the purpose of mapping and locating the use-wear traces consistently in an identical way. The outline of the standard samples was used as template for a grid of four areas. This was

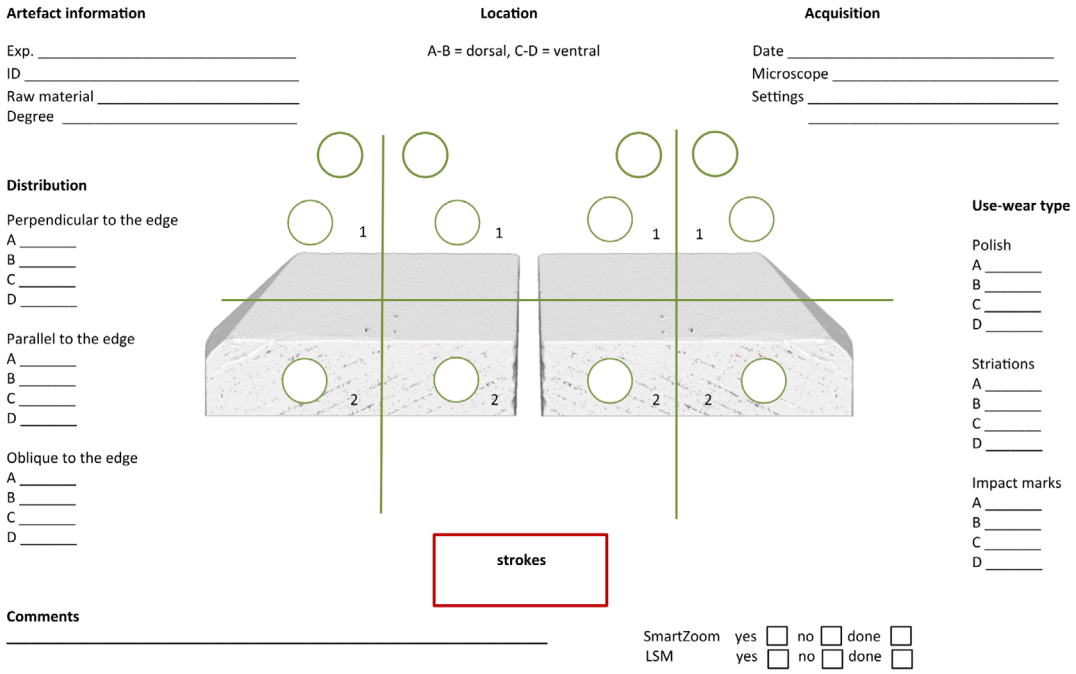

Fig. 40 Scheme used during the qualitative use-wear analysis for the documentation of the analysed standard samples from the experiments. The dorsal surface is indicated by A and B (surface with the angle) and the ventral surfaces by D and C (straight surface). Additionally, the scheme includes information about the analysed standard sample itself, the cycle within the experiment, the acquisition date and settings as well as information about the use-wear traces (location, distribution and type). The scheme also contains information about, whether further acquisition or analysis are needed (SmartZoom = digital microscope images, LSM = quantitative use-wear analysis).

done for the dorsal (A and B) as well as for the ventral (D and C) surface. The areas are numbered from one, as the part of the tool with the edge, to two, the lower part of the tool.

The qualitative use-wear analysis was done in a high-power approach by means of an upright light microscope (ZEISS Axio Scope.A1 MAT). The samples were studied with a 5×, 10× and 20× magnification. Traces were documented as an EDF image in black and white settings. While the eight samples from the »artificial VS. natural« experiment were analysed before and after each cycle, the eight samples from the tool function experiment were only analysed before and after the last cycle with 2000 strokes.

The quantitative use-wear analysis was done on the same total 16 samples, using the laser-scanning confocal microscope (ZEISS Axio Imager.Z2 Vario + ZEISS LSM 800 MAT). The objective C Epiplan-Apochromat 50× with the numerical apertures 0.95 was generally used. In a few cases, the C Epiplan 50× /0.75 had to be used. The field of view (FOV) was 255.6 × 255.6 µm. For the quantitative analysis, measurements were taken on samples only from before and after 2000 strokes, in the case of the tool function experiment only after 2000 strokes. On each sample, one use-wear spot was measured three times at a nearby but non-identical point. Only on two samples, a second use-wear spot was measured as well. In total, 28 measurements were taken on the experimental sample times three. Since the qualitative as well as the quantitative use-wear analysis was done after the experiments were finished, the measurements were taken from the moulds. Exceptions are the samples after 2000 strokes from the tool function experiment. In these cases, the original surface not the replicated mould's surface were measured.

The reason for doing the use-wear analysis on the experimental samples was firstly to see what kind of use-wear develops within the sequential and automated experiments and also to see how the use-wear created differs depending on the contact material used. The second important aspect was to observe how use-wear develops in general and also under the application of the two tested raw materials. Therefore,

each time it was important to measure the exact same spot before and after the experiments. This was possible due to the coordinate system on the samples. The use of the coordinate system should guarantee that a possible measured variability in the surfaces topography is only due to a surface alteration and not because of a positional inaccuracy. The LSM has an integrated module called Shuttle-and-Find (Calandra et al. 2019a). This module allows the relocating of a sample based on a defined coordinate system. Prior to a measurement, the coordinate system needed to be created and calibrated for each sample with the C Epiplan-Apochromat 10× /0.40. Firstly, the surface of the sample after 2000 strokes was analysed. This way, the spot with the use-wear trace could be defined and measured. Afterwards, the sample was exchanged with the corresponding sample from before the experiment. Based on the previously calibrated coordinate system, the software could automatically relocate the same spot on the surface with a horizontal positional repeatability of approximately 14 % of the FOV.
The acquired data was processed identically to the data form the quantitative use-wear analysis of the archaeological material (see chapter Quantitative use-wear analysis). The data of the two experiments was individually processed with templates in ConfoMap (a derivative of MountainsMap Imaging Topography developed by Digital Surf, Besançon, France; version ST 8.1.9286). The maximum of two templates had to be applied. The first template, the »resampling template«, was used to perform a resampling in x and y on all 108 surfaces, leading to an identical spacing. In the second and final template, that data was processed (»processing template«). The following procedure was performed: I.) Levelling (least squares method by subtraction), II.) From removal (polynomial of degree3), III.) Outliers removal (maximum slope of 80°), IV.) Thresholding the surface between 0.1 and 99.9 % material ratio to remove the aberrant positive and negative spikes, V.) Applying a robust Gaussian low-pass S-filter (S_1 nesting index = 0.425 µm, corresponding to about five pixels, end effects managed) to remove noise, VI.) Filling-in the non-measured points (NMP), VII.) Analysis: Calculation of 21 ISO 25178-2 parameters, three furrow parameters, three texture direction parameters, one texture isotropy parameter and the SSFA parameters *epLsar, Asfc, Smfc, HAsfc9 and HAsfc81*. The ConfoMap templates for both experiments in MNT and PDF formats are available on GitHub, including all original and processed surfaces, as well as the results.
Again, the open-source software R (version 4.0.2 through RStudio version 1.3.1073, RStudio Inc., Boston, USA) was used to perform all descriptive analyses. This includes the summary statistics, the scatter plots and PCA's. As packages openxlsx v. 4.1.5, R.utils v. 2.9.2, doBy v. 4.6.7, ggsci v. 2.9, patchwork v. 1.0.1, ggplot2 v. 3.3.2, tidyverse v. 1.3.0, wesanderson v. 0.3.6 were used. Reports of the analysis in HTLM format, created with knitr v. 1.29 and rmarkdown v. 2.3 are available on GitHub [https://github.com/lschunk/artificial_VS_natural-experiment; https://github.com/lschunk/tool_function-experiment]. Also the raw data, the scripts and the RStudio project are saved in the same repository.

Analysis sensor data

The sensor data recorded throughout the experiments with the SMARTTESTER® can be analysed. Three of the five sensors were predetermined factors: velocity, acceleration and force. This means, the sensors have to be seen as a controlling mechanism. The analysis of these sensor data shows how controlled the experiments were in the sense of permanently repeating actions. The other two sensors recorded the penetration depth in mm and the friction in N. While the friction is a topic for itself and goes into the direction of physics and mechanics and was therefore excluded from further analysis, the penetration depth was analysed. The penetration depth is of interest because it directly relates to aspects of tool efficiency and performance. During the experiment, the sensor data is saved per strokes and per sensor individually as TXT files.

By means of R (version 4.0.2 through RStudio version 1.3.1073, RStudio Inc., Boston, USA) the data from the »artificial VS. natural« experiment as well as the data from the tool function experiment was combined in one data frame respectively and exported as a XLSX file. The data was then statistically analysed and plotted. The following packages were used openxlsx v. 4.1.5, R.utils v. 2.9.2, doBy v. 4.6.7, ggrepel v. 0.8.2, patchwork v. 1.0.1, ggplot2 v. 3.3.2, tidyverse v. 1.3.0 were used. Reports of the analysis created with knitr v. 1.29 and rmarkdown v. 2.3 in HTLM format are available on GitHub [https://github.com/lschunk/Smarttester-data.git]. In the same repository the data, the scripts and the RStudio project can be found.

RESULTS

Within this chapter, the collected data resulting from applying the aforementioned methods and techniques is presented. First, the results from the raw material characterisation are addressed, followed by the results from the techno-typological analysis. For the techno-typological analysis, the data from the three archaeological sites are not separated but instead, addressed sequentially within each artefact category. This allows for direct inter-comparability of the artefacts. The results from the Upper site of Buhlen are always mentioned first, then the ones from Balver Höhle and at lastly the data concerning Ramioul. Within this structure, the results concerning the two artefact categories, *Keilmesser* and *Prądnik scraper* are addressed sequentially. *Prądnik spalls* as a third artefact category, are separately treated and thus mentioned after the data regarding *Keilmesser* and *Prądnik scrapers*. After this subchapter, the results regarding the quantification of the edge design, the use-wear analysis and the controlled experiments are mentioned. Scrapers and flakes – as outgroup – are not addressed in all chapters. The results concerning the scrapers and flakes are only of relevance in the chapters Quantification of edge design and Use-wear analysis.
For the analyses, in total n = 330 *Keilmesser* were studied (**tabs 3. 5. 7**). The selected assemblage from Buhlen yielded n = 130 *Keilmesser*, Balve n = 191 and n = 9 artefacts are from Ramioul. Not all of the *Keilmesser* are complete artefacts. Some of these pieces can be described as distal *Keilmesser* tips, some as fragmented or semi-finished tools. Whenever only complete *Keilmesser* have been involved in an analysis, it is mentioned within the text. *Prądnik scrapers* were analysed identically to *Keilmesser.* For the analyses, n = 54 *Prądnik scrapers* were studied in total. This assemblage is composed of n = 24 *Prądnik scrapers* from Buhlen, n = 27 from Balver Höhle and n = 3 from Ramioul. These n = 54 *Prądnik scrapers* are without exception complete tools.

RAW MATERIAL CHARACTERISATION

The sampled *Keilmesser* from Buhlen are with a clear majority (n = 128; 98.5 %) made of black silicified schist (**tab. 2**). The silicified schist appears locally within the wider region in Pleistocene terraces and immediately next to the site in and near the small riverbed. One artefact is made of a more greenish, less dark silicified schist. The only other raw materials from the studied Buhlen assemblage are items made of Baltic flint (n = 1 piece) and reddish yellow carnelian (n = 1 piece).
A similar picture as in Buhlen is becoming evident for Balve (**tab. 2**). The significant majority with 95.3 % (n = 182) of the *Keilmesser* was produced from the local silicified schist. Analogues to Buhlen, the silicified schist can be found in the small river stream next to the site. A few pieces (n = 10) are made of Baltic flint. The nearest source for flint is approximately a distance of 20 km to the north of the cave (Andree 1928; Günther 1988). The silicified schist within the Balve assemblage is not always as dark black as in Buhlen and tends to be more often light-black, greyish or green greyish.
The distribution of the raw material in Ramioul is different though (**tab. 2**). The sampled artefacts are mainly made of a local light-coloured flint. With n = 18 pieces this counts for 90.0 % of the assemblage. The other two artefacts are made of black silicified schist. The silicified schist, too, can be found in the local surroundings of the cave site.

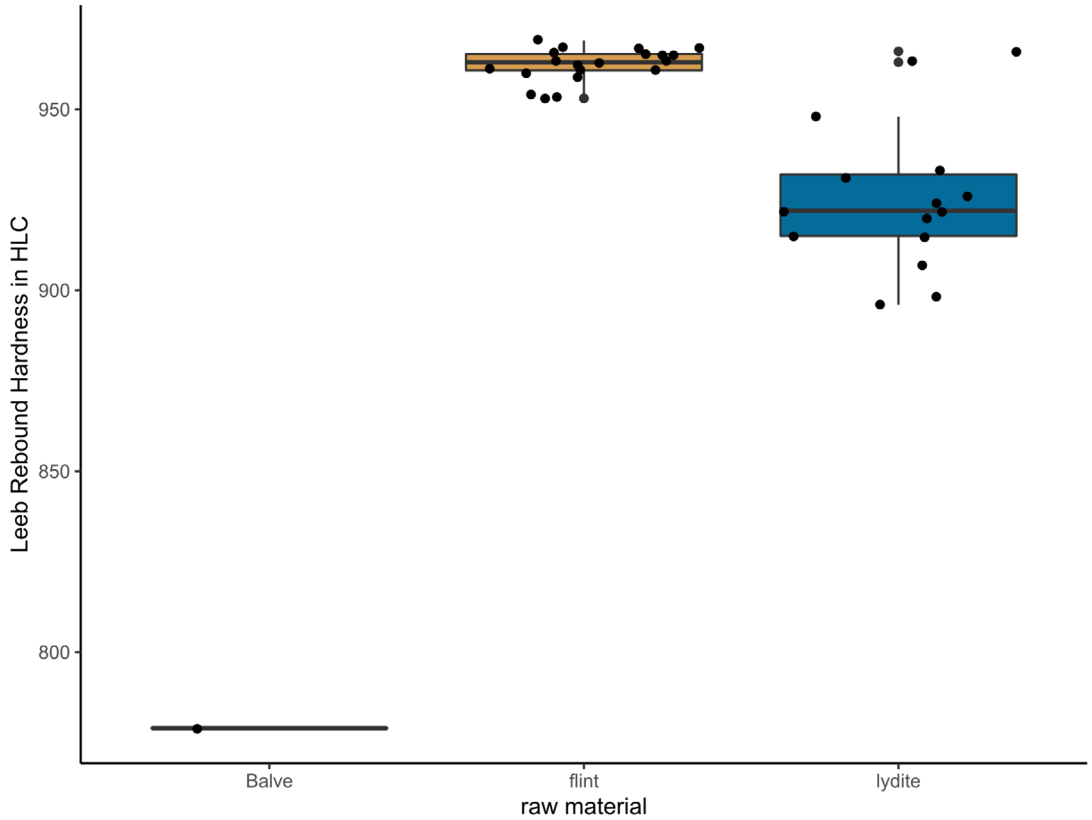

Fig. 41 Leeb Rebound Hardness in HLC measured for the two raw materials flint and lydite (samples initial experiment) and for the semi-finished tool from Balve (ID MU-278).

The *Keilmesser* from the three archaeological sites taken together result in a clear picture regarding the raw material. Nearly 94.2 % (n = 311) of the studied *Keilmesser* are silicified schist artefacts, 5.5 % (n = 18) are made of flint. The other one piece is made of carnelian.

A similar situation as described for the *Keilmesser* is documented for the *Prądnik scrapers*. The sampled *Prądnik scraper* assemblage (n = 24) from Buhlen consists without exception of tools made of black silicified schist.

In Balve, the situation is identical. All n = 27 *Prądnik scrapers* are made of silicified schist.

None of the n = 3 *Prądnik scrapers* from Ramioul is a silicified schist tool. They all are made of flint.

To summarise, 94.4 % (n = 51) of the *Prądnik scraper* assemblage from the three sites consists of tools made of silicified schist (**tab. 2**).

The properties of the two raw materials involved in the study – silicified schist (lydite) and flint – were measured. Surface roughness as well as hardness were considered for the material properties. To start, the hardness was measured with the Leeb rebound hardness tester (Proceq Equotip 550, Leeb C probe). The dataset can be found on GitHub [https://github.com/lschunk/Leeb_hardness]. As explained in the previous chapter, only one silicified schist artefact of the three assemblages fulfilled the necessary requirements to perform the hardness test. The measurements taken on this semi-finished tool from Balve (MU-278) resulted in a mean value of 779 HLC (**fig. 41**).

The same hardness test was applied for the standard samples later used in the experiments (Initial experiment and tool function experiment). Calculating properties such as the raw material hardness allows for a better understanding and also a prediction of aspects such as tool efficiency and durability (Key/Lycett 2017; Key/Fisch/Eren 2018; Key/Pargeter/Schmidt 2020; Key/Proffit/de la Torre 2020). The standard sam-

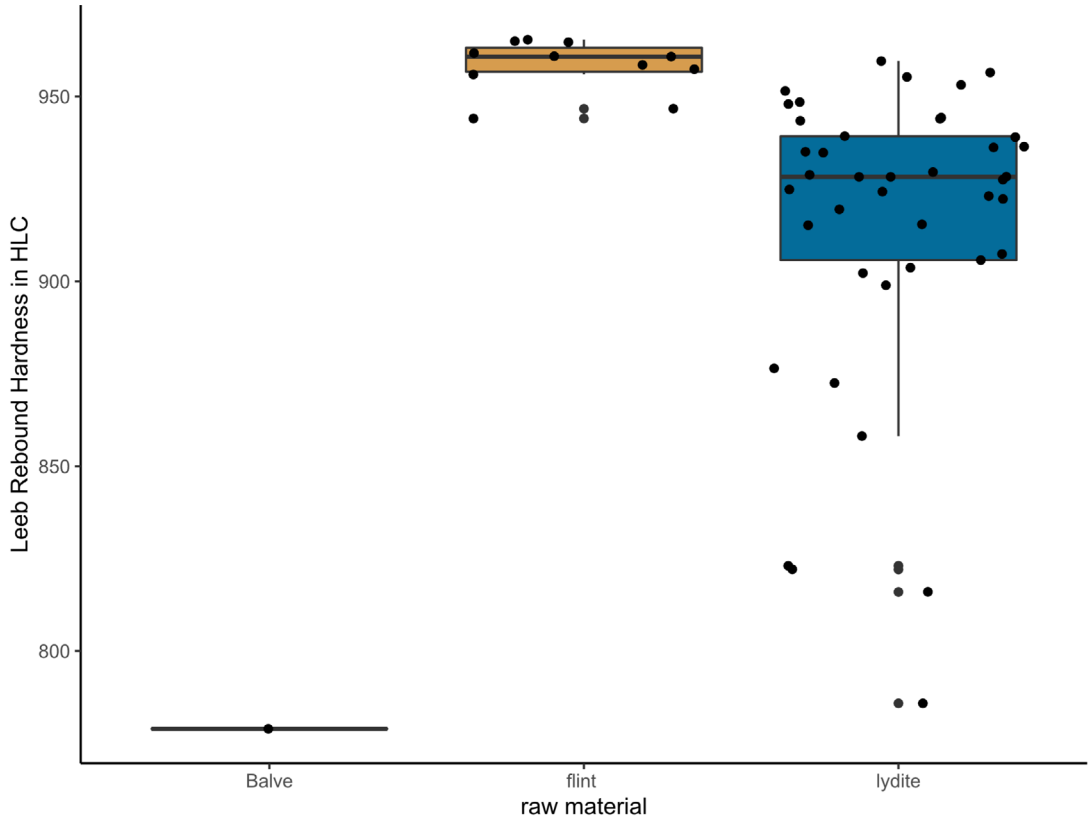

Fig. 42 Leeb Rebound Hardness in HLC measured for the two raw materials flint and lydite (samples tool function experiment) and for the semi-finished tool from Balve (ID MU-278).

ples, prepared for the experiment, are made of silicified schist and Baltic flint. The silicified schist was collected near the two sites Buhlen and Balver Höhle. These samples do have, since cut with the band saw, flat surfaces. Thus, the standard samples were perfectly suitable for the hardness measurement with the Leeb rebound tester. Neither the semi-finished *Keilmesser* from Balve nor the experimental standard samples fulfilled the size requirements. This could be compensated with some additional coupling paste, which connects the sample with the supporting base. Ten measurements per sample were taken in order to average the internal variance per sample. In total, n = 31 flint and n = 56 lydite standard samples were measured (for the experimental data lydite is here used as synonym to silicified schist). Not all of them were used in the experiments later. The measurements were mainly taken in order to get an idea, how similar or different the hardness of these two raw materials is. The Leeb rebound hardness test provides the answer for that (**fig. 42**). Based on the in total n = 87 tested samples, it is possible to say that flint has a higher HLC value than the tested silicified schist does. The arithmetic mean for the flint is 960.8 HLC while the one from silicified schist is 917.9 HLC. The hardness measurements do not only result in a value for the hardness, but they also illustrate another important aspect. The flint hardness ranges from 944.1 HLC to 969.0 HLC. However, the range for the lydite is from minimum 785.9 HLC to maximum 966.0 HLC. The variance for silicified schist is considerably higher compared to the flint. Likely, the reason for that can be seen in the schistosity planes or the banding of the lydite. Lydite is a finely layered, brittle sedimentary rock that fractures conchoidally. The raw material is also characterised by small cracks. By applying the Leeb rebound hardness test, an impact body, a small ball, is driven with a defined energy against the surface of the sample. The velocity of the impact body before and after the impact gets measured. Based on these measurements, the ratio between the impact velocity and rebound velocity defines the Leeb hardness (HL, here HLC). Whenever the

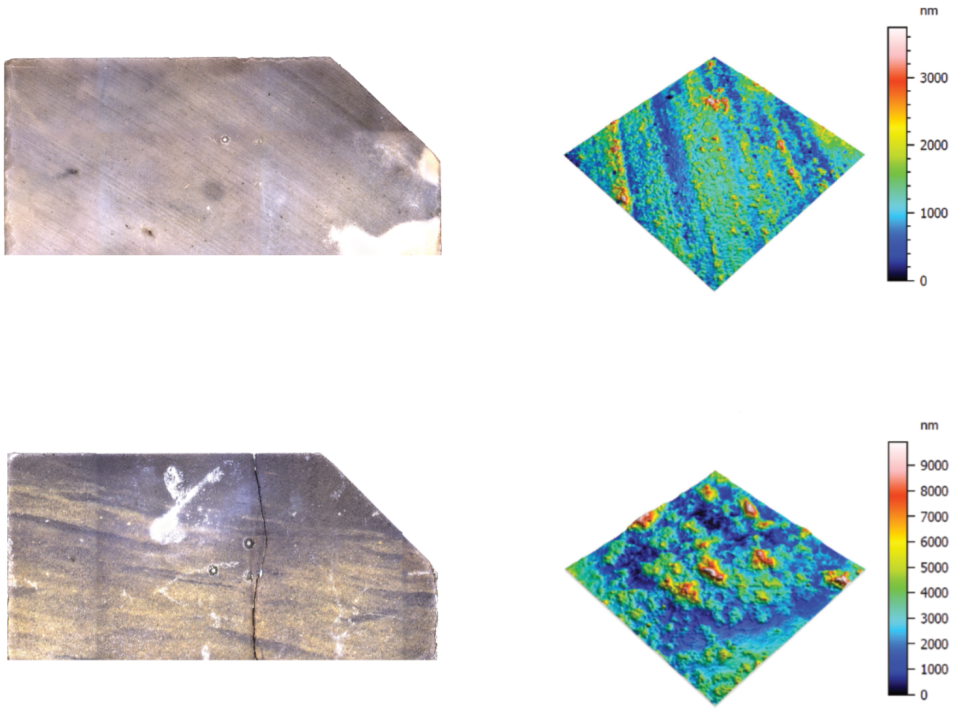

Fig. 43 Surface of unused standard samples for experimental approaches (left) and confocal micro-surface texture (right). The colour of the surfaces corresponds to the height on the z-axis. The upper row shows a flint sample, the lower row a lydite sample.

impact boy hits a less compact area of the surface (e. g. a crack underneath the surface), rebound energy gets lost and the Leeb hardness value will be smaller. This might be frequently the case for the silicified schist. Depending on the quality of the silicified schist, the Leeb hardness measurement will result in a lower or higher value per sample. When considering the range of the measured Leeb hardness of the lydite, the minimum values are comparable to the Leeb hardness of the semi-finished *Keilmesser* from Balve. The artefact has a Leeb hardness of 779 HLC and is thus similar to the lowest Leeb hardness value of 785.9 HLC from one of the standard samples.

As a second raw material property, the surface roughness was included in the raw material characterisation. Surface roughness can be measured with a confocal laser scanning microscope (for details see chapter Quantitative use-wear analysis). Unfortunately, the surface roughness of the archaeological samples were not considered during the data acquisition and thus not measured. Instead, measurements were taken on standard samples before they were used in the experiment (»artificial VS natural« experiment) (**fig. 43**). Surface roughness is a component of the surface texture and describes the unevenness of a surface height. Based on directional deviations from the surfaces, the surface roughness can be quantified. A large deviation stands therefore for rough surfaces while a small deviation is equal to smooth surfaces. In order to address the surface roughness of the measured standard sample here, *Sq*, the root mean square height, as one of the seven existing areal field parameters was chosen (for more information see Digital Surf, Besançon, France). Areal field parameters, especially *Sq*, are known to give more significant values. The results were calculated following the ISO 25178. The surface roughness was measured for n = 4 lydite as well as n = 4 flint standard samples. The arithmetic mean for the lydite samples is 22.392 µm while the one for the flint samples is 12.206 µm. Based on these values, flint surfaces are quantified as less rough than the lydite surface. It has to be pointed out that the measurements were taken on the standard samples, which are cut with a band saw (see chapter Controlled experiments). The traces from the band saw are macroscopically clearly visible on the sample surface. These traces surely affect the surface roughness. Unfortunately, there

is no reference collection or any comparable measurements taken on machine cut samples yet. Single comparable values measured on flint can be found in literature (Evans et al. 2014; Calandra et al. 2019c). These specific flint samples are knapped flakes and measured under similar (Evans et al. 2014) or even identical (Calandra et al. 2019c) settings than the standard samples within this project. The analysis for these flint samples was also done according to the ISO 25178. The measurements taken by Evans et al. lead to *Sq* values between 0.64 µm and 0.98 µm. The *Sq* values for other flint sample (Calandra et al. 2019c, supplementary table S3) ranges between 0.824 µm and 1.912 µm. Thus, these values are significantly lower than the values calculated on cut standard samples.
Additionally, the variance in the results from the standard samples has to be pointed out. While the measurements taken on the lydite samples ranging from 16.468 µm to 26.081 µm, the range is considerably bigger for the flint measurements. The minimum value for flint is 4.136 µm and the maximum is 28.733 µm. Without further measurements or a reliable reference collection, the variability within the calculated surface roughness values cannot be explained.
In general, although parameters such as the surface roughness are highly relevant, especially in the context of use-wear analysis and experimental design, they are not much explored yet in archaeology. The results presented here might indicate that lydite, even when both raw materials are cut identically with a band saw, has a higher surface roughness than flint. However, the existing information about the surface's roughness of the raw materials lydite and flint are not sufficient for further conclusions.

TECHNO-TYPOLOGICAL ANALYSIS

As mentioned above, the presentation of the results from the techno-typological analysis consider first the results from the *Keilmesser*, followed by the results from the *Prądnik scrapers*. In a later step, the focus is on the results gained from analysing the *Prądnik spalls*.

Blanks and cortex

In this part of the analysis, the distinction was made whether an artefact displays a core tool or not. This aspect is relevant to *Keilmesser* and *Prądnik scrapers*. Another interesting aspect in this context is the amount of cortex on the tool's surface, since it can provide some indications to which degree the blank was modified.
In Buhlen, 67.0 % (n = 87) of the *Keilmesser* could be defined as core tools (**fig. 44**). With 6.2 % (n = 8) only, flakes have been transformed into *Keilmesser* considerably less frequently. In 26.9 % (n = 35) of the artefacts the blank could not be determined as either core or flake. N = 55 of all *Keilmesser* are not covered with cortex at all. The remaining n = 75 artefacts have cortex. Most of them (n = 61) are core tools. Most of the time, the cortex can be found at the back of the tool (n = 38) or on the base (n = 22). Only in individual cases, the cortex is located in the proximal (n = 4) or medial (n = 9) tool area. The percentage of cortex measured on the complete tool surface is most often limited to less 25 % (n = 43). In one third (n = 25) of the tools with cortex, the percentage of cortex reaches up to 50 %.
In Balve, the majority of the tools, 71.2 %, were also manufactured as core tools with n = 136 artefacts (**fig. 45**). A comparable small number of *Keilmesser*, as in Buhlen, was produced on flakes (4.7 %, n = 9). The blank type was undeterminable in 24.1 % (n = 46) cases. The question, whether the *Keilmesser* from

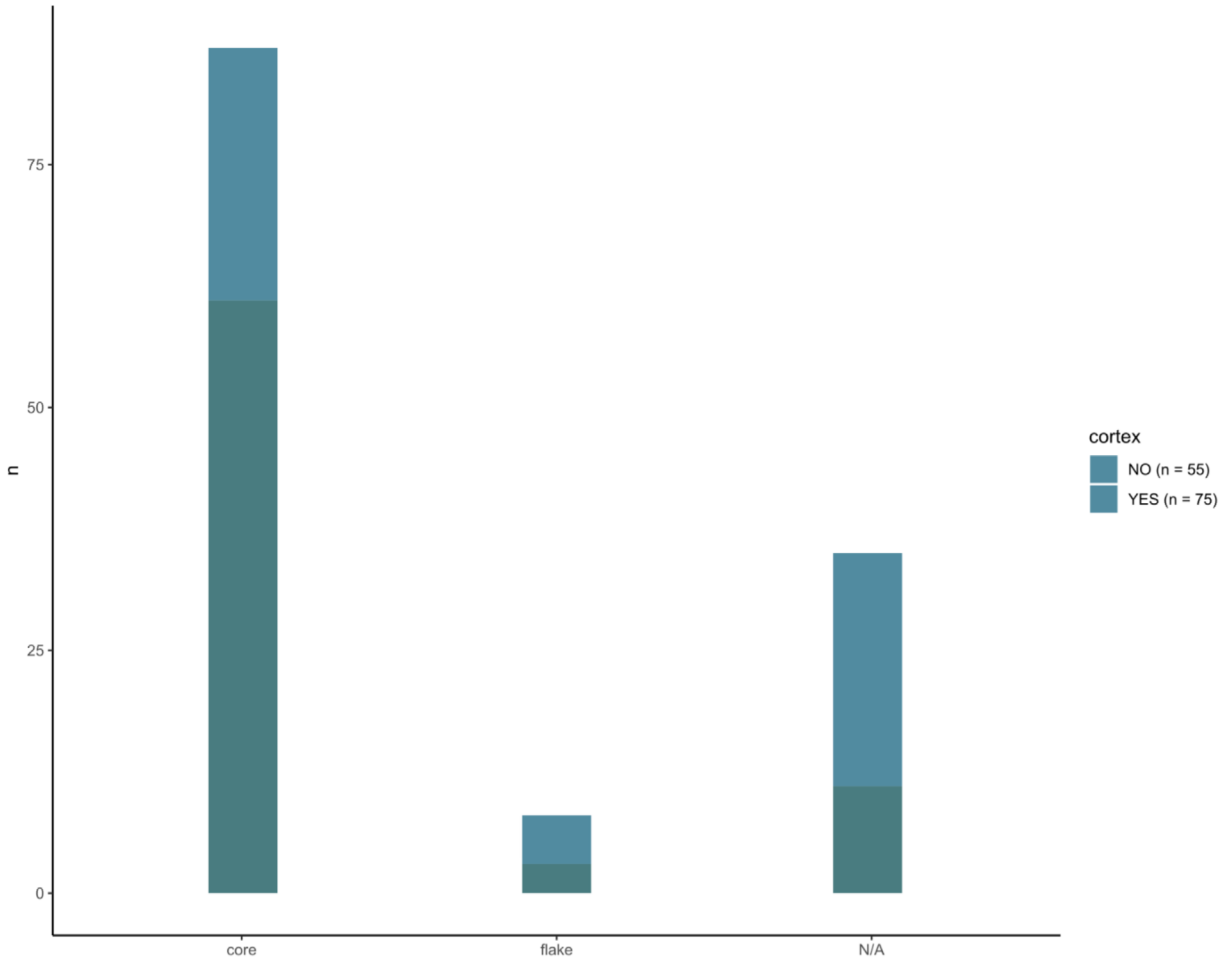

Fig. 44 Blank selection for the production of *Keilmesser* (n = 130) from Buhlen. Additionally, the figure includes the information whether an artefacts displays cortex or not.

the assemblage in Balve are covered with cortex or not, cannot be answered to full extent. One part of the assemblage was a short time loan from the LWL-Museum for Archaeology in Herne. When the material was studied a few years ago, this aspect was not part of the attribute analysis. Therefore, n = 35 *Keilmesser* need to be excluded. From the remaining n = 156 artefacts, n = 33 display no cortex. On the contrary, for n = 123 *Keilmesser*, cortex could be documented. Similar as in Buhlen, the cortex is by a majority (n = 95) located along the back of the tools. N = 6 pieces also show cortex on the tool base or in generally in the proximal area of the tool (n = 1). Cortex could be also documented in the medial (n = 14) or distal (n = 4) tool parts. N = 3 artefacts have cortex covering nearly the entire tool surface (except the active edge) with up to 75 % cortex. One of these three artefacts is a semi-finished tool. For the other tools with cortex, the same as in Buhlen counts. The percentage of cortex most commonly (n = 67) reaches up to 25 % of the surface. On n = 23 pieces, the amount of cortex is higher, but also limited to maximum 50 %.

Despite the small assemblage, the *Keilmesser* from Ramioul manufactured on cores also predominate the assemblage (**fig. 46**). 44.4 % (n = 4) are core tools, one artefact was made from a flake and again, 44.4 % (n = 4) could not be determined. All *Keilmesser*, except the one made from a flake, show cortex. The cortex is mostly located on the back (n = 7) and n = 1 artefacts has cortex on the proximal area of the dorsal tool surface. The percentage of cortex on the surface is comparable with the results from Buhlen and Balver Höhle. On only n = 2 *Keilmesser* up to 50 % of cortex could be documented. The other n = 6 artefacts display lower cortex percentages with maximum 25 %.

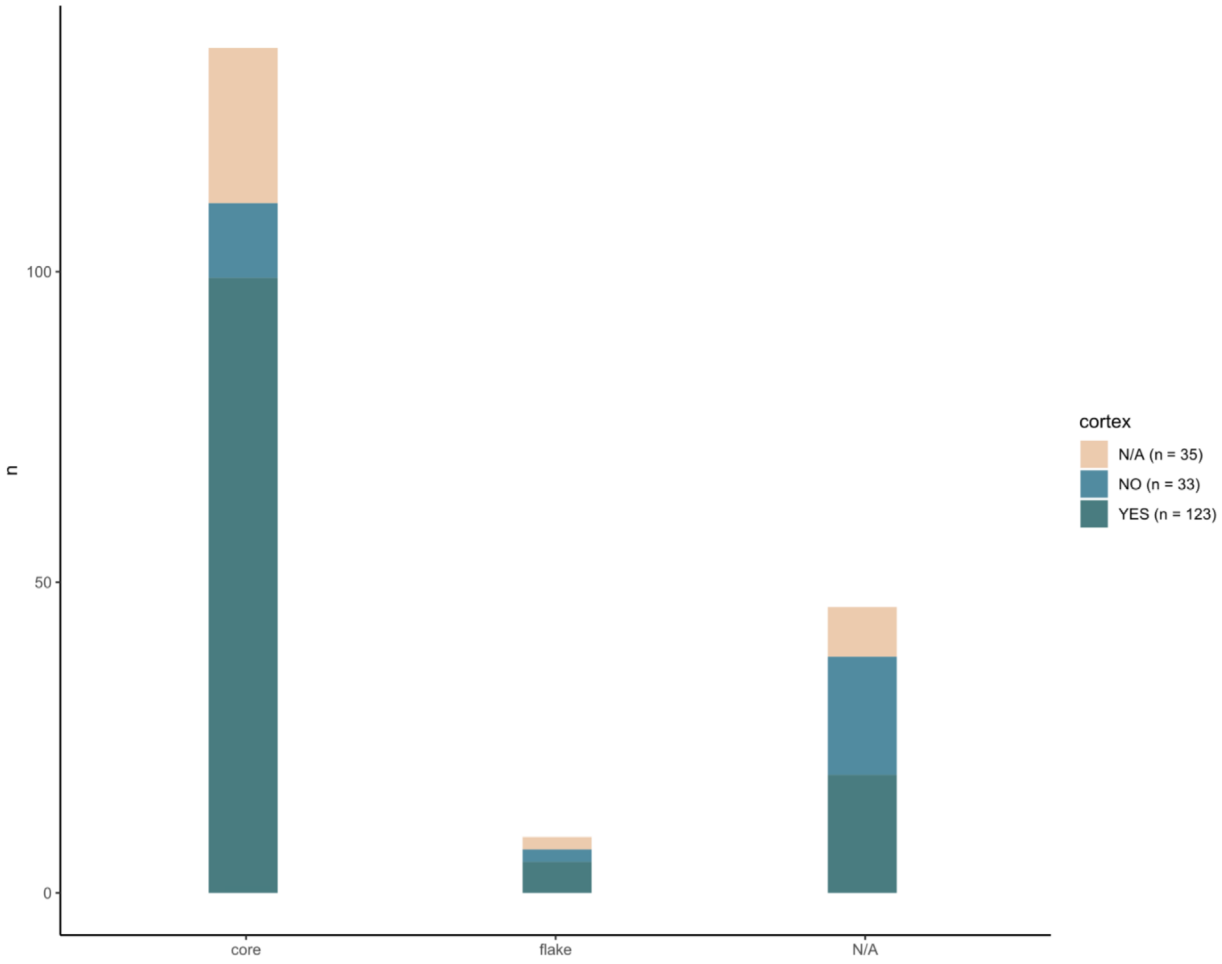

Fig. 45 Blank selection for the production of *Keilmesser* (n = 191) from Balver Höhle. Additionally, the figure includes the information whether an artefacts displays cortex or not. For some artefacts, this analysis was not done. Thus, these artefacts are labelled as N/A.

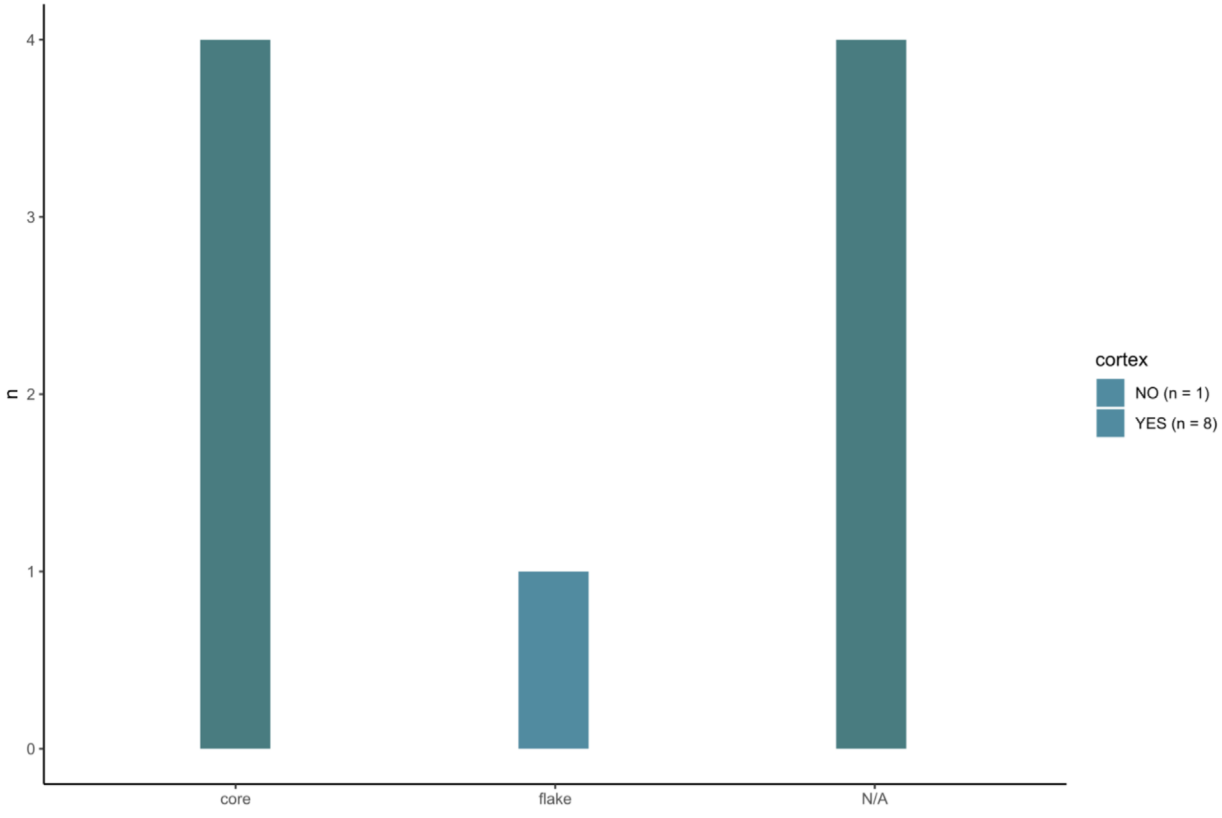

Fig. 46 Blank selection for the production of *Keilmesser* (n = 9) from Ramioul. Additionally, the figure includes the information whether an artefacts displays cortex or not.

These results combined for the three sites together illustrate a clear picture (**fig. 47**). The *Keilmesser* from these assemblages are by a majority of 68.8 % (n = 227) core tools. For only a small amount of 5.5 % (n = 18) a flake was used as a blank. For roughly a quarter (n = 85) of the tools the blank type could not be determined for sure.
Additionally, on the majority (69.8 %, n = 206) of the *Keilmesser,* cortex could be documented, covering up to 25 % of the surface (56.3 %, n = 116). Most often, the cortex was located on the back (68.0 %, n = 140) of the tools.
None of the *Prądnik scrapers* from the studied assemblages can be defined for sure as a core tool. In contrary, all *Prądnik scrapers* from Buhlen are clearly tools produced on a flake. The analysis for the quantity and location of cortex on the tool surfaces was done for the *Prądnik scrapers* as well. The results are contrasting to the ones from the *Keilmesser* though. However, considering the blanks chosen to produce the tools, the results are consistent. In Buhlen 79, 2 % (n = 19) of the *Prądnik scraper* do not show any cortex. The only n = 5 artefacts with cortex display up to 25 % cortex along the back (n = 4) or on the base (n = 1).
Also in Balve, n = 21 (77.8 %) artefacts could be documented as such. In the remaining n = 6 cases, the blank type was undeterminable. Nearly half (n = 13) of the *Prądnik scrapers* from the assemblage in Balve have no cortex. N = 8 artefacts display cortex along the back, n = 2 tools either has cortex in the medial or distal part of the tool. Except for one of these n = 10 *Prądnik scraper* the percentage of cortex per surface was less than 25 %. For n = 4 *Prądnik scraper* this analysis was not conducted.
The results for the *Prądnik scrapers* from Ramioul are equivalent to the ones from Buhlen; all *Prądnik scrapers* are produced from flakes. In Ramioul, no cortex could be documented on the *Prądnik scrapers.*
The results taken together illustrate that 88.9 % (n = 48) of the *Prądnik scrapers* are produced from flakes (**fig. 48**). For the other 10.1 % (n = 6) the blank type is unknown. With only 27.8 % (n = 15) the quantity of tools with cortex is lower than compared to the *Keilmesser*.

Morphometric quantitative analysis

The dimensions to address first are the length, width and thickness measurements. In general, the fragmented *Keilmesser* were omitted in this part of the analysis. The measurements of these tools can be found on GitHub [https://github.com/lschunk/Lithic_analysis_archaeology]. Additionally, the results from the complete *Keilmesser* are separated from the ones from the *Keilmesser* tips.
The complete *Keilmesser* from the here studied assemblage from Buhlen (n = 111) can be classified in a size range from 30.0 mm to 113.5 mm length (**figs 49. 52**). The arithmetic mean of the length is 53.0 mm. Concerning the width, the minimum and maximum are extending between 14.0 mm and 71.9 mm, with an arithmetic mean value of 32.9 mm (**fig. 53**). The thickness is ranging between 7.0 mm and 31.0 mm (**fig. 54**). The arithmetic mean amounts to 16.1 mm.
These measurements considered for the *Keilmesser* tips only, lead to the following picture. As to be expected, the n = 15 *Keilmesser* tips are significantly smaller in terms of the artefact length. The length ranges between 13.0 mm and 46.0 mm. The arithmetic mean is 28.1 mm. The minimum width measurement is 19.0 mm while the maximum is 42.0 mm. The arithmetic mean is similar to the one from the complete *Keilmesser* with 30.0 mm. The thickness is ranging from 8.0 mm to 20.0 mm with an arithmetic mean value of 12.6 mm.
In Balve, the results of the length, width and thickness measurements are based on n = 158 complete *Keilmesser*. The arithmetic mean of the length measurements is 55.5 mm with a minimum length of 29.7 mm and a maximum of 135.6 mm (**figs 50. 52**). With these values, the margin is bigger than in Buhlen, but

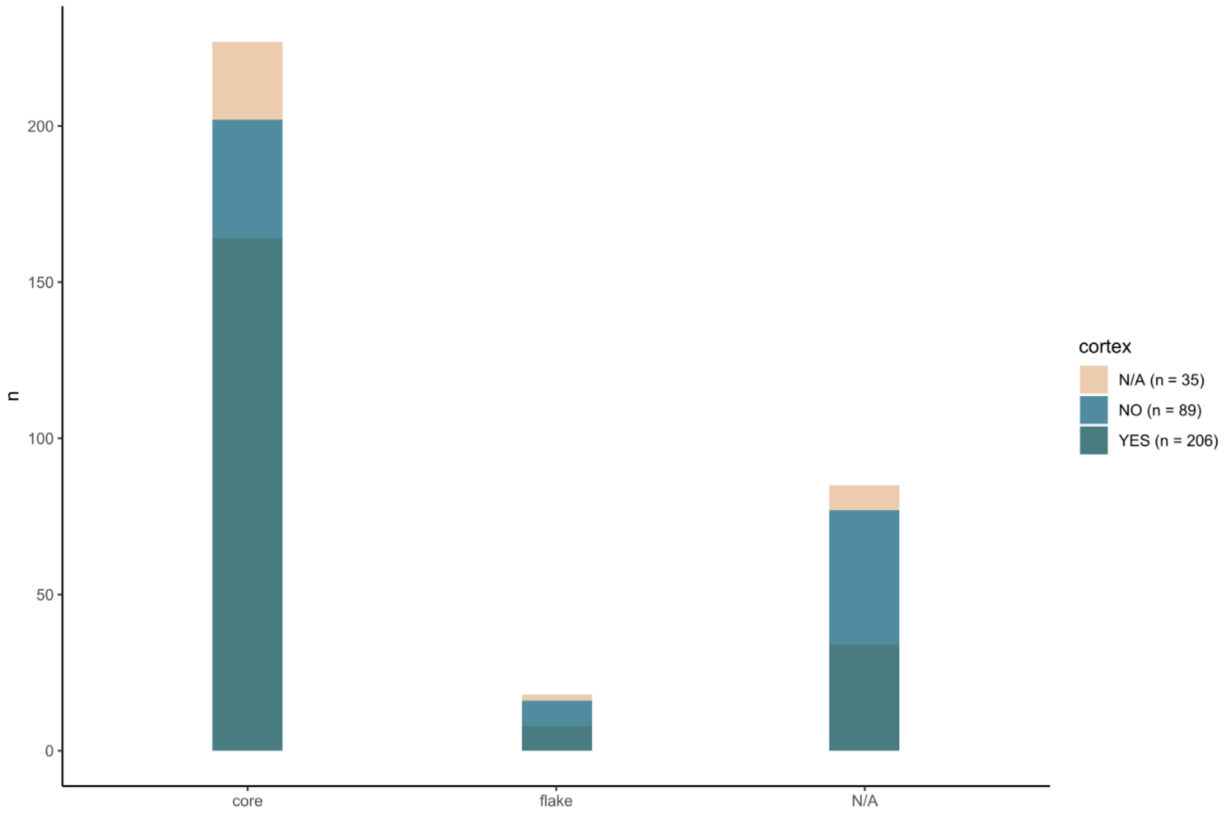

Fig. 47 Blank selection for the production of *Keilmesser* from Buhlen (n = 130), Balver Höhle (n = 191) and Ramioul (n = 9). Additionally, the figure includes the information whether an artefacts displays cortex or not. For some artefacts, this analysis was not done. Thus, these artefacts are labelled as N/A.

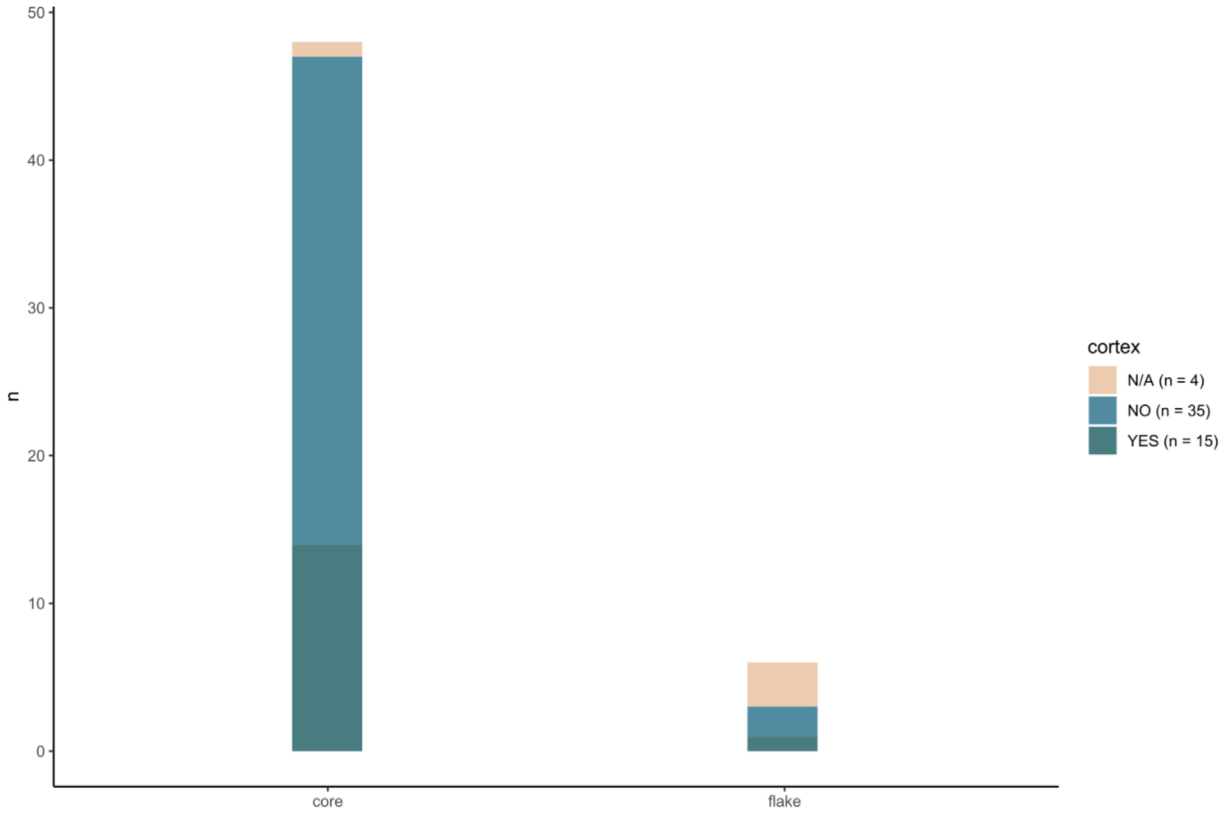

Fig. 48 Blank selection for the production of *Prądnik scraper* from Buhlen (n = 24), Balver Höhle (n = 27) and Ramioul (n = 3). Additionally, the figure includes the information whether an artefacts displays cortex or not. For some artefacts, this analysis was not done. Thus, these artefacts are labelled as N/A.

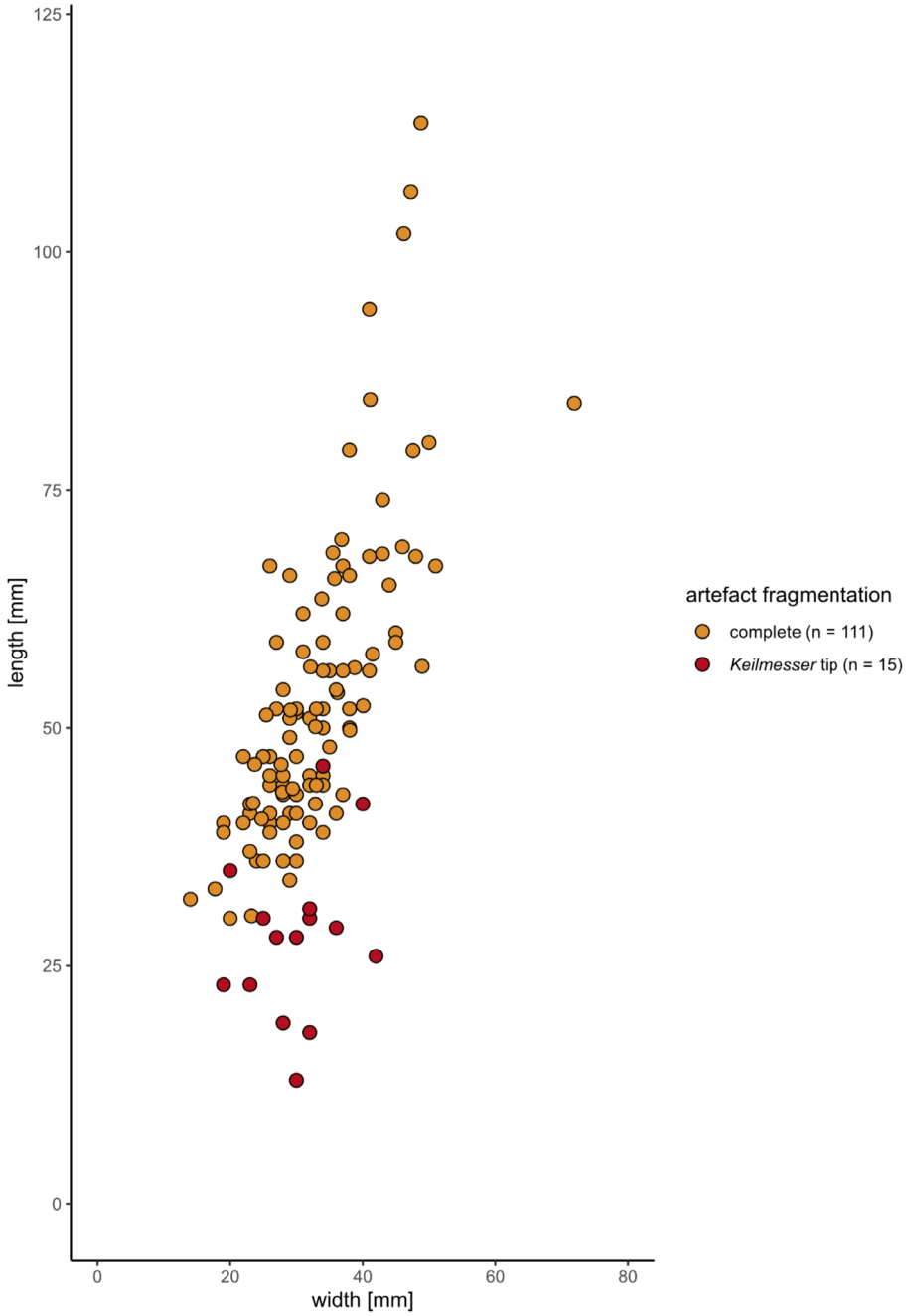

Fig. 49 Length-width ratio of the complete *Keilmesser* (n = 111) and *Keilmesser* tips (n = 15) from Buhlen.

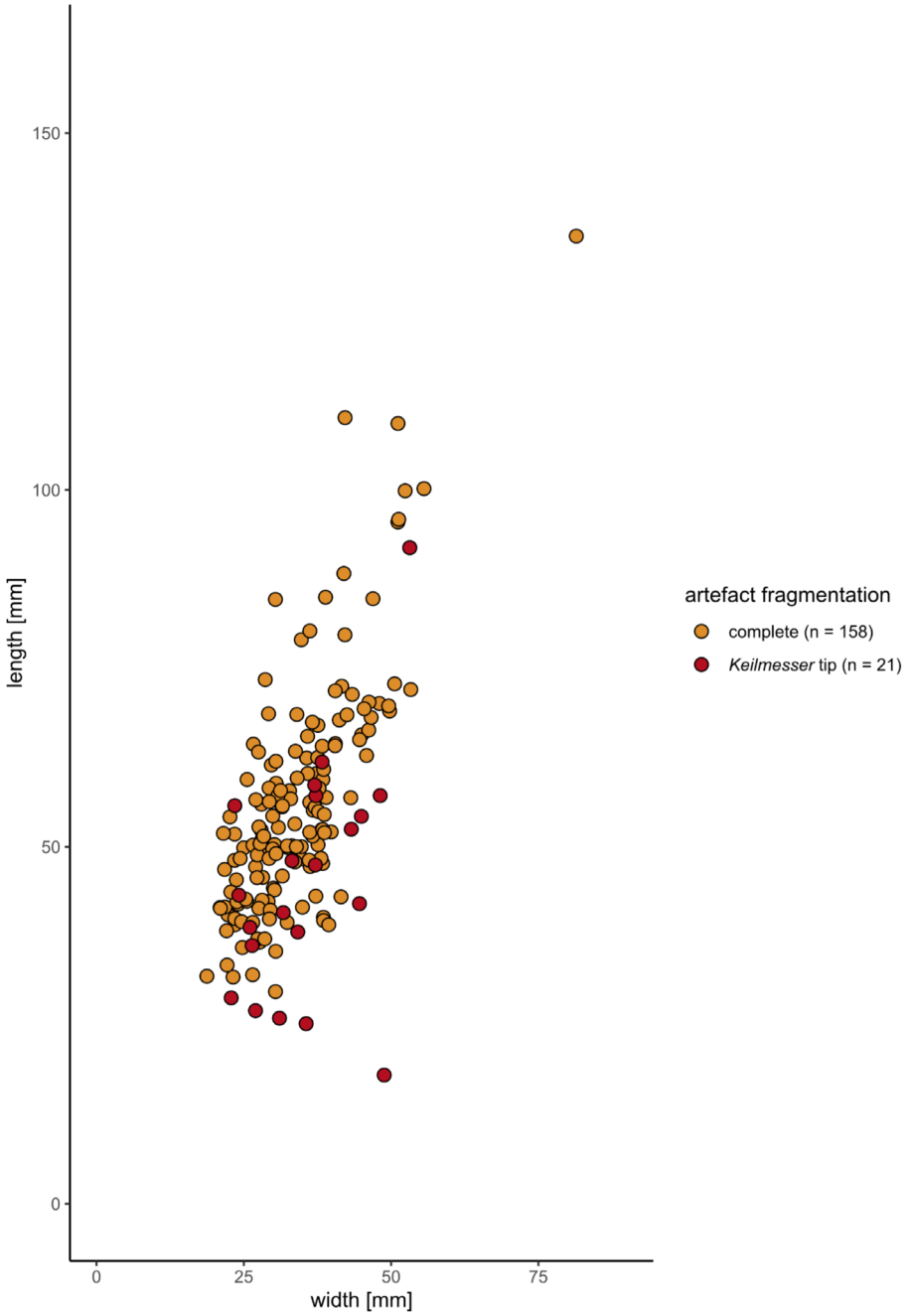

Fig. 50 Length-width ratio of the complete *Keilmesser* (n = 158) and *Keilmesser* tips (n = 21) from Balver Höhle.

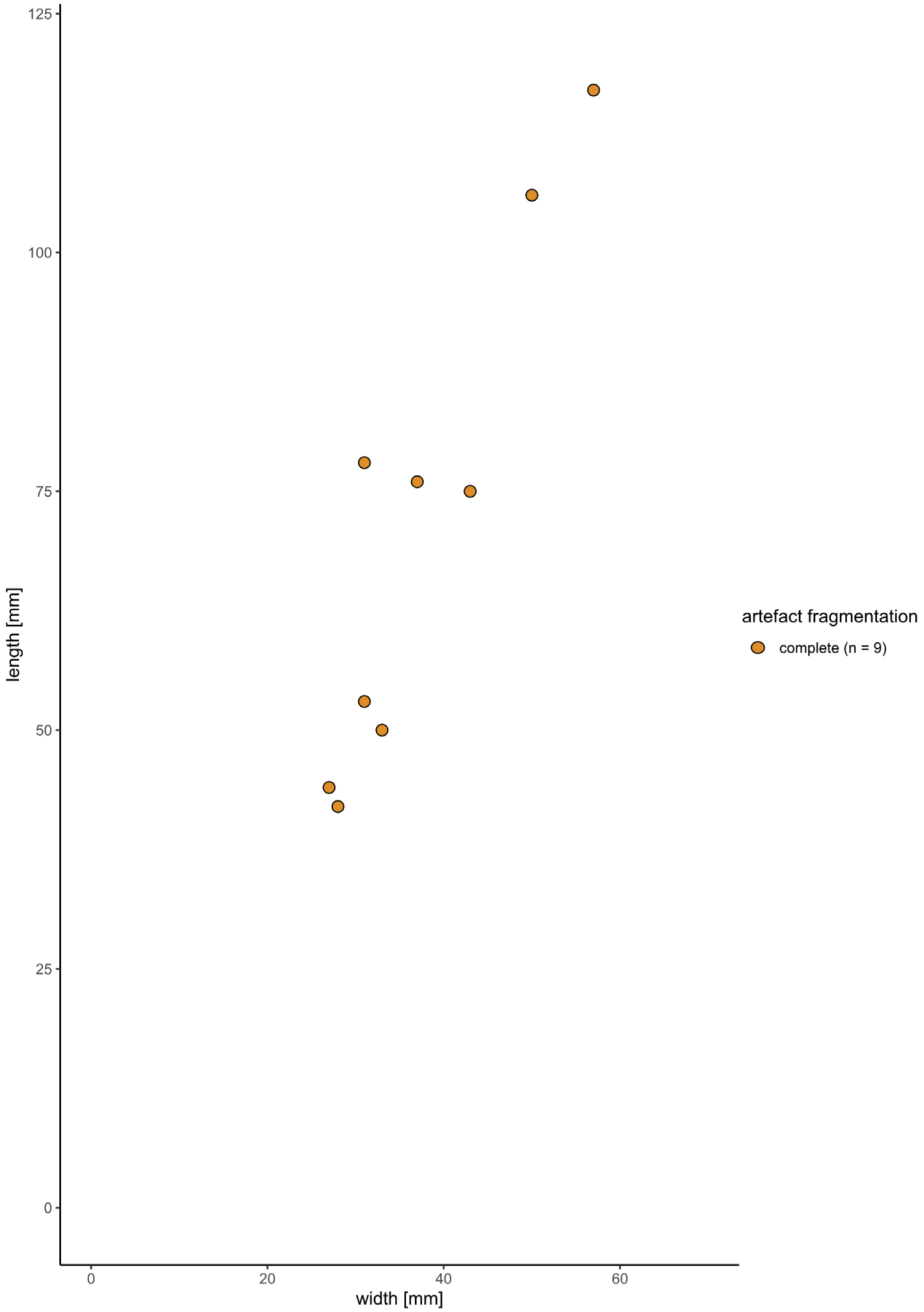

Fig. 51 Length-width ratio of the complete *Keilmesser* (n = 9) from Ramioul.

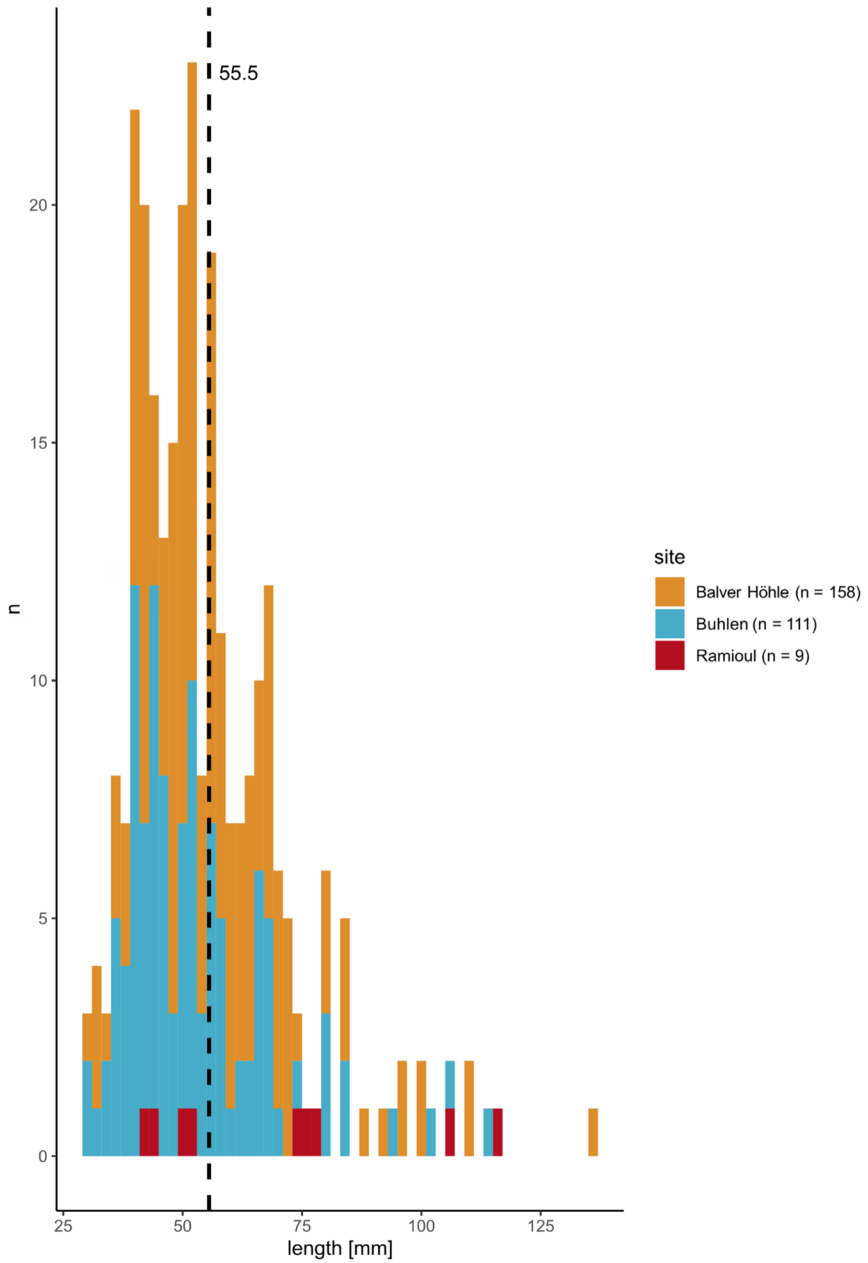

Fig. 52 Maximal length of the complete *Keilmesser* from Buhlen (n = 111), Balver Höhle (n = 158) and Ramioul (n = 9). The dashed line indicates the arithmetic mean value.

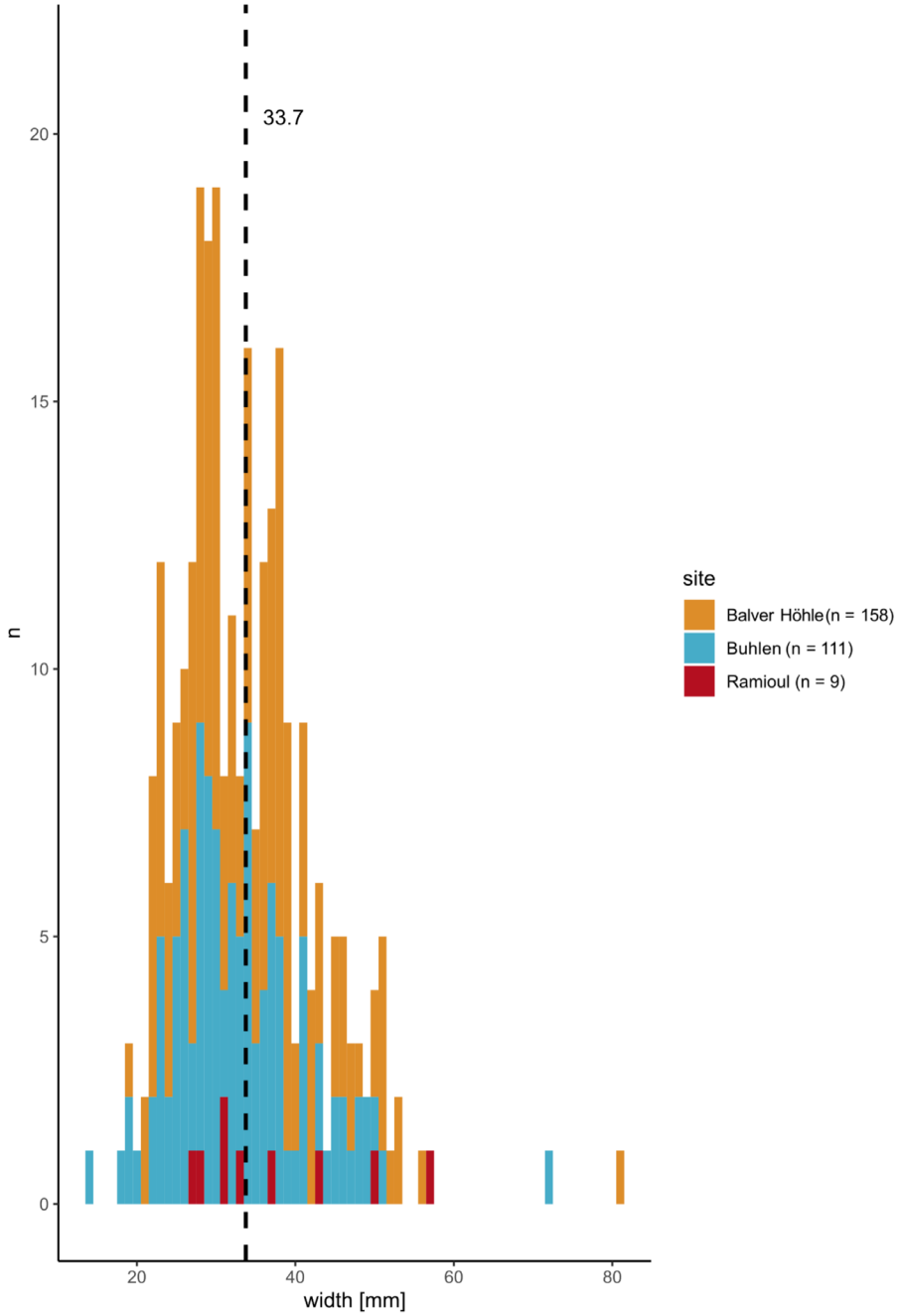

Fig. 53 Maximal width of the *Keilmesser* from Buhlen (n = 158), Balver Höhle (n = 111) and Ramioul (n = 9). The dashed line indicates the arithmetic mean value.

the mean values are comparable. The width is ranging between 18.7 mm and 81.4 mm with an arithmetic mean of 34.1 mm (**fig. 53**). The measured thickness values are similar to the ones from Buhlen (**fig. 54**). The margin is between 7.4 mm and 29.3 mm. The arithmetic mean value is 16.3 mm.

When looking at the *Keilmesser* tips only (n = 21), the measurements result in the following values. The length is ranging from 18.0 mm to 91.0 mm. The arithmetic mean amounts to 45.2 mm. The arithmetic mean value concerning the width is slightly higher than the one for the complete *Keilmesser* with 35.6 mm. The measured minimum value is thereby 22.9 mm and the maximum value 53.9 mm. The thickness margin is between 9.5 mm and 23.6 mm. The arithmetic mean is 15.5 mm.

In the same way as for Buhlen and Balve, the measurements were recorded for the *Keilmesser* from Ramioul. The results deviate not much from the results already mentioned, but since the assemblage from Rami-

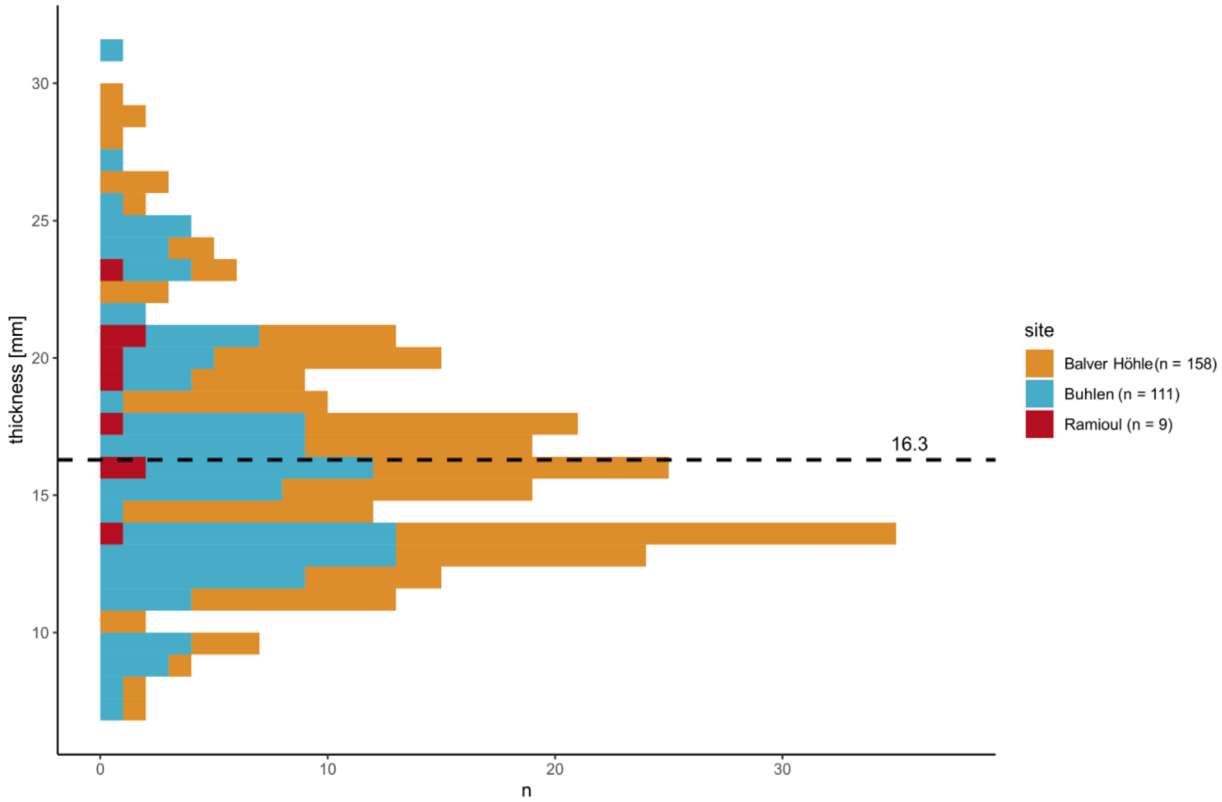

Fig. 54 Maximal thickness of the *Keilmesser* from Buhlen (n = 158), Balver Höhle (n = 111) and Ramioul (n = 9). The dashed line indicates the arithmetic mean value.

oul is significantly smaller (n = 9), the results are of little consequence (**figs 51-52**). The minimum length is 42.0 mm, while the maximum is 117.0 mm. The arithmetic mean can be calculated as 71.2 mm. Concerning the width, the minimum and maximum values extend between 27.0 mm and 57.0 mm, with an arithmetic mean value of 37.4 mm (**fig. 53**). The thickness of the *Keilmesser* ranges between 14.0 mm and 23.0 mm (**fig. 54**). The arithmetic mean is 18.7 mm.

The results from the three sites taken together reveal the following picture. *Keilmesser* (n = 278) extend in their length from 29.7 mm to 135.6 mm (**figs 52. 55**). The arithmetic mean is 55.5 mm. The width measurements ranging from 14.0 mm to 81.4 mm with an arithmetic mean value of 33.7 mm (**fig. 53**). The range for the thickness is between 7.0 mm and 31.0 mm (**fig. 54**). The arithmetic mean is 16.3 mm.

The dimensions – length, width and thickness – were measured for all *Prądnik scrapers.*

In Buhlen, the results of the length measurements are in a range between 27.0 mm and 78.0 mm (**figs 56. 59**). The arithmetic mean of the length is 43.5 mm. The mean value for the width is 28.5 mm with a minimum measurement of 18.0 mm and a maximum of 48.0 mm (**fig. 60**). The thickness of *Prądnik scrapers* is ranging between 4.0 mm and 15.8 mm with an arithmetic mean of 9.2 mm (**fig. 61**).

The *Prądnik scrapers* from Balve can be classified in a size range from 33.4 mm to 75.7 mm length (**figs 57. 59**). The arithmetic mean of the length is 50.5 mm. The width extends from 20.6 mm to 53.3 mm, with an arithmetic mean value of 32.8 mm (**fig. 60**). The thickness is ranging between 1.2 mm and 20.4 mm (**fig. 61**). The arithmetic mean is 13.9 mm.

The margins for the *Prądnik scraper* length from Ramioul are 45.0 mm and 52.0 mm (**figs 58-59**). The arithmetic mean value adds up to 48.3 mm. The minimum and maximum width values extend between 35.0 mm and 37.0 mm, with an arithmetic mean value of 35.7 mm (**fig. 60**). The arithmetic mean of the thickness is 12.0 mm (**fig. 61**). The measurements range from 11. 0 mm to 14.0 mm.

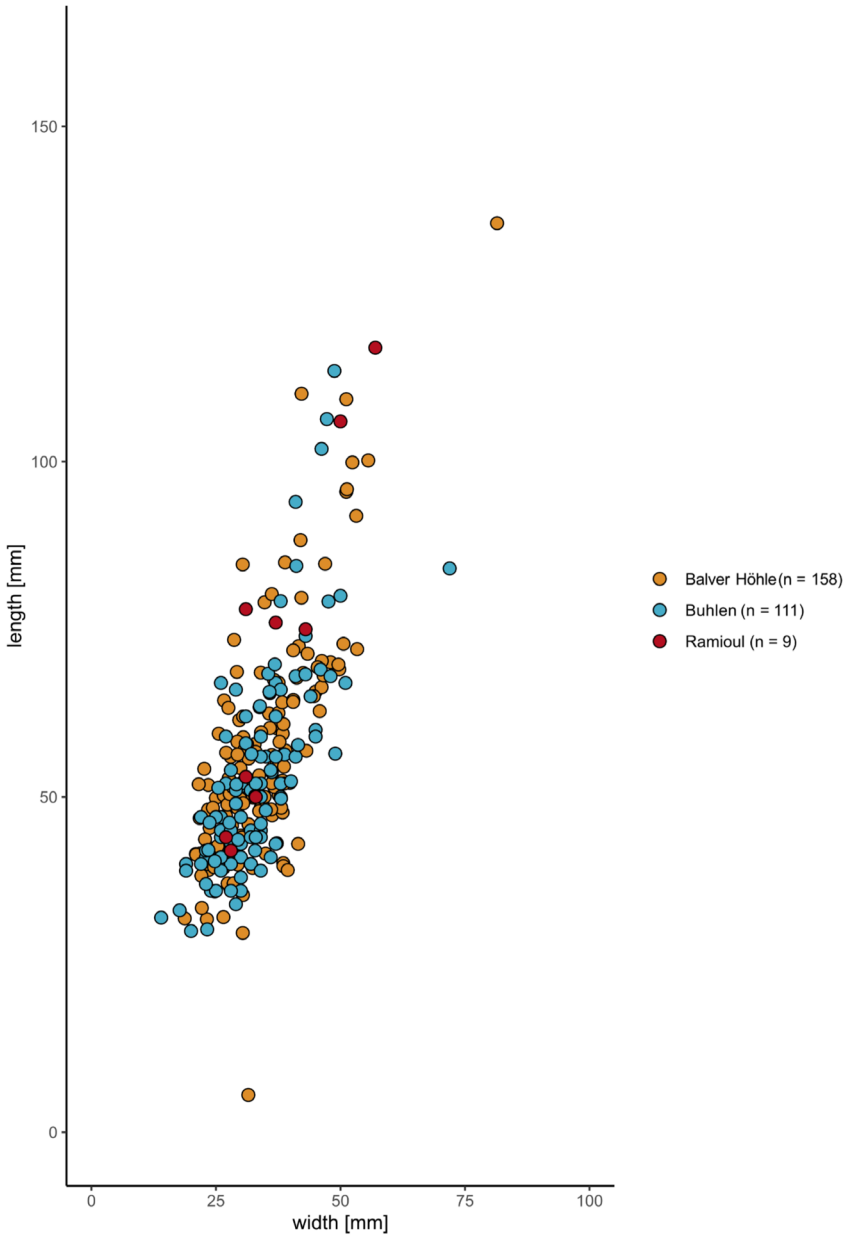

Fig. 55 Length-width ratio of the complete *Keilmesser* from Buhlen (n = 111), Balver Höhle (n = 158) and Ramioul (n = 9).

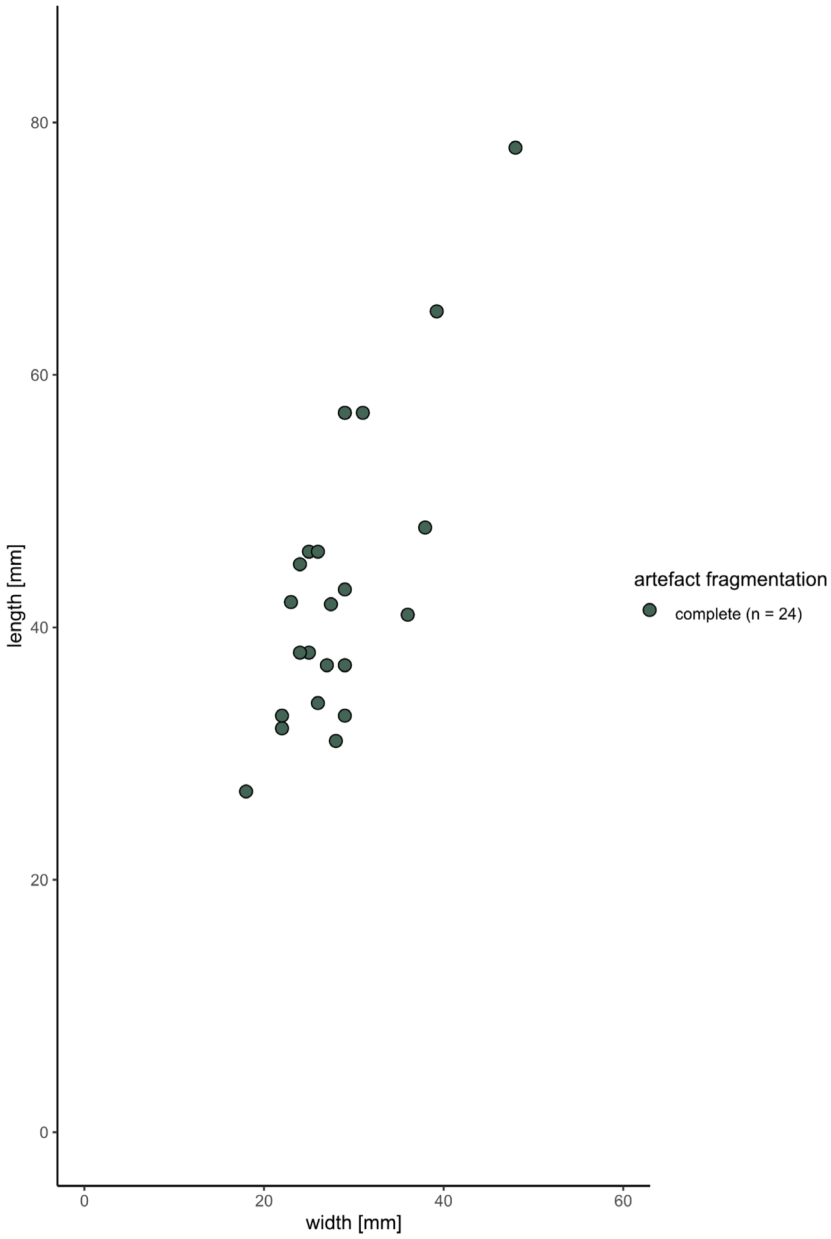

Fig. 56 Length-width ratio of the *Prądnik scrapers* (n = 24) from Buhlen.

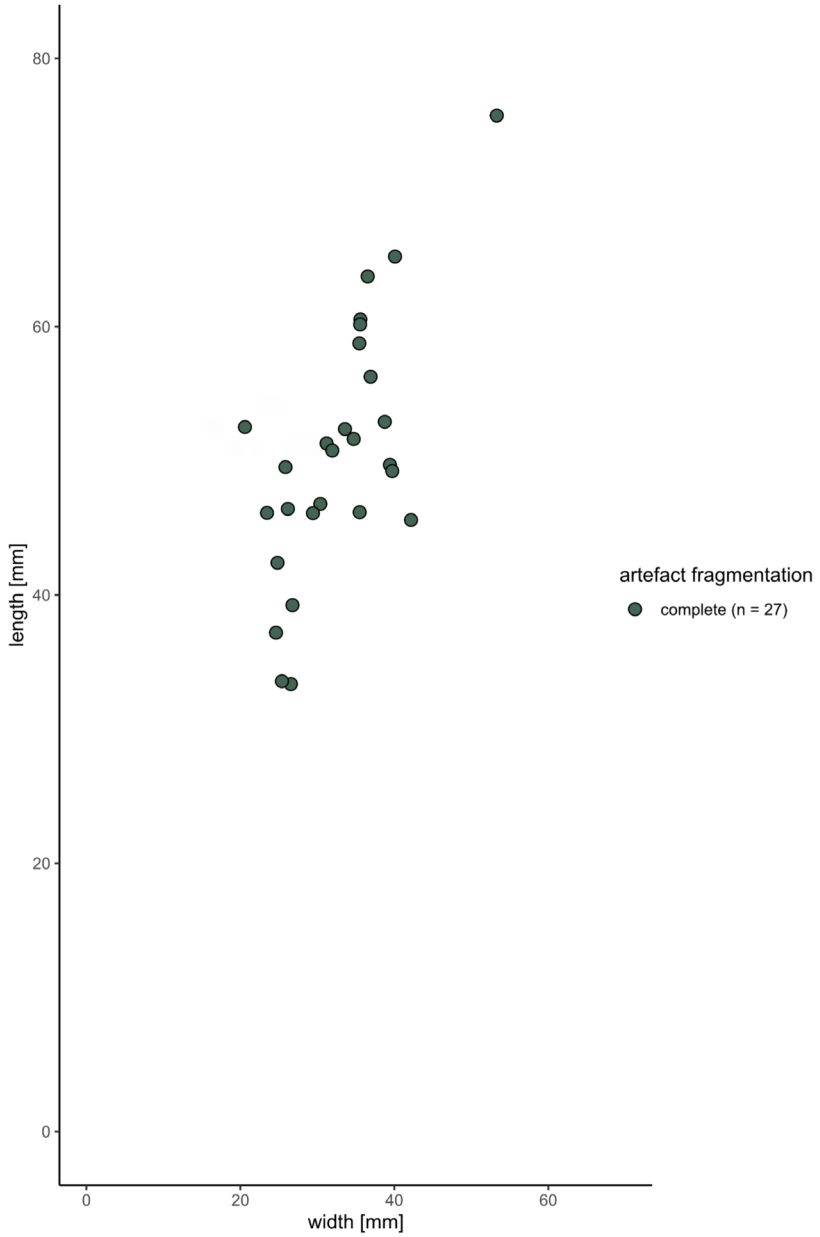

Fig. 57 Length-width ratio of the *Prądnik scrapers* (n = 27) from Balver Höhle.

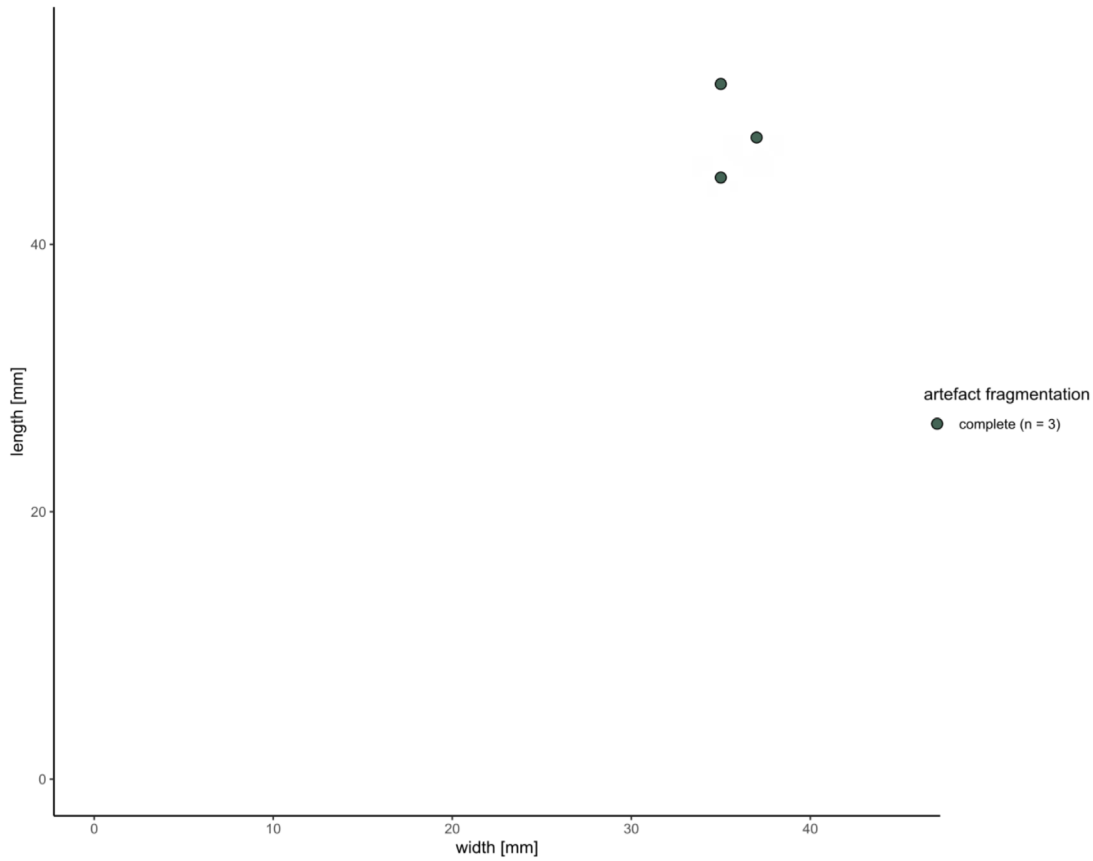

Fig. 58 Length-width ratio of the *Prądnik scrapers* (n = 3) from Ramioul.

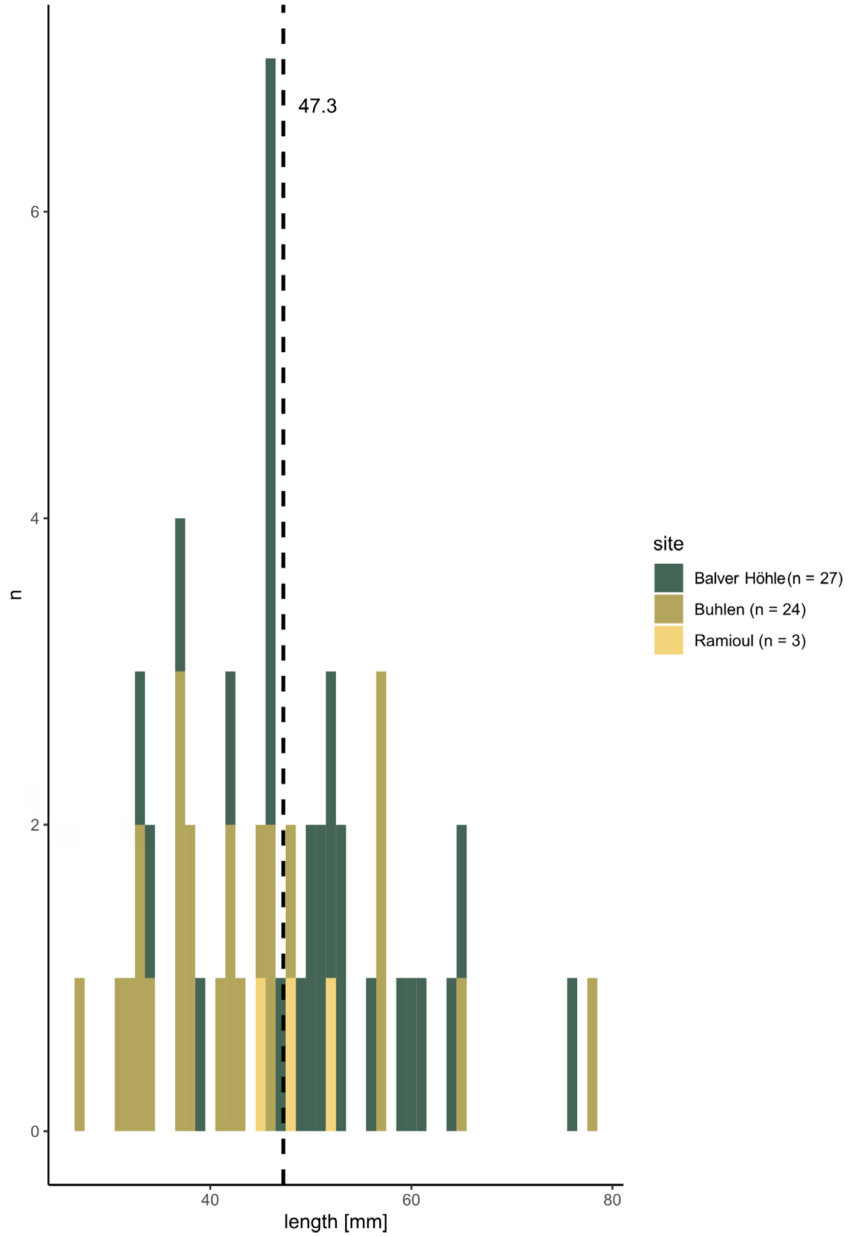

Fig. 59 Maximal length of the *Prądnik scrapers* from Buhlen (n = 24), Balver Höhle (n = 27) and Ramioul (n = 3). The dashed line indicates the arithmetic mean value.

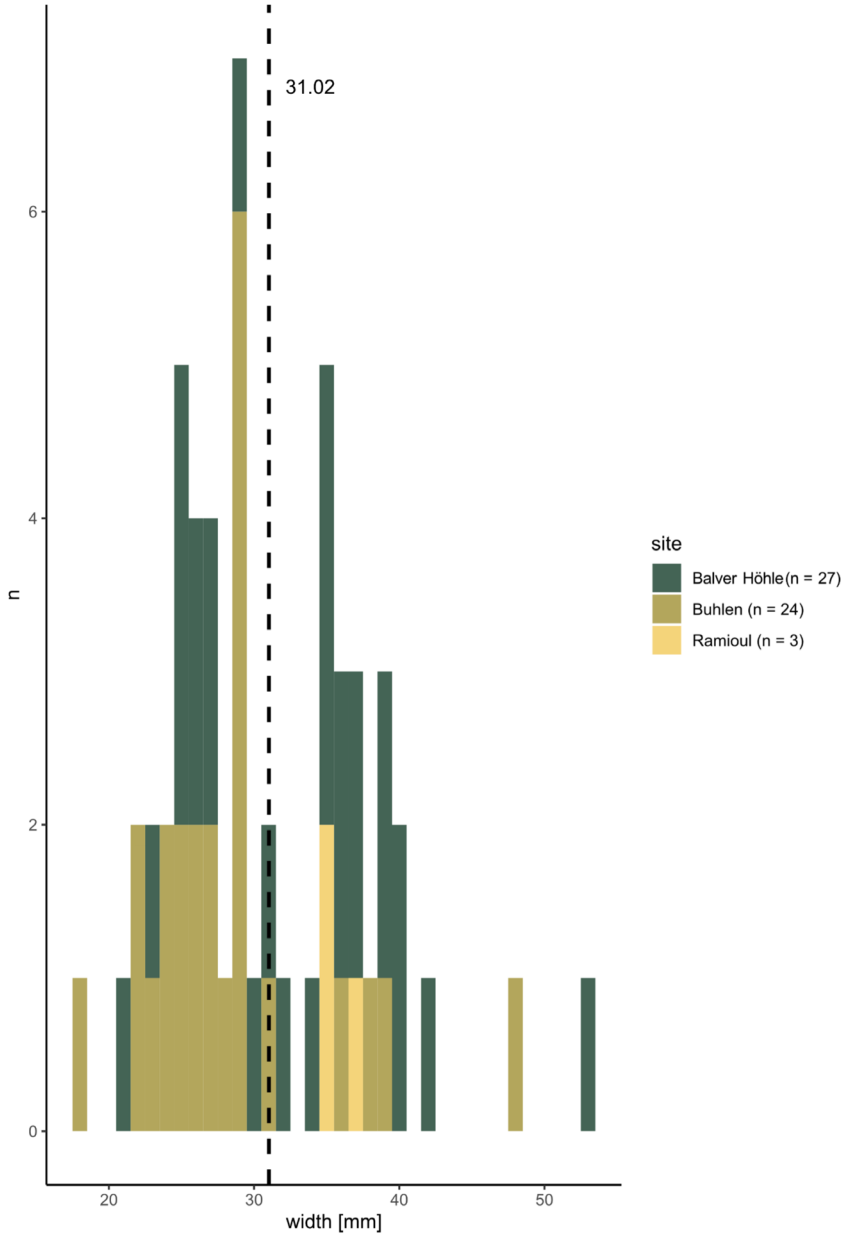

Fig. 60 Maximal width of the *Prądnik scrapers* from Buhlen (n = 24), Balver Höhle (n = 27) and Ramioul (n = 3). The dashed line indicates the arithmetic mean value.

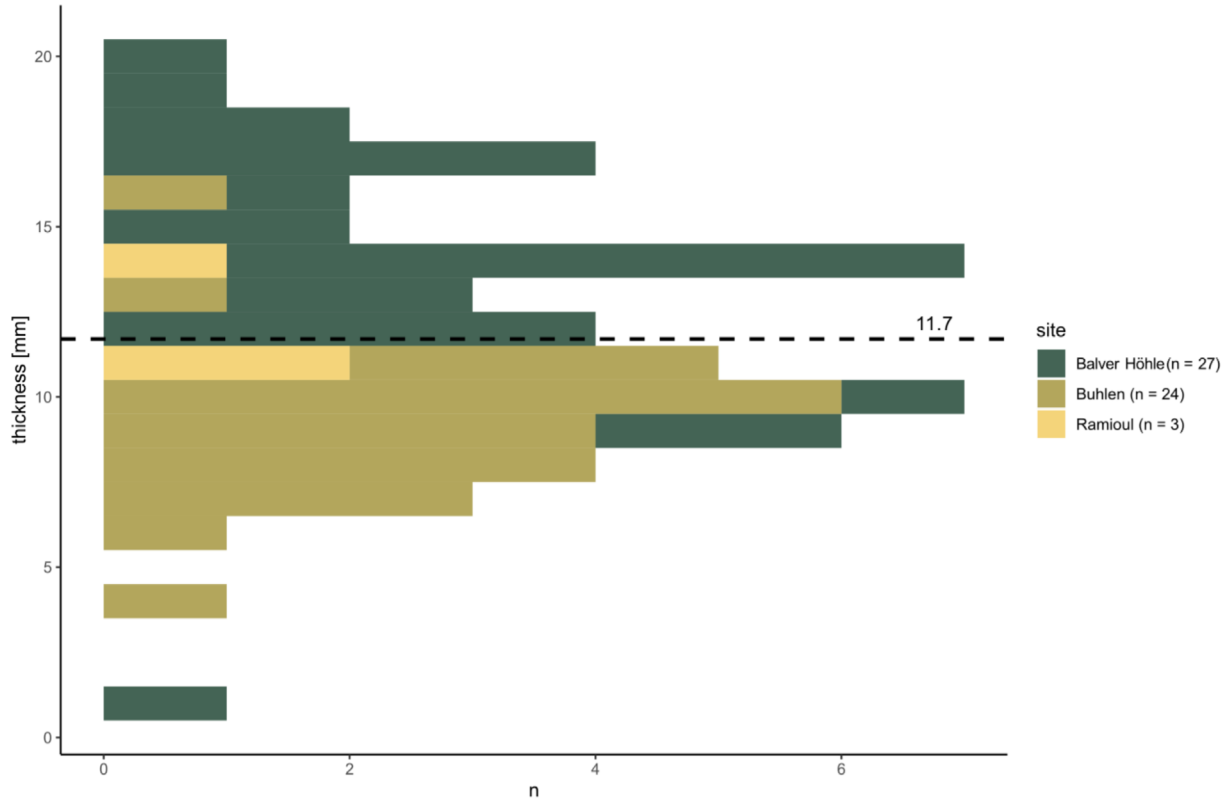

Fig. 61 Maximal thickness of the *Prądnik scrapers* from Buhlen (n = 24), Balver Höhle (n = 27) and Ramioul (n = 3). The dashed line indicates the arithmetic mean value.

Taken together, the measurements for the *Prądnik scrapers* length from the three sites result in a range from 27.0 mm to 78.0 mm with a mean value of 47.3 mm (**figs 59. 62**). All together, the *Prądnik scrapers* have a minimum width of 18.0 mm and a maximum of 53.3 mm (**fig. 60**). The arithmetic mean is 31.0 mm. The thickness of *Prądnik scrapers* ranges between 1.2 mm and 20.4 mm, with an arithmetic mean of 11.7 mm (**fig. 61**). The measurements from the *Prądnik scrapers* are in general smaller than the ones taken from the *Keilmesser.*

Tool back

This part of the qualitative analysis is about the characteristics of the back of the *Keilmesser*. Because locally used siliceous schist is mostly found in blocks, plates or barely rounded pebbles, the raw material piece itself mostly offers convenient striking angles for directed retouch. This aspect is the base to argue that the piece of raw material was carefully selected (Jöris 2001; Jöris/Uomini 2019). Following this argument, the raw material shape was integrated into the overall tool design. As a result, only few *Keilmesser* show clear traces of distinct knapping along the back.

This general observation is applicable to the studied assemblage from Buhlen. N = 46 pieces of the n = 111 complete *Keilmesser* are characterised by a natural back that is either unworked or covered with cortex (**fig. 63**). Some pieces with a natural cortex back display additional minimal retouch (n = 29). N = 18 artefacts can be described as partly retouched, n = 18 as retouched.

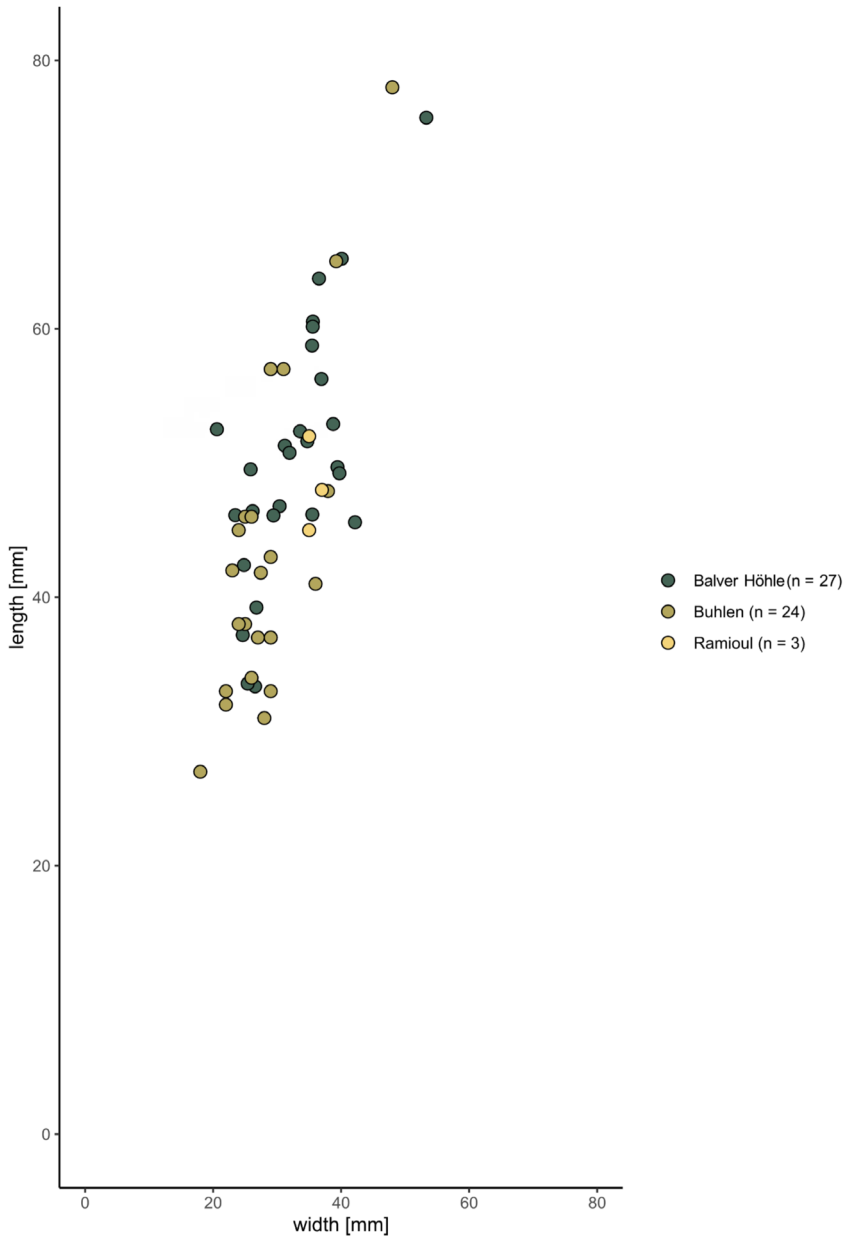

Fig. 62 Length-width ratio of the *Prądnik scrapers* from Buhlen (n = 24), Balver Höhle (n = 27) and Ramioul (n = 3).

Additionally, the thickness of the tool back was also recorded at the most pronounced part of the back (**fig. 67**). The thickness of the back ranges for the complete *Keilmesser* from 4.0 mm to 26.8 mm with an arithmetic mean of 11.9 mm.

A similar situation can be found for the *Keilmesser* from Balver Höhle (**fig. 64**). The majority of the tools with n = 77 artefacts do not display any work traces along the back of the tool. Frequently, the tools show small areas of retouch combined with the natural, unworked cortex (n = 35). The partly retouched back is characteristic for n = 23 artefacts, while n = 23 pieces show distinct retouch.

The thickness measurements of the back at its maximum extend was taken for all complete *Keilmesser* from Balve (**fig. 67**). The values ranging between 2.9 mm and 27.9 mm. The arithmetic mean amounts to 12.2 mm.

In Ramioul, n = 2 of the entire nine *Keilmesser* do not show work traces and thus display a natural back (**fig. 65**). Minimal traces of retouch along the back, showing also cortex, can be found on n = 5 artefacts.

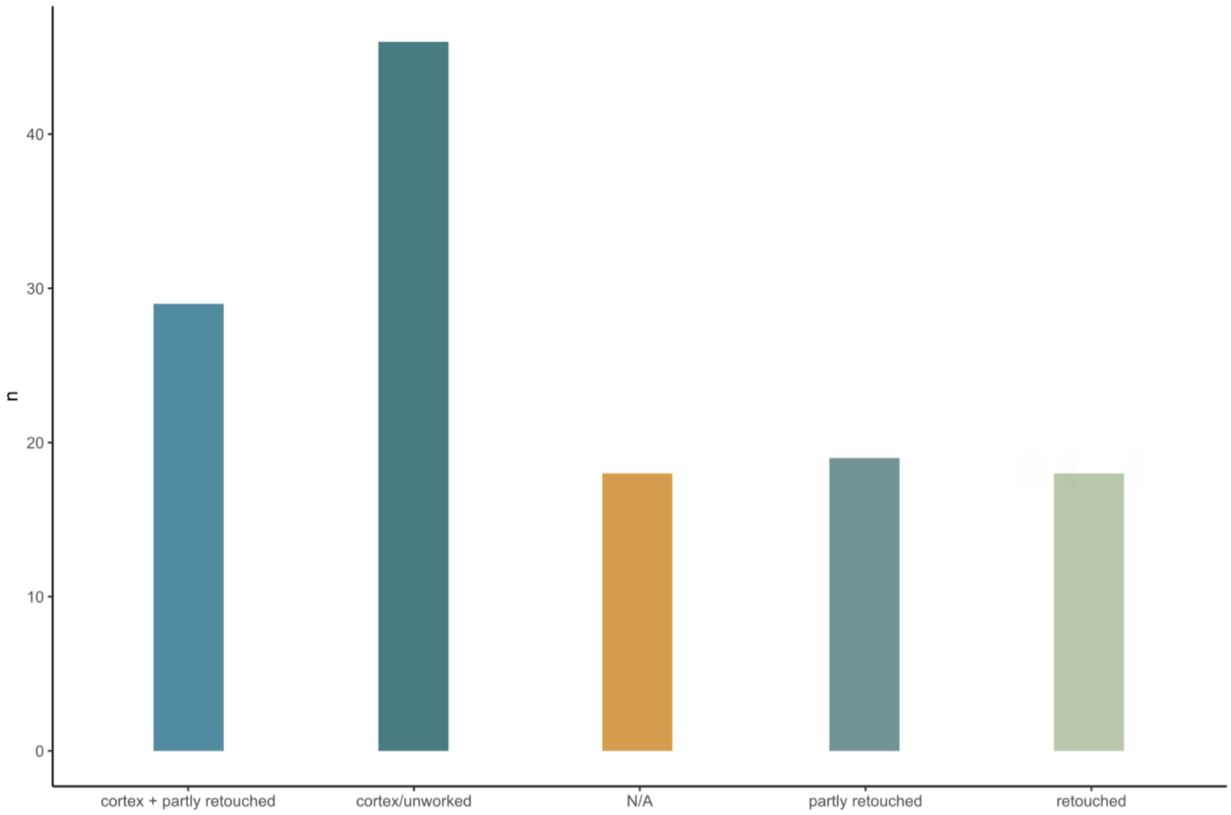

Fig. 63 Characteristics of the back of the complete *Keilmesser* (n = 111) from Buhlen.

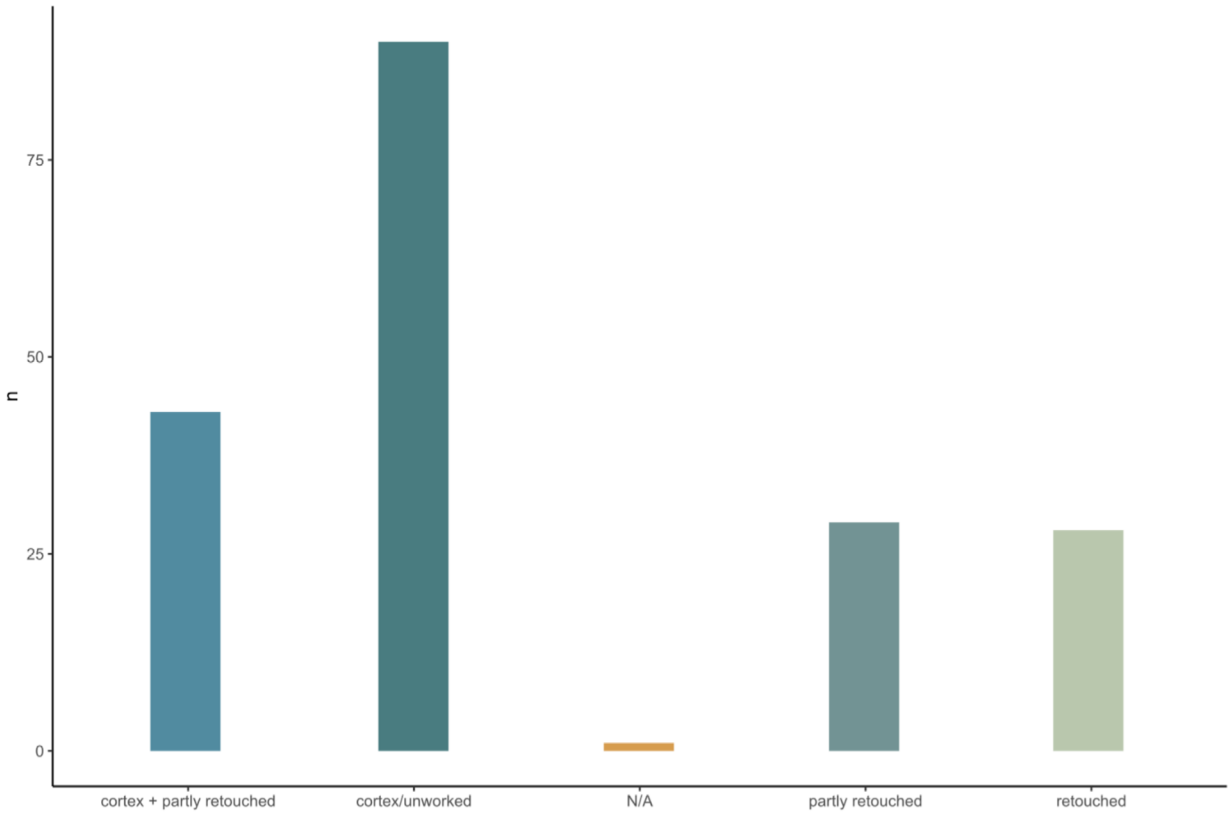

Fig. 64 Characteristics of the back of the complete *Keilmesser* (n = 158) from Balver Höhle.

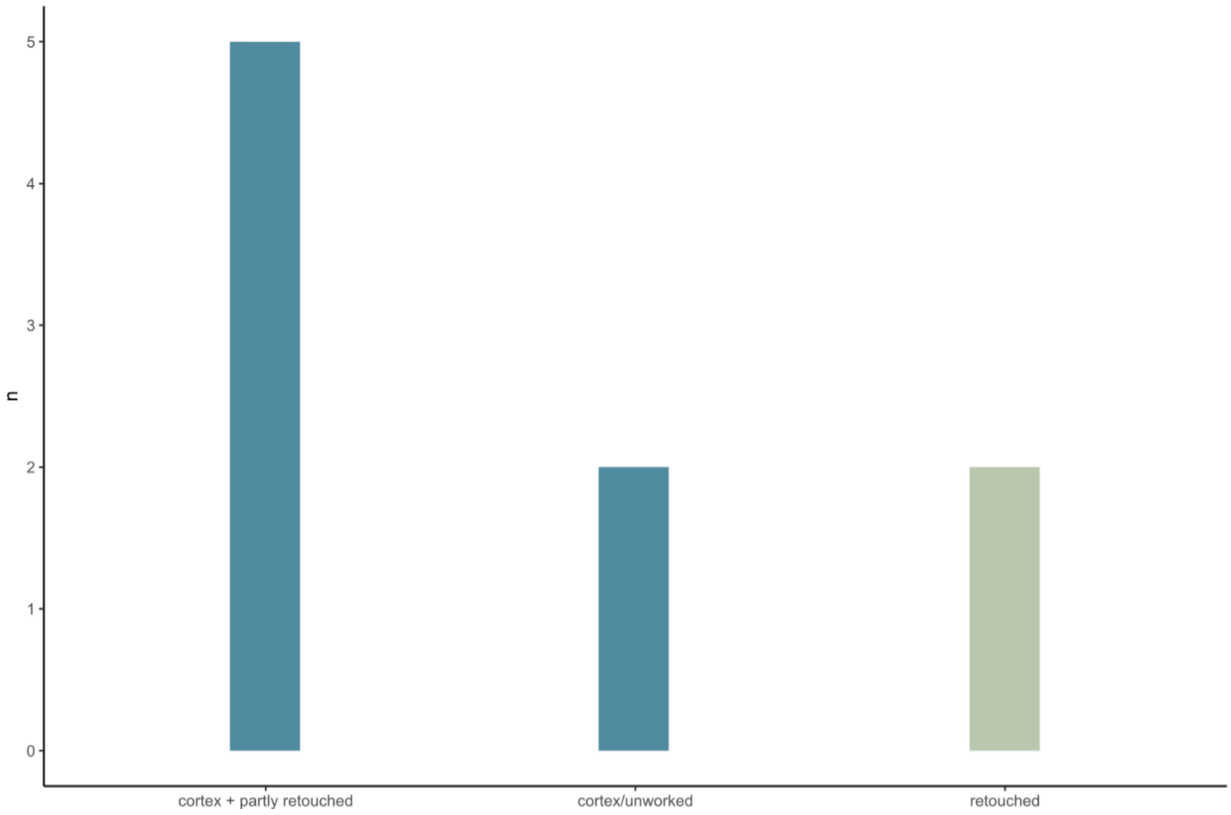

Fig. 65 Characteristics of the back of the complete *Keilmesser* (n = 9) from Ramioul.

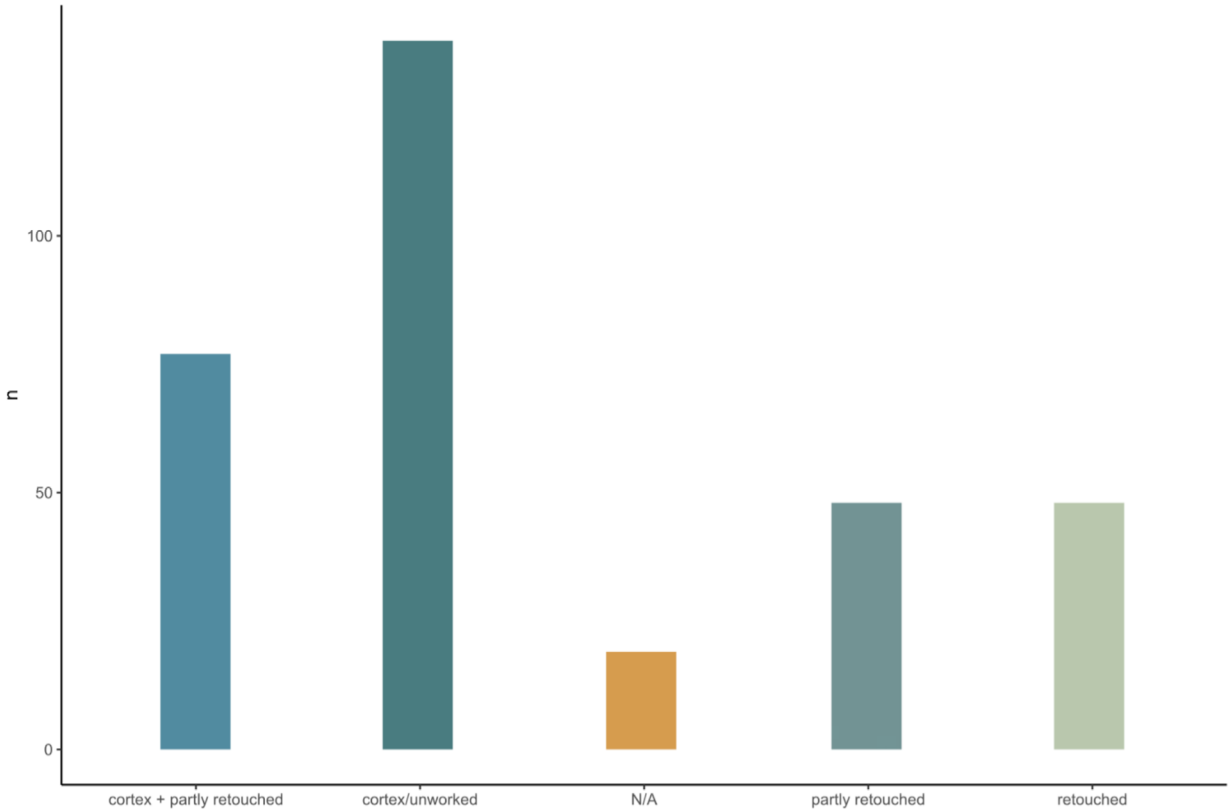

Fig. 66 Characteristics of the back of the complete *Keilmesser* from Buhlen (n = 111), Balver Höhle (n = 158) and Ramioul (n = 9).

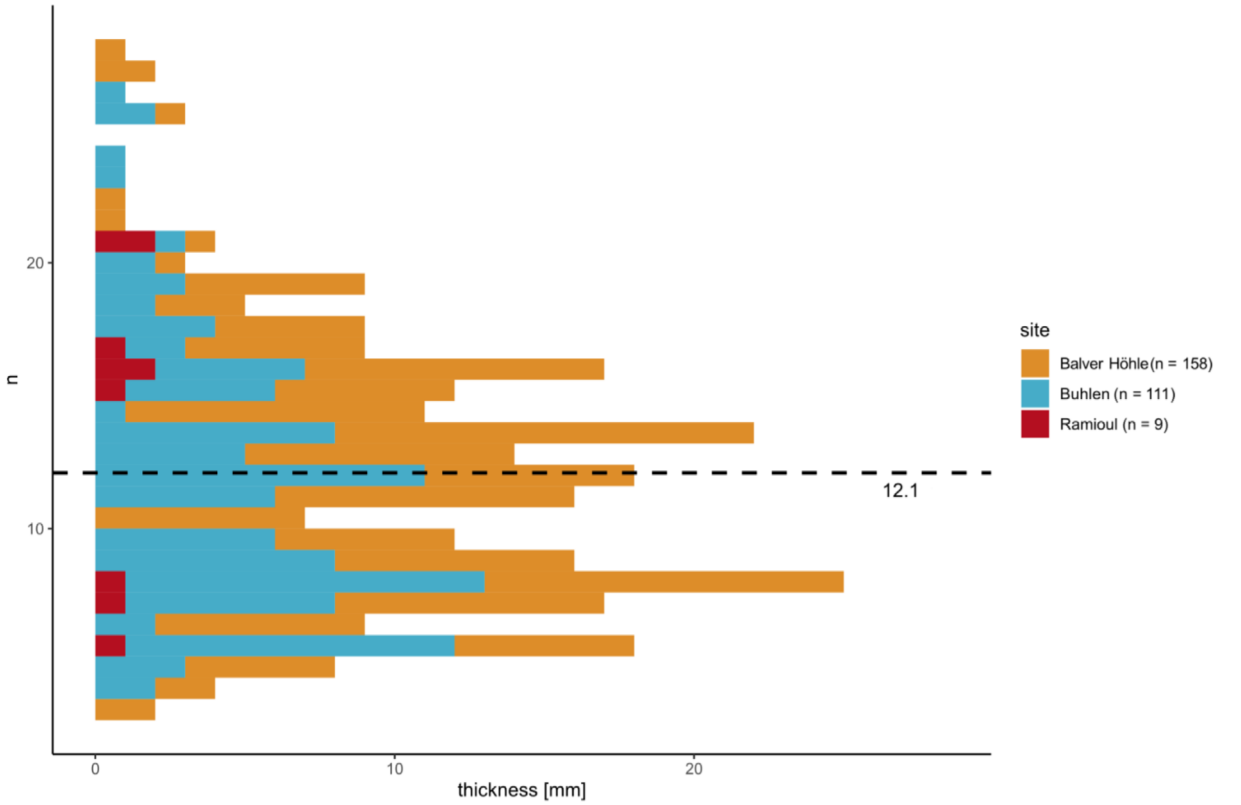

Fig. 67 Maximal thickness back of the *Keilmesser* from Buhlen (n = 111), Balver Höhle (n = 158) and Ramioul (n = 9). The dashed line indicates the arithmetic mean value.

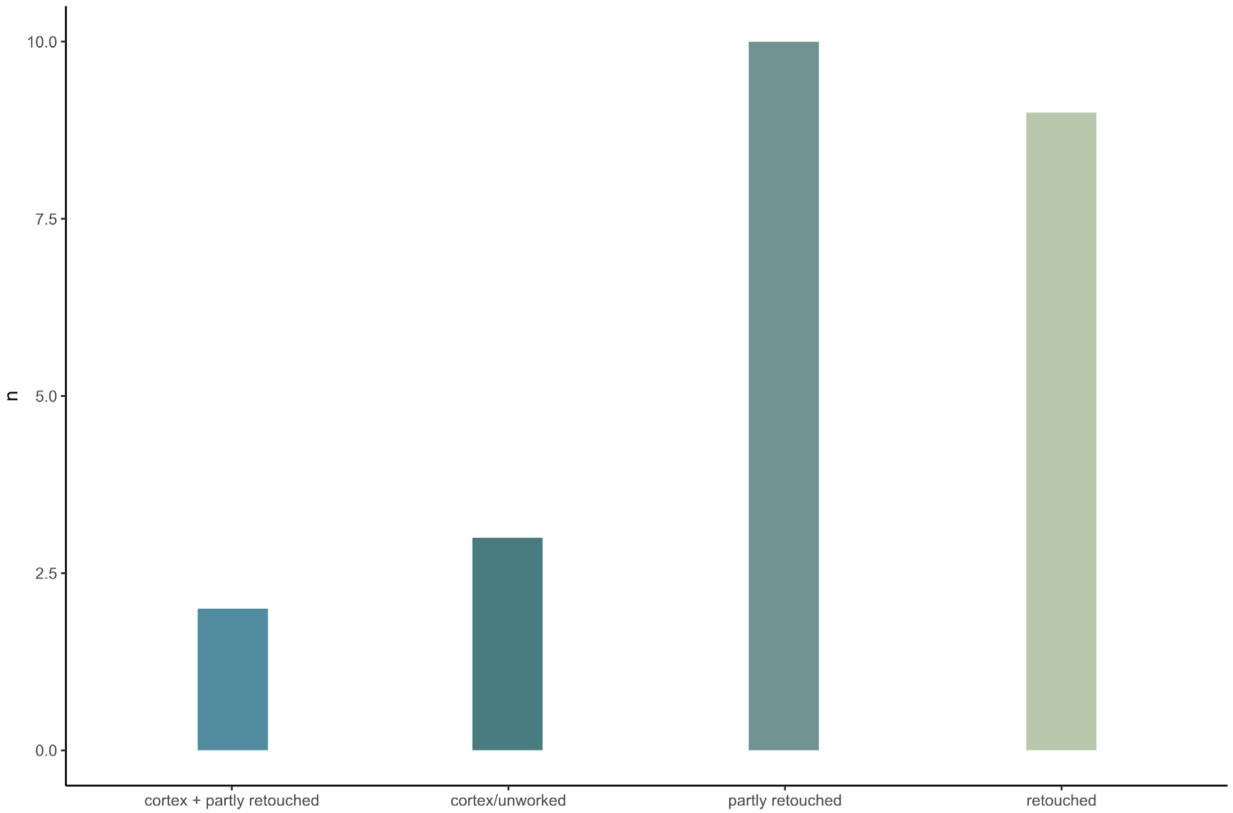

Fig. 68 Characteristics of the backs of the complete *Prądnik scrapers* (n = 24) from Buhlen.

N = 2 artefacts document clear retouch. Interestingly, the integration of the raw material piece in the tool manufacturing concept also seems to count for the artefacts which are made of flint and not only for the silicified schist tools. The assemblages from Ramioul is extremely small, but it shows that six out of eight flint *Keilmesser* are characterised by an either natural or slightly retouched back.
Additionally, the thickness of the tool back was also recorded, leading to a minimum value of 6.0 mm and a maximum of 21.0 mm for the artefacts from Ramioul (**fig. 67**). The mean value is 14.1 mm.
The three assemblages together document a clear picture (**fig. 66**). The back of these analysed *Keilmesser* is predominantly characterised by the absence of working traces (n = 125) or minimal modifications (n = 69). This makes 69.8 % of the artefacts, which can be described as tools with a natural back. Only for a small amount of 15.5 % of all *Keilmesser,* a distinct modification (retouch) can be documented.
Additionally, the thickness measurements of the back measured on all complete *Keilmesser* lead to similar ranges and arithmetic mean values for the three sites (**fig. 67**). The measurements taken together result in a range from 2.9 mm to 27.9 mm. The arithmetic mean value is reflected by the value 12.1 mm.
The characteristics of the tool back are also of interest concerning the *Prądnik scrapers*. Additionally, the retouch of the active edge opposed to the back is mentioned, too.
In Buhlen, the backs of the *Prądnik scrapers* are most often partly retouched (n = 10), sometimes even entirely retouched (n = 9; **fig. 68**). The fewest tools still display cortex (n = 3) or cortex with little retouch (n = 2) along the back. At the most pronounced part, the backs of the *Prądnik scrapers* have a thickness of 1.0 mm to 11.0 mm (**fig. 72**). The arithmetic mean amounts to 5.5 mm.
Comparable is the situation in Balve (**fig. 69**). The *Prądnik scrapers* from Balve are also mainly partly retouched (n = 11) along the back. Definite retouch is visible on n = 5 *Prądnik scrapers.* On the remaining tools could either cortex (n = 8) or cortex combined with slight retouch (n = 3) be documented. The minimum back thickness for the *Prądnik scrapers* is 4.6 mm and the maximum is 18.1 mm with a mean value of 9.9 mm (**fig. 72**).
The *Prądnik scrapers* from the assemblage in Ramioul are retouched (n = 3) in the back area (**fig. 70**). Additionally, the thickness of the tool back was recorded, leading to a minimum value of 5.0 mm and a maximum of 6.0 mm (**fig. 72**).
The results from this analysis are contrary to the ones from the *Keilmesser* (**fig. 71**). While the *Keilmesser* were most often not worked along the back, the *Prądnik scrapers* clearly display working traces and modifications. Modifications such as (partial) retouch taken together lead to a ratio of 70.4 % (n = 38) to 29.6 % (n = 16) of the tools. The 29.6 % of the *Prądnik scrapers* are thus natural or only slightly modified along the back.
The backs of all *Prądnik scrapers* from Buhlen, Balve and Ramioul have a thickness at its most pronounced part of 4.0 mm up to 20.4 mm, leading to a mean value of 7.7 mm (**fig. 72**).

Active edge retouch

Another recorded attribute was the retouch along the active edge. The active edges of the *Keilmesser* from Buhlen are to a percentage of 81.5 % (n = 106) bifacially retouched, some artefacts are semi-bifacially retouched (14.6 %, n = 19).
The *Keilmesser* from Balve do also mainly display a bifacially edge retouch (74.4 %, n = 142), followed by tools with a semi-bifacial retouch (20.4 %, n = 39).
In Ramioul, the *Keilmesser* are either bifacially retouched (44.4 %, n = 4) or semi-bifacially retouched (44.4 %, n = 4).

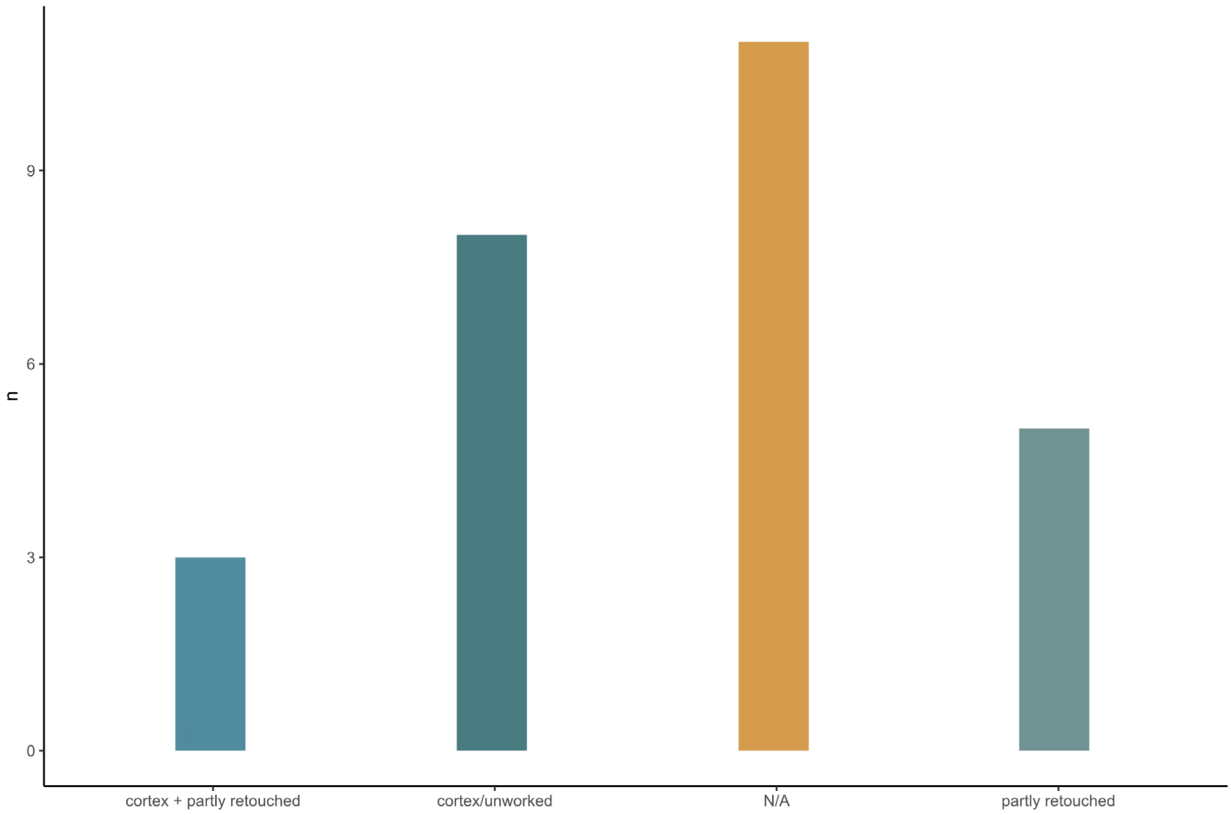

Fig. 69 Characteristics of the backs of the complete *Prądnik scrapers* (n = 27) from Balver Höhle.

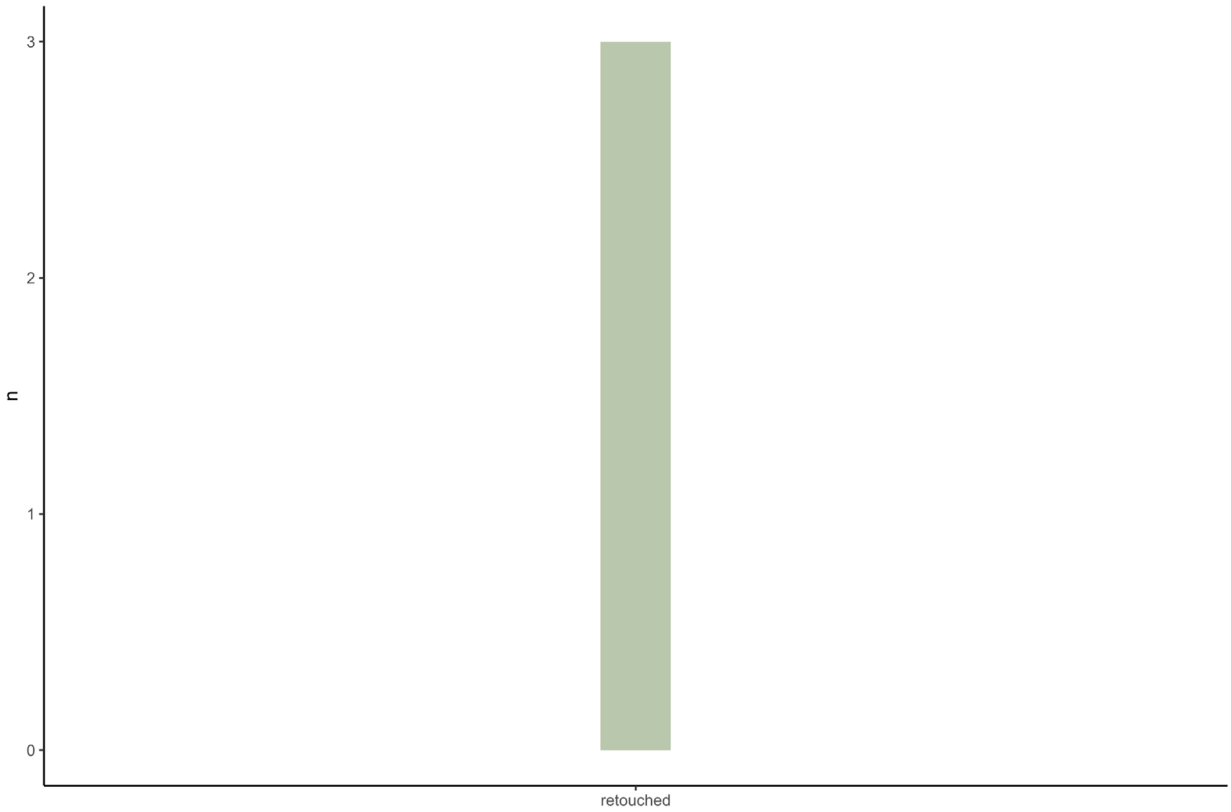

Fig. 70 Characteristics of the back of the complete *Prądnik scrapers* (n = 3) from Ramioul.

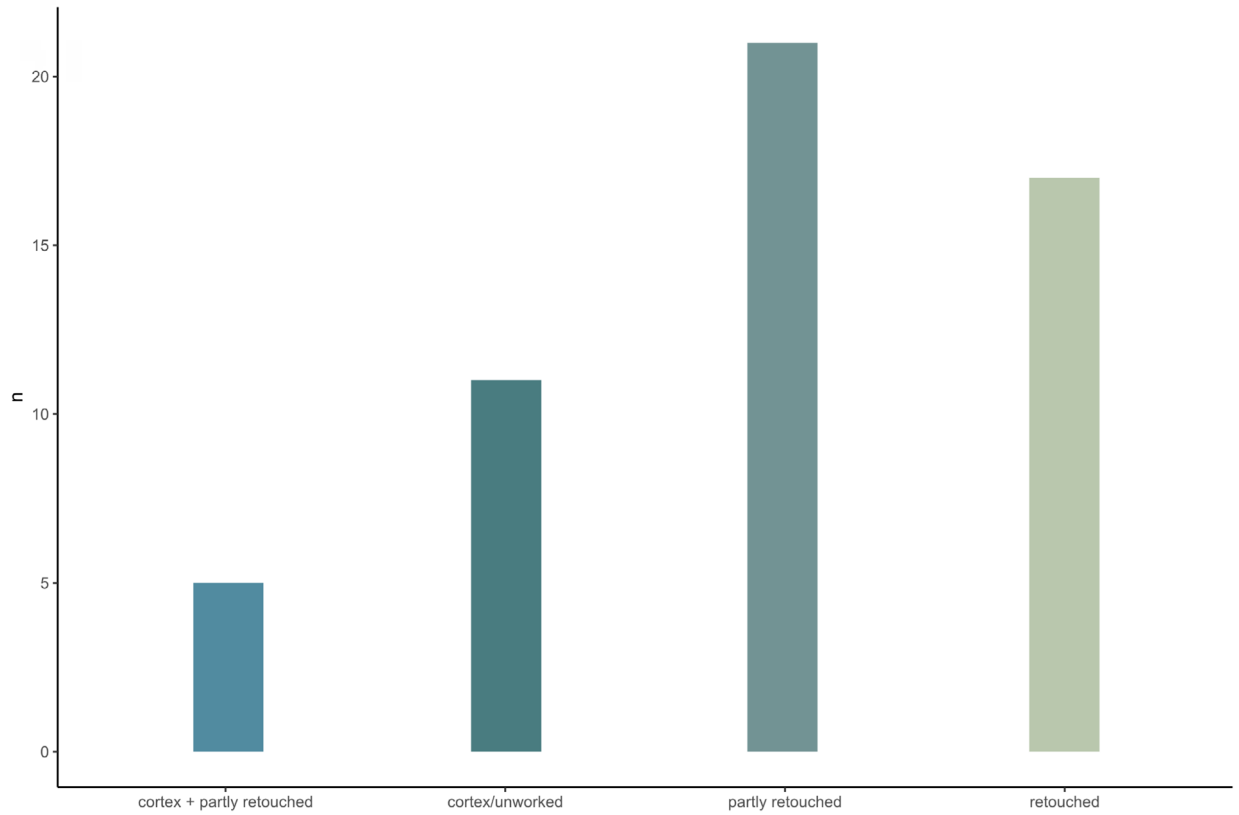

Fig. 71 Characteristics of the backs of the complete *Prądnik scrapers* from Buhlen (n = 24), Balver Höhle (n = 27) and Ramioul (n = 3).

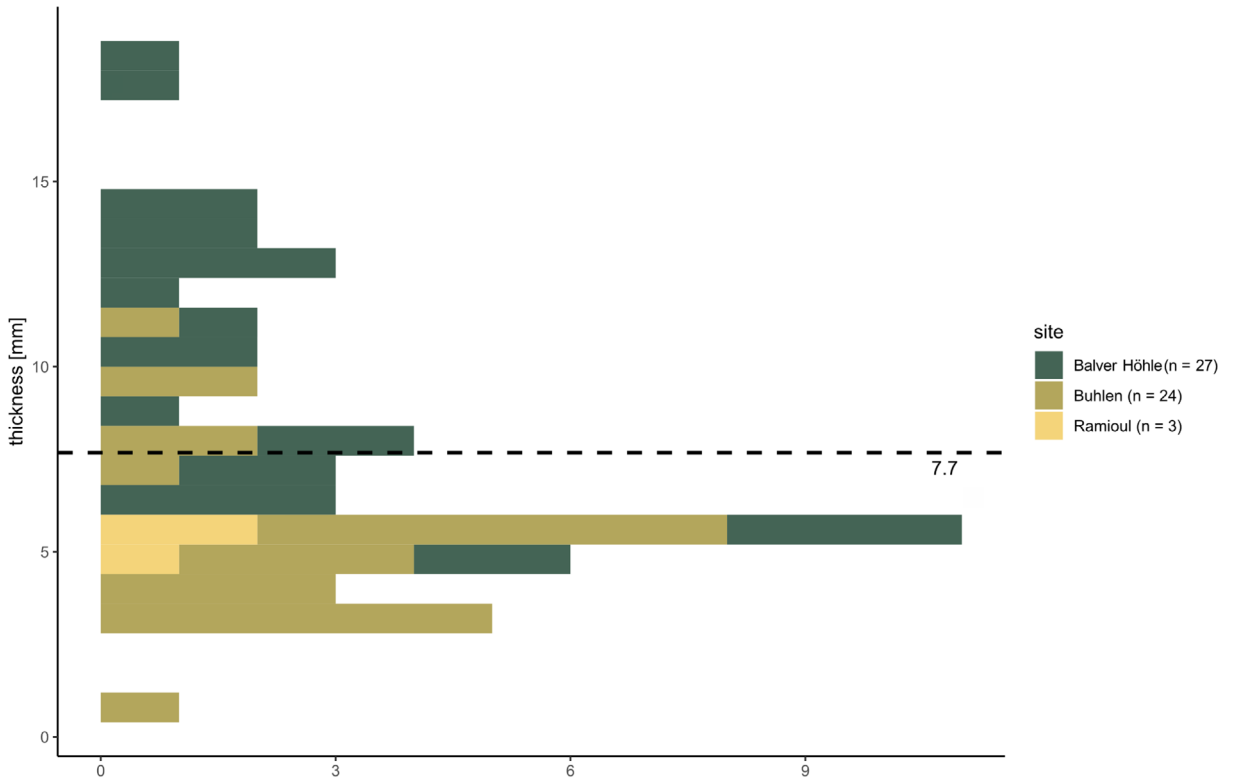

Fig. 72 Maximal back thickness of the *Prądnik scrapers* from Buhlen (n = 24), Balver Höhle (n = 27) and Ramioul (n = 3). The dashed line indicates the arithmetic mean value.

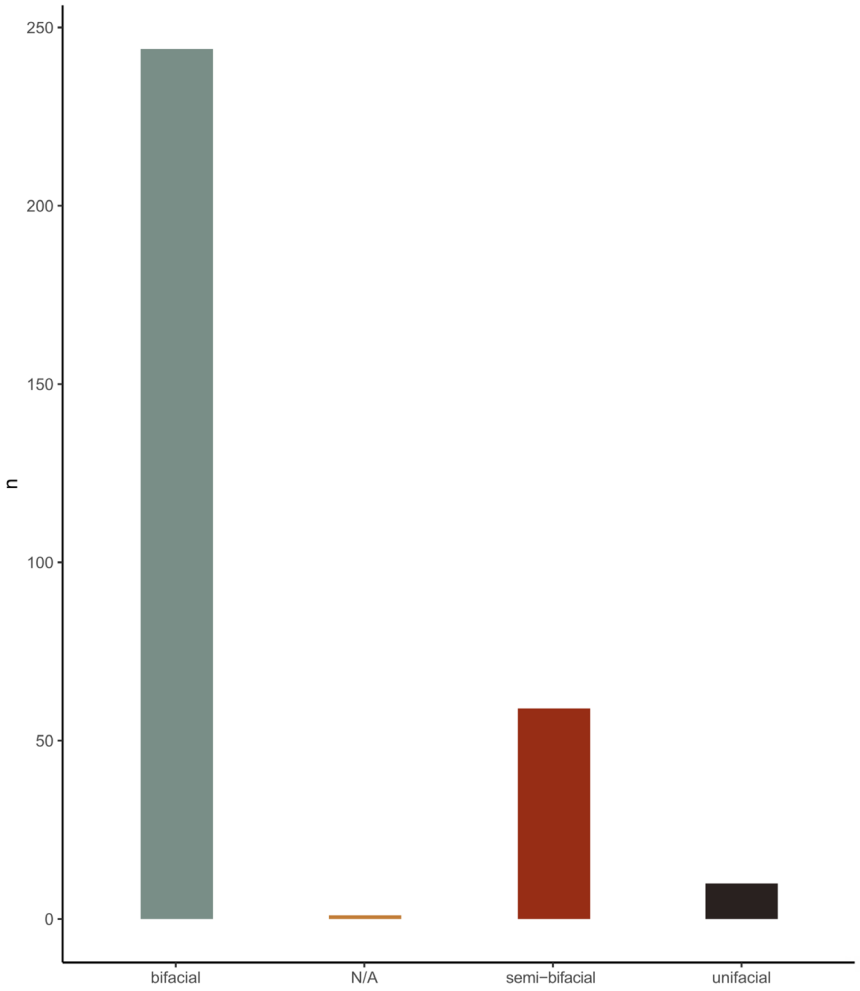

Fig. 73 Retouch type along the active edge of complete *Keilmesser* and *Keilmesser* tips from Buhlen (n = 111; n = 15), Balver Höhle (n = 158; n = 21) and Ramioul (n = 9). For a small part of the assemblage, this analysis was not done (N/A).

Keilmesser from the three sites are by a majority bifacially retouched (76.4 %, n = 252), some are semi-bifacially retouched (18.8 %, n = 62) and only a few pieces are unifacially retouched (3.3 %, n = 11; **fig. 73**). The active edge retouch was also documented for the *Prądnik scrapers* involved within this study. In Buhlen, the back of the *Prądnik scrapers* is most often (45.8 %, n = 11) opposed to a unifacially retouched active edge. Some artefacts are semi-bifacially retouched (29.2 %, n = 7) or bifacially retouched (25.0 %, n = 6).
In Balve, the active edge opposed to the back is mostly semi-bifacially retouched (44.4 %, n = 12), sometimes unifacially retouched (33.3 %, n = 9). One artefact is bifacially retouched. This analysis was initially not done for a small part of the assemblage (n = 5) and thus the data is missing.
The active edge of the studied *Prądnik scrapers* from Ramioul is either unifacially retouched (66.7 %, n = 2) or semi-bifacially retouched (33.3 %, n = 1).
To summarise these observations, the results concerning the active edge retouch of the *Prądnik scrapers* from the three analysed assemblages stands in contrast to the data recorded for the *Keilmesser* (**fig. 74**). A majority of 40.7 % (n = 22) of the *Prądnik scrapers* are only unifacaill retouched or 37.0 % (n = 20) are semi-bifacially retouched. Some artefacts display a bifacial edge retouch (13.0 %, n = 7).

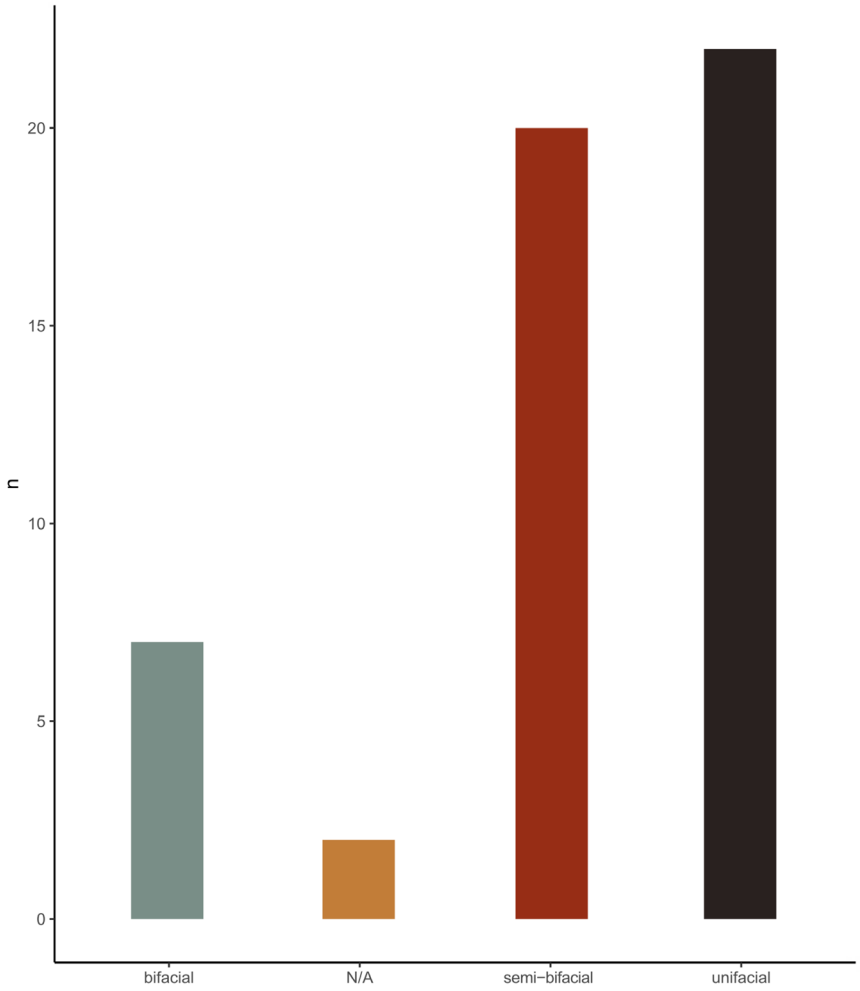

Fig. 74 Retouch type along the active edge of *Prądnik scrapers* from Buhlen (n = 24), Balver Höhle (n = 27) and Ramioul (n = 3). For a small part of the assemblage, this analysis was not done (N/A).

Lateralisation

Based on the asymmetry of *Keilmesser*, tool lateralisation can be defined.

A clear dominance of right-lateral tools can be documented in Buhlen (**tab. 12**). With n = 117 artefacts, the right-sided *Keilmesser* represent 90.0 % of the studied assemblage. A small amount of n = 10 artefacts were classified as left-lateral tools. For n = 3 *Keilmesser* the lateralisation could not be defined with certainty. Here, it should be pointed out again, that the studied assemblage from Buhlen does not reflect the entire amount of artefacts found in Buhlen. In particular the quantity of selected *Prądnik spalls* is considerably smaller. Thus, the mentioned results differ from already published ones (Jöris 2001; Jöris/Uomini 2019).

The same trend can be found in the *Keilmesser* assemblage from Balver Höhle (**tab. 12**). A clear majority (71.2 %, n = 136) of the tools were identified

site		*Keilmesser*			
		sin.	*dex.*	N/A	total
Buhlen	n	10	117	3	**130**
	%	7.7	90.0	2.3	100.0
Balve	n	50	136	5	**191**
	%	26.2	71.2	2.6	100.0
Ramioul	n	1	8	0	**9**
	%	11.1	88.9	0.0	100.0
total	**n**	**61**	**261**	**8**	**330**
	%	18.5	79.1	2.4	100.0

Table 12 Determination of the tool lateralisation for the *Keilmesser* from Buhlen, Balver Höhle and Ramioul.

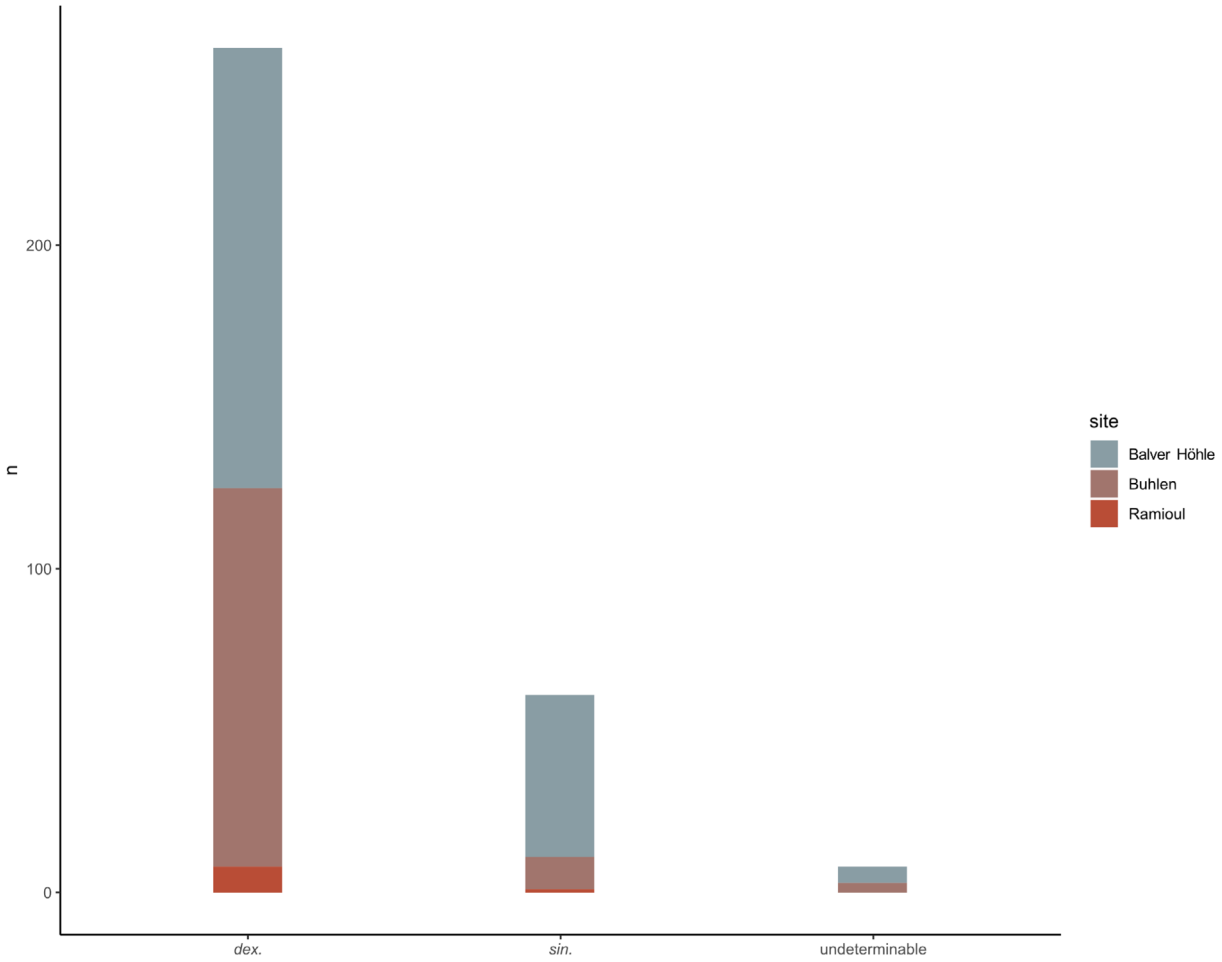

Fig. 75 Determination of the tool lateralisation for the *Keilmesser* from Buhlen (n = 130), Balver Höhle (n = 191) and Ramioul (n = 9).

as right-sided artefacts. As left-sided tools count 26.2 % (n = 50) of the *Keilmesser* in Balve. The laterality of n = 5 pieces could not be defined.

The right-sidedness of the *Keilmesser* also prevails in the assemblage from Ramioul (**tab. 12**). N = 8 tools could be documented as right-lateral tools, whereas only n = 1 counts as a left-sided tool.

In the three analysed sites, a clear tendency can be named (**fig. 75**; **tab. 12**). The *Keilmesser* are predominantly right-sided, represented by 79.1 % of the assemblages. Left-laterality is documented in 18.5 % of all *Keilmesser* only.

As *Keilmesser*, *Prądnik scrapers* display a morphological asymmetry. Therefore, the laterality of the *Prądnik scrapers* can be defined in the same way (**tab. 13**). The *Prądnik scraper* from Buhlen illustrate a clear dominance (n = 19) of right lateral tools. Only n = 3 *Prądnik scrapers* are documented as left lateral tools. For n = 2 of the in total n = 24 artefacts the tool laterality could not be defined.

site		*Prądnik scraper*			
		sin.	*dex.*	N/A	total
Buhlen	n	3	19	2	**24**
	%	12.5	79.2	8.3	100.0
Balve	n	4	23	0	**27**
	%	14.8	85.2	0.0	100.0
Ramioul	n	1	2	0	**3**
	%	33.3	66.7	0.0	100.0
total	**n**	**8**	**44**	**2**	**54**
	%	14.8	81.5	3.7	100.0

Table 13 Determination of the tool lateralisation for the *Prądnik scrapers* from Buhlen, Balver Höhle and Ramioul.

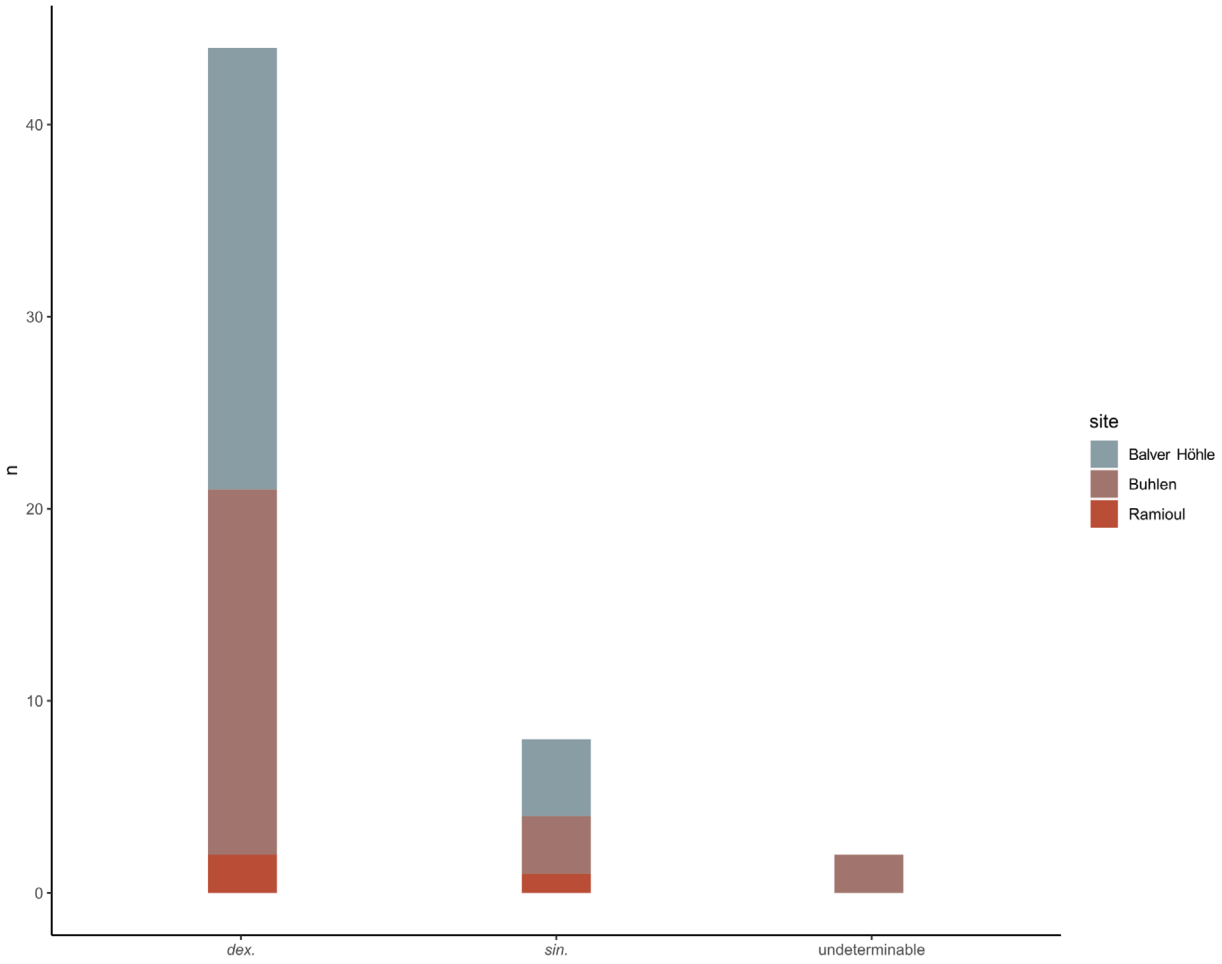

Fig. 76 Determination of the tool lateralisation for the *Prądnik scrapers* from Buhlen (n = 24), Balver Höhle (n = 27) and Ramioul (n = 3). The laterality of n = 2 artefacts could not be determined. These artefacts are excluded from the figure.

A similar picture is becoming evident for the *Prądnik scrapers* from Balve. By a majority of 85.2 % (n = 23), the tools are right-sided. N = 4 *Prądnik scrapers* count as left-sided artefacts.
N = 2 of the n = 3 *Prądnik scraper* from Ramioul display a right laterality, the other *Prądnik scraper* is left lateral.
To summarise, a predominance of right lateral *Prądnik scrapers* can be documented for the three studied sites Buhlen, Balve and Ramioul (**fig. 76**). The ratio of right lateral to left lateral tools is 81.5 % (n = 44) to 14.8 % (n = 8).

Morphological shape variability

The idea, to assign each *Keilmesser* to one of the previously described seven *Keilmesser* shapes were taken up in this subchapter. Only complete *Keilmesser* were involved in this part of the analysis. Due to some transitional morphology, it was not possible to ascribe every artefact strictly to one of the *Keilmesser* shapes. These tools are marked as undeterminable.
In Buhlen n = 111 *Keilmesser* could be assigned to a *Keilmesser* shape (**fig. 77**). While there is no *Königsaue Keilmesser* within the Buhlen assemblage, all other *Keilmesser* shapes are represented. Out of the remaining

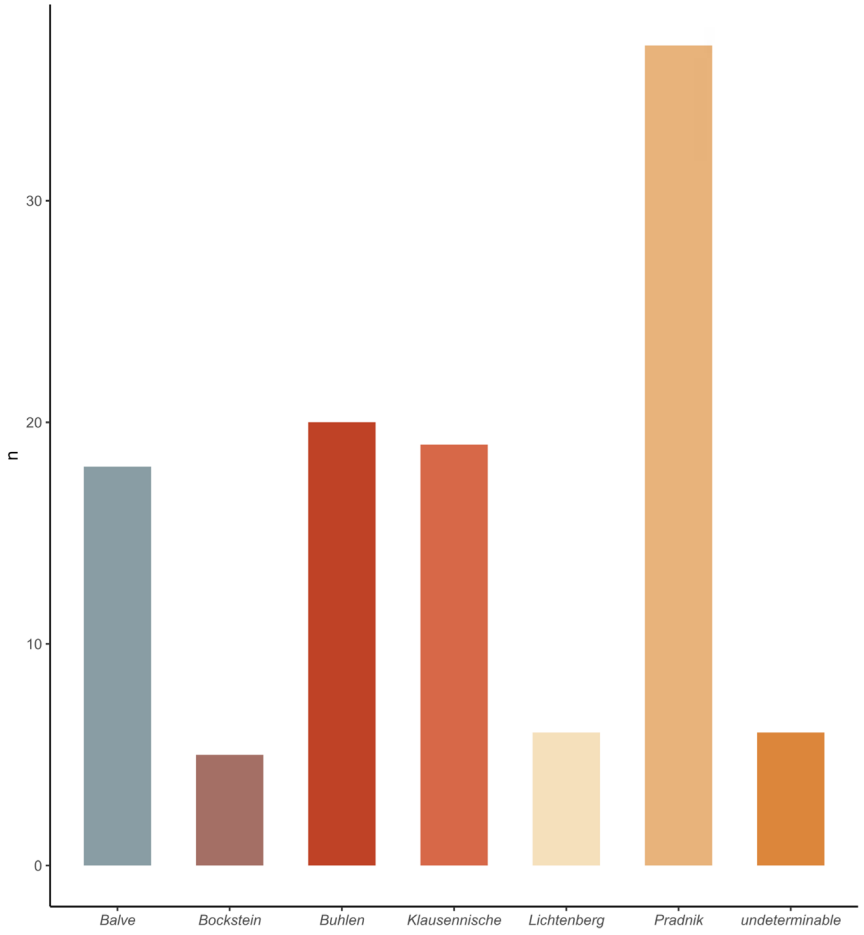

Fig. 77 Distribution of the complete *Keilmesser* (n = 111) from Buhlen to one of the described *Keilmesser* shapes.

six different types, one stands out slightly. Exactly one third (n = 37) of the tools are *Prądnik knives*. Subsequently, the *Keilmesser* shapes *Buhlen* (n = 20), *Klausennische* (n = 19) and *Balve* (n = 18) a part of the assemblage in about the same sum. Much scarcer are those tools, which can be morphologically assigned to the *Keilmesser* shapes *Bockstein* (n = 5) and *Lichtenberg* (n = 6).

A slightly different picture reveals the assignment of the *Keilmesser* shapes for the *Keilmesser* inventory from Balve (**fig. 78**). The type *Lichtenberg* is not represented at all. As in the Buhlen assemblage, the majority of *Keilmesser* can be ascribed as *Prądnik knives* (n = 47). This is followed by the *Keilmesser* shapes *Klausennische* (n = 37), *Balve* (n = 36) and *Bockstein* (n = 29). *Keilmesser* which can be morphologically defined as type *Buhlen* (n = 8) and *Königsaue* (n = 1) are rarely represented.

In Ramioul, the *Keilmesser* assemblage can only be ascribed to three of the seven *Keilmesser* shapes (**fig. 79**). The *Keilmesser* shapes *Balve, Klausennische and Prądnik* are present in equal parts (each n = 3).

Taken together, this means, the most often represented *Keilmesser* shape in the three studied assemblages is the *Prądnik knife* (n = 87; **fig. 80**). Together with the types *Balve* (n = 65) and *Klausennische* (n = 59) they compose three quarter of the artefacts.

In an additional step, the perimeter sections were measured for the *Keilmesser* from the three assemblages. For this analysis, only complete artefacts were suitable.

In Buhlen, the artefacts have a base and back length of minimum 33.0 mm and maximum 120.0 mm. The second perimeter section, the distal posterior part ranges from 6.0 mm to 92.0 mm. Some artefacts (n = 2), however, are characterized by a lack of this area. The determined values are therefore 0.0 cm. The active edge, as the third perimeter area, shows a size range from 21.0 mm to a maximum of 113.0 mm.

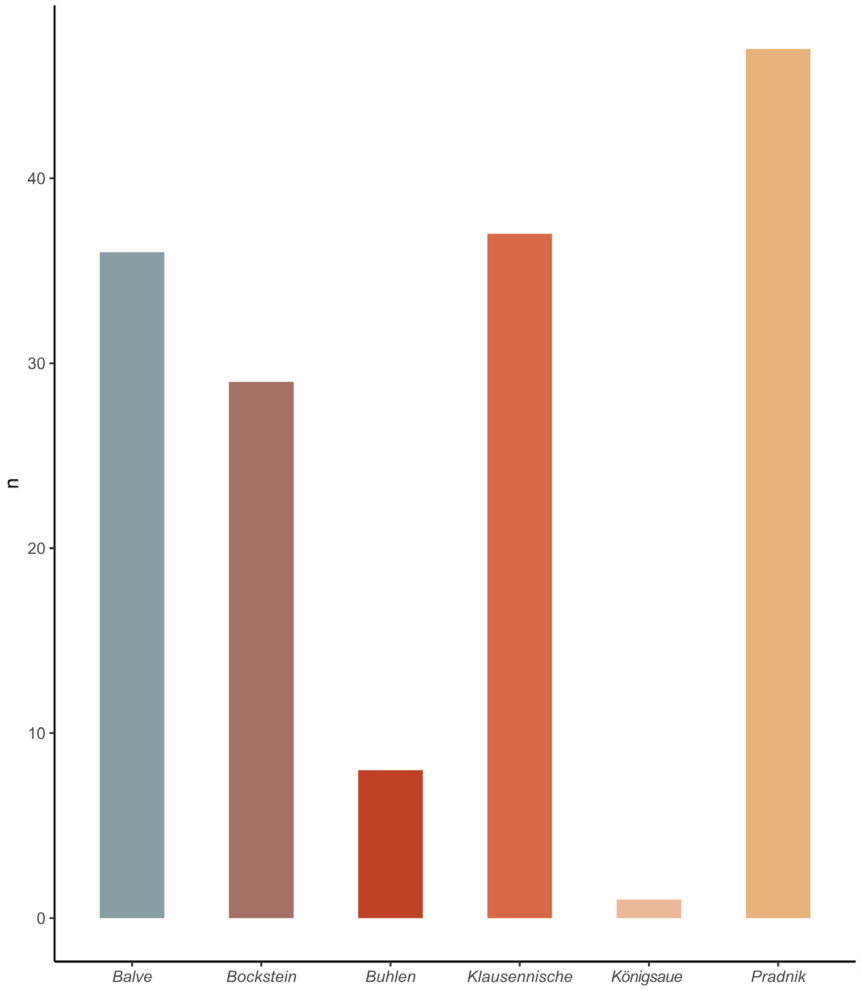

Fig. 78 Distribution of the complete *Keilmesser* (n = 158) from Balver Höhle to one of the described *Keilmesser* shapes.

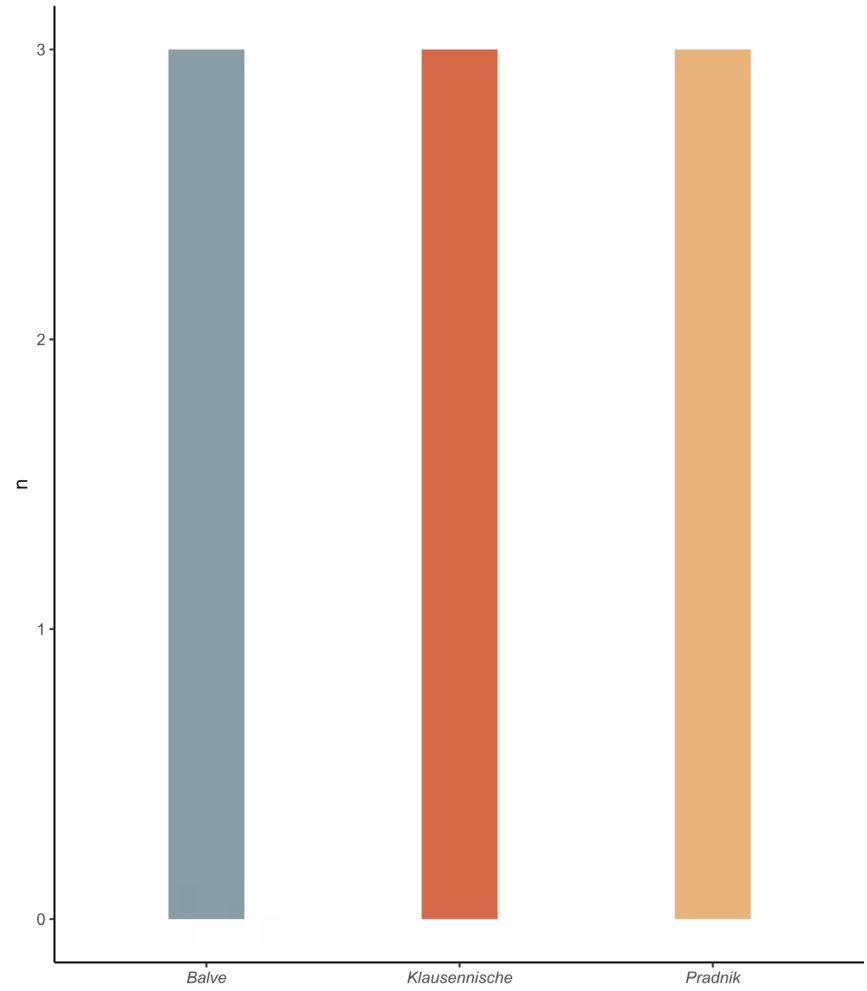

Fig. 79 Distribution of the complete *Keilmesser* (n = 9) from Ramioul to one of the described *Keilmesser* shapes.

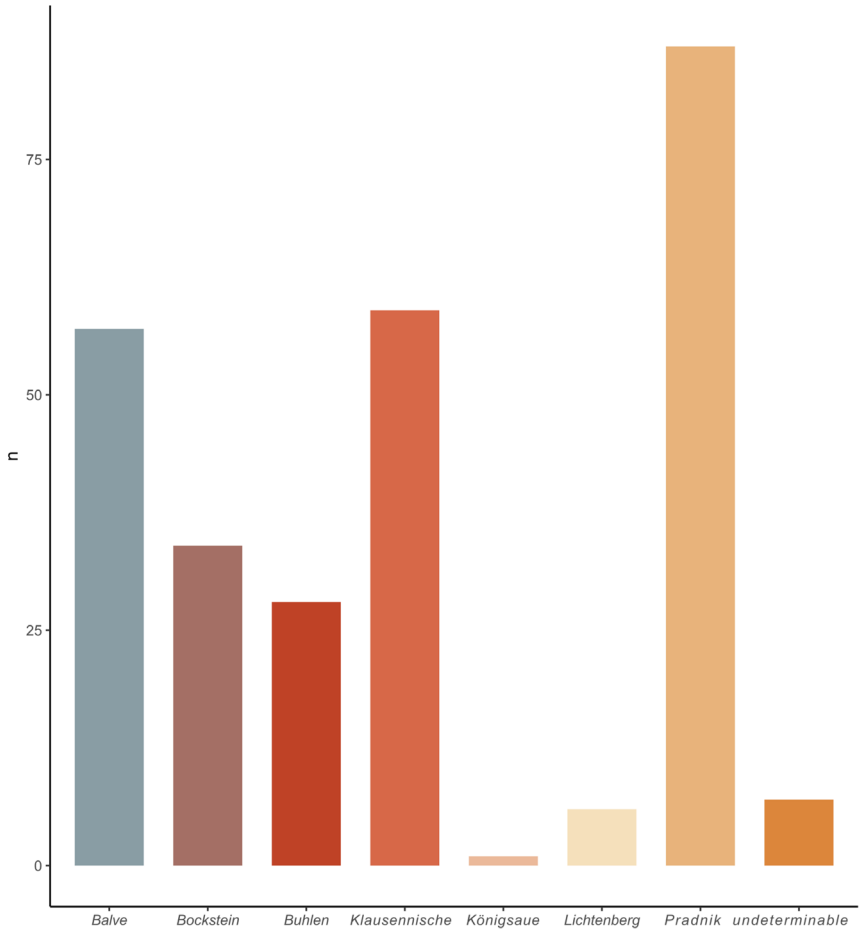

Fig. 80 Distribution of the complete *Keilmesser* from Buhlen (n = 111), Balver Höhle (n = 158) and Ramioul (n = 9) to one of the described *Keilmesser* shapes.

The results from the measurements taken from the Balve assemblage illustrate similar proportions. The section that spans from the base to the back ranges from 30.0 mm to 142.0 mm. The connecting section, the distal posterior part, has a minimum of 10.0 mm and maximum of 93.0 mm. Again, some artefacts do not have this section. In these cases (n = 24) the back directly connects to the active edge. The active edge displays a range between 26.0 mm and 127.0 mm.

In Ramioul, the first section – base and back – ranges from 57.0 mm to 105.0 mm. The margins for the distal posterior part are between 19.0 mm and 82.0 mm. The minimum measurement for the active edge is 13.0 mm while the maximum is 113.0 mm.

The analysis of the determined perimeter sections measured on all *Keilmesser* from the three sites illustrates the following: The proportions of the first section – base and back and the second perimeter section – the distal posterior part – seem to be closely related. The smaller the second section, the larger the dimensions of the back and base. Regardless of this, the length of the working edge is almost constant and occupies on average between 33 and 37 percent of the total perimeter.

In order to determine the actual relationship between the morphologically defined *Keilmesser* shapes and the metrically measured perimeter sections, the data was combined in one graph (**figs 81-84**). The dimensions were plotted in a ternary plot, comprising the mm measurements of the three perimeter sections together at once. The ascribed *Keilmesser* shapes were highlighted in different colours. In case, distinct *Keilmesser* shapes exist, they should cluster graphically grouped together. However, these clusters are not visible as such. Instead of clear clusters, there is a transition between the *Keilmesser* shapes represented by the individual data points. Only the *Keilmesser* classified as shape *Bockstein* separate from the rest of the

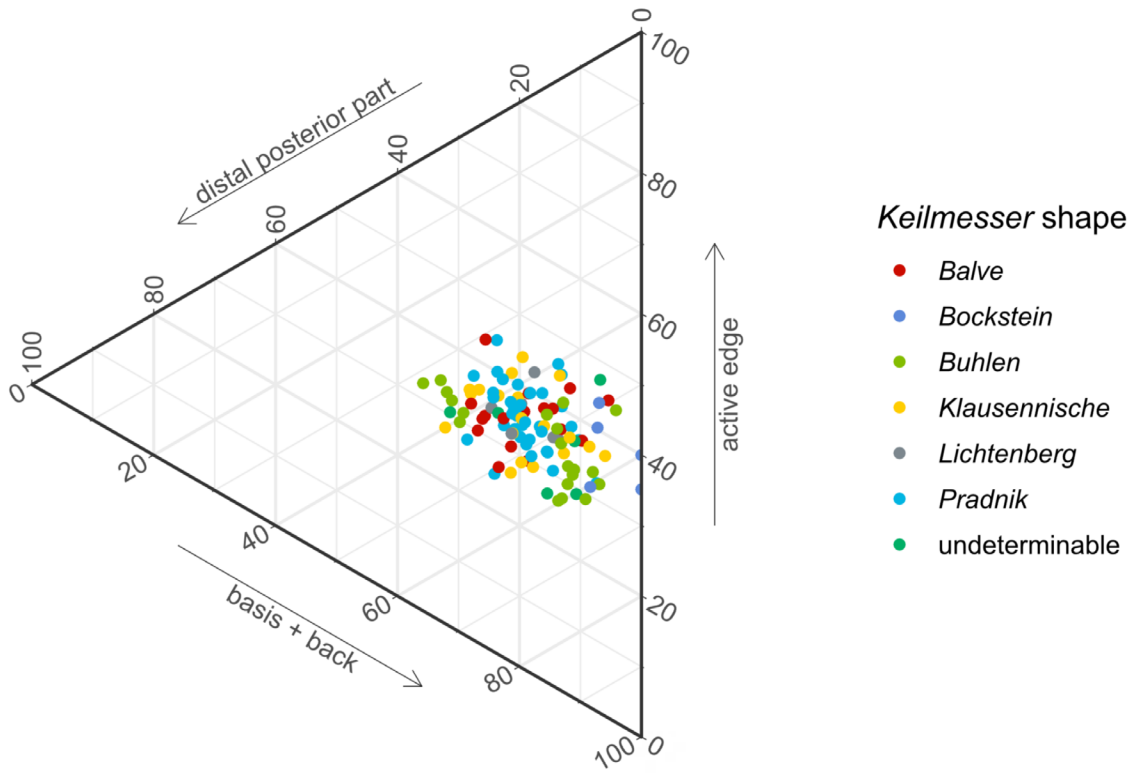

Fig. 81 Size-independent comparison of the shape variation in the perimeter of the complete *Keilmesser* from Buhlen, showing the ratio of the perimeter sections back and base, distal posterior part and active edge. The data points are coloured based on the assigned *Keilmesser* shape.

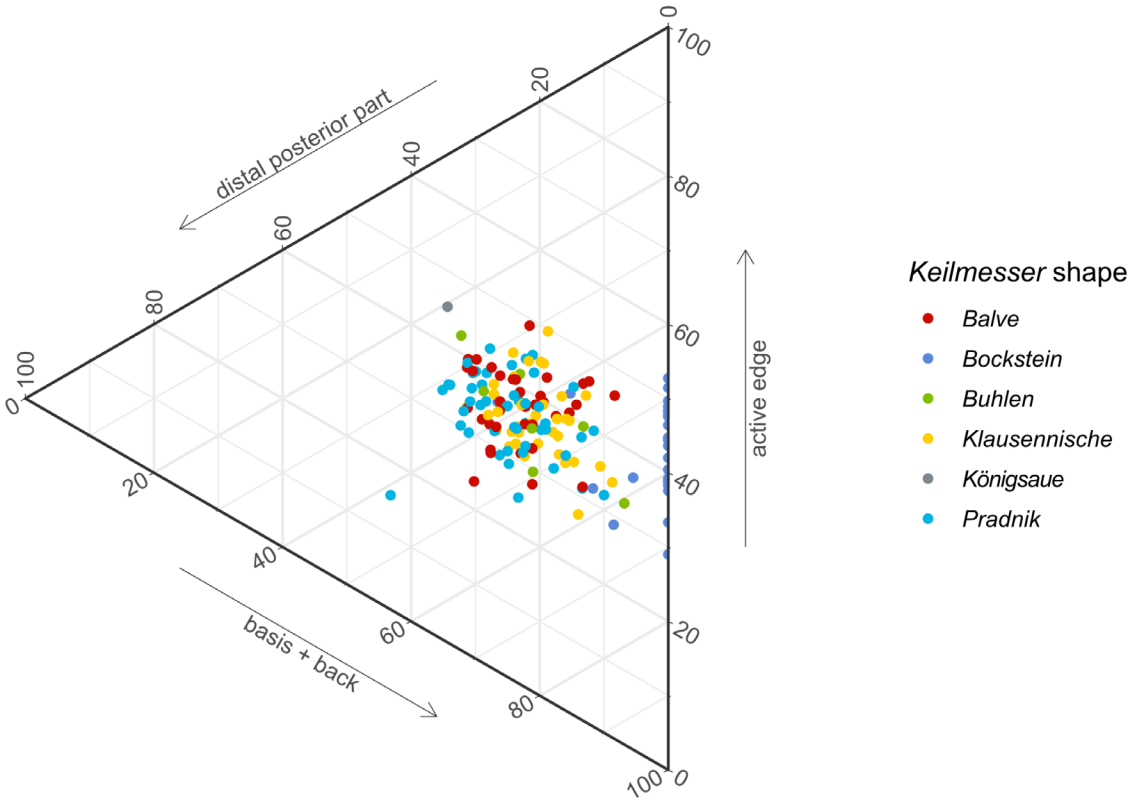

Fig. 82 Size-independent comparison of the shape variation in the perimeter of the complete *Keilmesser* from Balver Höhle, showing the ratio of the perimeter sections back and base, distal posterior part and active edge. The data points are coloured based on the assigned *Keilmesser* shape.

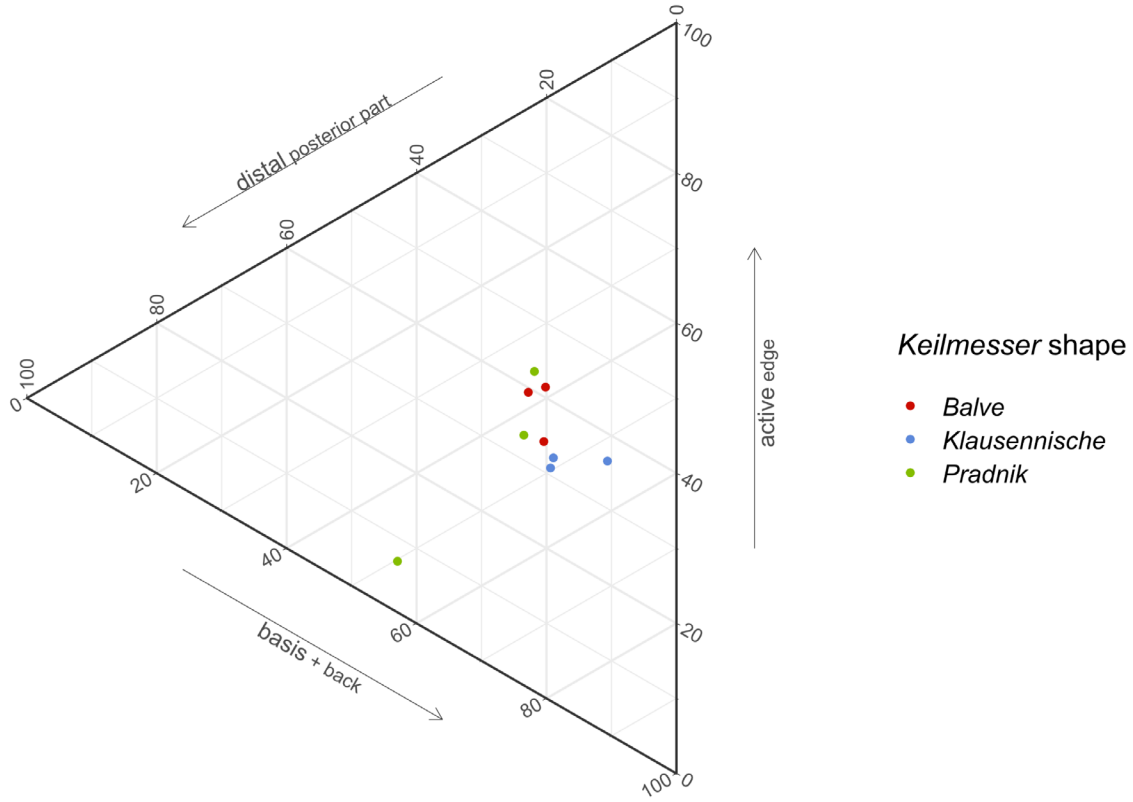

Fig. 83 Size-independent comparison of the shape variation in the perimeter of the complete *Keilmesser* from Ramioul, showing the ratio of the perimeter sections back and base, distal posterior part and active edge. The data points are coloured based on the assigned *Keilmesser* shape.

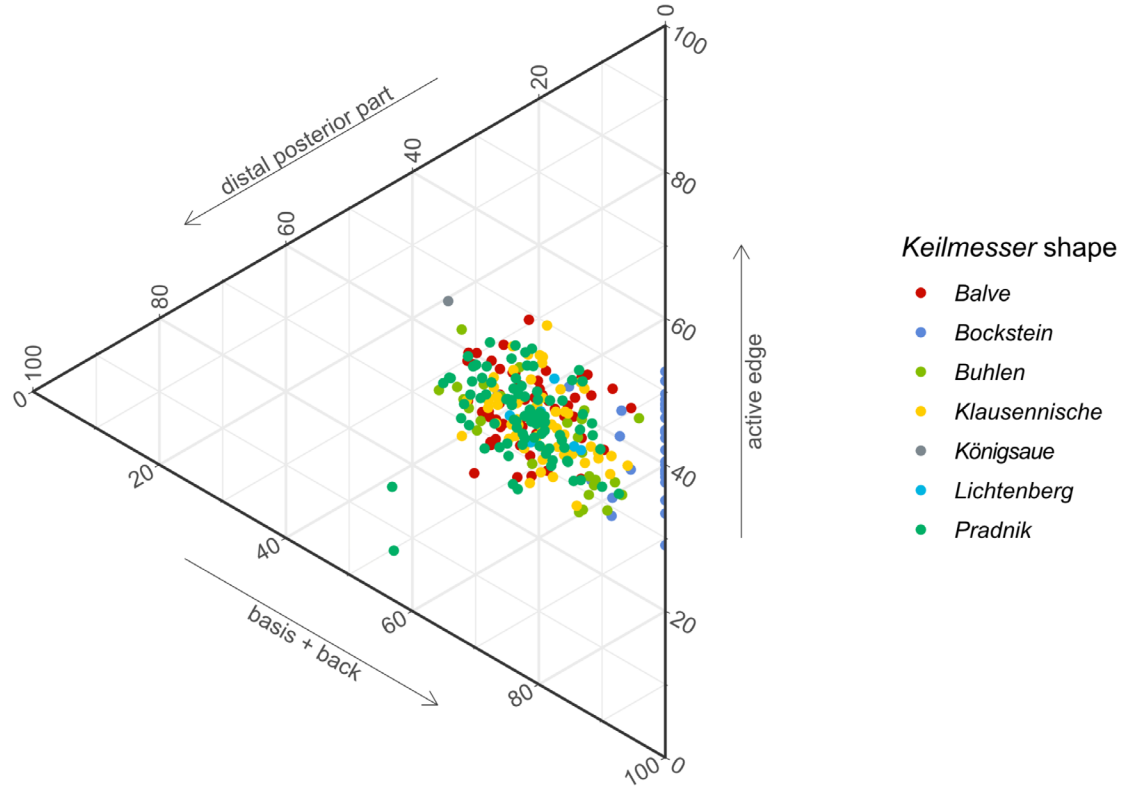

Fig. 84 Size-independent comparison of the shape variation in the perimeter of the complete *Keilmesser* from Buhlen, Balver Höhle and Ramioul, showing the ratio of the perimeter sections back and base, distal posterior part and active edge. The data points are coloured based on the assigned *Keilmesser* shape.

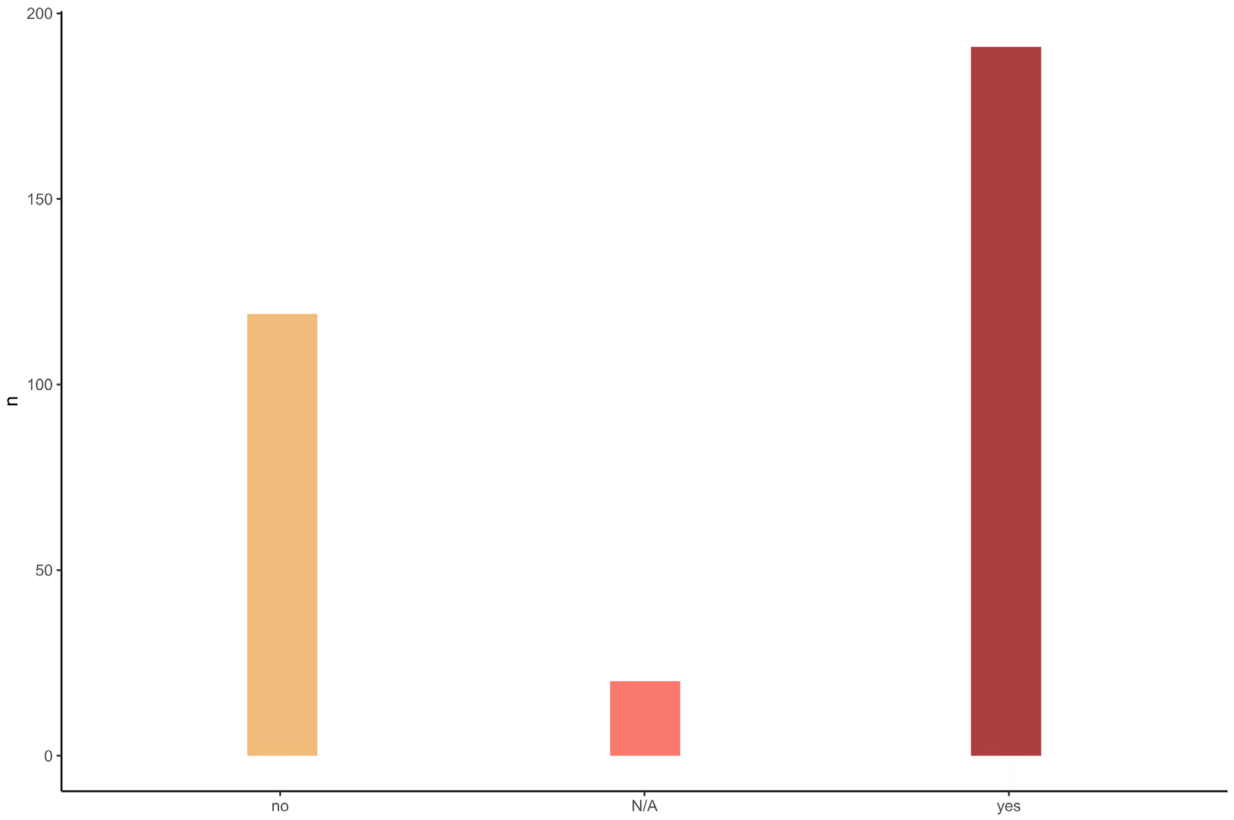

Fig. 85 Tool modification by the application of the *Prądnik method* for the complete *Keilmesser* and *Keilmesser* tips from Buhlen (n = 111, n = 15), Balver Höhle (n = 158, n = 21) and Ramioul (n = 9). In some cases (N/A), it was not possible to approve the application with certainty.

data. In the case of the *Bockstein Keilmesser*, the distal posterior part is missing (± 0 mm). Consequently, the *Keilmesser* of this shape can be found on one axis and not somewhere in the middle of the graph.
The described distribution of the data is relevant for the analysed *Keilmesser* from all three sites. The data taken together displays all data points distributed »randomly« together without clustering into distinct groups. Noticeable is the location of the plotted points. The data plots are not in the middle of the ternary plot, they all tend to be closer to the active edge axis. The other scenario would be expected if the proportions of the three perimeter sections are equal in length.
The fact that the measured values do not match with the morphologically defined *Keilmesser* shapes raises the question of the relevance or correctness of this classification. Rather, it should be questioned why the *Keilmesser* shapes seem to reflect some transitional stages and whether processes such as reworking, sharpening or transformation may cause the differences in the morphology of *Keilmesser* (Jöris 2001; 2004; Jöris/Uomini 2019).

Application of the *Prądnik method*

The majority of the *Keilmesser* from the three sites Buhlen, Balver Höhle and Ramioul display a special modification in the distal part of the tool. The application of the so-called *Prądnik method* is evident by one or multiple negatives on the tool surface resulting from the removal of an elongated lateral spall. For this part of the analysis, only complete and not fragmented *Keilmesser* were considered.

Nearly three quarter (73.0 %, n = 92) of the *Keilmesser* assemblage from Buhlen attests the edge modification by the application of the *Prądnik method*. Out of these, n = 77 display only one negative. It is therefore likely that the *Prądnik method* was applied only once. The remaining n = 15 artefacts of the assemblage are characterised by two or more superimposed negatives. A small amount of n = 26 *Keilmesser* show no evidence of a modification in the distal tool part. Some pieces are classified as undetermined. For these n = 8 artefacts it is not possible to approve the modification or not. In some of these cases, the artefacts are *Keilmesser tips*.
As mentioned above, also at Balve the *Prądnik method* was regularly applied to the *Keilmesser*. With n = 91 artefacts, this counts for half of the artefacts (50.8 %). Recognisable by superimposed negatives, n = 8 of these tools show evidence for the repeated application. More *Keilmesser* than in Buhlen, n = 82, do not display a modification in the distal tool part. For n = 6 *Keilmesser*, a point could not be made.
The same overall picture can be found in Ramioul. Almost all (n = 8) *Keilmesser* clearly document the application of the *Prądnik method*. One of these artefacts also displays a multiple application. Only one *Keilmesser* does not show a modification by the *Prądnik method* in the distal area of the tool.
The majority of *Keilmesser* from the three sites are bifacially retouched, but more interestingly regarding the edge design is the special modification in the distal area of the tool's active edge. The numbers taken together result in the following percentage distribution: 60.8 % (n = 191) of all *Keilmesser* are modified by the *Prądnik method* whereas 34.7 % (n = 109) are not (**fig. 85**). The reaming 4.5 % (n = 14) artefacts are undetermined regarding the application. A small percentage of 12.6 % (n = 24) is clearly characterised be a repeated application, indicated by superimposed negatives.

Prądnik spalls

The so-called *Prądnik spalls,* which result from the application of the *Prądnik method* on *Keilmesser* or *Prądnik scrapers,* are part of the studied inventories. In total, n = 159 *Prądnik spalls* were analysed. Due to the fact, that no *Prądnik spalls* from the assemblage in Ramioul could be selected for this study, this part of the analysis only focuses on the artefacts from Buhlen (n = 42) and Balve (n = 117).
The results presented in the following are based on a classification of the *Prądnik spalls* as primary or secondary spalls and the determination of the artefact laterality. In a further step, the dimensions of the *Prądnik spalls* will be addressed.

Morphometric quantitative analysis

The length, width and thickness of the *Prądnik spalls* was measured on the maximum extend, respectively. Only n = 36 of the n = 42 studied *Prądnik spalls* from Buhlen are complete and thus relevant for the analysis. The other *Prądnik spalls* are either distal (n = 3) or proximal (n = 3) fragments. The measurements of these pieces can be found on GitHub [https://github.com/lschunk/Lithic_analysis_archaeology]. The complete *Prądnik spalls* can be classified in a size range from 21.0 mm to 56.0 mm length (**figs 86. 89**). The arithmetic mean of the length is 35.1 mm. The minimum and maximum extension of the width are 8.0 mm and 31.0 mm, with an arithmetic mean value of 16.0 mm (**fig. 90**). The thickness is ranging between 2.0 mm and 13.0 mm (**fig. 91**). The arithmetic mean amounts to 4.7 mm.
As in Buhlen, not all *Prądnik spalls* from Balve are complete pieces. While the majority of the *Prądnik spalls* are complete (n = 110), also n = 4 distal and n = 3 medial fragments belong to the *Prądnik spall* assem-

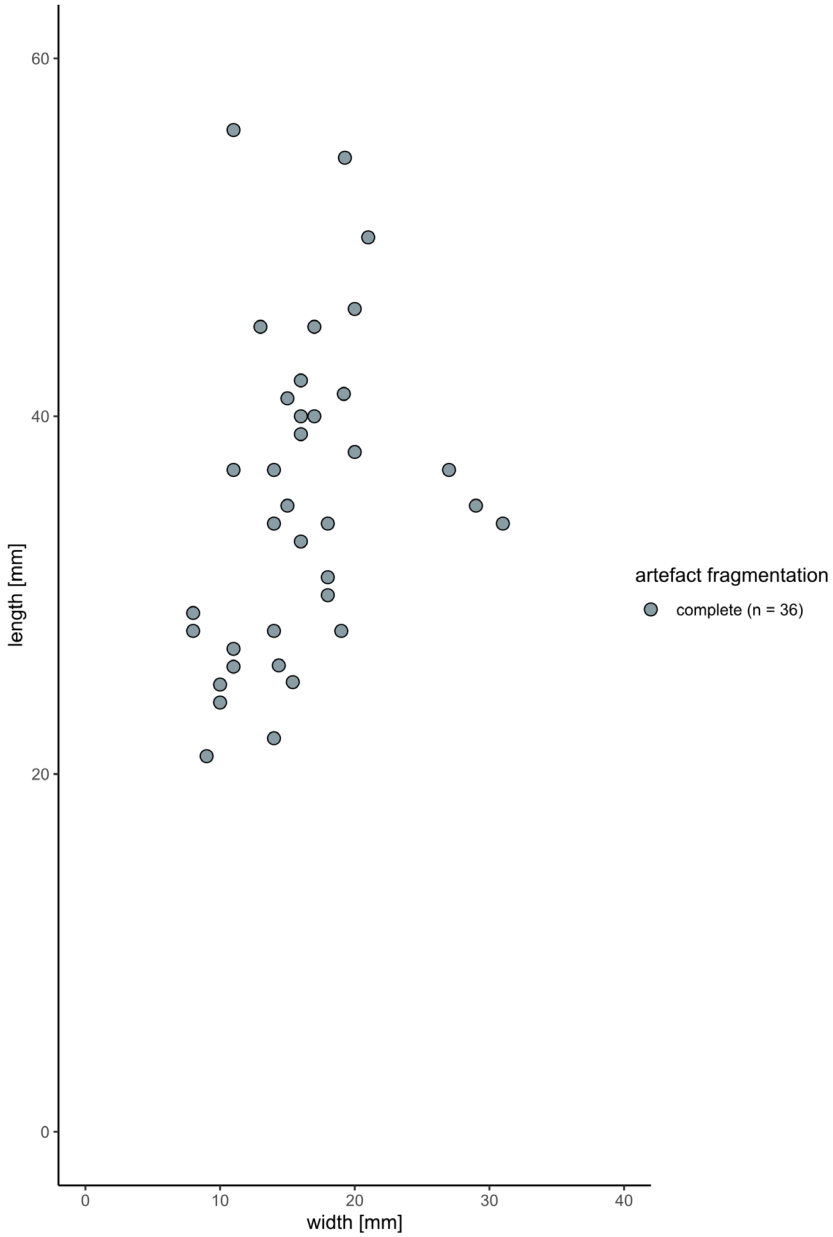

Fig. 86 Length-width ratio of the complete *Prądnik spalls* (n = 36) from Buhlen.

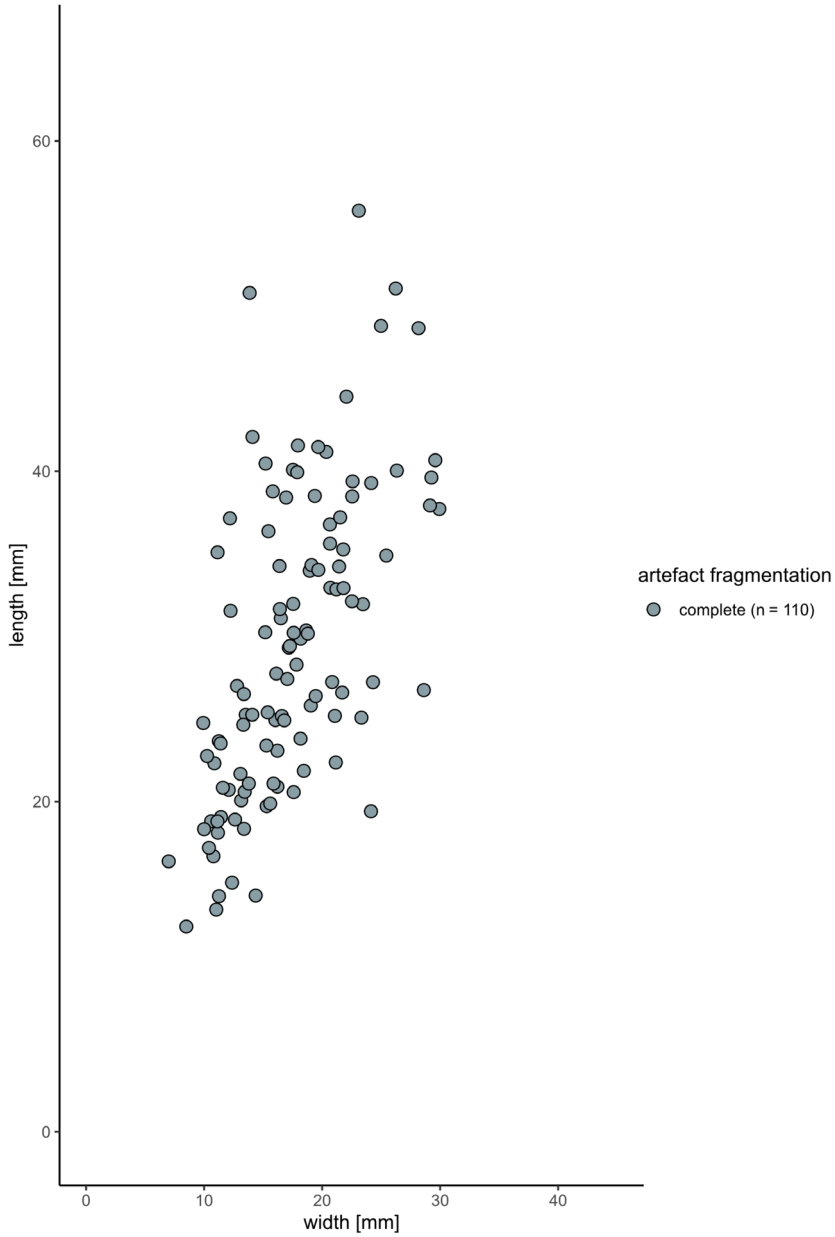

Fig. 87 Length-width ratio of the complete *Prądnik spalls* (n = 110) from Balver Höhle.

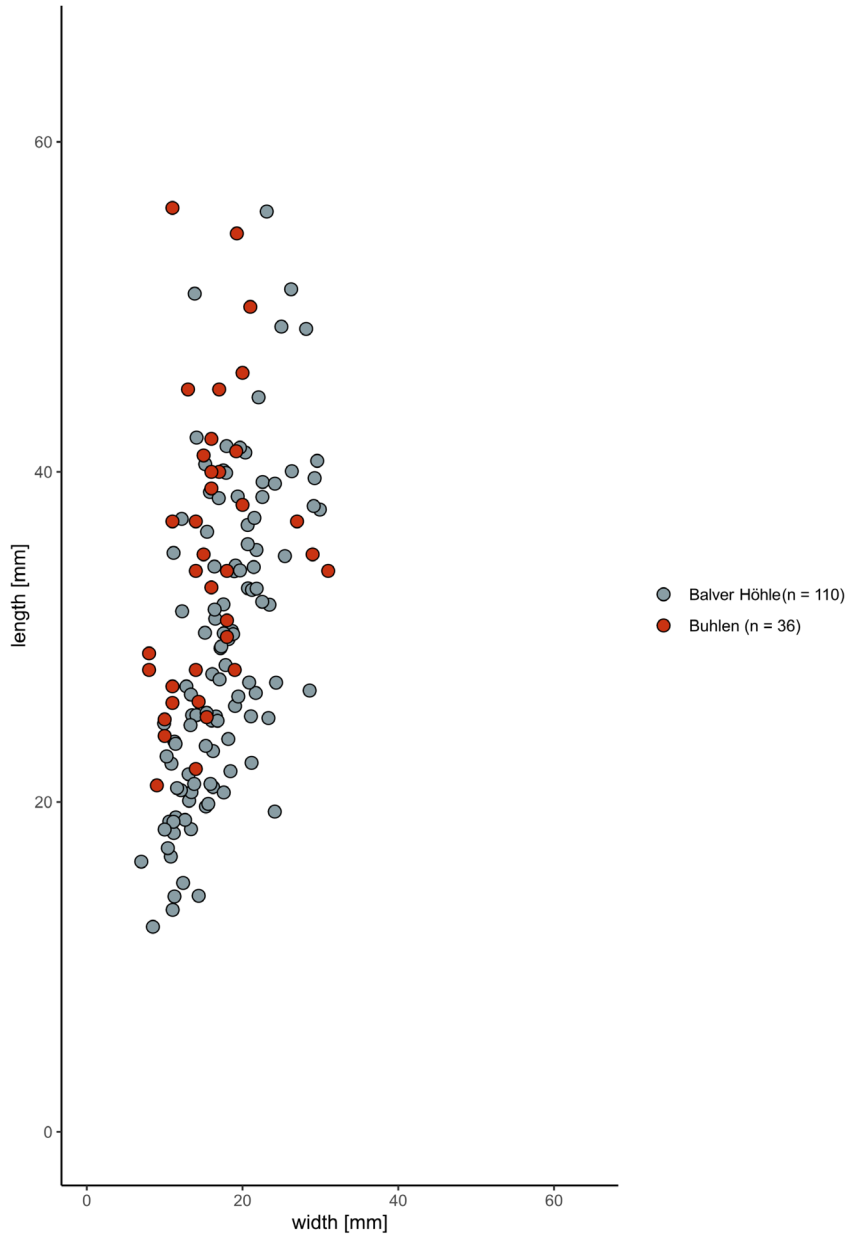

Fig. 88 Length-width ratio of the complete *Prądnik spalls* from Buhlen (n = 36) and Balver Höhle (n = 110).

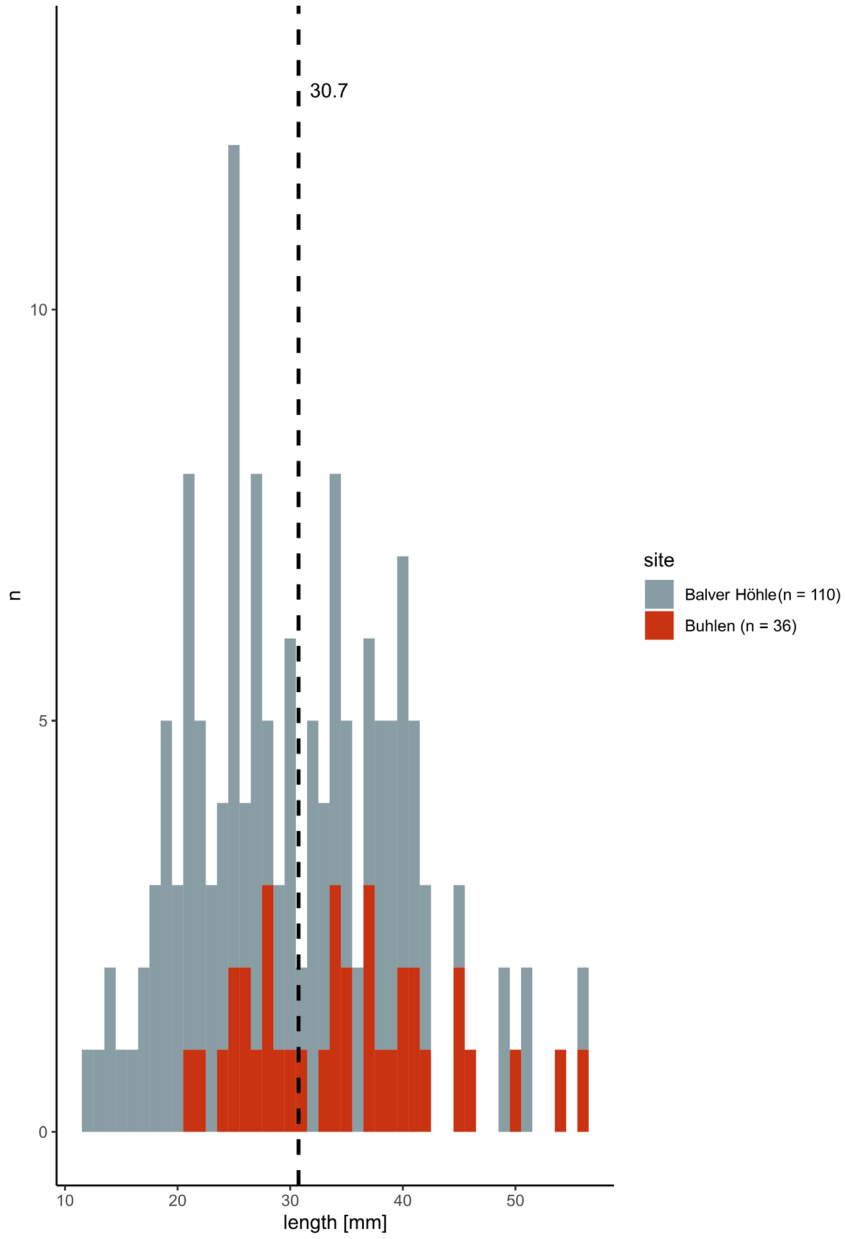

Fig. 89 Maximal length of the complete *Prądnik spalls* from Buhlen (n = 36) and Balver Höhle (n = 110). The dashed line indicates the arithmetic mean value.

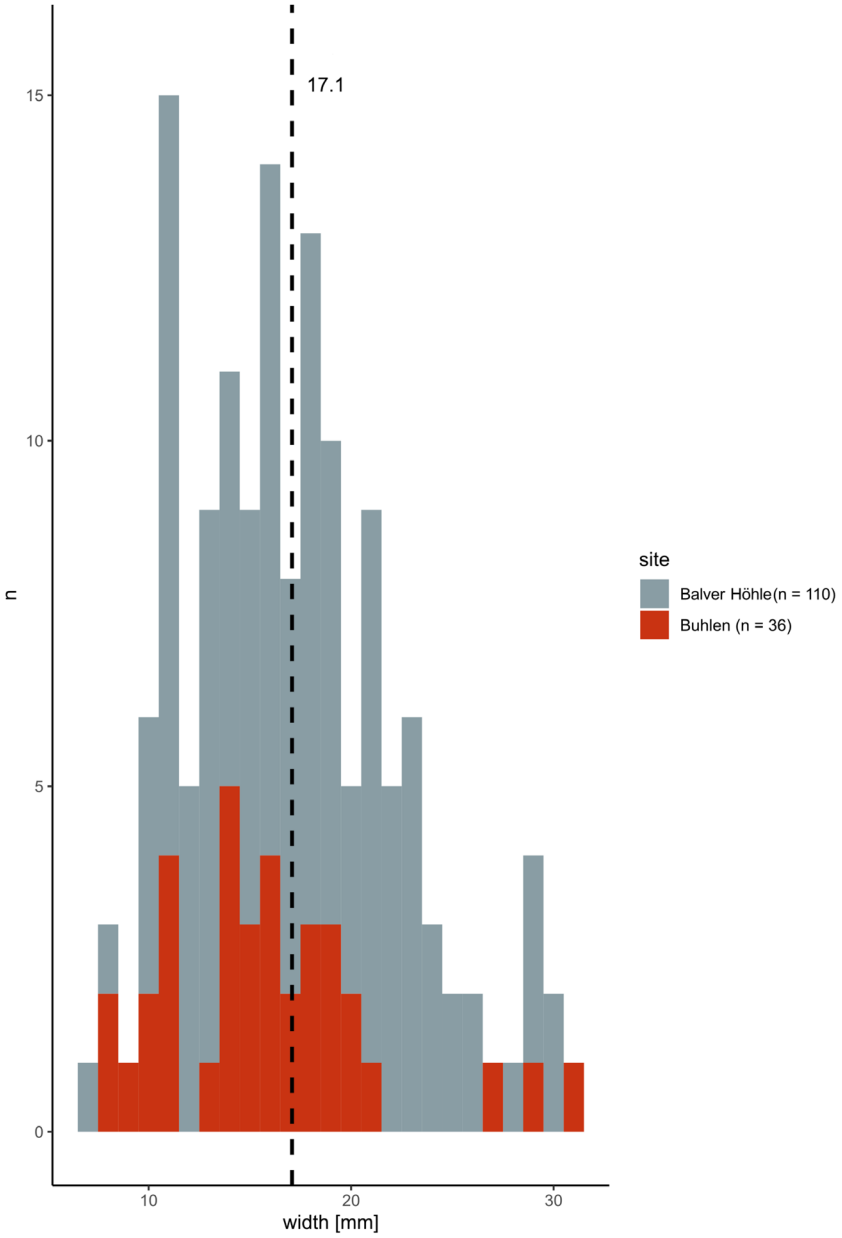

Fig. 90 Maximal width of the complete *Prądnik spalls* from Buhlen (n = 36) and Balver Höhle (n = 110). The dashed line indicates the arithmetic mean value of the complete and fragmented *Prądnik spalls* together.

blage. In Balve, the complete *Prądnik spall* length ranges between 12.4 mm and 55.8 mm (**figs 87. 89**). The arithmetic mean is 29.3 mm. The margin concerning the width is 7.0 mm and 29.3 mm with an arithmetic mean value of 17.4 mm (**fig. 90**). The minimum thickness of the *Prądnik spalls* is 2.14 mm and the maximum is 11.0 mm (**fig. 91**). The arithmetic mean amounts to 6.0 mm.

The data generated from the two sites shows, that the *Prądnik spalls* from Buhlen and Balve have comparable dimensions. To summarize, the analysed complete *Prądnik spalls* from the two sites together (n = 146) are between 12.4 mm and 56.0 mm long (**figs 88-89**). The arithmetic mean value thereby is 30.7 mm. The width extends from minimum 7.0 mm to maximum 31.0 mm with an arithmetic mean of 17.1 mm (**fig. 90**). The thickness is ranging between 2.0 mm and 13.0 mm (**fig. 91**). The arithmetic mean value for the thickness is 5.7 mm.

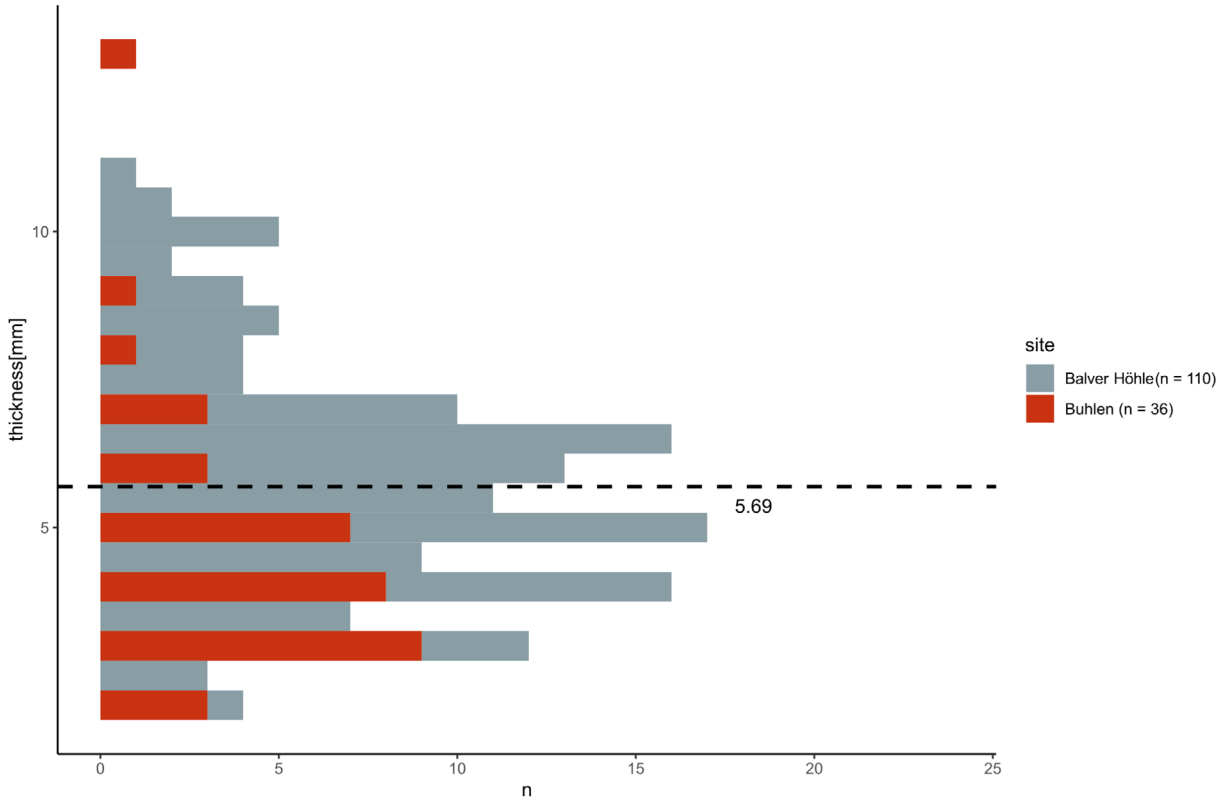

Fig. 91 Maximal thickness of the complete *Prądnik spalls* from Buhlen (n = 36) and Balver Höhle (n = 110). The dashed line indicates the arithmetic mean value of the complete and fragmented *Prądnik spalls* together.

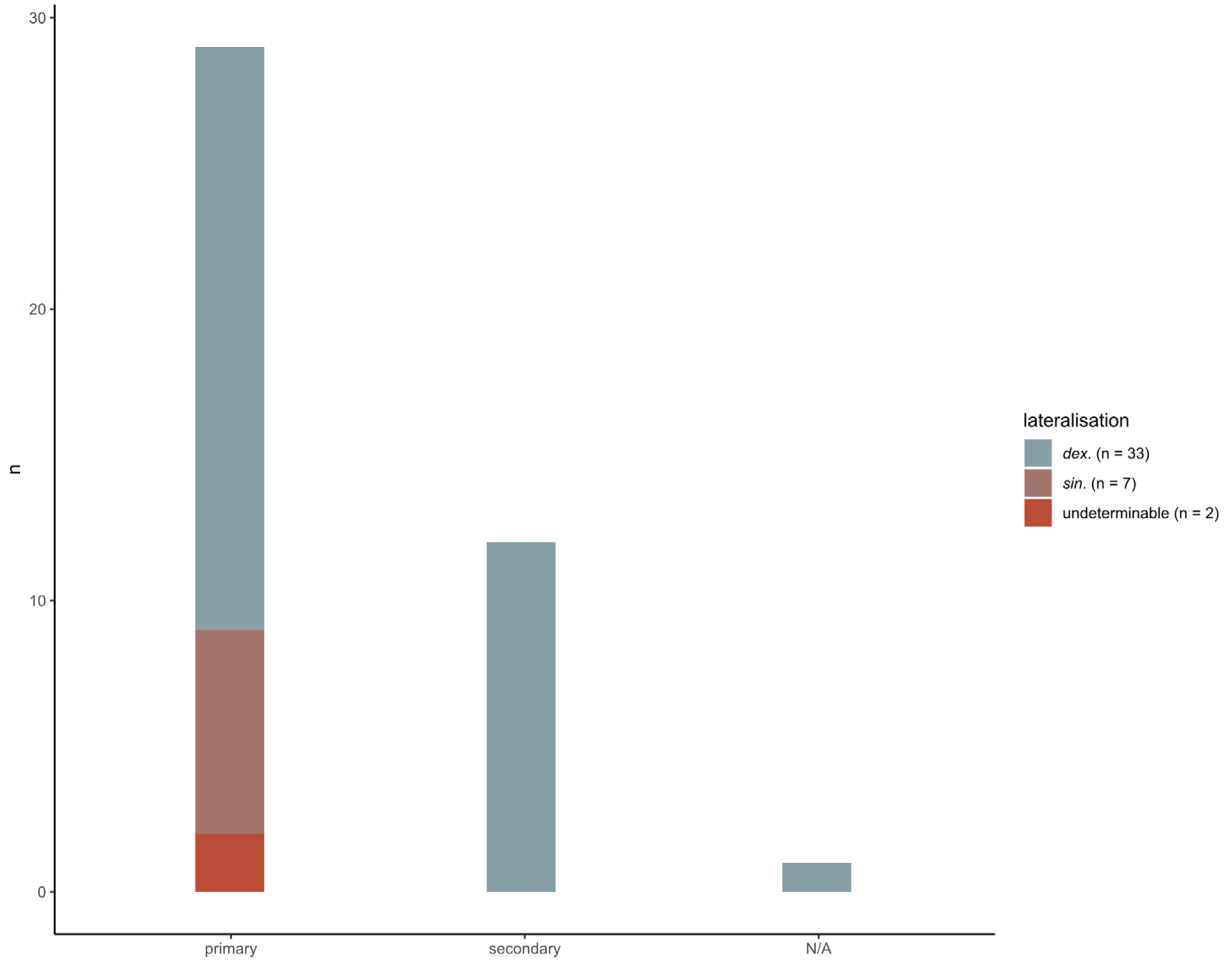

Fig. 92 Classification of the *Prądnik spalls* (n = 42) from Buhlen. The colours indicate the laterality of the artefacts.

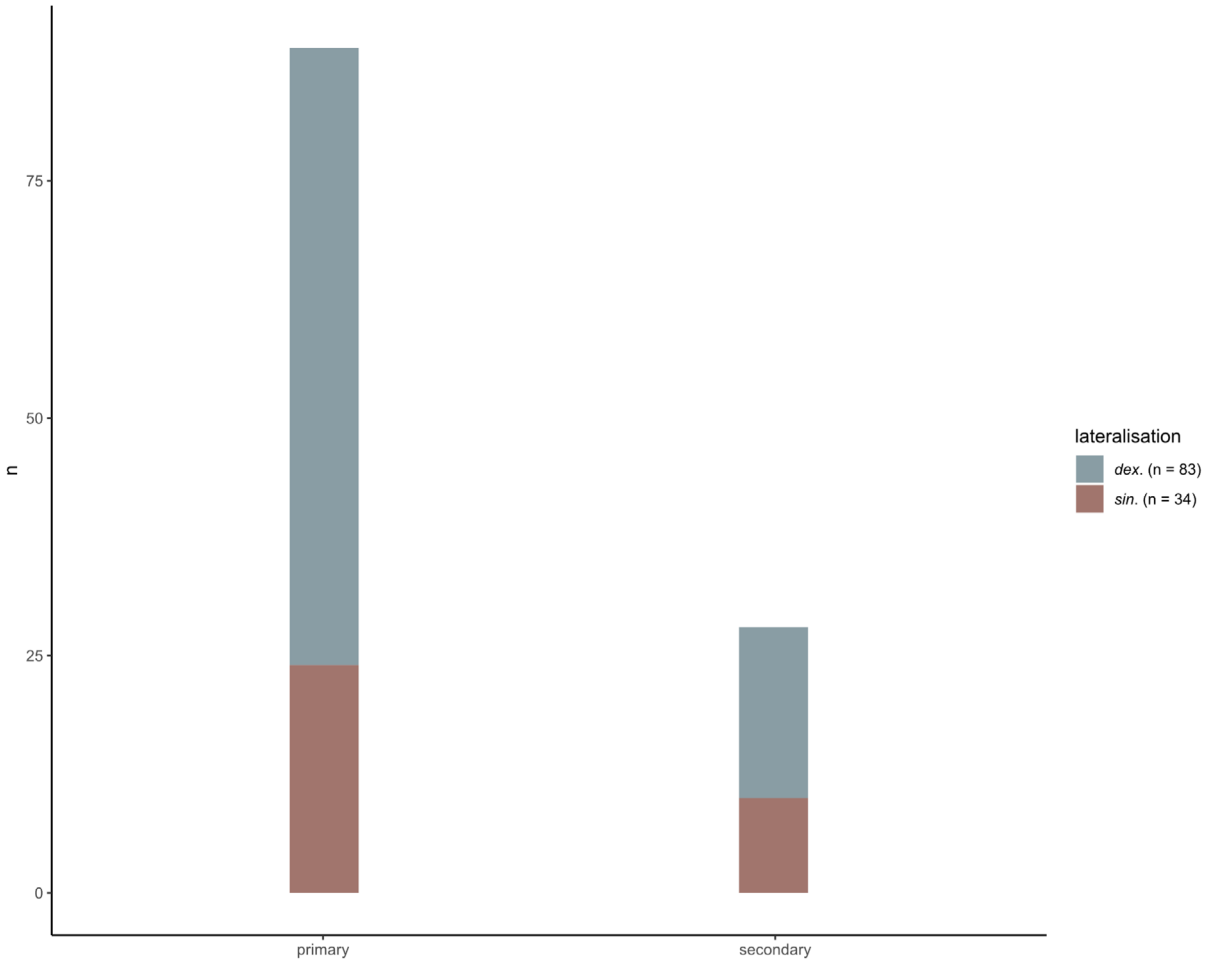

Fig. 93 Classification of the *Prądnik spalls* (n = 117) from Balver Höhle. The colours indicate the laterality of the artefacts.

Classification

The *Prądnik spalls*, which emerge by the application of the *Prądnik method*, can be subdivided in primary and secondary spalls. The n = 42 analysed *Prądnik spalls* from the Buhlen inventory can be separated in n = 29 primary and n = 12 secondary spalls (**fig. 92**). One artefact could not be attributed due to its fragmentation.
In Balve, in total n = 117 *Prądnik spalls* were analysed (**fig. 93**). Here, the primary *Prądnik spalls* predominate with n = 89 pieces, too. Secondary *Prądnik spalls* are represented with n = 28 artefacts.
The results from the two sites taken together lead to a percentage of 74.2 % primary to 25.2 % secondary *Prądnik spalls* (**fig. 94**).

Lateralisation

Similar as for the *Keilmesser* and *Prądnik scrapers*, a lateralisation can also be determined for the *Prądnik spalls* removed from these tools (**tab. 14**).

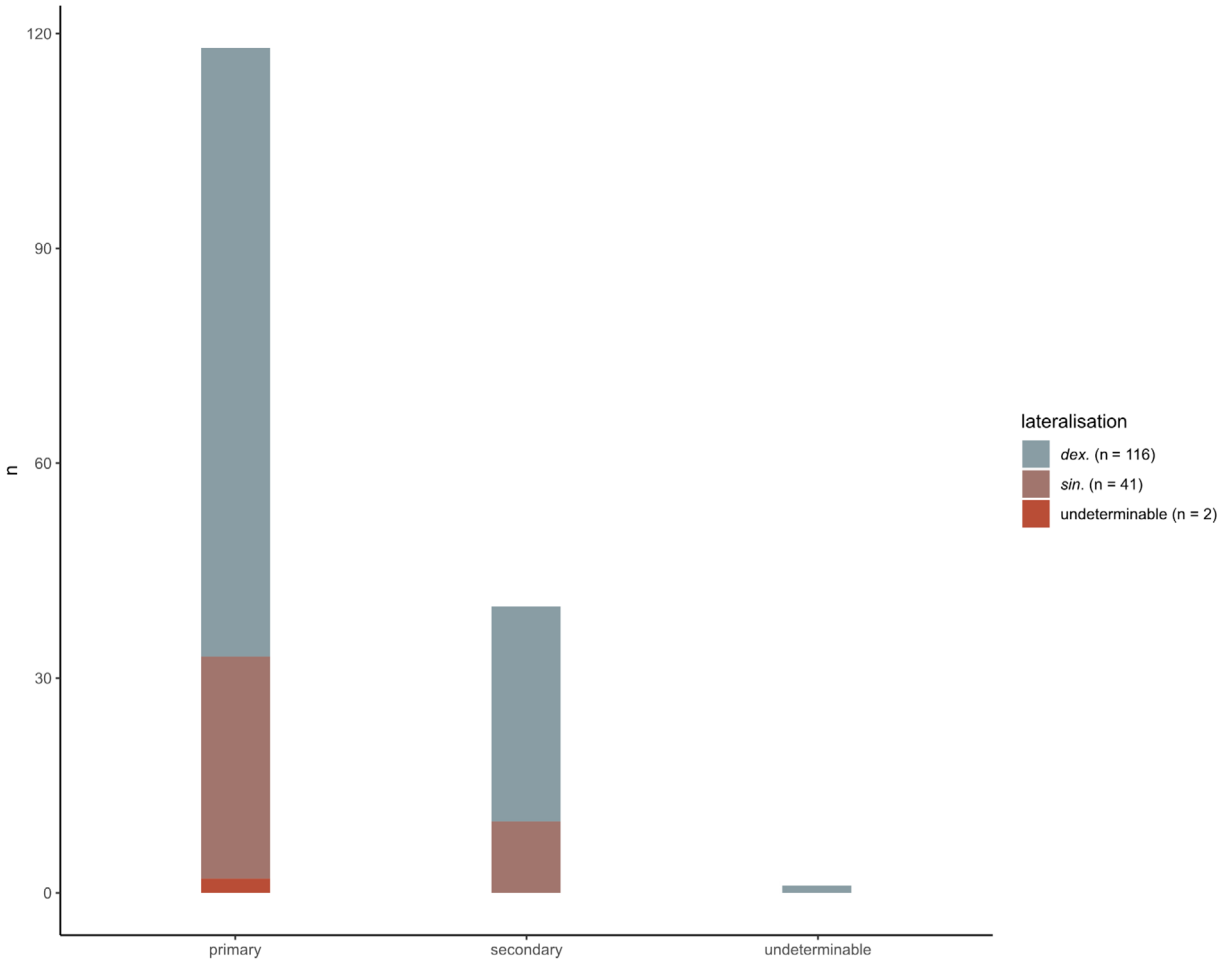

Fig. 94 Classification of the *Prądnik spalls* from Buhlen (n = 42) and Balver Höhle (n = 117). The colours indicate the laterality of the artefacts.

As for the tools, the *Prądnik spalls* from Buhlen are by a majority right-sided spalls (**fig. 94**). Next to the n = 29 right-lateral artefacts, n = 13 pieces are documented as left-lateral. These left-lateral *Prądnik spalls* are without exception primary spalls. However, the right-sided *Prądnik spalls* can be categorised as primary (n = 20) and secondary (n = 7) pieces.

A dominance of right-sided *Prądnik spalls* becomes also evident in the assemblage from Balve with n = 69 pieces. A description as left-lateral *Prądnik spalls* is possible for n = 28 artefacts. Both, right- as well as left-sided *Prądnik spalls* consist of primary and secondary spalls.

site		*Prądnik spall*		
		sin.	*dex.*	total
Buhlen	n	13	29	**130**
	%	31.0	69.1	100.0
Balve	n	34	83	**117**
	%	29.1	70.9	100.0
total	**n**	**47**	**112**	**159**
	%	29.6	70.4	100.0

Table 14 Determination of the tool lateralisation of the *Prądnik spalls* from Buhlen and Balver Höhle.

In total, 74.2 % (n = 118) of the analysed *Prądnik spalls* from Buhlen and Balve are documented as primary spalls, whereas 25.2 % (n = 40) of the pieces count as secondary spalls. The overall predominating right-sidedness of the *Keilmesser* and *Prądnik scrapers* is also reflected in the laterality of the *Prądnik spalls.* 61.2 % (n = 98) of the pieces are right-lateral, 25.8 % (n = 41) are left-lateral.

QUANTIFICATION OF EDGE DESIGN

One relevant aspect concerning tool design is the edge angle. Edge angle measurements have been taken on selected artefacts. The sampling strategy thereby was explained in the previous method chapter, resulting in a sub-sample of n = 226 artefacts (**tab. 8**). Only complete artefacts were selected. These artefacts can be divided in n = 157 *Keilmesser*, n = 18 *Keilmesser* tips, n = 20 *Prądnik scrapers* and n = 21 *Prądnik spalls*. Also for the edge angle measurements, artefacts not belonging to the selected artefact categories were relevant. Thus, n = 8 scraper as well as n = 2 flakes were sampled for reference as outgroup. The edge angles here was measured with a semi-automated, script-based method. Hence, the n = 226 artefacts have been scanned with a 3D scanner (AICON smartScan-HE R8, Hexagon, Germany) in order to create 3D models for the application of the method.

Edge angle variability

The edge angles of the scanned tools were calculated in order to understand the variability of the angle along the entire tool edge. Moreover, the specific method was also applied to document the changes of the edge angle from the intersection of dorsal and ventral surfaces towards the middle of the artefact. As pointed out already earlier, one mean value *per* tool is thus not sufficient and does not allow for any interpretation concerning the internal variability of the edge design within and between tools. In order to explain the resulting data, certain arithmetic mean values need to be mentioned here, though. Every individual measured angle can be review on GitHub [https://github.com/lschunk/edge_angle_analysis]. There, the raw data, the derived data and a plot of each single artefact can be found and accessed.
For each scanned artefact, ten horizontal sections were defined. Starting at the edge of the tool, each section had a length of 12 mm towards both surfaces (ventral and dorsal) (**figs 23-25**). Based on these horizontal sections, the measurements were taken in 1 mm steps starting at the intersection. Meaning, up to twelve measurements per section were taken.
As explained in the methods chapter, three different measurement procedures were applied for each tool. From earlier tests, which also have been done on objects with a known edge angle, it could be noticed, that the different measurement system led to slightly different results. While the »2-line« and the »best-fit« procedures produce similar results, the results from the »3-point« procedure vary more strongly. It is likely that the »3-point« measurement procedure deals well with simple structures and smooth surfaces. For instance, the »3-point' procedure works perfectly well on the experimental standard samples. The other two measurement procedures seem to be more suitable and reliable for complex structures and surface irregularities.
The results for the different artefact categories involved is presented and illustrated exemplarily for the three different measurement procedures respectively in the following. The data is split in the usual artefact categories *Keilmesser*, *Prądnik scrapers*, *Prądnik spalls*, scrapers and flakes. Additionally, the *Keilmesser* are furthermore separated in *Keilmesser* with and without negative of the *Prądnik spall* removal and *Keilmesser* tips. The data calculated for the *Prądnik spalls* refers always to the edge on the dorsal surface, which was the former active edge of the *Keilmesser* or *Prądnik scraper* before the spall was detached (**fig. 95**). In order to make the herein explained quantity of data a little more comprehensible, only the results for the measurements at 2 mm, 5 mm and 10 mm distance to the intersection will be mentioned. Moreover, when analysing the data, it became obvious, that the results of the first section (distal) as well as the tenth section (proximal) most often deviate from the results of the other eight sections. The reason for that can likely be found in the

length of the vertical polyline that follows the tool edge. This polyline often slightly extents toward the distal posterior part and the base of the tool. Meaning, these results would actually reflect not the edge angle measurements for the active edge, but rather for the adjacent perimeter section. Thus, to avoid any doubts, these two sections will be excluded when presenting the data. Whenever there will be a range discussed, it always refers to the range from the second (distal) to the ninth (proximal) horizontal section. The range does not necessarily reflect the minimum and maximum values. All mentioned edge angle values are in degrees.

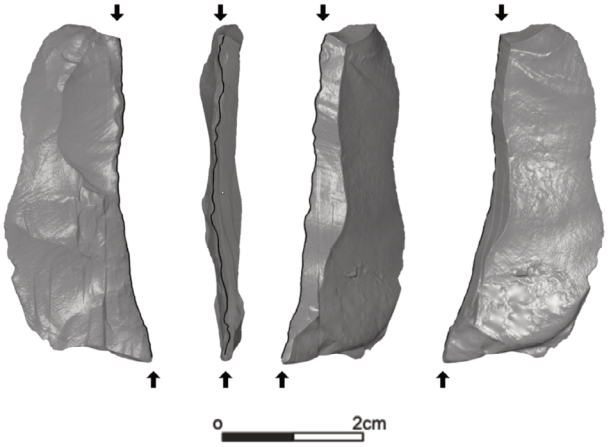

Fig. 95 3D scan of a secondary *Prądnik spall* from Buhlen (left: dorsal surface; middle: edge, right: ventral surface) illustrating on which edge (black line; indicated by the arrows) the angles have been calculated. – Not to scale.

»3-point« procedure

First, the results from the »3-point« measuring procedure is presented. The results for the *Keilmesser* are based on n = 57 artefacts (**tab. 8**). To start with the 2 mm distance, the edge angle ranges from 86.8° to 92.2° (**tab. 15**). The measurements at 5 mm distance result in a range from 70.4° to 79.6°. At the 10 mm distance, the values are 51.4° to 66.8°. For these three distances, the arithmetic mean is 89.1°, 75.3° and 61.6° respectively.

Keilmesser with a negative from the application of the *Prądnik method* are with n = 100 pieces part of the analysis (**tab. 16**). These measurements result in lower edge angles. At a distance of 2 mm from the intersection, the measurements are ranging from 79.8° to 86.1°, with an arithmetic mean value of 82.9°. The range for the 5 mm distance is from 67.0° to 74.0°. The arithmetic mean is 71.0°. At the 10 mm distance, the measurements are 54.6° to 61.2° and the arithmetic mean is 59.7°.

The next category is the *Keilmesser* tips. N = 18 pieces were scanned and analysed for the edge angle measurements (**tab. 17**). The results for the *Keilmesser* tips are similar to the previously mentioned results. Interesting here is, that n = 10 of the *Keilmesser* tips also display a negative resulting from the application of the *Prądnik method*. At the 2 mm distance, the values are 83.8° to 83.0°. The range at 5 mm is from 67.3°

section	distance to origin [in degrees]			mean per section (2-5)	mean per section (all)
	2 mm	5 mm	10 mm		
1	89.5	73.6	57.4	73.5	72.9
2	86.8	70.4	51.4	69.5	69.4
3	88.2	73.0	60.4	73.9	73.4
4	86.1	72.1	61.5	73.2	72.6
5	89.1	75.9	65.0	76.7	76.1
6	88.6	76.1	58.6	74.4	75.6
7	87.6	75.9	63.5	75.7	75.7
8	94.4	79.4	65.4	79.7	78.9
9	92.2	79.6	66.8	79.5	78.8
10	98.4	84.2	67.5	83.4	82.3

Table 15 Edge angle arithmetic mean values for *Keilmesser* (n = 57). The edge angles are calculated with the »3-point« measurement procedure.

section	distance to origin [in degrees]			mean per section (2-5)	mean per section (all)
	2 mm	5 mm	10 mm		
1	81.7	65.2	50.8	65.9	65.1
2	79.8	67.0	54.6	67.1	66.5
3	80.7	67.6	54.9	67.7	67.1
4	76.3	68.2	57.8	67.4	67.4
5	80.4	71.8	62.2	71.5	71.0
6	85.9	72.4	62.3	73.5	72.8
7	86.7	73.8	63.1	74.5	74.2
8	87.2	72.9	61.7	73.9	73.4
9	86.1	74.0	61.2	73.8	73.0
10	98.8	81.1	64.9	81.6	80.4

Table 16 Edge angle arithmetic mean values for *Keilmesser* modified by the *Prądnik method* (n = 100). The edge angles are calculated with the »3-point« measurement procedure.

section	distance to origin [in degrees]			mean per section (2-5)	mean per section (all)
	2 mm	5 mm	10 mm		
1	68.3	66.1	49.9	61.4	65.1
2	83.8	67.3	50.9	67.3	66.5
3	79.2	64.9	52.3	65.5	67.1
4	80.0	67.6	55.8	67.8	67.4
5	76.5	64.5	57.0	66.0	71.0
6	81.2	69.4	56.0	68.9	72.8
7	80.7	71.0	58.9	70.2	74.2
8	82.7	71.2	57.4	70.4	73.4
9	83.0	71.0	59.9	71.3	73.0
10	85.3	66.5	53.9	68.6	80.4

Table 17 Edge angle arithmetic mean values for *Keilmesser tips* (n = 18). The edge angles are calculated with the »3-point« measurement procedure.

section	distance to origin [in degrees]			mean per section (2-5)	mean per section (all)
	2 mm	5 mm	10 mm		
1	65.6	42.2	31.6	46.5	45.7
2	55.7	43.0	33.3	44.0	44.2
3	53.4	46.0	38.5	46.0	46.2
4	63.0	51.7	42.6	52.4	52.4
5	76.4	59.3	43.1	59.6	59.4
6	75.7	54.7	42.3	57.6	56.7
7	81.4	57.0	44.6	61.0	59.9
8	74.4	62.9	46.2	61.2	60.6
9	80.0	66.4	48.3	64.9	63.9
10	85.8	67.8	49.2	67.6	65.8

Table 18 Edge angle arithmetic mean values for *Prądnik scrapers* (n = 20). The edge angles are calculated with the »3-point« measurement procedure.

to 71.0°. At a distance of 10 mm from the intersection, the values are 50.9 to 59.9°. The arithmetic mean values amount to 80.9°, 68.4° and 56.0°.

N = 20 *Prądnik scrapers* were included in the analysis (**tab. 18**). From 55.7° to 80.0° is the range at the 2 mm distance. The measurements ranging from 43.0° to 66.4° at the 5 mm distance. Significantly lower are the values at 10 mm. They range from 33.3° to 48.3°. This leads to arithmetic mean values of 70.0°, 55.1° and 42.4° per mentioned distance.

Table 19 Edge angle arithmetic mean values for *Prądnik spalls* (n = 21). The edge angles are calculated with the »3-point« measurement procedure.

section	distance to origin [in degrees]			mean per section (2-5)	mean per section (all)
	2 mm	5 mm	10 mm		
1	54.3	32.1	19.6	35.3	37.4
2	59.5	38.8	17.9	38.7	38.9
3	63.4	41.6	17.2	40.7	40.8
4	64.4	40.0	18.9	41.1	41.0
5	64.5	41.8	19.5	41.9	41.6
6	72.0	46.6	20.9	46.5	45.5
7	72.5	44.7	22.0	46.4	45.0
8	73.4	45.6	22.3	47.1	45.1
9	69.4	42.1	20.4	44.0	42.7
10	56.4	35.4	18.4	36.7	36.8

Table 20 Edge angle arithmetic mean values for scrapers (n = 9). The edge angles are calculated with the »3-point« measurement procedure.

section	distance to origin [in degrees]			mean per section (2-5)	mean per section (all)
	2 mm	5 mm	10 mm		
1	79.4	55.2	52.5	62.4	59.4
2	72.3	58.5	47.1	59.3	58.3
3	89.0	65.3	55.3	69.9	69.4
4	56.8	51.2	48.6	52.2	51.8
5	74.3	57.5	49.5	60.4	59.5
6	78.8	60.3	53.6	64.2	63.3
7	76.0	59.9	50.4	62.1	61.1
8	82.4	62.6	55.7	66.9	66.2
9	80.7	71.9	61.6	71.4	70.3
10	108.9	106.7	95.6	103.7	105.1

The analysed n = 21 *Prądnik spalls* result in measurements of 59.5° and 69.4° at 2 mm distance with an arithmetic mean of 67.4° (**tab. 19**). At a distance of 5 mm, the values are 38.8° to 42.1°. The arithmetic mean values for the 5 mm distance is 42.7°. The range for the 10 mm distance is 17.9° to 20.4°. The arithmetic mean is 19.9°.

Additionally, n = 9 scrapers and n = 2 flakes were analysed as outgroup (**tab. 20**). The scrapers range at the 2 mm distance from 93.7° to 85.2°. At the 5 mm distance, the values are 74.9° to 75.2°. The measurements for the 10 mm distance are 55.0° and 75.8°. These measurements result in arithmetic mean values of 94.8°, 77.0° and 59.8° per distance respectively.

The flakes have a range of 72.3° to 80.7° at the 2 mm distance with an arithmetic mean of 76.3° (**tab. 21**). The measurements at 5 mm distance reach from 58.5° to 71.9°. The arithmetic mean value is 60.9°. At the 10 mm distance, the values are lower and range from 47.1° to 61.6°. The arithmetic mean is 52.7°.

»2-lines« procedure

With the second measuring procedure, the so-called »2-lines« procedure, deviating edge angle values were calculated.

section	distance to origin [in degrees]			mean per section (2-5)	mean per section (all)
	2 mm	5 mm	10 mm		
1	95.9	79.4	50.0	75.1	75.1
2	93.7	74.9	55.0	74.5	74.6
3	93.3	74.1	58.1	75.2	74.5
4	96.9	76.4	58.7	77.3	76.5
5	95.7	80.3	62.3	79.4	79.1
6	94.8	81.4	64.4	80.2	79.3
7	93.6	76.6	62.5	77.6	77.5
8	95.5	76.9	60.2	77.5	76.9
9	95.2	75.2	57.0	75.8	74.8
10	99.5	81.4	56.9	79.3	78.0

Table 21 Edge angle arithmetic mean values for flakes (n = 2). The edge angles are calculated with the »3-point« measurement procedure.

section	distance to origin [in degrees]			mean per section (2-5)	mean per section (all)
	2 mm	5 mm	10 mm		
1	76.5	53.9	28.2	52.9	52.6
2	73.7	51.3	28.2	51.1	49.5
3	71.9	59.2	39.2	56.8	55.9
4	72.3	58.4	45.0	58.6	58.4
5	74.3	60.8	47.0	60.7	61.1
6	77.3	59.3	45.7	60.8	59.9
7	73.7	62.8	43.8	60.1	59.7
8	81.3	60.2	40.6	60.7	60.8
9	78.4	62.7	43.1	61.4	61.9
10	83.9	66.1	43.9	64.6	63.0

Table 22 Edge angle arithmetic mean values for *Keilmesser* (n = 57). The edge angles are calculated with the »2-lines« measurement procedure.

section	distance to origin [in degrees]			mean per section (2-5)	mean per section (all)
	2 mm	5 mm	10 mm		
1	63.4	48.9	30.8	47.7	46.8
2	66.3	52.9	30.9	50.0	50.4
3	66.7	50.6	35.3	50.9	51.3
4	68.3	55.3	43.8	55.8	55.1
5	69.6	62.8	46.8	59.7	58.4
6	71.3	58.4	45.0	58.2	58.8
7	74.5	59.3	44.4	59.4	59.5
8	72.5	59.3	44.3	58.7	58.1
9	74.6	59.9	41.9	58.8	57.5
10	82.8	59.8	42.0	61.5	59.9

Table 23 Edge angle arithmetic mean values for *Keilmesser* modified by the *Prądnik method* (n = 100). The edge angles are calculated with the »2-lines« measurement procedure.

For *Keilmesser*, the range at 2 mm is from 73.7° to 78.4° (**tab. 22**). At a distance of 5 mm from the intersection, the values are 51.3° and 62.7°. The range at 10 mm is from 28.2° to 43°. The arithmetic means for these three distances are 75.4°, 59.3° and 41.5° respectively.

Keilmesser with a negative from the removed *Prądnik spall* do have slightly smaller values at the 2 mm and 5 mm distance compared to the beforehand mentioned results for the *Keilmesser* (**tab. 23**). At 2 mm dis-

Table 24 Edge angle arithmetic mean values for *Keilmesser* tips (n = 18). The edge angles are calculated with the »2-lines« measurement procedure.

section	distance to origin [in degrees]			mean per section (2-5)	mean per section (all)
	2 mm	5 mm	10 mm		
1	65.0	41.6	28.5	45.0	46.8
2	64.8	50.5	30.3	48.5	50.4
3	62.8	52.1	32.1	49.0	51.3
4	68.2	54.7	34.2	52.4	55.1
5	64.6	60.9	31.7	52.4	58.4
6	68.2	57.3	33.2	52.9	58.8
7	64.9	66.1	31.6	54.2	59.5
8	70.3	57.8	34.3	54.1	58.1
9	71.2	60.7	42.2	58.0	57.5
10	61.9	47.2	35.4	48.2	59.9

Table 25 Edge angle arithmetic mean values for *Prądnik scrapers* (n = 20). The edge angles are calculated with the »2-lines« measurement procedure.

section	distance to origin [in degrees]			mean per section (2-5)	mean per section (all)
	2 mm	5 mm	10 mm		
1	41.5	26.2	25.8	31.2	30.3
2	42.3	33.6	15.8	30.6	30.6
3	43.8	37.1	17.2	32.7	34.7
4	49.5	40.9	24.1	38.2	39.4
5	59.5	40.5	23.8	41.3	39.4
6	55.8	36.9	20.5	37.7	38.0
7	59.9	36.1	24.4	40.1	41.2
8	62.6	45.6	21.8	43.3	41.4
9	64.8	50.9	16.2	44.0	42.5
10	67.6	47.5	16.7	43.9	43.7

tance, these *Keilmesser* have a range of 66.3° to 74.6 ° with a mean value of 70.5°. The measurements at 5 mm range from 52.9° to 59.9°. The arithmetic mean is 57.3°. At the 10 mm distance, the measurements are 30.9° to 41.9° and the arithmetic mean is 41.6°. Thus, the arithmetic means at the 10 mm distance for *Keilmesser* and *Keilmesser* with negative are nearly identical. It is likely that the negative often does not reach up to 10 mm width on the surface.

The measurements for the *Keilmesser* tips result in the following values (**tab. 24**). The range at the 2 mm distance from the intersection is 64.8° to 71.2°. For the measurements at the 5 mm distance, the values are 50.5° and 60.7°. At 10 mm distance to the intersection, the values ranging from 30.3° to 42.2°. The edge angle measurements lead to arithmetic mean values of 66.9°, 57.5° and 33.7° per mentioned distance.

The calculated edge angles for the *Prądnik scrapers* result in measurements of 42.3° and 64.8° at 2 mm distance with an arithmetic mean of 54.8° (**tab. 25**). At a distance of 5 mm, the values are 33.6° to 50.9°. The arithmetic mean values for the 5 mm distance is 40.0°. The range for the 10 mm distance is 15.8° to 16.2°. The arithmetic mean is 20.5°.

For *Prądnik spalls*, the values measured at the 2 mm distance are 44.4° and 50.7° (**tab. 26**). At the 5 mm distance to the intersection, a range from 20.7° to 14.9° could be calculated. The values at 10 mm are ranging from 21.4° to 16.1°. The arithmetic mean for these three distances are 47.6°, 18.5° and 18.8° respectively. The measured scrapers display a range of 71.7° to 75.6° at the 2 mm distance with an arithmetic mean of 77.5° (**tab. 27**). The measurements at 5 mm distance reach from 53.7° to 52.2°. The arithmetic mean value is 55.2°. At the 10 mm distance, the values range from 22.9° to 25.8°. The arithmetic mean is 33.8°.

section	distance to origin [in degrees]			mean per section (2-5)	mean per section (all)
	2 mm	5 mm	10 mm		
1	32.8	18.3	21.7	24.3	24.9
2	44.4	20.7	21.4	28.8	28.5
3	43.9	20.5	21.1	28.5	28.5
4	44.4	18.1	20.3	27.6	26.7
5	43.9	17.7	17.8	26.5	26.5
6	53.1	18.5	21.3	31.0	29.5
7	47.5	20.3	16.9	28.2	27.6
8	52.7	17.3	15.6	28.5	27.6
9	50.7	14.9	16.1	27.2	25.6
10	35.3	10.2	13.3	19.6	20.5

Table 26 Edge angle arithmetic mean values for *Prądnik spalls* (n = 21). The edge angles are calculated with the »2-lines« measurement procedure.

section	distance to origin [in degrees]			mean per section (2-5)	mean per section (all)
	2 mm	5 mm	10 mm		
1	74.4	42.4	18.7	45.2	44.4
2	71.7	53.7	22.9	49.4	51.0
3	74.9	52.2	36.8	54.6	54.0
4	78.5	51.8	36.5	55.6	54.9
5	83.3	55.7	43.7	60.9	59.2
6	81.3	58.8	41.5	60.5	60.3
7	76.5	59.5	32.9	56.3	57.1
8	78.2	57.5	30.1	55.3	54.1
9	75.6	52.2	25.8	51.2	51.3
10	83.1	56.4	14.5	51.3	49.0

Table 27 Edge angle arithmetic mean values for scrapers (n = 9). The edge angles are calculated with the »2-lines« measurement procedure.

section	distance to origin [in degrees]			mean per section (2-5)	mean per section (all)
	2 mm	5 mm	10 mm		
1	54.3	30.3	24.8	36.5	39.5
2	59.6	39.7	35.5	44.9	43.3
3	69.4	48.2	39.2	52.3	53.0
4	49.9	47.3	33.9	43.7	46.2
5	55.6	44.2	40.2	46.7	46.8
6	58.3	48.7	43.3	50.1	50.7
7	60.7	42.0	44.2	49.0	48.8
8	58.3	50.6	42.8	50.6	52.5
9	78.4	52.7	51.0	60.7	59.1
10	99.9	109.9	61.5	90.4	91.3

Table 28 Edge angle arithmetic mean values for flakes (n = 2). The edge angles are calculated with the »2-lines« measurement procedure.

The flakes, also belonging to the selected outgroup, range at a distance of 2 mm to the intersection from 59.3° to 78.4° (**tab. 28**). The values displayed at the 5 mm distance are 39.7° and 52.7°. At the 10 mm distance, the measurements are 35.5° and 51.0°. For the three mentioned distances, the arithmetic means are 61.3°, 46.7° and 41.3°.

Table 29 Edge angle arithmetic mean values for *Keilmesser* (n = 57). The edge angles are calculated with the »Best-fit« measurement procedure.

section	distance to origin [in degrees]			mean per section (2-5)	mean per section (all)
	2 mm	5 mm	10 mm		
1	76.0	55.1	38.4	56.5	56.6
2	73.4	54.6	27.8	51.9	51.7
3	71.7	59.3	45.6	58.9	58.8
4	72.7	58.5	47.3	59.5	59.5
5	73.7	61.5	47.4	60.9	61.6
6	77.5	59.0	45.9	60.8	59.8
7	73.9	63.3	44.1	60.4	60.0
8	80.2	59.6	41.0	60.3	61.3
9	78.4	62.6	46.8	62.6	63.4
10	84.2	66.3	47.4	66.0	65.2

Table 30 Edge angle arithmetic mean values for *Keilmesser* modified by the *Prądnik method* (n = 100). The edge angles are calculated with the »Best-fit« measurement procedure.

section	distance to origin [in degrees]			mean per section (2-5)	mean per section (all)
	2 mm	5 mm	10 mm		
1	63.4	50.0	30.8	48.1	49.5
2	66.4	54.9	35.2	52.2	53.0
3	66.3	51.2	37.1	51.5	52.3
4	67.6	56.0	44.5	56.0	56.9
5	69.4	63.2	48.6	60.4	59.9
6	71.4	57.9	50.5	59.9	59.4
7	74.4	59.0	44.0	59.1	59.9
8	71.9	59.0	45.3	58.7	59.2
9	74.3	59.9	43.7	59.3	58.3
10	82.8	59.6	43.7	62.0	60.8

»Best-fit« procedure

Lastly, the results from the »best-fit« measurement procedure will be presented. These results are similar to the ones from the »2-lines« measurements. Since the two procedures are almost identical, except that the »best-fit« procedure interpolates the points between the 2 mm line, the similarity between the results is not surprising.

The measurements for the *Keilmesser* display a range from 73.4° to 78.4° at the 2 mm distance to the intersection (**tab. 29**). At 5 mm distance, the values range from 54.6° to 62.6°. The measurements for the 10 mm distance are 27.8° and 46.8°. The arithmetic means for these three distances are 75.2°, 59.8° and 43.2°.

Keilmesser with a negative from the application of the *Prądnik method* result again in lower edge angle values than the *Keilmesser* without modification (**tab. 30**). At a distance of 2 mm from the intersection, the measurements are ranging from 66.4° to 74.3°, with an arithmetic mean value of 70.2°. The range for the 5 mm distance is from 54.9° to 59.9°. The arithmetic mean is 57.6°. At the 10 mm distance, the measurements are 35.2° and 43.7° and the arithmetic mean is 43.6°. Also, in this case, the arithmetic mean value at the 10 mm distance is similar to the one from the *Keilmesser* without modification while the mean values at 2 mm and 5 mm are lower.

The calculated edge angles for the *Keilmesser* tips result in measurements of 63.8° and 71.1° at 2 mm distance (**tab. 31**). At a distance of 5 mm, the values are 50.4° and 62.5°. The range for the 10 mm distance is 42.5° to 41.7°. The arithmetic mean values amount to 66.7°, 58.6° and 40.3°.

section	distance to origin [in degrees]			mean per section (2-5)	mean per section (all)
	2 mm	5 mm	10 mm		
1	64.8	47.5	41.1	51.1	49.5
2	63.8	50.4	42.5	52.2	53.0
3	63.6	58.3	43.3	55.1	52.3
4	68.8	54.5	39.6	54.3	56.9
5	64.5	60.1	31.8	52.1	59.9
6	67.8	57.9	50.4	58.7	59.4
7	64.2	65.2	31.6	53.7	59.9
8	69.7	59.6	41.7	57.0	59.2
9	71.1	62.5	41.7	58.4	58.3
10	60.8	48.0	35.1	48.0	60.8

Table 31 Edge angle arithmetic mean values for *Keilmesser* tips (n = 18). The edge angles are calculated with the »Best-fit« measurement procedure.

section	distance to origin [in degrees]			mean per section (2-5)	mean per section (all)
	2 mm	5 mm	10 mm		
1	41.0	27.6	30.0	32.9	37.3
2	42.6	34.0	19.9	32.2	33.7
3	44.0	37.5	22.1	34.5	37.1
4	50.3	46.1	27.1	41.2	42.1
5	58.5	40.6	30.2	43.1	43.4
6	57.7	36.4	24.8	39.6	38.5
7	61.0	37.5	29.2	42.6	43.9
8	61.3	45.5	30.0	45.6	43.2
9	65.5	51.7	19.4	45.5	43.7
10	66.3	47.3	74.6	62.7	50.2

Table 32 Edge angle arithmetic mean values for *Prądnik scrapers* (n = 20). The edge angles are calculated with the »Best-fit« measurement procedure.

section	distance to origin [in degrees]			mean per section (2-5)	mean per section (all)
	2 mm	5 mm	10 mm		
1	37.0	19.3	23.9	26.7	34.0
2	46.0	21.9	33.3	33.7	36.6
3	43.4	20.6	23.7	29.2	31.0
4	53.5	27.5	34.0	38.3	38.7
5	43.6	18.8	27.3	29.9	32.0
6	54.0	33.6	32.0	39.9	36.6
7	47.7	19.8	24.4	30.6	33.0
8	55.1	27.3	15.6	32.7	35.0
9	54.9	15.4	25.2	31.8	33.8
10	47.4	21.0	38.3	35.6	28.0

Table 33 Edge angle arithmetic mean values for *Prądnik spalls* (n = 21). The edge angles are calculated with the »Best-fit« measurement procedure.

For the *Prądnik scrapers*, the following results were calculated with the »best-fit« measuring procedure (**tab. 32**). At the 2 mm distance to the intersection, the values are 42.6° and 65.0° with an arithmetic mean of 55.1°. The measurements at 5 mm range from 34.0° to 51.7°. The mean value is 41.2°. At the 10 mm distance, the measurements are 19.9° and 19.4° and the arithmetic mean is 25.3°.

Table 34 Edge angle arithmetic mean values for scrapers (n = 9). The edge angles are calculated with the »Best-fit« measurement procedure.

section	distance to origin [in degrees]			mean per section (2-5)	mean per section (all)
	2 mm	5 mm	10 mm		
1	72.7	41.3	34.2	49.4	46.6
2	71.1	67.8	23.1	54.0	53.6
3	74.7	50.8	53.9	59.8	55.4
4	77.7	51.6	35.9	55.1	54.9
5	82.9	55.9	45.0	61.3	59.3
6	81.8	58.0	41.3	60.4	61.6
7	76.7	60.8	32.2	56.6	57.1
8	77.6	58.4	30.5	55.5	55.7
9	74.9	52.1	43.8	56.9	54.6
10	82.6	56.5	14.3	51.1	49.3

Table 35 Edge angle arithmetic mean values for flakes (n = 2). The edge angles are calculated with the »Best-fit« measurement procedure.

section	distance to origin [in degrees]			mean per section (2-5)	mean per section (all)
	2 mm	5 mm	10 mm		
1	54.5	33.2	25.4	37.7	39.6
2	60.5	40.7	35.9	45.7	43.2
3	71.3	48.7	39.4	53.1	53.1
4	48.9	48.0	33.6	43.5	46.8
5	53.7	44.5	41.1	46.4	46.8
6	56.1	48.7	45.6	50.1	50.7
7	61.3	40.7	43.3	48.4	48.9
8	55.7	50.2	43.0	49.6	52.5
9	77.2	53.5	52.3	61.0	59.2
10	96.0	109.1	60.7	88.6	91.8

The analysed *Prądnik spalls* display at the 2 mm distance a range of 46.0° to 54.9° (**tab. 33**). At the 5 mm distance, the values range from 21.9° to 15.4°. The measurements at the 10 mm distance are 33.3° and 25.2°. The calculated arithmetic mean values of these three distances are 49.8°, 23.1° and 26.9°.
The scrapers, representing one artefact category of the sampled outgroup, display at the 2 mm distance measurements of 71.1° and 74.9° with an arithmetic mean value of 77.2 (**tab. 34**). The range for the 5 mm distance is from 67.8° to 52.1°. The arithmetic mean is 56.9°. At the 10 mm distance, the measurements are 23.1° and 43.8° and the arithmetic mean is 38.2°.
The measurements for the flakes result in a range of 60.5° to 77.2° at the 2 mm distance from the intersection (**tab. 35**). For the measurements at the 5 mm distance, the values are 40.7° and 53.5°. At 10 mm distance to the intersection, the values ranging from 35.9° to 52.3°. The edge angle measurements result in arithmetic mean values of 60.6°, 46.9° and 41.8° per mentioned distance.

Edge angle analysis

When taking all the data concerning the edge angle analysis into account, the differences in the results from the three measurement procedures are primarily noticeable. The differences between the »2-lines« and the »best-fit« procedures are comparable small. The measurements at 2 mm and 5 mm distance from the inter-

section display a variance of 0.2° up to 3.6°. Only at the 10 mm distance, a difference of 8.1° is noticeable between the results of the »2-lines' and the »best-fit« measurement procedures. The variance between these results and the results of the »3-point« measurement procedure is significantly higher. However, the results reflect the same tendencies and are not randomly different. Instead, the results calculated with the »3-point« procedure are always around 10° to 20° higher. Beforehand conducted, controlled tests with an artefact, an experimental flake and a calibrated standard angle (gauge block; edge angle known) led to the exact same conclusion. These tests were done in order to validate the reliability of the method. The results of the three measurement procedures reflect the same tendencies and patterns although the calculated edge angles with the »3-point« procedure are always higher. As mentioned earlier, it seems like the »3-point« measurement is leading to reliable results when edge angles of simple objects are measured. As soon as the object is more complex and does not have plain surfaces, the »2-lines« and the »best-fit« procedures seem to lead to more precise data.

Another striking aspect regarding the data are the different results calculated for the three presented distances to the intersection. In general, the variance between the distances is for all artefact categories higher that the variance along the edge. When considering all artefact categories, especially the distance at 2 mm stands out. This is not entirely unexpected. Two aspects are relevant when interpreting the data. The first one is the resolution of the 3D model. The data can only be as good as the resolution of 3D model. In particular, the acute edges of the artefacts are often difficult to document with a 3D scanner. When zooming extremely into a 3D model, the edges of the models always appear curved instead of sharp. Therefore, the results calculated for the first probably 1 to 3 mm should likely be higher than the edge angle values calculated for the following distances. The second aspect is the human factor. Although the method is predominantly script- and algorithm-based, some steps need to be done manually. One of these steps is the digitalisation of the edge by defining a vertical polyline. Placing this polyline in the correct position is complicated when the edge of the scanned artefact is curved. Thus, it can happen that the line was placed for instance 1 mm too far towards one tool surface. As a result, the edge angle value will be higher than it would be in reality. To summarize, the measurements taken really close to the edge are likely to be affected by at least one of the described issues. This should be reflected by higher edge angle values at the first few distances from the intersection.

After highlighting some general aspects, aspects concerning specific artefact categories are discussed in the following. First of all, it has to be mentioned that not only the edge angles for the active edge were calculated. *Per* tool, two edges (E1 and E2) have been digitalised. In the case of *Keilmesser* often even three edges (E3). The distinction between a back and an active edge is mostly simple. *Keilmesser* in particular often have such a pronounced and thick back, that the back can only be defined by two edges. Nevertheless, the idea was to calculate the edge angles from all existing edges *per* artefact in order to be as objective as possible. The results of this second and/or third edge per tool can be found on GitHub [https://github.com/lschunk/edge_angle_analysis]. The graphic representation of the measured edge angles for each artefact also includes all edges. Since the focus, when presenting the data, was only on the active edge, the results for the *Keilmesser* edges representing the back will be addressed here only briefly. In general, there is no recognisable trend that shows the edge angle values change along the edge. There is a variance along the edge, but the values do not increase towards the proximal part of the tool. The edge angle values along the edge as well as the ones from the different distances seem to be slightly higher compared to the values from the *Keilmesser* active edge. Although edge angle values around 70° were calculated, also values above 100° were documented.

The second topic refers to the artefact morphology. The tool morphology seems to be reflected in the data. Tools including *Keilmesser* and *Prądnik scrapers* but also scrapers have deviating edge angle values at 5 mm

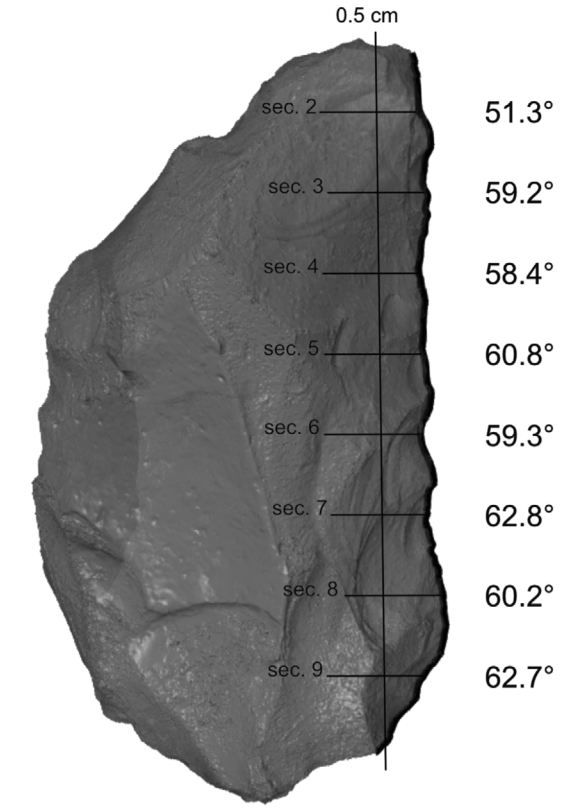

Fig. 96 Edge angle variability at 0.5 cm distance from the intersection for all measured *Keilmesser* (n = 57) without *Prądnik method* modification. The edge angle values display mean values calculated with the »2-lines« procedure. The 0.5 cm vertical line is only schematic. Normally, this line follows the shape of the digitalised active edge.

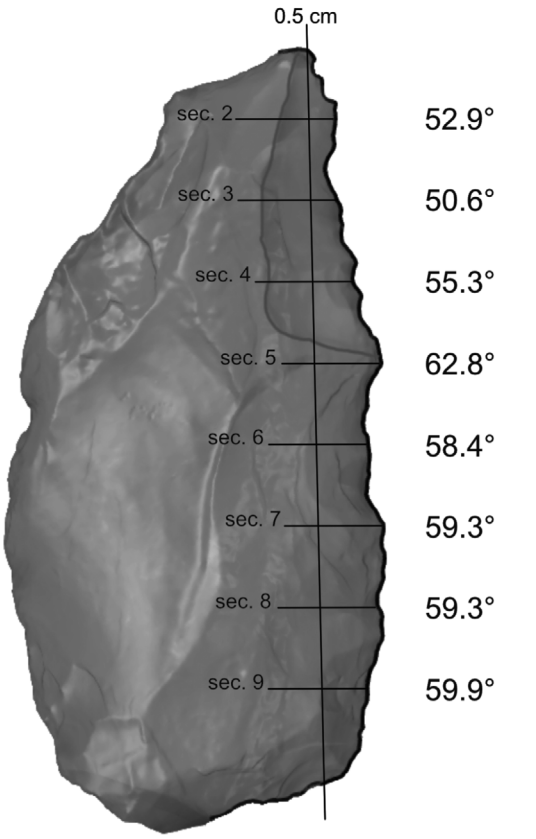

Fig. 97 Edge angle variability at 0.5 cm distance from the intersection for all measured *Keilmesser* (n = 100) with *Prądnik method* modification. The edge angle values display mean values calculated with the »2-lines« procedure. The 0.5 cm vertical line is only schematic. Normally, this line follows the shape of the digitalised active edge.

and 10 mm distance, while *Prądnik spalls* and flakes display no remarkable differences between the measurements. Since bifacially worked tools or especially *Keilmesser* and *Prądnik scrapers* do not necessarily have flat surfaces, the curvature of the surface will be reflected by changing edge angle values with increasing distance to the intersection. The *Prądnik spalls* and flakes do not reflect this change between the measurements at 5 mm and 10 mm distance.

Another aspect is the edge angle variability along the edge of *Keilmesser* (**figs 96. 98**). The data calculated for the *Keilmesser* (with and without modification) illustrates a change in the edge angle from the distal to the proximal part of the *Keilmesser* around approximately 10°. According to the data, the edge is on average more acute in the distal part of the tool than in the proximal area. The same is documented for the *Prądnik scrapers*.

Additionally, the *Keilmesser* with a modification through the *Prądnik method* do display a lower, sharper edge angle in the distal tool area than *Keilmesser* without the modification (**fig. 97**). This difference is only small and does not exceed 10°.

Prądnik scrapers do have more acute edge angles than *Keilmesser* (**fig. 99**). The calculated edge angles for the *Prądnik scraper* are on average 20° lower.

The *Prądnik spalls*, when excluding the measurements at the 2 mm distance to the intersection for the mentioned reasons, display significantly lower edge angles values compared to the tools (**fig. 100**). The values range

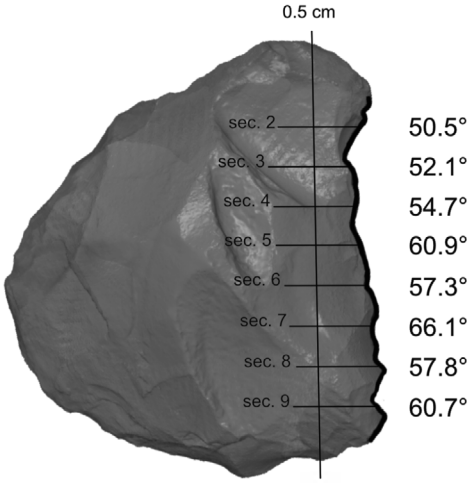

Fig. 98 Edge angle variability at 0.5 cm distance from the intersection for all measured *Keilmesser* tips (n = 18). The edge angle values display mean values calculated with the »2-lines« procedure. The 0.5 cm vertical line is only schematic. Normally, this line follows the shape of the digitalised active edge.

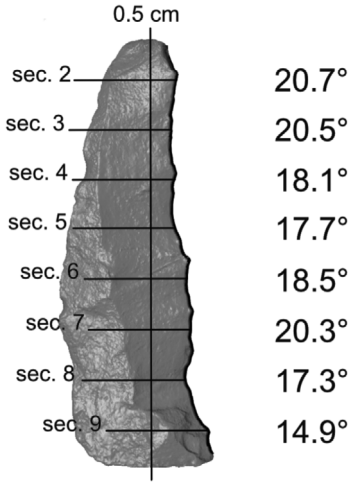

Fig. 100 Edge angle variability at 0.5 cm distance from the intersection for all measured *Prądnik spalls* (n = 21). The edge angle values display mean values calculated with the »2-lines« procedure. The 0.5 cm vertical line is only schematic. Normally, this line follows the shape of the digitalised active edge.

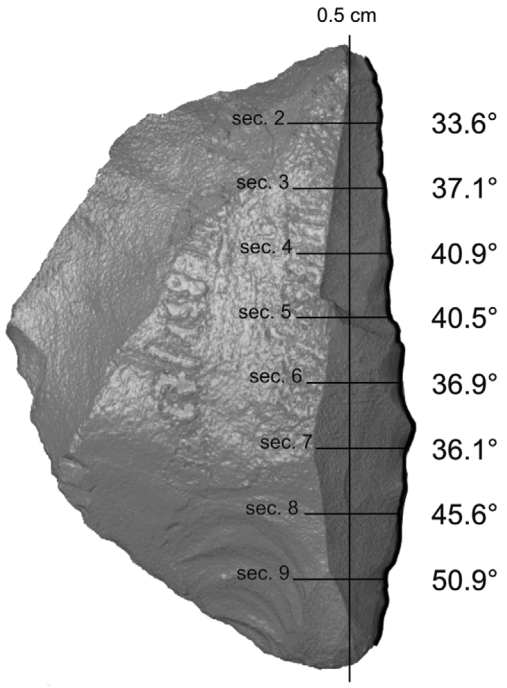

Fig. 99 Edge angle variability at 0.5 cm distance from the intersection for all measured *Prądnik scrapers* (n = 20). The edge angle values display mean values calculated with the »2-lines« procedure. The 0.5 cm vertical line is only schematic. Normally, this line follows the shape of the digitalised active edge.

between 20° and 25°. Additionally, the edge angle values for the *Prądnik spalls* display in general only a small variance (~ 5°) and are in comparison more constant along the edge and towards the surface.

The last aspect to address is the result from the outgroup. A small quantity of scrapers (**fig. 101**) and flakes (**fig. 102**) were included in the edge angle measurements in order to have a possibility to put the results from the *Keilmesser* and *Prądnik scraper* in context. The variability along the edge with the tendency of an increasing edge angle towards the proximal part of the tool as noticed for the *Keilmesser* and *Prądnik scraper* cannot be documented for the scrapers and flakes. Moreover, the edge angle values are in general lower. In particular, the flakes with edge angle values between 30° and 40° have more acute edges than *Keilmesser*. However, these values are similar to the measurements from the *Prądnik scrapers*.

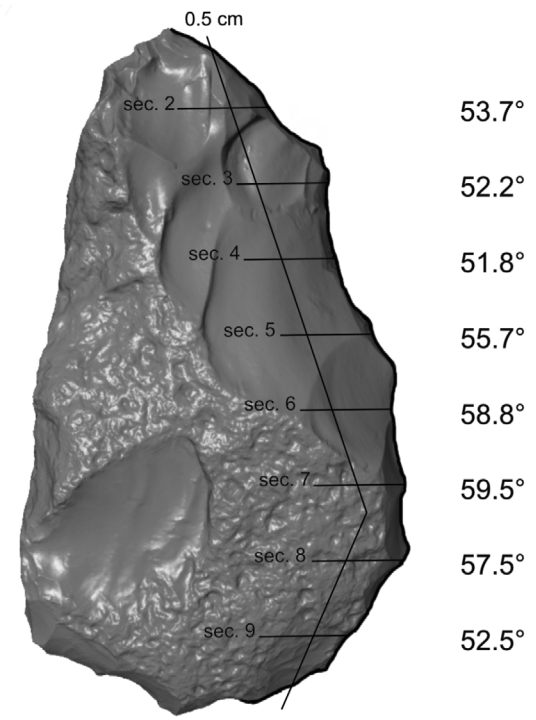

Fig. 101 Edge angle variability at 0.5 cm distance from the intersection for all measured scraper (n = 9). The edge angle values display mean values calculated with the »2-lines« procedure. The 0.5 cm vertical line is only schematic. Normally, this line follows the shape of the digitalised active edge.

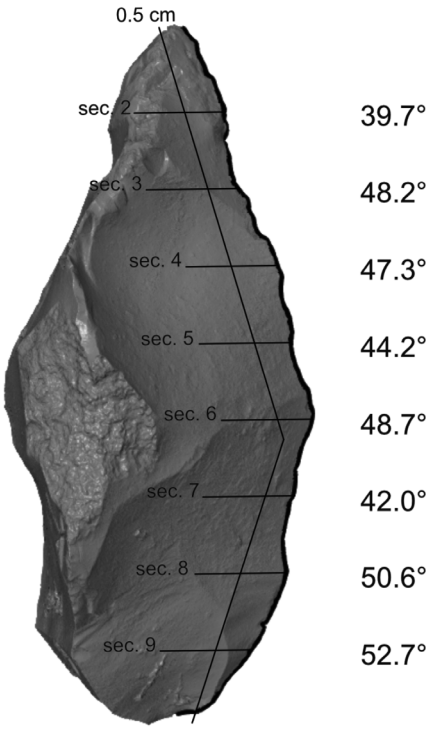

Fig. 102 Edge angle variability at 0.5 cm distance from the intersection for all measured flakes (n = 2). The edge angle values display mean values calculated with the »2-lines« procedure. The 0.5 cm vertical line is only schematic. Normally, this line follows the shape of the digitalised active edge.

USE-WEAR ANALYSIS

This subchapter addresses the results of the conducted use-wear analysis. First, the results of the qualitative assessment are presented. This includes the location, the orientation and the description of the use-were traces. Subsequently, the results of the quantitative use-wear are addressed.

Qualitative use-wear analysis

Use-wear analysis is a time-consuming approach. For that reason, a sub-sampling of the assemblage under study was needed. The sampling was done during the techno-typological analysis. The base for the sampling was thereby the research question. Since the research question focusses on specific tools – *Keilmesser* and *Prądnik scrapers* – these tools were predominantly selected. Also relevant in order to address the research question are the *Prądnik spalls*, which have been removed from the *Keilmesser* and *Prądnik scrapers* at a certain stage within the use-life history of the tools. In order to be able to put the results in relation with other artefact categories afterwards, some other tools were additionally sampled. A small number of scrapers and flakes was selected as outgroup. Only complete and well-preserved artefacts from the three archaeological assemblages were chosen for the use-wear analysis and all *Keilmesser* shapes were selected.

sites	use-wear	artefact category						
		Keilmesser	*Keilmesser* tip	*Prądnik* scraper	*Prądnik* spall	scraper	flake	total
Buhlen	with traces [n]	34 (33.6 %)	7 (6.9 %)	12 (11.9 %)	11 (10.9 %)	1 (1.0 %)	0 (0.0 %)	65 (64.3 %)
	without traces [n]	24 (23.8 %)	1 (1.0 %)	3 (3.0 %)	7 (6.9 %)	1 (1.0 %)	0 (0.0 %)	36 (35.7 %)
Balve	with traces [n]	40 (50.6 %)	2 (2.5 %)	2 (2.5 %)	16 (20.3 %)	8 (10.1 %)	0 (0.0 %)	68 (86.1 %)
	without traces [n]	2 (2.5 %)	0 (0.0 %)	3 (3.8 %)	5 (6.3 %)	1 (1.3 %)	0 (0.0 %)	16 (13.9 %)
Ramioul	with traces [n]	8 (40.0 %)	0 (0.0 %)	3 (15.0 %)	0 (0.0 %)	5 (25.0 %)	1 (5.0 %)	17 (85.0 %)
	without traces [n]	1 (5.0 %)	0 (0.0 %)	0 (0.0 %)	0 (0.0 %)	1 (5.0 %)	1 (5.0 %)	3 (15.0 %)
total	with traces [n]	82 (41.0 %)	9 (4.5 %)	17 (8.5 %)	27 (13.5 %)	14 (7.0 %)	1 (0.5 %)	150 (75.0 %)
	without traces [n]	27 (13.5 %)	1 (0.5 %)	6 (3.0 %)	12 (6.0 %)	3 (1.5 %)	1 (0.5 %)	50 (25.0 %)

Table 36 Numbers of artefacts per site and artefact category studied with a qualitative use-wear analysis. The percentages in brackets relate to the number of artefacts per assemblage.

Having this as a prerequisite, with n = 200 artefacts, more than one third of the entire assemblage was sampled for the qualitative use-wear analysis (**tab. 9**). These n = 200 sampled artefacts divide in n = 119 *Keilmesser*, whereas n = 10 of these are *Keilmesser* tips, n = 23 *Prądnik scrapers* as well as n = 39 *Prądnik spalls*. This means, more than one third (36.1 %) of the entire *Keilmesser* assemblage was part of the qualitative use-wear analysis, while nearly half of the *Prądnik scrapers* (42.6 %) have been studied. *Prądnik spalls* were less frequently involved in this analysis with 24.5 %. less frequently. The outgroup consist of n = 17 scrapers and n = 2 flakes. The n = 200 artefacts are not sampled equally from the three archaeological sites. Since the assemblage from Ramioul is comparatively small, the entire n = 20 samples were included for the qualitative use-wear analysis. The macroscopic preservation (e. g. no edge damage) in Buhlen seemed better than the one in Balve. Therefore, more artefacts from Buhlen were sampled. Thus, the sampled artefacts are to 50.5 % (n = 101) from Buhlen, to 39.5 % (n = 79) from Balve and to 10.0 % from Ramioul.

The samples were studied with an upright light microscope (ZEISS Axio Scope.A1 MAT) under a 5×, 10× and 20× magnification. By doing so, traces could be found on n = 150 pieces out of the sampled n = 200 artefacts (**tab. 36**). Although Buhlen was samples most numerously, the artefacts from Buhlen displayed the fewest use-wear traces. On only n = 65 artefacts traces could be documented. The preservation for the material from Balve was estimated as poorer and therefore less suitable for a use-wear analysis. Surprisingly, n = 68 out of n = 79 selected pieces displayed use-wear traces. The complete studied assemblage from Ramioul (n = 20) was selected for the use-wear analysis. The material from Ramioul appeared as less well preserved. Most of the edges and higher micro topographical areas seemed rounded and affected. Moreover, the light coloured, almost white flint made the detection of use-wear traces more complicated. Nevertheless, on n = 17 artefacts traces could be documented.

The tool areas displaying use-wear traces were documented as EDF stitching images with a digital microscope (ZEISS Smartzoom 5) by using a 1.6× objective and 34-× zoom. All use-wear traces are illustrated as figures in the supplementary material.

Analysis use-wear traces and spatial pattern recognition

During the performance of the qualitative use-wear analysis, all traces were documented in the beforehand described scheme (see chapter Qualitative use-wear analysis; **fig. 26**). Hence, not only the location of each trace on the artefacts was recorded, but also, if possible, the type (polish, striation or impact marks) and the orientation (perpendicular, parallel or oblique to the edge). After performing the qualitative use-wear, all documented traces of the n = 150 artefacts with use-wear were sorted and visually categorised (**appendix I**). Important criteria for the categorisation were the appearance of the traces, their extension, their orientation as well as the abrasiveness on the surface. In this way, nine types of traces were defined (described below).

The different types were named in a simple way by giving, as soon as a category was defined, a letter as a name, starting with the letter »A«. When two categories were nearly identical, but for instance, only the orientation of the striations was different, the addition »2« was given. In three cases, no clear category could be given. These traces appeared like a combination out of two already defined categories. Therefore, next to the seven categories, also »C/E«, »C/D« and »C/A« exist.

Afterwards, a reordering of these types was done in order to make the descriptions more comprehensible and the order more logical. However, the former names of the categories are additionally given since these names also appear in the plots. A description of the traces is given in the following (**fig. 103**; **tab. 37**).

I. The first category is characterised by small polished spots. These spots appear as bright, intact circles. The polish is only slightly abrasive and affects only the highest micro topography. An orientation is indeterminable. [A]
II. The second category is also a polish. This time the polish is not limited to a spot, instead it is extended to a small area. Again, only the highest topographical locations are affected. The abraded, polished areas appear bright and slightly scattered. The polish can be parallel or perpendicular to the tool edge or without clear orientation. [B]
III. The third type of polish is in its appearance identical to the second category (II/B), but the distribution is more extensive. The polished areas occur most often parallel to the tool edge. [B2]
IV. The fourth category is another type of polish. The polish is smooth and distinctly more compact. In terms of the extension, the polish is comparable with the second category (II/B) and only appears in small, sometimes elongated areas. Despite the compact appearance, the polish can be found only on the highest topographical locations. This polish has either no orientation or is parallel to the edge orientated. [E]
V. The fifth category is again a polish. The polish is extensive and continual and appears as bright and shiny. Not only the highest topographical locations are abraded, but also lower topography. The orientation is most often indeterminable or otherwise parallel to the edges. [C]
VI. Category six combines a smooth polish with randomly orientated striations. The traces are not selected, instead they are extended over small areas. The polish is abrasive, affects all topographical locations, the highest and the lowest topography. The striations do not reach deeper than the polish. In the majority, the traces do not have an orientation. [D]
VII. The seventh category is identical to the category described before (VI/D). The only difference can be found in the orientation. The striations are not randomly orientated, they are orientated towards one direction. Since the striations do have an orientation, it was also possible to define the orientation of the traces in general. Most often, the traces are orientated perpendicular to the tool edges. [D2]
VIII. The eighth category can be described by orientated striations, which are not extensive and limited in their dimensions. The linear scratches affect the lowest as well as the highest topographical locations. These traces can be either parallel, perpendicular or oblique towards the edges. [F]

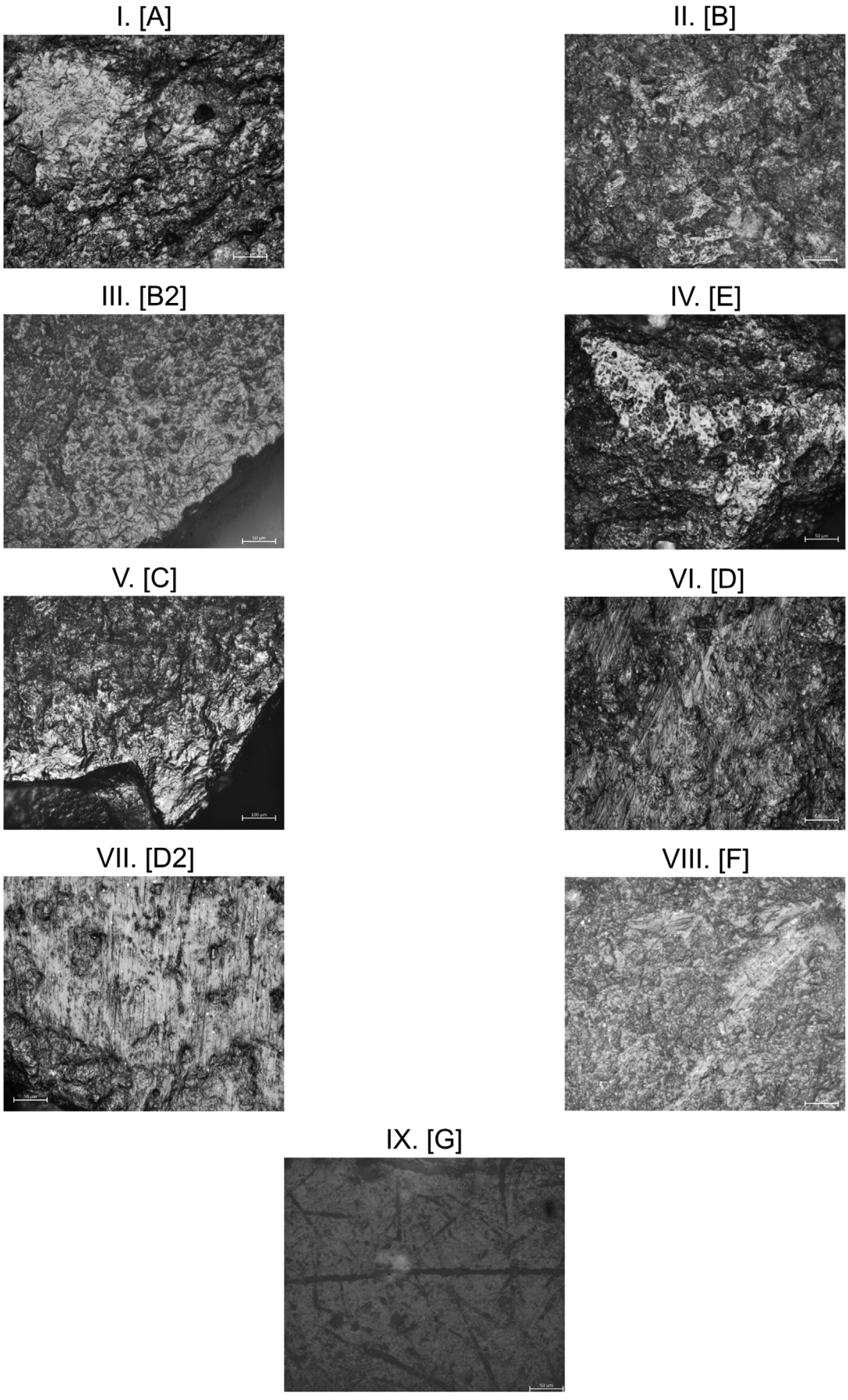

Fig. 103 Documented qualitative use-wear types (all images are taken with a 20× optical objective).

type	main features	description	topographical location
I. [A]	polish	small & bright polished circle	highest micro topography
II. [B]	polish	small & bright area of polish	highest micro topography
III. [B2]	polish	extended area of polish	highest micro topography
IV. [E]	polish	small areas of smooth & compact polish	highest micro topography
V. [C]	polish	extensive & continues and bright & shiny polish	lowest and highest micro topography
VI. [D]	polish & striation	smooth polish with randomly orientated striations; small area	lowest and highest micro topography
VII. [D2]	polish & striation	smooth polish with orientated striations; small area	lowest and highest micro topography
VIII. [F]	striation	small & orientated striations	lowest and highest micro topography
IX. [G]	polish, furrows & groves	dull & abrasive polish, deep furrows and groves	lowest and highest micro topography

Table 37 Description of the documented use-wear traces including their topographical location.

IX. The ninth and thus the last category displays a dull and abrasive polish. The polish is additionally combined with shallow or deep furrows and groves. The linear striations are randomly orientated and sometimes reach deeper than the polish. These traces are extensive and cover big areas of the surface while affecting all topographical locations, causing a surface deformation. The orientation is indeterminable. The category can be found close to the edge, but also extending towards the surface. [G]

Although the studied silicified schist samples clearly outnumber the flint samples, the mentioned use-wear types were documented on silicified schist as well as on flint samples. The categories do not differ depending on the raw material. However, one type was only documented on silicified schist, not on flint. This is type II. (B). However, type III. (B2) was documented and only differs concerning the extension of the trace.
In qualitative use-wear analysis, the first step is the recognition and the characterisation of use-wear types on the analysed artefacts. The aim of a use-wear analysis is to identify the observed traces in order to gain a functional interpretation of the different tools. In a qualitative use-wear analysis, this is solely based on visual identifications and characterisation. It is known that not only the worked material (Keeley 1980; Haslam 2009; Rots 2013), but also the raw material, the use intensity and the performed task haven an impact on the formation of the use-wear traces (Buc 2011; Marreiros et al. 2020). Without a widespread and highly reliable reference collection, the aim of a functional interpretation of the observed use-wear traces can barely be observed. For silicified schist, there is no such reference collection existing yet. Thus, the aspiration of identifying the use-wear traces based on a qualitative use-wear analysis will not be fulfilled within this project.
Despite this, one single interpretation regarding the described use-wear categories will be made. The interpretation refers to the ninth category (IX/G). The described features of the traces are distinctly different from the other categories. These features do not look like use-wear traces, instead, they will be interpreted as post-depositional traces.
After analysing the artefacts, observing, categorising and describing the traces, the location of these traces was transformed from the manually filled scheme into a geographical information system (QGIS, version 3.14.16). Each use-wear trace was illustrated by a coloured point. The points were coloured according to the use-wear type categorisation.

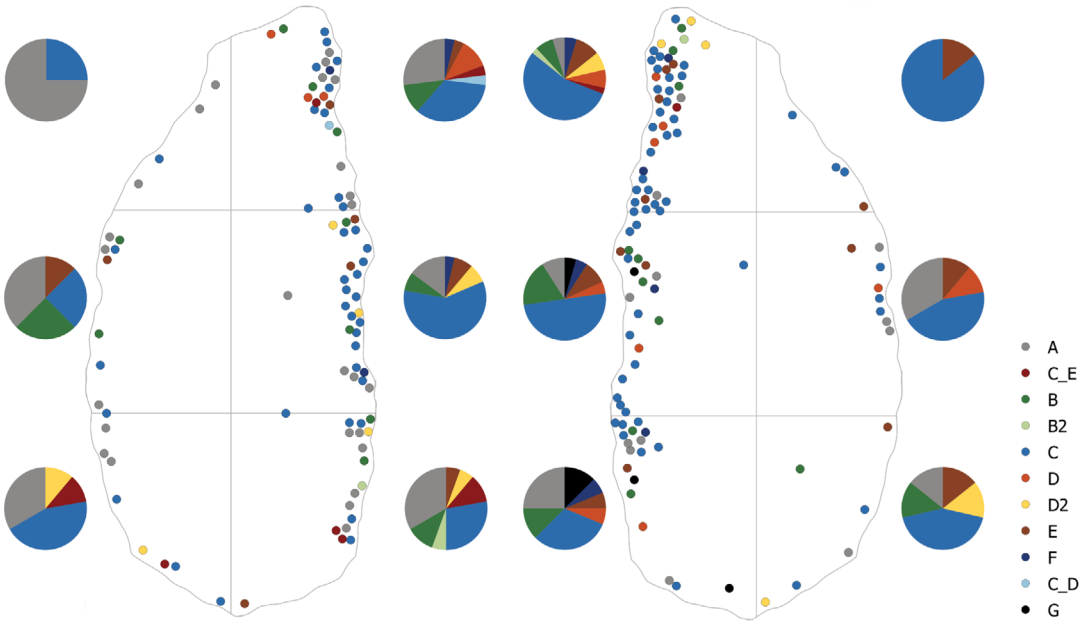

Fig. 104 Distribution of all the use-wear traces documented on *Keilmesser*. The left side illustrates the dorsal surfaces of the tool, the right side the ventral tool surface. The colours indicate the use-wear types.

The results of this graphical representation are presented in the following organised by artefact categories. Before doing so, one issue needs to be explained. Per tool category, one outline was used in order to locate the use-wear traces. These outlines were divided into areas, whereas A and B always displayed the dorsal and D and C the ventral surface of the tool. The orientation of these areas changed when looking at a left sided instead of a right sided tool. Since the specific lateralisation of the artefacts had no priority in the context of the location of the use-wear traces, all use-wear traces from left sided artefacts were transferred to the right sided scheme in order to fit a uniform scheme.

For *Keilmesser*, all described nine use-wear categories were documented (**fig. 104**). Surface modifications in the sense of use-wear or post-depositional traces could be documented on in total n = 195 locations (**tab. 38**). Although the surfaces of the tools were checked entirely, most of the use-wear traces can be found along the active edge. This counts for 77.4 % (n = 151) of the traces. The ventral surface shows thereby slightly more traces (n = 80) than the dorsal surface (n = 71). The traces are of all documented

artefact category	use-wear type [n]											
	I. (A)	II. (B)	III. (B2)	IV. (E)	V. (C)	VI. (D)	VII. (D2)	VIII. (F)	IX. (G)	V./ IV.	V./ VI.	total
Keilmesser	38	19	2	15	89	9	8	6	3	5	1	**195**
Prądnik scraper	9	0	0	0	19	0	1	0	3	1	0	**33**
Prądnik spall	7	4	0	0	33	2	0	2	0	5	0	**53**
scraper	4	3	1	5	18	0	2	2	4	1	0	**40**
total	**58**	**26**	**3**	**20**	**159**	**11**	**11**	**10**	**10**	**12**	**1**	321

Table 38 Number of documented use-wear traces on artefacts from Buhlen, Balver Höhle and Ramioul per use-wear type and artefact category.

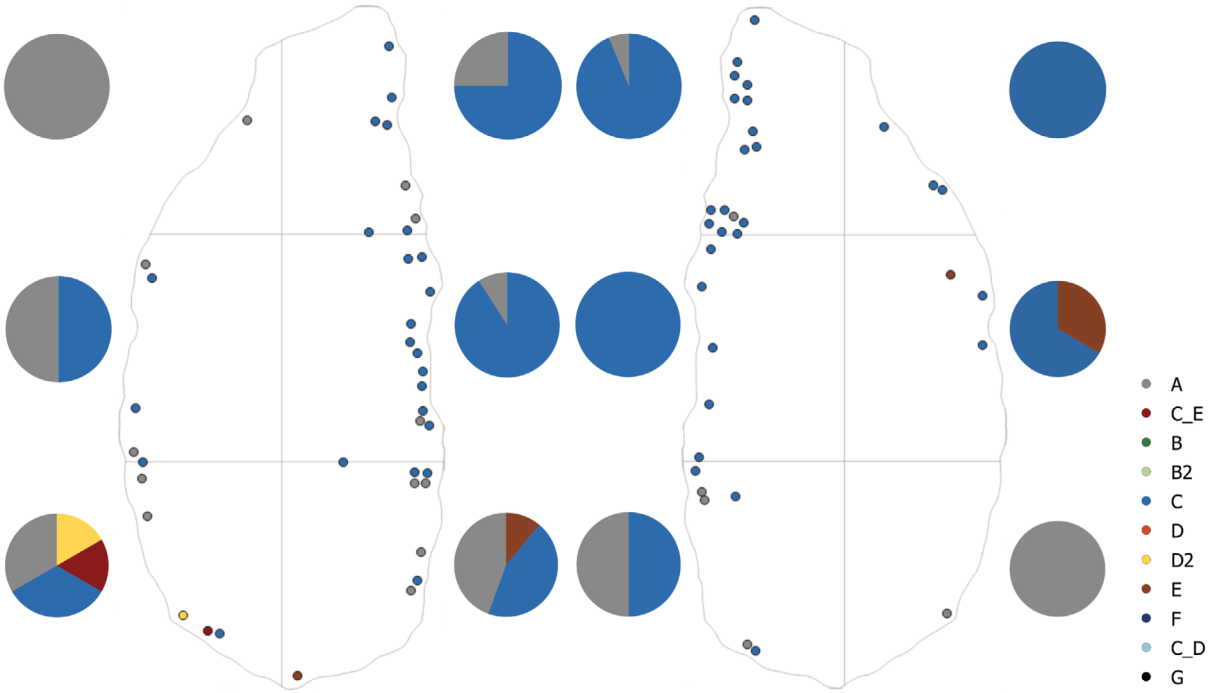

Fig. 105 Distribution of all the use-wear traces documented on *Keilmesser* from Buhlen. The left side illustrates the dorsal surfaces of the tool, the right side the ventral tool surface. The colours indicate the use-wear types.

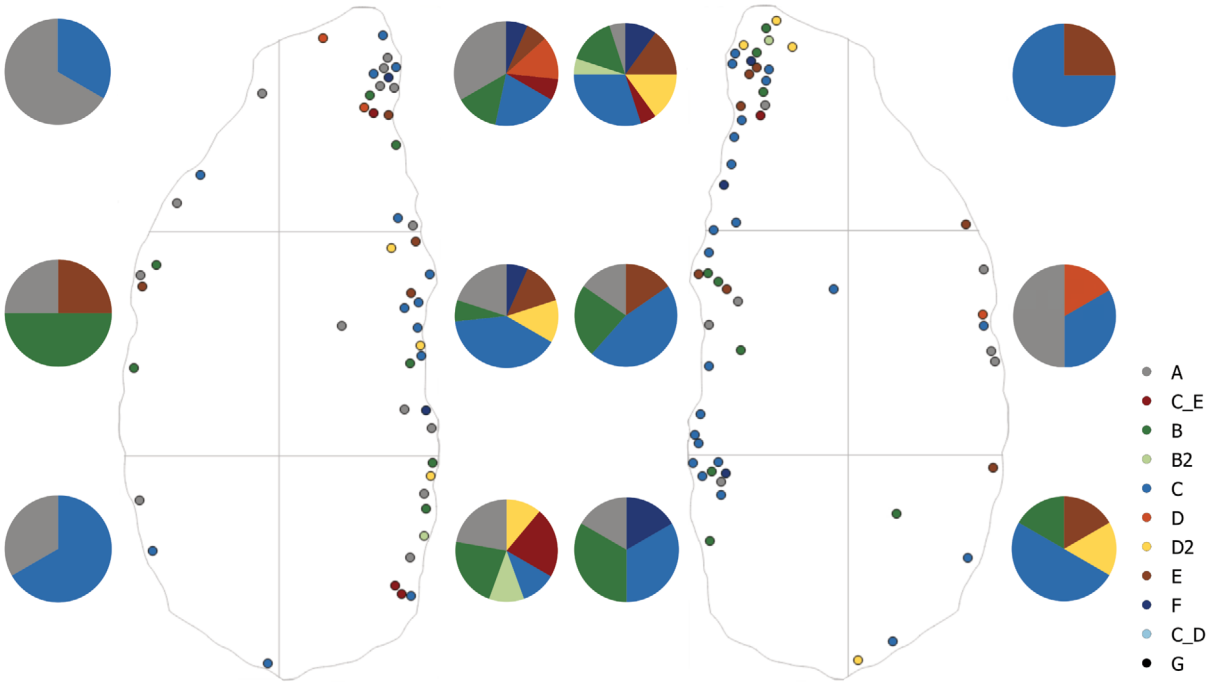

Fig. 106 Distribution of all the use-wear traces documented on *Keilmesser* from Balver Höhle. The left side illustrates the dorsal surfaces of the tool, the right side the ventral tool surface. The colours indicate the use-wear types.

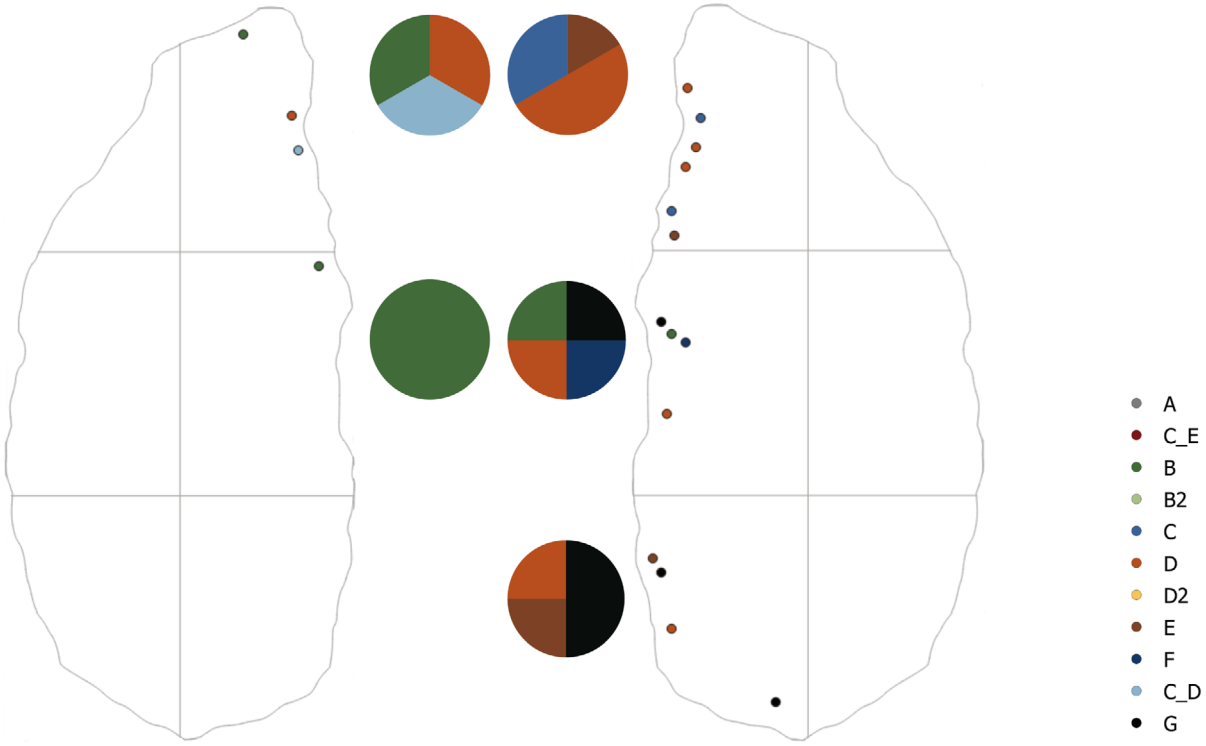

Fig. 107 Distribution of all the use-wear traces documented on *Keilmesser from Ramioul*. The left side illustrates the dorsal surfaces of the tool, the right side the ventral tool surface. The colours indicate the use-wear types

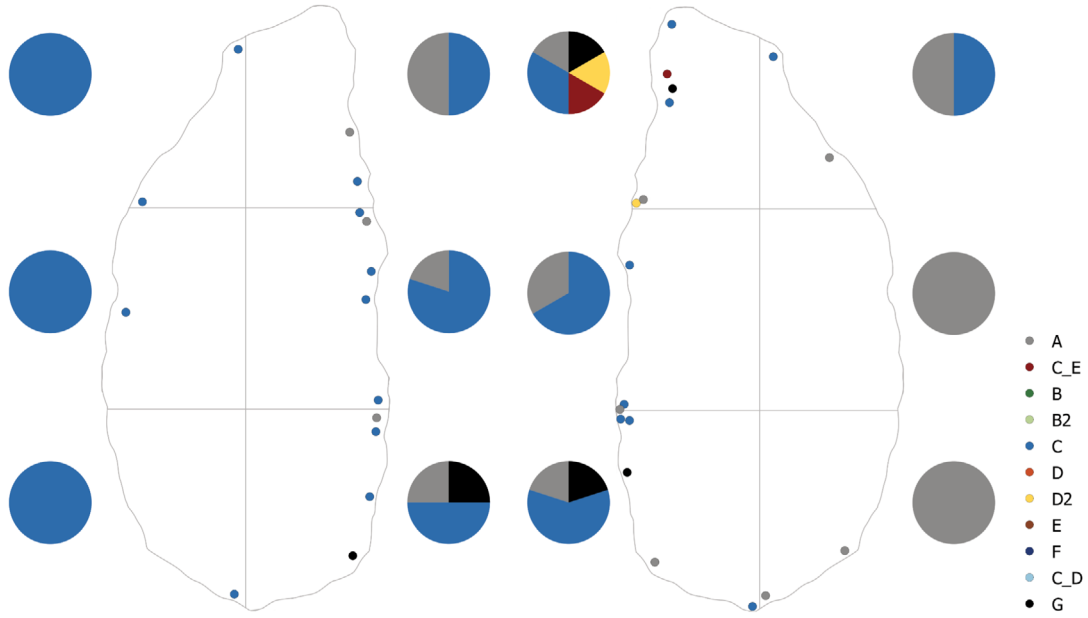

Fig. 108 Distribution of all the use-wear traces documented on *Prądnik scrapers*. The left side illustrates the dorsal surfaces of the tool, the right side the ventral tool surface. The colours indicate the use-wear types.

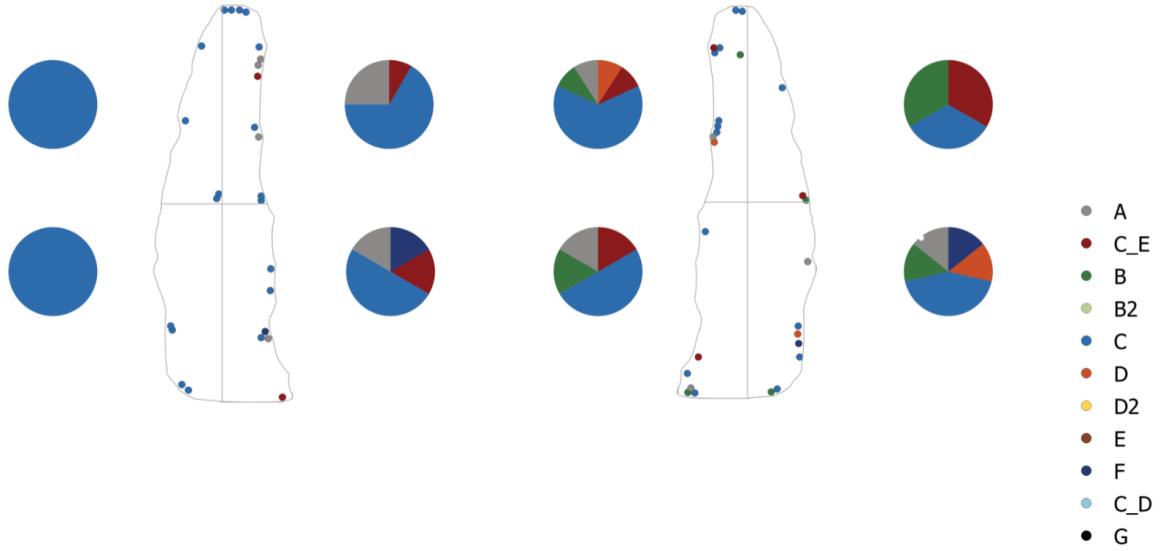

Fig. 109 Distribution of all the use-wear traces documented on *Prądnik spalls*. The left side illustrates the dorsal surfaces of the tool, the right side the ventral tool surface. The colours indicate the use-wear types.

types, but the majority (n = 37) can be categorised as V. (C). Conspicuously often (n = 26) along the edge is also the category I. (A). A third category, type II. (B), sticks out a little with n = 9 documented spots. The remaining categories could be documented on one to five locations.

These results differ when looking at the plotted traces from the three studied sites individually. All the aforementioned observations concerning the location of the use-wear traces is still valid. However, the occurrence of the documented use-wear types differ from site to site. The diversity of use-wear types reflected on all analysed *Keilmesser* together is not present on the *Keilmesser* from Buhlen only (**fig. 105**). Besides a few exceptions in the proximal part of the tools on the dorsal surface, the *Keilmesser* from Buhlen display solely use-wear traces of the category I. (A) or V. (C).

The documented traces on the artefacts in Balve do reflect the variety of use-wear types noticed for all *Keilmesser* from the three sites together (**fig. 106**). Eight of the nine use-wear categories can be found on the *Keilmesser* from Balve. The only missing category is type IX. (G), the type interpreted as post-depositional trace.

Despite the small quantity of analysed *Keilmesser* from the site Ramioul, the variety of documented use-wear traces is nearly comparable to the results from Balve (**fig. 107**). The observed traces are located only along the active edge. Except for the three use-wear categories I. (A), III. (B2) and VIII. (D2), all other types could be documented on the artefacts.

The results for the analysed *Prądnik scrapers* do look different (**fig. 108**). First of all, not many traces (n = 33) could be documented as measured by the smaller number of tools, compared to the *Keilmesser*. Most of the traces could be found again along the active edge (n = 25) with a majority of traces on the ventral surface (n = 14). Moreover, the diversity of use-wear types is also different. The surface modifications on *Prądnik scrapers* can be attributed to 84.9 % (n = 27) to the types V. (C) and I. (A), but type V. clearly predominates (n = 19). Three times, the category IX., interpreted as post-depositional traces, was found on two tools.

Within the qualitative use-wear analysis, n = 39 *Prądnik spalls* were microscopically checked for surface modifications. In total, n = 53 traces on n = 27 artefacts could be documented (**fig. 109**). The variance is higher than documented for the *Prądnik scrapers*, but not as high as for the *Keilmesser*. Five of the nine categories were found on the *Prądnik spalls*. The main frequency of the use-wear types is the same as for

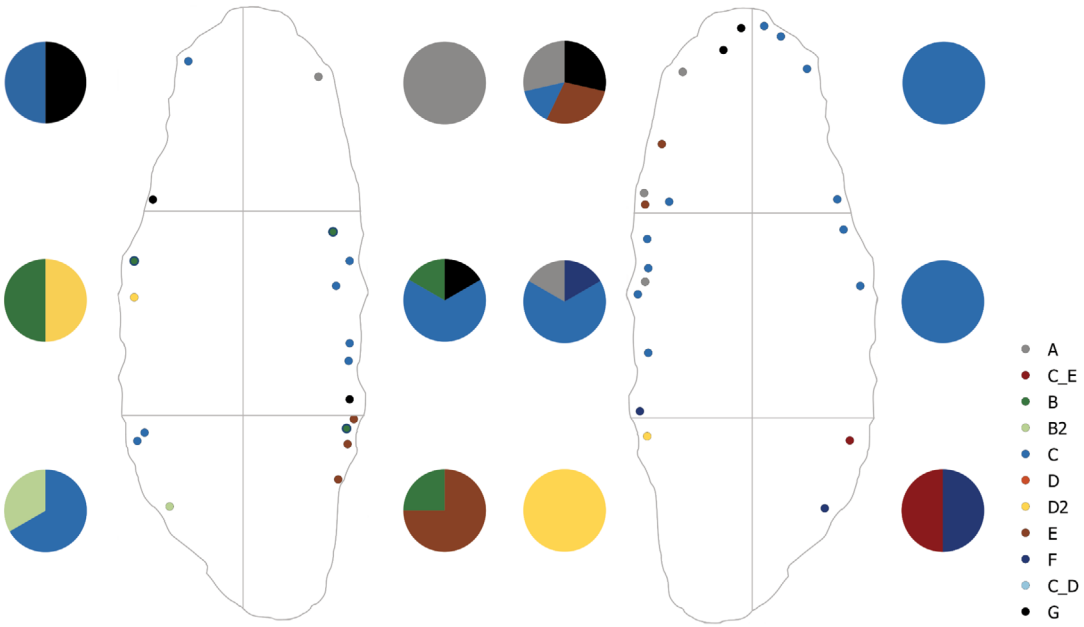

Fig. 110 Distribution of all the use-wear traces documented on scrapers. The left side illustrates the dorsal surfaces of the tool, the right side the ventral tool surface. The colours indicate the use-wear types.

Keilmesser. Category V. is again the most often documented use-wear type with n = 33 locations. The frequency of type I. (n = 7) is also slightly higher compared to other types as well as type II. (n = 4). The combination of category V. and category IV. was also documented for n = 5 locations. The distribution of the traces is not as clear as described for *Keilmesser* and *Prądnik scrapers*. The traces are still most often orientated along the active edge (former active edge of the tool) but also the number of traces along the opposite edge is proportionally high. The percentage distribution is 52.8 % for the active edge to 47.2 % for the opposed edge.

Additionally, the orientation of the striations on *Keilmesser*, *Prądnik scarpers* and *Prądnik spalls* was reviewed. This was done in order to see, whether the striations can support or contradict the interpreted tool lateralisation. To do so, only striations along the active edge with a clear orientation (type VII. and VIII.) can provide information. Furthermore, these striations have to be oblique towards the edge. Oblique striations could reflect the tool handling of the tool during its action in the sense of which surface was used. Therefore, striations of left-lateral tools should be thereby mirrored, compared to the ones on right-lateral tools. Unfortunately, none of the documented striations with an oblique orientation is located along the edge. Thus, the tool laterality cannot be correlated with results of the qualitative use-wear analysis.

The results of the analysed scrapers illustrate again a different picture (**fig. 110**). For the small number of analysed tools with some surface modification (n = 14), the quantity of documented traces is comparably high (n = 37). Additionally, the variance of use-wear types is also high. Seven of the nine categories are displayed on the scrapers. Although the most frequent category is again type V. (n = 18), there is no other prominent use-wear type. The other categories are all present with one to five locations. The distribution of these traces is more even towards all edges, although the traces along the active edge still prevail slightly (n = 25).

The only flake with use-wear traces displayed type V. on three different locations.

For all artefact categories from the three archaeological sites together, the following picture emerges. The traces clearly prevail along the active edges. About 38.9 % (n = 125) of the traces can be found close to the

site		artefact category						
		Keilmesser tip	*Prądnik scraper*	*Prądnik spall*	scraper	flake	total	
Buhlen	n	4	0	1	1	0	0	**6**
	%	66.7	0.0	16.7	16.7	0.0	0.0	100.1
Balve	n	25	2	0	3	3	0	**33**
	%	75.8	6.1	0.0	9.1	9.1	0.0	100.1
Ramioul	n	6	0	2	0	3	0	**11**
	%	54.6	0.0	18.1	0.0	27.3	0.0	100.0
total	n	**37**	**2**	**3**	**4**	**6**	**0**	**52**
	%	71.2	3.9	5.8	7.7	11.5	0.00	100.1

Table 39 Selected artefacts from Buhlen, Balve and Ramioul for the quantitative use-wear analysis.

active edge on the ventral surface, 34.6 % (n = 111) on the dorsal surface. The remaining 26.5 % of the traces are located on the edge opposed to the active edge, the posterior part, either on the ventral (n = 45) or on the dorsal surface (n = 40). The quantity of traces decreases in all areas (A to D) from the distal and medial to the proximal tool part. While the quantity of traces in the medial and proximal part is more or less equally distributed in the areas A, B and C, the frequency of traces in area D is considerably higher in the distal part of the tool (n = 66; medial n = 37, proximal n = 22).
Regarding the type of traces, there is also one category that clearly stands out. Out of the n = 321 in total documented traces on all tools, 49.5 % (n = 159) of the traces are ascribed as category V. The next more frequent category is I. with 18.1 % (n = 58). Worth mentioning are also use-wear type II. and IV., documented on 8.10 % (n = 26) and 6.2 % (n = 20) of the cases. The remaining categories are rarely present on the tools and make only up to 4 % of the traces respectively.
Some additional aspects should be highlighted, which are a consequence of the distribution and the occurrence of the different traces. As mentioned before, *Keilmesser* (Buhlen as an exception) display all of the aforementioned described use-wear categories. The only other artefact category that displays nearly all use-wear types too, are the scrapers. Interestingly, category VI. only appears on *Keilmesser* and *Prądnik spalls*. In general it seems the distribution of the use-wear types on *Prądnik spalls* are very similar to the distribution on *Keilmesser.* This makes sense when assuming that the traces result from tool use before the *Prądnik spalls* have been removed from the *Keilmesser*. At the same time, the traces on *Prądnik spalls* can be found on all edges, what makes it impossible to only be a consequence of a *Keilmesser* use. *Prądnik scrapers*, however, do not share these similarities with *Keilmesser* and *Prądnik spalls*. The use-wear types on *Prądnik scrapers* reflect almost no diversity and can be summarised be they types V. and I.

Quantitative use-wear analysis

The second part of the use-wear analysis was the quantitative use-wear analysis with the aim to acquire 3D surface topography data to measure and characterise the micro surface texture of the identified use-wear traces. The samples for the quantitative use-wear analysis have been selected based on the results from the previously performed qualitative use-wear analysis. From the n = 150 artefacts that displayed in total n = 321 traces, n = 50 traces provide the subsample for the quantitative use-wear analysis (**tab. 39**). These sampled traces correspond to n = 37 spots on *Keilmesser*, n = 3 on *Prądnik scrapers*, n = 4 on *Prądnik spalls*

and n = 6 traces on scrapers. This subsample does not only display the different artefact categories, but also the different use-wear types. Since the predominant use-wear type found on the artefacts was category V., this type was selected by a majority (n = 13). The remaining use-wear types were selected on the premise, that, if possible, the minimum number of use-wear types were represented by three samples. Each use-wear trace was measured three times. These measurements were taken at nearby but non-identical spots within the trace in order to review the homogeneity within each trace. Hence, n = 150 measurements were performed in total. As explained in the method chapter, the data was acquired with an upright light microscope coupled with a laser-confocal microscope (ZEISS Axio Imager.Z2 Vario + ZEISS LSM 800 MAT).

Surface micro texture data analysis

The acquired data was analysed according to the ISO 25178-2 parameters. Based on this international standard, 21 ISO 25178-2 parameters, three furrow parameters, three texture direction parameters, one texture isotropy parameter and the scale-sensitive fractal analysis (SSFA) parameters *epLsar, NewEplsar, Asfc, Smfc, HAsfc9 and HAsfc81* were calculated on each surface (**tab. 11**; further information about these parameters can be found in the »surface metrology guide« from Digital Surf; see Digital Surf, Besançon, France). Only one parameter, *Str*, could not be calculated on a small number of surfaces and is thus missing for n = 9 measurements. However, the parameter *isotropy* (texture direction parameter) is identical to the ISO 25178-2 *Str* parameter. The ConfoMap templates, the resulting data including plots for each measured parameter can be found on GitHub. In order to present the data here, nine out of the 34 parameters were considered. These nine parameters spanning the different categories of field parameters (Blateyron 2013) and some additional isotropy, furrow and SSFA parameters. The areal parameters separate in the three categories areal field, areal-scale and length-scale analysis. To start with the areal field parameters, *Sq* was chosen as an amplitude parameter expressing the root mean squared height. Thus, *Sq* is a measure of surface roughness. The higher the *Sq*, the higher the surface roughness. *Std*, a spatial parameter, calculates the main direction of the surface texture (texture direction). The parameter is defined relative to the y-axis. Thus, a surface with an orientation along the y-axis will return a *Std* of 0 degrees. Only when a surface is anisotropic, this parameter is of relevance or can be calculated. Interesting is, that *Std* can be used to detect the presence of a preliminary surface modification process, which is to be removed (succeeding modifications that lead to different texture directions). As a volume parameter of the areal field parameters, *Vmc* stands for the volume of the material. *Vmc* can be useful to understand how much material may be worn away for a given depth. *Sxp* is another functional parameter describing the peak extreme height. *Sxp* is a measure for the height differences between the average height of the surface and the highest peak by excluding 2.5 % of the highest points. High *Sxp* values indicate the existence of high peaks. A field parameter belonging to the category of areal scale analysis is the hybrid parameter *Sdr*. *Sdr* is a measure of surface complexity. The higher the value, the more complex the surface. Meaning, a value close to 0 % is equitable to a flat and smooth surface. Moreover, for the texture isotropy and periodicity the *isotropy* on surface was selected. The higher the *isotropy* value, the more the surface resembles itself in every direction. In other words, the *isotropy* decreases with an increasing directionality of the surface. For the furrow analysis, the *mean density of furrows* was selected as a parameter for detecting and characterising furrows on the surface. The last category are parameters of the fractal analysis. One of these parameters is *HAsfc9*. *HAsfc9* displays the heterogeneity of areal-scale fractal complexity. A high HAsfc9 value indicates a high-degree within-surface variation across different scales. EpLsar is another parameter of the fractal analysis, categorised as length-scale analysis. The parameter reflects the anisotropy of a texture and it thus the reverse of isotropy. The

epLsar values increase with increasing directionality. To summarise, for the quantitative characterisation of the surface micro texture these variables were considered: surface roughness, surface directionality, volume, height, surface complexity, isotropy, heterogeneity and anisotropy.

Based on these selected variables, representative for the different categories of parameters, some results are explained. Prior to this, it should be mentioned again that quantitative use-wear analysis is a comparable new approach in archaeology although the interest is clearly increasing (e. g. Martisius et al. 2018; Galland et al. 2019; Stemp/Macdonald/Gleason 2019; Álvarez-Fernández et al. 2020; Bradfield 2020; Martisius et al. 2020; Pedergnana et al. 2020b; Pedergnana/Ollé/Evan 2020). Following the international standards (ISO 25178-2) offers a secure way to analyse the data. However, which parameters are relevant or the most important ones to analyse use-wear traces on lithics, especially on silicified schist, is not sufficiently known yet. Quantitative use-wear analysis is a very promising approach with the great potential to be straightforward when explored and applied more regularly (Calandra et al. 2019b; Martisius et al. 2020; Pedergnana et al. 2020b). Large archaeological assemblages, such as the one presented here, have not been part of a qualitative use-wear analysis yet.

To check the results, the scatterplots (**figs 111-119**) of all measurements plotted *per* parameter give a first overview on the distribution of the values. The scatterplots show the measured values separated per artefact. Information about the raw material and the location (A to D, one to three) are given. The data points are coloured based on the interpreted use-wear types. In this way, different results within or between the raw materials, the artefact categories, the use-wear type classification and the locations can be compared. Unfortunately, the measured parameters lead to no obvious diagnostic results. No direct pattern between the results and the aforementioned variables is apparent. However, four measurements stand out. These measurements (MU-199 C3_01_a, MU-202 D2_01c, BU-173 C2-01_a and BU-173 C2-01_b) are noteworthy. Here, it should be pointed out again that from each trace, three measurements were taken in order to make an identification of measuring errors possible. The results of these three measurements *per* trace should be similar, otherwise the measurement is likely unreliable. However, this is the case for the four aforementioned samples. The variability within the results of the three measurements per traces respectively is conspicuous. A review of the four measurements could clearly identify them as outliers. When processing the data, existing noise is removed by a threshold. This data is interpreted as non-measured points. In a further step, such missing data gets filled. This is necessary in order to calculate some of the ISO and the SSFA parameters. In the case of the four outliers, the following happened: The measured areas were marginal and located closed to the tool edge. When scanning the surface, a small area beyond the edge was also included in the scan. Meaning, this area is treated as non-measured points. In order to calculate the parameters, the missing data needed to be filled in and the final results do not reflect the actual measured surfaces. Thus, these four measurements appear as outliers and should therefore be excluded when interpreting the data.

Although the data results in no immediately identifiable pattern, some aspects can be pointed out. The first aspect concerns the surface roughness (*Sq*). The *Sq* values calculated on flint are lower than the ones from lydite (**fig. 116**). The arithmetic mean values for flint is 98.6 µm while the mean value for lydite is 189.2 µm. It needs to be noted that the arithmetic mean value for lydite (n = 111) is based on more measurements than the flint (n = 39) one. When looking at the use-wear types, some can be categorised by higher *Sq* values then others. The surface roughness for the use-wear type I., II. and IV. seems slightly rougher compared to the other types. Contrary to that, the use-wear type V. appears to be smoother, which is reflected by lower *Sq* values.

In general, the three mentioned use-wear types I., II. and IV. differ from the other types not only concerning the surface roughness, but also concerning volume, height and surface complexity.

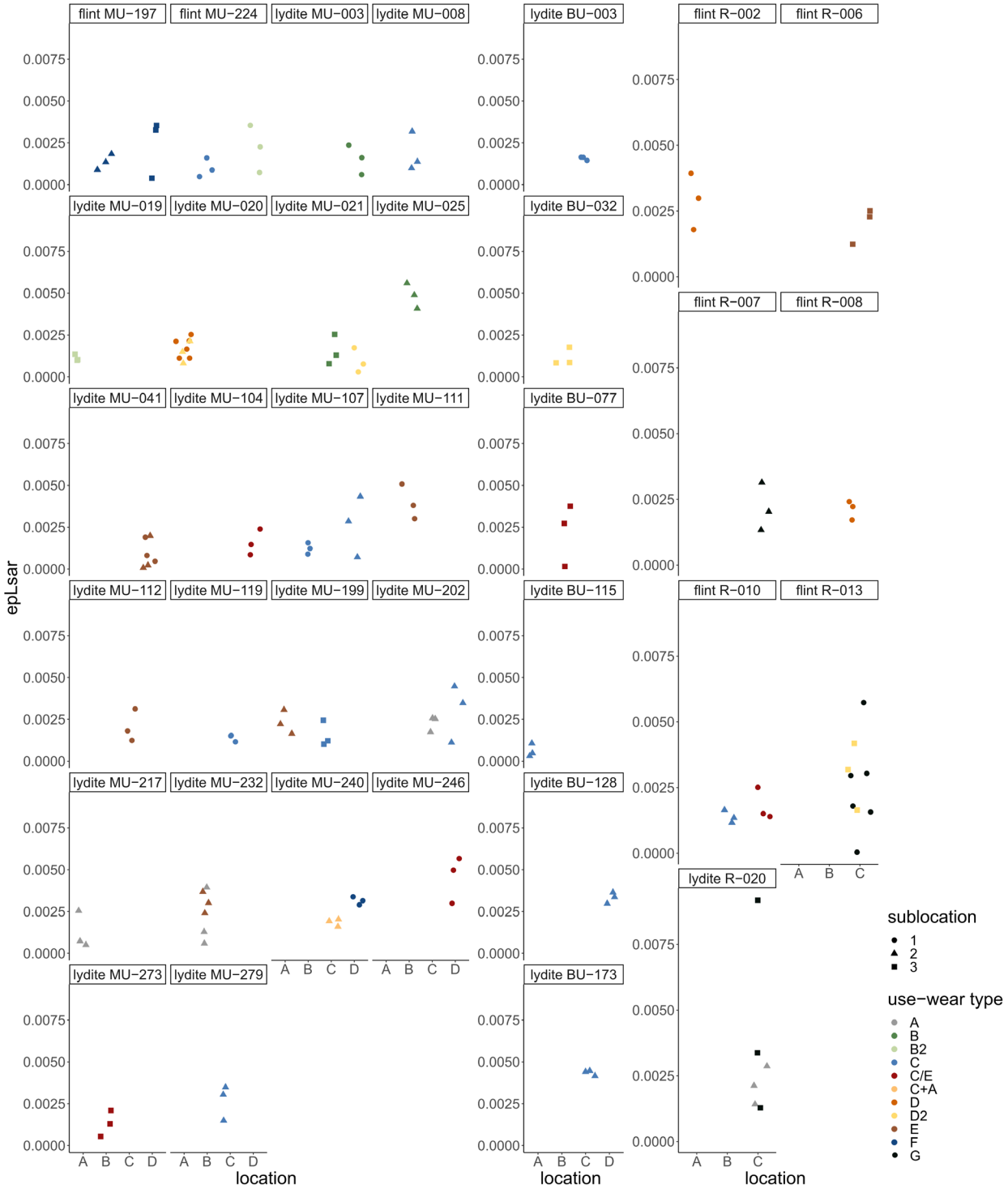

Fig. 111 *EpLsar* values for each analysed artefact (raw material [flint or lydite] plus ID). The parameter reflects the anisotropy of the texture. The epLsar value increases with increasing directionality. The plot indicates the location of the use-wear on the tool (A & B = dorsal, D & C = ventral) plus the sublocation (1, 2 or 3; sublocation stands for the number of use-wear traces *per* location). The three measurements per location and sublocation represent the three measurements *per* use-wear taken at non-identical but nearby spots. The data points are coloured based on the interpreted use-wear types.

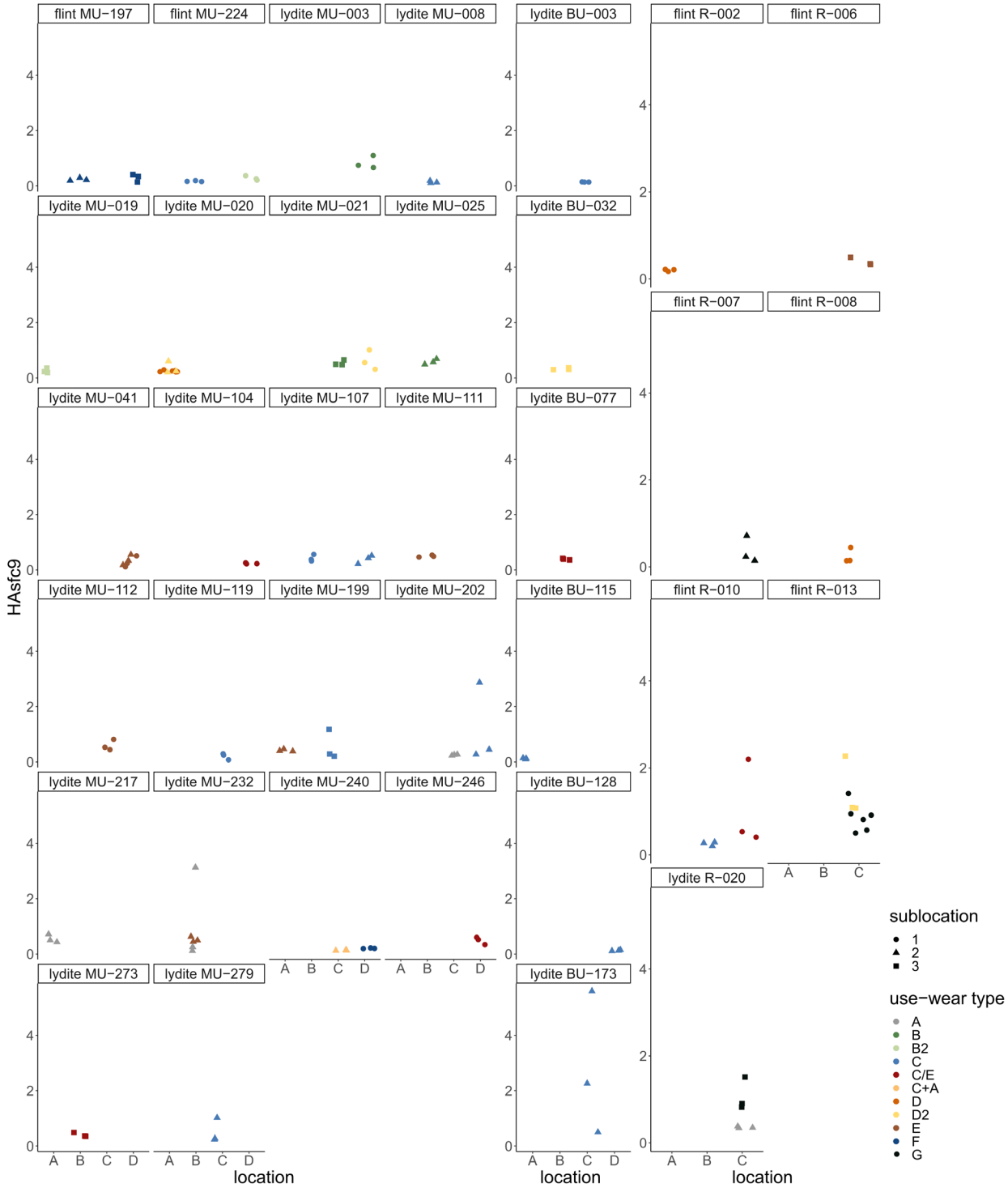

Fig. 112 *HAsfc9* values for each analysed artefact (raw material [flint or lydite] plus ID). HAsfc9 displays the heterogeneity of areal-scale fractal complexity. The plot indicates the location of the use-wear on the tool (A & B = dorsal, D & C = ventral) plus the sublocation (1, 2 or 3; sublocation stands for the number of use-wear traces *per* location). The three measurements per location and sublocation represent the three measurements *per* use-wear taken at non-identical but nearby spots. The data points are coloured based on the interpreted use-wear types.

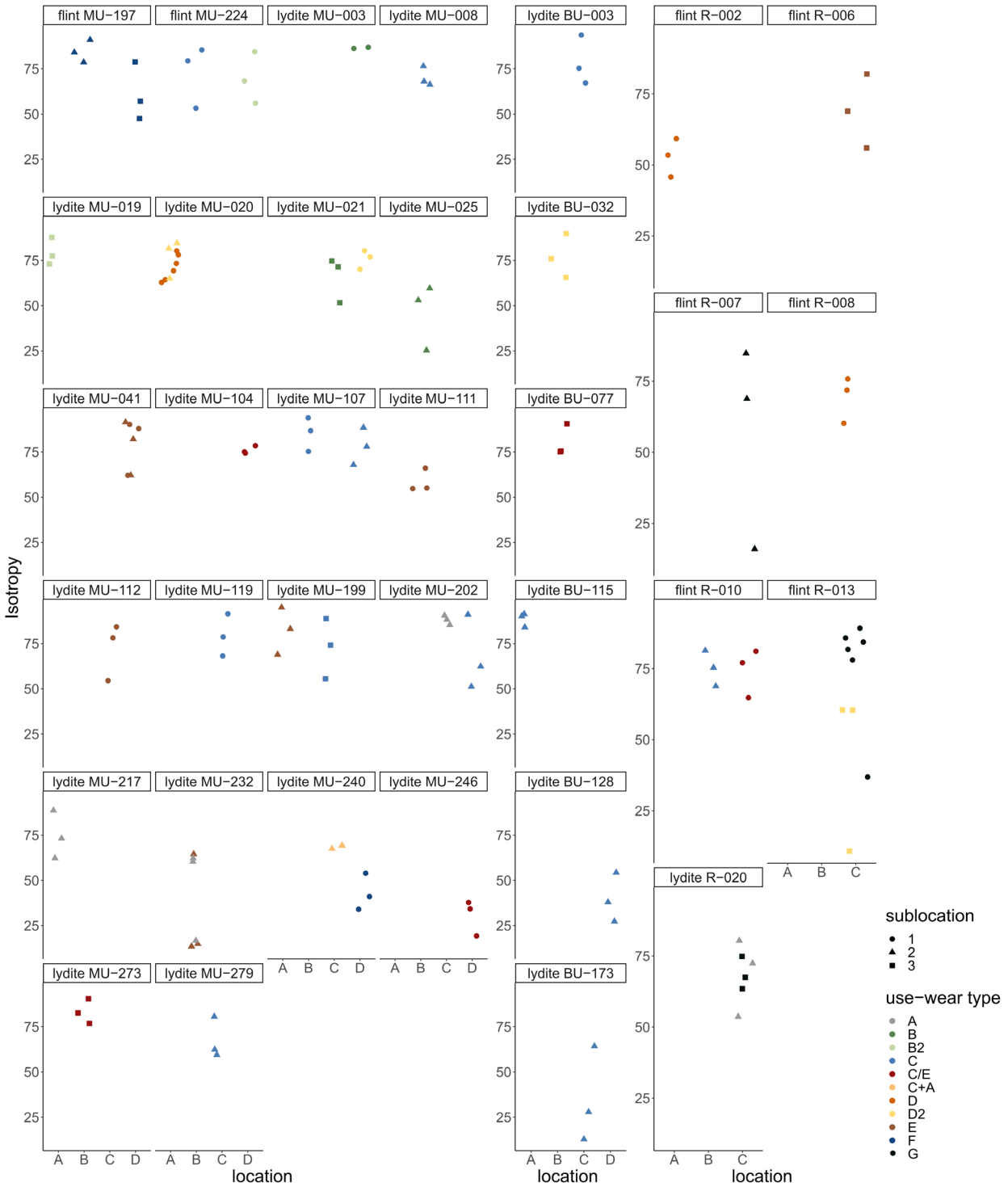

Fig. 113 *Isotropy* values for each analysed artefact (raw material [flint or lydite] plus ID). *Isotropy* reflects surface directionality. The value decreases with an increasing directionality of the surface. The plot indicates the location of the use-wear on the tool (A & B = dorsal, D & C = ventral) plus the sublocation (1, 2 or 3; sublocation stands for the number of use-wear traces *per* location). The three measurements per location and sublocation represent the three measurements *per* use-wear taken at non-identical but nearby spots. The data points are coloured based on the interpreted use-wear types.

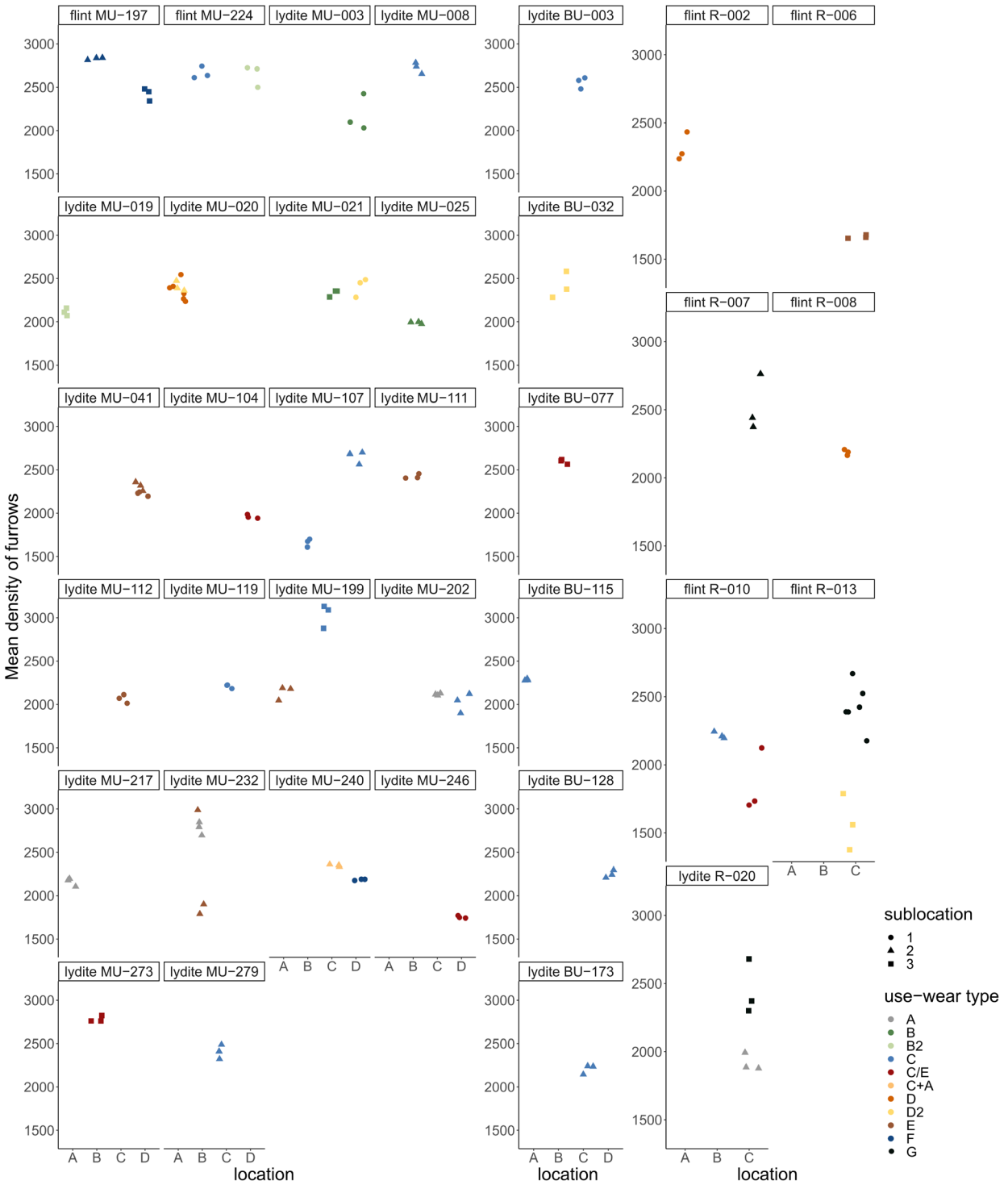

Fig. 114 *Mean density of furrow* values for each analysed artefact (raw material [flint or lydite] plus ID). *Isotropy* reflects surface directionality. The value reflects furrows on the surface. The plot indicates the location of the use-wear on the tool (A & B = dorsal, D & C = ventral) plus the sublocation (1, 2 or 3; sublocation stands for the number of use-wear traces *per* location). The three measurements per location and sublocation represent the three measurements *per* use-wear taken at non-identical but nearby spots. The data points are coloured based on the interpreted use-wear types.

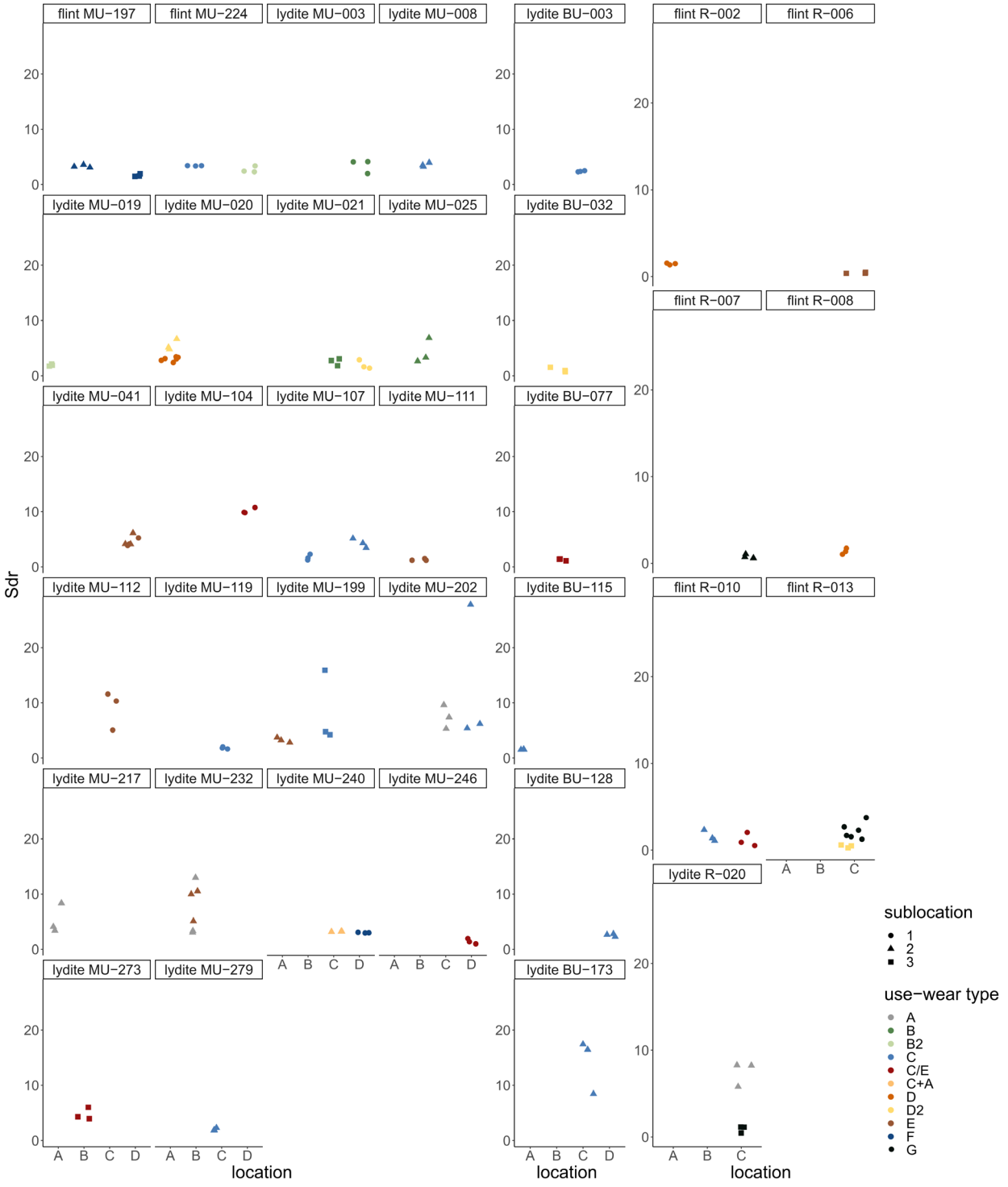

Fig. 115 *Sdr* values for each analysed artefact (raw material [flint or lydite] plus ID). *Sdr* is a measure of surface complexity. The higher the value, the more complex the surface. The plot indicates the location of the use-wear on the tool (A & B = dorsal, D & C = ventral) plus the sublocation (1, 2 or 3; sublocation stands for the number of use-wear traces *per* location). The three measurements per location and sublocation represent the three measurements *per* use-wear taken at non-identical but nearby spots. The data points are coloured based on the interpreted use-wear types.

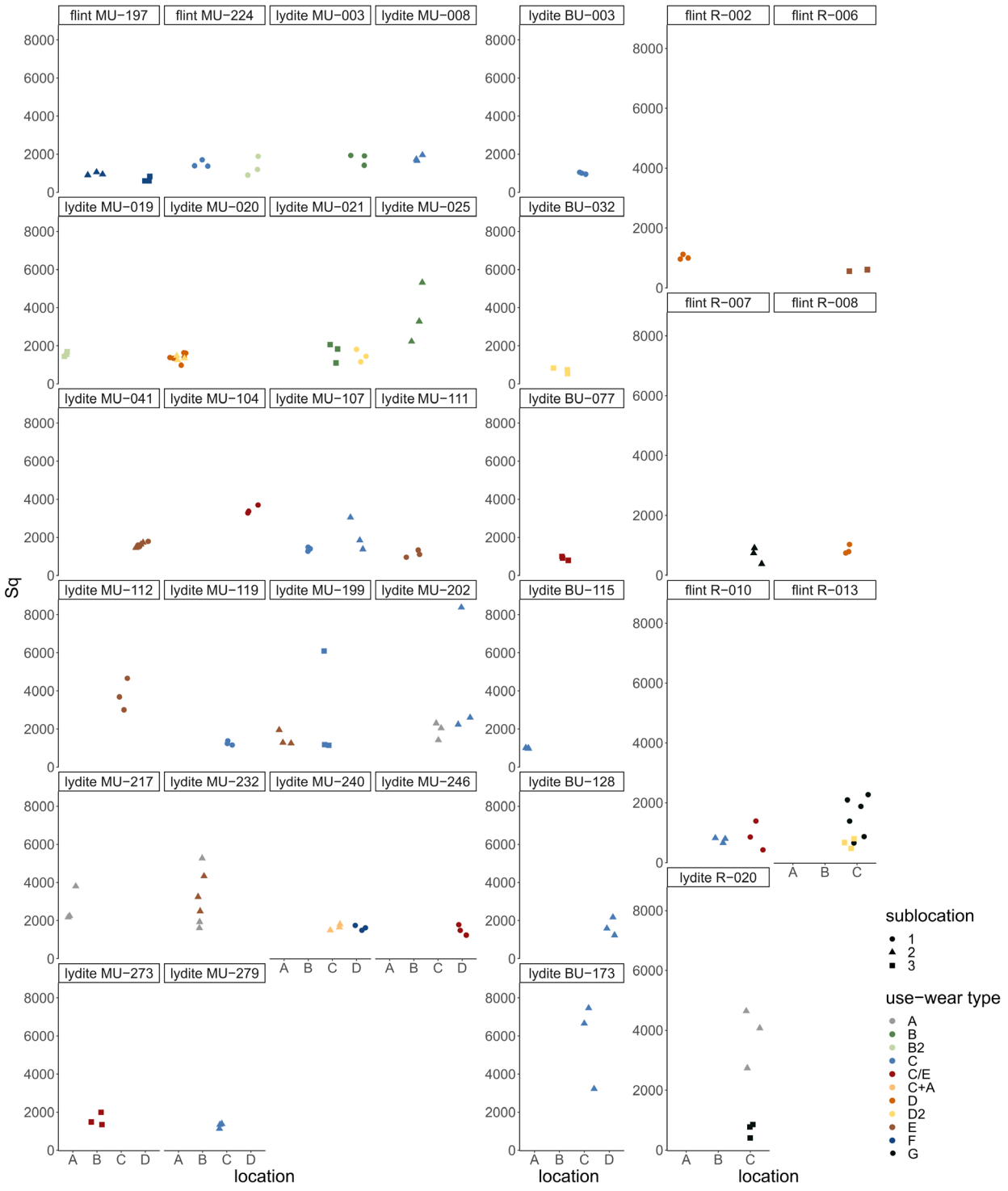

Fig. 116 *Sq* values for each analysed artefact (raw material [flint or lydite] plus ID). *Sq* is a measure of surface roughness. The higher the *Sq* value, the higher the surface roughness. The plot indicates the location of the use-wear on the tool (A & B = dorsal, D & C = ventral) plus the sublocation (1, 2 or 3; sublocation stands for the number of use-wear traces *per* location). The three measurements per location and sublocation represent the three measurements *per* use-wear taken at non-identical but nearby spots. The data points are coloured based on the interpreted use-wear types.

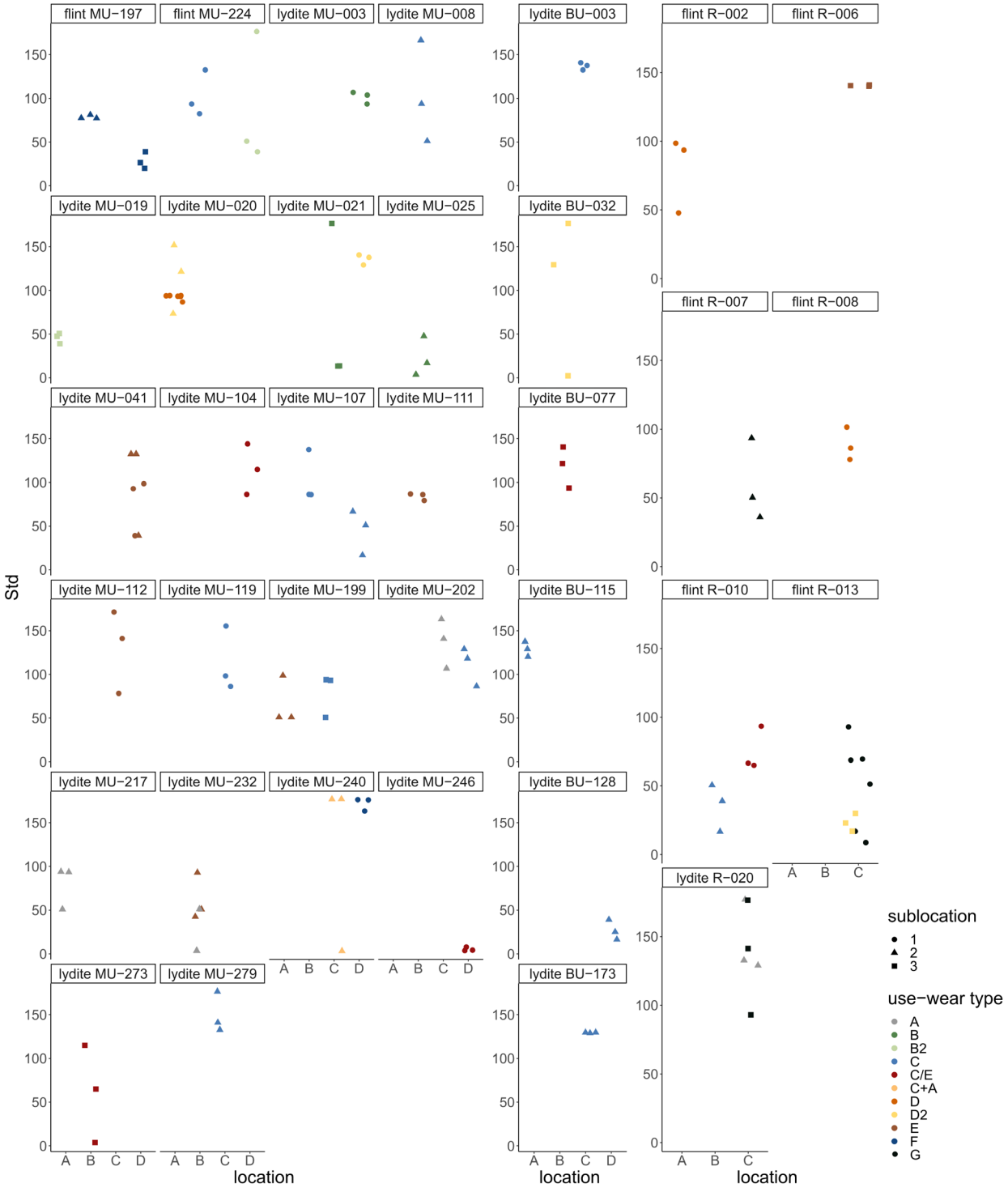

Fig. 117 *Std* values for each analysed artefact (raw material [flint or lydite] plus ID). *Std* reflects the main direction of the surface texture. The plot indicates the location of the use-wear on the tool (A & B = dorsal, D & C = ventral) plus the sublocation (1, 2 or 3; sublocation stands for the number of use-wear traces *per* location). The three measurements per location and sublocation represent the three measurements *per* use-wear taken at non-identical but nearby spots. The data points are coloured based on the interpreted use-wear types.

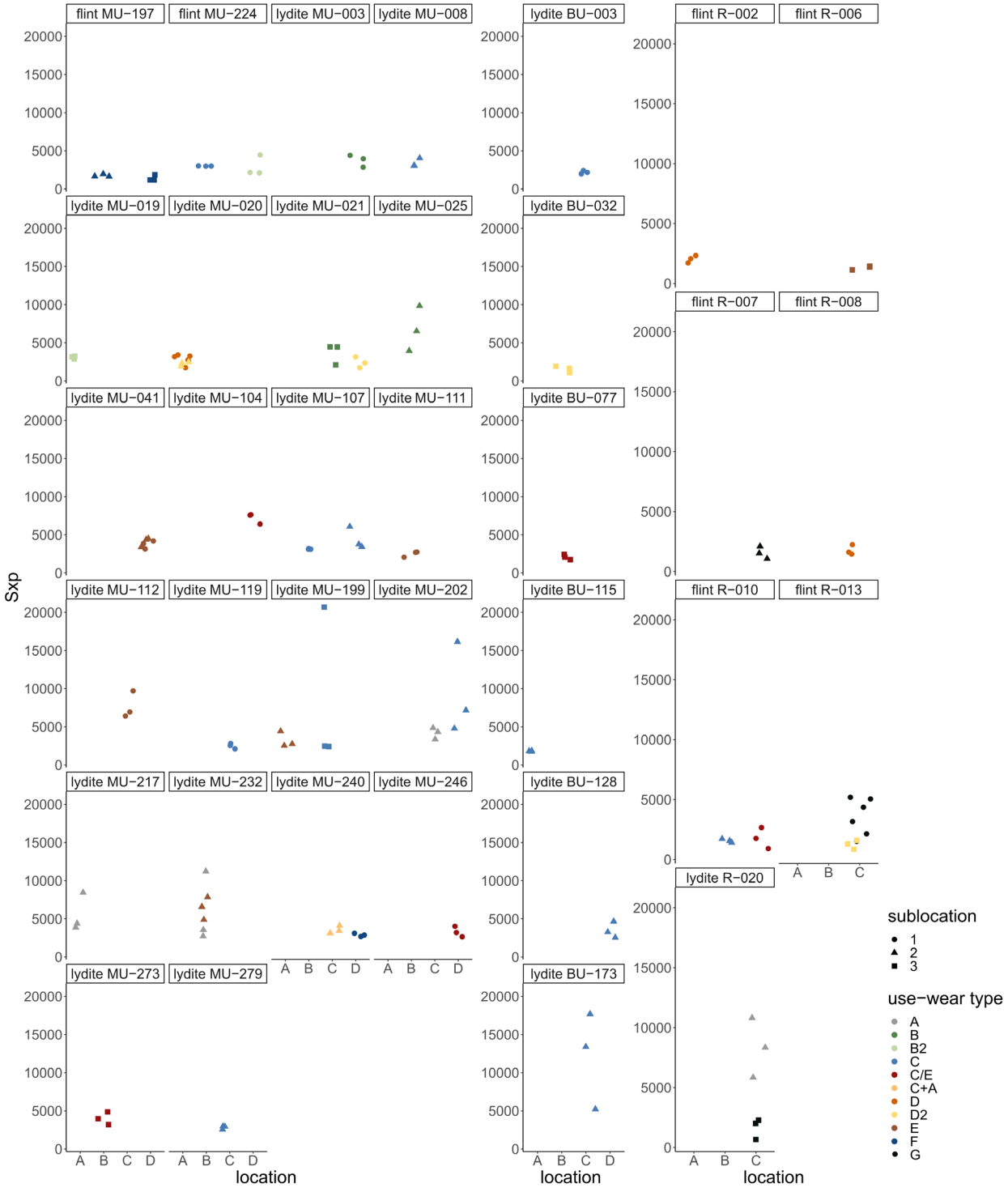

Fig. 118 *Sxp* values for each analysed artefact (raw material [flint or lydite] plus ID). *Sxp* is a measure for the height differences between the average height of the surface and the highest peak by excluding 2.5 % of the highest points. The plot indicates the location of the use-wear on the tool (A & B = dorsal, D & C = ventral) plus the sublocation (1, 2 or 3; sublocation stands for the number of use-wear traces *per* location). The three measurements per location and sublocation represent the three measurements *per* use-wear taken at non-identical but nearby spots. The data points are coloured based on the interpreted use-wear types.

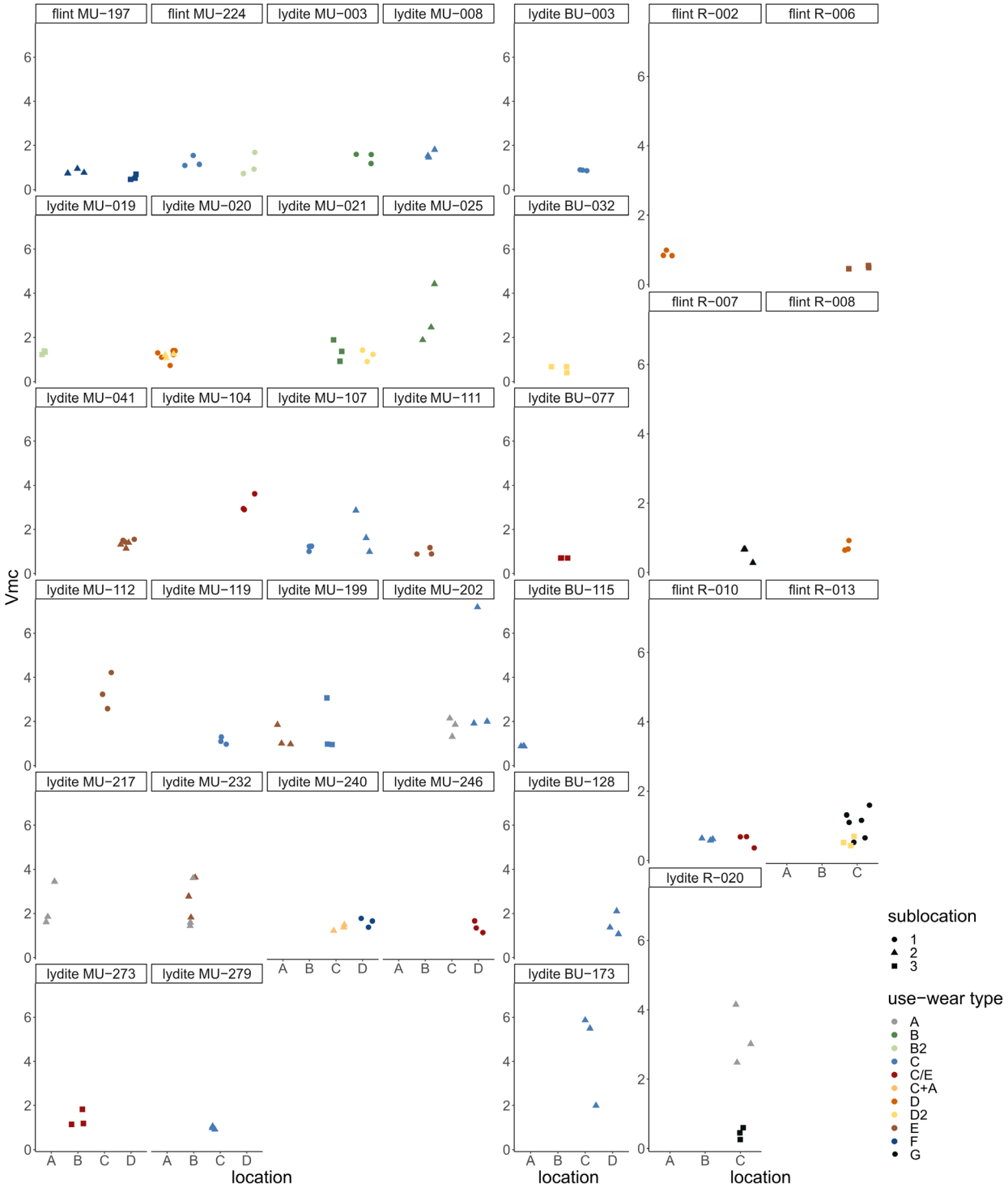

Fig. 119 *Vmc* values for each analysed artefact (raw material [flint or lydite] plus ID). *Vmc* stands for the volume of the material. The plot indicates the location of the use-wear on the tool (A & B = dorsal, D & C = ventral) plus the sublocation (1, 2 or 3; sublocation stands for the number of use-wear traces *per* location). The three measurements per location and sublocation represent the three measurements *per* use-wear taken at non-identical but nearby spots. The data points are coloured based on the interpreted use-wear types.

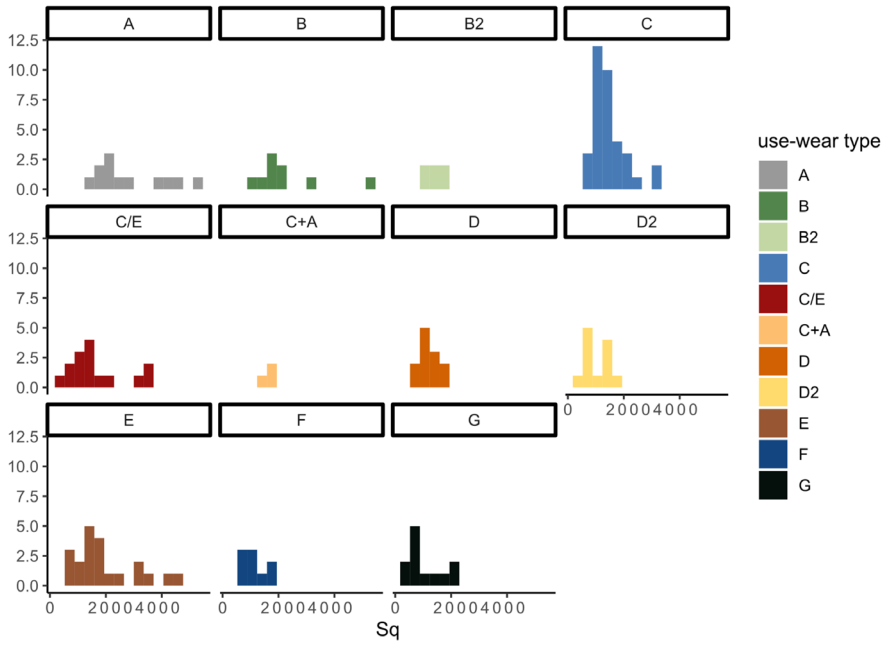

Fig. 120 *Sq* values and their frequency for the use-wear traces (n = 50) on the artefacts, categorised and coloured according to the interpreted use-wear types.

In order to bring the data a little more into question, the data was plotted in additional ways. For all these additional plots, the four measurements identified as outliers were excluded. Histograms of the use-wear types plotted *per* parameter support the aforementioned aspect (**fig. 120**). By a majority, the use-wear type V. displays a comparably low roughness based on the parameter *Sq*. Moreover, the observations that the types I., II. and IV. differ from other types, is also visible in the histograms.

The last mentioned aspect is also illustrated by the boxplots of the use-wear types plotted again per parameters (**fig. 121**). The boxplots include the information about the artefact category. Interestingly, the data measured on the scrapers set off against the other artefact categories.

Two parameters, *Vmc* and *Sq* were selected in order to plot the results of these parameters against each other in a scatterplot. In one plot, the data was coloured based on the interpreted use-wear types (**fig. 122**). The data points align in one direction without any significant correlation. The same can be reported for the second plot, in which the data points were coloured based on the two plotted artefact categories *Keilmesser* and *Prądnik scrapers* (**fig. 123**). The data representing the *Keilmesser* spread more over the plot, but is numerically also more represented. Other parameters were plotted in the similar way. The parameters are *epLsar* and *Asfc* (**fig. 124**) as well as *Mean density of furrows* against *mean depth of furrows* (**fig. 125**). The plots reflecting the different use-wear types lead to no new insights. However, in the plot *epLsar* against *Asfc* a separation of the use-wear types I. (A) and IV. (E) is visible. These two types do not cluster differently, but the data points spread further towards a higher *Asfc* value.

A last attempt to explore the data was done by a principal component analysis (PCA). A first PCA was applied on seven components reflecting the variance in the artefact categories (**fig. 126**). These components are the parameters *Sq, Ssk, Vmc, Mean density of furrows, Isotropy, Asfc* and *HAsfc9*, spanning the different categories of field parameters. The variance in *Sq, Vmc* and *Asfc* is represented by Principal Component 1 (PC1), which accounts for 38.55 %. Principal component 2 (PC2) reflected 21.29 % of the explained variance with *Ssk, Mean density of furrows, Isotropy* and *HAsfc9*. This dimensionality reduction illustrates an overlap of the data with the data scattering mainly on the right half of the PC1 axis. The data cluster from the four different artefact categories – *Keilmesser*, *Prądnik scraper*, *Prądnik spall* and *scraper* – clearly overlap, whereas the data points from the *Keilmesser* spread the most. The cluster built by the data points from the *Prądnik spacers* do differ from the other data.

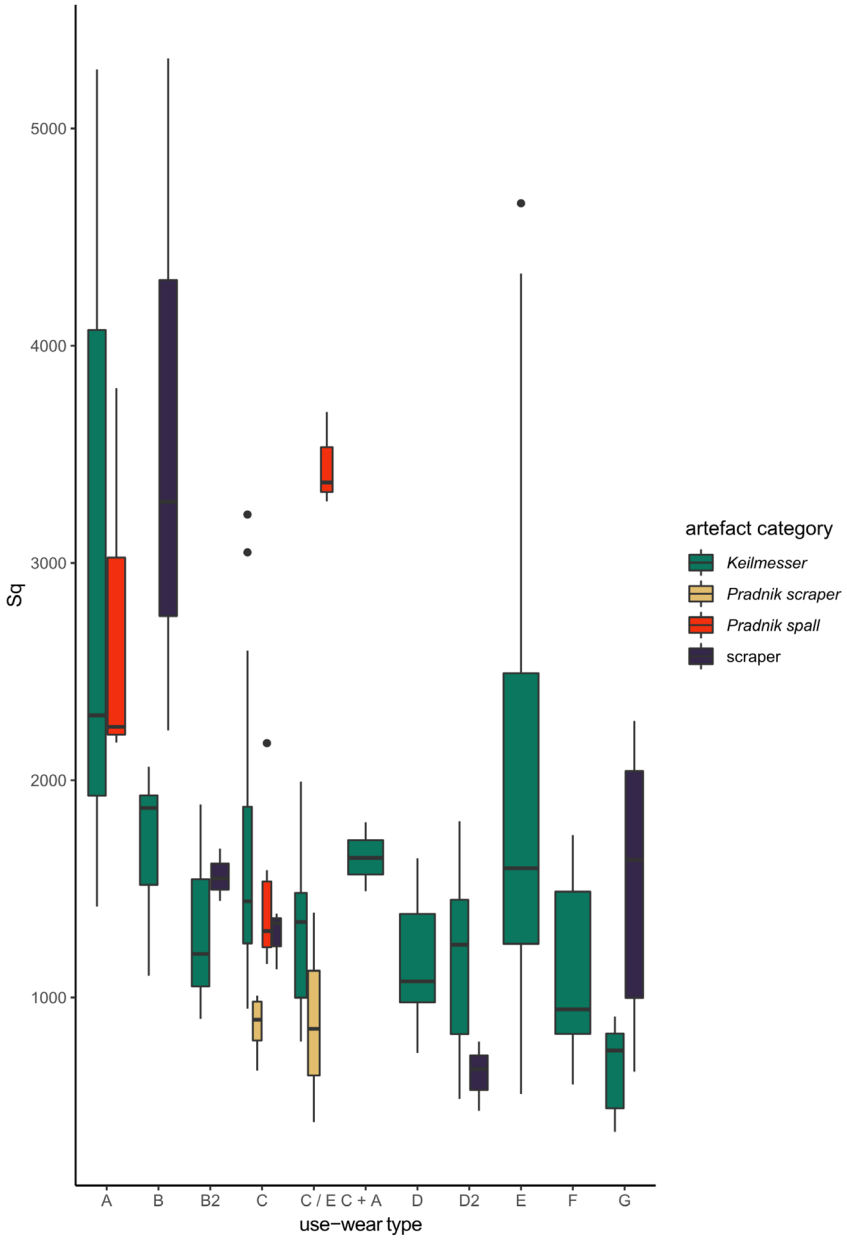

Fig. 121 Distribution of *Sq* values for the measured use-wear traces (n = 50) on the artefacts. The data is categorised according to the interpreted use-wear types and coloured based on the artefact type.

A second PCA visualises the variance of the different use-wear types based on the same seven components (**fig. 127**). Again, the data scatters mainly on the right part of the PC1 axis. However, the clusters illustrating the use-wear types I. (A), II. (B), IV. (E) and also the combination of V. (C) and IV. (E) stretch towards the left PC1 axis. In particular use-wear type I. (A) varies from the other clusters and does not overlap with the use-wear types III. (B2), VI. (D) and IX. (G).

Although the interpretation of these data enters a new field in archaeology and needs to be explored in more detail, the quantitative use-wear analysis proved to have the potential to complement and improve qualitative use-wear analysis. Based on the presented data, it can be noticed that *Sq* as a parameter for the surface texture roughness indicates differences when combined with the defined use-wear types. Some use-wear types (e. g. type V.) seem to reflect a lower surface-roughness than other types. However, the parameters associated with the surface directionality (e. *g. isotropy, epLsar* or *NewEpLsar*) are more complex and thus, the combination between the results of the qualitative and this quantitative use-wear analysis might be more complicated.

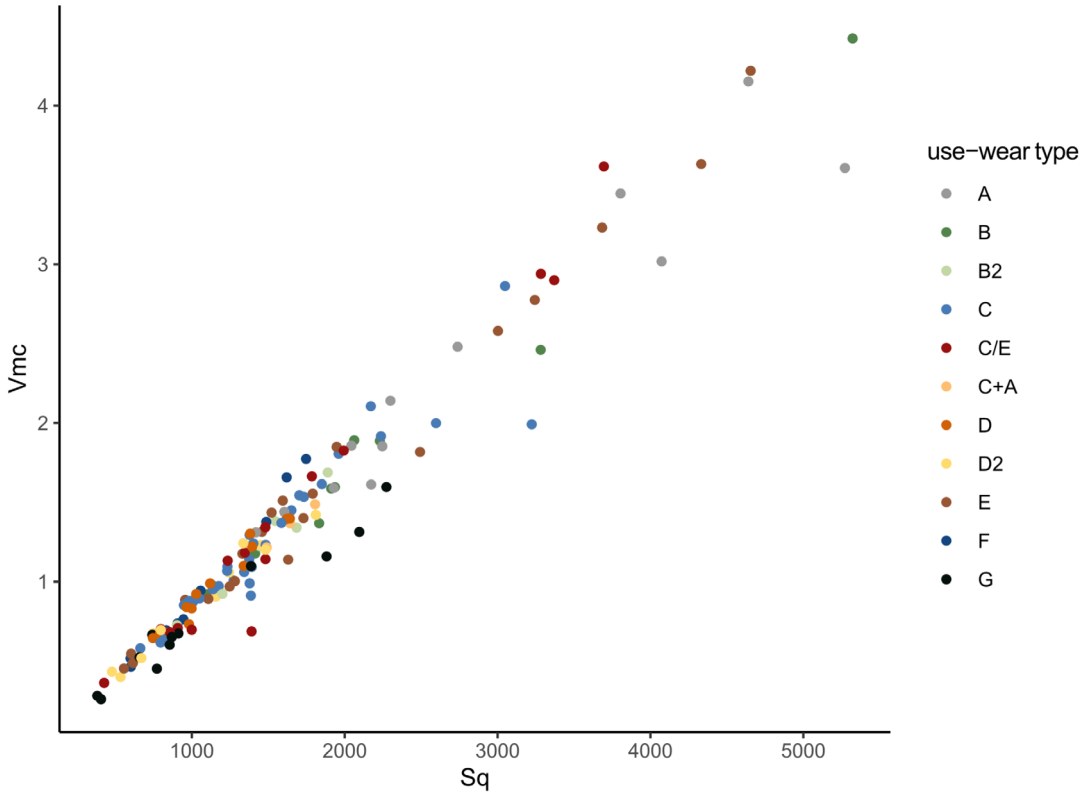

Fig. 122 *Vmc* and *Sq* values of the measured use-wear traces (n = 50) on the artefacts plotted against each other. The data points are coloured according to the interpreted use-wear type.

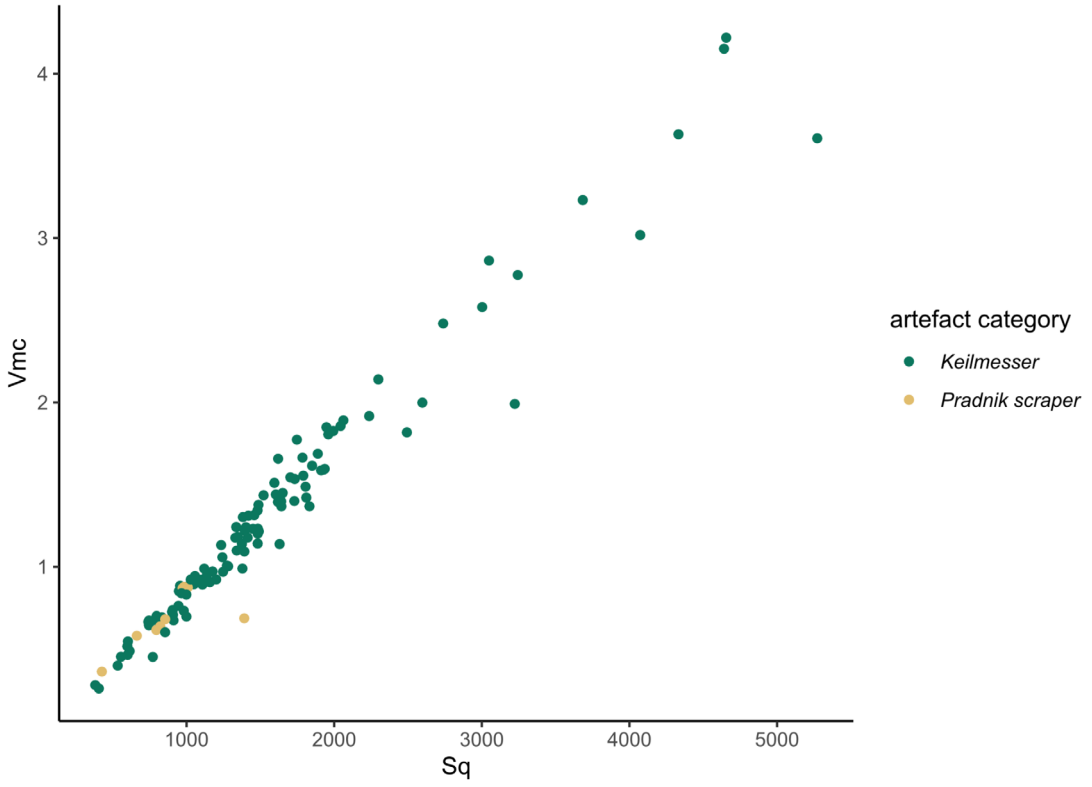

Fig. 123 *Vmc* and *Sq* values of the measured use-wear traces (n = 50) on the artefacts plotted against each other. The data points are coloured according to the artefact category.

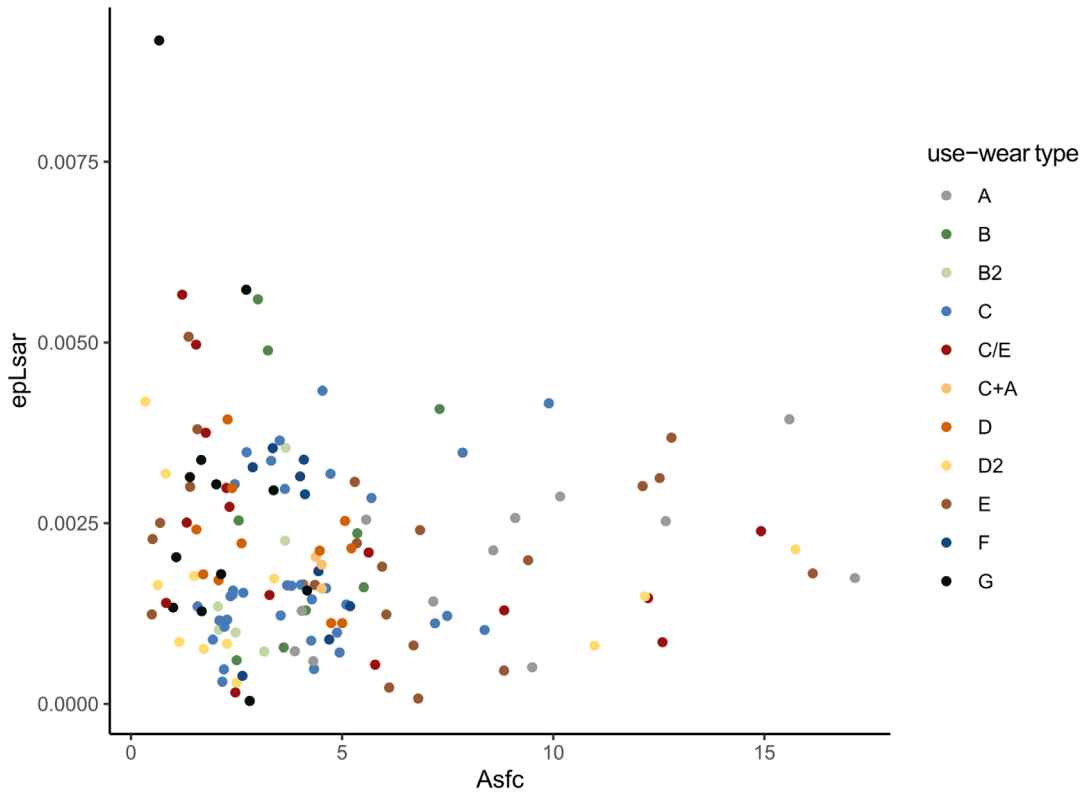

Fig. 124 *EpLsar* and *Asfc* values of the measured use-wear traces (n = 50) on the artefacts plotted against each other. The data points are coloured according to the interpreted use-wear type.

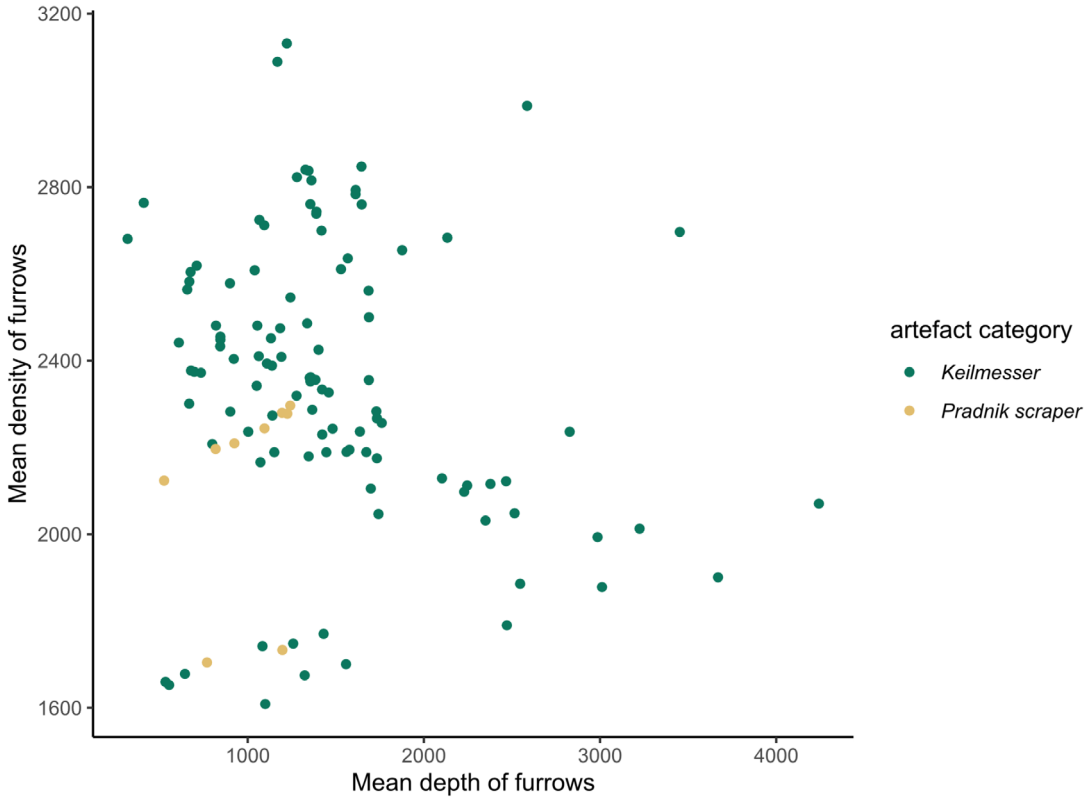

Fig. 125 *Mean density of furrows* and *Mean depth of furrows* values of the measured use-wear traces (n = 50) on the artefacts plotted against each other. The data points are coloured according to the artefact category.

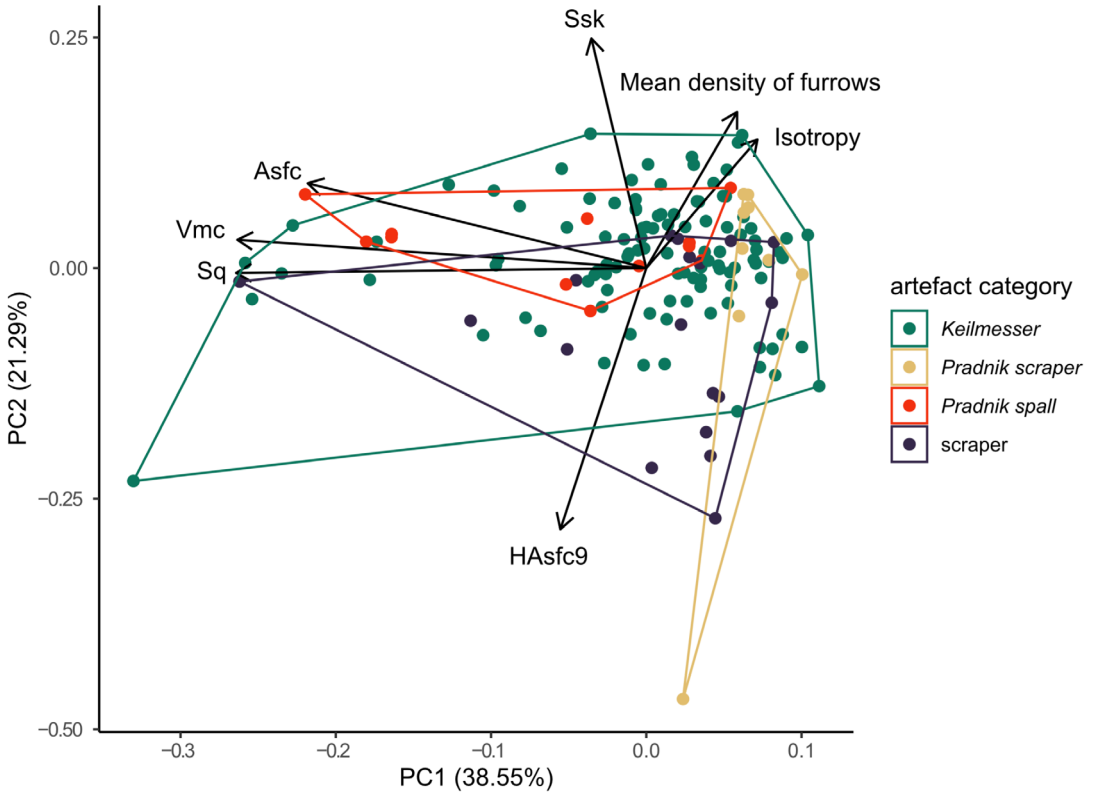

Fig. 126 Principal component analysis applied on the measured use-wear traces (n = 50) of the artefacts, reflecting variation regarding the artefact category.

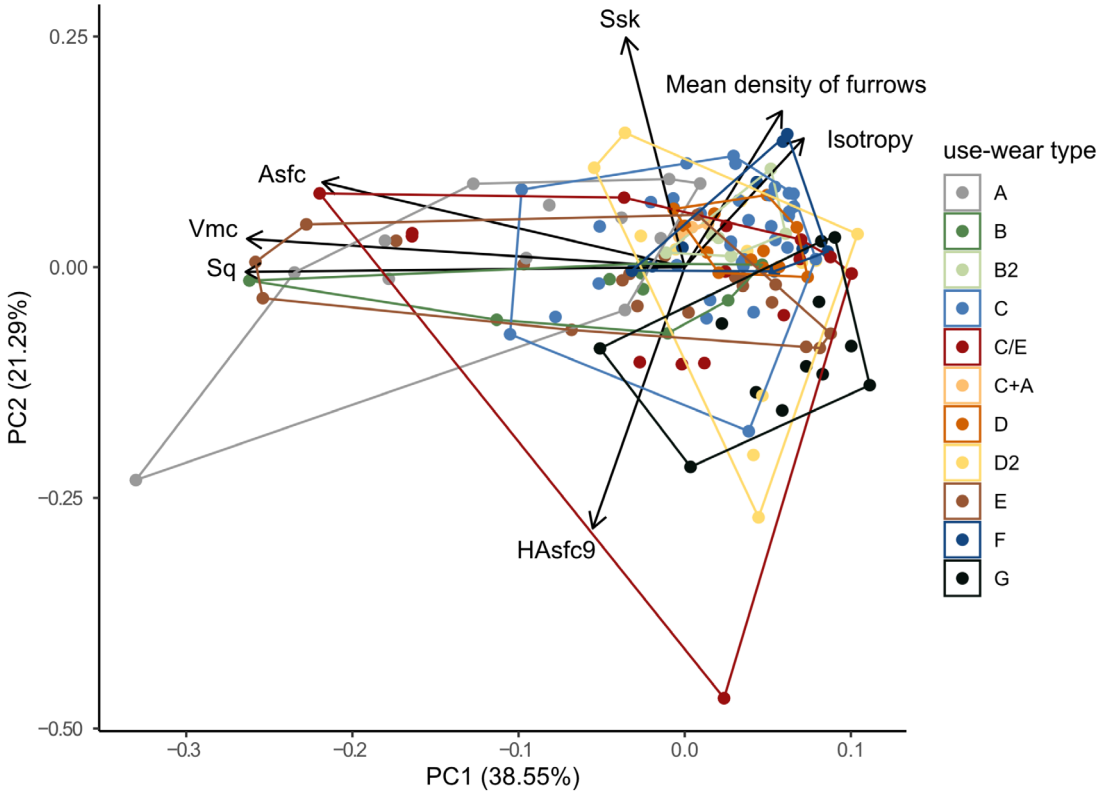

Fig. 127 Principal component analysis applied on the measured use-wear traces (n = 50) of the artefacts, reflecting variation regarding the interpreted use-wear types.

CONTROLLED EXPERIMENTS

The last subchapter refers to the results from the conducted so-called controlled or *second generation experiments* (*sensu* Marreiros et al. 2020). These experiments aimed at understanding the influence of specific, individually tested variables. These independent variables were the raw material and the edge angle of the standard samples, the contact material and the performed task. In order to test the effect-causation of these variables within a complex system, a mechanical device, the modular material tester SMARTTESTER®, was used to perform defined actions. Designed as sequential experiments, this also allowed for investigating the mechanics affecting tool performance and the formation of-use wear traces. Together, the execution of the experiments aimed at understanding the tool design of *Keilmesser* from a mechanical and practical point of view. At the same time, they were meant to test the possibility of successfully performing the two tasks, cutting and carving, with a specific edge design. In the following subchapter, the results are presented in the exact order, the experiments have been conducted: initial experiment, »artificial VS. natural« experiment and tool function experiment.

Data analysis – initial experiment

The first in the sequence of experiments was the so-called initial experiment (**fig. 36**). The purpose of this experiment was to test the experimental setup and to receive a first impression on the influence of the chosen variables within the setup. In total n = 7 standard samples (3× silicified schist 40°, 2× silicified schist 60°, 1× flint 40°, 1× flint 60°) were tested in a linear cutting movement on an artificial bone plate. Each sample had to perform in four cycles. Based on the uniform documentation of the standard samples before and after each cutting cycle it is possible to reveal precisely at which stage and location alteration in the sense of material loss, fractures, retouch etc. occur throughout the sequential experiment. In general, alteration has been documented via 3D scans and EDF images taken with a digital microscope as well as measurements based on the weight and the volume. However, the volume could not be calculated in the case of the samples from the initial experiment. The proximal part of the standard samples were fixed in a metal sample holder (**fig. 128**). This was done in order to guarantee that the samples can be fixed easily and cannot move in the sample holder of the SMARTTESTER®. During the course of the initial experiment, the metal attachment turned out as a weak point in the experimental setup. Thus, the metal attachment was slightly modified for the second experiment. After testing it on a few samples again, it was finally discarded. It became evident that an additional sample holder was not needed. Whenever a sample had this additional metal attachment, it was difficult to scan this area due to the high reflections of the material. Most of the time, the metal area was covered with a black fabric during the scanning process so that it was excluded from the documentation. Hence, the 3D models from the standard samples are missing their base. 3D models, which do not have an entirely closed mesh, are unsuitable for calculating the volume.
One important characteristic of a *second generation experiment* is the repeatability of the experiment and with thus the reproducibility of the data. As explained beforehand, the SMARTTESTER® was connected to five sensors throughout the experiments. In this way, the predetermined factors velocity, acceleration and force were sensor recorded. Two additional sensors measured the penetration depth and the friction. The initial experiment was meant to test the reliability of these controlling mechanisms. Thus, the data was checked frequently. The data set can be found on GitHub [https://github.com/lschunk/Initial_experiment-sensor_recording]. As shown by the data plot (**fig. 129**), force, friction, velocity (including acceleration) and depth are controlled throughout the experiment. Shown here are the measurements for one cycle of

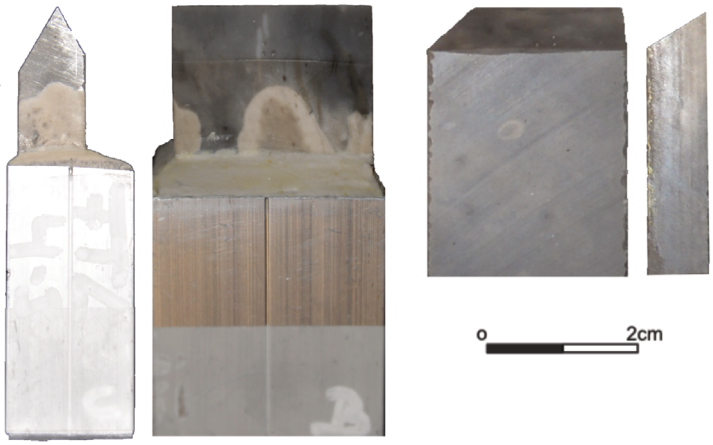

Fig. 128 Design of two standard sample (flint) illustrating the changes in design from the initial experiment to the later ones. The sample on the left side is fixed in a metal sample holder as used during the initial experiment. Moreover, the sample is bifacially cut. The sample on the right has no sample holder and is only unifacially cut. Additionally, this sample is modified by a 45° chamfered edge. – Scale 1:1.

50 strokes made with one standard sample (LYDIT1-2). Except for a few outliers in the force plot, the lines displaying each stroke are always following the same pattern. The data produced by the depth sensor at the bottom right, documents the increased depth of penetration by the standard sample with every cut.
All seven samples were used to perform the four cycles. Within these cycles of in total 2000 cutting strokes, the progressive alteration of the standard sample surfaces is recognisable (**fig. 130**). When looking at the samples with the 40° edge angle, the tool damage on the flint specimen is lower than the damage on the

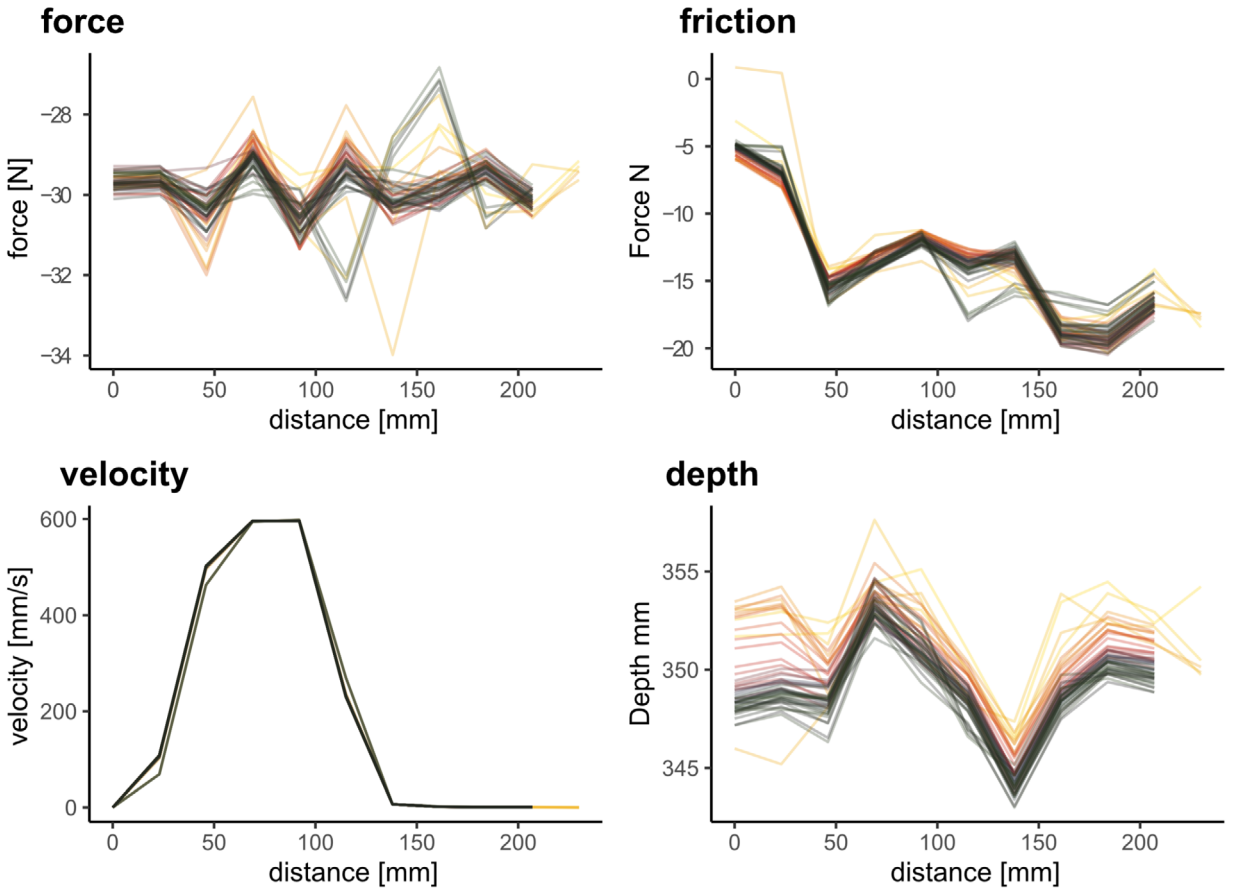

Fig. 129 Sensor data from a cycle of 50 cutting strokes performed with the SMARTTESTER® using the sample LYDIT4-2. Each line reflects one cutting stroke. The first stroke is in yellow and with increasing stroke number, the colour of the line turns darker. The graph illustrates that the predetermined factors force, friction and velocity stayed constant (as set) throughout the experiment. The graph in the lower right corner (depth) displays the achieved penetration depth, which increases throughout the 50 performed cutting stokes.

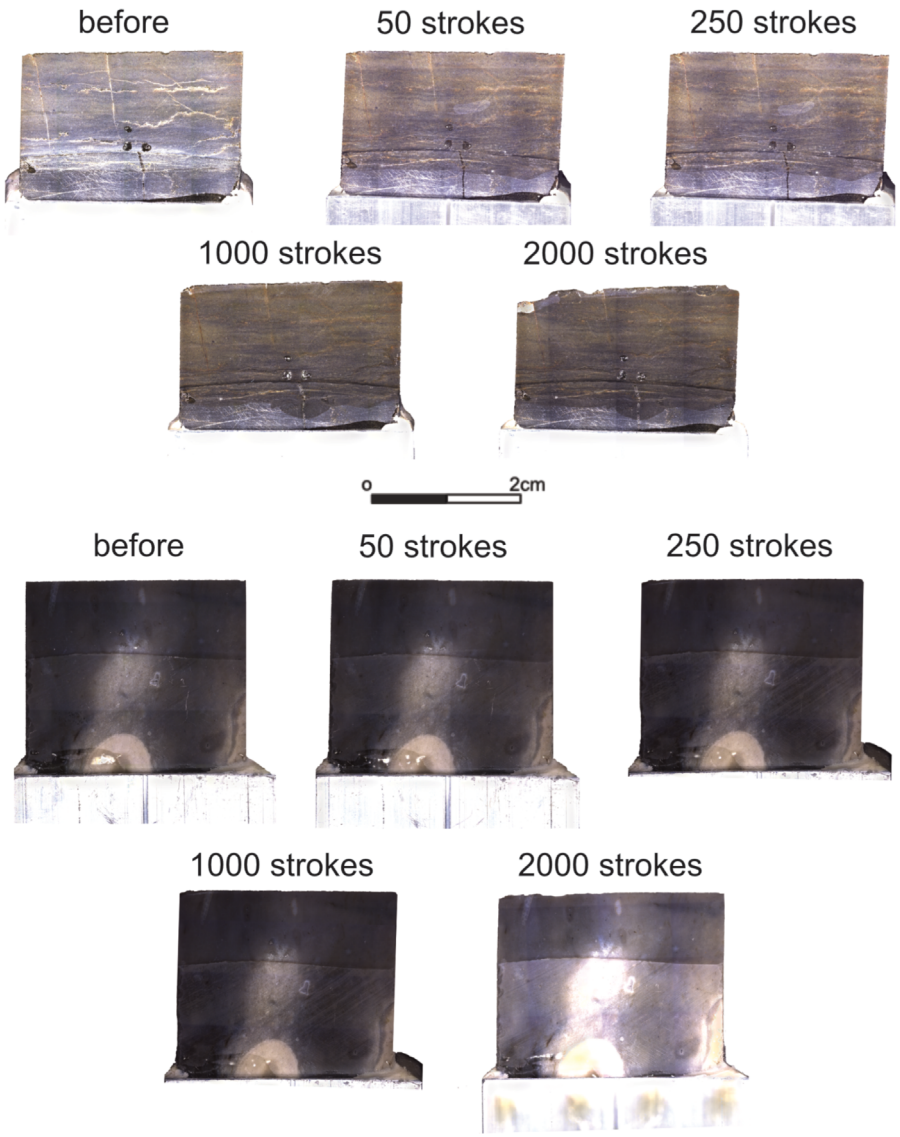

Fig. 130 Standard samples made of lydite (row one and two) and flint (row three and four) illustrating the alteration experience throughout the sequential experiment. – Scale 1:1

lydite samples. The material loss is also reflected in the weight measurements. In fact, one lydite sample (LYDIT1-4) performed only 1368 strokes instead of the targeted 2000 strokes. The cycle had to be ended at that point, because the sample could not perform the task anymore due to a breakage. Standard samples with the 60° edge angle do not show this difference between the raw materials. Only minor edge fragmentation (barley macroscopically visible) could be documented in both raw materials. Higher fragmentation changes the edge angle as well as the tool performance. Tool performance was only assessed based on visual estimations. As defined, tool performance describes how well a task, here the cutting, was accomplished. This can be assessed by correlating the cutting depth with the material loss on the standard sample and on the contact material. Since one factor, the calculation of the material loss based on the standard sample volume was not possible, this was not done for this initial experiment. Nevertheless, the tool performance can be partially assessed based on the contact material, the artificial bone plate. The first aspect that can be noticed is the quality of the cuts. The first three cuts on the bone plate are made by lydite samples, the fourth by a flint sample (**fig. 131**). All four samples had a 40° edge angle. While the flint sample cut appears as a thin line, the cut created with the lydite samples are broader and less fine. The same can be noticed for cuts produced with the 60° samples. The lydite cuts are not only wider they also achieve a greater cutting depth. A new line needed to be used for one sample (LYDIT3-2) during the last cycle. After

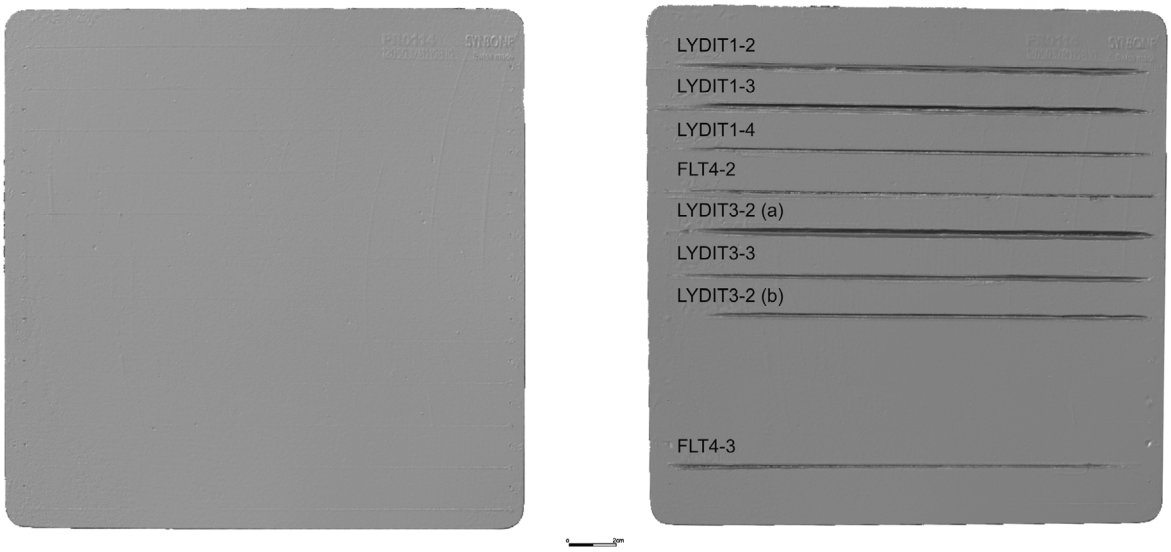

Fig. 131 3D scan of the artificial bone plate used during the initial experiment. The left side shows the plate before the use, the right side after 2000 strokes performed with seven standard samples.

1000 strokes, the generated cutting depth was nearly equal to the thickness of the bone plate. In order to avoid a damage of the mechanics below the bone plate, a new cutting track was started. Visually judged, this above mentioned lydite sample was not the only sample creating a deep cut. It seems as if the cutting depth generated by the lydite samples in general is deeper than the ones from the flint samples. Likely, this aspect can be combined with the edge angle changes of the samples.

The edge angles of all samples were calculated before and after each cycle. This was done based on the 3D models, as previously explained. Although the edge angles were calculated with the three different measurement procedures respectively, only the results from the »3-point« procedure will be presented here (fig. 132). The entire dataset can be found on GitHub [https://github.com/lschunk/edge_angle_experiments]. The data as well as the plot illustrates clearly, that the 40° and 60° flint samples change the edge angle in the course of the experiment only insignificantly. The same counts for the two 60° lydite samples. The change of the edge angles in these samples is about maximum 3° and thus also in the threshold of the expected inaccuracy of the measurement method. The 40° lydite samples did change more significantly. Throughout the first 250 strokes, the edge angles of the three lydite samples altered only slightly as described for the other samples. Distinct changes occurred during the penultimate and especially during the last cycle. While this means a difference of about 10° from the initial 40° edge angle in two lydite samples, one sample altered much more. The edge angle of the sample LYDIT1-4 changed from 40° to roughly 50° after 1000 strokes and above 100° throughout the last cycle.

Altogether, the preliminary observations made during the initial experiment show a reproducible trend: lydite breaks more easily than flint when the tool has a low edge angle (= 40°). With a higher edge angle of 60° this difference between flint and lydite can no longer be observed (Schunk et al. 2019). At the same time, lydite seems more efficient in the sense of the achieved cutting depth. The more fragile the raw material, the bigger the risk of damages, which can affect the durability. In the case of the more fragile lydite, increasing the edge angle leads to an improved durability. Efficiency and durability both play a role when evaluating tool performance.

Neither a qualitative nor a quantitative use-wear analysis was done on the samples from the initial experiment.

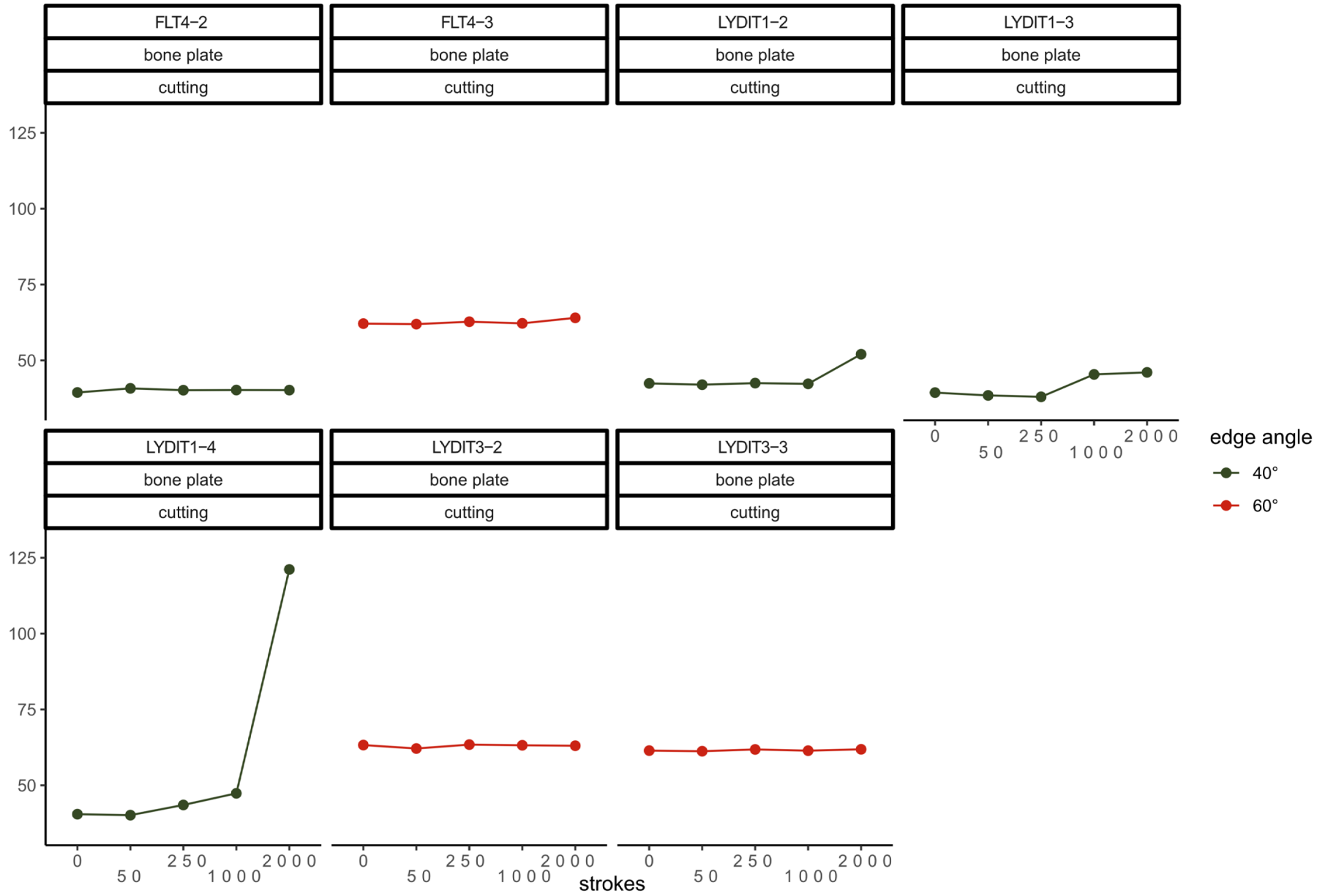

Fig. 132 Edge angle values calculated per sample used during the initial experiment (calculated with the »3-point« procedure; mean value of section 2 to 8 and distance 3 to 6). The data points per sample represent the values after the performance of each cycle (0, 50, 250, 1000 and 2000 cutting strokes).

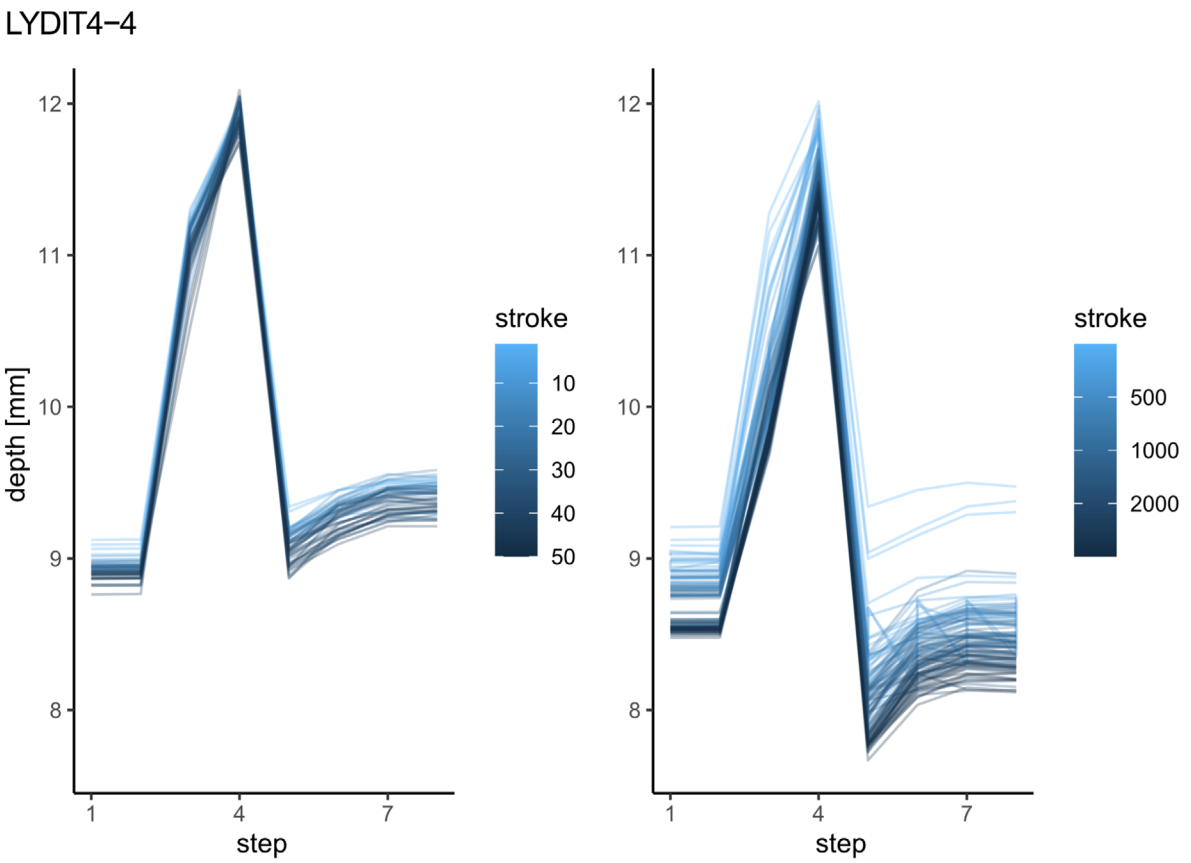

Fig. 133 Sensor recorded penetration depth achieved with a cutting movement performed with the SMARTTESTER® during the »artificial VS. natural« experiment. Exemplarily presented here the recording of sample LYDIT4-4. The left graph shows each cutting stroke within the first cycle (0 to 50 strokes). The right graph shows each 40th cutting stroke within all cycles (0 to 2000 strokes). The darker the colour, the greater the penetration depth.

Data analysis – »artificial VS. natural« experiment

The second experiment was the »artificial VS. natural« experiment (**fig. 37**). The goal of the experiment was to evaluate, whether standardised, artificial contact materials lead to comparable results as the use of natural contact material does. Simultaneously, this experiment was meant to add more data on how the independent variables – here raw material and contact material – influences tool efficiency, durability and performance. Concerning the use-wear, this experiment was also meant to provide data in order to test and understand the mechanics behind the formation of use-wear traces. Moreover, the reflection of these processes in the quantitative data should be investigated.

The twelve lydite and the twelve flint samples were all unifacially cut with a 60° edge angle. The samples were tested in four cycles on a bone plate with a rubber skin layer, a fresh cow scapula, a soft tissue pad and a piece of natural pork skin. All 24 samples passed through the four cycles and completed the 2000 cutting strokes respectively.

The first analysed aspects were the sensor data from the SMARTTESTER®. As explained in the method chapter, the focus thereby was lying on the data from the depth sensor. The penetration depth for each sample was recorded throughout the entire experiment. The data was plotted per sample (**fig. 133**). The plots always show in one plot each single stroke from the first cycle (n = 50 strokes) and every 40th stroke

from all the four cycles together in a second plot. These plots illustrated a continuous increase in depth with a rapid penetration during the first 250 strokes (dependant on the contact material). Unfortunately, some issues with the software of the SMARTTESTER® can be noticed similarly. Some of the plots show clear outliers with sudden changes in depth. These are part of the data, but could be identified as wrong recoding due to problems with the software. Moreover, the absolute penetration depth per sample was calculated (**figs 134-135**). The plots of these calculations reveal some interesting aspects. First of all, the samples reached a greater cutting depth on the natural contact materials compared to the artificial contact materials. More surprisingly is that the lydite samples performed better than the flint ones. Except for the skin pad, where the results are similar between the samples from the two raw materials, lydite tends to achieve a higher cutting depth.

Identical to the initial experiment, the edge angle values of all samples during the different stages were calculated (**fig. 136**). Before explaining the results, it has to be mentioned that a few data points are misleading. The scans from one sample, LYDIT4-9, are slightly problematic. The scans after 50 strokes and after 1000 strokes displayed some small holes on the edge, indicating that the edge was not perfectly scanned. These holes needed to be filled in order to calculate the edge angle values. Apparently, the filling was not accurate enough. These two data points are wrong and do not display the real edge angle values. That these data points are incorrect can be reconstructed by inspecting the raw data of the 3D models and the EDF pictures of the edge. For the mentioned two samples, no visible change occurred during the corresponding cycles. One other sample displays misleading results. The sample FLT4-7 got damaged right before it was used in the experiment. Due to this damage, the cutting edge of the standard sample was partly modified. One half of the edge was still complete and displayed the typical diamond band saw cut, the other half looked retouched (**fig. 137**). Since it takes many hours to produce such a standard sample, it was decided to use this sample as initially planned. The sample was documented again and treated as any other new sample. However, the edge angle of the retouched part of the standard sample was slightly higher than the targeted 60°. Therefore, the mean edge angle of sample FLT4-7 deviates with ~ 66° from the other standard samples. For the remaining edge angle calculations, no mistake could be identified. For the twelve samples (lydite and flint) used on the soft materials, natural pork skin and artificial soft tissue pad, no significant change could be documented. All edge angle changes are within the approximated 3° threshold of the expected impreciseness of the measurement method. The results differ when looking at the samples used to cut the hard contact material, fresh cow scapula. The samples used on the fresh cow scapula are characterised by alteration along the standard sample edge. The alteration occurs directly during the first cycle and proceeds continuously throughout each cycle. The edge angle values shift about 3° to 9°, whereas the edge alternation is slightly bigger for the lydite samples than for the flint samples. The results for the samples used on the second hard material, the artificial bone plate, are comparable to the results from the soft contact material. One exception should be mentioned. Sample LYDIT4-2 displays a small alternation of the edge of about 6° in total. Here, the modification is also characterised by a continuous process starting already during the first cycle. To summarize, the hard contact material favours alteration of the standard samples. This process was documented on the flint standard samples as well as on the lydite standard samples. However, this effect is stronger in lydite. The last aspect is emphasised by the results from sample LYDIT4-2.

The qualitative and quantitative use-wear analysis was done for eight samples from the »artificial VS. natural« experiment (see **appendix II**). These eight standard samples have been selected systematically so that four flint and four lydite samples were involved in the analysis. *Per* raw material, there was one sample respectively tested from each of the four contact materials. For the qualitative use-wear analysis, the »dorsal« (A and B) and the »ventral« surface (D and C) were analysed with the upright light microscope (ZEISS Axio Scope.A1 MAT). All use-wear traces are illustrated as figures in the supplementary material.

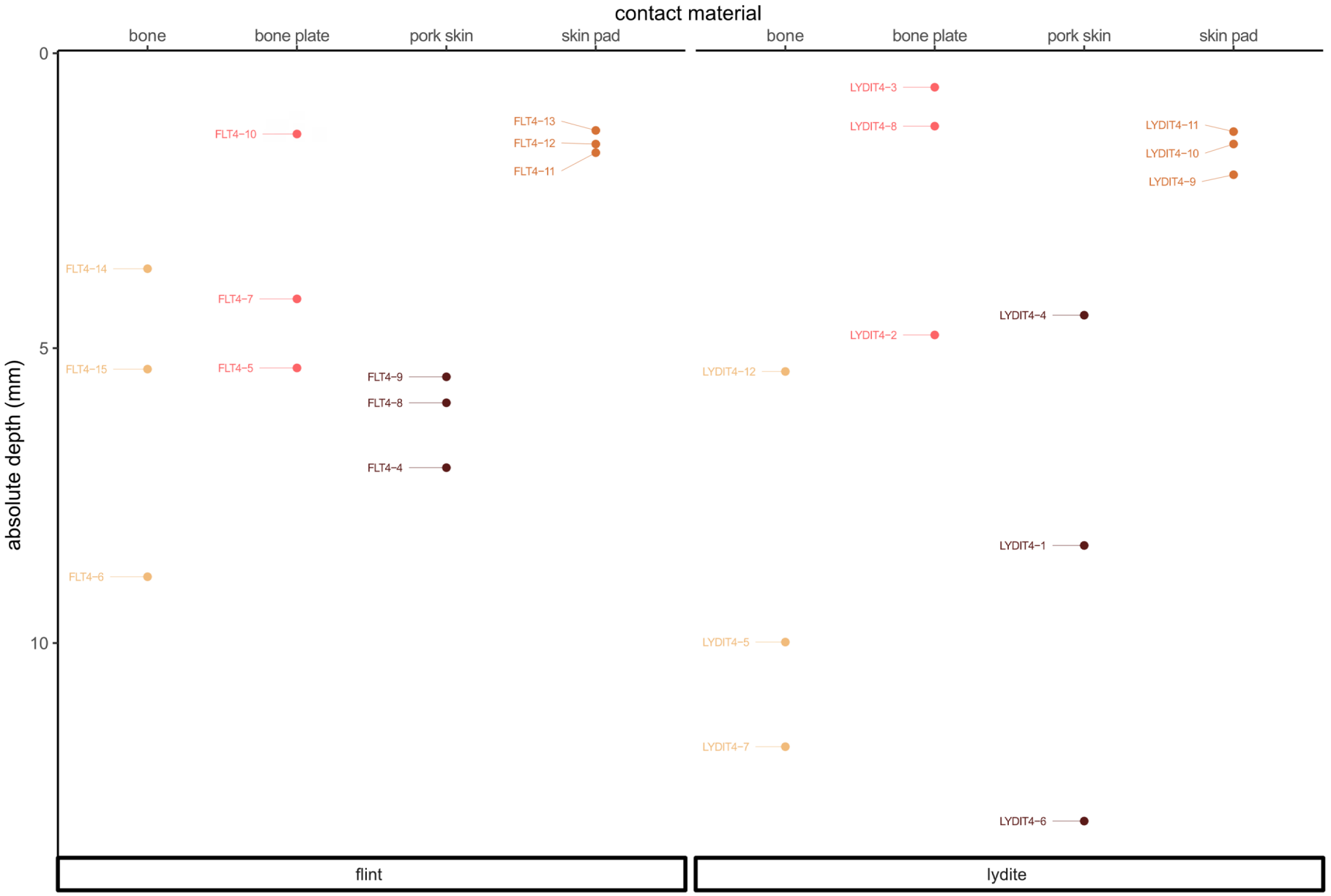

Fig. 134 Absolute cutting depth of all samples used during the »artificial VS. natural« experiment. The samples are organised according to the standard sample raw material and the contact material.

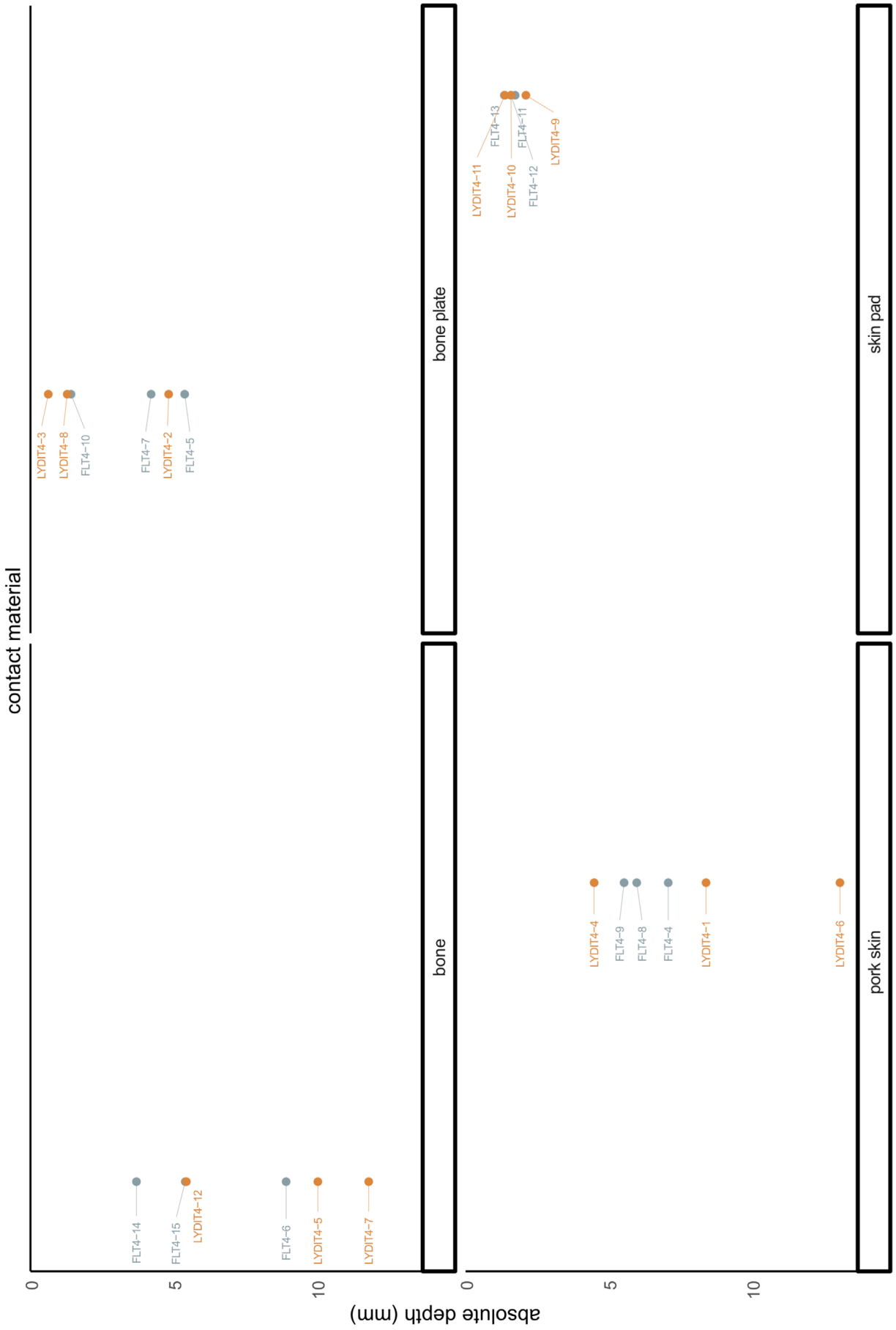

Fig. 135 Absolute cutting depth of all samples used during the »artificial VS. natural« experiment. The samples are organised according to the contact material.

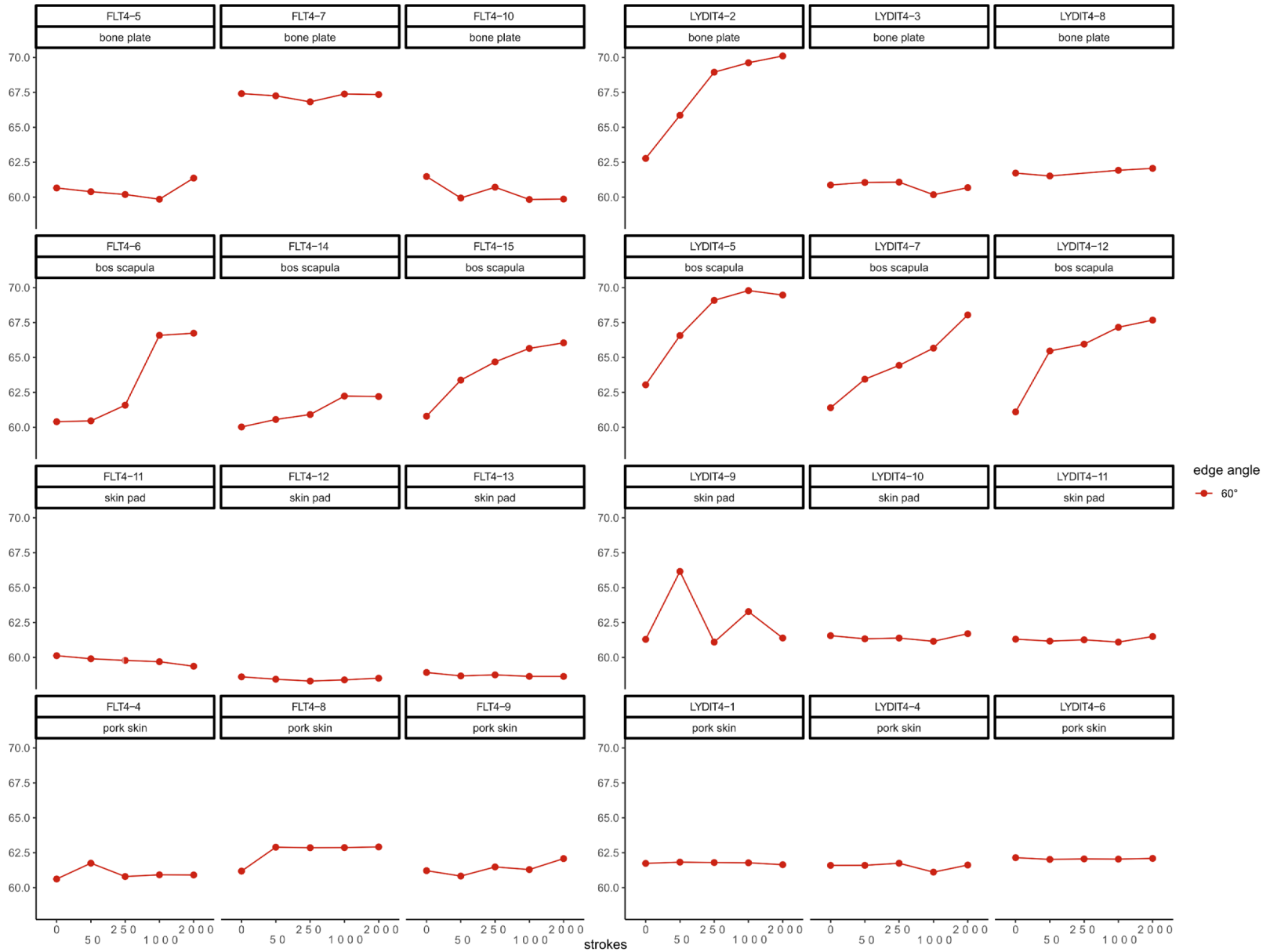

Fig. 136 Edge angle values calculated per sample used during the »artificial VS. natural« experiment (calculated with the »3-point« procedure; mean value of section 2 to 8 and distance 3 to 6). The data points per sample represent the values after the performance of each cycle (0, 50, 250, 1000 and 2000 cutting strokes).

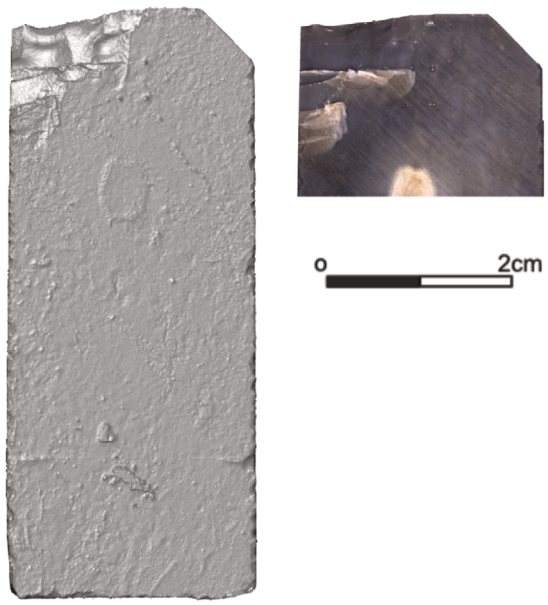

Fig. 137 Flint standard sample FLT4-7 as 3D scan (left) and EDF-stitching image of the edge (right) used during the »artificial VS. natural« experiment. The sample is damages on the left side. – Not to scale.

The question behind the use-wear analysis was to see how, where and when use-wear develops on the standard samples. Another question was, whether or not the use-wear traces produced with the natural contact material differ from the ones produced with the artificial contact material or vice versa. To answer these questions, the selected eight samples (moulds) were microscopically analysed before and after each cycle. To start with the soft contact material again, first the results for the natural pork skin will be explained (**figs 138-139**). On the flint sample (FLT4-4), there is no development of use-wear visible until 1000 strokes. Use-wear is visible on the »dorsal« (B) surface. The spot is further developed after 2000 strokes. The lydite sample (LYIT4-1) used on the natural pork skin starts to develop some use-wear traces after 250 strokes (D), but identifiable use-wear traces are only visible after 2000 strokes (A, B, D). However, the surface shows in the beginning clear traces of the diamond band saw cut and these traces turned weaker within the first cycles. The same can be noticed for the lydite sample (LYDIT4-9) used on the artificial soft tissue pad. Throughout the cycles, the initially visible traces from the diamond band saw abrade and disappear, the »natural« surface seems to appear and during the last cycle, use-wear traces develop (B). The situation is similar for the corresponding flint sample (FLT4-12). The flint sample (FLT4-7) used on the artificial bone plate only displays clear use-wear traces (A, B) after 2000 strokes. By contrast, use-wear traces (A, C) on the lydite sample (LYDIT4-2) are already visible after 50 strokes. Both samples (FLT4-15 and LYDIT4-5), which were used on the fresh cow scapula, show traces right after the first (lydite: A, B) and second cycle (flint: B, D). Only the traces on the »ventral« surface (D) of the lydite sample occur as distinct traces not until 1000 strokes.

The qualitative analysis could prove that use-wear traces do develop on the standard samples, although they are missing the surface texture characteristic for the material. Moreover, these observations clearly show that the harder the contact material, the easier is it for use-wear traces to develop. At the same time, a modification of the standard sample surface occurs faster on lydite than on flint. The answer for the comparability between natural and artificial contact materials is less straightforward though. Visually inspected, the traces produced by both groups of contact material do appear similar. The developed polished areas do look typical for hard and soft contact materials. However, the process, when the traces develop, is not always comparable. The results for the lydite samples are identical on the natural as well as on the artificial contact materials. The lydite samples used on both soft contact materials display use-wear traces after 250 and 1000 strokes, the ones used on both hard contact materials after 50 strokes. The situation for the flint samples is different. While cutting, the natural soft contact material led to use-wear traces after 1000 strokes, the artificial soft contact material did not produce use-wear traces before the 2000 stroke cycle. The sample used on the natural hard contact material developed traces after 50 strokes, while traces from the artificial hard contact material appeared not until 1000 strokes. Unfortunately, only one sample per raw material and contact material was analysed, so that the results are not statistically evaluable.

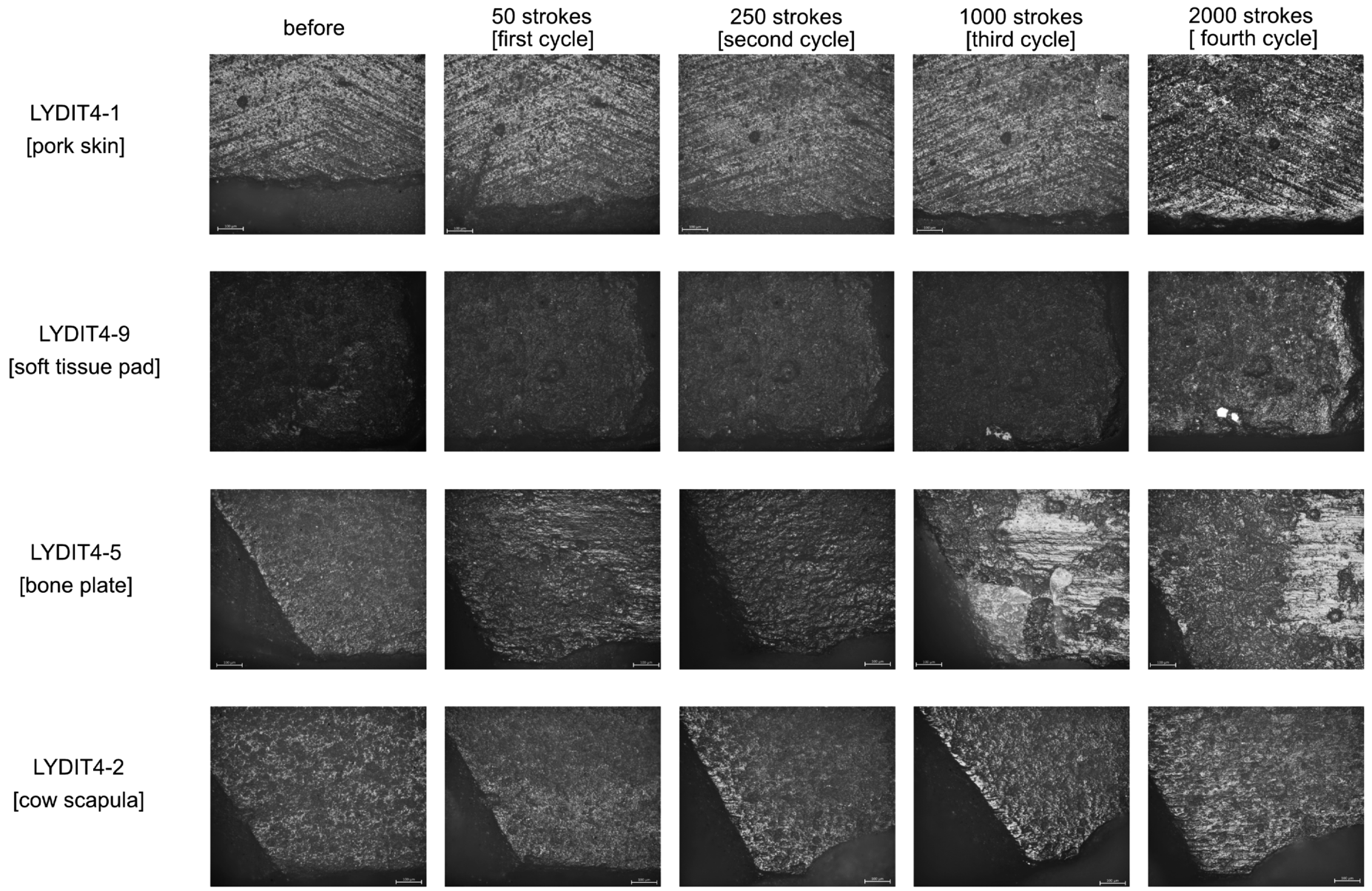

Fig. 138 Use-wear formation on the analysed lydite standard samples during the four cycles of the »artificial VS. natural« experiment (all images are taken with a 10× optical objective).

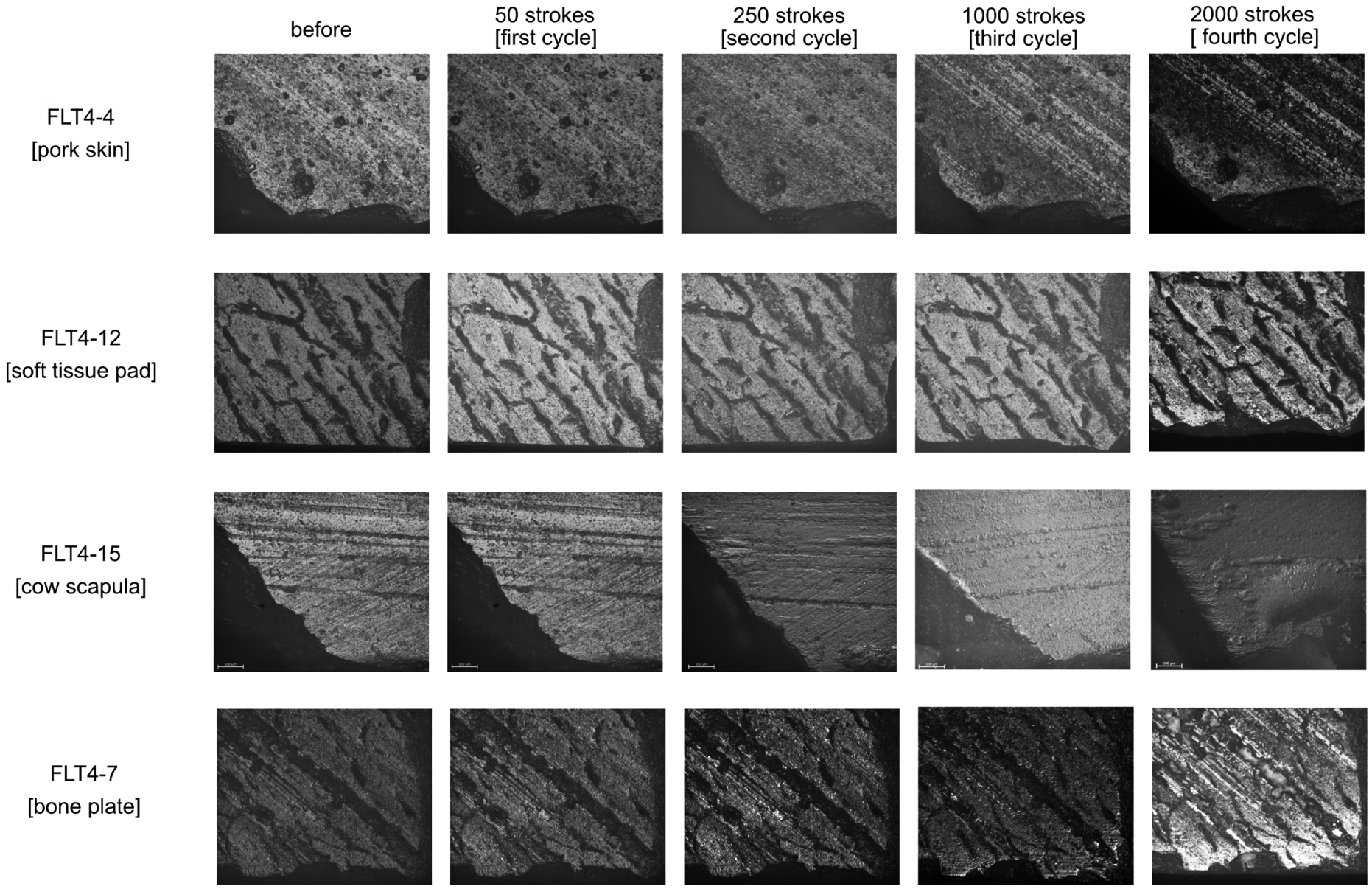

Fig. 139 Use-wear formation on the analysed flint standard samples during the four cycles of the »artificial VS. natural« experiment (all images are taken with a 10× optical objective).

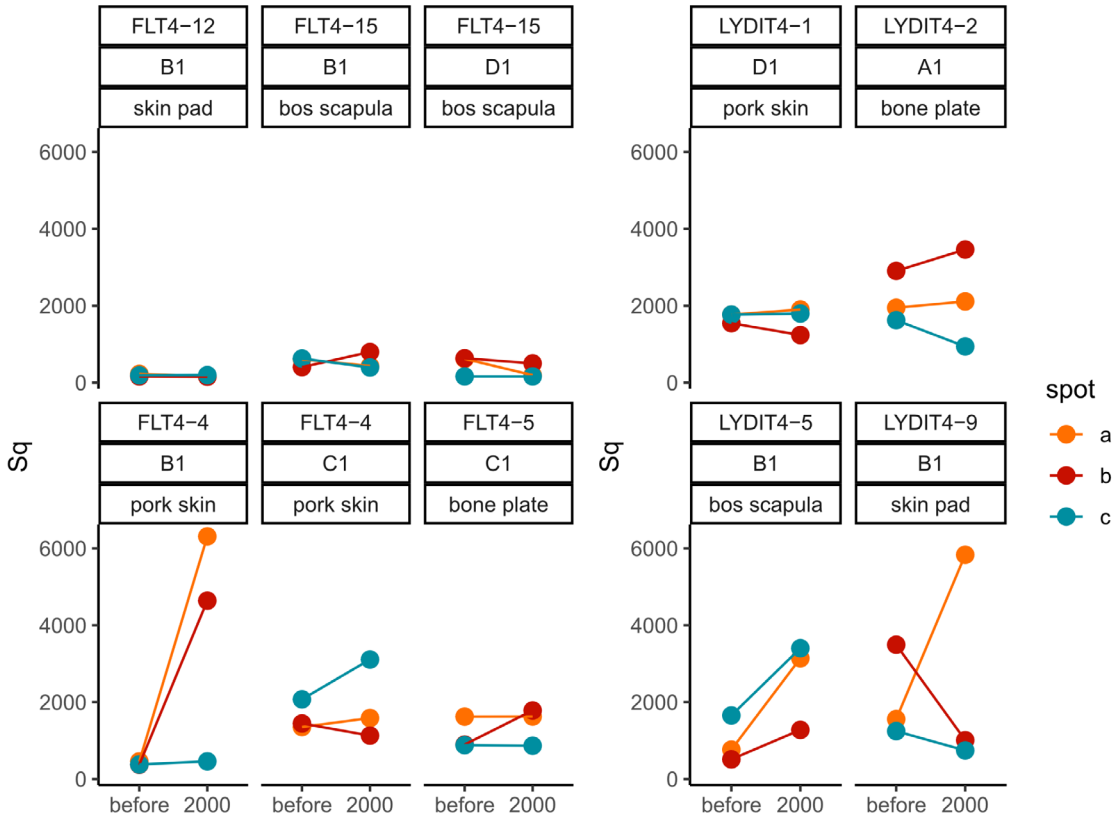

Fig. 140 *Sq* values before and after 2000 cutting strokes measured on identical spots on each standard sample used during the »artificial VS. natural« experiment respectively. Spot a, b and c refers to the three measurements taken per use-wear trace.

Additionally, a quantitative use-wear analysis was conducted. The same eight samples were used for the analysis, but only the moulds from before the experiment and after 2000 strokes were analysed. Thanks to the coordinate system (beads; Calandra et al. 2019a) on each tool surface, it was possible to relocate to the identical spot on the before and after surface. Thus, variability due to positional inaccuracy could be excluded. Generally, one spot per sample was selected for the quantitative use-wear analysis. Two samples constitute an exception: on two flint samples (FLT4-14 and FLT4-15) two instead of one spot were measured. Scans were acquired on well-developed polished areas (after 2000 strokes). As done already for the quantitative use-wear analysis from the archaeological material, each use-wear trace was measured three times (a-c) on nearby, but not identical spots. In total, n = 30 measurements were taken on the samples from before the experiments and n = 30 on the samples from after 2000 strokes. Identical to the qualitative use-wear analysis performed on the archaeological samples, the data was acquired to the ISO 25178-2. Furthermore, the same 21 ISO 25178-2 parameters, three furrow parameters, three texture direction parameters, one texture isotropy parameter and the SSFA parameters *epLsar, NewEplsar, Asfc, Smfc, HAsfc9 and HAsfc81* were calculated on each surface (**tab. 11**).

A first attempt to review the data was done by plotting the data in a scatterplot per parameter (**figs 140-141**). These scatterplots include information about the sample, the raw material and the contact material as well as the location (A-D). The data is illustrated in a way that the results from before and after 2000 strokes can be compared directly.

Four data points, identified as outliers, need to be mentioned. Since the use-wear on the standard samples is extremely marginal due to the low penetration depth into the contact material, it was often difficult to acquire the data without scanning beyond the edge. Whenever this happens, such areas are interpreted

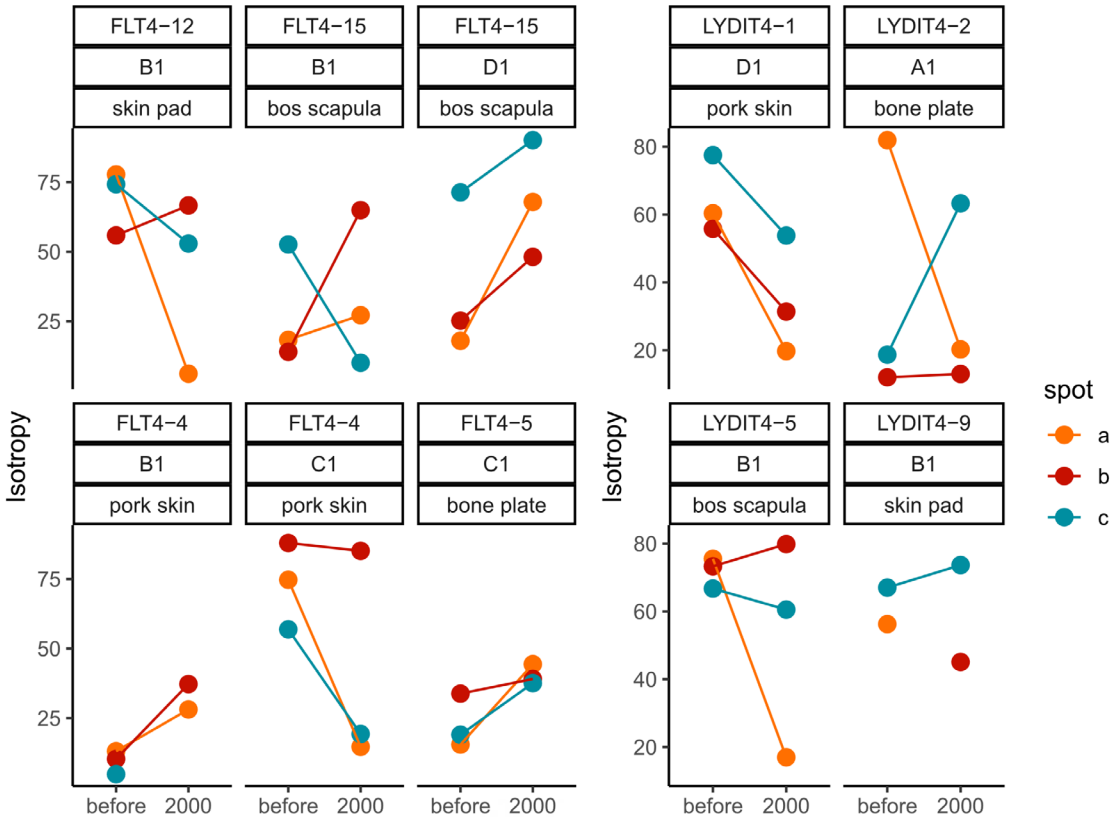

Fig. 141 *Isotropy* values before and after 2000 cutting strokes measured on identical spots on each standard sample used during the »artificial VS. natural« experiment respectively. Spot a, b and c refers to the three measurements taken per use-wear trace.

as non-measured points. Filling these data points to calculate the parameters leads to divergent results. Unfortunately, that happened in four cases. The samples LYDIT4-9-B1-b (before), FLT4-4-B1-a, FLT4-4-B1-b and LYDIT4-9-B1-a (all 2000 strokes) need to be treated as outliers and excluded from interpretations. Most of the parameters, as for instance *Sq*, *Vmc, Sxp* or *Sdr* change from before to after 2000 strokes only insignificantly. For single samples, as for example the sample LYDIT4-5, the surface roughness seems to increase after 2000 strokes. Clear changes are noticeable when looking at the *isotropy* or *epLsar* (equal to anisotropy) (**fig. 141**). With some exceptions within the flint samples (FLT4-5-C1, FLT4-15-D1), the *isotropy* values decrease from before towards 2000 strokes. This means, the directionality of the surface is getting higher, and the surface is getting less similar in all directions. It seems as if directionality of the surface, characterised by the diamond band saw cut, stands in contrast to the directionality of the use-wear traces. In another plot type, the three measurements per use-wear traces were taken together and the arithmetic mean values per use-wear trace were calculated (**fig. 142**). These plots only emphasize, what was pointed out before. Based on the calculated ISO parameters, there is no significant recognisable change between before and after the 2000 strokes. The only exception still, is sample LYDIT4-5 use on fresh bone. Nevertheless, it seems as if the initial surface texture roughness influences how significant the change from before to after the use is. Samples with an initially higher surface roughness seem to experience more change than samples with an initially lower surface roughness. However, a clear shift can be noticed concerning the texture isotropy parameter and the SSFA parameters.

On seven selected parameters, a principal component analysis (PCA) was applied. The same parameters as for the last PCA (see chapter Surface micro texture data analysis) were chosen in order to perform the PCA.

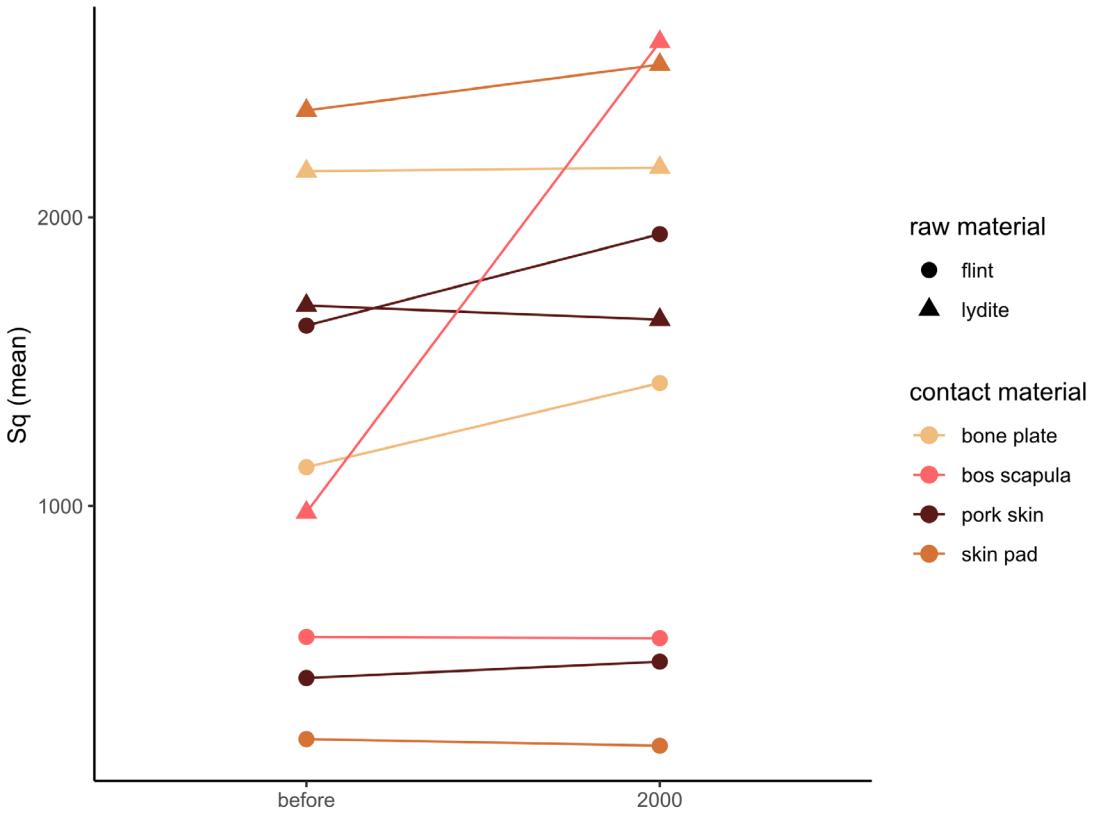

Fig. 142 *Sq* values before and after 2000 cutting strokes measured on identical spots on each standard sample used during the »artificial VS. natural« experiment, respectively. *Sq* reflects the mean value of the three measured spots taken per use-wear trace. The colours indicate the contact material the tool was used on.

These parameters are *Sq, Ssk, Vmc, Mean density of furrows, Isotropy, Asfc* and *HAsfc9*, spanning the different categories of field parameters. The first PCA reflects the variance between the samples used on the four contact materials (**fig. 143**). Principal component 1 (PC1) reflects 39.74 % of the variance in *Sq, Vmc*, and *Asfc*. The variance in *Ssk, Mean density of furrows, Isotropy* and *HAsfc9* is represented by Principal Component 2 (PC2), which accounts for 21.17 %. The data cluster from the four contact materials overlap. Unfortunately, the cluster from the natural contact material and the corresponding artificial contact material differ distinctly in both cases.

A second PCA visualises the variance in the two categories before and after 2000 strokes (**fig. 144**). The two cluster overlap mainly in the left part of the PC1 axis. At the same time, the data points from after 2000 strokes scatter more over the plot. The cluster from before is denser, pointing to more homogeneous data. The results of the quantitative use-wear analysis illustrate the diversity within the measured, individual use-wear traces. While the homogeneity for the three measured spots (a, b and c) *per* use-wear trace is given, this does not count for the use-wear traces on the different samples. The acquired data emphasise that within the selected use-wear traces, a variance exists. This means, the use-wear traces on the flint samples and the use-wear traces on the lydite samples produced on identical contact material respectively, already differ. The same results count for the comparison between the natural and the artificial contact material. The analysis highlights the importance of the amount of data and the relevance of replicas. Here, the acquired data is not statistically evaluable since only one sample per raw material and contact material was part of the quantitative use-wear analysis. Otherwise, it would be interesting to see, whether the data acquired on the replicas used within the experiment would lead to different results within each analysed category.

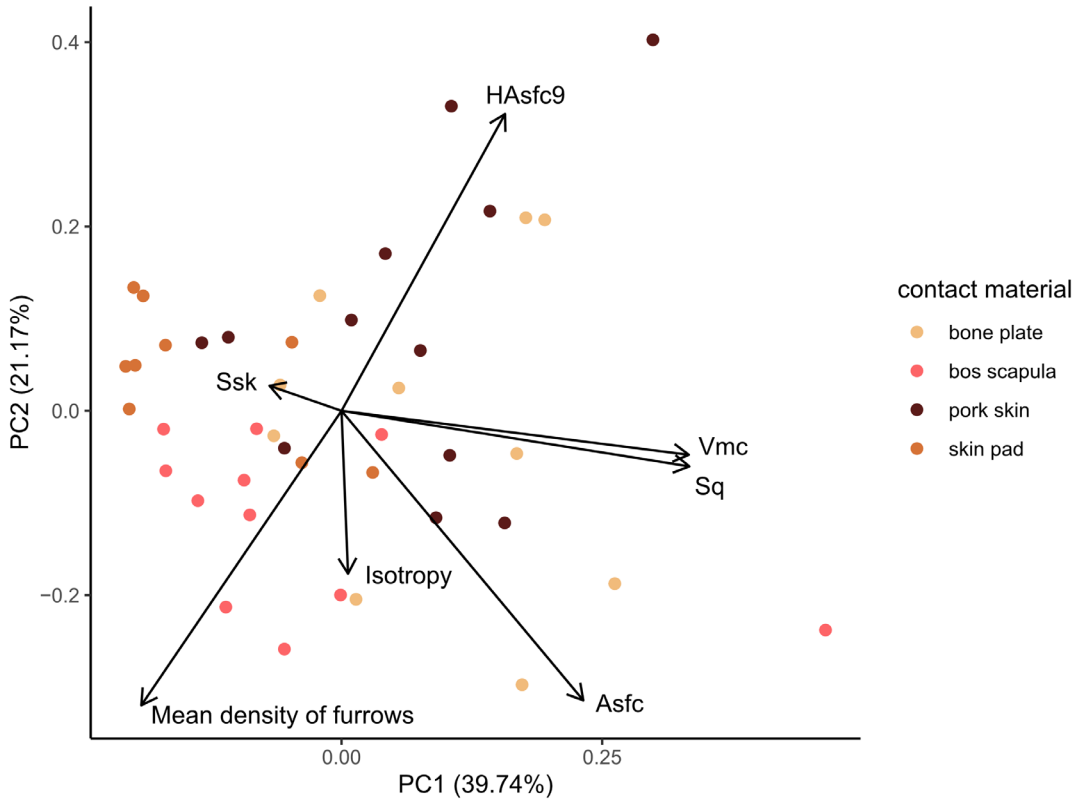

Fig. 143 Principal component analysis applied on the measured use-wear traces of the analysed standard samples from the »artificial VS. natural« experiment after 2000 cutting strokes, reflecting variation regarding the contact material.

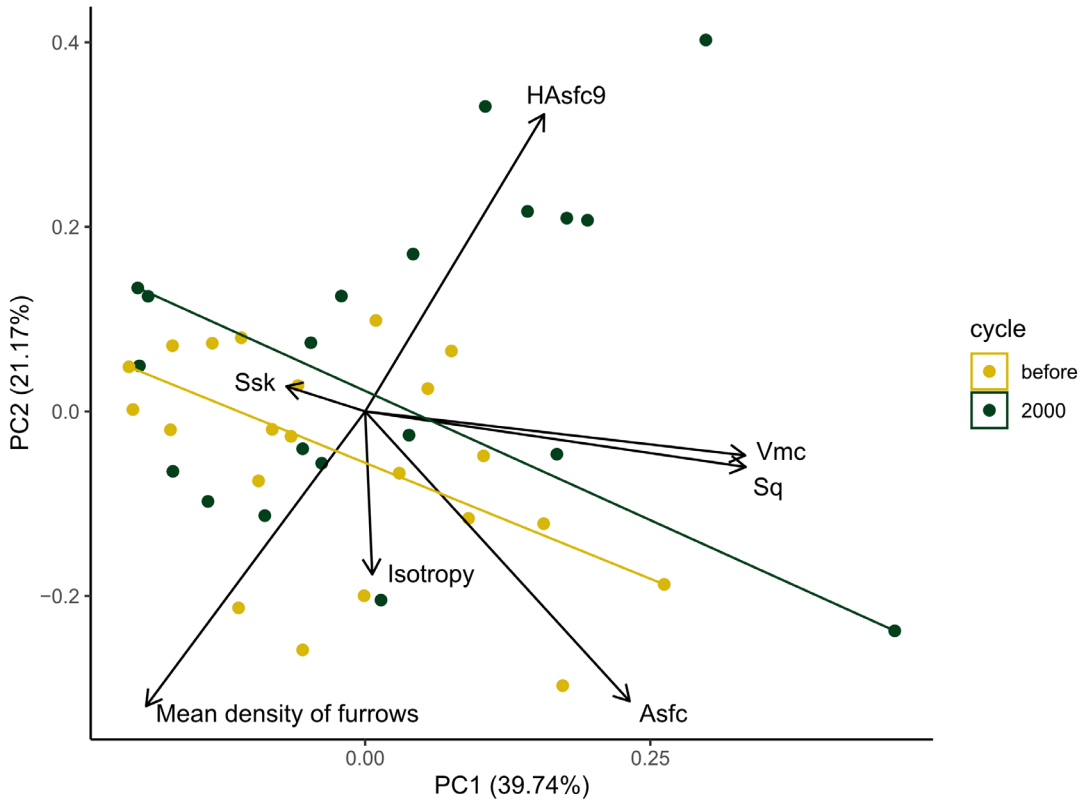

Fig. 144 Principal component analysis applied on the measured use-wear traces of the analysed standard samples from the »artificial VS. natural« experiment, reflecting variation regarding before and after 2000 cutting strokes.

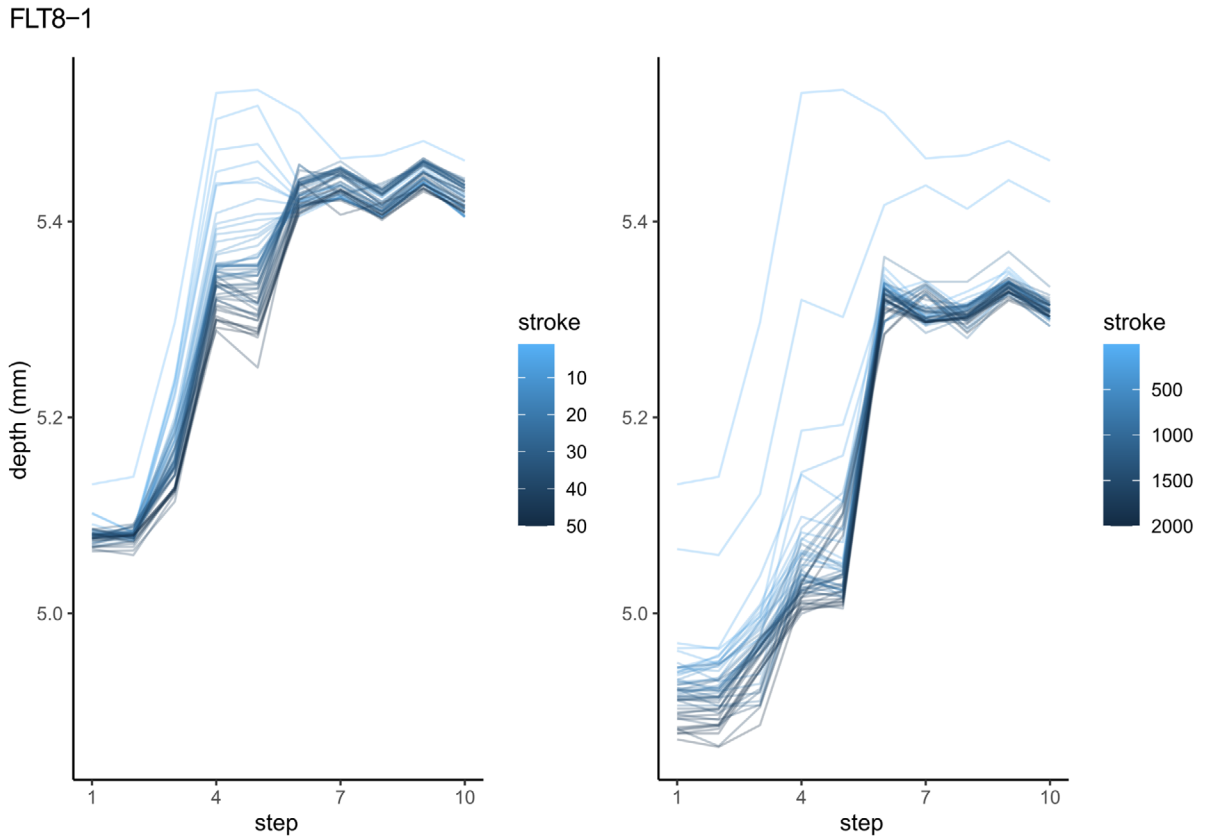

Fig. 145 Sensor recorded penetration depth achieved with a cutting movement performed with the SMARTTESTER® during the tool function experiment. Exemplarily presented here the recording of sample FLT8-1. The left graph shows each cutting stroke within the first cycle (0 to 50 strokes). The right graph shows each 40th cutting stoke within all cycles (0 to 2000 strokes). The darker the colour, the more increased is the penetration depth.

Data analysis – tool function experiment

The final experiment was the tool function experiment (**fig. 38**). Raw material, edge angle and movement served as independent variables. Tool efficiency, durability and performance were tested on artificial bone plates. In total 24 unifacially cut standard samples were used. The samples can be separated in the following groups: twelve flint and twelve lydite standard samples with six times 35° and 45° edge angle each. Three samples per category were used for cutting, three samples per category for carving.

In a first step analogous to the experiment before, the sensor data from the SMARTTESTER® will be presented. In the focus of this analysis stands again the data recorded with the depth sensor. The individual results per sample are accessible as plots showing the first 50 strokes and additionally each 40th stroke combined (**fig. 145**). The plots illustrate a continuous increase in penetration depth throughout the experiment with an especially rapid increase during the first strokes. In order to put the efficiency, here only measured as penetration depth, in relation to all 24 samples, the absolute depth achieved per sample was calculated. As reported for the previous experiment, sometimes software issues with the SMARTTESTER® appeared, leading to wrong recordings. These wrong recordings are identifiable in the plots. Within the recorded data, recorded data for single strokes reaches values beyond the possible moving radius of the mechanical device. Thus, some outliers are included in the data. The outliers are not only visible when checking the individual penetration depth per stroke and sample (**fig. 146**), but also in the plots showing the absolute penetration

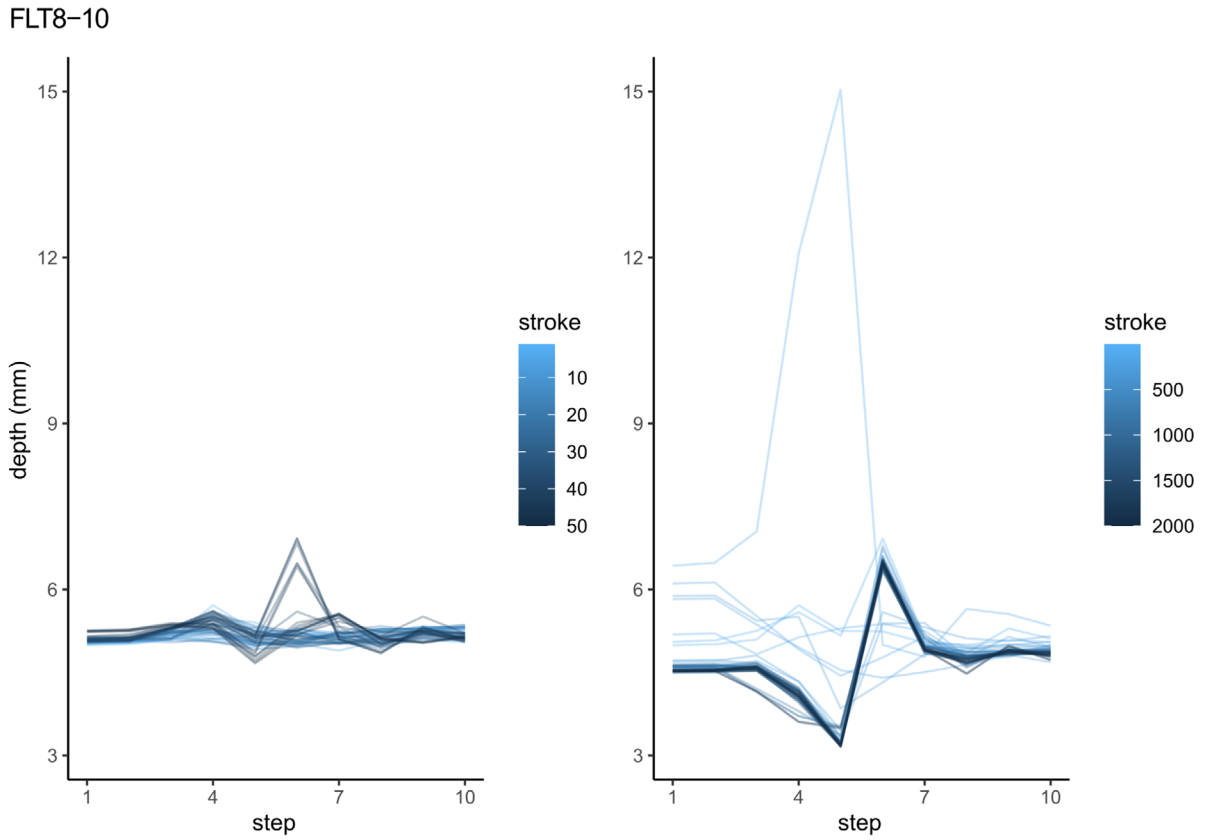

Fig. 146 Sensor recorded penetration depth achieved with a carving movement performed with the SMARTTESTER® during the tool function experiment. Exemplarily presented here the recording of sample FLT8-1. The left graph shows each cutting stroke within the first cycle (0 to 50 strokes). The right graph shows each 40th cutting stoke within all cycles (0 to 2000 strokes). The recording includes outliers as displayed with the light blue line reaching up to 15 mm depth. The darker the colour, the more increased is the penetration depth.

depth. This specific plot (**fig. 147**) includes next to the penetration depth also the information about the sample, the raw material, the edge angle and the movement. Three samples, FLT8-3, FLT8-4 and FLT8-10 differ from the other samples. These are the three identified outliers. In order to get a better resolution of the correctly displayed data, the outliers have been removed (**fig. 148**). The biggest penetration depth was reached with a lydite sample (LYDIT5-7). With the exception of this sample, the penetration depth reached during cutting is comparable between the 35° and the 45° samples. Concerning the carving, the 45° samples achieved a comparable higher penetration depth than the 35° samples. A general tendency is that the lydite samples penetrated deeper into the contact materials than the flint samples. While this observation is not so clear for carving, it is undoubtedly seen for cutting.

In regard of tool efficiency, the edge angle measurements need to be mentioned. As for the other two experiments, the edge angles of the n = 24 samples were measured before and after each cycle (**fig. 149**). Before explaining the data, one outlier has to be reported. The first edge angle calculation (before) for sample FLT8-3 is not reflecting the accurate value. This sample was produced with 45° edge angle, but displays a 55° edge angle. An examination of the raw data revealed small holes in the 3D data along the edge. Apparently, also in this case, filling the holes changed the edge angle. However, this is the only data point, which needs to be excluded for interpretation.

The results for cutting differ depending on the edge angle. While the shift in the edge angle is only minimal for the three flint and lydite standard samples with 45°, the results are different for the 35° samples. For one flint sample (FLT8-6), only minimal changes could be observed, but the two other samples (FLT8-4 and

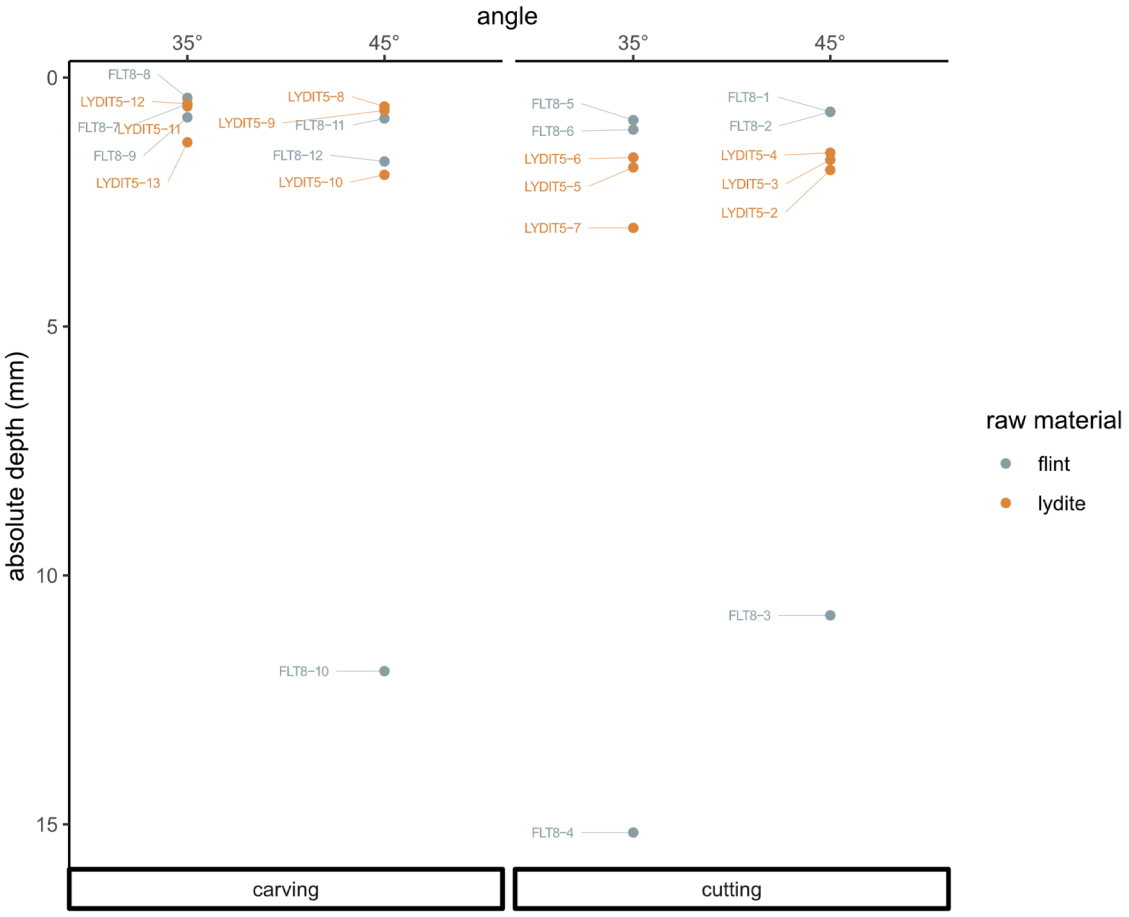

Fig. 147 Absolute cutting depth of all samples used during the tool function experiment. The samples are organised according to the performed task and the edge angle of the standard sample.

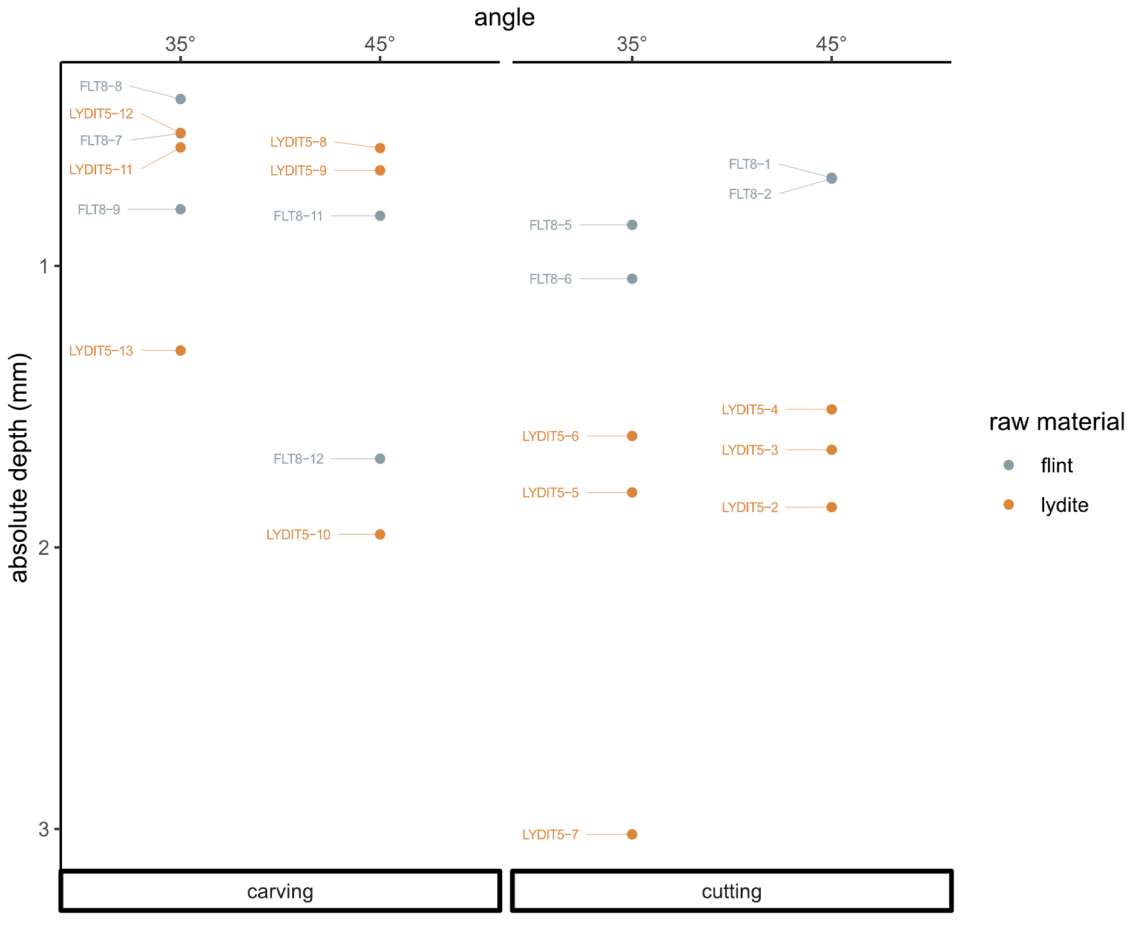

Fig. 148 Absolute cutting depth of all samples used during the tool function experiment. The samples are organised according to the performed task and the edge angle of the standard sample. Outliers removed.

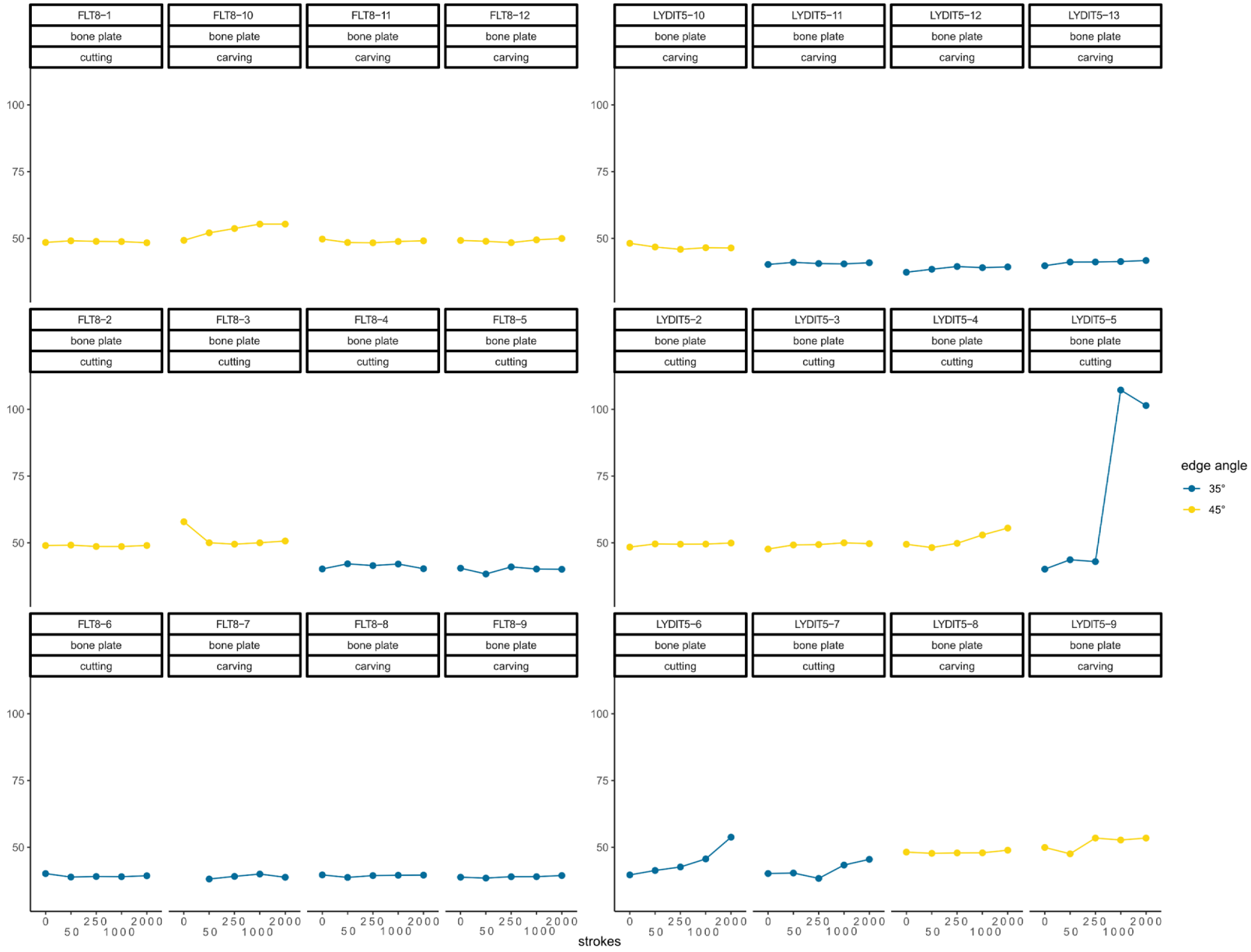

Fig. 149 Edge angle values calculated per sample used during the tool function experiment (calculated with the »3-point« procedure; mean value of section 2 to 8 and distance 3 to 6). The data points per sample represent the values after the performance of each cycle (0, 50, 250, 1000 and 2000 cutting strokes).

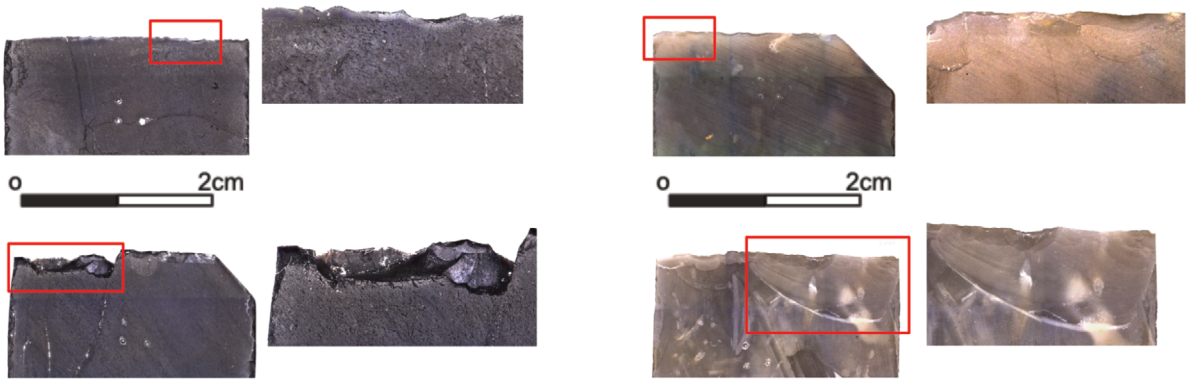

Fig. 150 Tool alteration on standard samples made of lydite (left) and flint (right) after 2000 strokes used during the tool function experiment. – Not to scale.

FLT8-5) display material loss and thus, a slight shift in edge angle values towards increased bluntness. For the three lydite samples with a 35° edge angle, a decrease in acuteness is clearly visible and illustrated by continuous material loss throughout the experiment. One sample changed from 35° to approximated 75° due to a fracture. Surprisingly the six samples with a 35° used for carving did not change significantly. The same counts for a majority of the 45° samples used for carving. Nevertheless, two samples, one flint and one lydite sample, experienced some alternation after 50 strokes, leading in both cases to a continuous but small increase in the edge angle.

In general, the 10° difference between the two sets of standard samples (35° and 45°) seems to make a difference in durability when used to perform cutting strokes. Although, none of the samples were altered or damaged in a way that it could not function anymore. All 24 samples completed the 2000 strokes. However, the 35° samples exhibit more damage in the sense of small fractures and material loss. This observation cannot be transferred to the results from the carving movement. Irrespective of the raw material, more alteration could be documented for the 45° samples.

The edge angle measurements can be correlated with the volume loss of the standard samples. The volume of each sample was calculated based on the 3D models. Thus, the measurements can only be as precise as the quality of the 3D model allows. On average, lydite samples experience a volume loss of 0.21 % (~ 0.37 mm³). Flint samples display a slightly higher volume loss of 0.36 % (~ 0.52 mm³). These values could be verified with the weight measurements. Although the lydite samples fracture more and thus also experience more frequent and significant damage, on average, the material loss is only minor. However, the lydite samples appear more fragile and tiny particles break away, which is reflected in the edge angle measurements (**fig. 150**). By contrast, the flint samples more often display material loss comparable to retouch and not fractures. The retouch-like material loss might go further on the surface and could explain the bigger loss in volume and weight. Moreover, this type of material loss might not change the edge angle in a way that the breaking particles do on the lydite.

Another aspect is the quality of the cuts or scratches produced on the bone plates (**fig. 151**). Quality can be defined by the regularity, the uniformity and the width of the cuts or scratches. In this sense, quality is one relevant aspect in order to evaluate tool performance. As already mentioned for the initial experiment, the cuts produced with flint samples optically differ slightly from the ones produced with the lydite samples. This observation is only based on a visual assessment. The flint cuts appear as thin lines, whereas the lydite cuts seem thicker and less precise. In particular the cuts produced with the 35° lydite samples seem broader. For the majority of the traces left on the bone plates during carving, no significant difference between the

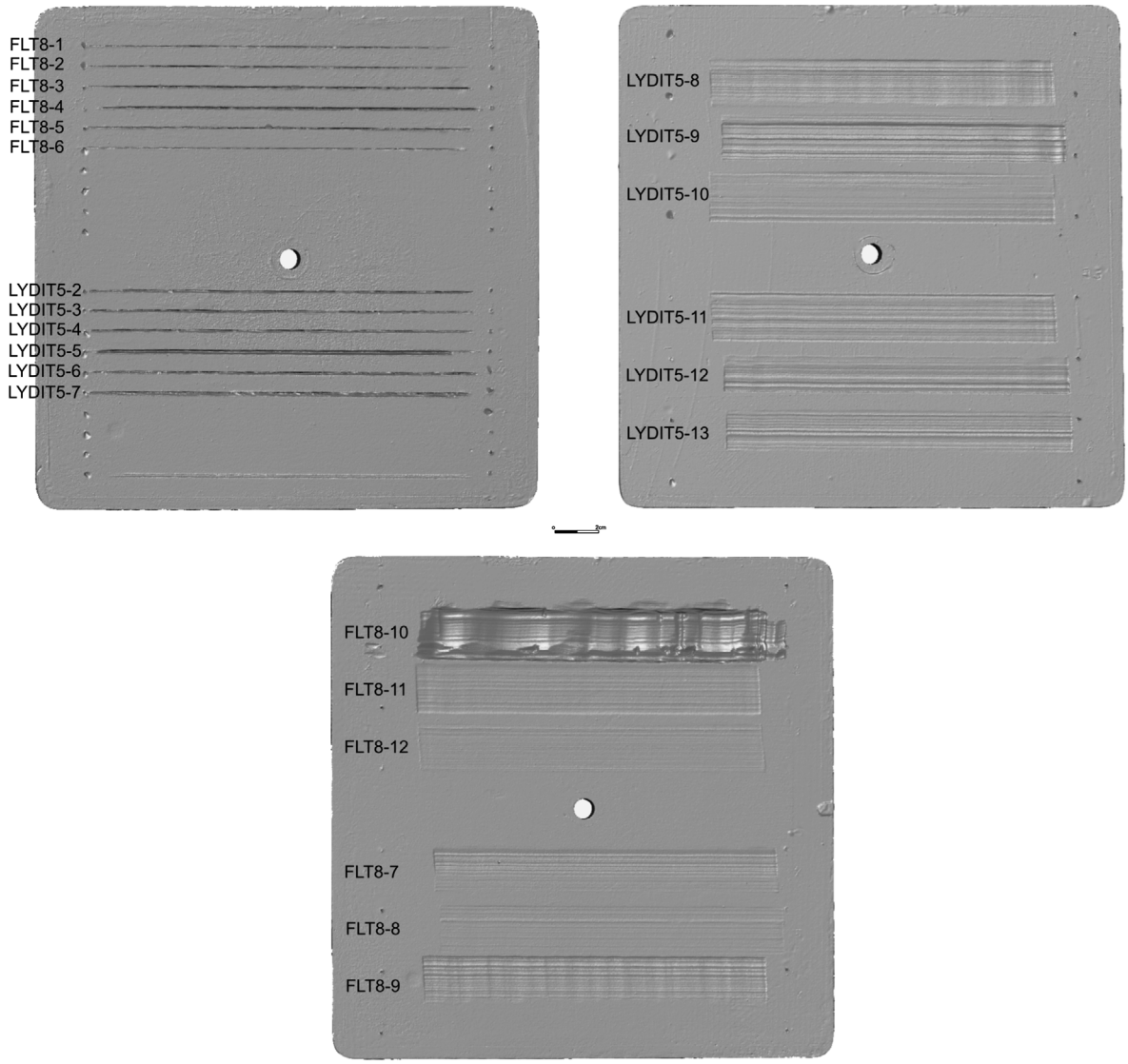

Fig. 151 3D scans of the artificial bone plates used during the tool experiment after 2000 strokes. The upper left scan shows the plate used for cutting, the upper right scan the plate used for carving with lydite samples. The lower scan illustrates the scan of the bone plate used for carving with flint samples.

traces caused by the flint samples and the ones caused by the lydite samples is noticeable. One exception is the trace left by the flint sample FLT8-10. This sample achieved a comparable high penetration depth. During the first cycle, the sample was not perfectly fixed in the sample holder and was able to move a little. Thus, the contact between the sample and the bone plate did not happen exactly parallel to each other. During the second cycle, this problem was solved, and the samples could not move anymore in the sample holder. As a result of the first cycle, the surface of the bone plate (the trace) was a bit uneven causing more resistance and friction which in turn caused more alteration on the tool.

A qualitative and quantitative use-wear analysis was conducted for eight samples from the tool function experiment (see **appendix II**). These eight samples always include one sample *per* raw material, edge angle and movement. For the qualitative use-wear analysis, only the samples from before and after 2000 strokes were analysed. All images of the use-wear analysis can be found as figures in the supplementary material. All four samples used for cutting developed use-wear throughout the four cycles of the experiment (**fig. 152**). The use-wear traces are visible on the »dorsal« as well as the »ventral« surface of the standard

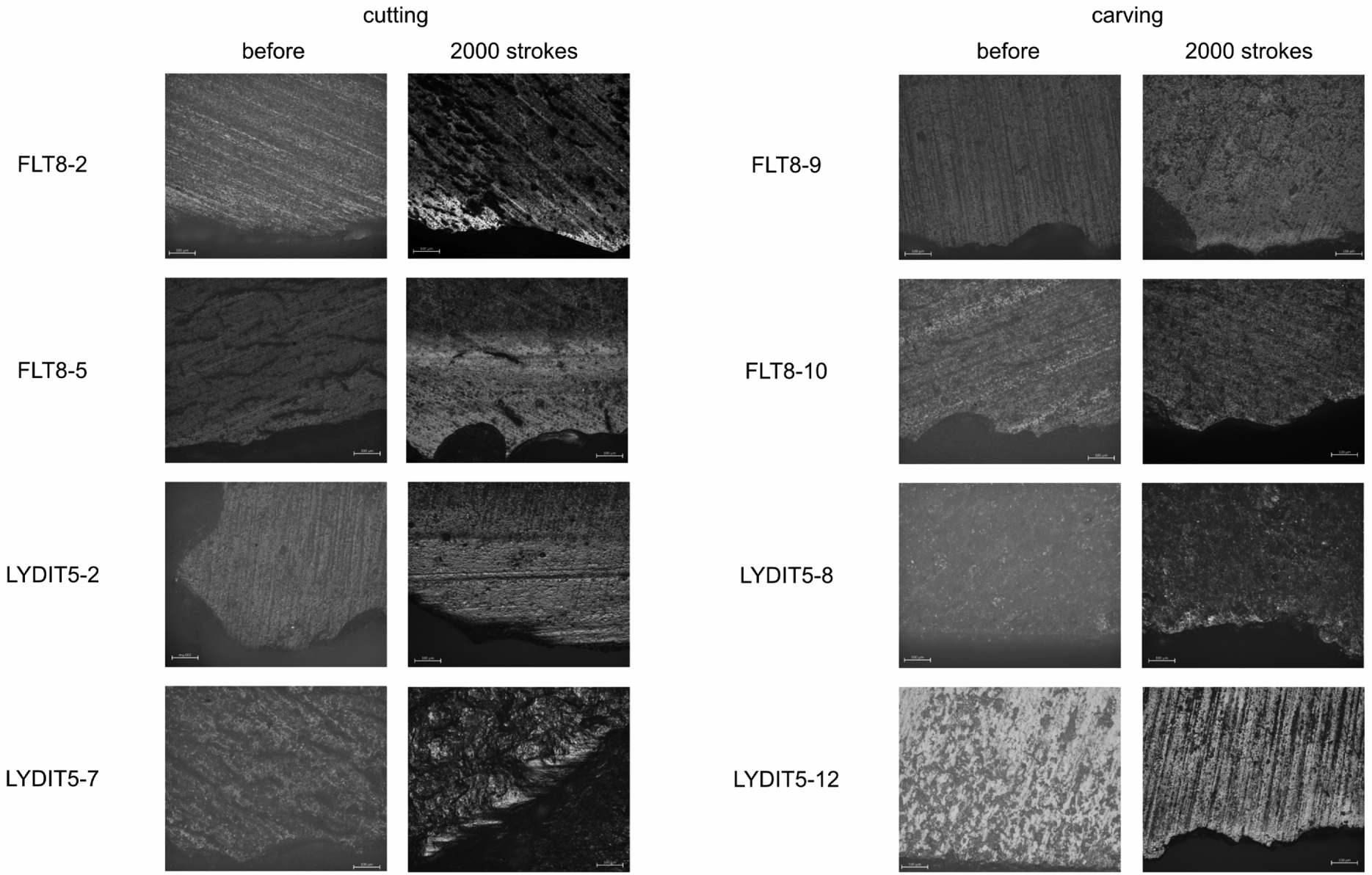

Fig. 152 Use-wear formation on the analysed flint and lydite standard samples before and after (2000 strokes) performing the tool function experiment. The left side shows the samples used for cutting, the right side the samples used for carving (all images are taken with a 10× optical objective).

samples. One exception is the flint sample FLT8-2, which did only develop use-wear on the »ventral« surface (D). The samples used for the carving movement also developed use-wear within the 2000 strokes. However, the use-wear traces are often marginal. The reason for that can likely be seen in the low penetration depth into the contact material. Thus, there was less possibility of friction between the samples and the contact material. While the flint sample FLT8-9 displays use-wear traces on both surfaces, the other three samples developed use-wear traces only either on the dorsal or ventral surface.

The same eight samples were selected for the quantitative use-wear analysis, whereas the data was only acquired on the samples after 2000 strokes. Well-developed use-wear traces were selected for the analysis. The eight traces were measured three times each, as done similarly for the other performed qualitative use-wear analyses. Again, the data was calculated based on the identical 34 parameters (see **tab. 10**). Scatterplots from each parameter combined with information about the sample, the raw material, the task and the edge angle display the results (**fig. 153**). Prominent within these scatterplots are two data points. Both of the data points belong to the categories flint and carving. One of the samples has a 35° edge angle (FLT8-9-B1-01-a), the other one a 45° edge angle (FLT8-10-C1-01-b). These tow samples clearly differ from the corresponding tow measurements per use-wear trace. A review of the raw data made an identification of these two data points as possible outliers. In one case, the acquired data included some data from next to the use-wear trace, in the other case the scan went beyond the edge. In both cases, the results are misleading and should be thus excluded as outliers. Although the data analysis leads to no significant results, differences between the categories are visible. The data acquired on the flint samples used for carving shows a variance between the 35° edge angle results and the 45° edge angle results. Moreover, the results from the sample with the 35° edge angle tend to be more homogeneous. The lydite samples also display differences between the 35° and 45° edge angles, whereas the results are homogeneous in both cases. A significant variance between the two groups of raw material, flint and lydite, are not noticeable.

The data was explored further with a principal component analysis. The PCA was applied on the identical seven components used for the previously described PCAs, the parameters *Sq, Ssk, Vmc, Mean density of furrows, Isotropy, Asfc* and *HAsfc9*. The variance in *Sq, Vmc* and *Mean density of furrows* is explained by Principal component 1 (PC1), reflecting 53.06 % of the variance. Principal component 2 (PC2) accounts for 19.47 % of the variance with *Ssk, Isotropy, Asfc* and *HAsfc9*. The first PCA reflects this variance combined with the movement, cutting and carving (**fig. 154**). The data scatters mainly on the right part of the PC1 axis and clearly overlaps.

A second PCA visualises the variance of the raw material of the standard samples based on the same seven components (**fig. 155**). Although the data overlaps again in the right part of the PC1 axis, the data scatters in different directions.

The only PCA that results in distinct clusters is the third applied PCA (**fig. 156**). This PCA reflects the variance combined with the edge angles, 35° and 45°. The results are consistent with the results mentioned from the scatterplots mentioned before. The cluster from the 35° edge angle is narrow, while the cluster from the 45° is scattered more, likely due to the less homogeneous data.

The data from the quantitative use-wear analysis acquired on the samples from the tool function experiment leads to unexpected results. Neither the raw material of the standard samples nor the performed movement seems to affect the measured features of the use-wear traces. However, the edge angles of the standard samples seem to have an effect.

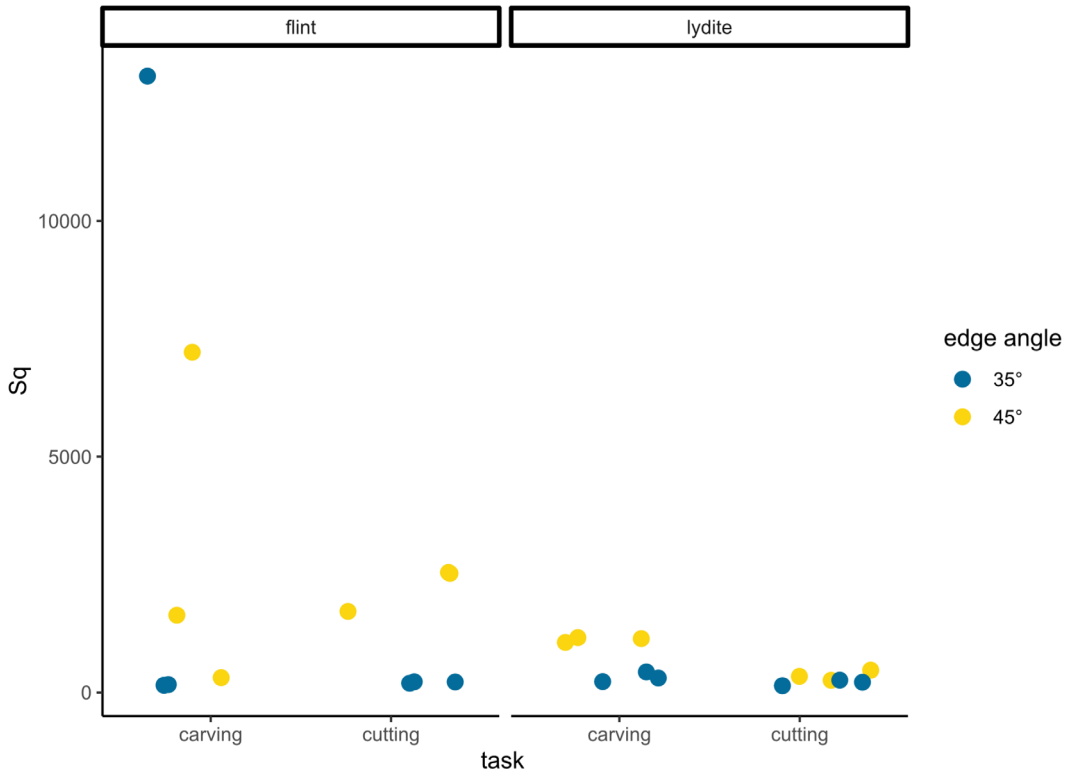

Fig. 153 *Sq* values measured on the flint and lydite samples after 2000 strokes used during the tool function experiment. Three data points are shown per sample, reflecting the three measurements taken per use-wear trace (spot a, b and c). The data is categorised according to the performed task. The colour indicates the edge angle of the standard samples.

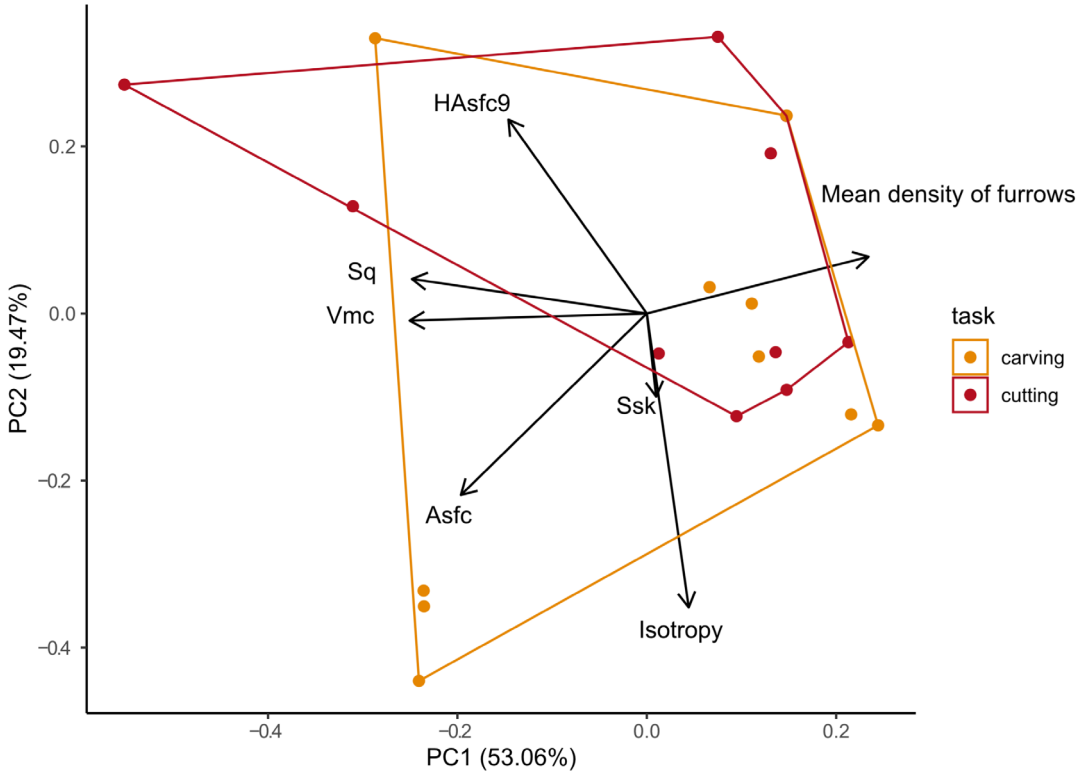

Fig. 154 Principal component analysis applied on the measured use-wear traces of the analysed standard samples from the tool function experiment, reflecting variation regarding the performed task.

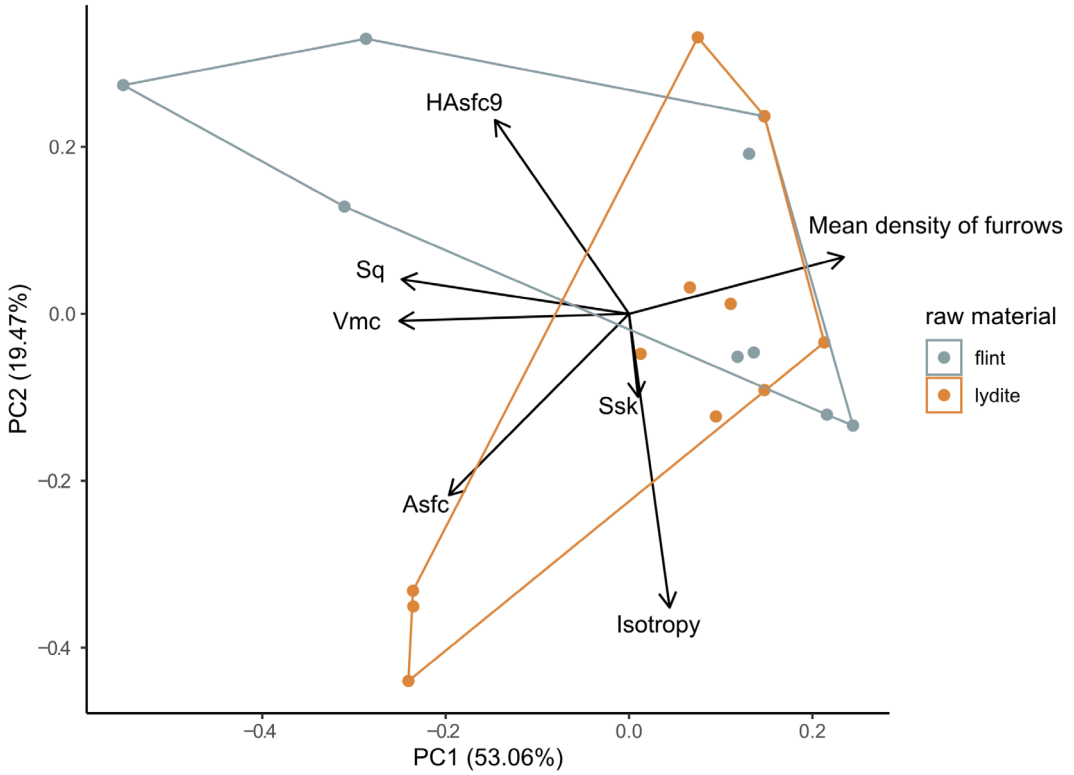

Fig. 155 Principal component analysis applied on the measured use-wear traces of the analysed standard samples from the tool function experiment, reflecting variation regarding the raw material of the standard samples.

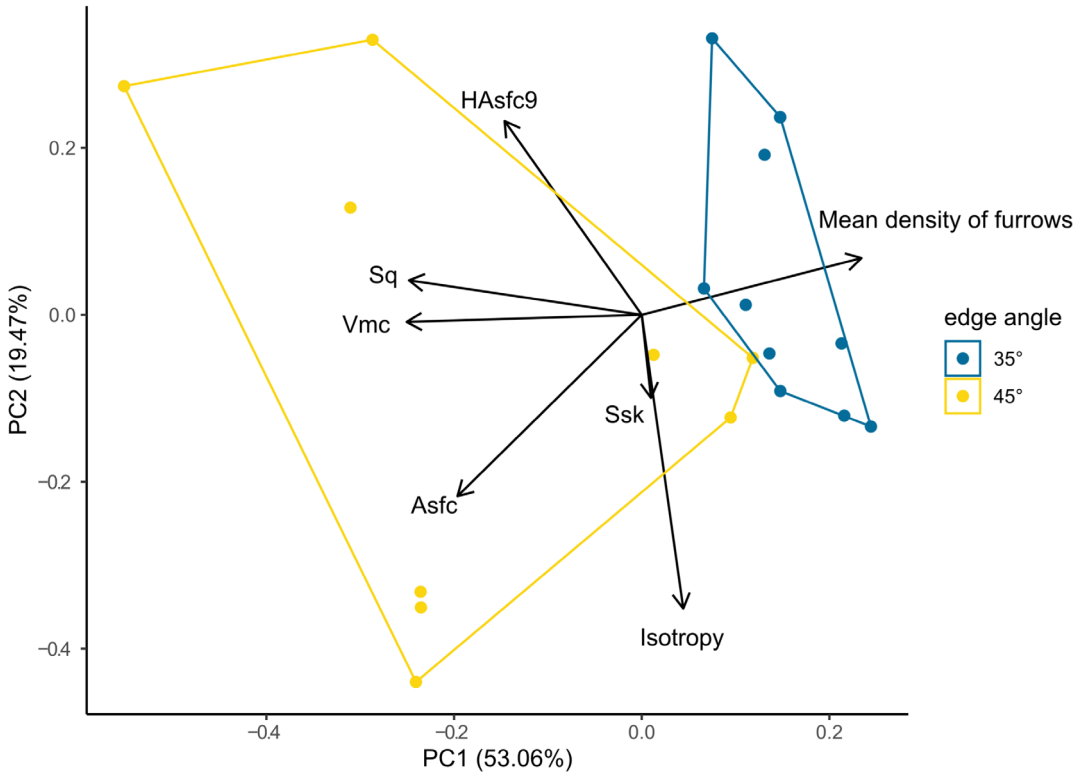

Fig. 156 Principal component analysis applied on the measured use-wear traces of the analysed standard samples from the tool function experiment, reflecting variation regarding the edge angle of the standard samples.

Combined data of the experiments

It was possible to combine the data from the three experiments in several ways. First, the alteration of the tool and thus the change of the edge angle will be addressed. Throughout the three experiments, a reproducible trend could be noticed: The lower the edge angle, the more alteration occurs on the tool's edge. This trend gets strengthened through two additional impacts, the raw material of the standard samples and the characteristics of the contact material. Concerning the raw material, flint seems to be more durable than lydite, which is likely due to the raw material properties of the tool. The hardness of the contact material seems also to be of influence. However, the hardness of the contact material might not be the only relevant aspect concerning the material properties. The artificial bone plates do have a comparable shore hardness to the fresh cow scapula used during the »artificial VS. natural« experiment. Still, the cow scapula had a stronger effect on the tool alteration than the artificial bone plate. The mentioned trend could be observed for cutting movements, not for carving. The standard samples with the lower 35° edge angle used for carving display only minimal alteration compared to the samples with the 45° edge angles.
The results from the qualitative use-wear analysis of the »artificial VS. natural« experiment and the tool function experiment can be compared. The comparison is possible for all samples used for cutting on artificial bone plates. All samples belonging to this category developed use-wear traces within the 2000 strokes. Interestingly, visible use-wear traces on flint samples only formed after 2000 strokes. By contrast, lydite samples displayed use-wear traces already after 50 strokes.
Moreover, some results from the quantitative use-wear analysis of the »artificial VS. natural« and the tool function experiment have been combined. While all the data from the tool function experiment could be used for a comparison, only the data acquired on the 60° samples used for cutting on bone plates from the »artificial VS. natural« experiment was included. To do so, data was combined in one plot per parameter (fig. 157). The results from the samples with the 35° edge angle are, compared to the 45° and 60° samples, more homogenous. This observation was already mentioned beforehand, but in combination with 60° samples, it becomes more obvious. The data obtained on the samples with the 60° edge angle clearly differs from the other data points.
To summarise, the standard samples made of lydite turned out to be more fragile and more easily affected by alteration (e. g. due to hardness, schistosity). Furthermore, the raw material promotes the formation and development of use-wear traces. At the same time, the lydite samples are more efficient in cutting when judged by the penetration depth solely. However, efficiency defines the ratio between cost and benefits. Benefits, in this case, can be measured based on the achieved penetration depth. Costs are the loss of material and volume. In this sense, lydite exhibits a greater loss when judged by single artefacts. In one case (initial experiment, LYDIT1-4), the loss was so severe, that it affected the durability. In the course of the experiment, the sample fractured so much, that the functionality could not be retained. Thus, the sample was not able to achieve the goal (2000 strokes). However, the lydite sample described above is an exception. Although the other lydite samples used for cutting or carving experienced material loss, the loss was not enough to lose the functionality. Measured on the change in volume and weight (tool function experiment), the loss of raw material is slightly higher on flint samples. Nevertheless, likely due to the raw material properties, the flint samples alter in a different way than the lydite samples. While material loss on flint samples appears more as retouch-like, material loss on lydite samples displays fractures and breakages. This observed difference is also expressed in the shift of the edge angle values.

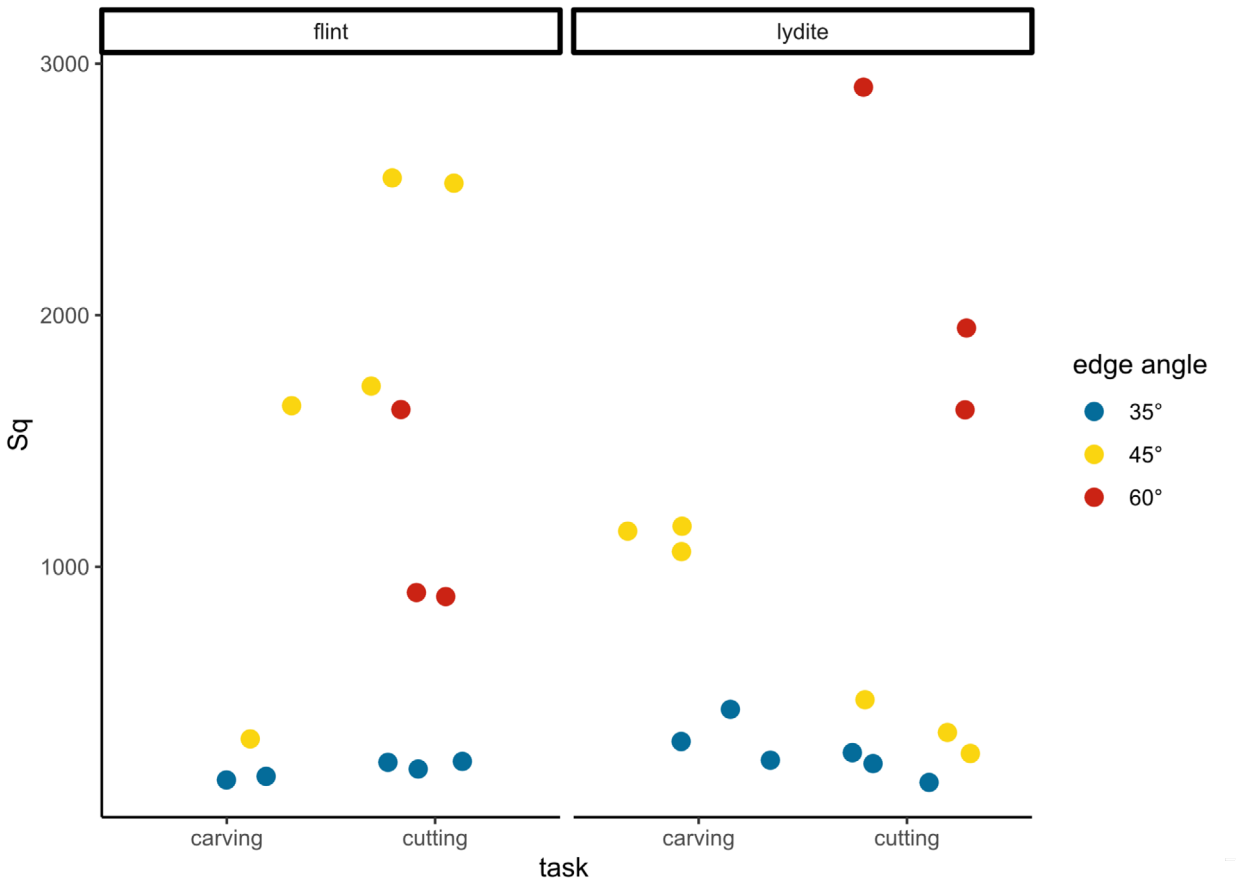

Fig. 157 *Sq* values measured on the flint and lydite samples after 2000 strokes used during the tool function experiment and the »artificial VS. natural« experiment. Three data points are shown per sample, reflecting the three measurements taken per use-wear trace (spot a, b and c). The data is categorised according to the performed task. The colour indicates the edge angle of the standard samples. The 35° and 45° samples have been used during the tool function experiment, the 60° samples during the »artificial VS. natural« experiment.

DISCUSSION

The Late Middle Palaeolithic in Central and Eastern Europe is often characterised by lithic inventories comprising asymmetric tools. One of these artefact categories are the well-known *Keilmesser*. *Keilmesser* are defined by an interaction of certain technological and typological characteristics. From exactly the combination of both, technological and typological features, *Keilmesser* are well studied, resulting in a multitude of interpretations and models not only concerning production and manufacturing strategies, but also about tool function and use (**tab. 1**). Based on the analysis of *Keilmesser* inventories from three relevant, central European sites, given interpretations were called into question. A multidisciplinary approach served the purpose.

TOOL STANDARDISATION

Tool dimensions and the effect of reduction

Keilmesser are referred to as highly standardised tools (e. g. Veil et al. 1994; Richter 1997; Jöris 2001; 2006; 2012; Wiśniewski et al. 2020) with (recurrent) stages of reduction or shape transformation. Their manufacture, reduction, (re-) sharpening and shape transformation seems to follow an underlying socially learned and transmitted concept. The tool dimensions provide a first impression of the degree of tool standardisation. Relevant are absolute sizes such as the length, the width and the thickness; proportional measures such as the ratio between the length and the width and lastly the perimeter measures from the artefact outline. Thereby, indications can be found in each assemblage and in the comparison of the three assemblages. When looking at the results from Buhlen, Balve and Ramioul individually, it becomes evident that the dimensions, for example the length, the width and the thickness do range around certain measurements, but the range of these absolute dimensions can likely be explained as a consequence of diverging use-life histories (Richter 1997; Jöris 2001; 2006; Pastoors/Schäfer 1999; Pastoors 2001). More interestingly, the variability of dimensions (including proportional ratios) from the artefacts from the three sites does not differ significantly within and across assemblages. On the contrary, the results indicate similar ranges for the length, the width, the thickness as well as a rather standardised thickness of the tools' back in the three studied assemblages. Not only the ranges are similar, also the arithmetic mean values are nearly identical. Therefore, the morphological concept of a *Keilmesser* seems to be represented in the studied assemblages, characterised by artefacts with similar dimension ratios. This becomes more evident when looking at the length-width ratio (**fig. 158**) of the analysed samples. The analysis supports the idea that the individual *Keilmesser* represent artefacts with diverging tool biographies. Consequently, *Keilmesser* in their preserved form reflect a morphology, shaped by previous use and reduction. Due to use, a resharpening of the tools is eventually inevitable, resulting in changing dimensions, but not in its technological design. In *Keilmesser*, resharpening is seen as an inherent part of the tool concept (Richter 1997; Jöris 2001; 2006; 2012; Weiss et al. 2018). Resharpening influenced thereby mainly the length and the width of the tools. Nevertheless, the dimensions seem not to change randomly, but the shift in the length and width dimensions follows a ratio. This indicates repeated standardised phases of retouch, mostly in the distal part of the tool's active edge. Iovita (2010) already suggested after analysing artefacts from Buhlen, that *Keilmesser* change isometrically

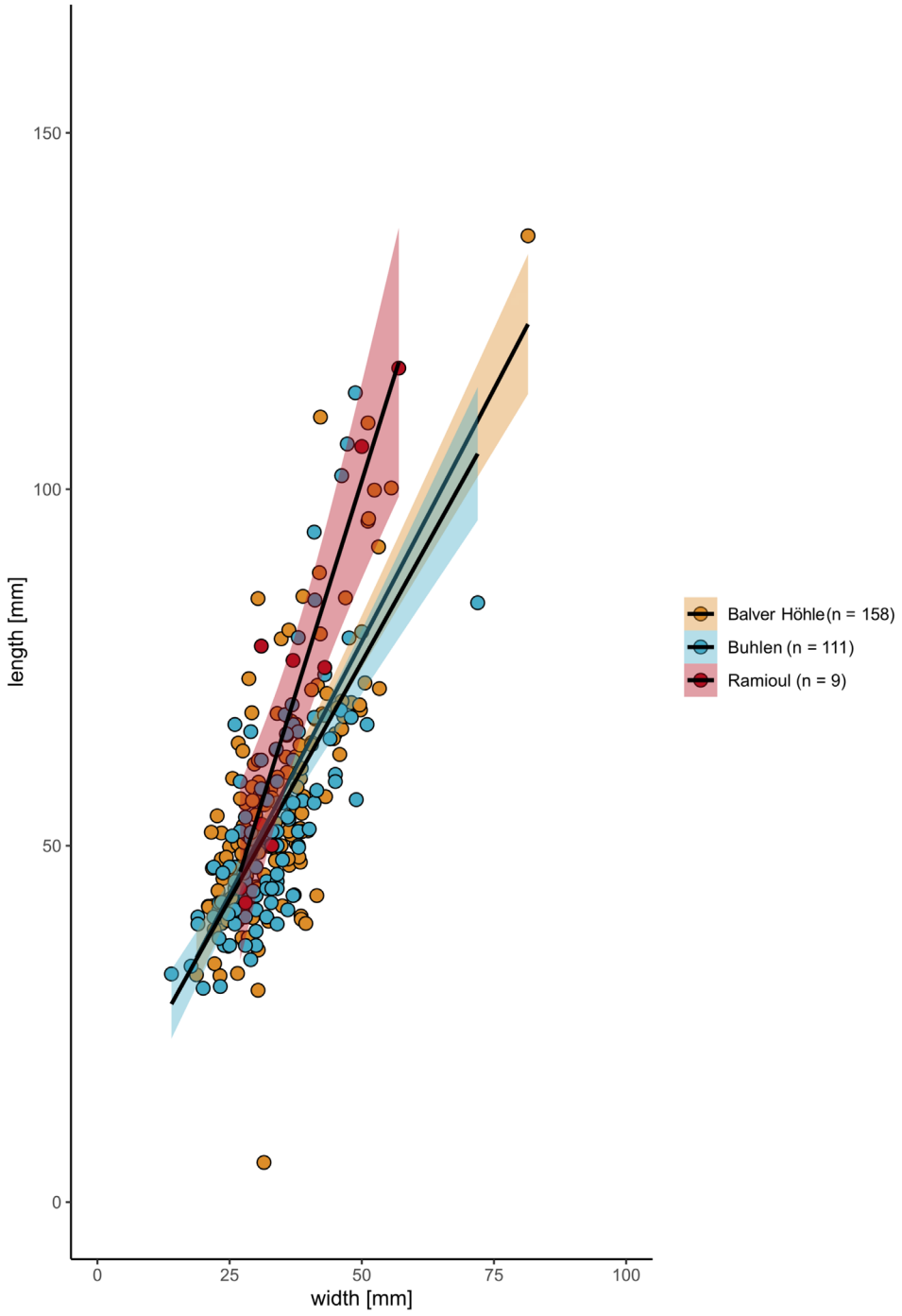

Fig. 158 Length-width ratio of all complete *Keilmesser* from Buhlen, Balver Höhle and Ramioul. The regression line per site shows the overall trend of the data set.

in relation to their perimeter sections (base + back, distal posterior part and active edge). Reduction has thus no direct impact on the length-width ratios of the tool outline (Jöris 2001).

According to their morphological characteristics, also the so-called *Keilmesser* tips are part of this *Keilmesser* tool concept. *Keilmesser* tips could be documented for the assemblages from Buhlen and Balve. The analysis of the dimensions confirmed that *Keilmesser* tips are substantially shorter, comparable with the shortest complete *Keilmesser*. However, the *Keilmesser* tips display the same length-width ratio and fit in the size variability of *Keilmesser* (**figs 49-50**). Thus, also here, the techno-typological analysis supports the theory that, when a point was reached so that resharpening of the tool was not possible anymore, *Keilmesser* were transformed into other shapes by removal of their tips. According to Jöris (2001; Jöris/Uomini

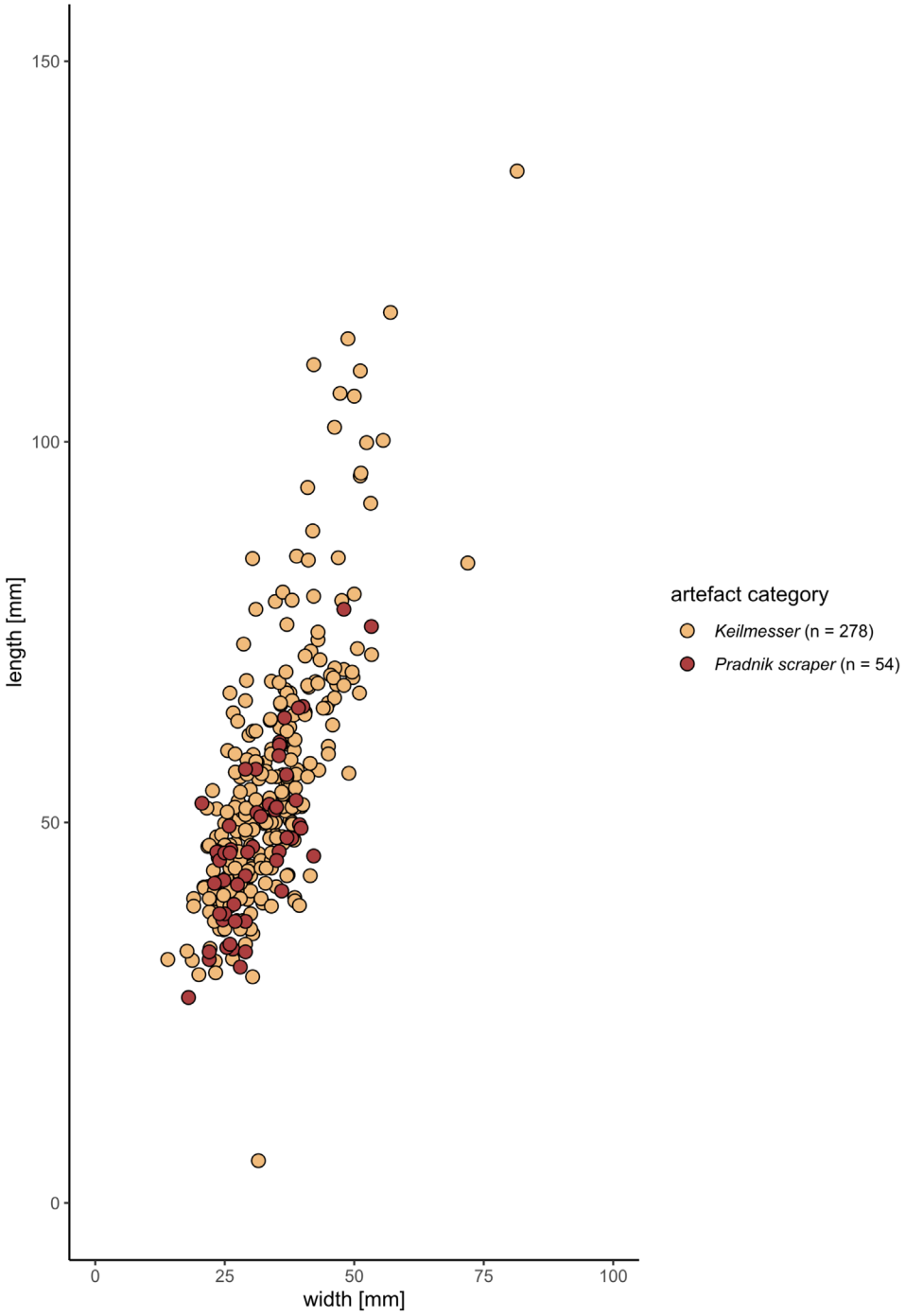

Fig. 159 Length-width ratio of all complete *Keilmesser* and *Prądnik scraper* from Buhlen (n = 111, n = 24), Balver Höhle (n = 158, n = 27) and Ramioul (n = 9, n = 3).

2019) additional thinning (back and distal posterior part, convex upper surface) and lateral sharpening led to the desired shape.

Moreover, also the dimensions of the *Prądnik scrapers* are comparable to the ones from *Keilmesser* (**fig. 159**). However, the ratios of *Keilmesser*, including the shortest and longest *pieces,* scatter more widely than the ones from *Prądnik scrapers*. The variance in length as well as in thickness of the back is smaller and thus to emphasise. However, the quantity of studied *Keilmesser* is also bigger compared to the studied *Prądnik scraper* assemblage, which could also affect these results. Nevertheless, *Prądnik scrapers* provide the impression of varying less in their dimensions and appearing slightly more static compared to *Keilmesser*. Contrary to *Prądnik scrapers*, *Keilmesser* display more often traces of resharpening and reworking accompanied with

decreasing dimensions. Indications of reworking such as the removal of the tip as described for the *Keilmesser* could not be documented for the *Prądnik scrapers*.

Shape variability in *Keilmesser*

In line with these thoughts are the observations made regarding the classification of the different *Keilmesser* shapes. Based on the measurements of the individual perimeter sections, the relation between these sections could be illustrated in a size-independent comparison together with the defined *Keilmesser* shapes (fig. 84). In this way, the previously expressed assumption (see also Urbanowski 2003; Migal/Urbanowski 2006; Jöris 2012; Jöris/Uomini 2019; Weiss 2020) could be strengthened: based on their morphometry, there are no strict *Keilmesser* shapes. The different shapes might be the combined results of the natural variability of the raw material and its shape, the blank type used as well as the result of tool modification during and after use. Resharpening and reworking most often effects the distal posterior part and the active edge (Migal/Urbanowski 2006; Iovita 2010; Jöris/Uomini 2019; Weiss 2020). The perimeter proportions shift, leading to a slight change in shape. These observations contradict the idea of shape variability as a chronological sequence (Bosinski 1967; 1969). Instead, the classification of the *Keilmesser* shapes should be seen as an artificially constructed categorisation. Although these tools display a certain shape variability, they all have morphological features in common, which can be summarised under the concept *Keilmesser*.

Transmission of skills and knowledge

The results gained through the techno-typological analysis of the three sites Buhlen, Balver Höhle and Ramioul build on existing evidence concerning the given degree of tool standardisation in *Keilmesser*. The results referring to the tool dimensions, attributes and shapes indicate that *Keilmesser* were manufactured and curated following a certain scheme. This is indicated on the one hand by the data from the sites respectively and on the other hand through the data of the inter-site comparison, which led to nearly identical results. The similarities between the assemblages from Buhlen, Balve and Ramioul imply that the standards, which define the tool production and curation to a certain degree, are not only present in one of the sites, instead, they can be documented in all assemblages. What becomes evident is, that these standards must have been established and maintained over extended periods of time, rooted in the technological behaviour of Neanderthals (Jöris 2004; Ruebens 2013; 2014; Kozłowski 2014; for a contrasting opinion see Iovita 2014; Weiss et al. 2018). The sites Buhlen and Balver Höhle do reflect long, recurrent settlements of human occupation. Due to the palimpsest situation, an extended temporal depth is reflected in the archaeological assemblages. Based on these similarities in the artefacts, *Keilmesser* likely indicate regional, common features or regional technological traditions. Traditions are the result of a continuous transmission of for instance action pattern and social conventions. These include simple actions such as the manufacturing of tools or complex ones such as language. The social component is indispensable for the development of traditions. The formation of traditions requires social interaction (see Shennan 2008 for a review). Traditions are not inherited, they have to be learned and passed on either horizontally (within a social group) or vertically (across generations). The standardised production of a *Keilmesser* presumably reflects the result of such social interaction (Jöris/Uomini 2019). The manufacturing and the curation of *Keilmesser* has likely been a skill passed on from generation to generation. This would explain the similarities within the tools, described as underling tool concept, visible not only within the temporal depth of each site, but also across assemblages as the

inter-site comparison emphasises. It is exactly this constant transmission of knowledge, action patterns or conventions across generations that defines traditions (Langlois 2001; Lycett/Von Cramon-Taubadel/Eren 2016; see also Shils 1971; Handler/Linnekin 1984).

TOOL DESIGN: TECHNOLOGICAL CHOICES AND EDGE DESIGN

The *Keilmesser* concept

Tool design reflects conscious and unconscious human decision-making as part of human cognitive behaviour. *Keilmesser* with their complex and sophisticated morphology offer the possibility to investigate several aspects related to tool design. Some of these aspects have been addressed within this project. The first point to mention is the raw material choice for the tool production, giving insights into technological and ecological adaptations. The fact, that the shape of the raw material was often an integral part in the tool manufacturing concept, has been stated several times (Jöris 2001; 2006; 2012; Frick/Heckert 2019; Jöris/Uomini 2019; Delpiano/Uthmeier 2020). This could be already demonstrated by Jöris (2001) for Buhlen, but the same approach concerning the tool production is reflected in the artefacts from Balve and Ramioul, too. Nearly 70 % of the analysed *Keilmesser* could be classified as core tools (also in the sense of raw pieces), while in only 5.5 % of the cases a flake was used as a blank. In line with this observation are the results concerning the morphology of the back. In total, for more than two thirds of the studied tools (68.0 %), a cortical back could be documented. The data suggest that the natural morphology of the back was already considered from the tool production onwards and the raw material was accordingly selected. Since the silicified schist, in Buhlen, but also in Balve, appears regionally as angular, barely rounded river pebbles (Jöris/Uomini 2019), the raw pieces could directly be modified by retouch. *Keilmesser* from Ramioul, which are mainly made of flint, are not an exception. Also, these artefacts are characterised by a mainly natural and cortical back.

A second aspect related to tool design is the *Keilmesser* morphology created during the manufacturing process. This topic was already touched on in the previous subchapter, but should be discussed further here. According to Weiss et al. (2018; see also Jöris 2004; Frick/Herkert 2019; Delpiano/Uthmeier 2020), *Keilmesser* do reflect a high shape variability (compared to e. g. hand axes, bifacial points or scrapers) but are standardised in their perimeter sections base and back, distal posterior part and the active edge. As explained before, the artefacts do vary in their shape, especially in their length and width dimensions. Moreover, the tools can be, based on their morphology, ascribed to (artificially categorised) *Keilmesser* shapes. The description of *Keilmesser* as tools with a high shape variability is thus not unsubstantiated. Nevertheless, the characteristics or the morphological definitions of *Keilmesser* are based on their attributes and perimeter sections. Interestingly, the analysis of the perimeter sections of the studied assemblages showed the following: the relation between the base and back as well as the distal posterior part seems to be highly dependent. The smaller the distal posterior part, the larger the dimensions of the back and the base. Regardless of this, the length of the active edge is nearly constant. These findings are supported by the observation from Weiss et al. (2018), stating that the distal posterior part is the more variable part in the tool morphology (see also Bosinski 1969).

Additionally, edge angle maintenance is seen as a crucial and determining factor in the design of *Keilmesser* (Iovita 2010; 2014). Following the ideas by Iovita (2010) and Weiss (2020), edge angle maintenance does not change the presence of the individual perimeter sections. Meaning, the ratio between the sections is

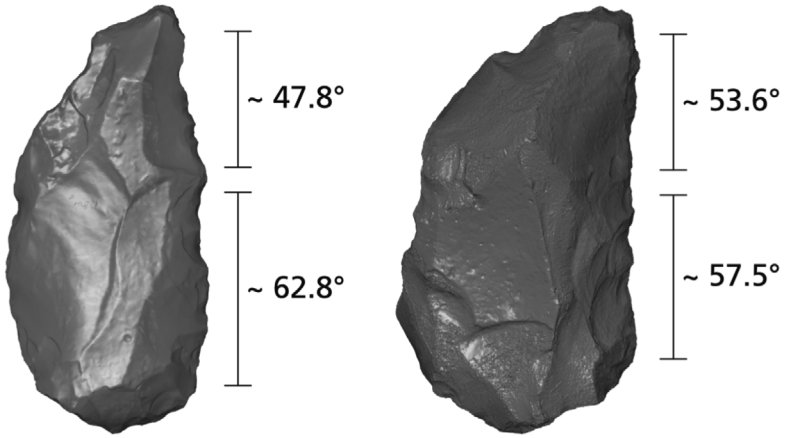

Fig. 160 3D scan of a *Keilmesser* modified by the application of the *Prądnik method* (left; Balve, ID MU-202) and of a *Keilmesser* without this modification (right; Balve, ID MU-197), illustrating the average edge angle in the distal and proximal part of the tool (calculated with the »best-fit« procedure; mean value of section 2 to 4 and distance 3 to 6).

interpreted as needed in order to retain the tool functionality (Weiss 2018). Is it possible to say that the focus of the *Keilmesser* design is concentrated on the active edge and the maintenance of the active edge angle? Within this project, the techno-typological analysis did not go that far in-depth in order to reconstruct retouch sequences or resharpening trajectories. However, this topic can also be addressed from the edge design point of view, including the study of edge angle variance. As common for *Keilmesser*, the active edge of the studied artefacts is most often bifacially worked (76.4 %), sometimes semi-bifacial (18.8 %) and only rarely unifacially worked (3.33 %). Moreover, the majority of *Keilmesser* (60.8 %) are modified by the application of the *Prądnik method*. The result of the modification is usually seen as the production of a stable, straight and/or acute active edge (Jöris 2001; 2006; Frick et al. 2017; Frick/Herkert 2019; Jöris/Uomini 2019). While this is visually recognisable and surely the case, other hypothesis are not so easy to evaluate. One of these hypotheses presumes a reduction of the edge angle by the application of the *Prądnik method*; the other suggests the creation of a bipartite morphology along the edge for differing functions (e. g. cutting and scraping). With the help of the acquired data concerning the edge angles, the first hypothesis can be tested, however, the second hypothesis cannot conclusively be addressed solely with this data, but can be with the results from the use-wear analysis.

Keilmesser edge design

The general results from the edge angle measurements taken from all *Keilmesser* indicate a correlation between the removal of a *Prądnik spall* and an acute edge angle. *Keilmesser* with a modification through the *Prądnik method* display on average a lower, sharper edge angle in the distal tool area than *Keilmesser* without the modification. However, this difference is not immense, usually ranging between a few degrees and rarely exceeding ten degrees. In order to illustrate these results, two examples are given. The first example is a bifacially retouched *Keilmesser* with a clear *Prądnik spall* removal. For this *Keilmesser* from Balve with the ID MU-202 (**fig. 160**) an edge angle of 47.8° could be calculated (»best-fit« procedure; mean value of section two to four and distance three to six) for the distal part of the active edge, where the *Prądnik spall* was removed. The proximal part of the active edge shows an increased edge angle value of 62.8° (»best-fit« procedure; mean value of section five to nine and distance three to six). The second example describes a *Keilmesser* with a bifacial edge retouch, but without any further modification. The edge angles have been calculated in an identical way as noted for the first example. For this *Keilmesser*, *Keilmesser* MU-197 from Balve (**fig. 160**), an edge angle of 53.6° was calculated for the distal and an edge angle of 57.5° for the proximal active edge area. Hence, this *Keilmesser* also shows lower values in the distal tool area, but the

variance is smaller. In general, independent of a *Prądnik method* modification, this is a trend documented for all *Keilmesser*. The calculated data illustrates a shift in the edge angle towards higher values from the distal to the proximal part of the tool. Following this, the active edge of *Keilmesser* is more acute in the distal tool area than in the proximal one. Thus, the data analysis supports the theory that the application of the *Prądnik method* reduces the edge angle and leads to a more acute active edge in the area of the removal in the distal part of the tool. This is also in line with other research, demonstrating that the application of a similar method to remove lateral tranchet blows, changed the angle of the tool's active edge by about 10° (Zaidner/Grosman 2015; Prévost/Centi/Zaidner 2020). The researchers concluded the production of a regular, straight and sharp edge as the aim of this tool modification. The second theory about the edge angle design of *Keilmesser* suggested a bi-functional morphology (Jöris 2001; 2006; Frick et al. 2017; Frick/Herkert 2019).

As mentioned above, the distal active edge area of *Keilmesser* commonly displays a more acute edge angle as the proximal area. The acuteness of edge angles often plays a role in the interpretation of the tool's function. Different ranges of edge angle values are thus associated with certain tasks, reflecting technological variability. A comparison with modern cutting edges can underline this aspect. Modern cutting and splitting implements are task specific designed. The values range commonly from low edge angles with less than 20° (e. g. razor blade, scalpel), medium values up to 40° (e. g. Japanese knife, standard cooking knife) to higher edge angles around 50° and 60° (e. g. hatchet, axe) (Hainsworth/Delaney/Rutty 2007; see also ISO 8442-5). Similar functional classification is assumed for Palaeolithic tools. Edge angles below 60° count as acute edge angles (Veil et al. 1994). An ascribed function could be cutting. Edge angles above 60° are more often associated with tasks such as scraping and carving. Based on the calculated edge angle, the interpretation of tools with bipartite morphology along the active edge and bipartite function cannot be refuted for the majority of analysed *Keilmesser* from the assemblages.

Tool handling

Another aspect of tool design, also related to tool functionality, concerns the tool handling. Due to their morphological concept, *Keilmesser* are usually interpreted as handheld tools (Jöris 2001; Frick et al. 2017; Frick/Herkert 2019; Jöris/Uomini 2019). Sometimes, the perimeter sections are also used to infer functional units (Iovita 2010; Weiss et al. 2018; Frick/Herkert 2019; Weiss 2020). Thereby, the base and the back fulfil a prehensile function, the distal posterior part is described as an edge connecting to the tip and used, among others, as a striking platform for thinning. The retouched active edge is seen as the active zone. Assuming the base and the back are the prehensile part of the tool, then, in the case of hafting, the presence of use-wear traces should confirm that. To current knowledge, the only published results of use-wear analysis on *Keilmesser* have been performed on artefacts from the Late Middle Palaeolithic site Sesselfelsgrotte (Rots 2009). From the n = 14 analysed *Keilmesser*, Rots interpreted four of these tools as possibly hafted. These findings cannot be transferred to the results obtained during the analysis of the studied *Keilmesser* from Buhlen, Balve and Ramioul. Based on the observed use-wear traces, hafting can likely be ruled out. None of the different types of the documented use-wear traces could clearly be correlated with hafting, neither due to the location of the traces. Individual artefacts show traces at remarkable positions. However, none of these traces is conclusive in a sense that the location of the traces is consistent on the dorsal and ventral artefact surface. Even so, one example should be given here even so. This example is not classified as *Keilmesser*, but as a *Prądnik scraper*. *Prądnik scrapers* do not reflect deviating results concerning hafting. The tool with the ID BU-099 is a unifacially retouched *Prądnik scraper* from Buhlen (**fig. 161**). The traces are

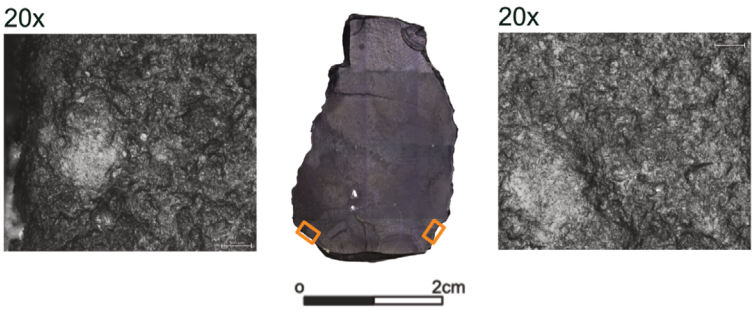

Fig. 161 EDF stitching image of the ventral surface of a *Prądnik scraper* (Buhlen, ID BU-099). The images on the left and right show use-wear traces (images are taken with a 20× optical objective).

located on the ventral surface of the tool in the proximal area to the left and right of the bulb. The traces are not located on exposed areas and are difficult to relate to potential use. Nevertheless, for an interpretation as a hafted tool, these indications are too limited. Thus, the use-wear analysis performed on tools from Buhlen, Balve and Ramioul supports the theory that *Keilmesser* as well as *Prądnik scrapers* are handheld tools. To summarise, the tool design of *Keilmesser* includes certain technological choices (e. g. raw material and blank selection) combined with functional aspects (e. g. edge retouch), often described as the *Keilmesser* concept (Jöris 2001; 2012; Jöris/Uomini 2019; Weiss et al. 2018; Frick/Herkert 2019; Weiss 2020). The recurrent application of this concept during the manufacturing, the curation and the reworking of the tools convey the idea of standardisation.

Prądnik scrapers and the *Keilmesser* concept

Next to *Keilmesser*, *Prądnik scrapers* as an asymmetrical artefact category have also been addressed within this project in order to investigate these tools more closely. When considering the *Keilmesser* concept not as a rigid one, but as one that combines the mentioned aspects and attributes, how do *Prądnik scrapers* fit into this concept? *Prądnik scrapers* do share morphological traits with *Keilmesser* (Jöris 2001; Jöris/Uomini 2019). In the case of the three studied assemblages, the tools were made of the same raw material. Despite this, the vast majority (88.9 %) of *Prądnik scrapers* are produced from flakes. The flakes, however, seem to be selected carefully, since more than half of the studied artefacts display an asymmetric shape. Additionally, some items illustrate cortical or natural backs, sometimes combined with minor retouch (29.6 %). Other tools show modification, indicating an intentional blunting of the edge in the posterior tool part, giving the impression of the preparation of an »artificial back«. The opposed active edge is mostly not bifacially retouched (13.0 %), as it is in the case for *Keilmesser*. Most of the *Prądnik scrapers* do have a unifacially retouched edge (40.7 %), some a semi-bifacially retouched edge (37.0 %). Furthermore, these scrapers are modified by the application of the *Prądnik method*, which is what differentiates them from other scrapers. These observations have led to the assumption that *Prądnik scrapers* could illustrate a simplistic or ad hoc version of *Keilmesser* (Jöris 2001; 2004; Jöris/Uomini 2019; see also Weiss et al. 2018) and may have been produced by less experienced knappers (e. g. children), trying to mimic *Keilmesser* (Jöris/Uomini 2019). The data obtained during the techno-typological analysis, does not contradict these interpretations. However, if a *Prądnik scraper* resembles a *Keilmesser*, then the function should be similar, too. The conducted use-wear analysis can add information on that. Out of the analysed n = 23 artefacts, n = 17 pieces display use-wear traces. First of all, the majority of the documented traces is located along the active edge, confirming the interpretation of a tool with only a single active edge. Surprisingly, the large variety of traces documented for *Keilmesser* is not reflected in the studied *Prądnik scraper* assemblage. On the contrary, the surface modifications documented on the *Prądnik scrapers* are mainly from one use-wear type, type V. (C),

a few from type I. (A) (**fig. 108**). This means for example, that with one exception, only polish could be found on the tool's surfaces. Interestingly, the use-wear category V. (C) is defined as extensive, shiny polish affecting the highest as well as the lowest topographical locations. Interpreted here as use-wear trace resulting from intense use. With this information, the results can now be set against the previously mentioned assumptions. To begin with, it is difficult to argue, that *Prądnik scrapers* should have the same or a similar function than *Keilmesser*. The documented traces indicate at least less versatility as the results for *Keilmesser* indicate. The question is, whether *Prądnik scrapers* would have been produced spontaneously or *ad hoc*, maybe as a reaction to a problem, or in order to learn the tool production. Would that be a tool used for such a long duration, so that use-wear traces as documented on the analysed tools can develop? The generalisation of the results is limited by the comparably small sample size and should thus not be overvalued, but the data suggests that *Prądnik scrapers* could be a simplistic version of *Keilmesser*. Simplistic in the sense of sharing the same morphological traits, which can be summarised under the umbrella term *Keilmesser* concept, but with less complex manufacturing und curation processes. The abbreviated production sequence for *Prądnik scrapers* (e. g. unifacial retouch compared to bifacial retouch) led probably to a less sophisticated active edge without the aspect of bi-functionality. Although the bipartite morphology is clearly given due to the application of the *Prądnik method*, the results of the use-wear analysis do not support a diverging use of the edge. Moreover, the results of the edge angle analysis also seem to contradict this idea to some degree. The calculated edge angle values for the *Prądnik scrapers* result in lower and therefore more acute edge angles along their active edges. One example is a *Prądnik scraper* from Ramioul. The tool, R-010, is a *Prądnik scraper* manufactured from a flake (**fig. 162**). The active edge is characterised by a unifacial retouch and one distinct *Prądnik spall* scar. This tool has an edge angle of 41.4° in the distal area where also the negative of the *Prądnik spall* removal is located (»best-fit« procedure; mean value of section two to four and distance three to six). In the proximal tool area, the active edge has an arithmetic mean value of 46.4°. This example illustrates that the active edge of *Prądnik scrapers* is slightly more acute compared to the majority of *Keilmesser*. Furthermore, the edge angle values in the proximal part are also lower in comparison. A decrease in acuteness along the active edge towards the proximal tool area is documented for the *Prądnik scrapers,* but this shift is considerably smaller, hence, the proximal tool area is barely reaching the 60°. Considering this, the mean value for the entire edge of *Prądnik scrapers* is on average 20° lower than the one for *Keilmesser*. The low edge angles might have given fewer possibilities for further retouch. At least that could explain the limited indications for retouch intensity and the absence of indications for reworking in contrast to *Keilmesser* (Jöris 2001; Jöris/Uomini 2019). In fact, a multiple application of the *Prądnik method* on *Prądnik scrapers* could only be documented three times. As demonstrated, based on the edge angle calculations, that *Prądnik scrapers* might not have a bipartite edge morphology, the assumption of a bi-functional edge is also invalid. A more plausible explanation for the edge modification with the *Prądnik method* could be seen in the aim to create a stable, straight and

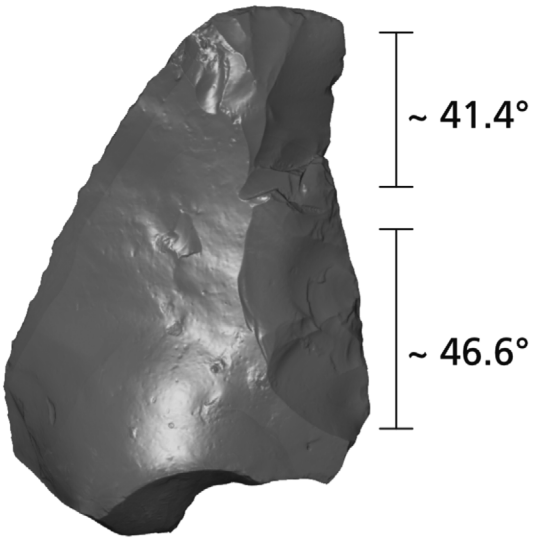

Fig. 162 3D scan of a *Prądnik scraper* (Ramioul, ID R-010) illustrating the average edge angle in the distal and proximal part of the tool (calculated with the »best-fit« procedure; mean value of section 2 to 4 and distance 3 to 6).

slightly sharper edge as suggested for *Keilmesser* as well (Jöris 2001; 2006; Frick et al. 2017; Frick/Herkert 2019; Jöris/Uomini 2019).
The analysis of the three assemblages from Buhlen, Balve and Ramioul demonstrate that *Keilmesser* are produced following a specific design. Broadly speaking, the tool concept integrates morphological attributes as the back and the base, likely used as prehensile area, the distal posterior part and the active edge. The mostly bifacially worked active edge of *Keilmesser* is characterised by a bipartite morphology or more precisely by an increase of acuteness towards the distal part of the edge. These aspects taken together form the characteristic asymmetric *Keilmesser* morphology. This morphology implies, and the results of the use-wear analysis supports the idea of *Keilmesser* as handheld and thus not hafted tools. The *Keilmesser* design, here described as *Keilmesser* concept, includes, when seen as an inclusive rather than a strict concept, also *Prądnik scrapers*. Despite the fact that *Prądnik scrapers* vary in aspects such as the blank selection and edge retouch, they are designed following the same underlying scheme as *Keilmesser* and therefore display the same morphological attributes. However, *Prądnik scrapers* seem not to have a bi-functional active edge, based on the results from the use-wear analysis and edge angle analysis. Thus, the presented data provides the idea that *Keilmesser* as well as *Prądnik scrapers* were produced according to similar tool design aspects but did not fulfil the same functional aspects. How the specific edge design of *Keilmesser* actually affects their use and if the interpretation of a multifunctional tool is supported by the results from the use-wear analysis, is discussed in one of the subsequent subchapters.

TOOL LATERALISATION AND THE IMPLICATIONS FOR HUMAN HAND PREFERENCES

Technology and use-wear to infer tool laterality

Handedness is a unique trait of humans (Uomini/Ruck 2019). As argued, handedness is closely related to brain lateralisation and cognitive evolution (Corballis/Badzakova-Trajkov/Häberling 2012; Ruck/Broadfield/Brown 2015; Cai/van der Haegen 2015; Uomini/Ruck 2018). Human behaviour related aspects such as the development of language and social learning are linked with handedness (Corballis 2003; Steele/Uomini 2008; Uomini 2009; Poza-Rey/Lozano/Arsuaga 2017; Uomini/Ruck 2019). Unfortunately, evidence for human handedness is difficult to find in the Palaeolithic record. Nevertheless, indications exist (e. g. proportions of right- and left-hand prints and stencils found on rocks and cave walls, asymmetries in fossil skeletons, striations on fossil tees; see e. g. Bermúdez de Castro/Bromage/Jalvo 1988; Trinkaus/Churchill/Ruff 1994; Frayer et al. 2010; 2012; Volpato et al. 2012; Fiore et al. 2015; Condemi et al. 2017; Frayer et al. 2016; Lozano et al. 2017), sometimes based on lithic studies (Semenov 1964; Cornford 1986; Uomini 2008; 2009; Ruck/Broadfield/Brown 2015; Jöris/Uomini 2019; Prévost/Centi/Zaidner 2020; Rodriquez et al. 2020). Although the recognition of (extinct) human hand preference is clearly limited, a bias towards right-handedness has been pointed out (Uomini 2011). Asymmetric tools such as *Keilmesser* and *Prądnik scrapers* may provide indications for human handedness. Due to their overall tool asymmetry, the tools can be distinguished in left-lateral and right-lateral tools, as demonstrated by Jöris and Uomini (2019). Thus, the tool laterality was accessed within this project. To begin with, the results from the analysis of the *Keilmesser* are addressed. In total, 79.1 % of the assemblage was defined as right-sided tools. Interestingly, in Buhlen as well as in Ramioul, the percentage of right-lateral tools is in each assemblage around 90 %. In Balve, the clear majority with 71.2 % of the *Keilmesser* were identified as right-sided artefacts and 26.2 % as left-sided artefacts. The total amount of left-lateral tools is 18.5 % of the three assemblages. The results

obtained from the *Prądnik scrapers* are similar, leading to a predominance of right lateral tools with a ratio of 81.5 % to 14.8 %. In this case, the results for the three assemblages are similar. Additionally, the *Prądnik spalls* reflect the laterality of the tools they have been removed from. The predominating right-sidedness of the *Keilmesser* and *Prądnik scrapers* is also illustrated by the *Prądnik spalls.* 61.2 % of the pieces are right-lateral, 25.8 % are left-lateral.

Taking the results of this analysis as a proxy for human handedness would indicate a clear predominance of right-handedness based on the studied assemblages. However, it should be pointed out again that the studied artefacts from Buhlen do not reflect the entire assemblage from the site. In particular the selected *Prądnik spalls* only display a small sample (n = 42 here studied *Prądnik spalls* out of 1661 existing *Prądnik spalls*; see Jöris 2001). Thus, the obtained results differ from the results published by Jöris (2001; Jöris/Uomini 2019). Having this as a constraint, further interpretation of the results would have no impact. Nevertheless, the results from the two other sites, Balve and Ramioul, do not contradict the observations made for the Palaeolithic record. As mentioned earlier, handedness may be influenced through social learning (Bradshaw/Nettleton 1982; Steele/Uomini 2009; Uomini 2009; Jöris/Uomini 2019). In this context, the standardised tool design of *Keilmesser* has been argued to be a result of continuous transmission as a skill passed on from generation to generation, as mentioned earlier (Jöris/Uomini 2019). This topic can be addressed further, and the implications of the results can be discussed in detail, but this is beyond the topic of this project. Nevertheless, based on the conducted use-wear analyses, an attempt was done to further investigate tool laterality based on the directionality of the use-wear traces.

The idea to investigate tool lateralisation based on qualitative use-wear analyses is not new (Semenov 1970), but has rarely been applied. A recent study on use-wear directionality is based on an experimental data set (Rodriguez et al. 2020). To current knowledge, tool laterality has not been linked with quantitative use-wear yet. Within this project, a first effort was done. To start with, the results of the qualitative use-wear analysis should be explained. Unfortunately, only a minority of documented use-wear traces displays a clear directionality. However, none of these traces is located in a way that indications about the directionality and thus the tool handling (in which hand the tool was hold) could be given. The results for all analysed tools suggested the slight predominance of use-wear traces along the active edge on the ventral tool surface. This general observation is similar for the n = 16 qualitatively analysed *Keilmesser* defined as left-sided tools. On these artefacts, n = 14 traces have been documented on the ventral edge, n = 15 on the dorsal edge. Assuming all the use-wear would be on the dorsal tool surface, it would be likely, that the tools defined as left-sided have been used in an identical way as the right-sided tools, presumably in the right hand. Since the results are nearly identical for both surfaces and thus inconclusive, the interpreted tool laterality can be neither supported nor denied. Unfortunately, also with the additional quantitative use-wear analysis no explicit results could be achieved. In theory, parameters such as the *isotropy, anisotropy, epLsar* or *NewEpLsar* provide information about the surface texture directionality. These parameters have been calculated for the studied artefacts, leading to no significant results so far. Significant results means that no pattern could be recognised or the data could not be interpreted in a meaningful way. As already indicated, quantitative use-wear analysis has not been applied in connection to tool laterality yet and needs to be further explored in future. Thus, there is no reference collection or any comparable data, which would help to usefully access the obtained data.

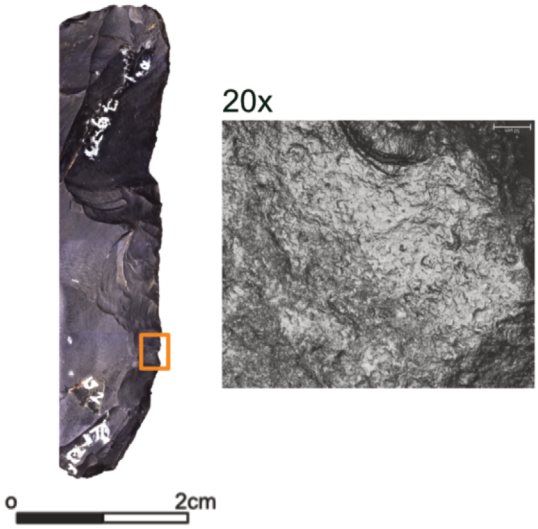

Fig. 163 EDF stitching image of the dorsal surface of a *Keilmesser* (Buhlen, ID BU-057). The image on the right shows the documented use-wear (image is taken with a 20× optical objective).

RESHARPENING AND RECYCLING BEHAVIOUR

Resharpening address by a functional analysis

An envisaged long use-life involving the option of recurrent resharpening has been documented as an inherent part of the *Keilmesser* concept (Jöris 1994; Richter 1997; Jöris 2001; Pastoors 2001, Weiss 2020). Based on technological studies and the reconstruction of the entire *chaînes opératoire*, long usages for *Keilmesser* could be demonstrated, highlighting the presence of several phases of retouch (Jöris 2001; Frick 2016b). Within this project, resharpening has only been addressed via the documentation of the (repeated) application of the *Prądnik method*. While in total 60.8 % of the studied *Keilmesser* are modified by a *Prądnik spall* removal, only a small percentage of 12.6 % is clearly characterised by a repeated application. An additional n = 36 distal tips of *Keilmesser* are part of the analysed assemblages, interpreted as a possibility to facilitate a longer tool use by creating new striking platforms (Jöris 2001). These elements are interpreted with respect to tool transformation (*Keilmesser* tips) and as elements involved in tool finishing and resharpening (*Prądnik spalls*). One interesting aspect is the retouch intensity of *Keilmesser* made of flint compared to the ones made of lydite. Unfortunately, the flint assemblage is rather small. Nevertheless, based on the *Prądnik method* application, a first impression can be gained. Surprisingly, nearly 62 % of both, lydite and flint samples, are modified by the *Prądnik method*. A multiple application could be documented for 12.4 % of the lydite samples and for 9.1 % of the flint samples. These observations indicate a similar resharpening intensity independent from the tool's raw material. How this is reflected in use-wear, has not been discussed yet. In order to address this aspect, the results for individual artefacts are explained exemplarily for the entire assemblage. To start with, a *Keilmesser* from Buhlen, BU-057 (**fig. 163**), with a distinct scar from the *Prądnik spall* removal, displays a use-wear trace in the dorsal, proximal tool area of the active edge. This use-wear trace is defined as type V. (C), associated with relatively longer-term or intense use. The distal area of the tool, which displays the *Prądnik spall* scar, shows no use-wear traces. Moreover, the negative of the *Prądnik spall* removal gives the impression of being fresh, not least due to the lack of (intentional) retouch within this area. Taking this information together, the artefact BU-057 might represent a *Keilmesser* that was eventually modified with the *Prądnik method*. Before this, the tool has likely being used. Simultaneously, this example can be seen as an argument against the idea of the *Prądnik method* application as a tool finishing method, otherwise the scar should also display use-wear traces similar to the proximal tool part. A *Keilmesser* from Balve with the ID MU-202 (**fig. 164**) illustrates another situation. The tool displays use-wear traces along the active edge within the area of the *Prądnik spall* negative. The use-wear is categorised as type II. (B), a low-intense use-wear trace. Additionally, the same tool shows use-wear traces on the ventral surface at a comparable location to the previously described use-wear spot. These traces, however, are defined as type V. (C), a more intense use-wear. It could be argued that the tool was used and eventually, the *Prądnik spall* was removed. Hence, the less intense use-wear traces on the dorsal surface could be explained in comparison to the traces on the ventral surface. Another example is a *Keilmesser*, BU-051, with a clear *Prądnik spall* negative extending almost over the entire length of the active edge (**fig. 165**). This scar appears as rela-

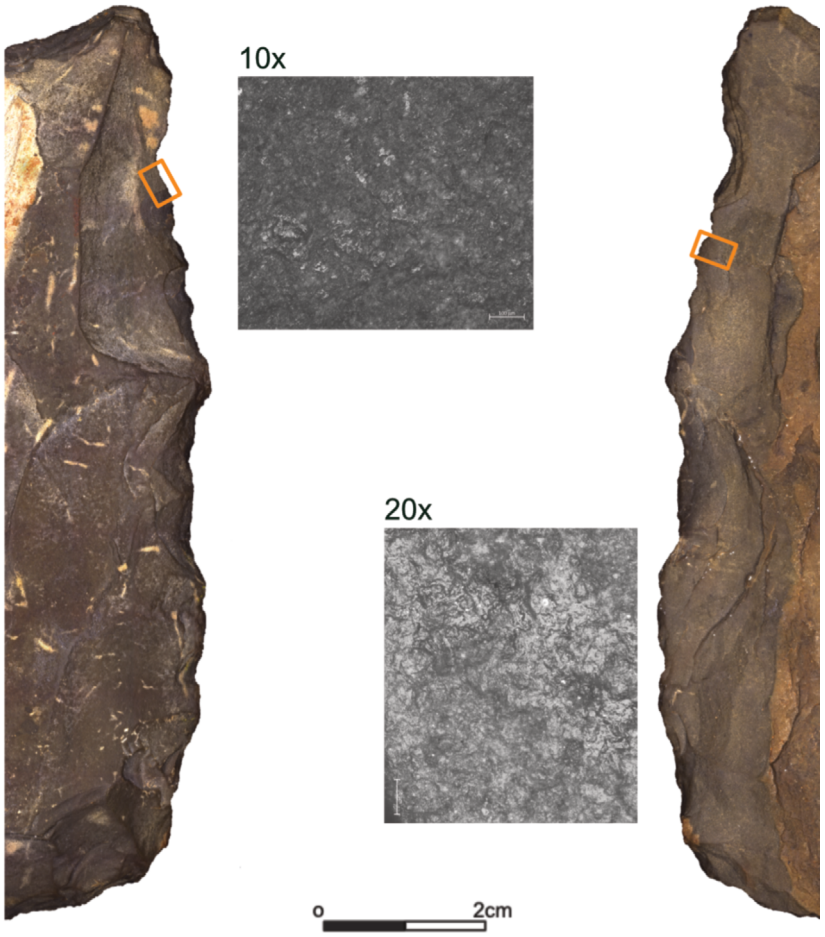

Fig. 164 EDF stitching image of the dorsal (left) and ventral (right) surfaces of a *Keilmesser* (Balve, ID MU-202). The images in the middle show the documented use-wear (images are taken with a10× and 20× optical objective).

tively fresh too, despite some minimal retouch along the edge. Nevertheless, the tool displays a use-wear trace of type I. (A) near the active edge in the area of the *Prądnik spall* negative. This use-wear category is interpreted as resulting from non-intense use. Thus BU-051 probably illustrates a tool, that was finished or (re-)sharpened and used short-term or with little intensity thereafter, resulting in minor, unintentional retouch and use-wear along the edge.

Not only can the tools help when assessing the intentionality of the *Prądnik method* application, but also the removed *Prądnik spalls* themselves. A qualitative use-wear analysis has been performed for a total of n = 39 *Prądnik spalls*. This analysis resulted in the documentation of use-wear traces on n = 27 artefacts. Beneath these spalls are n = 14 primary *Prądnik spalls* displaying use-wear traces. One example is an artefact from Buhlen with the ID BU-

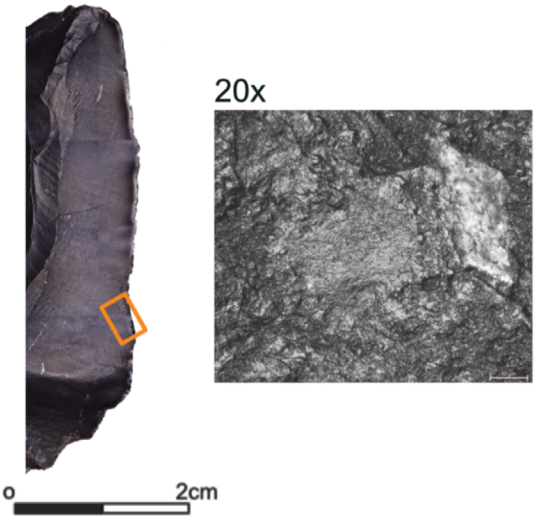

Fig. 165 EDF stitching image of the dorsal surface of a *Keilmesser* (Buhlen, ID BU-051). The image on the right shows the documented use-wear (image is taken with a 20× optical objective).

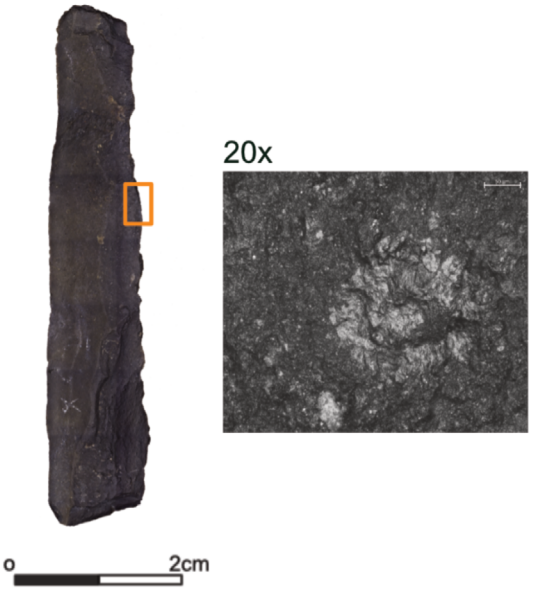

Fig. 166 EDF stitching image of a primary *Prądnik spall* (Buhlen, ID BU-129). The image on the right shows the documented use-wear (image is taken with a 20× optical objective).

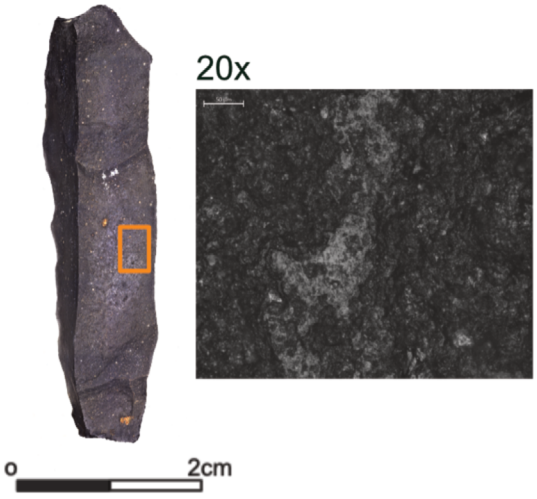

Fig. 167 EDF stitching image of the ventral surface of a primary *Prądnik spall* (Buhlen, ID MU-104). The image on the right shows the documented use-wear (image is taken with a 20× optical objective).

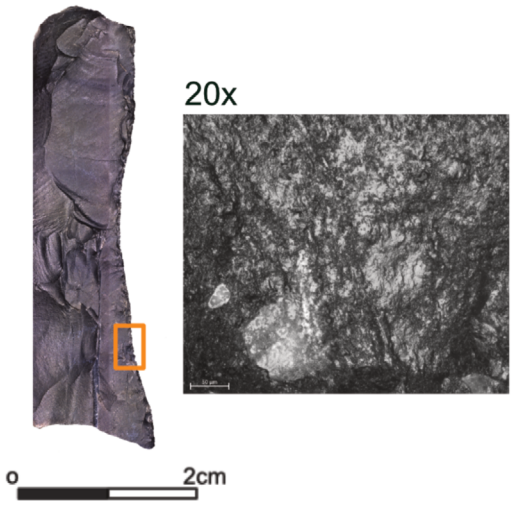

Fig. 168 EDF stitching image of a secondary *Prądnik spall* (Buhlen, ID BU-136). The image on the right shows the documented use-wear (image is taken with a 20× optical objective).

129 (**fig. 166**). On this *Prądnik spall*, a use-wear trace defined as type I. (A) could be documented. This indicates a use of the *Prądnik spall* before it was removed from the tool. However, this interpretation should be given with some caution. The majority of the documented use-wear traces on *Prądnik spalls* is not documented on the former active edge, but for instance on the ventral surface of the spall. This surface of the *Prądnik spall* was before the removal from the *Keilmesser* or *Prądnik scraper* attached to the tool and by no means could this surface have been exposed to use. One example is a primary *Prądnik spall* from Balve, MU-104 (**fig. 167**). This artefact shows intense use-wear of type V. (C) / VI. (D). Additionally, on n = 13 secondary *Prądnik spalls* use-wear could be documented. Only six of them show use-wear along the former active edge, so that the use could result from before the removal of the spall from the *Keilmesser* or *Prądnik scraper*. One example is a *Prądnik spall* from Buhlen with the ID BU-136 (**fig. 168**). The artefact shows use-wear defined as type V. (C). Findings as these support the interpretation of the *Prądnik method* as a technological option to sharpen and refresh the tool's edge.

The existence of use-wear traces on other locations besides the former active edge does not exclude the idea of reflecting the use of the *Keilmesser* or *Prądnik scraper* before the *Prądnik spall* was removed. However, the data also provides the idea that *Prądnik spalls* have been used as tools in their own right after having been produced. Interestingly, *Prądnik spalls* do reflect a comparatively high variability in the documented use-wear types, but this variability is shown on the ventral surface and not on the former active edge. The

calculated edge angle values for *Prądnik spalls* (measured on the former active edge) could explain why they are likely to have been used as independent tools. The measured edge angles are significantly lower than for all other sampled and analysed artefact categories. The values range between 20° and 25°. Thus, *Prądnik spalls* do have acute edges comparable to modern razor plates. It is not difficult to imagine that *Prądnik spalls* could have been used for tasks other than those performed by *Keilmesser* or scrapers for instance.

RAW MATERIAL PROPERTIES AND THEIR IMPLICATIONS FOR TOOL PERFORMANCE

Material loss, tool damage and blunting

In this study, the large majority of the lithics are made of silicified schist, the minority of flint. The properties of these two raw materials differ to some extent. The raw material hardness and the surface roughness have been the focus of the study. Based on the analysis of the two mentioned properties, flint can be pointed out as the harder raw material (according to the Leeb rebound hardness measured with the probe C). In addition, the surface roughness of flint is lower. Not only due to the lower hardness, but especially due to the schistosity planes, the banding or the natural cracks, lydite appears as the more brittle and fragile raw material. However, in the studied archaeological assemblages, lydite has been used more often for the tool production than flint. One reason for that is unequivocally the local occurrence of the raw material near the sites. In the course of the three conducted experiments, another potential reason might has evolved. The raw material properties, as studies on Pleistocene stone tool use have long argued, influence the way the tools perform during their use. As seen on the analysed standard samples, the effect that use has on these samples differs slightly for the samples made of flint and lydite respectively. In most cases, the damage on flint samples was, especially concerning acute edge angles (e. g. 40°) smaller, and the breaking pattern was visually often similar to retouch. Thus, the flint samples were less often affected by a change or increase of the edge angle. By contrast, the lydite samples experienced alteration in the sense of material loss. Especially during cutting, samples with acute edge angles were more often affected by alteration. The material loss on the lydite samples can be described as microfracturing and small breakages. These alterations do affect the tool performance to some extent, but rarely tool functionality. At the same time, tool performance based solely on efficiency and measured on the achieved penetration depth *per* tool (material displacement), was better for lydite samples.

Interestingly, the data suggests that the raw material effects tool performance and maybe human recycling behaviour too. An important aspect thereby is the tool sharpness. Sharpness has rarely been addressed on Palaeolithic tool studies (Key 2016; Key/Fisch/Eren 2018). However, studies focusing on the sharpness of metal knives point out the influence that sharpness has on aspects such as grip force, durability (McGorry/Dowd/Dempsey 2003), the contact material and the force needed to perform a task (Schuldt et al. 2013; 2016). According to Key, Fisch and Eren (2018) sharpness can be tested by the measurement of force, material displacement and work combined with the tool performance. Two aspects might be relevant in order to measure sharpness. These are the tool edge angle as well as the tip radius (Atkins 2009; McCarthy/Annaidh/Gilchrist 2010; Schuldt et al. 2013). These thoughts are important when considering the results of the experiments. As described before, the lydite samples experienced more alteration in the sense of microfracturing. Meaning, during the experiments, when the contact between the lydite sample and the contact material was given, alteration occurred. This likely caused constant »self-refreshing«. The flint samples, however, did not alter significantly. What likely happens is that the use of the flint samples

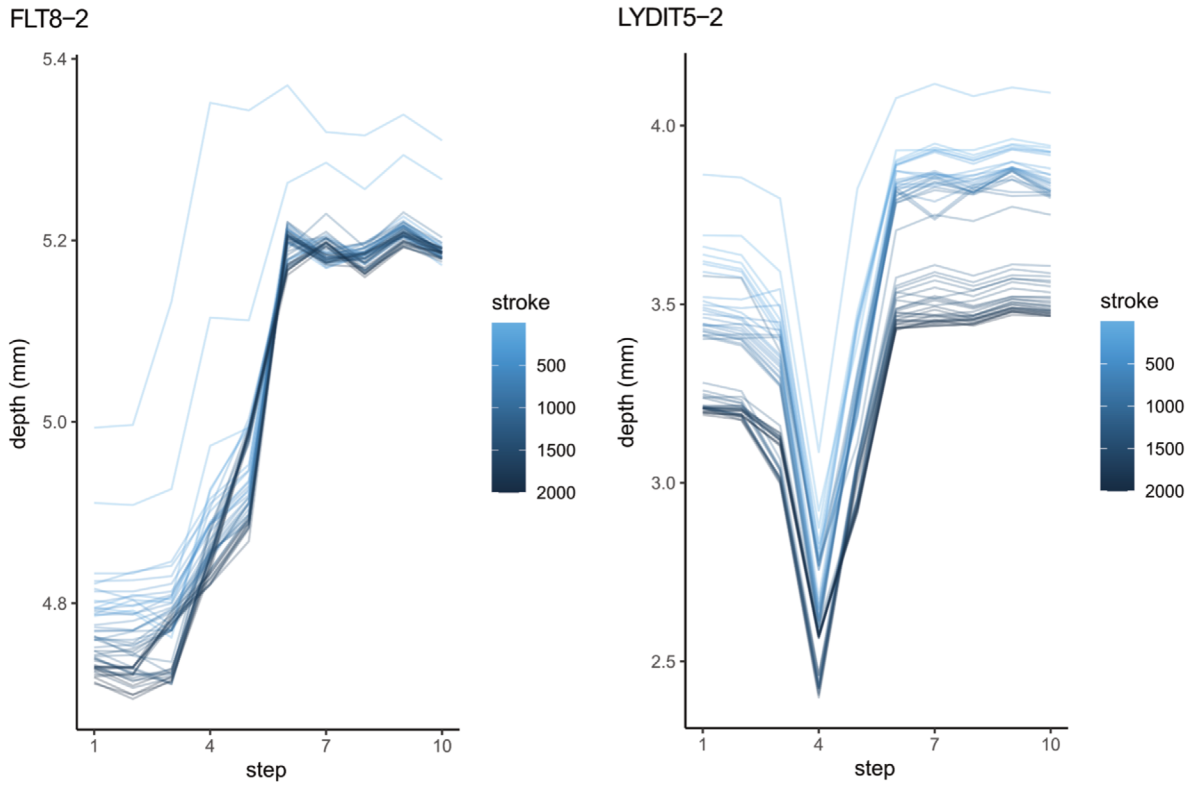

Fig. 169 Sensor recorded penetration depth achieved with a cutting movement with the SMARTTESTER® during the tool function experiment. On the left is the recording of the sample FLT8-2 and on the right the recording of the sample LYDIT5-2. The graphs show each 40th cutting stroke within all cycles (0 to 2000 strokes). The darker the colour, the more increased the penetration depth.

causes blunting through abrasion, finally resulting in a smoothening. This would explain why the lydite samples were more efficient in the sense of material displacement, as they were rather »refreshed« than smoothened. Early stage blunting can be counteracted by increasing force. Force is clearly an aspect influencing tool performance. During the experiments, force could be excluded as a relevant variable, because it was set and standardised during the experiments. Nevertheless, this means, in order to achieve the same penetration depth with flint as with lydite, the application of more force would have been needed. Due to its more fragile material properties, lydite seems to overcome the effect of early blunting by the loss of small fragments, which keeps the edge sharp to a certain degree. Experimental research on edge blunting with a variety of chert samples demonstrated that already one abrasive cutting stroke has to be compensated by 38 % increase if force and 70 % increase in work in order to achieve identical performance results (Key 2016; Key/Fisch/Eren 2018). These observation are also supported by the analysis of the penetration depth, which was sensor recorded in the course of the conducted experiments here. When looking at the results in detail, it is possible to see differences between the results obtained with the lydite and the flint samples. As an example, the samples FLT8-2 and LYDIT5-2 can be mentioned. Both samples are 45° samples used for cutting on a bone plate during the tool function experiment. The flint sample gives the impression of a continuous increase of the penetration depth during the first 100 to 150 cutting strokes (**fig. 169**). After that, the increase is only minimal. The lydite sample, however, also displays a rapid increase in penetration depth from the first stroke onwards. Moreover, the increase seems to occur stepwise. Whenever the material displacement during the cutting seems only negligible, a few strokes later, the sample penetrated deeper again. This observation demonstrates a likely correlation between the documented microfracturing of the lydite samples and the inherent »self-refreshing« properties of the raw material through microfracturing.

Which implications do these results have for the interpretations of the archaeological record? The results presented indicate that the raw material properties of lydite, which at first appearance only seem to have negative consequences for the tool use, might actually be beneficial during tool use. In order to perform a task with a tool made of silicified schist, less force and thus less work needs to be applied compared to performance with a flint tool. Of course, there might be a threshold of how much force lydite can tolerate before breaking. This threshold is likely higher for flint due to its elevated hardness values. However, there is also a limit of how much force can be applied by a human hand. These aspects are out of the scope of the study presented and discussed here, and therefore, in future, they need to be experimentally investigated further.

TOOL-USE AND FUNCTIONALITY

The multifunctional aspect of *Keilmesser*

Based on the design of the active edge and the general tool morphology, *Keilmesser* are commonly interpreted as tools with a singular bi- or multifunctional active edge (Jöris 2001, Urbanowski 2003; Jöris 2006; Rots 2009; Jöris 2012; 2014; Golovanova et al. 2017; Frick/Herkert 2019; Frick 2020b). The conducted use-wear analysis could clearly indicate that the main focus during tool use is on the active edge. The majority of the use-wear traces could be documented along the active edge. With 77.4 % of the traces, this result is unambiguous. The documented traces slightly prevail on the ventral than on the dorsal surface.
Concerning the functionality of the tools, the answer to the question is more complex. In order to assess the topic, the interpretation of the documented use-wear types should be discussed first. As mentioned in the previous chapter, the qualitative use-wear analysis performed within this project does not aim at a functional interpretation and the identification of the contact material. The reason for that is mainly given by the lack of a reliable reference collection for use-wear traces on silicified schist. Nevertheless, some aspects concerning the intensity of the traces and their implications can be discussed. First of all, the defined categories of use-wear traces can be separated into two main features: polish and striations (the latter which may appear in tandem together with polish). Within these categories, there are noticeable intensity nuances (**fig. 103**; **tab. 37**). Polish as use-wear is defined by the categories I. to V. While category I. (A) describes small spots of polish, which are only slightly abrasive and only effect the highest topography, category V. (C) is extensive polish affecting the lowest as well as the highest topographical levels. The traces displaying striations (VI. – VIII.) affect all topographical levels. The analysis of the use-wear traces indicates a correlation between the intensity of the use-wear traces and the duration of the tool use. Following this interpretation, short-term or less intense use only leaves small traces on the highest topography of the surface. With increasing duration of the tool use, the traces are getting more extensive and abrasive. Measured on the abrasiveness of the traces with striations, these traces reflect also high intensity or long-term tool use. Based on this interpretation, the resulting consequences can be discussed. Following this interpretation, use-wear traces reflecting a long-term use should be predominantly located along the active edge. This is the case in this study, but at the same time, there are also such use-wear traces (e. g. category V., VI. and VII.) located on the back of the *Keilmesser*. At first glance, this sounds contradictory. Assuming that only the active edge of *Keilmesser* has been used, then traces along the back should only display traces of short-term activities, post-depositional traces or traces resulting from unintended use. However, they also display traces associated with a longer or more intense use. For example n = 20 out of n = 44 traces documented along the back of *Keilmesser* are

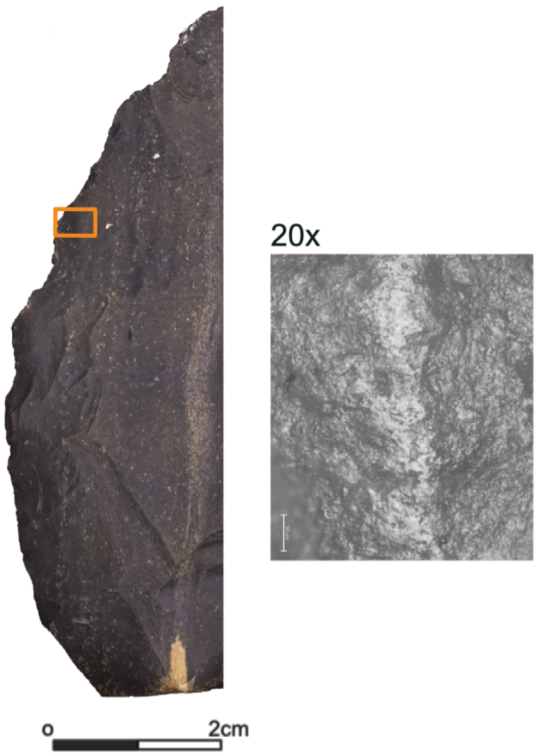

Fig. 170 EDF stitching image of a *Keilmesser* (Balve, ID MU-199). The image on the right shows the documented use-wear (image is taken with 20× optical objective).

defined as use-wear type V. (C). These n = 20 traces have been observed on in total n = 16 *Keilmesser*. Interestingly, the majority of these 16 *Keilmesser* (n = 10) are partly retouched or retouched along the edge of the back and distal posterior part (n = 4 are unworked, n = 2 are undefined) (e. g. *Keilmesser* MU-199; (**fig. 170**). These findings do not contradict the idea of *Keilmesser* as tools with one active edge. The numerously documented traces along the active edge still support this statement. However, a small amount of tools also display traces along the back associated with long-term or intense use. Most of these *Keilmesser* are retouched in the corresponding areas of the back. These results indicated that the use of *Keilmesser* might have been more versatile or the handling less static than expected.

In general, within the studied artefact categories, *Keilmesser* illustrate the highest variability of documented use-wear types. A nearly, but not comparable high variance is documented for the scrapers, which built an outgroup within the study. Further indications regarding the tool function and use are given through the distribution of the use-wear traces. Following the interpretation of *Keilmesser* as a multifunctional tool with an active edge designed for different actions, this should be reflected in the accumulation, the distribution and potentially in the type of use-wear traces along the active edge. In order to address this topic more specifically, the results of individual samples will be discussed exemplarily. Assuming a *Keilmesser* would have been used with the distal part of the tool for a different action than the proximal part of the tool. This would likely lead to diverging use-wear traces. A tool, which could have been used for these minimum two actions could be the *Keilmesser* with the ID MU-111 (**fig. 171**). The application of the *Prądnik method* is clearly visible by an elongated negative in the distal part of the active edge. This sample displays intense use-wear (type IV.) in the exact same, distal tool area. Parallel to these traces, similar use-wear can be found on the same location, but on the ventral tool surface. The use-wear on the ventral surface is of the same type, but extends less. Additionally, the tool displays use-wear traces in the proximal part of the tool on the ventral surface. This documented use-wear spot is defined as use-wear type III. and thus, categorised as a polish, too, but resulting from a less intense use. The fact that the differing use-wear traces are documented on the ventral, flat surface of the tool, makes it difficult to imagine that they could have formed simultaneously during one type of action. Assuming these traces are the result of a cutting movement, involving the entire length of the active edge, it would be difficult to explain why the traces in the distal tool area are more intense than in the proximal area although the surface is flat and even. Thus, the sample MU-111 could be an example for a *Keilmesser* with a multifunctional active edge. Moreover, there are *Keilmesser* supporting the idea of a tool with a versatile purpose. Following this interpretation does not mean that the tool was actually used for all possible purposes, but that it was in general designed to perform varying tasks. Consequently, there are *Keilmesser* displaying traces either only in the distal, the medial or in the proximal area of the active edge. *Keilmesser* MU-246 is such an example (**fig. 172**). Intense polish (type V. / VI.) was documented in the distal

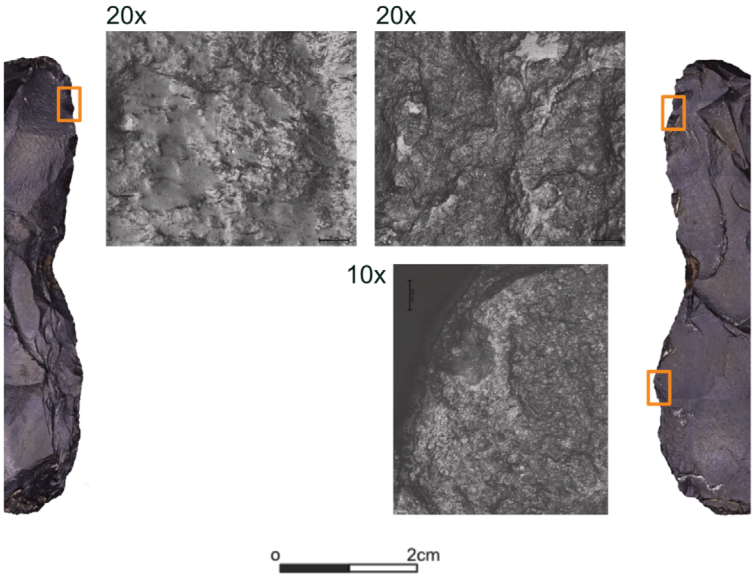

Fig. 171 EDF stitching image of a *Keilmesser* (Balve, ID MU-111). The images in the middle show the documented use-wear (images are taken with 20× optical objective).

part of the tool on the dorsal as well as the ventral surface. The quantitative use-wear analysis results in an arithmetic mean value of 1.5 µm for *Sq*, expressing the root mean squared height, and thus reflecting the micro surface roughness. A *Sq* value of 1.5 µm in the context of the studied material is comparably small and thus supports the interpretation of a surface modification affecting the highest and the lowest surface topographies as described for the use-wear types V. and VI. Despite this intense polish in the distal part of the tool, no further use-wear traces could be documented. Based on these observations, it seems likely, that the tool was only used in the distal tool area and not with the entire length of the active edge. Here, a correlation with the location of the traces and the tool handling seems likely. The *Keilmesser* illustrates no indications for a tool hafting and is a comparably small tool with 5.4 cm in average length. A tool handling

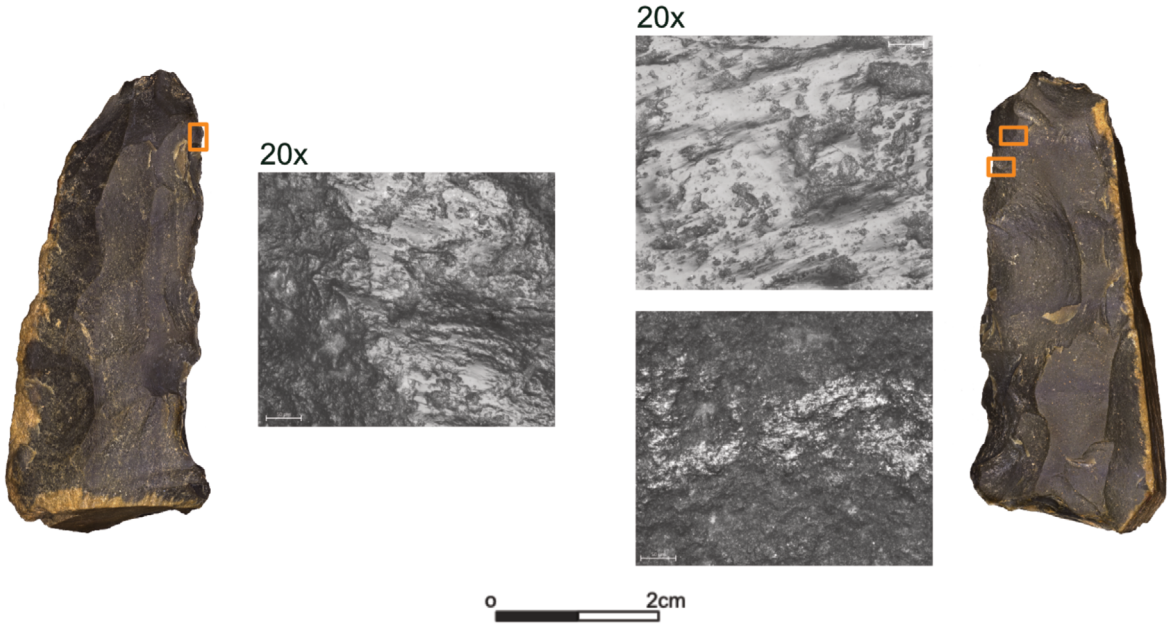

Fig. 172 EDF stitching image of a *Keilmesser* (Balve, ID MU-246). The images in the middle show the documented use-wear (images are taken with a 20× optical objective).

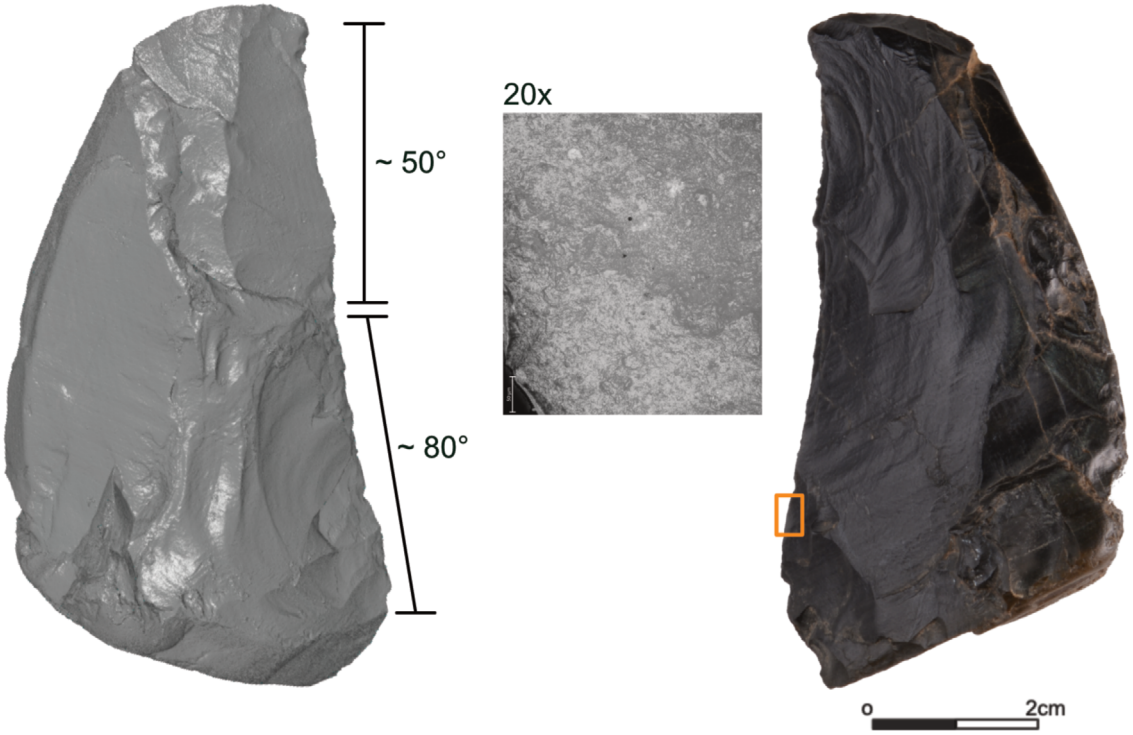

Fig. 173 3D scan (left) and EDF stitching image (right) of a *Keilmesser* (Buhlen, ID BU-158). The image in the middle shows the documented use-wear (image is taken with a 20× optical objective). The 3D scan indicates the average edge angle in the distal and proximal part of the tool (calculated with the »best-fit« procedure, mean value of section 2 to 9 at the 3 mm to 6 mm distance to the intersection).

as suggested by Frick et al. (2017) or Jöris and Uomini (2019) for a carving movement could explain the absence of use-wear traces in areas other than the distal tool part. According to these descriptions, the index finger (Frick et al. 2017) or the thumb (Jöris/Uomini 2019) is pressing against the back of the tool, while the other fingers embrace the base and thus the proximal part of the tool. Following this interpretation, only the distal tool area would be exposed to use. At the same time, there are tools within the studied material, which are characterised by the absence of traces in the distal part of the tool, while the proximal part of the tool displays traces. One example is the *Keilmesser* with the ID BU-158 (**fig. 173**). Use-wear type V. could be documented on the ventral surface of the *Keilmesser*. The tool is modified by a removal of a *Prądnik spall* on the dorsal surface. The changing character or quality of the active edge from the distal to the proximal tool area is also expressed by the edge angle values. The average edge angle for the upper part of the tool is 50°, the mean value for the lower, proximal part is 80° (»best-fit« procedure, mean value of section two to nine at the 3 mm to 6 mm distance to the intersection). In general, as previously explained, edge angles below 60° are seen as acute edge angles suitable for tasks such as cutting. Edge angles above 60° are too blunt for cutting and therefore more suitable for carving and scraping tasks (Veil et al. 1994; Weiss 2020). This observation separates the active edge of the described *Keilmesser* into two morpho-functional parts. Taking all these aspects together, the interpretation of the tool only used with the proximal part for instance for a scraping or carving movement cannot be denied. At least, only there, the use led to the formation of use-wear traces. Contrary to these examples, there are also tools displaying identical use-wear traces along the entire active edge. One example is the *Keilmesser* MU-214 (**fig. 174**). On the ventral surface of the tool, three spots of use-wear, categorised as use-wear type V. (C), could be documented. The dorsal surface does not display use-wear traces. Interestingly, this *Keilmesser* is characterised by the application of the *Prądnik*

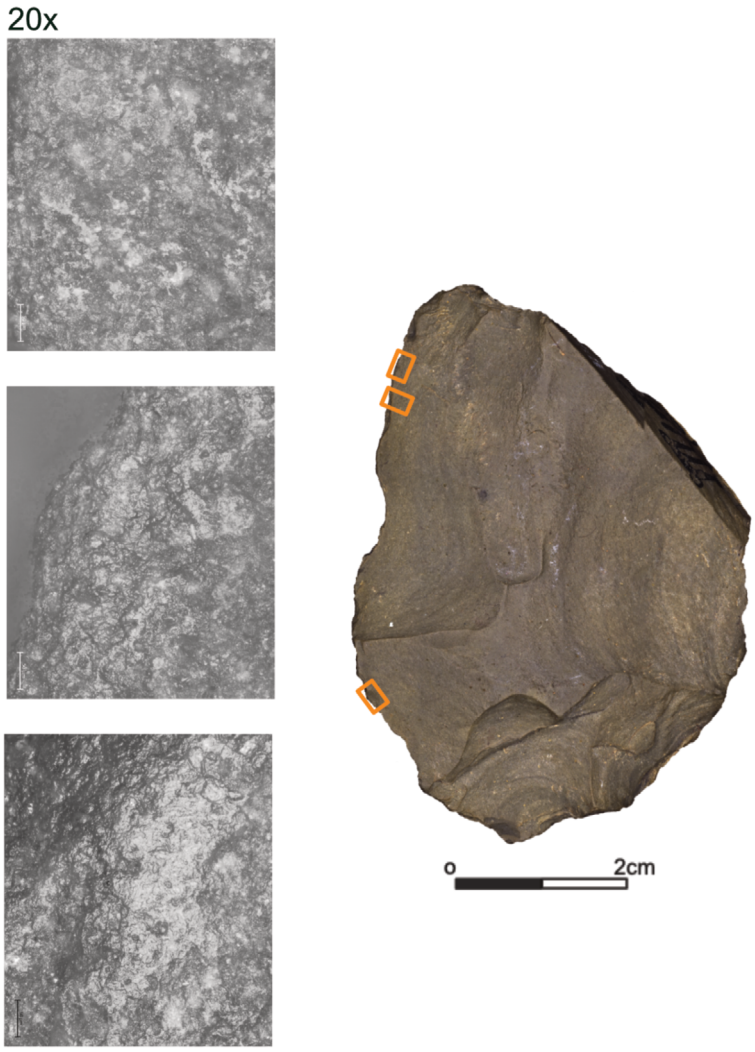

Fig. 174 EDF stitching image of the ventral surface of a *Keilmesser* (Balve, ID MU-214). The images on the left show the documented use-wear (images are taken with 20× optical objective).

method, but represents one of a few exceptions with a negative of the *Prądnik method* on the ventral surface. Therefore, the documented use-wear traces on the ventral surface are located in the negative left by the removal of the *Prądnik spall* and below in the proximal tool area. Based on the documented use-wear traces solely, this *Keilmesser* offers no indication for versatile use. Here, the question needs to be raised, what tool multifunctionality implies? Assuming multifunctionality describes a tool, designed in a way that several (or at least two) tasks could be potentially performed in a useful way. If only the aspect concerning the design is of relevance, then it is not important, whether the tool was actually used for multiple purposes or not. Considering this, the results of the presented examples, which are in place of all studied *Keilmesser*, are in line with the interpretation of *Keilmesser* as multifunctional tools (Jöris 2001; 2006; Rots 2009; Jöris 2012; 2014; Golovanova et al. 2017; Frick/Herkert 2019). Generally speaking, the results from the qualitative use-wear analysis indicate that *Keilmesser* illustrate tools with a versatile application. Derived from the distribution of the use-wear traces and types, an identical handling and use for all tools is inconceivable. As described, the idea concerning a versatile tool functionality is supported by the edge angle calculation. However, it is not imperative, that all *Keilmesser* were used for multiple purposes. Based on the results from the use-wear analysis solely, it seems as if most of the *Keilmesser* do reflect traces resulting from a single activity only.

Tool use in site context

With the just discussed results in mind, it should be mentioned again, that the results from the use-wear analysis performed on the *Keilmesser* from Buhlen led to a slightly diverging picture. In general, as explained, from Balve and Ramioul, *Keilmesser* do reflect a variety of use-wear types. However, the analysed *Keilmesser* from Buhlen differ in this aspect (**fig. 105**). In this sample, mainly use-wear traces from the category I. (A) and V. (C) could be documented. This observation raises the question, whether *Keilmesser* from Buhlen were used for different purposes than in Balve and Ramioul? Based on the identified use-wear types, it is clear that no striations could be documented along the active edge, narrowing the base for arguments for a multifunctional from a use-wear point of view. In order to answer this question fully, additional artefact categories from the site need to be analysed. This would allow to investigate the aspect, whether *Keilmesser* in Buhlen have not been used as multifunctional tools, but instead, for a specific purpose. Nevertheless, the *Keilmesser* from Buhlen do display less (I.) as well as more intense use-wear (V.). The use-wear of type V. is thus also often located along the active edge in the distal area of the tool. The quantity of lateral *Prądnik spalls* in Buhlen is extremely high, outnumbering the quantity of *Keilmesser* and *Prądnik scrapers* (Jöris 2001). If it would be the case that mainly use-wear traces resulting from short-term or low intense use are reflected in the distal tool area, then it can be advocated that the tools were likely frequently resharpened. However, the intense use-wear traces in this tool area make it difficult to argue, and different use of the *Keilmesser* from Buhlen compared to Balve and Ramioul is thus unlikely. Nevertheless and interestingly enough, the *Keilmesser* from Buhlen reflect less striations, limiting the arguments for a multifunctional tool use.

Tool performance and variables affecting it

In order to access tool use and function for the studied asymmetric tools further, the results of the conducted controlled experiments should be include and discussed. Before delving into the results, the overarching goal of the experiments should be stressed again. The individually conducted, *second-generation experiments* aimed at identifying the influence of certain independent variables within the chosen experimental settings. Within the three experiments, the tested independent variables were raw material, edge angle, contact material as well as movement. It should be pointed out, that the goal was not to produce a use-wear reference collection for a comparison with the archaeological record. Instead, the influence of each mentioned independent variable on tool performance should be explored. At the same time, the experiments were meant to document the formation and the development of use-wear traces under controlled conditions. In this context, the mechanics behind the use-wear formation should be questioned based on the results of the quantitative use-wear analysis. The results concerning the differences in tool performance, depending on the raw material of the standard sample, measured on the penetration depth and the tool alteration (edge angle change) have been shortly addressed in the previous subchapter. Thus, this topic is not dealt with here again. Instead, the result from the tool function experiment regarding the edge angle and the movement should be mentioned. First of all, it has to be noticed that independent from the raw material and the edge angle of the sample, both tasks – cutting and carving – could be performed without the standard samples losing functionality. Since the edge angles have been extrapolated from the 3D models of the analysed *Keilmesser*, with reservation, the data can be transferred to the archaeological record. Meaning, the design of the average *Keilmesser* active edge should allow in theory for movements such as cutting and carving. Based on common interpretations, also scraping is assumed as a possible function of *Keilmesser* (Frick et al. 2017; Jöris/Uomini 2019) and should therefore be tested in future experiments.

The evaluation of the results from the qualitative use-wear analysis indicated that cutting more easily leads to the development of use-wear traces. The penetration depth into the contact material can likely explain this observation. During cutting, the standard samples went deeper into the contact material, increasing the area of contact between the standard sample and the contact material. During carving, the penetration depth was lower and the contact zone smaller. Thus, the developed use-wear on the standard samples used for carving is only marginal. Interestingly, the quantitative data obtained from the standard samples used during the experiment led to no identifiable differences regarding the movement. Meaning, based on these quantitative results only, the performed movement could not be identified. However, more relevant than the movement from the quantitative point of view proved to be the edge angle. The quantitative data correlated with the information about the edge angle of the samples formed distinct data clusters (**fig. 156**).

Surface texture roughness and the formation of use-wear traces

In the context of the experiments, the results from the quantitative use-wear analysis should be elaborated a bit further. In order to access the influence of the tested independent variables, the calculated (ISO) parameters should be mentioned. Each of the measured 34 parameter can potentially give some indications concerning a surface variation. Within these parameters, *Sq* (surface texture roughness) appeared as a prominent parameter. This is not only reasoned in the fact that quantitative use-wear studies most often refer to areal field parameters such as the amplitude parameters (e. g. *Sq, Ssk, Sa*) (Martisius et al. 2020; Pedergnana et al. 2020b), leading to a slightly better understanding of this parameter, but also due to the clear indications the data provides. When referring to the »artificial VS. natural« experiment, the results gained through the use of the four different contact materials are revealing. Before going into detail, it should be noted again that the measured *Sq* values for the standard samples made of flint, resulted in a lower micro-surface roughness than the lydite samples. Eight of the standard samples used during the »artificial VS. natural« experiment have been quantitatively analysed before and after (2000 strokes) the experiment. The results of this quantitative use-wear analysis provide a new insight into the relationship between the original surface texture roughness of the tools and the development of use-wear traces on that surface. The standard samples with an initial low surface texture roughness (mainly the flint samples) did not change significantly in the course of the experiment (**fig. 142**). Standard samples with an original rougher surface resulted in a modified surfaces roughness with a tendency of increasing values. In other words, a rough surface gets rougher after intensive use. The data indicates that a surface with a high surface texture roughness is more prone to abrasion processes than a low surface roughness. These findings are in line with the interpretation of polish formation as a result of abrasion processes (Schmidt et al. 2020). Within the conducted experiments, the surface texture of the raw material seems thereby of more relevance than the properties of the contact material. While these observations are important to understand the mechanics behind the formation of use-wear, they can also be transferred to some extent to the archaeological record. In order to explain this, one example is given. The example is a *Keilmesser* from Balve with the ID MU-224 (**fig. 175**). Use-wear traces could be documented in the distal part of the tool on the dorsal as well as on the ventral surface. While the use-wear trace on the dorsal surface is defined as type III. (B2), the use-wear trace on the ventral surfaces is categorised as type V. (C). Both use-wear traces have been analysed quantitatively. Since both spots are documented on the same tool, the initial surface texture roughness of this flint sample can be assumed as identical on both surfaces. Although the visual difference between the two use-wear traces is not extreme, the results indicate a diverging surface texture roughness. The calculated *Sq* value for the spot of type III. is 1.33 µm and for the other spot, type V., is 1.49 µm. This data supports the interpreta-

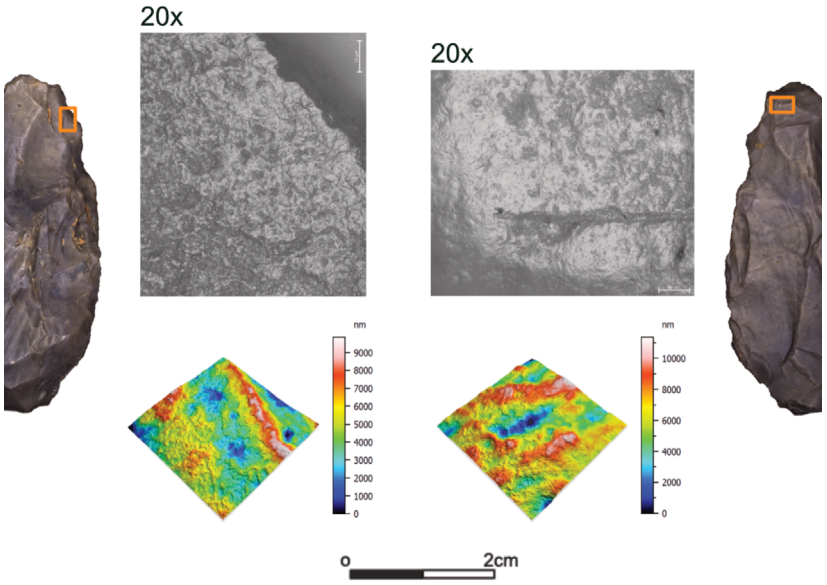

Fig. 175 EDF stitching images of the dorsal (left) and ventral right surfaces of a *Keilmesser* (Balve, ID MU-224). The images in the middle show the documented use-wear (images are taken with 20× optical objective) and the corresponding micro-surface texture. The colour of the surfaces corresponds to the height on the z-axis.

tion of the defined use-wear traces as a main result of varying use duration and/ or intensity. Moreover, this implies another aspect: *Sq*, when combined with the original surface texture roughness, can likely serve as an indicator for the duration or the intensity of the tool use. In order to underline this theory, the quantitative data from the archaeological samples was plotted together with the data from the standard samples (**fig. 176**). All plots can be found on GitHub in the corresponding repository [https://github.com/lschunk/use_wear-archaeology_meets_experiment]. The boxplots show the archaeological data separated in the use-wear types and with the artefact categories highlighted in different colours. Additionally, the data from the standard samples are included in the plot separated as before and after 2000 strokes. When looking at the boxplot from the parameter *Sq*, the previously described observations are supported. The combined *Sq* values of all analysed standard samples tend to vary more after usage. However, it should be noted that a direct comparison is not given, since the data results on the one hand from archaeological samples and on the other hand from machine cut standard samples, but the underlying trend seems to be comparable.

Contact material and use intensity

The here mentioned observations resulting from the quantitative use-wear analysis also help to answer another question. Among others, one aim of the »artificial VS. natural« experiment was to identify whether the use of standardised contact material can be justified over the use of natural contact material measured on tool performance and the development of use-wear traces. The answer to this question needs to be given from two diverging point of views. The use of standardised contact material within an experimental setup with the goal of producing a reference collection for a comparison with archaeological samples should be only done with reservation. Although the produced use-wear traces visually resemble the traces developed through the use of natural contact material, this does not need to be the case for traces on knapped material. Within the course of the conducted experiments, only standardised samples have been used. The use of the standard samples was necessary in order to exclude certain variables. However, this aspect illustrates the limitations of *second generation experiments*. The obtained conclusions need to undergo further testing in a more realistic scenario (*third generation experiment*, see Marreiros et al. 2020) before being conclusively transferred to the archaeological record. Another answer can be given when using standardised contact

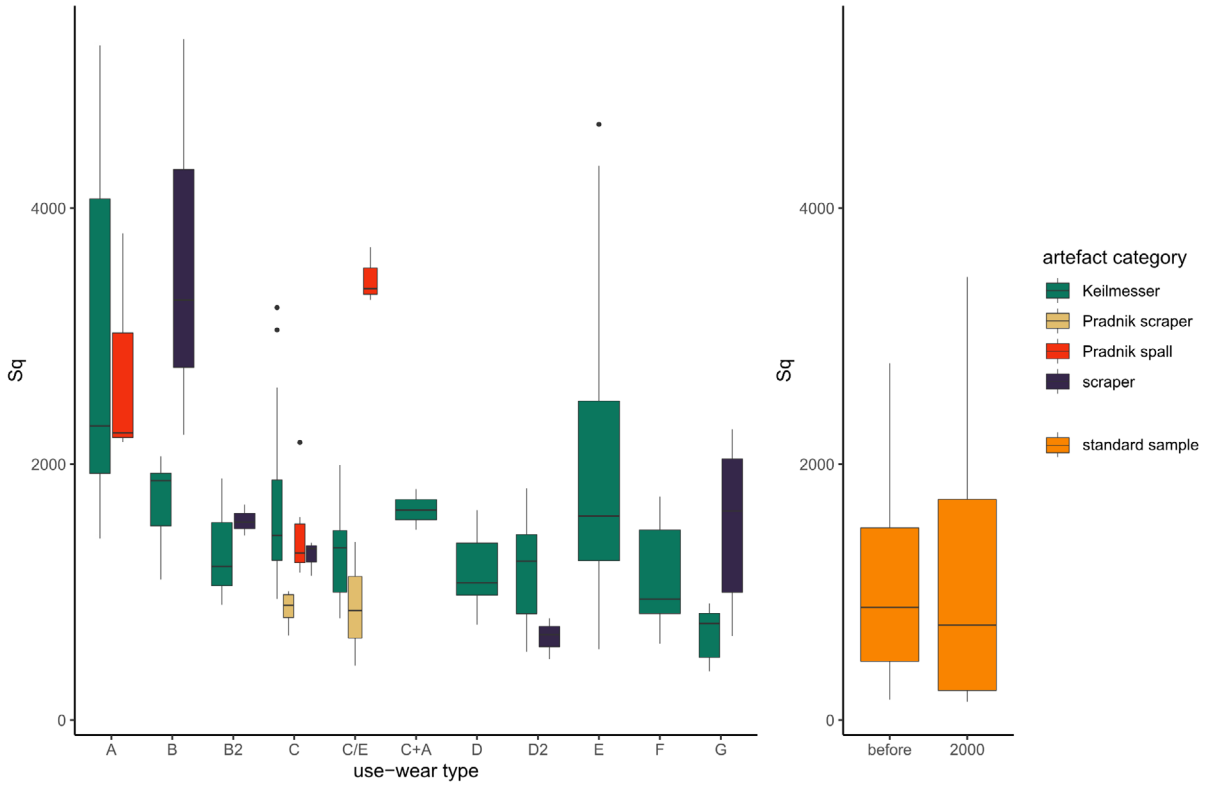

Fig. 176 Distribution of *Sq* values for the measured use-wear traces (n = 50) on the archaeological artefacts (left), combined with the measured use-wear traces (n = 28) from the »artificial VS. natural« and tool function experiment (right). The data is categorised according to the interpreted use-wear types and coloured based on the artefacts type.

material in an experimental setup, in order to investigate the influence of a specific variable within the setup. For example, here, it was the goal to investigate tool performance and the formation of use-wear traces as well as the mechanics behind both. In such a scenario, the use of standardised contact material should be compulsory. In the case of the conducted »artificial VS. natural« experiment, the use of both types of contact materials in comparison results in similar observations. One of them concerns the raw material of the standard samples. The use of natural as well as the use of artificial contact materials led to the suggestion that the correlation between the formation of use-wear traces and the raw material of the sample might be of more impact than the one between the formation of use-wear traces and the contact material. Moreover, this formation is highly correlated with the duration or the intensity of the tool use. This idea is supported by the results from the qualitative as well the quantitative use-wear analysis. All analysed standard samples (»artificial VS. natural« and tool function experiment) developed within the course of the experiments use-wear. The data taken together indicate that the use-wear formation under the tested conditions is dependent on several aspects. The order of these aspects based on their implications should likely be as follows: 1) the raw material of the sample, 2) the intensity or duration of the use, and 3) the contact material.

Within this chapter, several aspects concerning asymmetric tools such as *Keilmesser* and *Prądnik scrapers* have been discussed and interpreted within and between artefact categories. To do so, only a multidisciplinary approach allowed for testing previous interpretations regarding these tools. The chosen approach allowed for new data to be gained, providing new insights and a more distinct picture about these Late Middle Palaeolithic tools. Seen as major evidence to understand how humans produced, designed and used their tools in the past, this new information have an impact on contextualising technological behavioural choices of Neanderthals.

CONCLUSION

The research presented and discussed in this dissertation aimed to gain a more precise picture about asymmetric tools from the Late Middle Palaeolithic by testing common interpretations concerning their tool design and function. As a case study, *Keilmesser* and *Prądnik scrapers* as well as their resharpening debris, *Prądnik spalls,* from three sites – Buhlen, Balver Höhle and Ramioul – have been studied. Based on a multidisciplinary approach, including a functional analysis combined with controlled experiments, new data could be collected. To summarise the main findings, the addressed aspects concerning tool design are given in combination with the obtained results. The following conclusions can be drawn based on the data gained through the application of interrelated methods and techniques.

To start with, the first aspect concerns the results achieved through the raw material characterisation, which indicates the importance of raw material analyses in functional studies. The significance of the raw material regarding tool performance and wear formation could be clearly observed based on the results of the conducted experiments and quantitative use-wear analysis. During the sequential experiments, the observation could be made that lydite standard samples performed better than flint standard samples. Performance is thereby measured based on tool efficiency and durability. Although the lydite samples experienced more material loss and changes in the edge angles during usage, this did not affect the tool function. With one exception, all samples performed 2000 strokes without any maintenance processes. The flint standard samples displayed less material loss, but material loss is visually more similar to retouch than edge damage. The efficiency was evaluated via the contact material displacement and recording the penetration depth when constant force was applied. Lydite could be documented as less hard, but with a higher surface roughness compared to flint. Moreover, lydite contains schistosity planes and natural cracks, leading altogether to a more fragile impression. These raw material properties likely explain the better performance of the lydite samples in the course of the experiments. The material loss documented on the flint samples can be described as microfracturing, which is likely leading to the promotion of continuous »refresh« during tool use. In contrast, the minimal material loss observed on the flint samples seemed to have caused a blunting of the tool's edge in early stages. To achieve the same penetration depth with a flint sample compared to a lydite sample, additional force would need to be applied.

During the quantitative use-wear analysis, a second aspect related to the raw material of the samples became evident: the raw material properties of lydite promote the formation of use-wear traces more than the properties of flint do. As previously mentioned, the surface roughness of the machine-cut lydite samples is higher than the one from the flint samples. In the course of the sequential experiments, it could be documented, that from a qualitative point of view, the surface begins to change earlier than the surface from the flint samples. The results from the quantitative use-wear analysis performed for the »artificial VS. natural« experiment support this observation. It could be demonstrated that samples with initially higher *Sq* values (surface texture roughness), experienced more abrasion during the use, which is visible on the samples' surface as use-wear. To generalise, some raw materials seem to be, due to their properties, more prone to surface abrasion and thus, develop use-wear more easily. At the same time, *Sq* as a parameter for the surface texture roughness, can be pointed out as an indicator for tool use duration or intensity as it reflects surface abrasion processes. Correlated with the initial surface roughness of the artefact, the measured parameters for the use-wear traces can be put into relation. The observation from the experiments and the quantitative use-wear analysis taken together, emphasise the need of raw material characterisation in functional studies to create a framework for reliable and meaningful interpretations (Lerner 2014). Moreover, the results raise

a question, which requires further investigation; to which degree do the properties of the raw materials influence for instance the active edge design and tool resharpening?
Regarding the tool design, information could be gained through a techno-typological analysis, the quantification of the edge angles and the use-wear analysis. The overall tool design is often seen as standardised, following an underlying concept for tool production and curation (Jöris 1994; Veil et al. 1994; Richter 1997; Jöris 2001; Pastoors 2001; Migal/Urbaowski 2006; Jöris 2012). The results of the techno-typological analysis of the studied artefacts confirm this perspective. The individual tools from each archaeological assemblage share many features regarding the selected blanks, dimensions (e. g. relative standardised back thickness) and edge retouch (in particular regarding the perimeter attributes). This is not only the case for the artefacts *per* site, but applies also to the inter-site comparison.
The perimeter sections are seen as functional units (Jöris 2001; Iovita 2010; Frick et al. 2017; Weiss et al. 2018; Weiss 2020). The base and the back serve as a prehensile area. The distal posterior part is the most variable perimeter section, serving in many specimens as a striking platform for thinning the distal end of the tool, which further allowed edge angle maintenance of the active edge. These aspects could not be disproven based on the techno-typological results. On the contrary, the results of the perimeter section analysis support the idea of *Keilmesser* as being shape variable while changes occur isometrically in relation to the perimeter sections. Additionally, the qualitative use-wear analysis verified that the active edge is the area, concentrating the highest number of traces, and therefore, is interpreted as the used part of the tool. The amount of documented use-wear traces along the back and the base is significantly lower, which could be due to function as a prehensile area. Clear traces indicating a hafting of the tools could not be found, supporting the idea of *Keilmesser* as handheld tools (Jöris 2001; Jöris/Uomini 2019).
Additionally, *Keilmesser* are described as tools with a distinct laterality (Jöris/Uomini 2019; Frick/Herkert 2019). Laterality is seen as a proxy for handedness. This means, *Keilmesser* are either made by and/ or for individuals with a certain hand preference. The lateralisation of the studied artefacts was recorded, leading to an overall majority of right-lateral artefacts in Buhlen, Balve and Ramioul. Although evidence or indications for handedness in the Palaeolithic exist, these are often individual cases, not leading to any percentage figures. Nevertheless, several research studies indicate a bias towards the right-handedness (Ruck/Broadfield/Brown 2015; Uomini/Ruck 2019), as still valid for our modern population worldwide. Hence, the data obtained from the three archaeological assemblages builds on existing evidence concerning the predominance of right-handedness starting in early hominin populations. The laterality of the studied artefacts was addressed within the project, to see if the tool laterality can be confirmed by the use-wear analysis. Unfortunately, the data obtained with the qualitative and quantitative use-wear analysis did not provide significant evidence that could add more information to this topic.
Part of the overall tool design is the design of the active edge. To analyse the design, edge angle values along the entire tool active edge have been calculated. In the distal part of the tool, edge angles are more acute and increase in value towards the proximal part of the tool. The change amounts to a shift of 10° on average. The data for the proximal tool area is often near or above 60°, which is seen as a threshold for cutting tasks (Veil et al. 1994). This observation applies for *Keilmesser* with and without the modification by the application of the *Prądnik method*. However, *Keilmesser* characterised by a scar of the *Prądnik spall* removal at the distal part tend to have slightly more acute edges in this specific tool area. The difference is only small though and ranges between a few and maximum ten degrees. All *Keilmesser* display the same trend of diverging edge angle values in the distal and proximal tool parts. Thus, the data is in line with the morphological interpretation and supports the idea of *Keilmesser* as tools with bipartite edge morphology, whereas the focus lies on the distal tool edge. Thereby, the application of the *Prądnik method* likely fulfilled the purpose of resharpening the edge by creating more acute angles.

The aforementioned observation could also be addressed based on the results of the use-wear analysis performed on the *Prądnik spalls*. The results indicate the use of the tools, before the *Prądnik spalls* were removed. At least, some of the analysed primary *Prądnik spalls* show use-wear traces along the former active edge of the *Keilmesser* or *Prądnik scrapers.* This contradicts the idea, that the spalls were removed before the tool was subjected to use. The numerous secondary *Prądnik spalls* attest repeated (re-) sharpening sequences. Here again, the use-wear analysis could confirm traces along the former active edge of the *Keilmesser* or *Prądnik scrapers* on some pieces.

The idea of primary *Prądnik spalls* as a result of the tool finishing to create a bipartite active edge has led to the common interpretation of *Keilmesser* as multifunctional tools (Jöris 2001; 2006; Frick/Herkert 2019; Jöris/Uomini 2019; Frick 2020). Next to the edge angle calculation, the conducted use-wear analysis could provide further information regarding the type (e. g. polish, striations), the intensity and the location of use-wear. The results indicate a more versatile use compared to the other studied artefact categories, *Prądnik scrapers* and scrapers. Versatile means thereby that some artefacts show identical use-wear traces along the entire tool edge, some display traces either only in the distal or in the proximal part of the tool and others again illustrate diverging use-wear traces in both sections of the active edge. In general, data suggests that *Keilmesser* were either used for more than one single activity or that at least the handling (in the sense of how to hold the tool and how to perform a task) was not static, resulting in different locations and intensities of use-wear along the active edge. However, this does not exclude the possibility of some *Keilmesser* only being used for a single task solely. The conducted *second generation* experiments could confirm the suitability of certain edge angle values (extrapolated from the archaeological assemblages) for the performance of cutting as well as carving movements.

Keilmesser are not always the only asymmetric tools in Late Middle Palaeolithic assemblages. Some, as the three studied assemblages, also yield similar tools, here called *Prądnik scrapers.* One interpretation of *Prądnik scrapers* refers to them as simple, spontaneous and therefore less carefully produced versions of *Keilmesser* (Jöris 2001; 2004; Jöris/Uomini 2019; see also Weiss et al. 2018); another interpretation argues that *Prądnik scrapers* could have been produced by less experienced knappers, who imitate or copy more experienced knappers (Jöris/Uomini 2019). *Prądnik scrapers* do resemble *Keilmesser* in many ways. While the underlying tool concept as explained for *Keilmesser*, can also be in parts retrieved in *Prądnik scrapers*, other aspects differ. Both have the asymmetric shape in common, which is derived from the morphological components. In addition, *Prądnik scrapers* are modified by the application of the *Prądnik method*. Contrary to *Keilmesser*, the vast majority of *Prądnik scrapers* are produced from flakes and only unifacially or semi-bifacially retouched along the active edge. Moreover, (re-)sharpening processes, which go beyond the application of a primary *Prądnick spall* removal, and reworking are rarely documented for *Prądnik scrapers*. In summation, these results support the idea of *Prądnik scraper* as an »*ad hoc*« version of *Keilmesser*. However, the use-wear analysis does not support the idea of *Prądnik scrapers* mimicking, concerning their function. Based on these results, *Prądnik scrapers* do not display a versatile use in the sense of diverging use-wear types such as polish and striations, or the combination of those in different locations. However, the use-wear traces reflect a long-term or intense usage of the *Prądnik scrapers*. Additionally, the calculated edge angle values indicate a considerably more acute active edge with fewer differences in the values along the entire edge. Thus, due to their tool design, the data taken together supports the idea of *Prądnik scrapers* as a simplistic version of *Keilmesser*. At the same time, the results also suggest that *Prądnik scrapers* show less versatility in their handling and function than *Keilmesser*. Based on these findings, an alternative interpretation, which sees *Prądnik scrapers* as morphologically simplistic versions of *Keilmesser* with only a single function, will be proposed.

Additionally, new information about *Prądnik spalls* could be gained through the conducted qualitative use-wear analysis. Next to use-wear traces along the former active edge of the *Keilmesser* or *Prądnik scrapers*,

several use-wear traces could be documented in other locations on the dorsal as well as the ventral surface. The results of this analysis indicate that *Prądnik spalls* likely have been used as a tool after being removed from *Keilmesser* or *Prądnik scraper*. The edge angle calculation for the *Prądnik spalls* resulted in low values around 20° to 25° on average. Perhaps, these acute edge angles made them more suitable for certain tasks than other tools.

To summarise, asymmetric tools from the Late Middle Palaeolithic seem to be designed as standardised tools following a specific concept, which creates the typical morphology and allows for maintaining this morphology throughout the life-history of each individual tool. This observation is strengthened by the fact that these alleged standards are not only visible within the temporal resolution of one archaeological assemblage, but also across sites. Thus, these aspects taken together with the documented tool laterality, which, when seen as proxy for human handedness can be linked with social learning, knowledge transmission and the existence of certain rules and regulations, point towards the emerge of regional traditions. The *Keilmesser* tool concept would thereby be passed on as a skill from generation to generation.

In *Keilmesser*, the active edge design offers the possibility to perform different tasks. Based on the edge angle calculations and the results of the use-wear analysis, it seems as if these traits assign a unique role to *Keilmesser* within the studied artefact categories, but maybe also in *Keilmesser* assemblages in general.

As mentioned earlier, *Keilmesser* are well studied from a techno-typological point of view. However, use-wear on *Keilmesser* has rarely been addressed (Rots 2009); and, as a consequence, experiments focusing on tool use and function have not yet been conducted. This is precisely why a multidisciplinary approach promised the greatest chance of achieving new insights. As demonstrated, the results from the techno-typological approach only, could confirm the existing interpretations about *Keilmesser*. Interestingly, the data also showed that the three studied assemblages – Buhlen, Balve and Ramioul – share many similarities. However, the raw material analysis, the use-wear analysis and the conducted *second generation experiments* could enhance the data relating to this research topic. The calculation of the edge angle values made it possible to first quantify edge geometry and second, to verify assumptions about this design. From this point of view, the experiments fulfilled a similar goal. By conducting the experiments, the interpretations of the *Keilmesser* functionality could be tested. It could be demonstrated that the various tested edge angles (35°, 40°, 45° and 60°) can be used to perform unidirectional cutting as well as carving movements. At the same time, these sequential experiments made it possible to gain information about the mechanics behind tool abrasion and the formation of use-wear. To current knowledge, this project is the first one to illustrate this, applying qualitative and quantitative use-wear analysis to a lithic assemblage of this size. In particular the combination of both use-wear disciplines is new for lithic studies. Together, these two analyses led to new data concerning the use of *Keilmesser*, *Prądnik scrapers* and *Prądnik spalls*, especially to their use intensity.

While the application of the mentioned methods and techniques could provide a more distinct picture about asymmetric tools from the Late Middle Palaeolithic, they also have their limitations. The first limitation relates to the experiments. *Second generation experiments*, such as the conducted ones, focus on basic fundamental mechanics by testing the effect of individual variables. This means at the same time, the obtained results are only valid within the exact same experimental framework. The results cannot directly be transferred to the archaeological record. Certainly, the results can be extrapolated, but still, they need to be tested again within another experimental setup. Thus, a *second generation experiment* in itself is limited. To overcome this limitation, a subsequent *third generation experiment* should be conducted (Marreiros et al. 2020), incorporating the human variability and testing the models detected during the previous generation of experiments. The second limitation could be experienced regarding the quantitative use-wear analysis. Quantitative use-wear analysis is a relatively new approach in archaeology. This means, reference collections or interpretations of the data are rarely existing. Most quantitative use-wear studies have been applied on

experimental samples (Stemp/Stemp 2001; 2003; Lerner et al. 2007; Evans/Donahue 2008; Evans/Macdonald 2011; Stemp/Chung 2011; Giusca et al. 2012; Ibáñez/Lazuen/González-Urquijo 2018; Galland et al. 2019; Stemp/Macdonald/Gleason 2019; Álvarez-Fernández et al. 2020; Pedergnana et al. 2020b), some on archaeological bone samples (d'Errico/Backwell 2009; Martisius et al. 2018; Bradfield 2020; Martisius et al. 2020). Quantitative use-wear studies on lithic artefacts are not published yet and especially a raw material such as silicified schist has not been the focus of such studies yet. Unfortunately, that makes the interpretation of the data insecure and complicated, in particular when trying to infer on the contact material. Although, following international standards (ISO 25178-2) for data analysis offers a secure way, it does not explain the data itself. The relevance of the individual parameters for lithic studies is not conclusively known yet.

Based on these conclusions, the following recommendations for future research can be made. Firstly, the importance of raw material characterisation should again be stressed. The raw material properties play an important role concerning various aspects such as tool production, curation and performance as well as material abrasion, and therefore, the formation of use-wear traces. To obtain reliable results throughout quantitative use-wear analyses, besides the use-wear traces, the original surface should also be measured. The identification of properties such as the surface texture roughness will provide information necessary to understand how the use-wear formed. Since the development of use-wear is the result of surface abrasion (Schmidt et al. 2020), these processes are highly dependent on the raw material of the used sample. Without analysing these properties, the mechanics behind the use-wear formation cannot be incorporated in the overall interpretation. As demonstrated, within the experimental frame, the raw material properties likely play a more important role than the contact material. Further research is needed to determine the effects of the contact material in the process of use-wear formation. However, since the mechanics, which affect the sample during use, are not entirely understood, functional interpretations of diagnostic use-wear traces should be made with caution. Without this important background information, a judgment regarding the performed task or the contact material can only result in speculation. These observations lead to a second aspect. Use-wear studies would benefit from the incorporation of tribology. An interdisciplinary research approach including tribology would help to understand principles such as friction and lubrication and the cause-effect relation of wear formation. To better understand the implications of these observations, future studies could address these tribological principles, in order to build a framework to transfer theoretical and experimental results to the archaeological record.

Lithic artefacts provide key insights into early hominin behaviour. The study of stone tools such as Late Middle Palaeolithic artefacts helps to contextualise technological adaptability, innovations and dynamics in Neanderthal behavioural choices. By analysing the three *Keilmesser* assemblages from Buhlen, Balver Höhle and la Grotte de Ramioul new data concerning tool design, usage and functionality could be gathered. *Keilmesser* represent thereby such a complex and sophisticated artefact category, offering the potential to address numerous fundamental aspects. These aspects cover nearly the entire range of features that are possible to study on lithics. This includes raw material selection, tool production, maintenance and reworking, tool handling, functionality and use. In *Keilmesser*, all these features are combined in one specific tool design. Moreover, this tool design illustrates a technology, which has been kept and transmitted over long periods of time, giving clear indications on Neanderthal behaviour. Together, this makes it likely, that this tool design fulfilled a specific purpose. The data could be achieved through the employment of different methods and scales of analysis. For the first time, *Keilmesser* have been studied by combining techno-typological analyses with controlled experiments as well as qualitative and quantitative use-wear analysis. Consequently, the research presented herein provides a more holistic view on *Keilmesser.* Thus, this study adds a significant piece to the puzzle of our understanding of the evolutionary trajectory of past human behaviour.

REFERENCES

Agam/Zupancich 2020: A. Agam / A. Zupancich, Interpreting the Quina and demi-Quina scrapers from Acheulo-Yabrudian Qesem Cave, Israel: Results of raw materials and functional analyses. Journal of Human Evolution 144, 2020, 102798.

Álvarez-Fernández et al. 2020: A. Álvarez-Fernández / R. García-González / B. Márquez / J. M. Carretero / J. L. Arsuaga, Butchering or wood? A LSCM analysis to distinguish use-wear on stone tools. Journal of Archaeological Science Reports 31, 2020, 102377.

Ambrose 2001: S. H. Ambrose, Paleolithic technology and human evolution. Science 29, 2001, 1748-1783.

Andree 1928: J. Andree, Das Paläolithikum der Höhlen des Hönnetals in Westfalen. Mannus-Bibliothek 42 (Leipzig 1928).

Andrefsky 1994: W. Andrefsky, Raw-Material Availability and the Organization of Technology. American Antiquity 59, 1994, 21-34.

1998: W. Jr. Andrefsky, Lithics. Cambridge Manuals in Archaeology (Cambridge 1998).

2009: W. Jr. Andrefsky, The Analysis of Stone Tool Procurement, Production, and Maintenance. Journal of Archaeological Research 17, 2009, 65-103.

Archer et al. 2018: W. Archer / C. M. Pop / Z. Rezek / S. Schlager / S. C. Lin / M. Weiss / T. Dogandžić / D. Desta / S. P. McPherron, A geometric morphometric relationship predicts stone flake shape and size variability. Archaeological Anthropology Science 10, 2018, 1991-2003.

Astruc/Vargiolu/Zahouani 2003: L. Astruc / R. Vargiolu / H. Zahouani, Wear assessments of prehistoric instruments. Wear 255, 2003, 341-347.

Baales 2013: M. Baales, Die Balver Höhle – eine Ausgrabung zwischen Theater-und Konzertaufführungen. In: M. Baales / H.-O. Pollmann / B. Stapel (eds), Westfalen in der Alt- und Mittelsteinzeit (Münster 2013) 84-85.

Bahnschulte 1940: B. Bahnschulte, Die Balver Höhle – Eine Früheiszeitliche Mammutjägerstation und Werkstätte des Urmenschen. Mitteilungsblatt des NS Lehrerbundes, Gauverwaltung Westfalen-Süd H. 911, 1940.

Bamforth 1988: D. B. Bamforth, Investigating microwear polishes with blind tests: The institute results in context. Journal of Archaeological Science 15, 1988, 11-23.

Bar-Yosef/Kuhn 1999: O. Bar-Yosef / S. L. Kuhn, The Big Deal about Blades: Laminar Technologies and Human Evolution. American Anthropology 101, 1999, 322-338.

Bermúdez de Castro/Bromage/Jalvo 1988: J. Bermúdez de Castro / T. G. Bromage / Y. F. Jalvo, Buccal striations on fossil human anterior teeth: evidence of handedness in the middle and early Upper Pleistocene. Journal of Human Evolution 17, 1988, 403-412.

Beyries/Delamare/Quantin 1988: S. Beyries / F. Delamare / J.-C. Quantin, Tracéologie et rugosimétrie tridimensionnelle. In: S. Beyries (ed.), Industries Lithiques: Tracéologie et Technologie. BAR International Series 411 (Oxford 1988) 115-132.

Binford 1962: L. R. Binford, Archaeology as anthropology. American Antiquity 28, 1962, 217-225.

1986: S. R. Binford / L. R. Binford, Archeology in Cultural Systems (New York [1]1986).

Blateyron 2013: F. Blateyron, The areal field parameters. In: R. Leach (ed.), Characterisation of Areal Surface Texture (Berlin, Heidelberg 2013) 15-43.

Boëda 2001: É. Boëda, Détermination des unités techno-fonctionnelles de pièces bifaciales provenant de la couche acheuléenne C'3 base du site de Barbas I. In: D. Cliquet (ed.), Les industries à outils bifaciaux du Paléolithique moyen d'Europe occidentale. Actes de la Table Ronde internationale, Caen, 14-15 octobre 1999. Études et Recherches Archéologiques de l'Université de Liège 98, 2001, 51-75.

2013: É. Boëda, Technologique & technologie: une paléohistoire des objets lithiques tranchants (Paris 2013).

Borel/Dobosi/Mocel 2017: A. Borel / V. Dobosi / M. H. Moncel, Neanderthal's microlithic tool production and use, the case of Tata (Hungary). Quaternary International 435, 2017, 5-20.

Borel et al. 2014: A. Borel / A. Ollé / J. M. Vergès / R. Sala, Scanning electron and optical light microscopy: Two complementary approaches for the understanding and interpretation of usewear and residues on stone tools. Journal of Archaeological Science 48, 2014, 46-59.

Bosinski 1967: G. Bosinski, Die mittelpaläolithischen Funde im westlichen Mitteleuropa. Fundamenta Monographien zur Urgeschichte Reihe A 4 (Köln 1967).

1969: G. Bosinski, Eine Variante der Micoque-Technik am Fundplatz Buhlen, Kreis Waldeck. Jahresschrift für Mitteldeutsche Vorgeschichte 53, 1969, 59-74.

Bosinski/Kulick 1973: G. Bosinski / J. Kulick, Der mittelpaläolithische Fundplatz Buhlen, Kr. Waldeck. Vorbericht über die Grabungen 1966-1969. Germania 51, 1973, 1-41.

Bradfield 2020: J. Bradfield, The perception of gloss: A comparison of three methods for studying intentionally polished bone tools. Journal of Archaeological Science Reports 32, 2020, 102425.

Bradshaw/Nettleton 1982: J. L. Bradshaw / N. C. Nettleton, Language lateralization to the dominant hemisphere: Tool use, gesture and language in hominid evolution. Current Psychological Reviews 2, 1982, 171-192.

Brantingham 2003: P. J. Brantingham, A Neutral Model of Stone Raw Material Procurement. American Antiquity 68, 2003, 487-509.

Braun et al. 2009: D. R. Braun / T. Plummer / J. V. Ferraro / P. Ditchfield / L. C. Bishop, Raw material quality and Oldowan hominin toolstone preferences: evidence from Kanjera South, Kenya. Journal of Archaeological Science 36(7), 2009, 1605-1614.

Brown et al. 2009: K. S. Brown / C. W. Marean / A. I. R. Herries / Z. Jacobs / C. Tribolo / D. Braun / D. L. Roberts / M. C. Meyer / J. Bernatchez, Fire as an engineering tool of early modern humans. Science, 325, 2009, 859-862.

Buc 2011: N. Buc, Experimental series and use-wear in bone tools. Journal of Archaeological Science 38(3), 2011, 546-557.

Burdukiewicz 2000: J. M. Burdukiewicz, The Backed Biface Assemblages of East Central Europe. In: A. Ronen / M. Weinstein-Evron (eds), Toward Modern Humans: The Yabrudian and Micoquian 400-50 k-years ago. BAR International Series 850 (Oxford 2000) 155-165.

Burroni et al. 2002: D. Burroni / R. E. Donahue / A. M. Pollard / M. Mussi, The surface alteration features of flint artefacts as a record of environmental processes. Journal of Archaeological Science 29(11), 2002, 1277-1287.

Cai/van der Haegen 2015: Q. Cai / L. Van der Haegen, What can atypical language hemispheric specialization tell us about cognitive functions? Neuroscience Bulletin 31, 2015, 220-226.

Calandra/Gneisinger/Marreiros 2020: I. Calandra / W. Gneisinger / J. Marreiros, A versatile mechanized setup for controlled experiments in archeology. Science & Technology of Archaeological Research 6, 2020, 30-40.

Calandra et al. 2019a: I. Calandra / L. Schunk / A. Rodriguez / W. Gneisinger / A. Pedergnana / E. Paixao / T. Pereira / R. Iovita / J. Marreiros, Back to the edge: relative coordinate system for use-wear analysis. Archaeological Anthropology Science 11, 2019, 5937-5948.

2019b: I. Calandra / A. Pedergnana / W. Gneisinger / J. Marreiros, Why should traceology learn from dental microwear, and vice-versa? Journal of Archaeological Science 110, 2019, 105012.

2019c: I. Calandra / L. Schunk / K. Bob / W. Gneisinger / A. Pedergnana / E. Paixao / A. Hildebrandt / J. Marreiros, The effect of numerical aperture on quantitative use-wear studies and its implication on reproducibility. Scientific Reports 9, 2019, 6313.

Carr 1995: C. Carr, Building a Unified Middle-Range Theory of Artifact Design: Historical Perspectives and Tactics. In: C. Carr / J. E. Neitzel (eds), Style, Society, and Person: Archaeological and Ethnological Perspectives. Interdisciplinary Contributions to Archaeology (Boston MA 1995) 151-170.

Cashmore/Uomini/Chapelain 2008: L. Cashmore / N. Uomini / A. Chapelain, The evolution of handedness in humans and great apes: A review and current issues. Journal of Anthropological Sciences 86, 2008, 7-35.

Coles 1979: J. M. Coles, Experimental archaeology (London 1979).

Collins 2008: S. Collins, Experimental investigations into edge performance and its implications for stone artefact reduction modelling. Journal of Archaeological Science 35(8), 2008, 2164-2170.

Condemi et al. 2017: S. Condemi / J. Monge / S. Quertelet / D. W. Frayer / J. Combier, Vergisson 4: a left-handed Neandertal. American Journal of Physical Anthropology 162(1), 2017, 186-190.

Corballis 2003: M. C. Corballis, From mouth to hand: Gesture, speech, and the evolution of right-handedness. Behavioral and Brain Sciences 26(1), 2003, 199-208.

Corballis/Badzakova-Trajkov/Häberling 2012: M. C. Corballis / G. Badzakova-Trajkov / I. S. Häberling, Right hand, left brain: Genetic and evolutionary bases of cerebral asymmetries for language and manual action. Wiley Interdisciplinary Reviews: Cognitive Science 3(1), 2012, 1-17.

Cornford 1986: J. M. Cornford, Specialized resharpening techniques and evidence of handedness. In: P. Callow / J. M. Cornford (eds), La Cotte de St. Brelade 1961-1978. Excavations by C. B. M. McBurney (Norwich 1986).

Corkum et al. 2018: A. G. Corkum / Y. Asiri / H. El Naggar / D. Kinakin, The Leeb Hardness Test for Rock: An Updated Methodology and UCS Correlation. Rock Mechanics and Rock Engineering 51, 2018, 665-675.

Debénath/Dibble 1994: A. Debénath / H. Dibble, Handbook of Paleolithic Typology 1: Lower and Middle Paleolithic of Europe (Philadelphia PA 1994).

Debert/Sherriff 2007: J. Debert / B. L. Sherriff, Raspadita: a new lithic tool from the Isthmus of Rivas, Nicaragua. Journal of Archaeological Science 34(11), 2007, 1889-1901.

Del Bene 1979: T. A. Del Bene, Once Upon a Striation: Current Models of Striation and Polish Formation. In: Hayden 1979, 167-177.

Delgado-Raack/Gómez-Gras/Risch 2009: S. Delgado-Raack / D. Gómez-Gras / R. Risch, The mechanical properties of macrolithic artifacts: a methodological background for functional analysis. Journal of Archaeological Science 36(9), 2009, 1823-1831.

Derndarsky/Ocklind 2001: M. Derndarsky / G. Ocklind, Some preliminary observations on subsurface damage on experimental and Archaeological Quartz tools using CLSM and dye. Journal of Archaeological Science 28(11), 2001, 1149-1158.

d'Errico/Backwell 2009: F. d'Errico / L. Backwell, Assessing the function of early hominin bone tools. Journal of Archaeological Science 36(8), 2009, 1764-1773.

Dibble 1985: H. L. Dibble, Raw-Material Variation in Levallois Flake Manufacture. Current Anthropology 26(3), 1985, 391-393.

1987: H. L. Dibble, The Interpretation of Middle Paleolithic Scraper Morphology. American Antiquity 52(1), 1987, 109-117.

1995: H. L. Dibble, Middle paleolithic scraper reduction: Background, clarification, and review of the evidence to date. Journal of Archaeological Method and Theory 2, 1995, 299-368.

Dibble/Bernard 1980: H. L. Dibble / M. C. Bernard, A Comparative Study of Basic Edge Angle Measurement Techniques. American Antiquity 45, 1980, 857-865.

Dibble et al. 2005: H. L. Dibble / U. A. Schurmans / R. P. Iovita / M. V. McLaughlin, The Measurement and Interpretation of Cortex in Lithic Assemblages. American Antiquity 70(3), 2005, 545-560.

Dibble et al. 2017: H. L. Dibble / S. J. Holdaway / S. C. Lin / D. R. Braun / M. J. Douglass / R. Iovita / S. P. McPherron / D. I. Olszewski / D. Sandgathe, Major Fallacies Surrounding Stone Artifacts and Assemblages. Journal of Archaeological Method and Theory 24, 2017, 813-851.

Dogandžić et al. 2020: T. Dogandžić / A. Abdolazadeh / G. Leader / L. Li / S. P. McPherron / C. Tennie / H. L. Dibble, The results of lithic experiments performed on glass cores are applicable to other raw materials. Archaeological Anthropology Science 12, 2020, 44.

Dumont 1982: J. Dumont, The quantification of microwear traces: A new use for interferometry. World Archaeology 14(2), 1982, 206-217.

Eerkens/Lipo 2007: J. W. Eerkens / C. P. Lipo, Cultural transmission theory and the archaeological record: Providing context to understanding variation and temporal changes in material culture. Journal of Archaeological Research 15, 200, 239-274.

Eren et al. 2016: M. I. Eren / S. J. Lycett / R. J. Patten / B. Buchanan / J. Pargeter / M. J. O'Brien, Test, Model, and Method Validation: The Role of Experimental Stone Artifact Replication in Hypothesis-driven Archaeology. Ethnoarchaeology 8(2), 2016, 103-136.

Evans/Donahue 2005: A. A. Evans / R. E. Donahue, The elemental chemistry of lithic microwear: An experiment. Journal of Archaeological Science 32(12), 2005, 1733-1740.

Evans/Macdonald 2011: A. A. Evans / D. MacDonald, Using metrology in early prehistoric stone tool research: Further work and a brief instrument comparison. Scanning 33, 2011, 294-303.

Evans et al. 2014: A. A. Evans / D. A. Macdonald / C. L. Giusca / R. K. Leach, New method development in prehistoric stone tool research: Evaluating use duration and data analysis protocols. Micron 65, 2014, 69-75.

Faulks et al. 2011: N. R. Faulks / L. R. Kimball / N. Hidjrati / T. S. Coffey, Atomic force microscopy of microwear traces on Mousterian tools from Myshtylagty Lagat (Weasel Cave), Russia. Scanning 33, 2011, 304-315.

Féblot-Augustins 1993: J. Féblot-Augustins, Mobility strategies in the late middle palaeolithic of central europe and western europe: Elements of stability and variability. Journal of Anthropological Archaeology 12(3), 1993, 211-265.

1997: J. Féblot-Augustins, Middle and Upper Paleolithic raw material transfers in western and central Europe: assessing the pace of change. Journal of Middle Atlantic Archaeology 13, 1997, 57-90.

2008: J. Féblot-Augustins, Europe: Paleolithic raw material provenance studies. In: D. M. Pearsall (ed.), Encyclopedia of Archaeology (Amsterdam, San Diego CA 2008) 1187-1198.

Fiore et al. 2015: I. Fiore / L. Bondioli / J. Radovčić / D. W. Frayer, Handedness in the Krapina Neandertals: a re-evaluation. PaleoAnthropology 2015, 19-36.

Floss 1994: H. Floss, Rohmaterialversorgung im Paläolithikum des Mittelrheingebietes. Monographien des RGZM 21 (Bonn 1994).

2012: H. Floss (ed.), Steinartefakte. Vom Altpaläolithikum bis in die Neuzeit. Tübingen Publications in Prehistory (Tübingen 2012).

Frayer et al. 2010: D. W. Frayer / I. Fiore / C. Lalueza-Fox / J. Radovčić / L. Bondioli, Right handed Neandertals: Vindija and beyond. Journal of Archaeological Science 88, 2010, 113-27.

2012: D. W. Frayer / M. Lozano / J. M. Bermúdez de Castro / E. Carbonell / J. L. Arsuaga / J. Radovčić / I. Fiore / L. Bondioli, More than 500,000 years of right-handedness in Europe. Laterality 17(1), 2012, 51-69.

2016: D. W. Frayer / R. J. Clarke / I. Fiore / R. J. Blumenschine / A. Pérez-Pérez / L. M. Martinez / F. Estebaranz / R. Holloway / L. Bondioli, OH-65: The earliest evidence for right-handedness in the fossil record. Journal of Human Evolution 100, 2016, 65-72.

Frick 2016a: J. A. Frick, A Late Middle Palaeolithic assemblage containing Levallois and bifacial objects from Saône-et-Loire, France: GH 3 at Grotte de la Verpillière II à Germolles. Journal of Lithic Studies 3(2), 2016, 273-308.

2016b: J. A. Frick, On technological and spatial patterns of lithic objects. Evidence from the Middle Paleolithic at Grotte de la Verpillière II, Germolles, France [diss. Univ. Tübingen 2016].

2020a: J. A. Frick, Reflections on the term Micoquian in Western and Central Europe. Change in criteria, changed deductions, change in meaning, and its significance for current research. Archaeological Anthropology Science 12, 2020, 12-38.

2020b: J. A. Frick, New study and complementary analyses on the Keilmesser with tranchet blow from the site Abri du Musée at Les Eyzies (Dordogne, France). Nouvelle étude et analyses complémentaires sur le Keilmesser avec coup de tranchet du site de l'abri du Musée aux Eyzies (Dordogne, France). Paléo 30(2), 2020, 138-162.

Frick/Floss 2017: J. A. Frick / H. Floss, Analysis of bifacial elements from Grotte de la Verpillière I and II (Germolles, France). Quaternary International 428, 2017, 3-25.

Frick/Herkert 2019: J. A. Frick / K. Herkert, Flexibility and Conceptual Fidelity in the Production of Keilmesser with Tranchet Blow. Journal of Paleolithic Archaeology 3, 2019, 682-718.

Frick et al 2017: J. A. Frick / K. Herkert / C. T. Hoyer / H. Floss, The performance of tranchet blows at the Late Middle Paleolithic site of Grotte de la Verpillière I (Saône-et-Loire, France). PLoS ONE 12(11), 2017.

Galland et al. 2019: A. Galland / A. Queffelec / S. Caux / J. G. Bordes, Quantifying lithic surface alterations using confocal microscopy and its relevance for exploring the Neanderthal-Châtelperronian association at La Roche-à-Pierrot (Saint-Césaire, France). Journal of Archaeological Science 104, 2019, 45-55.

Giusca et al. 2012: C. Giusca, A. Evans / D. Macdonald / R. Leach, The effect of use duration on surface roughness measurements of stone tools. National Physical Laboratory Report ENG 35 (Teddington 2012).

Golovanova et al. 2017: L. V. Golovanova / E. V. Doronicheva / V. B. Doronichev / I. G. Shirobokov, Bifacial scraper-knives in the Micoquian sites in the North-Western Caucasus: Typology, technology, and reduction. Quaternary International 428, 2017, 49-65.

Goodale/Andrefsky 2015: N. Goodale / W. Andrefsky, Lithic Technological Systems and Evolutionary Theory, Lithic Technological Systems and Evolutionary Theory (Cambridge 2015).

Grace 1989: R. Grace, Interpreting the function of stone tools: the quantification and computerisation of microwear analysis. BAR International Series 474 (Oxford 1989).

1996: R. Grace, Review Article Use-Wear Analysis: The State of the Art. Archaeometry 38(2), 1996, 209-229.

Grace/Graham/Newcomer 1985: R. Grace / I. D. G. Graham / M. H. Newcomer, The quantification of microwear polishes. World Archaeology 17, 1985, 112-120.

Günther 1964: K. Günther, Die altsteinzeitlichen Funde der Balver Höhle. Bodenaltertümer Westfalens 8 (Münster 1964).

1988: K. Günther, Alt- und mittelsteinzeitliche Fundplätze in Westfalen. Teil 2: Altsteinzeitliche Fundplätze in Westfalen. Einführung in die Vor- und Frühgeschichte Westfalens 6 (Münster 1988).

Hahn 1993: J. Hahn, Erkennen und Bestimmen von Stein- und Knochenartefakten. Einführung in die Artefaktmorphologie. Archaeologica Venatoria 10 (Tübingen 1993).

Hainsworth/Delaney/Rutty 2007: S. V. Hainsworth / R. J. Delaney / G. N. Rutty, How sharp is sharp? Towards quantification of the sharpness and penetration ability of kitchen knives used in stabbings. International Journal of Legal Medicine 122(4), 2007, 281-291.

Hardy/Garufi 1998: B. L. Hardy / G. T. Garufi, Identification of woodworking on stone tools through residue and use-wear analyses: Experimental results. Journal of Archaeological Science 25(2), 1998, 177-184.

Haslam 2009: M. Haslam, Archeological science under a microscope. Terra Australis 30, 2009, 47-79.

Hay 1977: C. Hay, Use-scratch morphology: a functionally significant aspect of edge damage on obsidian tools. Journal of Field Archaeology 4, 1977, 491-494.

Hayden 1979: B. Hayden (ed.), Lithic Use-Wear Analysis. Studies in Archaeology (New York, San Francisco, London 1979).

Hovers/Belfer-Cohen 2006: E. Hovers / A. Belfer-Cohen, »Now You See it, Now You Don't« – Modern Human Behavior in the Middle Paleolithic. In: E. Hovers / S. L. Kuhn (eds), Transitions Before the Transition: Evolution and Stability in the Middle Paleolithic and Middle Stone Age. Interdisciplinary Contributions to Archaeology (Boston MA 2006) 295-304.

Hurcombe 1988: L. Hurcombe, Some criticisms and suggestions in response to Newcomer et al. Journal of Archaeological Science 15(1), 1988, 1-10.

Ibáñez/Lazuen/González-Urquijo 2018: J. J. Ibáñez / T. Lazuen / J. González-Urquijo, Identifying experimental tool use through confocal microscopy. Journal of Archeological Method and Theory 26, 2018, 1176-1215.

Iovita 2004: R. Iovita, The role of edge angle maintenance in explaining technological variation in the production of Late Middle Paleolithic bifacial and unifacial tools. Quaternary International 350, 2004, 105-115.

2009: R. Iovita, Ontogenetic scaling and lithic systematics: method and application. Journal of Archaeological Method and Theory 36, 2009, 1447-1457.

2010: R. Iovita, Comparing stone tool resharpening trajectories with the aid of elliptical fourier analysis. In: S. J. Lycett / P. R. Chauhan (eds), New Perspectives on Old Stones: Analytical Approaches to Paleolithic Technologies (New York et al. 2010) 235-253.

Iovita/McPherron 2011: R. Iovita / S. P. McPherron, The handaxe reloaded: A morphometric reassessment of Acheulian and Middle Paleolithic handaxes. Journal of Human Evolution 61, 2011, 61-74.

ISO 25178: International Organization for Standardization. ISO 25178-2 – Geometrical product specifications (GPS) – Surface texture: Areal – Part 2: Terms, definitions and surface texture parameters (Geneva 2012).

ISO 8442: International Organization for Standardisation. ISO 8442-5:2004 – Materials and articles in contact with foodstuffs – Cutlery and table hollowware – Part 5: Specification for sharpness and edge retention test of cutlery (Geneva 2004).

Jöris 1992: O. Jöris, Pradniktechnik im Micoquien der Balver Höhle. Archäologisches Korrespondenzblatt 22, 1992, 1-22.

1994: O. Jöris, 1994. Neue Untersuchungen zum Mittelpaläolithikum von Buhlen, Hessen. Technologische Studien zur Pradniktechnik in Horizont IIIb des Oberen Fundplatzes. Ethnographisch-Archäologische Zeitschrift 35, 1994, 88-97.

2001: O. Jöris, Der spätmittelpaläolithische Fundplatz Buhlen (Grabungen 1966-69): Stratigraphie, Steinartefakte und Fauna des oberen Fundplatzes. Universitätsforschungen zur Prähistorischen Archäologie 73 (Bonn 2001).

2004: O. Jöris, Zur chronostratigraphischen Stellung der spätmittelpaläolithischen Keilmessergruppen. Der Versuch einer kulturgeographischen Abgrenzung einer mittelpaläolithischen Formengruppe in ihrem europäischen Kontext. Bericht der Römisch-Germanischen Kommission 84, 2004, 49-154.

2006: O. Jöris, Bifacially backed knives (Keilmesser) in the Central European Middle Palaeolithic. In: N. Goren-Inbar / G. Sharon (eds), Axe age: acheulian tool-making from Quarry to discard (London, Oakville CT 2006) 287-310.

2012: O. Jöris, Keilmesser. In: Floss 2012, 297-308.

Jöris/Uomini 2019: O. Jöris / N. T. Uomini, Evidence for Neanderthal hand-preferences from the late Middle Palaeolithic site of Buhlen, Germany – insights into Neanderthal learning behaviour. In: O. Jöris / Y. Nishiaki (eds), Learning Among Neanderthals and Palaeolithic Modern Humans. Archaeological Evidence. Replacement of Neanderthals by Modern Humans Series (Singapore 2019).

Kamminga 1979: J. Kamminga, The Nature of Use-Polish and Abrasive Smoothing on Stone tools. In: Hayden 1979, 143-158.

Keely 1974: L. H. Keeley, Technique and methodology in microwear studies: A critical review. World Archaeology 5(3), 1974, 323-336.

1980: L. H. Keeley, Experimental Determination of Stone Tool Uses: A Microwear Analysis. Prehistoric Archeology and Ecology Series (Chicago 1980).

Keeley/Newcomer 1977: L. H. Keeley / M. H. Newcomer, Microwear analysis of experimental flint tools: a test case. Journal of Archaeological Science 4(1), 1977, 29-62.

Key 2016: A. J. M. Key, Integrating Mechanical and Ergonomic Research within Functional and Morphological Analyses of Lithic Cutting Technology: Key Principles and Future Experimental Directions. Ethnoarchaeology 8(1), 2016, 69-89.

Key/Lycett 2014: A. J. M. Key / S. J. Lycett, Are bigger flakes always better? An experimental assessment of flake size variation on cutting efficiency and loading. Journal of Archaeological Science 41, 2014, 140-146.

2015: A. J. M. Key / S. J. Lycett, Edge angle as a variably influential factor in flake cutting efficiency: An experimental investigation of its relationship with tool size and loading. Archaeometry 57(7), 2015, 911-927.

2017: A. J. M. Key / S. J. Lycett, Form and function in the lower palaeolithic: History, progress, and continued relevance. Journal of Archaeological Science 95, 2017, 67-108.

2018: A. J. M. Key / S. J. Lycett, Biometric variables predict stone tool functional performance more effectively than tool-form attributes: a case study in handaxe loading capabilities. Archaeometry 61(3), 2018, 539-555.

2020: A. Key / S. J. Lycett, Torque creation and force variation along the cutting edges of Acheulean handaxes: implications for tip thinning, resharpening and tranchet flake removals. Journal of Archaeological Science 120, 2020, 105189.

Key/Fisch/Eren 2018: A. Key / M. R. Fisch / M. I. Eren, Early stage blunting causes rapid reductions in stone tool performance. Journal of Archaeological Science 91, 2018, 1-11.

Key/Pargeter/Schmidt 2020: A. Key / J. Pargeter / P. Schmidt, Heat treatment significantly increases the sharpness of silcrete stone tools. Archaeometry 63(3), 2020, 447-466.

Key/Proffitt/de la Torre 2020: A. Key / T. Proffitt / I. de la Torre, Raw material optimization and stone tool engineering in the Early Stone Age of Olduvai Gorge (Tanzania). Journal of The Royal Society Interface 17, 2020, 20190377.

Kimball/Kimball/Allen 1995: L. R. Kimball / J. F. Kimball / P. E. Allen, Microwear polishes as viewed through the atomic force microscope. Lithic Technology 20(1), 1995, 6-28.

Kimball et al. 2017: L. R. Kimball / T. S. Coffey / N. R. Faulks / S. E. Dellinger / N. M. Karas / N. Hidjrati, A Multi-instrument Study of Microwear Polishes on Mousterian Tools from Weasel Cave (Myshtulagty Lagat), Russia. Lithic Technology 42(2-3), 2017, 61-76.

Kindler 2012: L. Kindler, Die Rolle von Raubtieren in der Einnischung und Subsistenz jungpleistozäner Neandertaler. Archäozoologie und Taphonomie der mittelpaläolithischen Faune aus der Balver Höhle (Westfalen). Monographien des RGZM 99 (Mainz 2012).

Klein 2000: R. G. Klein, Archeology and the evolution of human behavior. Evolutionary Anthropology 9(1), 2000, 17-36.

Kovler/Wang/Muravin 2018: K. Kovler / F. Wang / B. Muravin, Testing of concrete by rebound method: Leeb versus Schmidt hammers. Materials and Structures / Materiaux et Constructions 51, 2018, 138.

Kozłowski 2014: J. K. Kozłowski, Middle palaeolithic variability in Central Europe: Mousterian vs Micoquian. Quaternary International 326-327, 2014, 344-363.

Krukowski 1939: S. Krukowski, Paleolit. In: S. Krukowski / R. J. Kostrezewski (eds), Prehistoria ziem polskich. Encyklopedia Polska 4 (Krakow 1939) 1-117.

Kuhn 1990: S. L. Kuhn, A geometric index of reduction for unifacial stone tools. Journal of Archaeological Science 17(5), 1990, 583-593.

1992: S. L. Kuhn, On Planning and Curated Technologies in the Middle Paleolithic. Journal of Archaeological Research 48(3), 1992, 185-214.

1994: S. Kuhn, A Formal Approach to the Design and Assembly of Mobile Toolkits. American Antiquity 59(3), 1994, 426-442.

Langlois 2001: S. Langlois, Traditions: Social. In: N. J. Smelser / P. B. Baltes (eds), International Encyclopedia of the Social & Behavioral Sciences (Pergamon 2001) 15829-15833.

Lepot 1993: M. Lepot, Approche techno-fonctionnelle de l'outillage lithique Moustérien: essai de classification des parties actives en termes d'efficacité technique. Application a la couche M2e sagittale de Grand Abri de la Ferrassie [mémoire de maitrise, Nanterre, Univ. Paris X 1993].

Lerner 2014: H. J. Lerner, Intra-raw material variability and use-wear accrual: A continuing exploration. Journal of Lithic Studies 1, 2014, 165-186.

Lerner et al. 2007: H. Lerner / X. Du / A. Costopoulos / M. Ostoja-Starzewski, Lithic raw material physical properties and use-wear accrual. Journal of Archaeological Science 34(5), 2007, 711-722.

Lin/Marreiros 2020: S. C. Lin / J. Marreiros, Quina Retouch Does Not Maintain Edge Angle Over Reduction. Lithic Technology 46(1), 2020, 45-59.

Lin/Režek/Dibble 2018: S. C. Lin / Z. Režek / H. L. Dibble, Experimental Design and Experimental Inference in Stone Artifact Archaeology. Journal of Archaeological Method and Theory 25, 2018, 663-688.

Lombard 2005: M. Lombard, Evidence of hunting and hafting during the Middle Stone Age at Sibidu Cave, KwaZulu-Natal, South Africa: A multianalytical approach. Journal of Human Evolution 48(3), 2005, 279-300.

2008: M. Lombard, Finding resolution for the Howiesons Poort through the microscope: micro-residue analysis of segments from Sibudu Cave, South Africa. Journal of Archaeological Science 35(1), 2008, 26-41.

Longacre 2010: W. A. Longacre, Archaeology as Anthropology Revisited. Journal of Archaeological Method and Theory 17, 2010, 81-100.

Lozano et al. 2017: M. Lozano / A. Estalrrich / L. Bondioli / I. Fiore / J. M. Bermúdez de Castro / J. L. Arsuaga, E. Carbonell / A. Rosas / D. W. Frayer, Right-handed fossil humans. Evolutionary Anthropology 26(6), 2017, 313-324.

Lycett 2015: S. J. Lycett, Cultural evolutionary approaches to artifact variation over time and space: Basis, progress, and prospects. Journal of Archaeological Science 56, 2015, 21-31.

Lycett/Chauhan 2010: S. J. Lycett / P. R. Chauhan, New Perspectives on Old Stones: Analytical Approaches to Paleolithic Technologies (New York 2010).

Lycett/Von Cramon-Taubadel / Eren 2016: S. J. Lycett / N. Von Cramon-Taubadel / M. I. Eren, Levallois: Potential Implications for Learning and Cultural Transmission Capacities. Lithic Technology 41, 2016, 19-38.

Macdonald/Harman/Evans 2018: D. A. Macdonald / R. Harman / A. A. Evans, Replicating surface texture: Preliminary testing of molding compound accuracy for surface measurements. Journal of Archaeological Science Reports 18, 2018, 839-846.

Mania 1990: D. Mania, Auf den Spuren des Urmenschen. Die Funde aus der Steinrinne von Bilzingsleben (Berlin 1990).

Mania/Toepfer 1973: D. Mania / V. Toepfer, Königsaue. Gliederung, Ökologie und mittelpaläolithische Funde der letzten Eiszeit (Berlin 1973).

Mansur-Franchomme 1983: M. E. Mansur-Franchomme, Scanning electron microscopy of dry hide working tools: The role of abrasives and humidity in microwear polish formation. Journal of Archaeological Science 10, 1983, 223-230.

Marreiros/Pereira/Iovita 2020: J. Marreiros / T. Pereira / R. Iovita, Controlled experiments in lithic technology and function. Archaeological Anthropology Science 12, 2020, 10.

Marreiros et al. 2015: J. Marreiros / N. Mazzucco / J. F. Gibaja / N. Bicho, Use-Wear and Residue Analysis in Archaeology. Manuals in Archaeological Method, Theory and Technique (Cham 2015).

2020: J. Marreiros / I. Calandra / W. Gneisinger / E. Paixão / A. Pedergnana / L. Schunk, Rethinking Use-Wear Analysis and Experimentation as Applied to the Study of Past Hominin Tool Use. Journal of Paleolithic Archaeology 3, 2020, 475-502.

Martisius et al. 2018: N. L. Martisius / I. Sidéra / M. N. Grote / T. E. Steele / S. P. Mcpherron / E. Schulz-Kornas, Time wears on: Assessing how bone wears using 3D surface texture analysis. PLoS ONE 13(11), 2018, e0206078.

2020: N. L. Martisius / S. P. McPherron / E. Schulz-Kornas / M. Soressi / T. E. Steele, A method for the taphonomic assessment of bone tools using 3D surface texture analysis of bone microtopography. Archaeological Anthropology Science 12, 2020, 251.

Mazzucco 2018: N. Mazzucco, The Human Occupation of the Southern Central Pyrenees in the Sixth-Third Millennia cal BC: a traceological approach to flaked stone assemblages. BAR International Series 2905 (Oxford 2018).

McCarthy/Annaidh/Gilchrist 2010: C. T. McCarthy / A. N. Annaidh / M. D. Gilchrist, On the sharpness of straight edge blades in cutting soft solids: Part II – Analysis of blade geometry. Engineering Fracture Mechanics 77(3), 2010, 437-451.

McGorry/Dowd/Dempsey 2003: R. W. McGorry / P. C.Dowd / P. G. Dempsey, Cutting moments and grip forces in meat cutting operations and the effect of knife sharpness. Applied Ergonomics 34(4), 2003, 375-382.

McPherron et al. 2010: S. P. McPherron / Z. Alemseged / C. W. Marean / J. G. Wynn / D. Reed / D. Geraads / R. Bobe / H. A. Béarat, Evidence for stone-tool-assisted consumption of animal tissues before 3.39 million years ago at Dikika, Ethiopia. Nature 466, 2010, 857-860.

Meignen/Delagnes/Bourguignon 2009: L. Meignen / A. Delagnes / L. Bourguignon, Patterns of Lithic Material Procurement and Transformation During the Middle Paleolithic in Western Europe. In: B. Adams / B. S. Blades (eds), Lithic Materials and Paleolithic Societies (Hoboken NJ 2009) 15-24.

Migal/Urbanowski 2006: W. Migal / M. Urbanowski, Pradnik knives reuse. Experimental approach. In: A. Wisniewski / J. M. Burdukiewicz / T. Plonka (eds), The Stone Technique and Technology (Wroclaw 2006) 73-89.

Monnier/Ladwig/Porter 2012: G. F. Monnier / J. L. Ladwig / S. T. Porter, Swept under the rug: The problem of unacknowledged ambiguity in lithic residue identification. Journal of Archaeological Science 39(10), 2012, 3284-3300.

Morales/Lorenzo/Vergès 2015: J. I. Morales / C. Lorenzo / J. M. Vergès, Measuring Retouch Intensity in Lithic Tools: A New Proposal Using 3D Scan Data. Journal of Archaeological Method and Theory 22, 2015, 543-558.

Morgan et al. 2015: T. J. H. Morgan / N. T. Uomini / L. E. Rendell / L. Chouinard-Thuly / S. E. Street / H. M. Lewis / C. P. Cross / C. Evans / R. Kearney / I. De La Torre / A. Whiten / K. N. Laland, Experimental evidence for the co-evolution of hominin tool-making teaching and language. Nature Communications 6, 2015, 6029.

Moss 1987: E. H. Moss, A review of »Investigating microwear polishes with blind tests.« Journal of Archaeological Science 14, 1987, 473-481.

Neruda 2017: P. Neruda, GIS analysis of the spatial distribution of Middle Palaeolithic artefacts in Kůlna Cave (Czech Republic). Quaternary International 435, 2017, 58-76.

Newcomer/Grace/Unger-Hamilton 1986: M. H. Newcomer / R. Grace / R. Unger-Hamilton, Investigating microwear polishes with blind tests. Journal of Archaeological Science 13(3), 1988, 203-217.

1988: M. H. Newcomer / R. Grace / R. Unger-Hamilton, Microwear methodology: A reply to Moss, Hurcombe and Bamforth. Journal of Archaeological Science 15(1), 1986, 25-33.

Nonaka/Bril/Rein 2010: T. Nonaka / B. Bril / R. Rein, How do stone knappers predict and control the outcome of flaking? Implications for understanding early stone tool technology. Journal of Human Evolution 59(2), 2010, 155-167.

Odell 1975: G. H. Odell, Micro-wear in perspective: A sympathetic response to Lawrence H. Keeley. World Archaeology 7, 1975, 226-240.

1981: G. H. Odell, The mechanics of use-breakage of stone tools: Some testable hypotheses. Journal of Field Archaeology 8, 1981, 197-209.

2000: G. H. Odell, Stone tool research at the end of the millennium: Procurement and technology. Journal of Archaeological Research 8, 2000, 269-331.

2001: G. Odell, Stone Tool Research at the End of the Millennium: Classification, Function, and Behavior. Journal of Archaeological Research 9, 2001, 45-100.

Odell/Odell-Vereecken 1980: G. H. Odell / F. Odell-Vereecken, Verifying the Reliability of Lithic Use-Wear Assessments by »Blind Tests«: The Low-Power Approach. Journal of Field Archaeology 7(1), 1980, 87-120.

Ollé/Vergès 2014: A. Ollé / J. M. Vergès, The use of sequential experiments and SEM in documenting stone tool microwear. Journal of Archaeological Science 48, 2014, 60-72.

Ollé et al. 2016: A. Ollé / A. Pedergnana / J. L. Fernández-Marchena / S. Martin / A. Borel / V. Aranda, Microwear features on vein quartz, rock crystal and quartzite: A study combining Optical Light and Scanning Electron Microscopy. Quaternary International 424(7), 2016, 154-170.

Outram 2008: A. K. Outram, Introduction to experimental archaeology. World Archaeology 40, 2008, 1-6.

Pastoors 2001: A. Pastoors, Bifazielle Werkzeuge als Informationsträger. In: L. Bourguignon / I. Ortega/ M.-C. Frère-Sautot (eds), Préhistoire et Approche Experimentale. Préhistoires 5 (Montagnac 2001) 375-442.

Pastoors/Schäfer 1999: A. Pastoors / J. Schäfer, Analyse des états techniques de transformation, d'utilisation et états post dépositionelles illustrée par un outil bifacial de Salzgitter-Lebenstedt (FRG). Préhistoire Européenne 14, 1999, 33-47.

Pastoors/Tafelmaier 2010: A. Pastoors / Y. Tafelmaier, Bladelet production, core reduction strategies, and efficiency of core configuration at the Middle Palaeolithic site Balver Höhle (North Rhine Westphalia, Germany). Quartär 57, 2010, 25-41.

Pedergnana 2020: A. Pedergnana, »All that glitters is not gold«: Evaluating the Nature of the Relationship Between Archeological Residues and Stone Tool Function. Journal of Paleolithic Archaeology 3, 2020, 225-254.

Pedergnana/Ollé 2017: A. Pedergnana / A. Ollé, Monitoring and interpreting the use-wear formation processes on quartzite flakes through sequential experiments. Quaternary International 427, 2017, 35-65.

Pedergnana/Ollé/Evans 2020: A. Pedergnana / A. Ollé / A. A. Evans, A new combined approach using confocal and scanning electron microscopy to image surface modifications on quartzite. Journal of Archaeological Science: Reports 30, 2020, 102237.

Pedergnana et al. 2016: A. Pedergnana / L. Asryan / J. L. Fernández-Marchena / A. Ollé, Modern contaminants affecting microscopic

residue analysis on stone tools: A word of caution. Micron 86, 2016, 1-21.

2020a: A. Pedergnana / I. Calandra / K. Bob / W. Gneisinger / E. Paixão / L. Schunk / A. Hildebrandt / J. Marreiros, Evaluating the microscopic effect of brushing stone tools as a cleaning procedure. Quaternary International 569-570, 2020, 263-276.

2020b: A. Pedergnana / I. Calandra / A. A. Evans / K. Bob / A. Hildebrandt / A. Ollé, Polish is quantitatively different on quartzite flakes used on different worked materials. PLoS One 15(12), 2020, e0243295.

Pfleging et al. 2015: J. Pfleging / M. Stücheli / R. Iovita / J. Buchli, Dynamic monitoring reveals motor task characteristics in prehistoric technical gestures. PLoS One 10(8), 2015, e0134570.

Picin 2016: A. Picin, Short-term occupations at the lakeshore: a technological reassessment of the open-air site Königsaue (Germany). Quartär 63, 2016, 7-23.

Plisson 1985: H. Plisson, Etude founctionelle d'outillages lithiques prehistoriques par l'analyse des micro-usures: recherché metodologique et archeologique [diss. Univ. Paris 1985].

Plisson et al. 1998: H. Plisson / S. Beyries / J. Shea / A. Marks / J. M. Geneste, Pointes ou outils triangulaires? Données fonctionnelles dans le Moustérien levantin [with Commentry]. Paléorient 24, 1998, 5-24,

Pop 2013: C. M. Pop, The effects of raw material properties on edge attrition: a high-resolution study of unretouched experimental flakes. In: O. N. Crandell / V. Cotiugă (eds), »Stories Written in Stone«. International Symposium on Chert and Other Knappable Materials (Iași 2013) 56.

Porter/Roussel/Soressi 2019: S. T. Porter / M. Roussel / M. Soressi, A Comparison of Châtelperronian and Protoaurignacian Core Technology Using Data Derived from 3D Models. Journal of Computer Applications in Archaeology 2(1), 2019, 41-55.

Poza-Rey/Lozano/Arsuaga 2017: E. M. Poza-Rey / M. Lozano / J. L. Arsuaga, Brain asymmetries and handedness in the specimens from the Sima de los Huesos site (Atapuerca, Spain). Quaternary International 433, 2017, 32-44.

Prévost/Centi/Zaidner 2020: M. Prévost / L. Centi / Y. Zaidner, The use of the lateral tranchet blow technique at Nesher Ramla (Israel): A new cultural marker in the Levantine Middle Paleolithic? Quaternary International 2000 [in press].

Quinif et al. 2011: Y. Quinif / L. Barchy / T. Camelbeeck / S. Delaby / J.-P. Tshibangu / S. Vandycke / M. Van Ruymbeke, Considérations karstogénétiques sur le système de Ramioul. Bulletin de la Société Royale Belge d'Etudes Géologiques et Archéologiques 3, 2011, 79-96.

Režek et al 2018: Ž. Režek / H. L. Dibble / S. P. McPherron / D. R. Braun / S. C. Lin, Two million years of flaking stone and the evolutionary efficiency of stone tool technology. Nature ecology & evolution 2(4), 2018, 628-633.

Richter 1997: J. Richter, Der G-Schichten-Komplx der Sesselfelsgrotte. Zum Verständnis des Micoquien. Sesselfelsgrotte III. Quartär-Bibliothek 7 (Saarbrücken 1997).

2016: J. Richter, Leave at the height of the party: A critical review of the Middle Paleolithic in Western Central Europe from its beginnings to its rapid decline. Quaternary International 411, 2016, 107-128.

Rodriguez et al. 2020: A. Rodriguez / E. Pouydebat / M. G. Chacón / M. H. Moncel / R. Cornette / A. Bardo / L. Chèze / R. Iovita / A. Borel, Right or left? Determining the hand holding the tool from use traces Journal of Archaeological Science: Reports 31, 2020, 102316.

Rodríguez-Rellán 2016: C. Rodríguez-Rellán, Variability of the rebound hardness as a proxy for detecting the levels of continuity and isotropy in archaeological quartz. Quaternary International 424, 2016, 191-211.

Rolland/Dibble 1990: N. Rolland / H. L. Dibble, A New Synthesis of Middle Paleolithic Variability. American Antiquity 55(3), 1990, 480-499.

Rots 2009: V. Rots, The functional analysis of the Mousterian and Micoquian assemblages of Sesselfelsgrotte, Germany: aspects of tool use and hafting in the European Late Middle Palaeolithic. Quartär 56, 2009, 37-66.

2013: V. Rots, Prehension and Hafting Traces on Flint Tools. A Methodology (Leuven 2013).

Ruck/Broadfield/Brown 2015: L. Ruck / D. C. Broadfield / C. T. Brown, Determining hominid handedness in Lithic Debitage: A review of current methodologies. Lithic Technology 40, 2015, 171-188.

Ruebens 2013: K. Ruebens, Regional behaviour among late neanderthal groups in Western Europe: A comparative assessment of late middle palaeolithic bifacial tool variability. Journal of Human Evolution 65, 2013, 341-362.

2014: K. Ruebens, Late Middle Palaeolithic bifacial technologies across northwest Europe: Typo-technological variability and trends. Quaternary International 350, 2014, 130-146.

Sahle et al. 2013: Y. Sahle / W. K. Hutchings / D. R. Braun / J. C. Sealy / L. E. Morgan / A. Negash / B. Atnafu, Earliest stone-tipped projectiles from the Ethiopian rift date to >279,000 years ago. PLoS One 8, 2013, e0126064.

Schiffer 1979: M. Schiffer, The place of lithic use-wear studies in behavioural archeology. In: Hayden 1979, 15-25.

Schmidt/Mackay 2016: P. Schmidt / A. Mackay, Why was silcrete heat-treated in the Middle Stone Age? An early transformative technology in the context of raw material use at Mertenhof rock shelter, South Africa. PLoS One 11, 2016, e0149243.

Schmidt et al. 2020: P. Schmidt / A. Rodriguez / K. Yanamandra / R. K. Behera / R. Iovita, The mineralogy and structure of use-wear polish on chert. Scientific Reports 10, 2020, 21512.

Schuldt et al. 2013: S. Schuldt / G. Arnold / J. Roschy / Y. Schneider / H. Rohm, Defined abrasion procedures for cutting blades and comparative mechanical and geometrical wear characterization. Wear 300, 2013, 38-43.

2016: S. Schuldt / G. Arnold / J. Kowalewski / Y. Schneider / H. Rohm, Analysis of the sharpness of blades for food cutting. Journal of Food Engineering 188, 2016, 13-20.

Schunk et al. 2019: L. Schunk / I. Calandra / W. Gneisinger / O. Jöris / J. Marreiros, Is a knife a knife? Testing bifacial backed knives in controlled experiments. PESHE 8, 2019, 173.

Scott et al. 2005: R. S. Scott / P. S. Ungar / T. S. Bergstrom / C. A. Brown / F. E. Grine / M. F. Teaford / A. Walker, Dental microwear texture analysis shows within-species diet variability in fossil hominins. Nature 436, 2005, 693-695.

2006: R. S. Scott / P. S. Ungar / T. S. Bergstrom / C. A. Brown / B. E. Childs / M. F. Teaford / A. Walker, Dental microwear texture analysis: technical considerations. Journal of Human Evolution 51, 2006, 339-349.

Semenov 1957: S. Semenov, Pervobytnaja technika. Materialy i Issledovania po Archeologii SSSR 54 (Moscow, Leningrad 1957).

1964: S. Semenov, Prehistoric technology: an experimental study of the oldest tools and artefacts from traces of manufacture and wear (London 1964).

1970: S. A. Semenov, Forms and functions of the oldest stone tools. Quartär, 21, 1970, 1-20.

Serwatka 2014: K. Serwatka, Shape variation of middle palaeolithic bifacial tools from southern Poland: A geometric morphometric approach to Keilmessergruppen handaxes and backed knives. Lithic 35, 2014, 18-32.

2015: K. Serwatka, Bifaces in plain sight: testing elliptical Fourier analysis in identifying reduction effects on Late Middle Palaeolithic bifacial tools. Litikum 3, 2015, 13-25.

Shanks et al. 2001: O. C. Shanks / R. Bonnichsen / A. T. Vella / W. Ream, Recovery of protein and DNA trapped in stone tool microcracks. Journal of Archaeological Science 28(9), 2001, 965-972.

Shea 2011: J. J. Shea, Stone tool analysis and human origins research: Some advice from uncle Screwtape. Evolutionary Anthropology 20(2), 2011, 48-53.

Shennan 2008: S. Shennan, Evolution in archaeology. Annual Review of Anthropology 37, 2008, 75-91.

Shils 1971: E. Shils, Tradition. Comparative Studies in Society and History 13(2), 1971, 122-159.

Shott/Trail 2010: M. J. Shott / B. W. Trail, Exploring New Approaches to Lithic Analysis: Laser Scanning and Geometric Morphometrics. Lithic Technology 35, 2010, 195-220.

Solecki/Solecki 2001: R. L. Solecki / R. S. Solecki, Bifaces and the Acheulian industries of Yabroud Shelter I, Syria. In: M. Toussaint / C. Draily / J.-M. Cordy (eds), General Sessions and Posters. Section 4: Human Origins and the Lower Palaeolithic. Acts of the XIVth UISPP Congress. BAR International Series 1272 (Oxford 2001) 37-39.

Steele/Uomini 2008a: J. Steele / N. Uomini, Can the archaeology of manual specialization tell us anything about language evolution? A survey of the state of play. Cambridge Archaeological Journal 19(1), 2008, 97-110.

Stemp/Chung 2011: W. J. Stemp / S. Chung, Discrimination of surface wear on obsidian tools using LSCM and RelA: Pilot study results (area-scale analysis of obsidian tool surfaces). Scanning 33(5), 2011, 279-293.

Stemp/Stemp 2001: W. J. Stemp / M. Stemp, UBM laser profilometry and Lithic use-wear analysis: A variable length scale investigation of surface topography. Journal of Archaeological Science 28(1), 2001, 81-88.

2003: W. J. Stemp / M. Stemp, Documenting stages of Polish development on experimental stone tools: Surface characterization by fractal geometry using UBM laser profilometry. Journal of Archaeological Science 30(3), 2003, 287-296.

Stemp/Lerner/Kristant 2013: W. J. Stemp / H. J. Lerner / E. H. Kristant, Quantifying microwear on experimental mistassini quartzite scrapers: Preliminary results of exploratory research using LSCM and scale-sensitive fractal analysis. Scanning 35(1), 2013, 28-39.

Stemp/Macdonald/Gleason 2019: W. J. Stemp / D. A. Macdonald / M. A. Gleason, Testing imaging confocal microscopy, laser scanning confocal microscopy, and focus variation microscopy for microscale measurement of edge cross-sections and calculation of edge curvature on stone tools: Preliminary results. Journal of Archaeological Science Reports 24, 2019, 513-525.

Thomas et al. 2001: T. R. Thomas / B. G. Rosén / H. Zahouani / L. Blunt / M. El Mansori, Traceology, quantifying finishing machining and function: A tool and wear mark characterisation study. Wear 271, 2001, 553-558.

Tringham et al. 1974: R. Tringham / G. Cooper / G. Odell / B. Voytek, A. Whitman, Experimentation in the formation of edge damage: A new approach to lithic analysis. Journal of Field Archaeology 1, 1974, 171-196.

Trinkaus/Churchill/Ruff 1994: E. Trinkaus / S. E. Churchill / C. B. Ruff, Postcranial robusticity in Homo. II: Humeral bilateral asymmetry and bone plasticity. American Journal of Physical Anthropology 93(1), 1994, 1-34.

Ulrix-Closset 1975: M. Ulrix-Closset, Le paleolithique moyen dans le bassin mosan en Belgique. Bibliothèque de la Faculté de Philosophie et Lettres de l'Université de Liège, Publications Exceptionnelles 3 (Wetteren 1975).

Uomini 2008: N. Uomini, In the knapper's hands: identifying handedness from lithic production and use. In: L. Longo / N. Skakun (eds), »Prehistoric Technology« 40 years later: functional studies and the Russian legacy. BAR International Series 1783 (Oxford 2008) 51-62.

2009: N. T. Uomini, The prehistory of handedness: Archaeological data and comparative ethology. Journal of Human Evolution 57, 2009, 411-419.

2011: N. T. Uomini, Handedness in Neanderthals. In: N. J. Conard / J. Richter (eds), Neanderthal Lifeways, Subsistence and Technology. One Hundred Fifty Years of Neanderthal Study. Vertebrate Paleobiology and Paleoanthropology (Dordrecht 2011) 139-154.

Uomini/Ruck 2018: N. T. Uomini / L. Ruck, Manual laterality and cognition through evolution: An archeological perspective. Progress in Brain Research 238, 2018, 295-323.

2019: N. Uomini / L. Ruck, Testing Models of Handedness in Stone Tools. In: K. A. Overmann / F. L. Coolidge (eds), Squeezing Minds From Stones: Cognitive Archaeology and the Evolution of the Human Mind (Oxford 2019) 225-236.

Urbanowski 2003: M. Urbanowski, Pradnik knives as an element of Micoquian techno-stylisitc specifics [diss. Univ. Warsaw 2003].

Valde-Nowak et al. 2014: P. Valde-Nowak / B. Alex / B. Ginter / M. T. Krajcarz / T. Madeyska / B. Miekina / K. Sobczyk / D. Stefański / P. Wojtal / M. Zajac / K. Zarzecka-Szubińska, Middle paleolithic sequences of the ciemna cave (Pradnik valley, Poland): The problem of synchronization. Quaternary International 326-327, 2014, 125-145.

2016: P. Valde-Nowak / B. Alex / B. Ginter / M. T. Krajcarz / T. Madeyska / B. Miękina / K. Sobczyk / D. Stefański / P. Wojtal / M. Zając / K. Zarzecka-Szubińska, Late middle palaeolithic occupations in Ciemna Cave, southern Poland. Journal of Field Archaeology 41, 2016, 193-210.

Valletta et al. 2020: F. Valletta / U. Smilansky / A. N. Goring-Morris / L. Grosman, On measuring the mean edge angle of lithic tools based on 3-D models – a case study from the southern Levantine Epipalaeolithic. Archaeological Anthropology Science 12, 2020, 49.

Van Gijn 1990: A. Van Gijn, A. The wear and tear of flint: Principles of functional analysis applied to Dutch Neolithic assemblages. Analecta Praehistorica Leidensia 22, 1990, 1-181.

2014: A. L. Van Gijn, Science and interpretation in microwear studies. Journal of Archaeological Science 48, 2014, 166-169.

Vandebosch 1921: A. Vandebosch, 1921. La Grotte de Ramioul. Bulletin des Chercheurs de la Wallonie 6, 1921, 1-61.

1929: A. Vandebosch, Les Néolithiques à Ramioul. Bulletin des Chercheurs de la Wallonie 9, 1929, 128-130.

1957: A. Vandebosch, Les grottes de Ramioul, hydrologie souterraine. Bulletin des Chercheurs de la Wallonie 16, 1957, 172-178.

Vaquero et al. 2015: M. Vaquero / A. Bargalló / M. G. Chacón / F. Romagnoli / P. Sañudo, Lithic recycling in a middle paleolithic expedient context: Evidence from the Abric Romaní (Capellades, Spain). Quaternary International 361, 2015, 212-228.

Vaughan 1985: P. C. Vaughan, Use-Wear Analysis of Flaked Stone Tools (Tucson AZ 1985).

Veil et al. 1994: S. Veil / K. Breest / H.-C. Höfle / H.-H. Meyer / H. Plisson / B. Urban-Küttel / G. A. Wagner / L. Zoller, Ein mittelpaläolithischer Fundplatz aus der Weichsel-Kaltzeit bei Lichtenberg, Ldkr. Lüchow-Dannenberg. Zwischenbericht über die archäologischen und geowissenschaftlichen Untersuchungen 1987-1992. Germania 72, 1994, 1-66.

Volpato et al. 2012: V. Volpato / R. Macchiarell / D. Guatelli-Steinberg / I. Fiore / L. Bondioli / D. W. Frayer, Hand to mouth in a Neandertal: Right-handedness in Regourdou 1. PLoS One 7, 2012, e43949.

Weiss 2015: M. Weiss, Stone tool analysis and context of a new late Middle Paleolithic site in western central Europe – Pouch-Terrassenpfeiler, Ldkr. Anhalt-Bitterfeld, Germany. Quartär 62, 2015, 23-62.

2020: M. Weiss, The Lichtenberg Keilmesser – It's all about the angle. PLoS One 15(10), 2020, e0239718.

Weiss/Otcherednoy/Wiśniewski 2017: M. Weiss / A. Otcherednoy / A. Wiśniewski, Using multivariate techniques to assess the effects of raw material, flaking behavior and tool manufacture on assemblage variability: An example from the late Middle Paleolithic of the European Plain. Journal of Archaeological Science 87, 2017, 73-94.

Weiss et al. 2018: M. Weiss / T. Lauer / R. Wimmer / C. M. Pop, The Variability of the Keilmesser-Concept: a Case Study from Central Germany. Journal of Paleolithic Archaeology 1, 2018, 202-246.

Wetzel 1958: R. Wetzel, Die Bocksteinschmiede mit dem Bocksteinloch, der Brandplatte und dem Abhang sowie der Bocksteingrotte. Ein Beitrag zur europäischen Urgeschichte des Lonetals und zur geschichtlichen Morphologie des Menschen. Veröffentlichungen aus der prähistorischen Abteilung des Ulmer Museums 1 (Stuttgart 1958).

Wetzel/Bosinski 1969: R. Wetzel / G. Bosinski, Die Bocksteinschmiede im Lonetal. Veröffentlichungen des Staatlichen Amtes für Denkmalpflege Stuttgart A15 (Stuttgart 1969).

Whiten/Schick/Toth 2009: A. Whiten / K. Schick / N. Toth, The evolution and cultural transmission of percussive technology: integrating evidence from palaeoanthropology and primatology. Journal of Human Evolution 57, 2009, 420-435.

Wilkins et al. 2012: J. Wilkins / B. J. Schoville / K. S. Brown / M. Chazan, Evidence for early hafted hunting technology. Science 338, 2012, 942-946.

Williams-Hatala et al. 2018: E. M. Williams-Hatala / K. G. Hatala / M. Gordon / A. Key / M. Kasper / T. L. Kivell, The manual pressures of stone tool behaviors and their implications for the evolution of the human hand. Journal of Human Evolution 119, 2018, 14-26.

Wiśniewski et al. 2020: A. Wiśniewski / M. Chłoń / M. Weiss / K. Pyżewicz / W. Migal, On Making of Micoquian Bifacial Backed Tools at Pietraszyn 49a, SW Poland. Journal of Paleolithic Archaeology 3, 2020, 856-888.

Yaşar/Erdoğan 2004: E. Yaşar / Y. Erdoğan, Estimation of rock physicomechanical properties using hardness methods. Engineering Geology 71, 2004, 281-288.

Yilmaz/Sendir 2002: I. Yilmaz / H. Sendir, Correlation of Schmidt hardness with unconfined compressive strength and Young's modulus in gypsum from Sivas (Turkey). Engineering Geology 66, 2002, 211-219.

Zaidner/Grosman 2015: Y. Zaidner / L. Grosman, Middle Paleolithic sidescrapers were resharped or recycled? A view from Nesher Ramla, Israel. Quaternary International 361, 2015, 178-187.

APPENDIX I

Results of the qualitative and quantitative use-wear analyses performed on samples from the archaeological sites Buhlen, Balver Höhle and Ramioul

PLATES A1-156

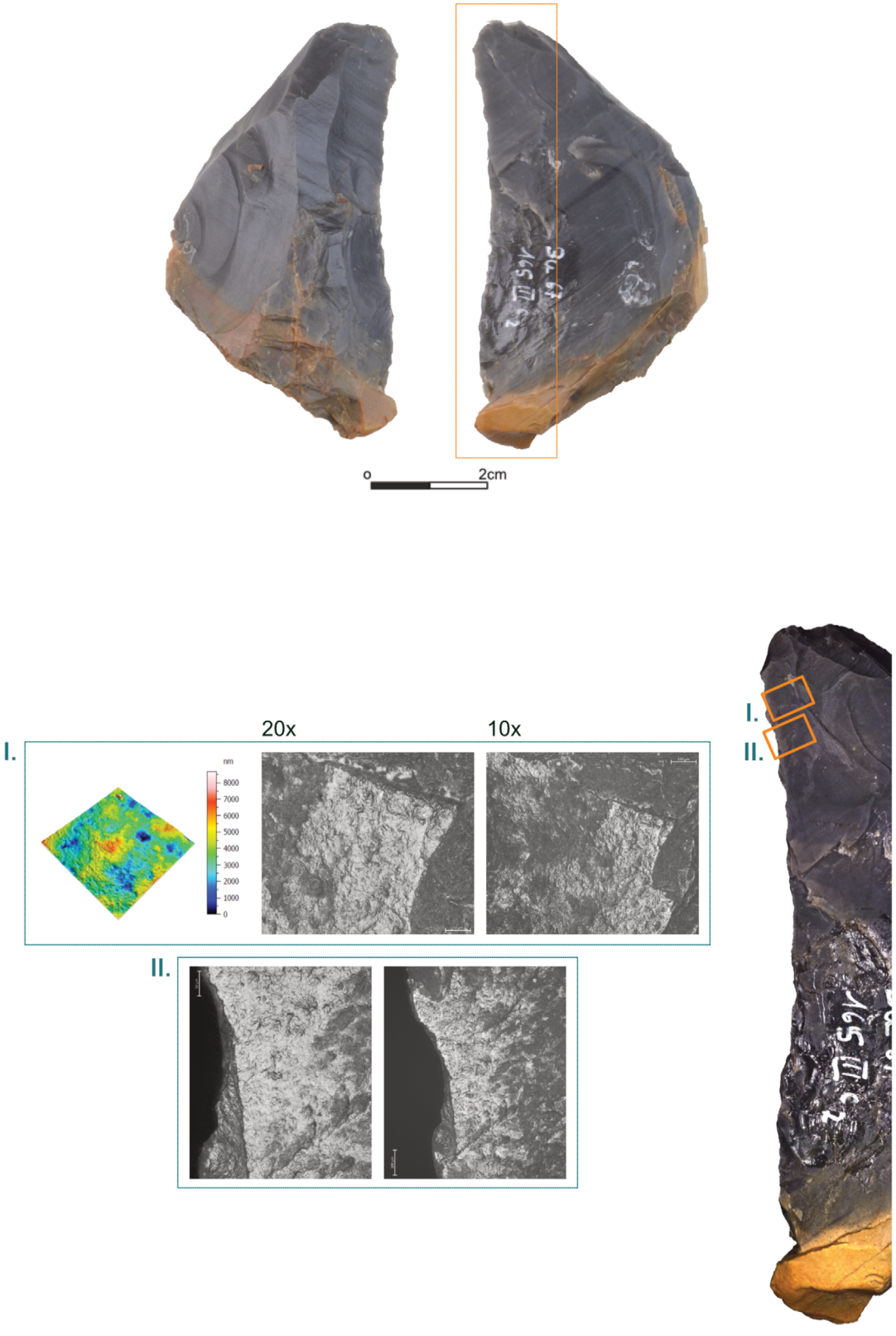

Buhlen, *Keilmesser* [ID BU-003]. The topmost image displays the artefact in original size. The other illustrations are magnifications acquired with a 1.6× objective and a 34-× zoom. The use-wear traces are acquired at magnification of 10× and 20× (I. type V.; II. type V.). The micro-surface displays the processed result of the confocal data acquisition with the 50× objective.

Plate A2

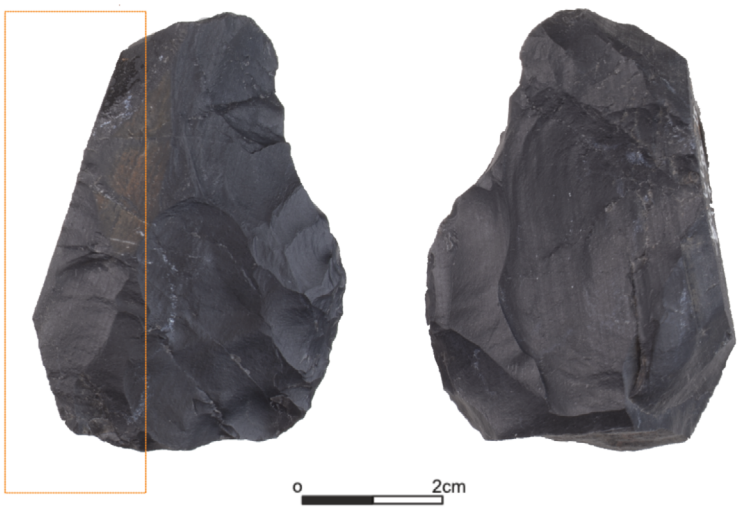

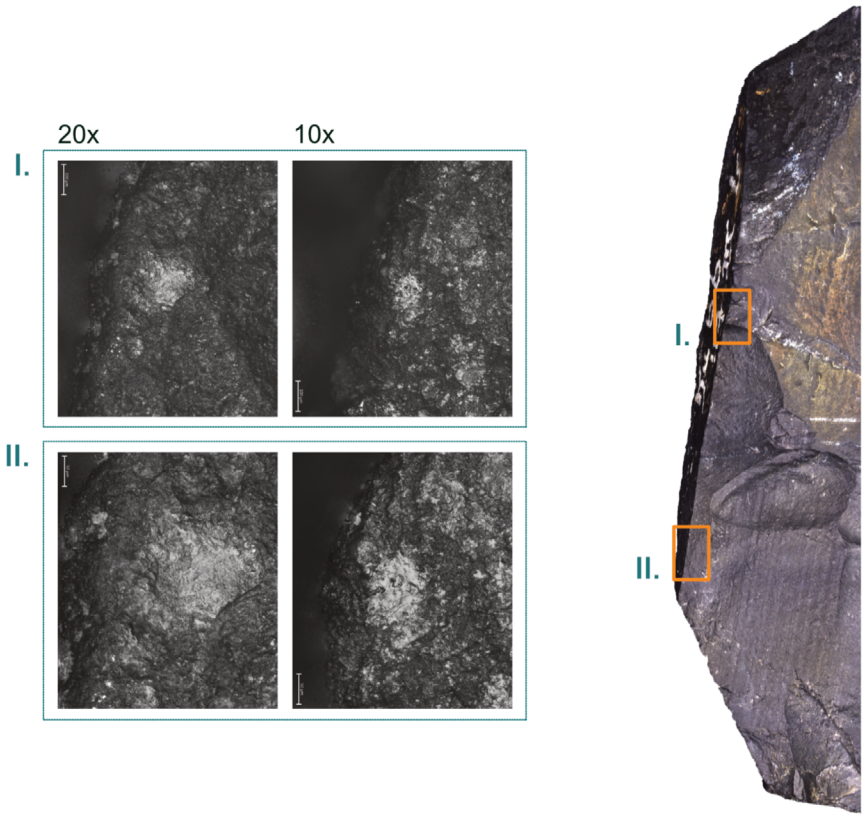

Buhlen, *Keilmesser* [ID BU-004]. The topmost image displays the artefact in original size. The other illustrations are magnifications acquired with a 1.6× objective and a 34-× zoom. The use-wear traces are acquired at magnification of 10× and 20× (I. type I.; II. type I.).

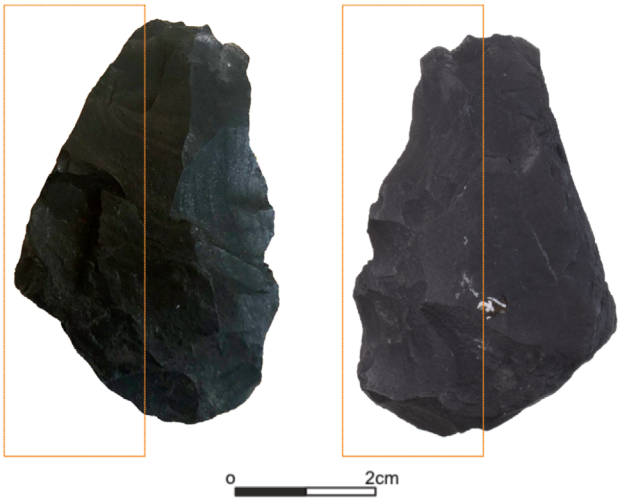

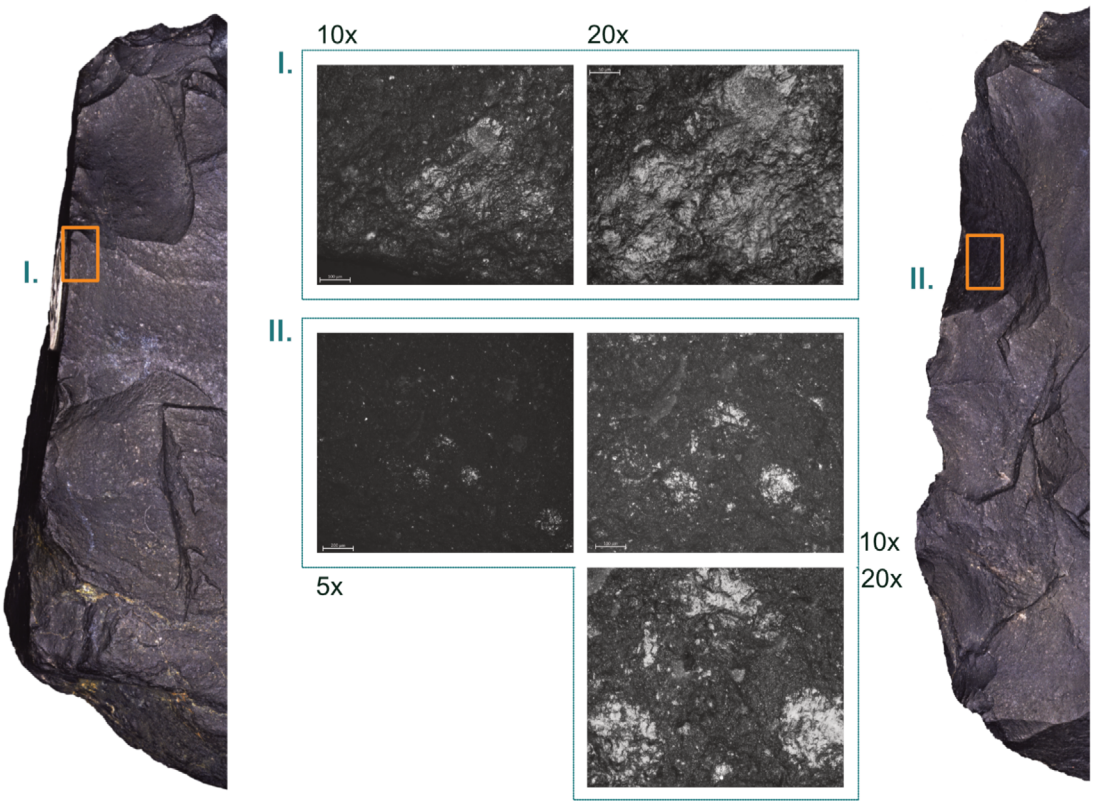

Buhlen, *Keilmesser* [ID BU-006]. The topmost image displays the artefact in original size. The other illustrations are magnifications acquired with a 1.6× objective and a 34-× zoom. The use-wear traces are acquired at magnification of 5×, 10× and 20× (I. type V.; II. type I.).

Plate A4

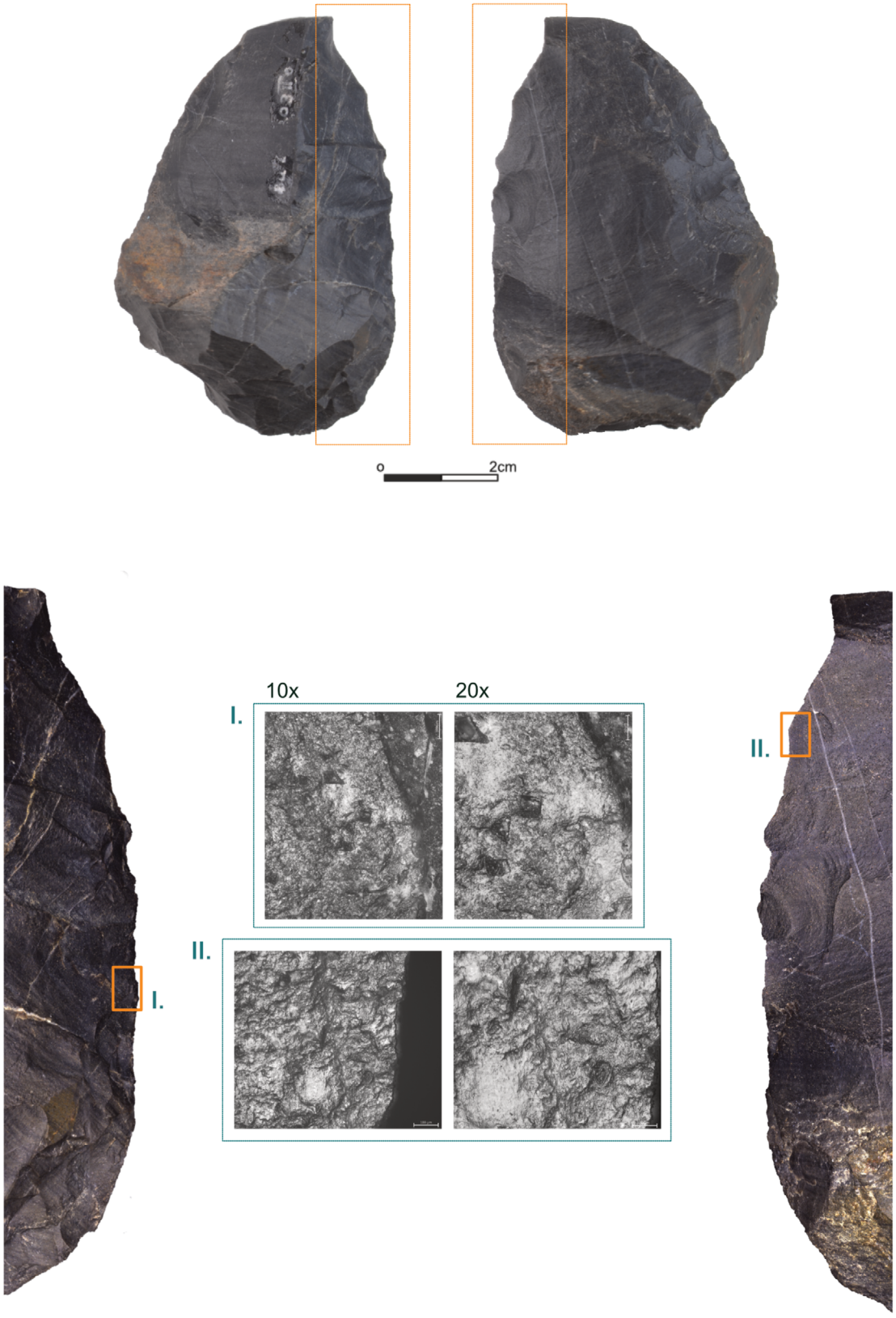

Buhlen, *Keilmesser* [ID BU-009]. The topmost image displays the artefact in original size. The other illustrations are magnifications acquired with a 1.6× objective and a 34-× zoom. The use-wear traces are acquired at magnification of 10× and 20× (I. type V.; II. type V.).



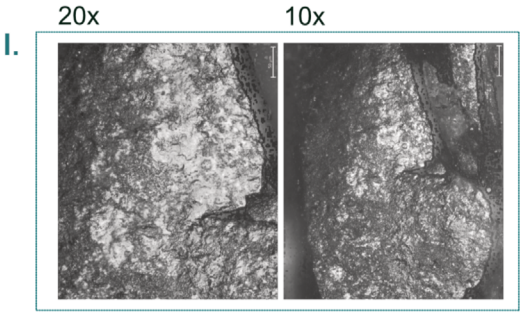



Buhlen, *Keilmesser* [ID BU-012]. The topmost image displays the artefact in original size. The other illustrations are magnifications acquired with a 1.6× objective and a 34-× zoom. The use-wear trace is acquired at magnification of 10× and 20× (I. type V.).

Plate A6



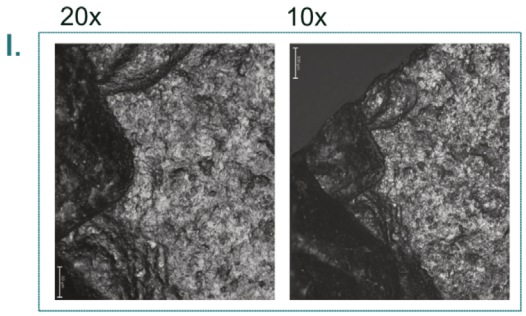



Buhlen, *Keilmesser* [ID BU-016]. The topmost image displays the artefact in original size. The other illustrations are magnifications acquired with a 1.6× objective and a 34-× zoom. The use-wear trace is acquired at magnification of 10× and 20× (I. type V.).



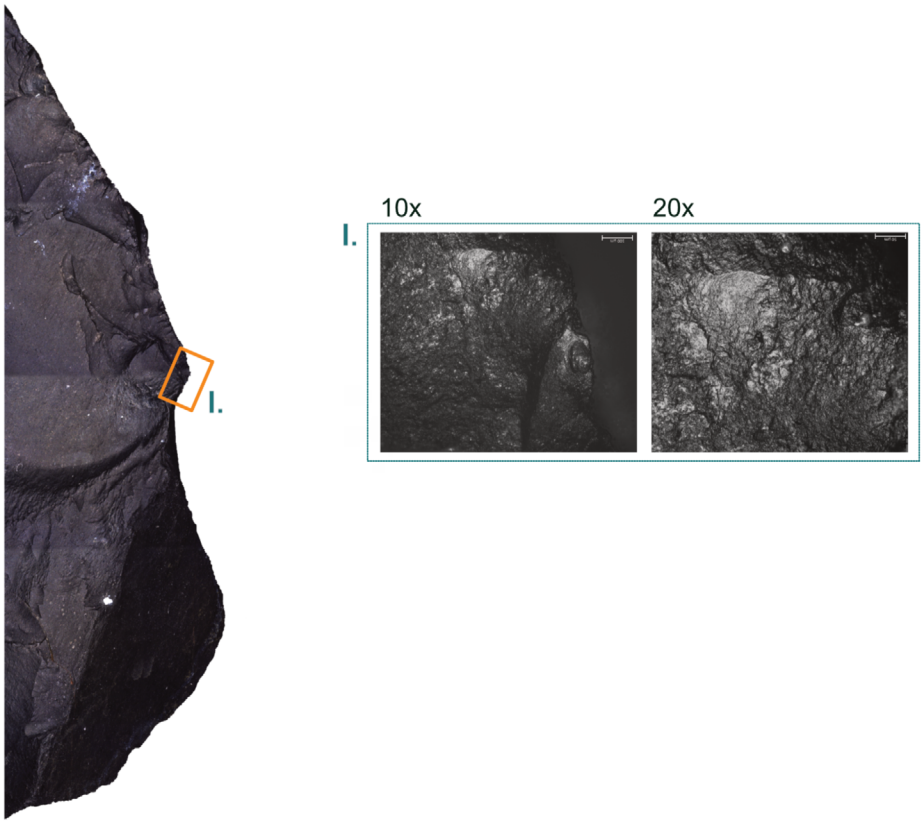

Buhlen, *Keilmesser* [ID BU-017]. The topmost image displays the artefact in original size. The other illustrations are magnifications acquired with a 1.6× objective and a 34-× zoom. The use-wear trace is acquired at magnification of 10× and 20× (I. type V.).

Plate A8



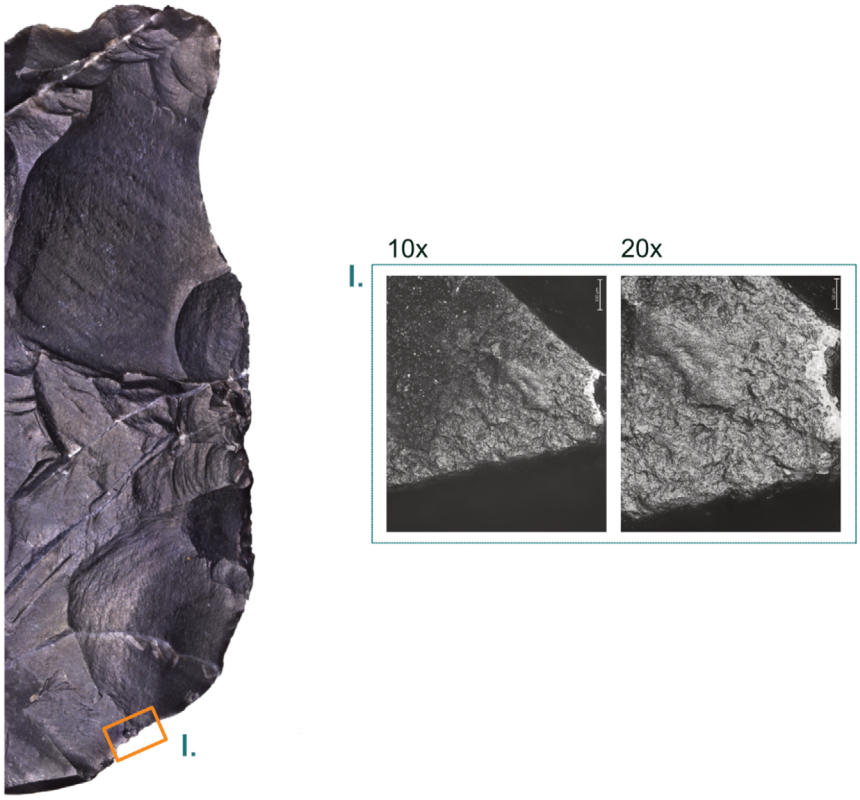

Buhlen, *Keilmesser* [ID BU-019]. The topmost image displays the artefact in original size. The other illustrations are magnifications acquired with a 1.6× objective and a 34-× zoom. The use-wear trace is acquired at magnification of 10× and 20× (I. type IV.).



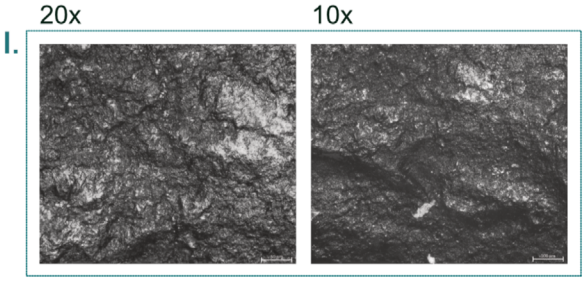



Buhlen, *Keilmesser* [ID BU-024]. The topmost image displays the artefact in original size. The other illustrations are magnifications acquired with a 1.6× objective and a 34-× zoom. The use-wear trace is acquired at magnification of 10× and 20× (I. type I.).

Plate A10



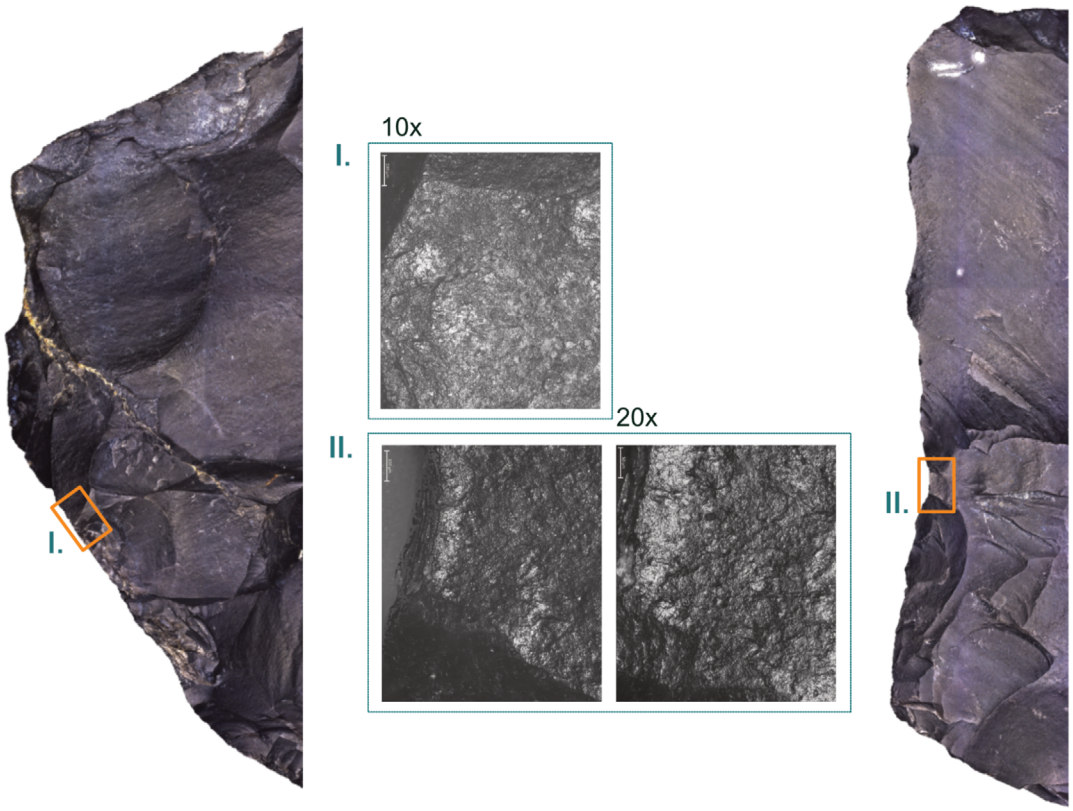

Buhlen, *Keilmesser* [ID BU-028]. The topmost image displays the artefact in original size. The other illustrations are magnifications acquired with a 1.6× objective and a 34-× zoom. The use-wear traces are acquired at magnification of 10× and 20× (I. type I.; II. type V.).

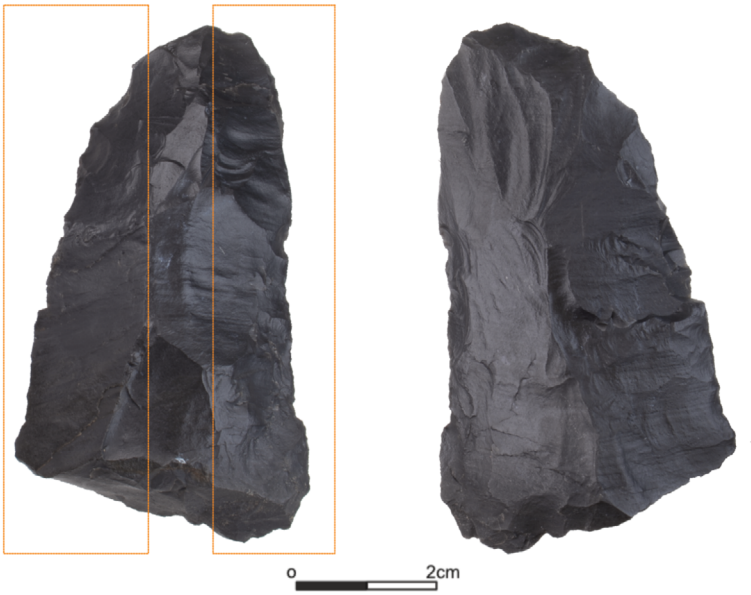

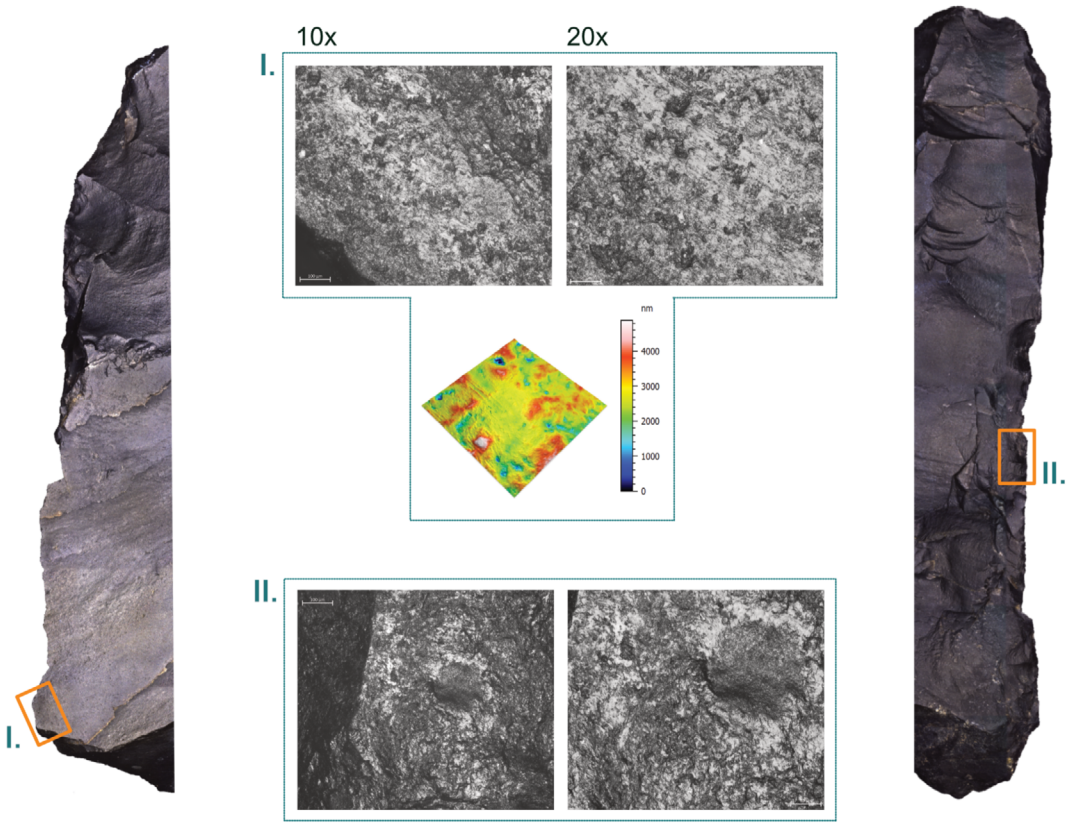

Buhlen, *Keilmesser* [ID BU-032]. The topmost image displays the artefact in original size. The other illustrations are magnifications acquired with a 1.6× objective and a 34-× zoom. The use-wear traces are acquired at magnification of 10× and 20× (I. type VII.; II. type V.). The micro-surface displays the processed result of the confocal data acquisition with the 50× objective.

Plate A12

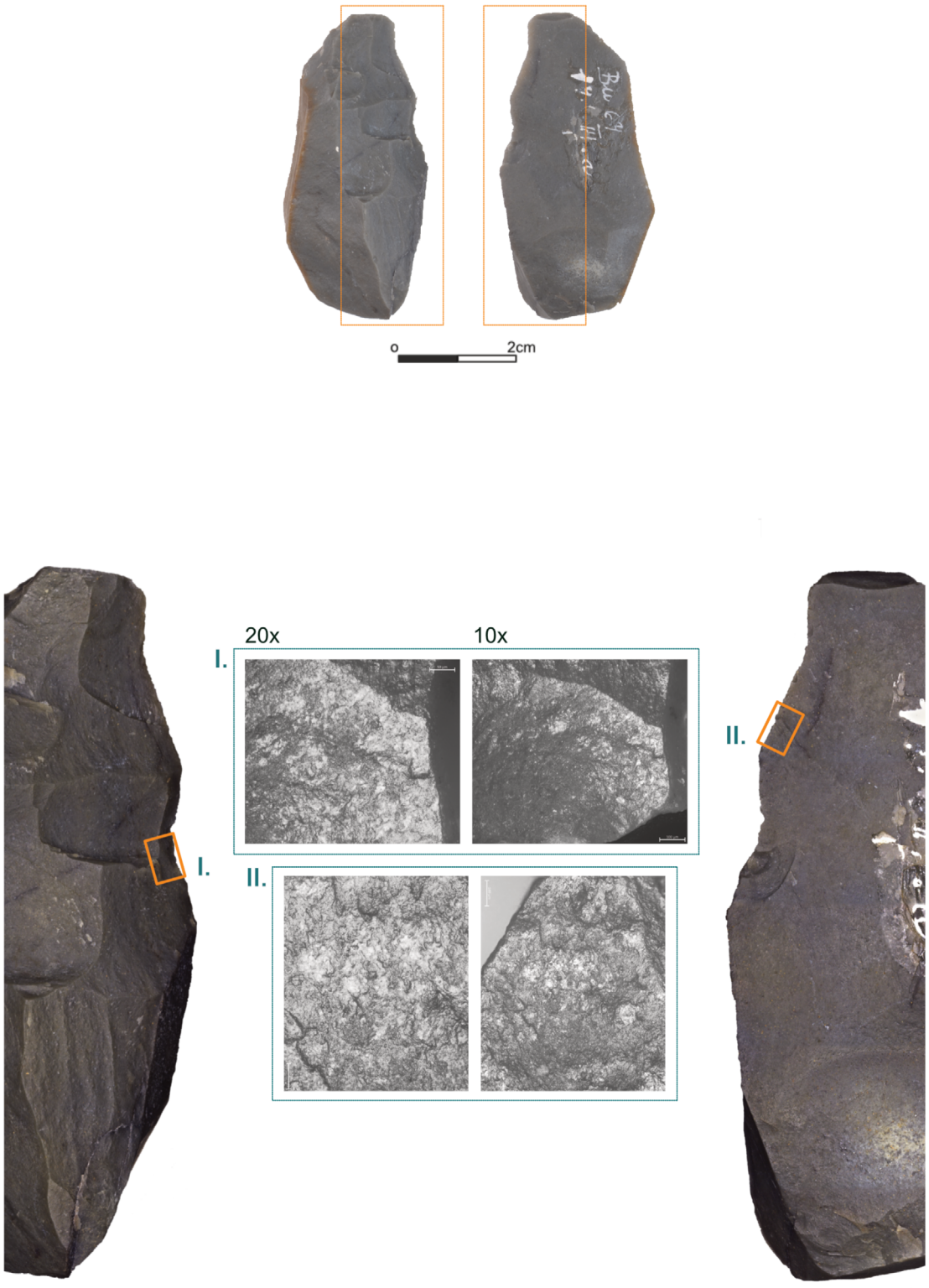

Buhlen, *Keilmesser* [ID BU-036]. The topmost image displays the artefact in original size. The other illustrations are magnifications acquired with a 1.6× objective and a 34-× zoom. The use-wear traces are acquired at magnification of 10× and 20× (I. type V.; II. type V.).

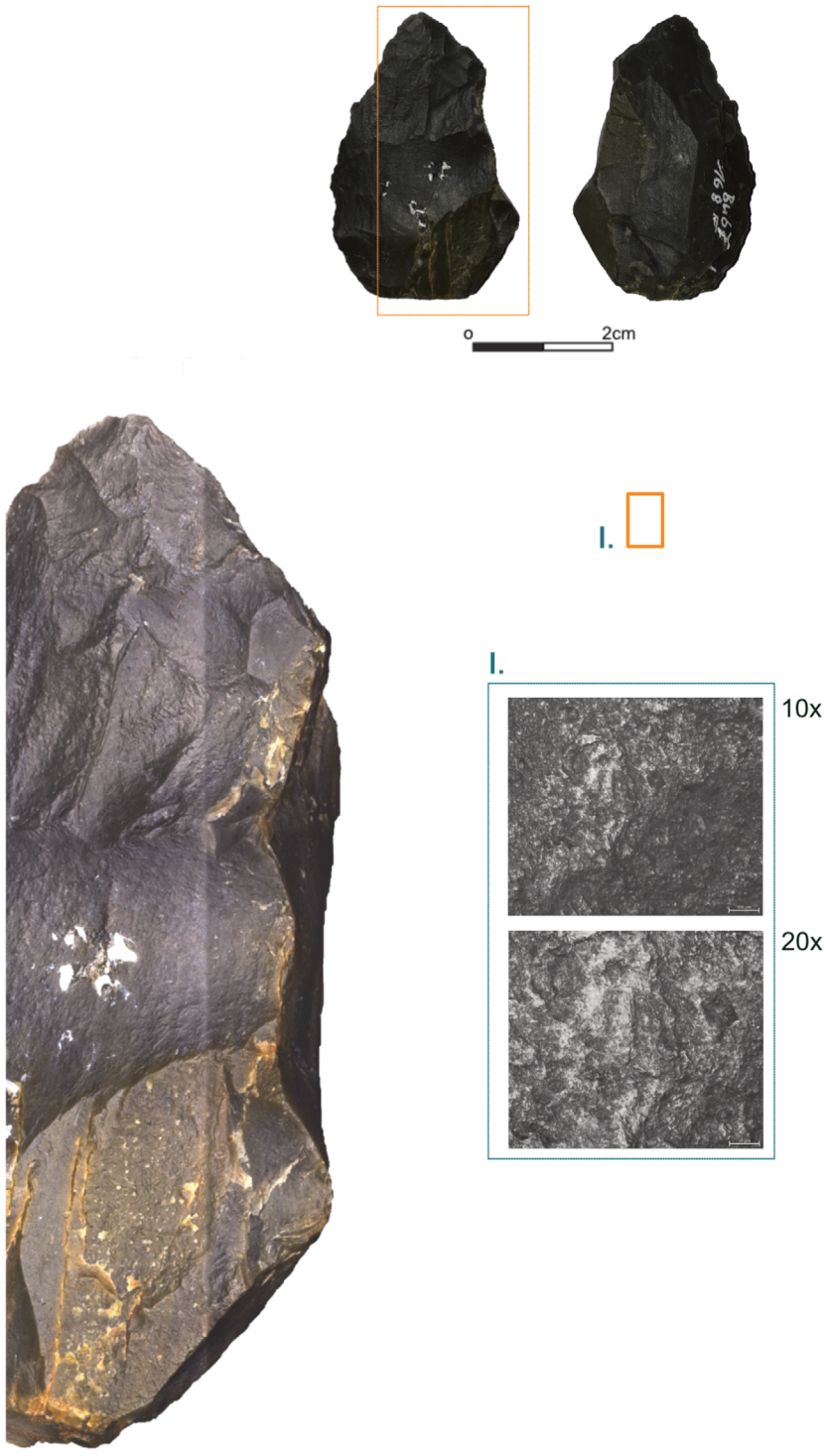

Buhlen, *Keilmesser* [ID BU-039]. The topmost image displays the artefact in original size. The other illustrations are magnifications acquired with a 1.6× objective and a 34-× zoom. The use-wear trace is acquired at magnification of 10× and 20× (I. type V.).

Plate A14

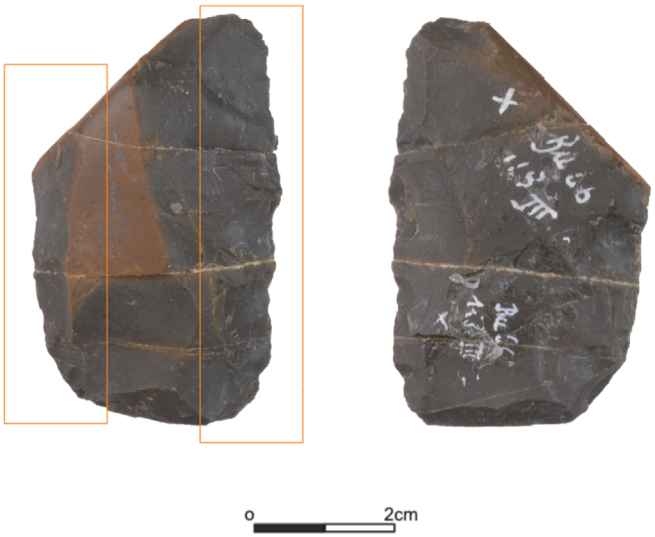

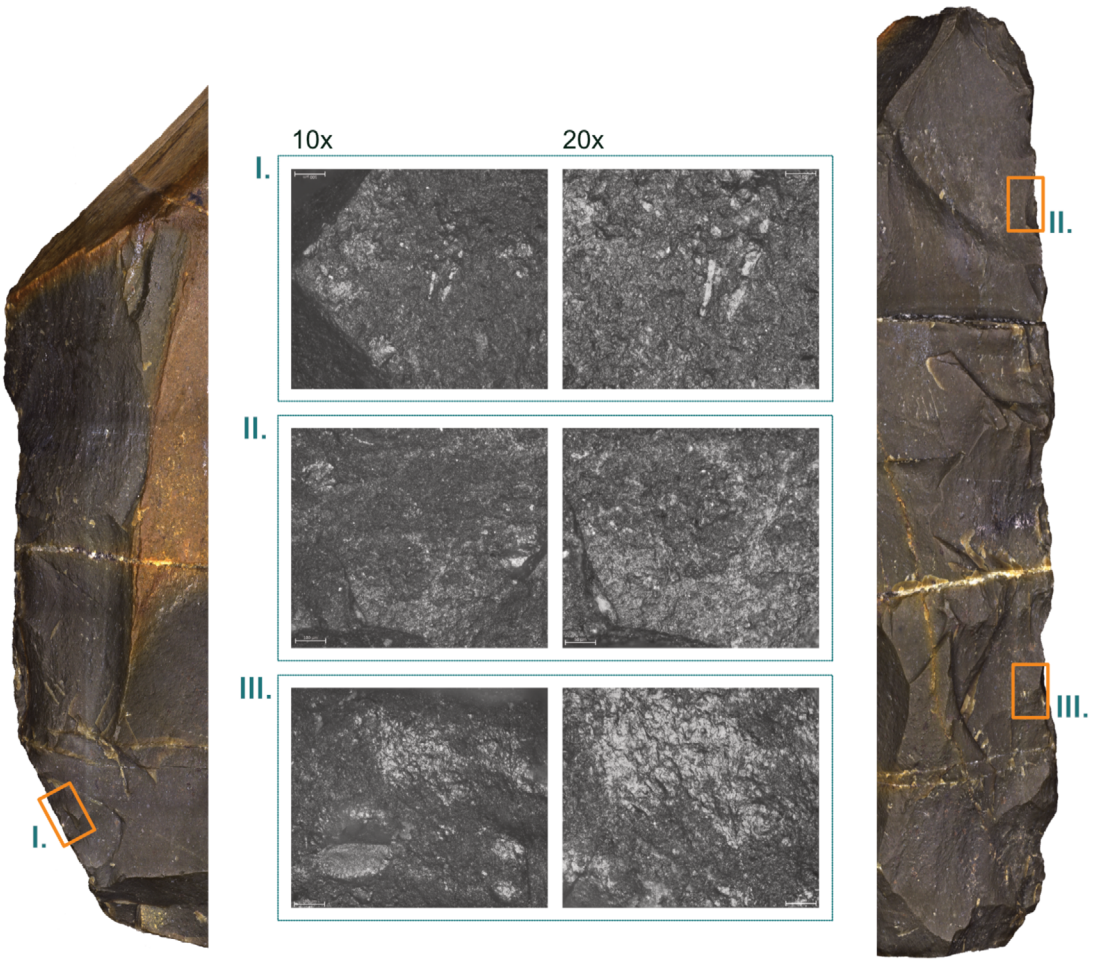

Buhlen, *Keilmesser* [ID BU-040]. The topmost image displays the artefact in original size. The other illustrations are magnifications acquired with a 1.6× objective and a 34-× zoom. The use-wear traces are acquired at magnification of 10× and 20× (I. type I.; II. type V.; III. type V.).

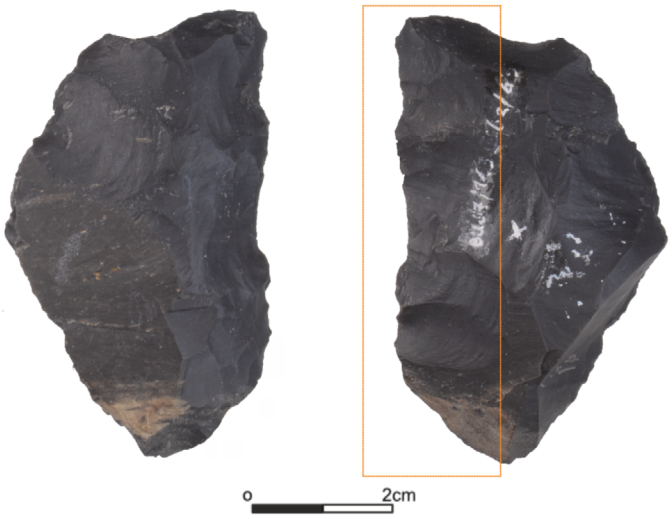

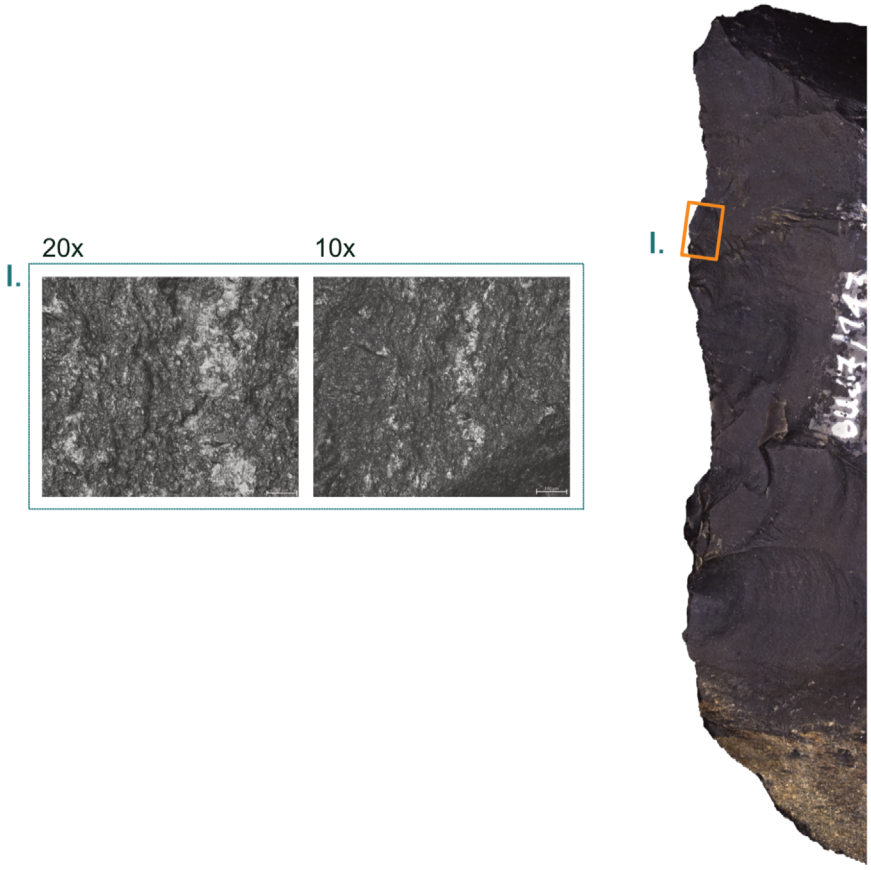

Buhlen, *Keilmesser* [ID BU-046]. The topmost image displays the artefact in original size. The other illustrations are magnifications acquired with a 1.6× objective and a 34-× zoom. The use-wear trace is acquired at magnification of 10× and 20× (I. type V.).

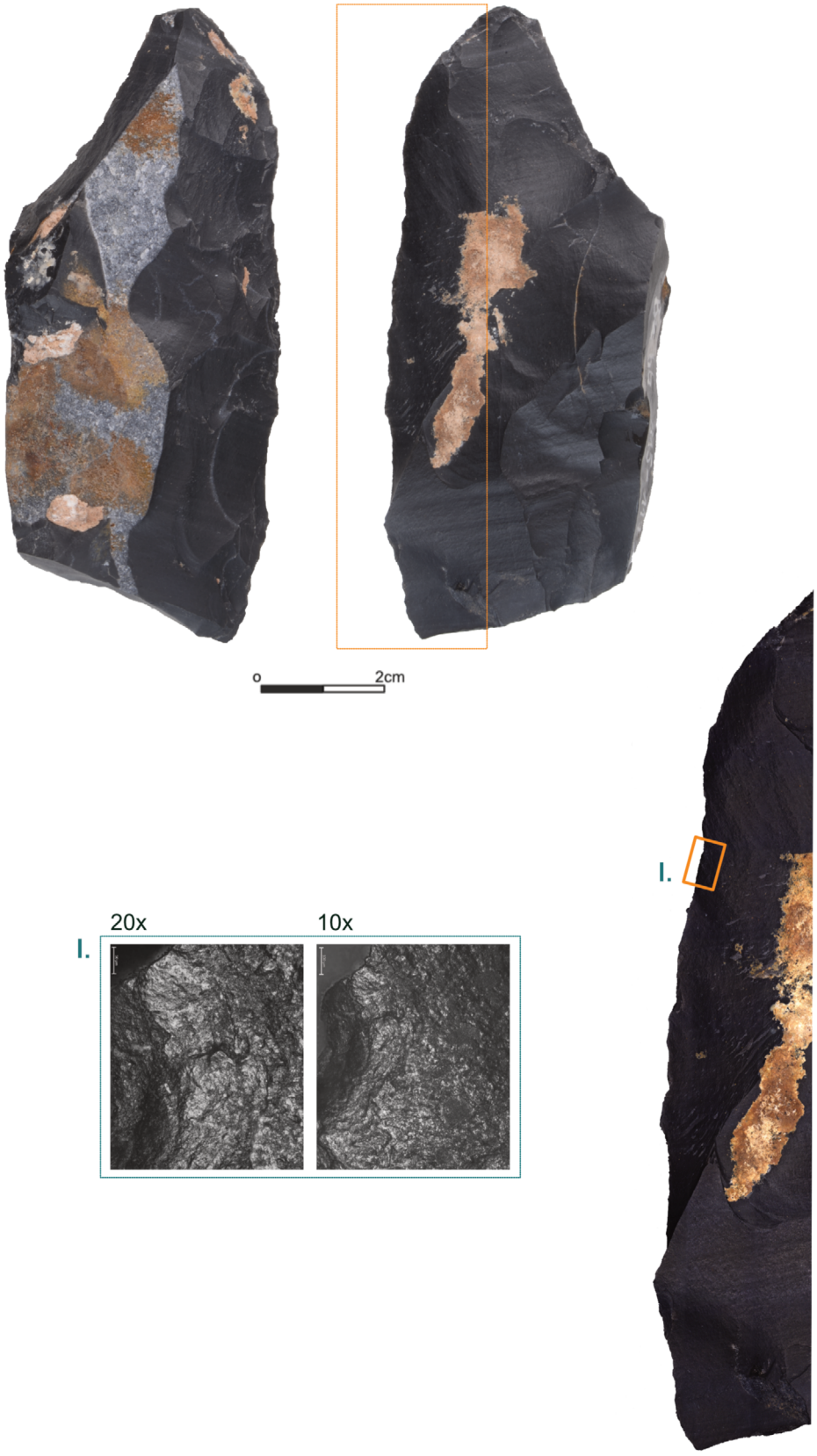

Buhlen, *Keilmesser* [ID BU-048]. The topmost image displays the artefact in original size. The other illustrations are magnifications acquired with a 1.6× objective and a 34-× zoom. The use-wear trace is acquired at magnification of 10× and 20× (I. type V.).



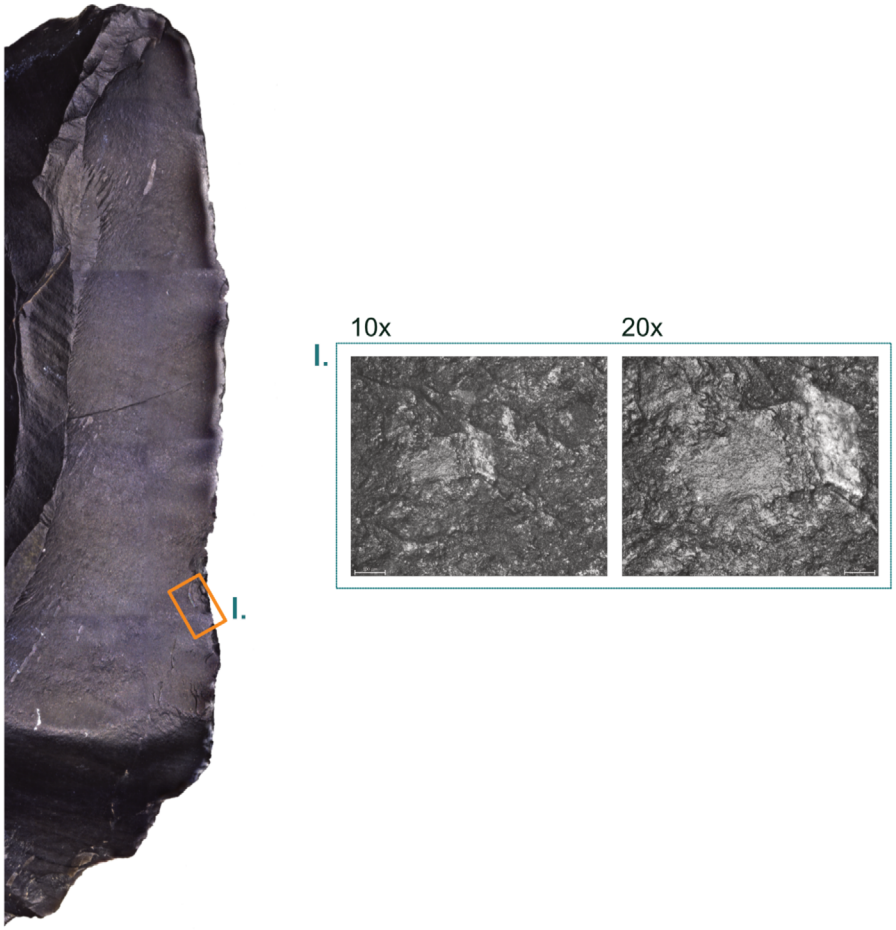

Buhlen, *Keilmesser* [ID BU-051]. The topmost image displays the artefact in original size. The other illustrations are magnifications acquired with a 1.6× objective and a 34-× zoom. The use-wear trace is acquired at magnification of 10× and 20× (I. type I.).

Plate A18

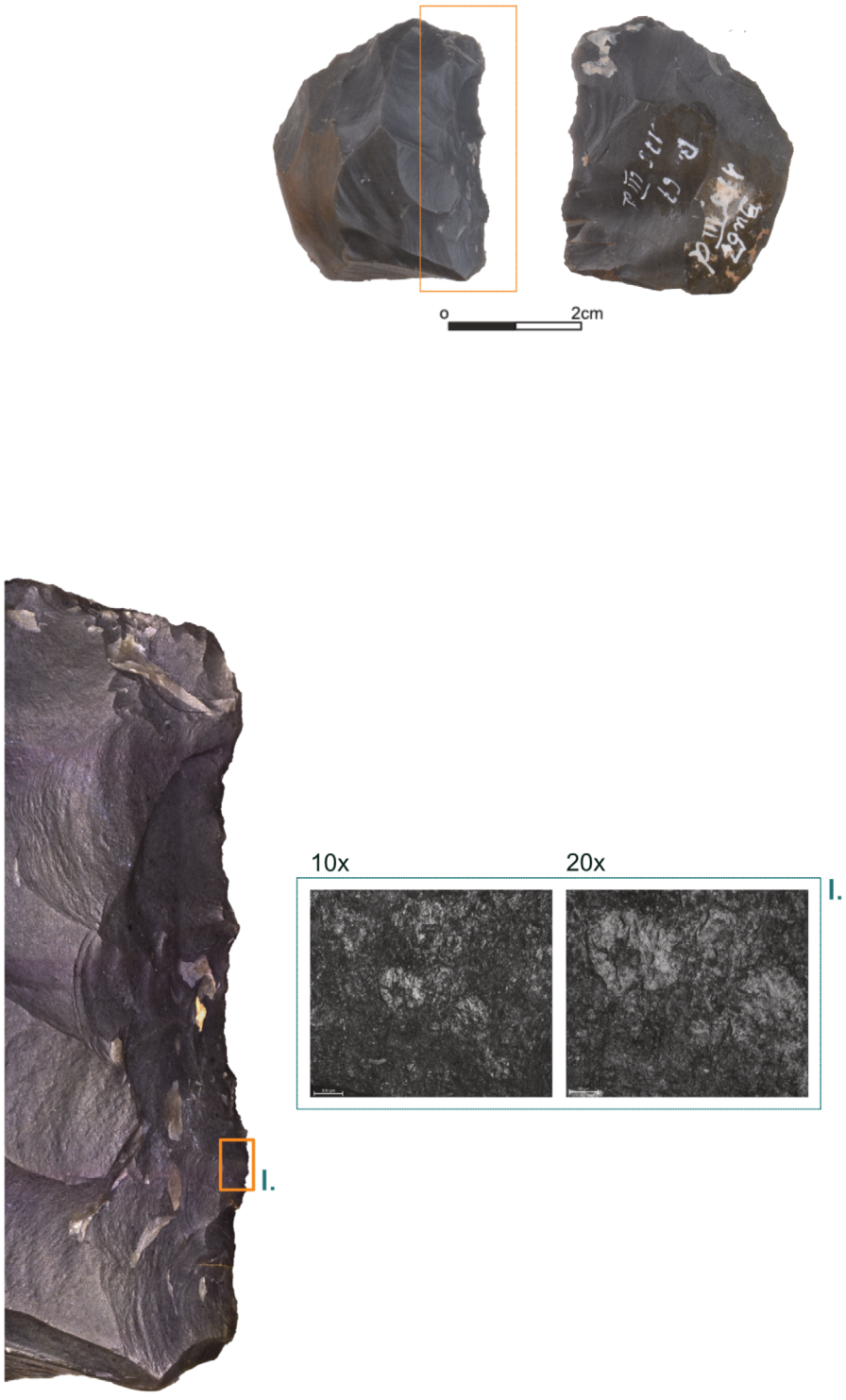

Buhlen, *Keilmesser* [ID BU-054]. The topmost image displays the artefact in original size. The other illustrations are magnifications acquired with a 1.6× objective and a 34-× zoom. The use-wear trace is acquired at magnification of 10× and 20× (I. type I.).

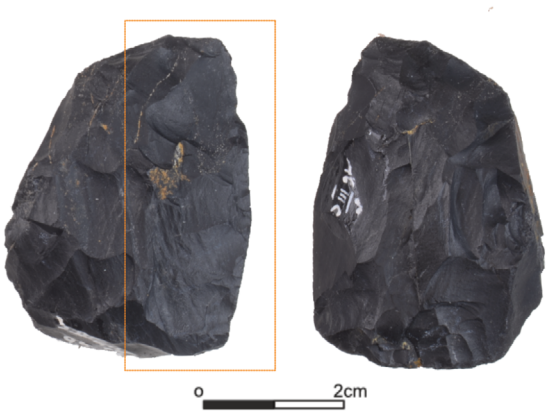

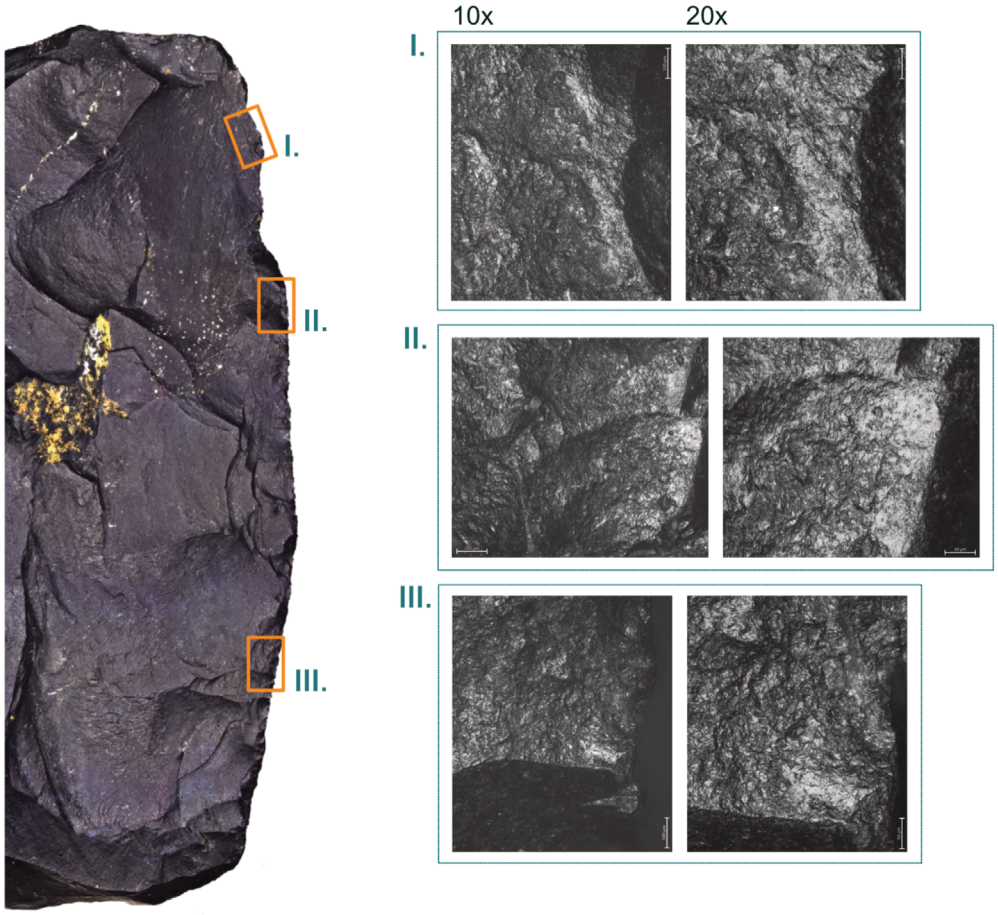

Buhlen, *Keilmesser* [ID BU-056]. The topmost image displays the artefact in original size. The other illustrations are magnifications acquired with a 1.6× objective and a 34-× zoom. The use-wear traces are acquired at magnification of 10× and 20× (I. type V.; II. type V.; III. type V.).

Plate A20





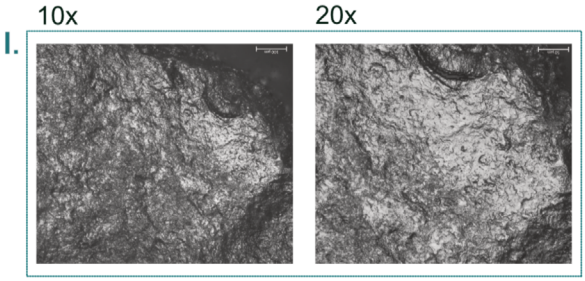

Buhlen, *Keilmesser* [ID BU-057]. The topmost image displays the artefact in original size. The other illustrations are magnifications acquired with a 1.6× objective and a 34-× zoom. The use-wear trace is acquired at magnification of 10× and 20× (I. type V.).



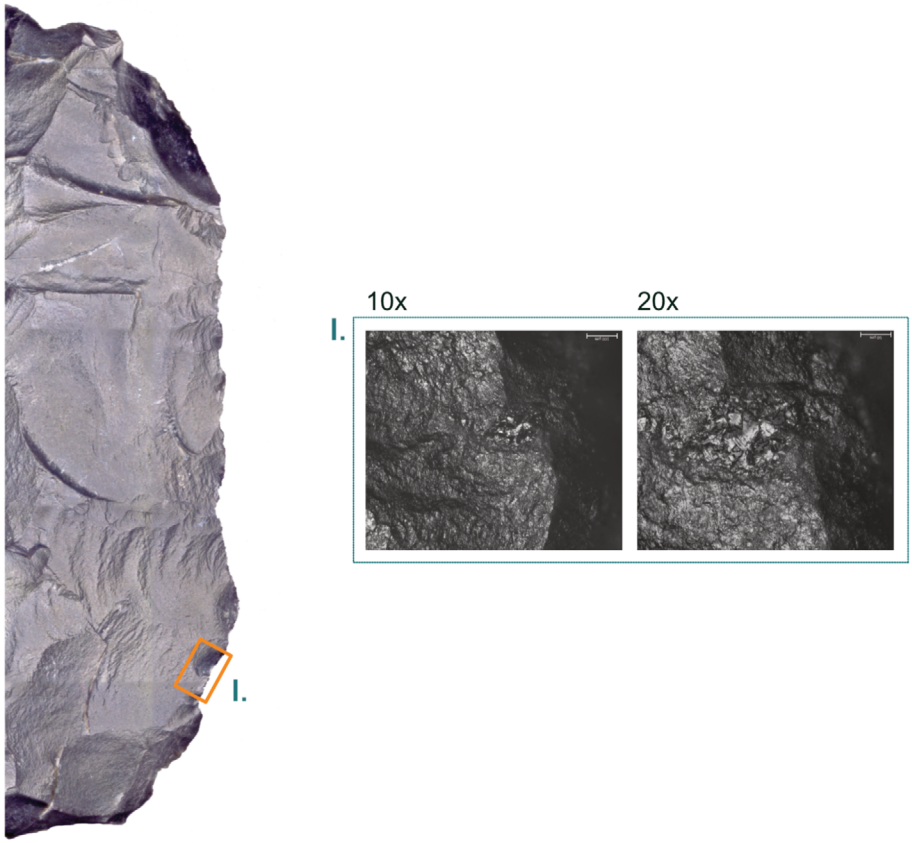

Buhlen, *Keilmesser* [ID BU-058]. The topmost image displays the artefact in original size. The other illustrations are magnifications acquired with a 1.6× objective and a 34-× zoom. The use-wear trace is acquired at magnification of 10× and 20× (I. type I.).

Plate A22

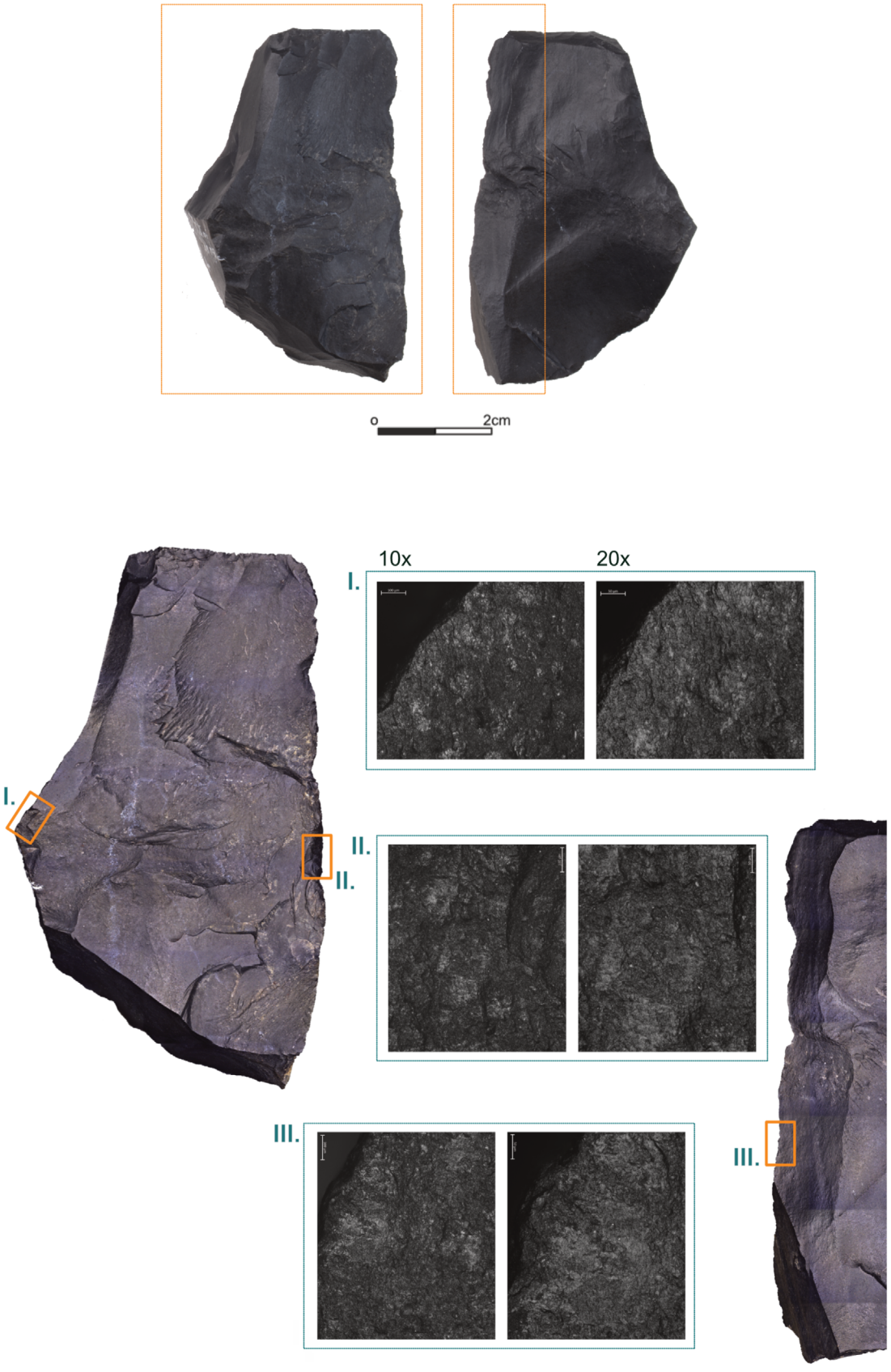

Buhlen, *Keilmesser* [ID BU-060]. The topmost image displays the artefact in original size. The other illustrations are magnifications acquired with a 1.6× objective and a 34-× zoom. The use-wear traces are acquired at magnification of 10× and 20× (I. type V.; II. type V.; III. type V.).

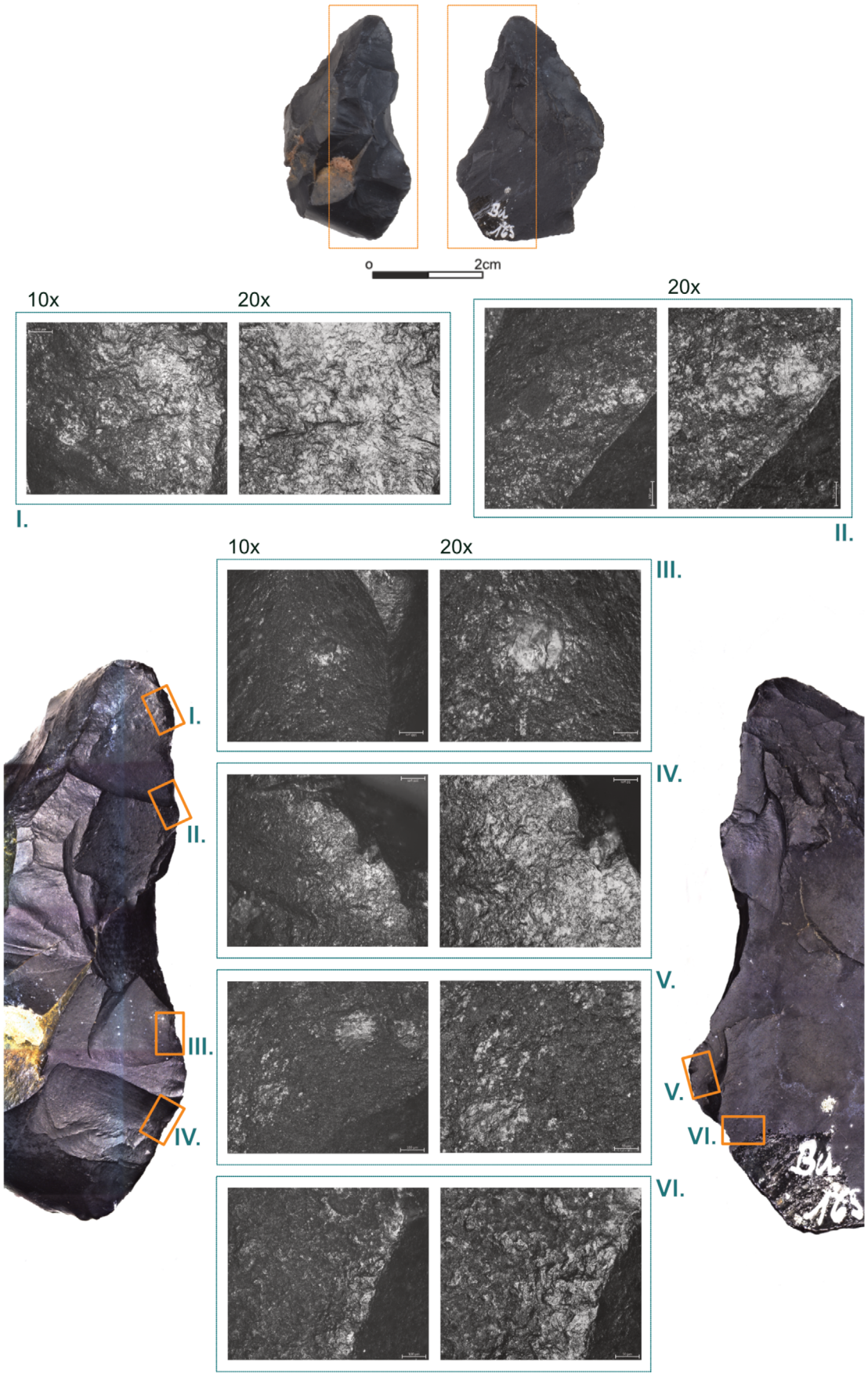

Buhlen, *Keilmesser* [ID BU-066]. The topmost image displays the artefact in original size. The other illustrations are magnifications acquired with a 1.6× objective and a 34-× zoom. The use-wear traces are acquired at magnification of 10× and 20× (I. type V.; II. type V.; III. type I.; IV. type I.; V. type I.; VI. type V.).

Plate A24

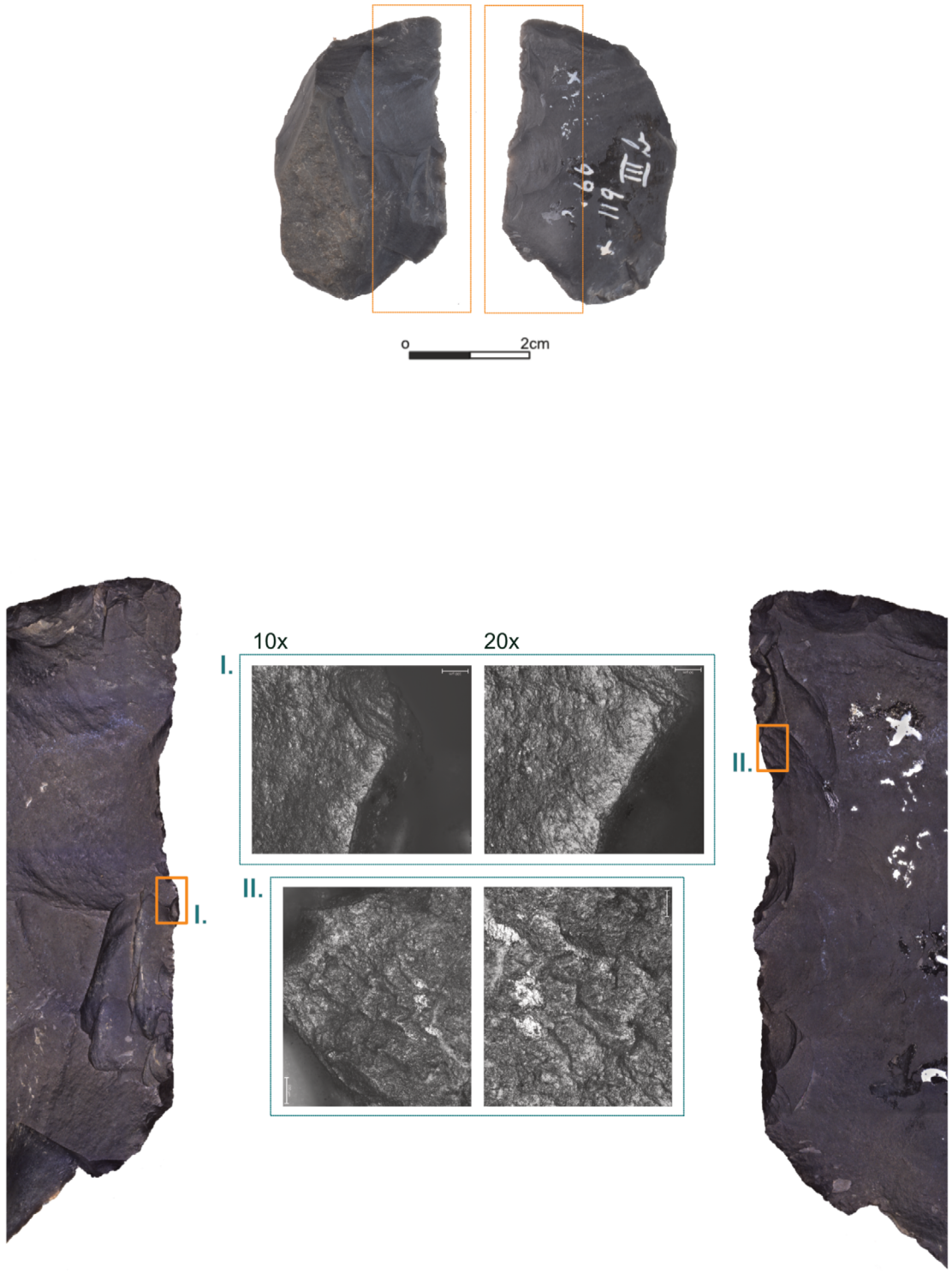

Buhlen, *Keilmesser* [ID BU-069]. The topmost image displays the artefact in original size. The other illustrations are magnifications acquired with a 1.6× objective and a 34-× zoom. The use-wear traces are acquired at magnification of 10× and 20× (I. type V.; II. type V.).



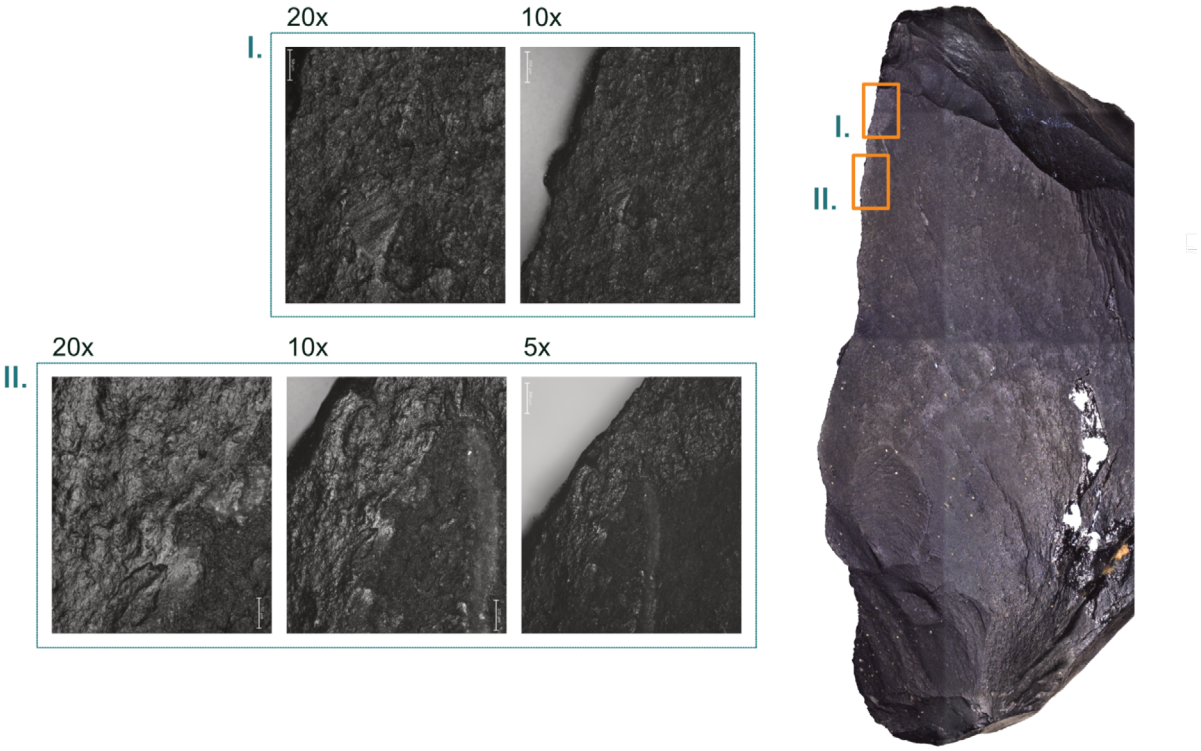

Buhlen, *Keilmesser* [ID BU-074]. The topmost image displays the artefact in original size. The other illustrations are magnifications acquired with a 1.6× objective and a 34-× zoom. The use-wear traces are acquired at magnification of 5×, 10× and 20× (I. type V.; II. type V.).

Plate A26

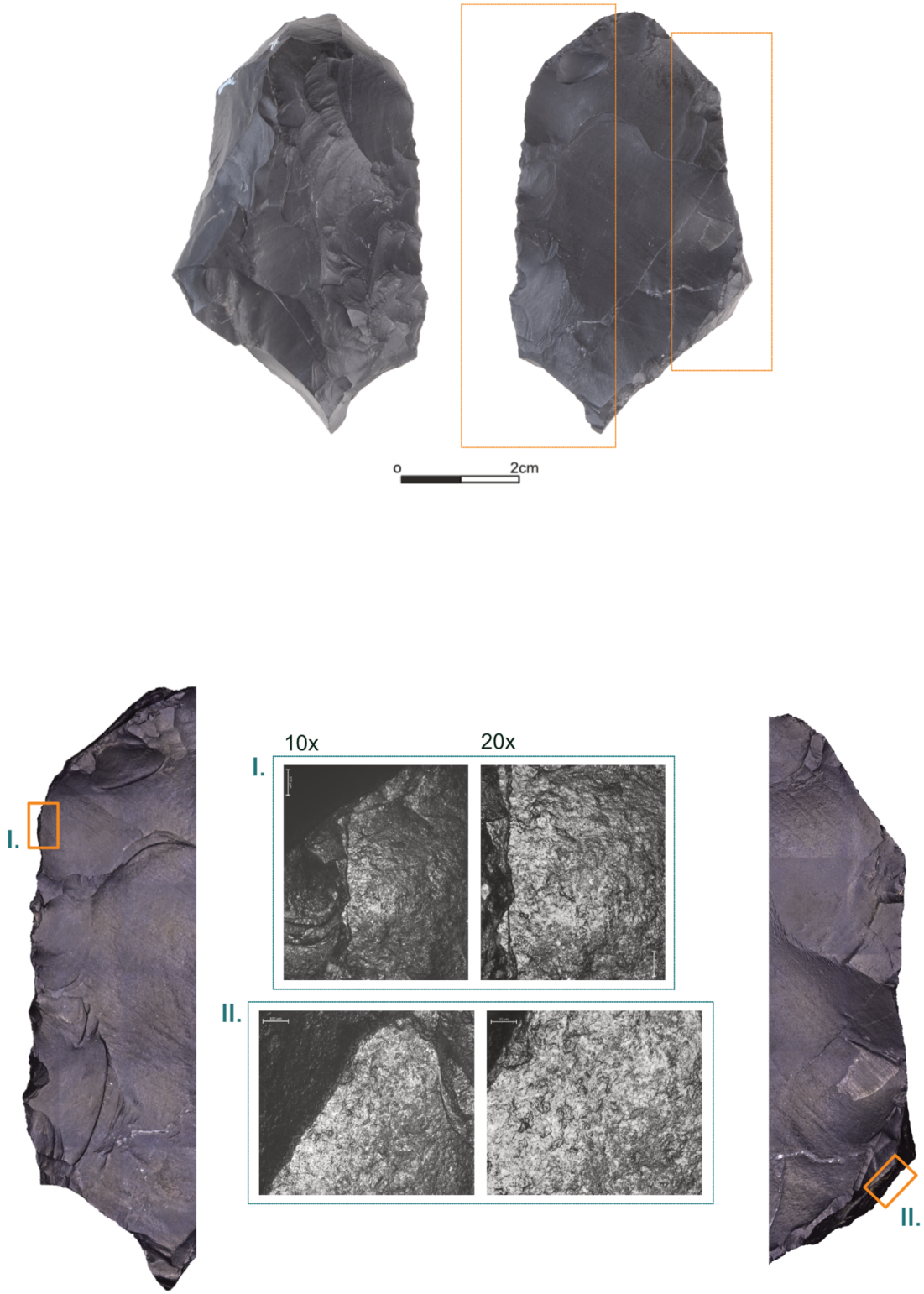

Buhlen, *Keilmesser* [ID BU-076; dorsal]. The topmost image displays the artefact in original size. The other illustrations are magnifications acquired with a 1.6× objective and a 34-× zoom. The use-wear traces are acquired at magnification of 10× and 20× (I. type V.; II. type V.).

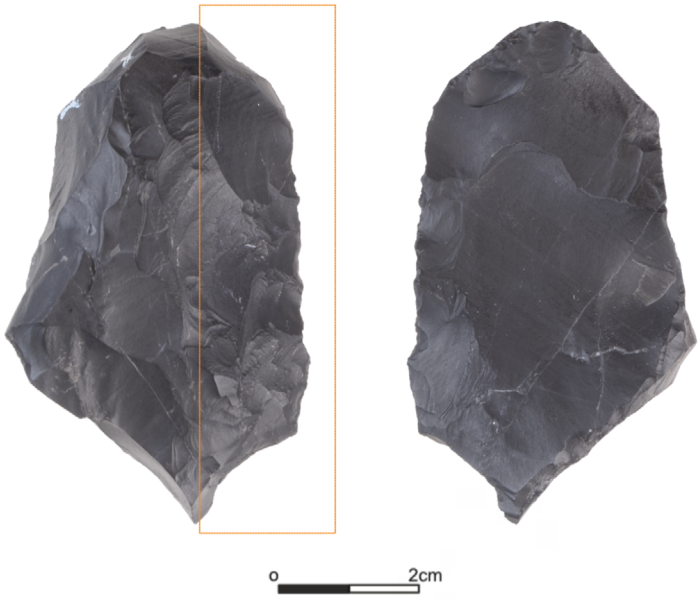

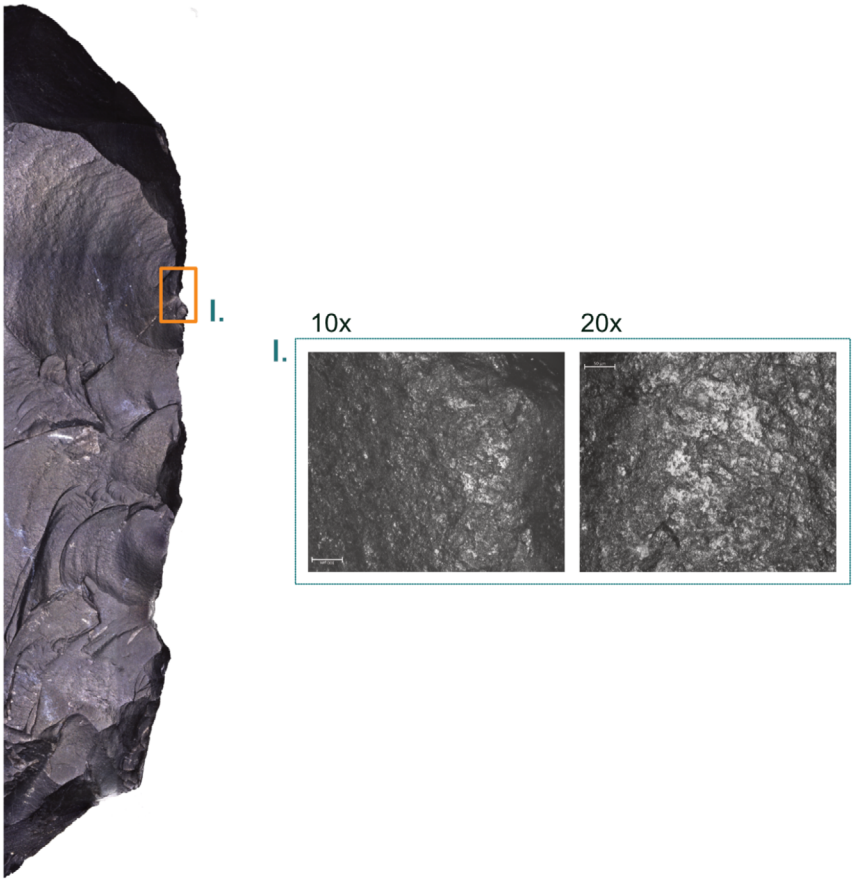

Buhlen, *Keilmesser* [ID BU-076; ventral]. The topmost image displays the artefact in original size. The other illustrations are magnifications acquired with a 1.6× objective and a 34-× zoom. The use-wear trace is acquired at magnification of 10× and 20× (I. type V.).

Plate A28

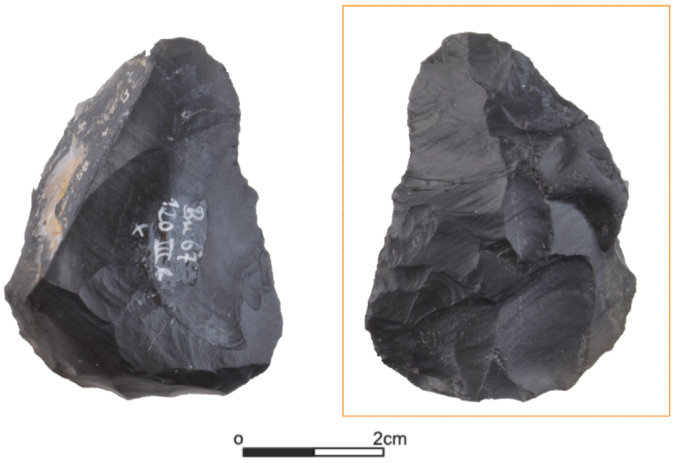

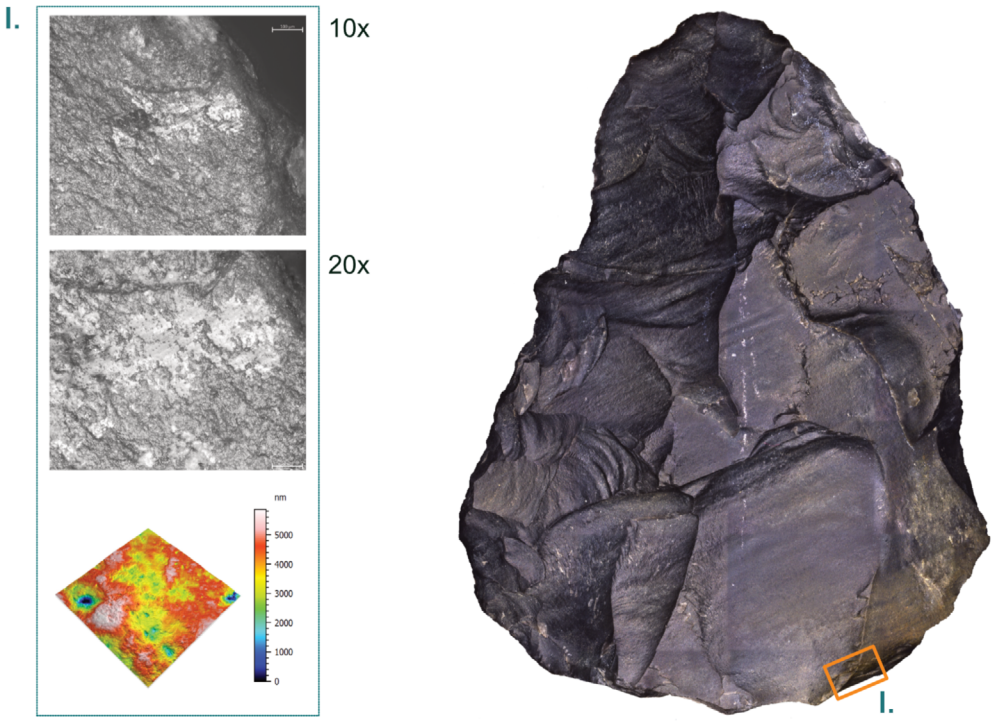

Buhlen, *Keilmesser* [ID BU-077]. The topmost image displays the artefact in original size. The other illustrations are magnifications acquired with a 1.6× objective and a 34-× zoom. The use-wear trace is acquired at magnification of 10× and 20× (I. type V. / IV.). The micro-surface displays the processed result of the confocal data acquisition with the 50× objective.

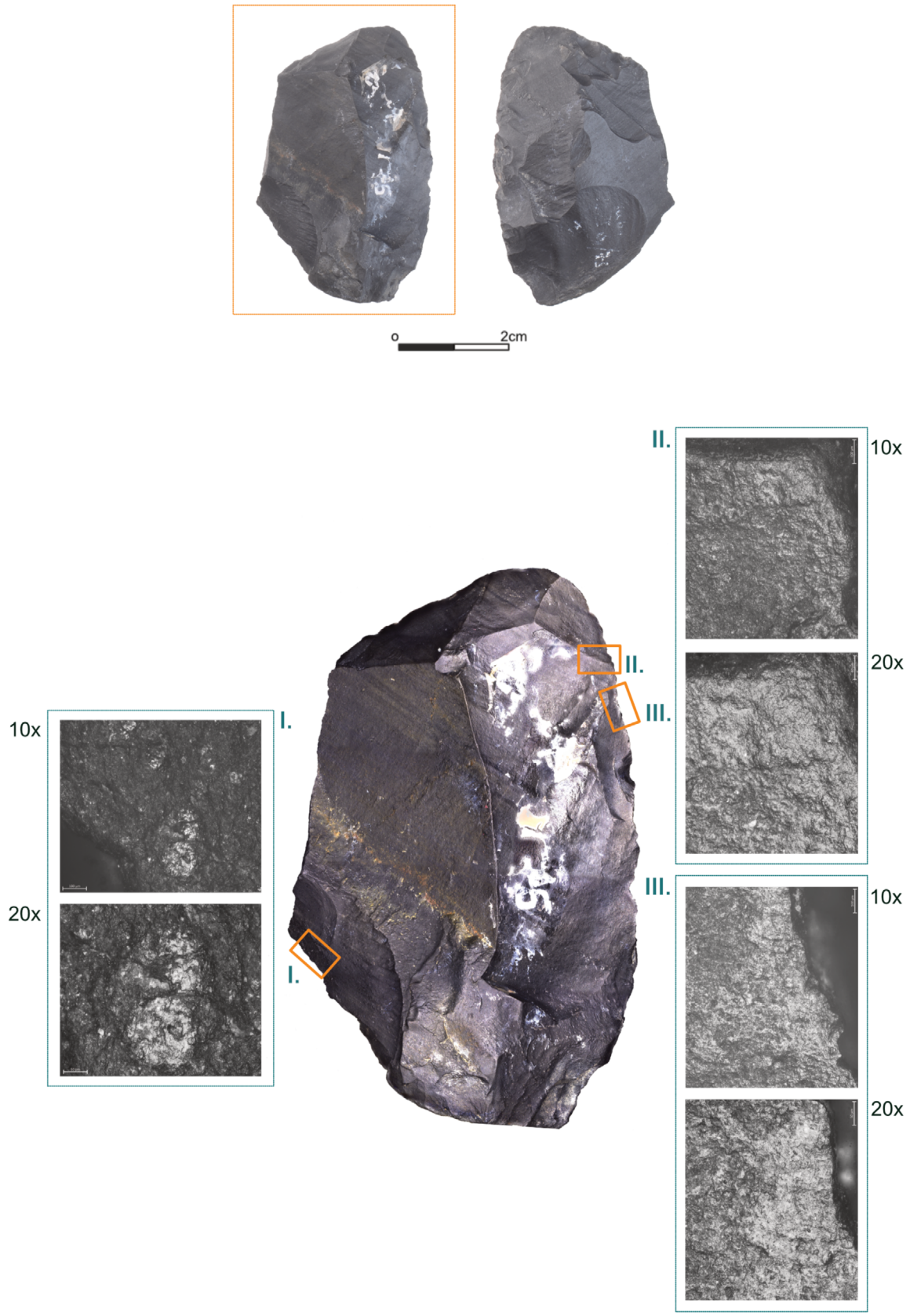

Buhlen, *Keilmesser* [ID BU-078; dorsal]. The topmost image displays the artefact in original size. The other illustrations are magnifications acquired with a 1.6× objective and a 34-× zoom. The use-wear traces are acquired at magnification of 10× and 20× (I. type I.; II. type V.; III. type V.).



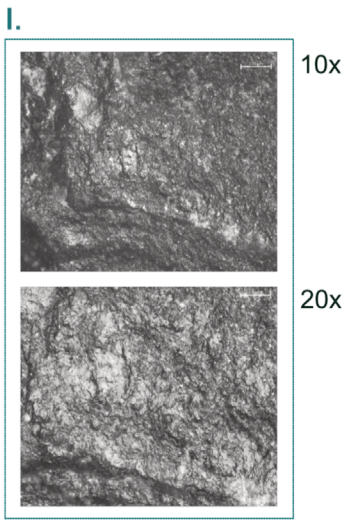



Buhlen, *Keilmesser* [ID BU-078; ventral]. The topmost image displays the artefact in original size. The other illustrations are magnifications acquired with a 1.6× objective and a 34-× zoom. The use-wear trace is acquired at magnification of 10× and 20× (I. type V.).



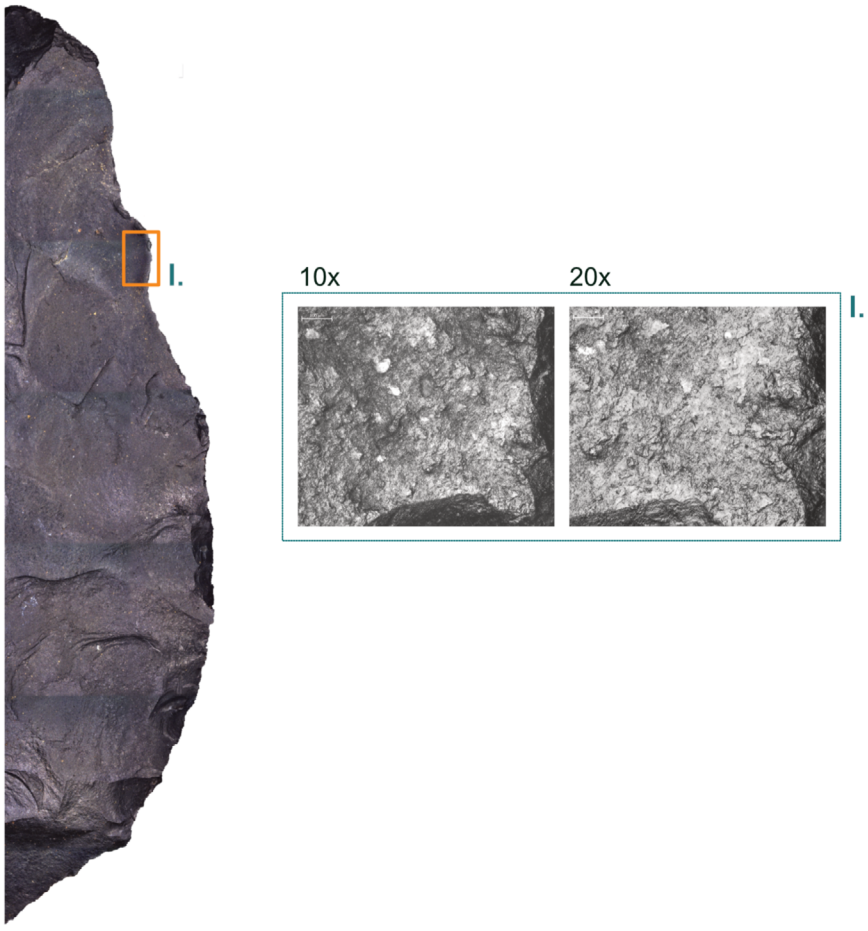

Buhlen, *Keilmesser* [ID BU-079]. The topmost image displays the artefact in original size. The other illustrations are magnifications acquired with a 1.6× objective and a 34-× zoom. The use-wear trace is acquired at magnification of 10× and 20× (I. type V.).

Plate A32

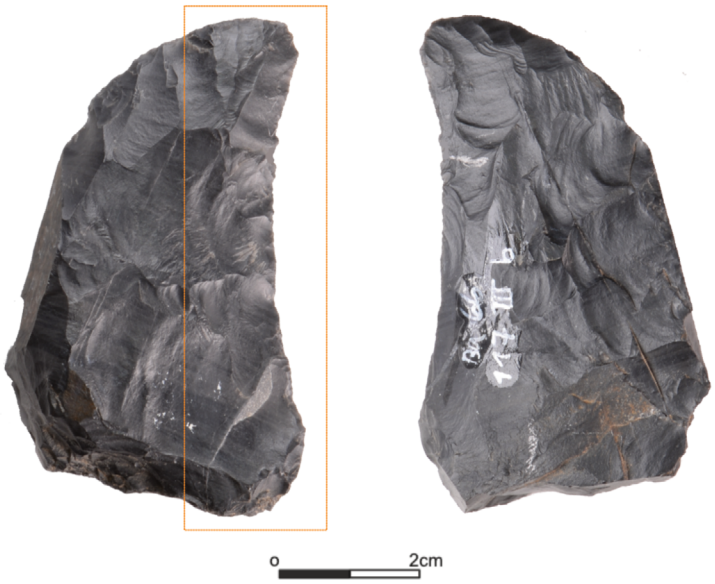

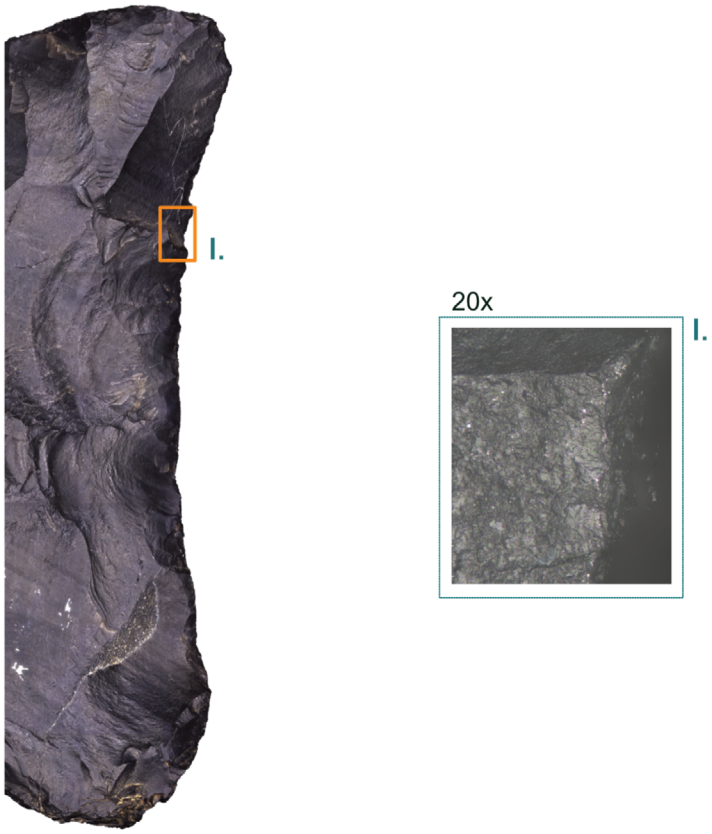

Buhlen, *Keilmesser* [ID BU-160]. The topmost image displays the artefact in original size. The other illustrations are magnifications acquired with a 1.6× objective and a 34-× zoom. The use-wear trace is acquired at magnification of 20× (I. type V.).



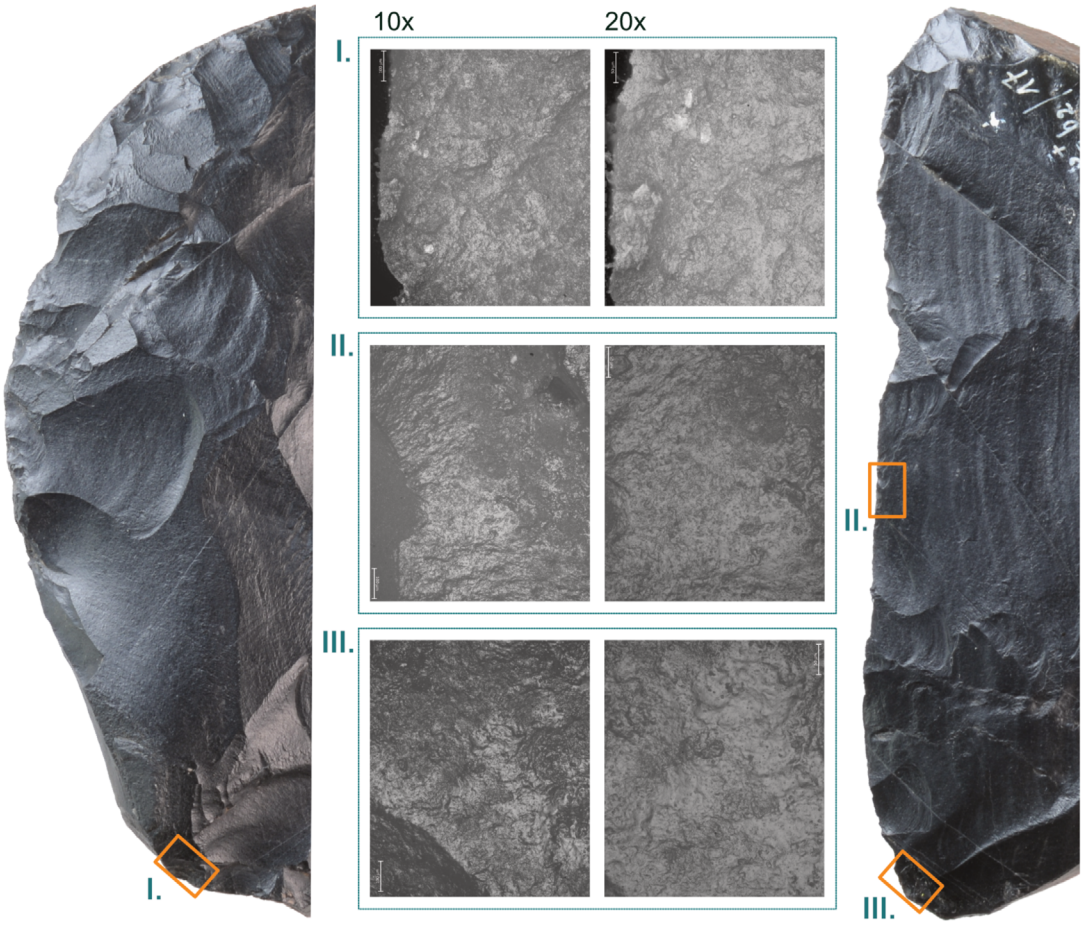

Buhlen, *Keilmesser* [ID BU-163]. The topmost image displays the artefact in original size. The other illustrations are magnifications acquired with a 1.6× objective and a 34-× zoom. The use-wear traces are acquired at magnification of 10× and 20× (I. type V.; II. type I.).

Plate A34



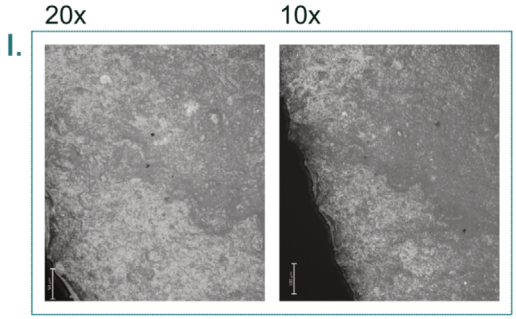



Buhlen, *Keilmesser* [ID BU-158]. The topmost image displays the artefact in original size. The other illustrations are magnifications acquired with a 1.6× objective and a 34-× zoom. The use-wear trace is acquired at magnification of 10× and 20× (I. type V.).

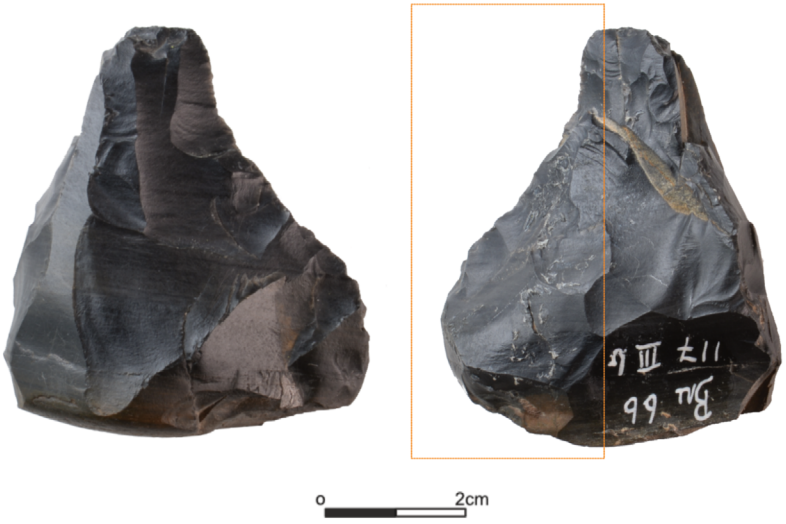

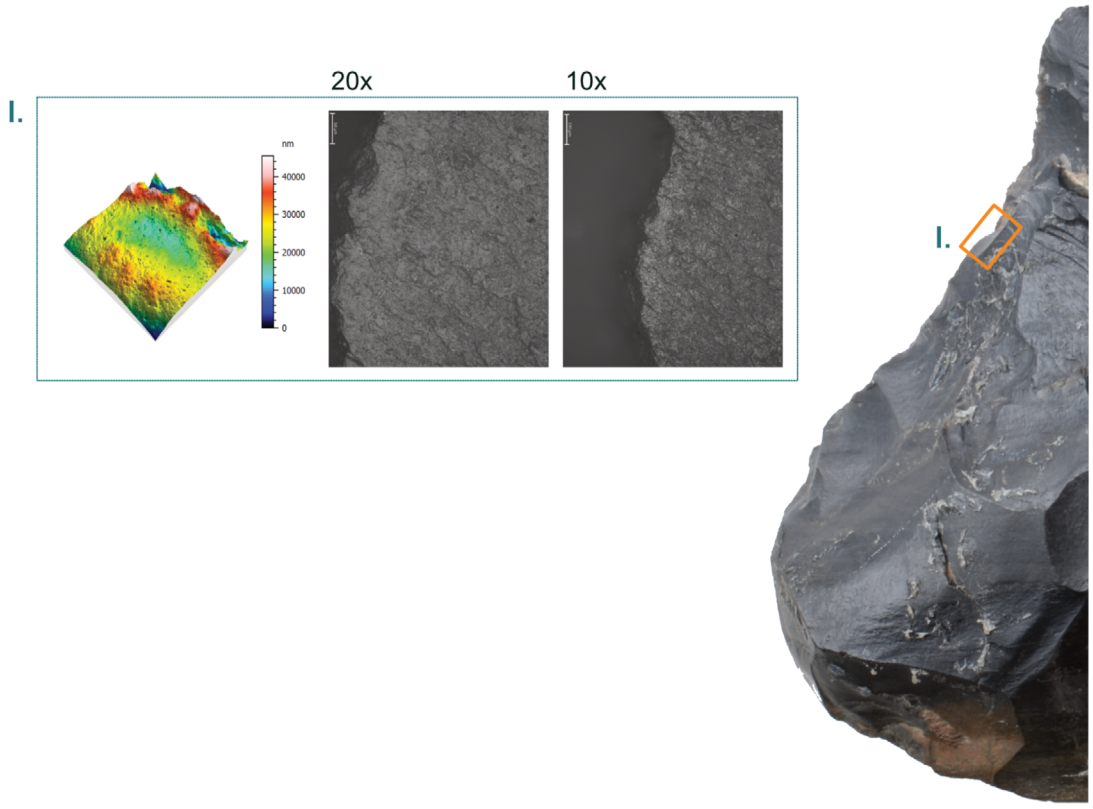

Buhlen, *Keilmesser* [ID BU-173]. The topmost image displays the artefact in original size. The other illustrations are magnifications acquired with a 1.6× objective and a 34-× zoom. The use-wear trace is acquired at magnification of 10× and 20× (I. type V.). The micro-surface displays the processed result of the confocal data acquisition with the 50× objective.

Plate A36





Buhlen, *Keilmesser* [ID BU-174]. The topmost image displays the artefact in original size. The other illustrations are magnifications acquired with a 1.6× objective and a 34-× zoom. The use-wear trace is acquired at magnification of 10× (I. type V.).

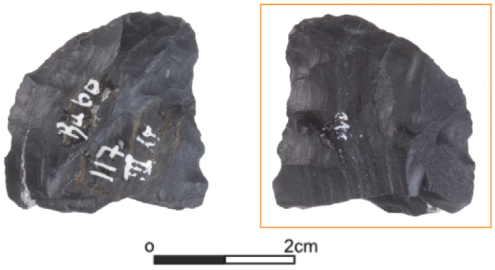

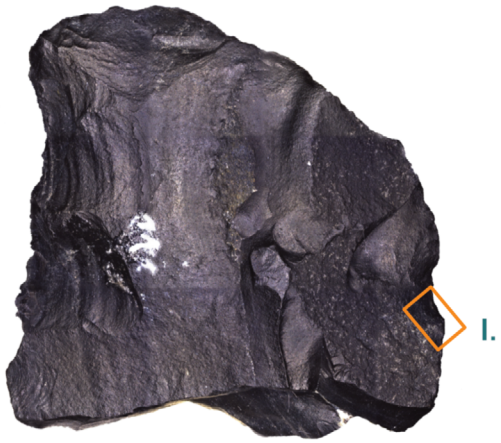

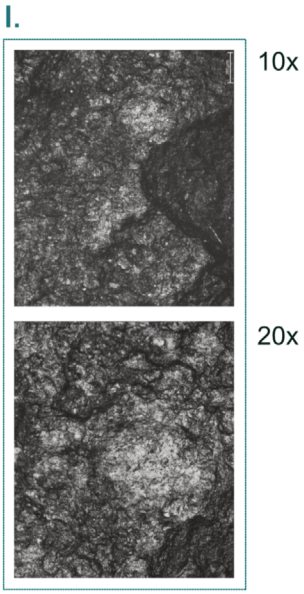

Buhlen, *Keilmesser* tip [ID BU-085]. The topmost image displays the artefact in original size. The other illustrations are magnifications acquired with a 1.6× objective and a 34-× zoom. The use-wear trace is acquired at magnification of 10× and 20× (I. type V.).

Plate A38

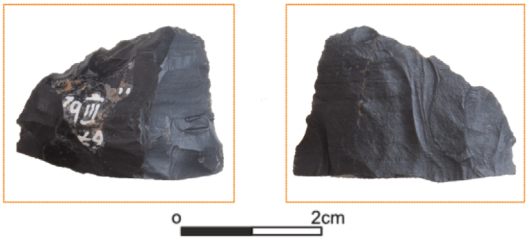

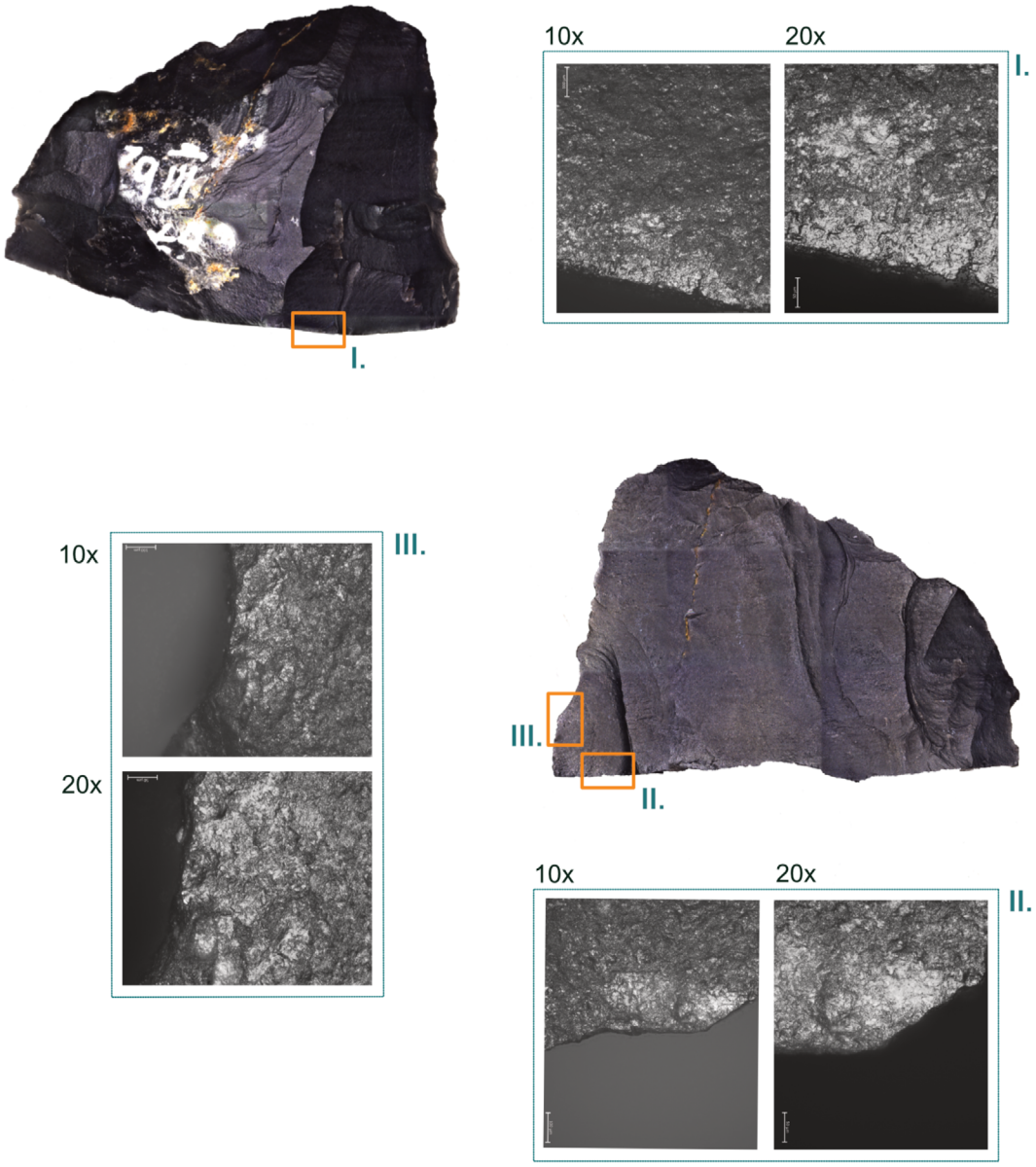

Buhlen, *Keilmesser* tip [ID BU-086]. The topmost image displays the artefact in original size. The other illustrations are magnifications acquired with a 1.6× objective and a 34-× zoom. The use-wear traces are acquired at magnification of 10× and 20× (I. type V.; II. type V.; III. type V.).

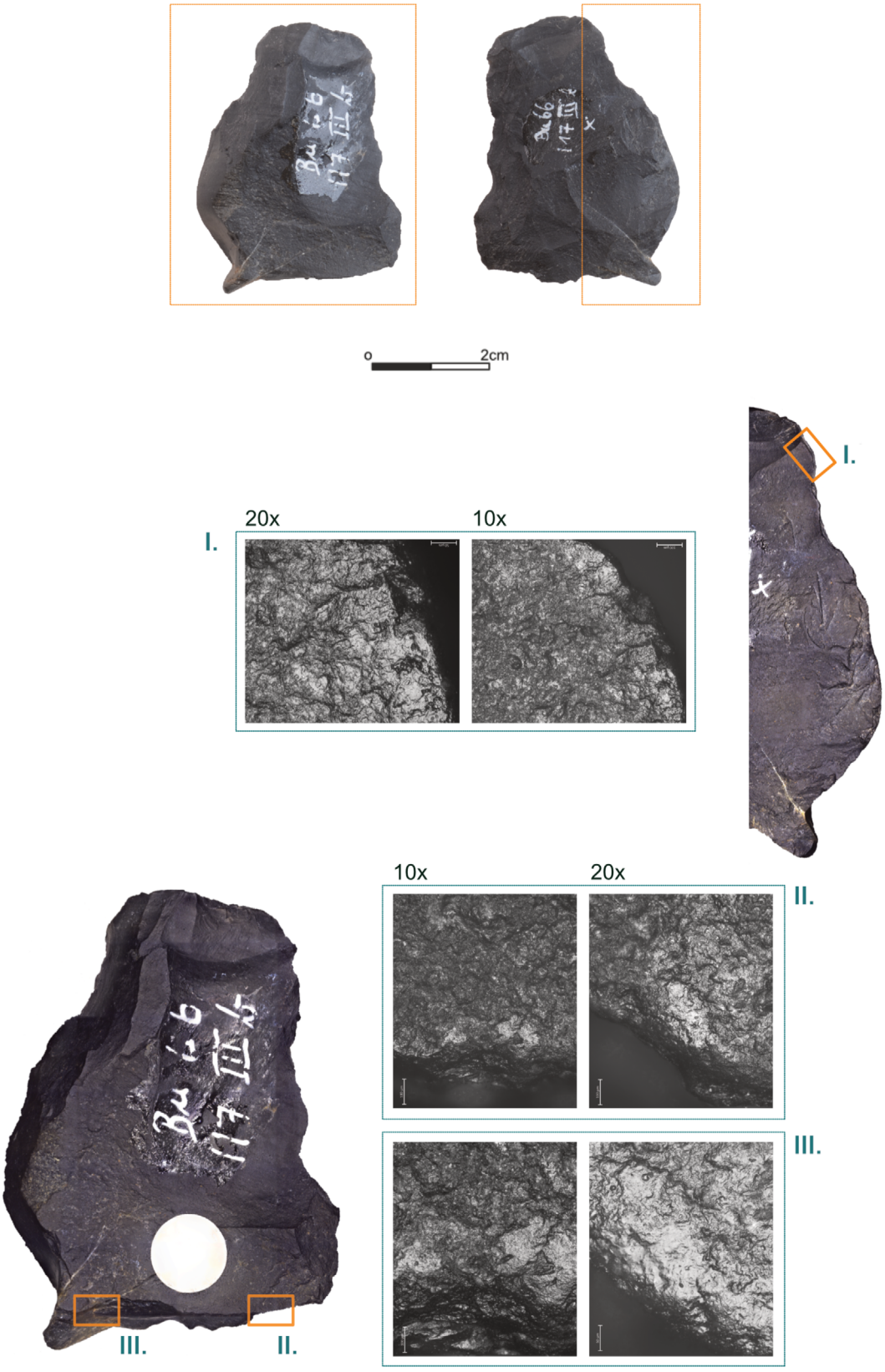

Buhlen, *Keilmesser* tip [ID BU-087]. The topmost image displays the artefact in original size. The other illustrations are magnifications acquired with a 1.6× objective and a 34-× zoom. The use-wear traces are acquired at magnification of 10× and 20× (I. type V.; II. type V.; III. type V.).

Plate A40

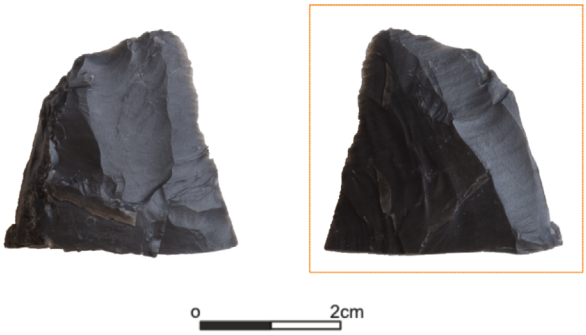

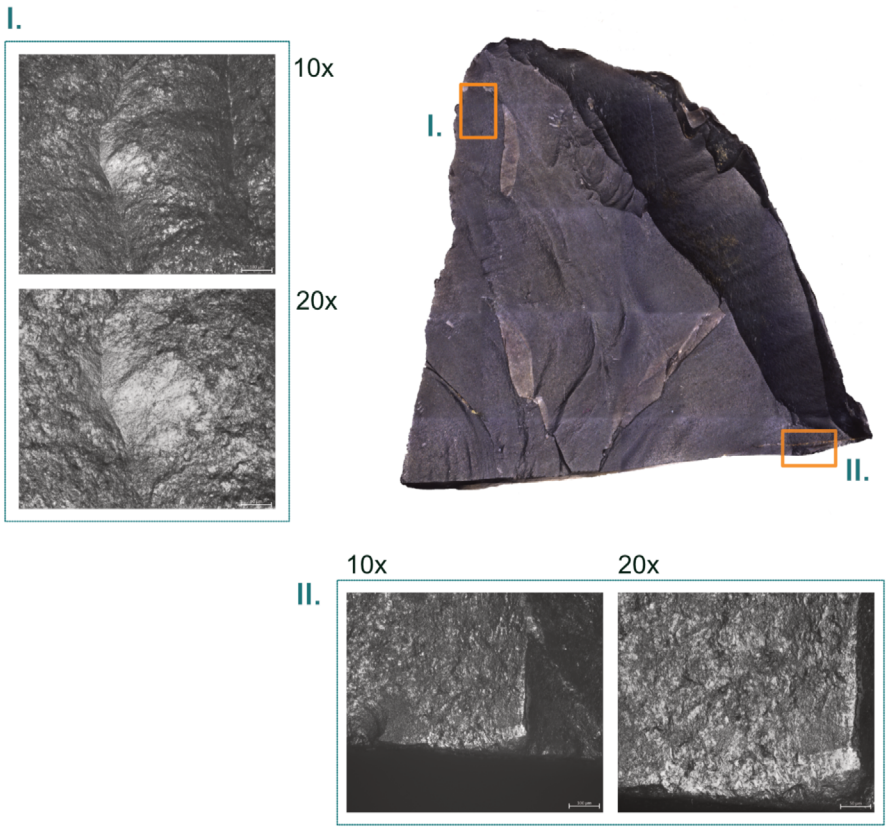

Buhlen, *Keilmesser* tip [ID BU-088]. The topmost image displays the artefact in original size. The other illustrations are magnifications acquired with a 1.6× objective and a 34-× zoom. The use-wear traces are acquired at magnification of 10× and 20× (I. type V.; II. type IV.).

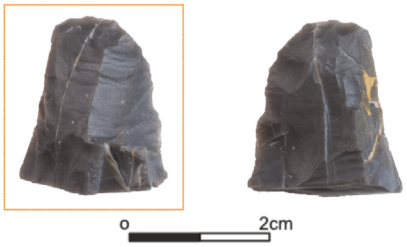

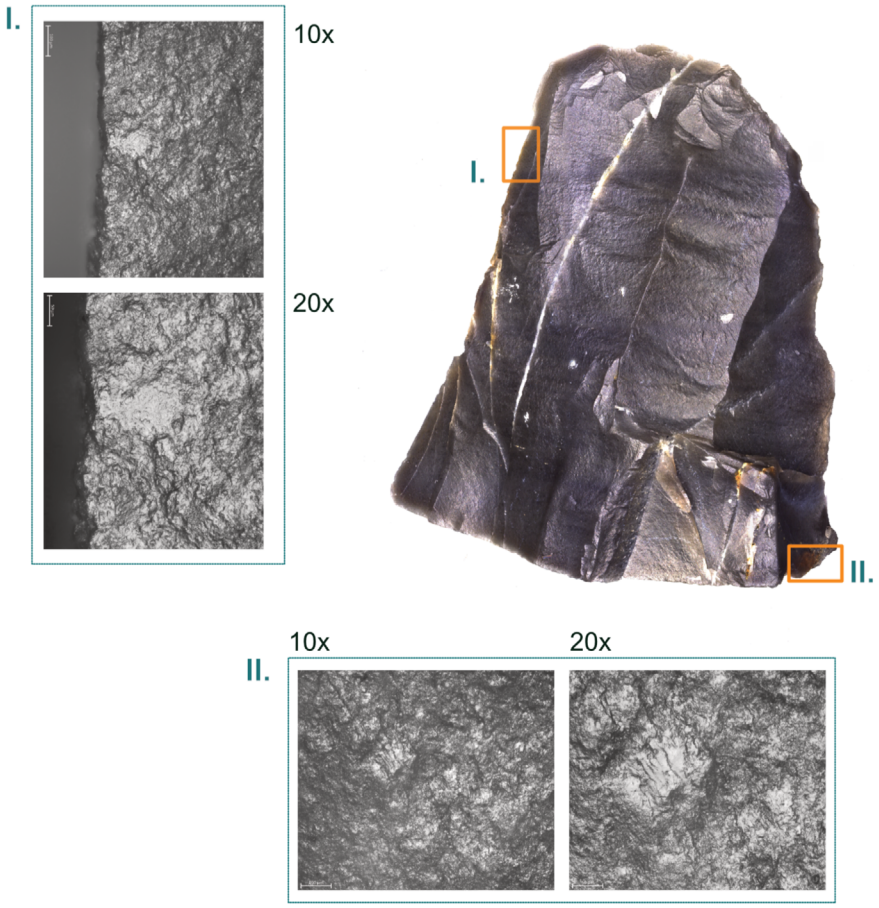

Buhlen, *Keilmesser* tip [ID BU-090]. The topmost image displays the artefact in original size. The other illustrations are magnifications acquired with a 1.6× objective and a 34-× zoom. The use-wear traces are acquired at magnification of 10× and 20× (I. type I.; II. type V.).

Plate A42



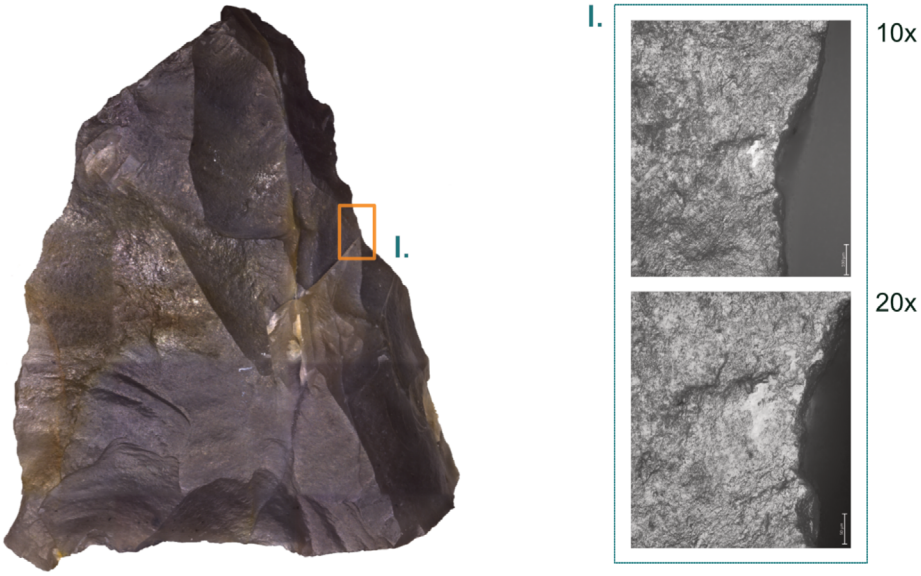

Buhlen, *Keilmesser* tip [ID BU-093]. The topmost image displays the artefact in original size. The other illustrations are magnifications acquired with a 1.6× objective and a 34-× zoom. The use-wear trace is acquired at magnification of 10× and 20× (I. type I.).

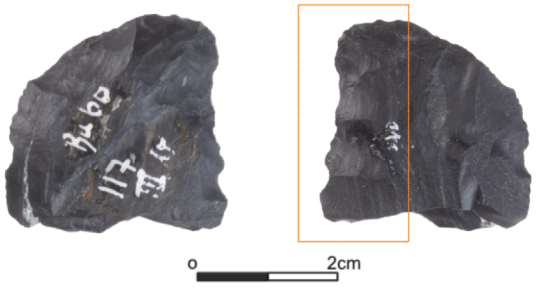

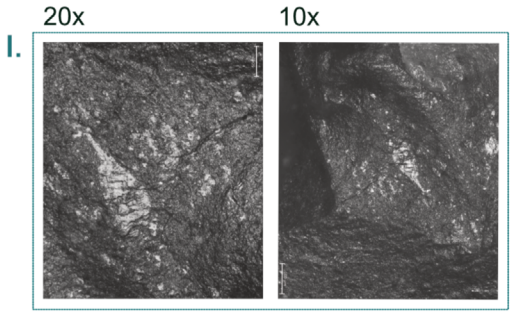



Buhlen, *Keilmesser* tip [ID BU-097]. The topmost image displays the artefact in original size. The other illustrations are magnifications acquired with a 1.6× objective and a 34-× zoom. The use-wear trace is acquired at magnification of 10× and 20× (I. type I.).

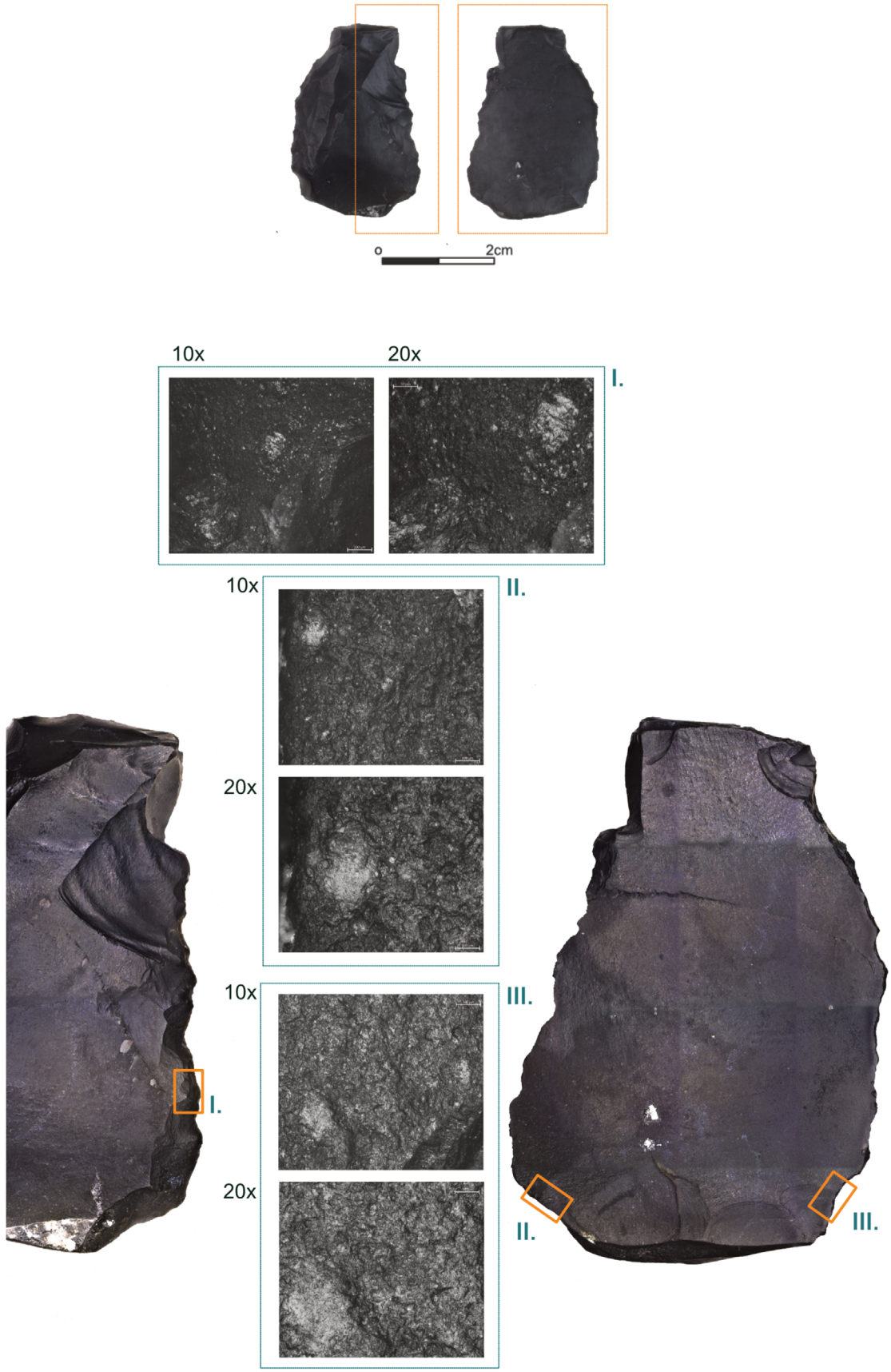

Buhlen, *Prądnik scraper* [ID BU-099]. The topmost image displays the artefact in original size. The other illustrations are magnifications acquired with a 1.6× objective and a 34-× zoom. The use-wear traces are acquired at magnification of 10× and 20× (I. type I.; II. type I. III. type I.).

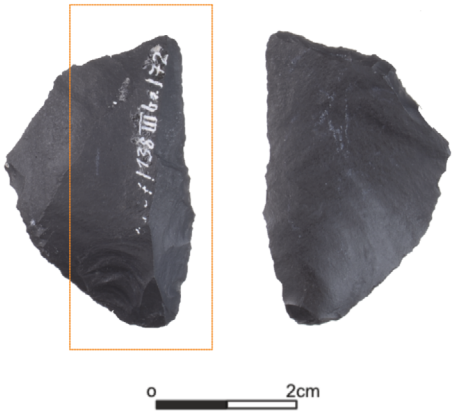

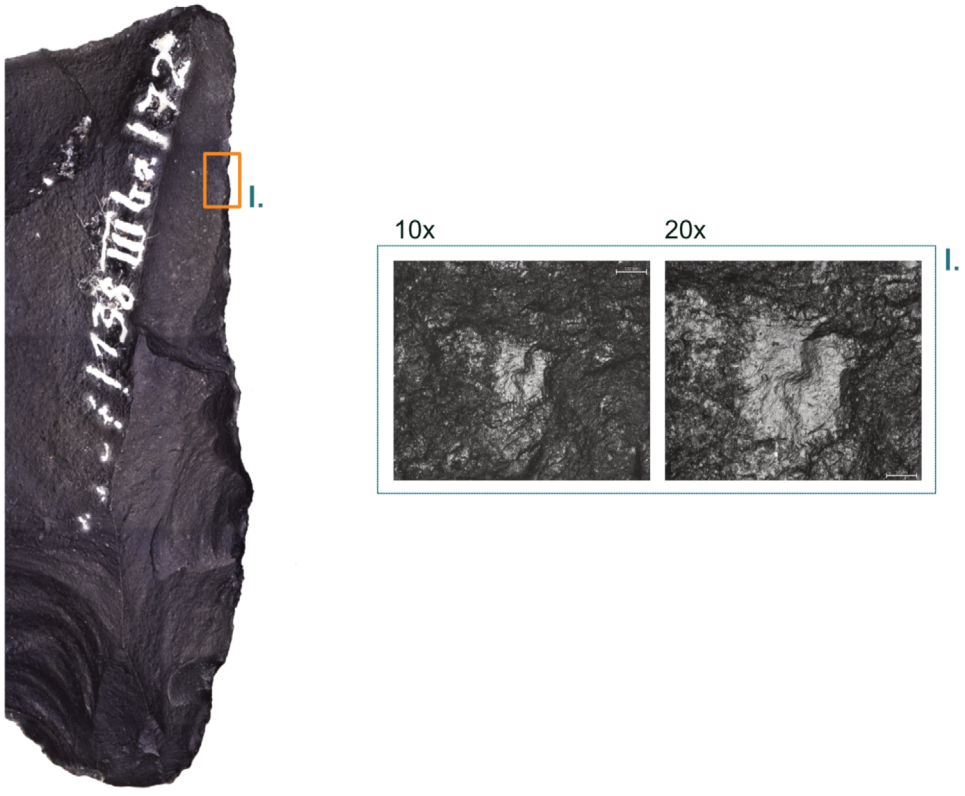

Buhlen, *Prądnik scraper* [ID BU-100]. The topmost image displays the artefact in original size. The other illustrations are magnifications acquired with a 1.6× objective and a 34-× zoom. The use-wear trace is acquired at magnification of 10× and 20× (I. type I.).



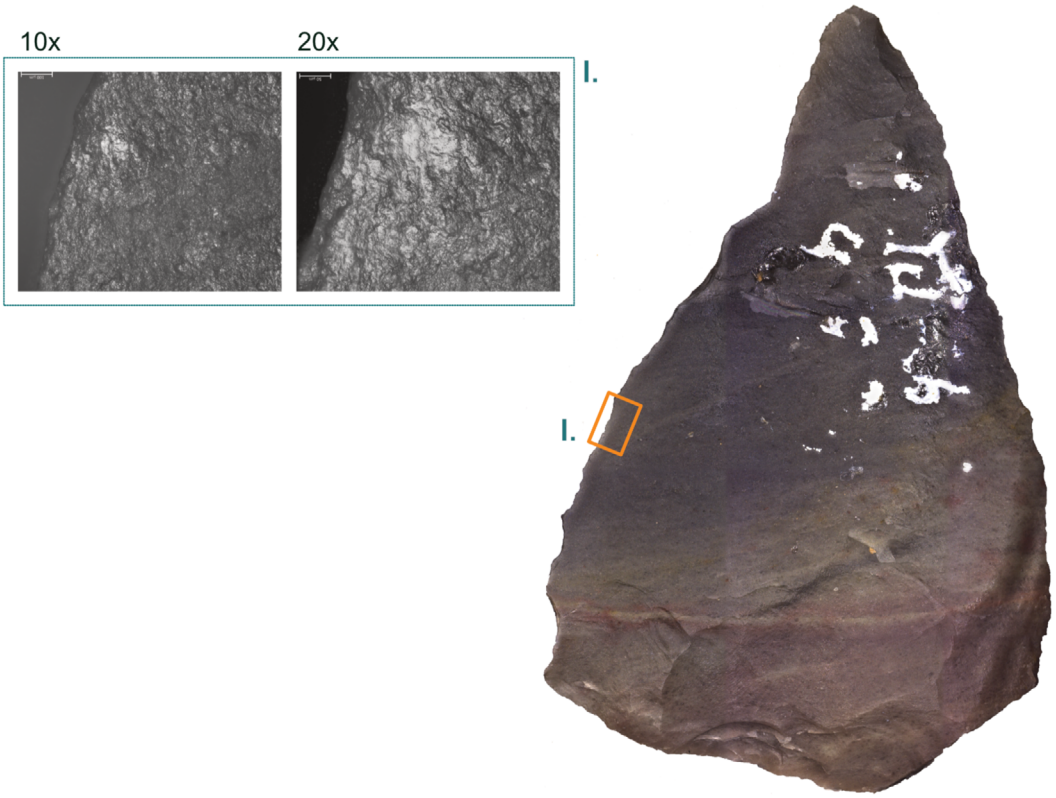

Buhlen, *Prądnik scraper* [ID BU-101]. The topmost image displays the artefact in original size. The other illustrations are magnifications acquired with a 1.6× objective and a 34-× zoom. The use-wear trace is acquired at magnification of 10× and 20× (I. type V.).

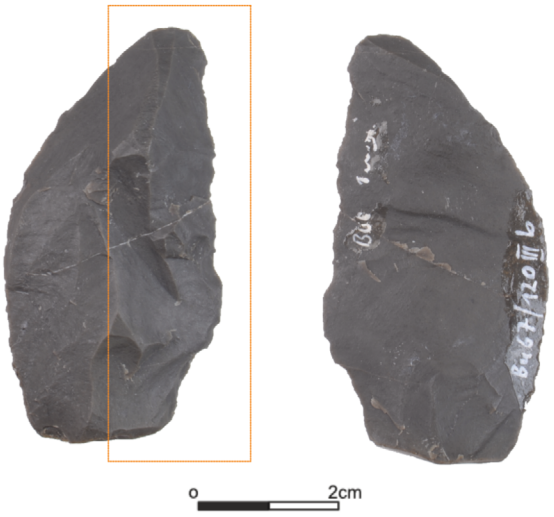

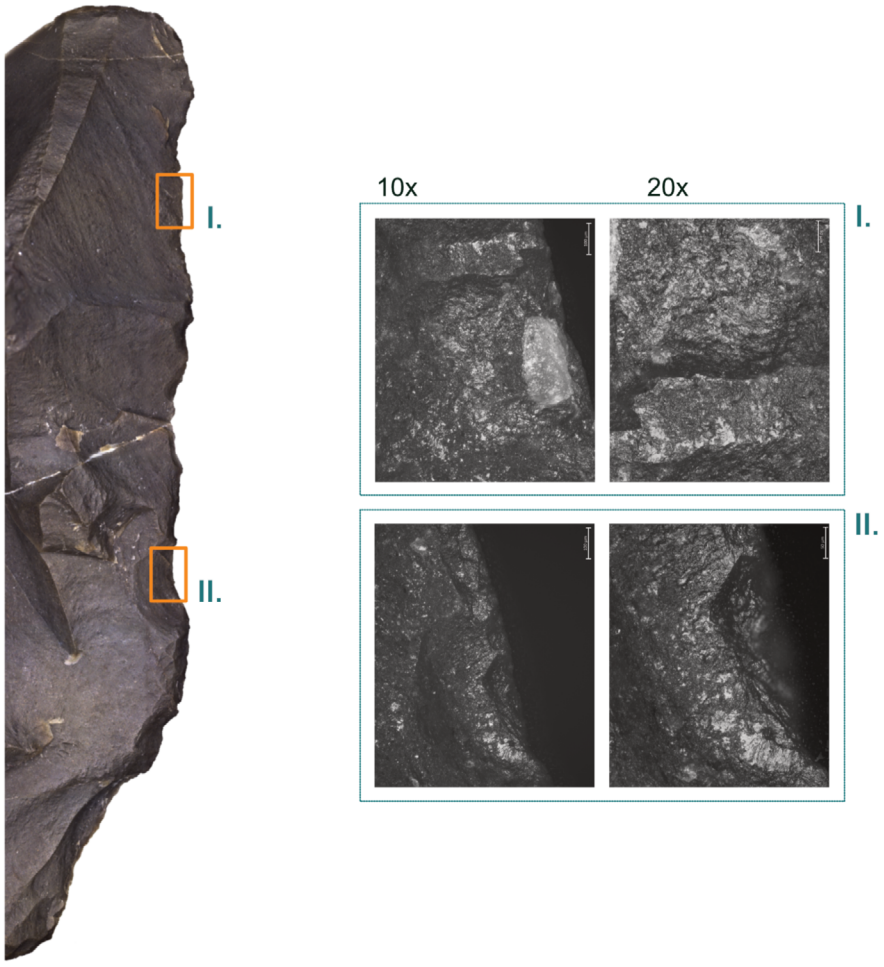

Buhlen, *Prądnik scraper* [ID BU-103]. The topmost image displays the artefact in original size. The other illustrations are magnifications acquired with a 1.6× objective and a 34-× zoom. The use-wear traces are acquired at magnification of 10× and 20× (I. type V.; II. type V.).

Plate A48

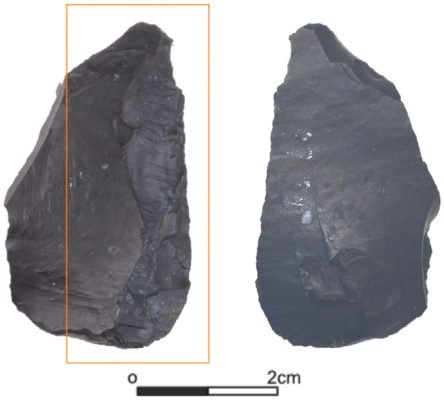

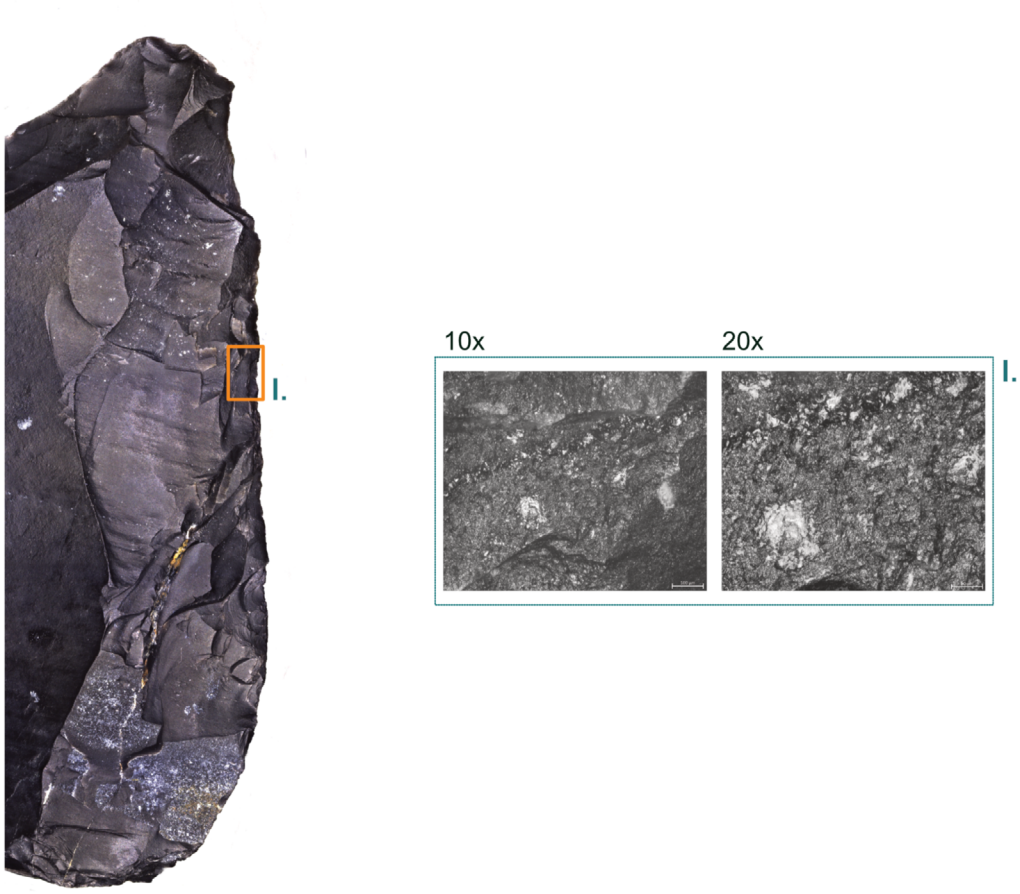

Buhlen, *Prądnik scraper* [ID BU-104]. The topmost image displays the artefact in original size. The other illustrations are magnifications acquired with a 1.6× objective and a 34-× zoom. The use-wear trace is acquired at magnification of 10× and 20× (I. type I.).

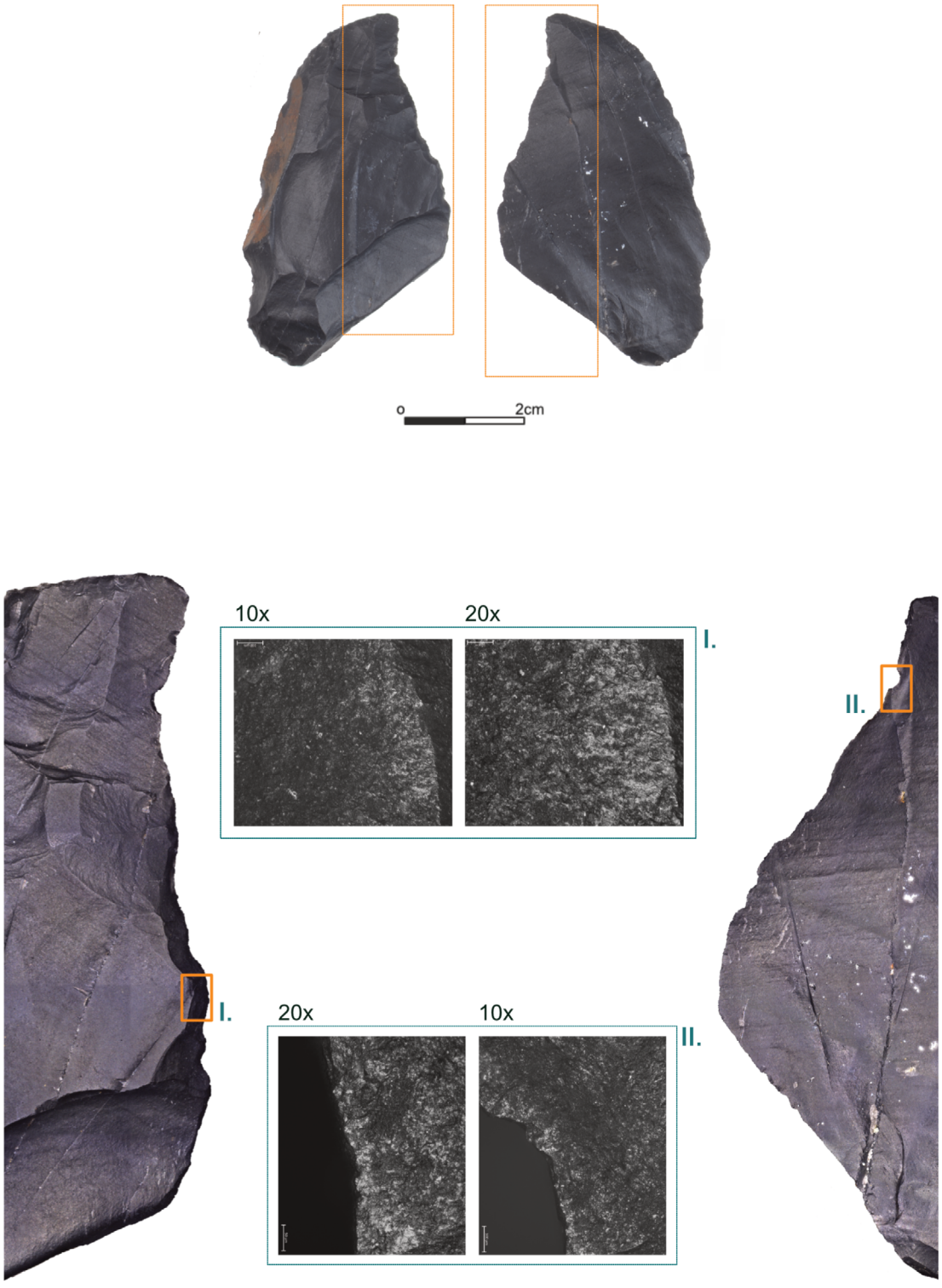

Buhlen, *Prądnik scraper* [ID BU-105]. The topmost image displays the artefact in original size. The other illustrations are magnifications acquired with a 1.6× objective and a 34-× zoom. The use-wear traces are acquired at magnification of 10× and 20× (I. type V.; II. type V.).

Plate A50

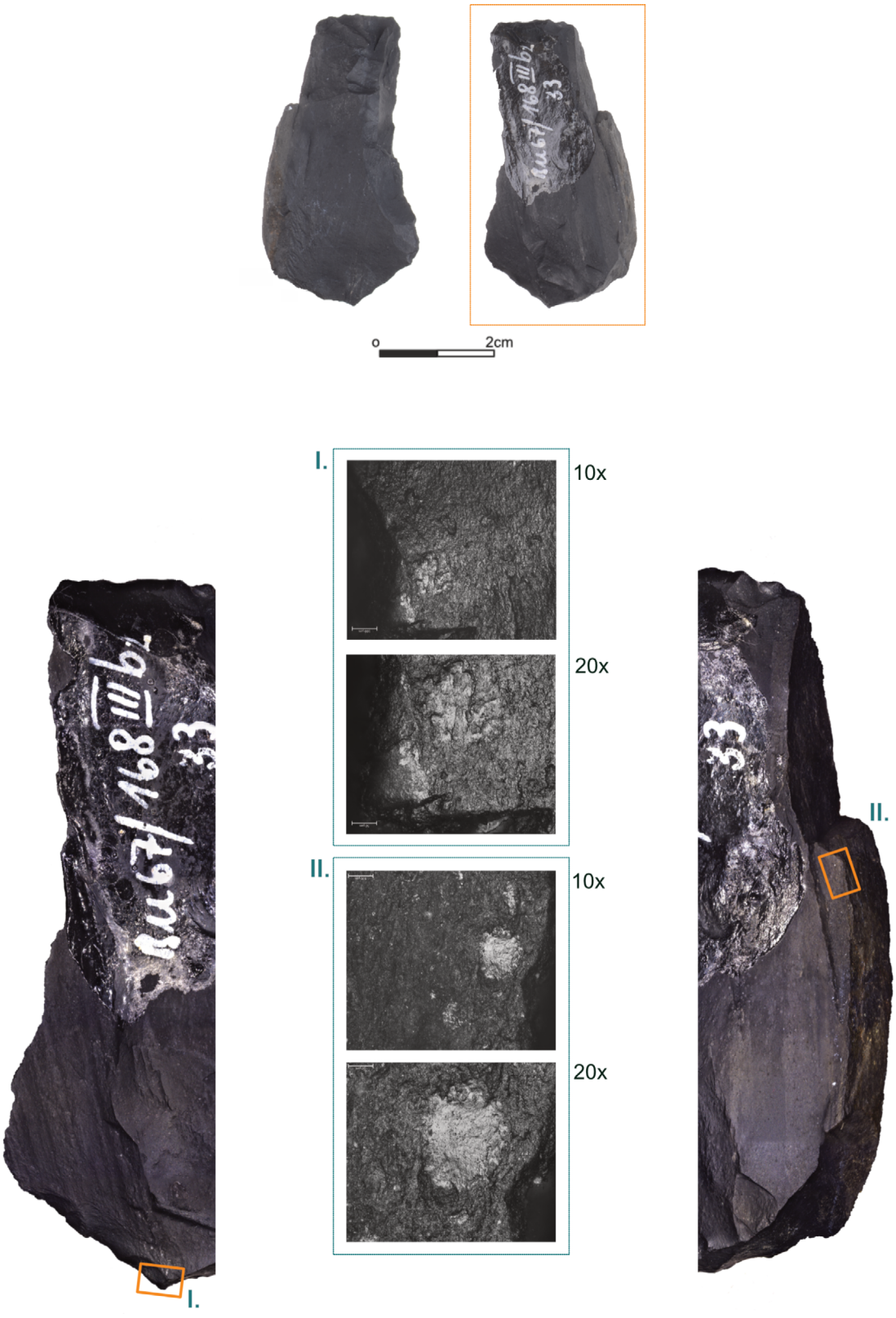

Buhlen, *Prądnik scraper* [ID BU-106]. The topmost image displays the artefact in original size. The other illustrations are magnifications acquired with a 1.6× objective and a 34-× zoom. The use-wear traces are acquired at magnification of 10× and 20× (I. type I.; II. type V.).

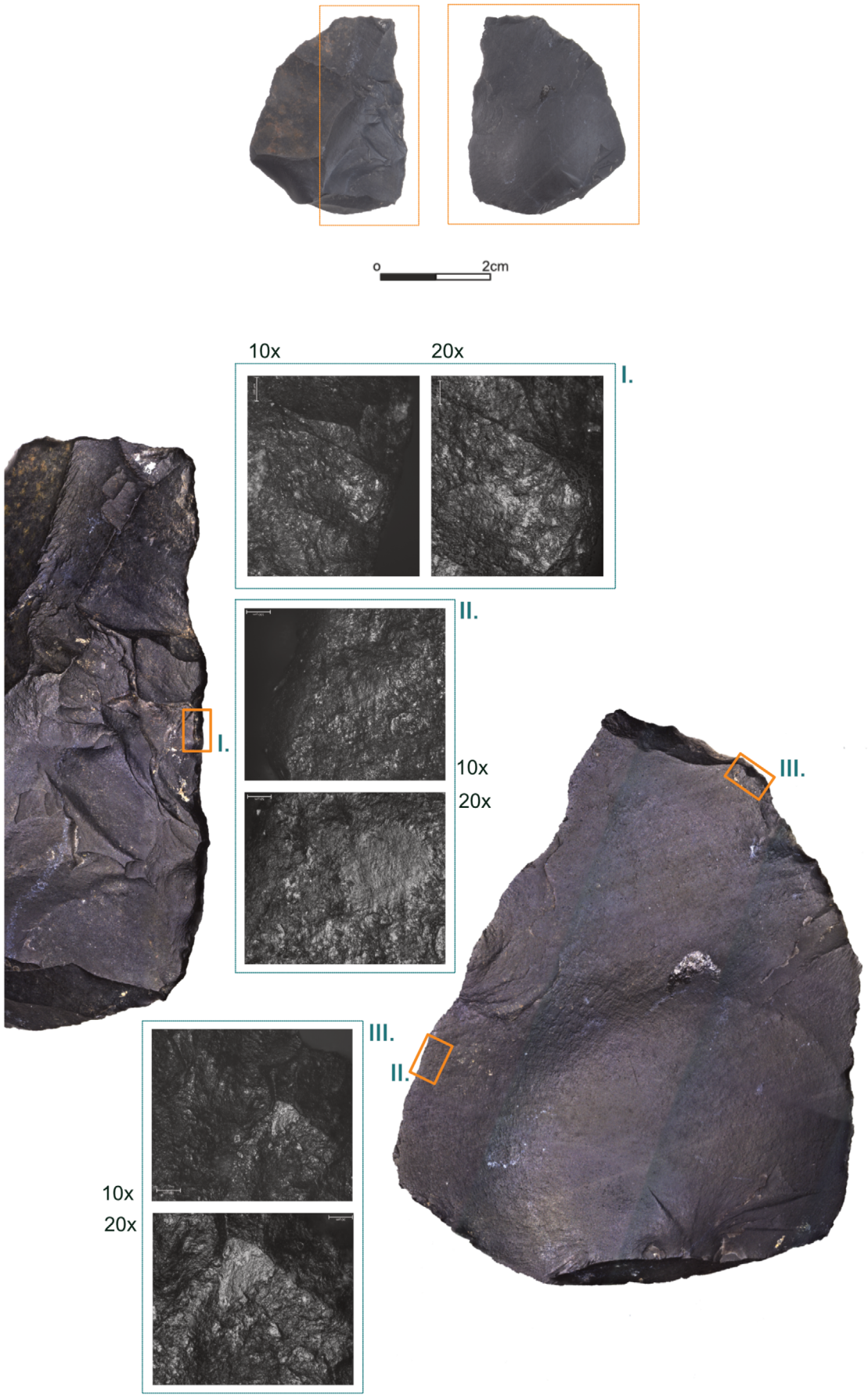

Buhlen, *Prądnik scraper* [ID BU-107]. The topmost image displays the artefact in original size. The other illustrations are magnifications acquired with a 1.6× objective and a 34-× zoom. The use-wear traces are acquired at magnification of 10× and 20× (I. type V.; II. type IX.; III. type V.).

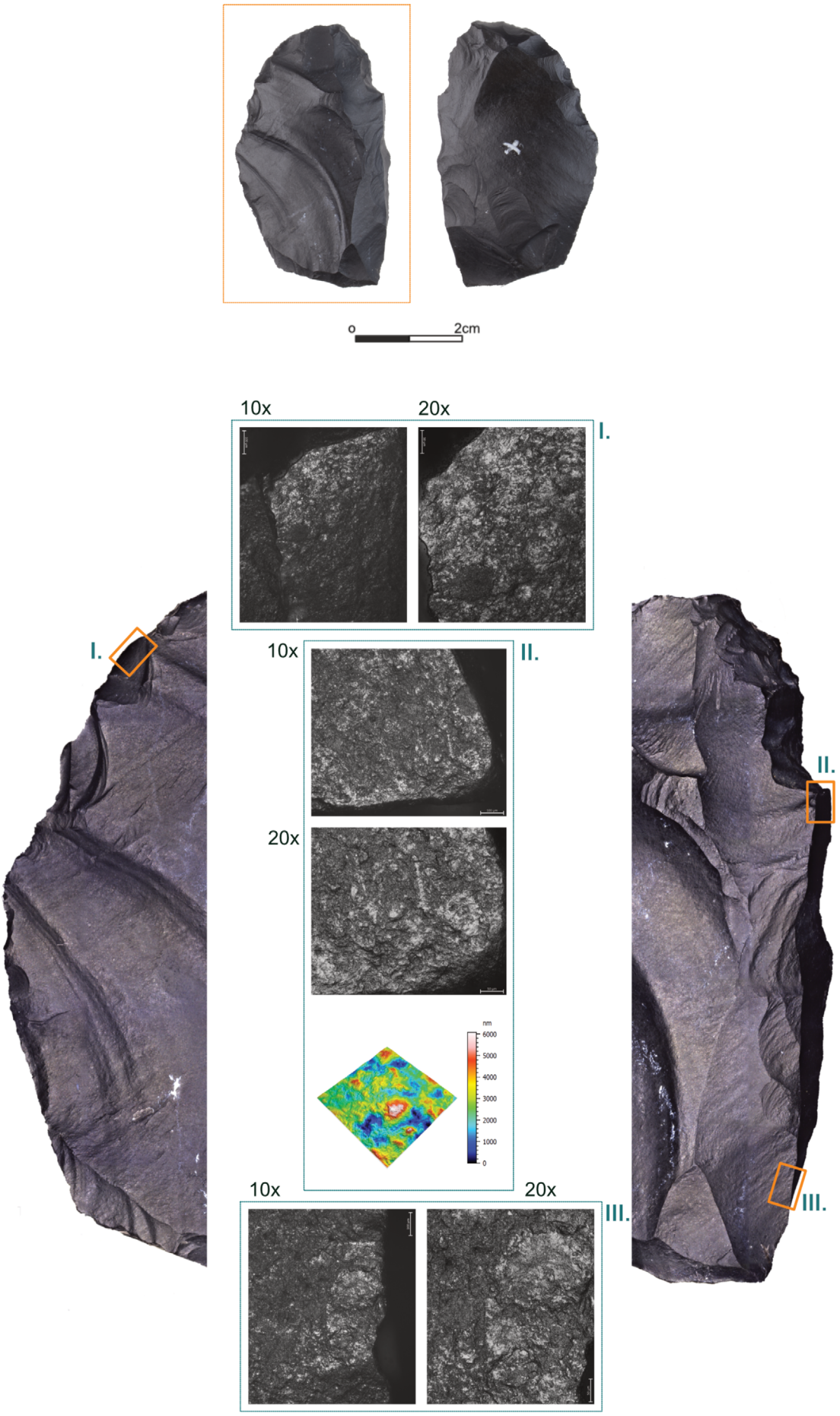

Buhlen, *Prądnik scraper* [ID BU-115; dorsal]. The topmost image displays the artefact in original size. The other illustrations are magnifications acquired with a 1.6× objective and a 34-× zoom. The use-wear traces are acquired at magnification of 10× and 20× (I. type V.; II. type V.; III. type V.).

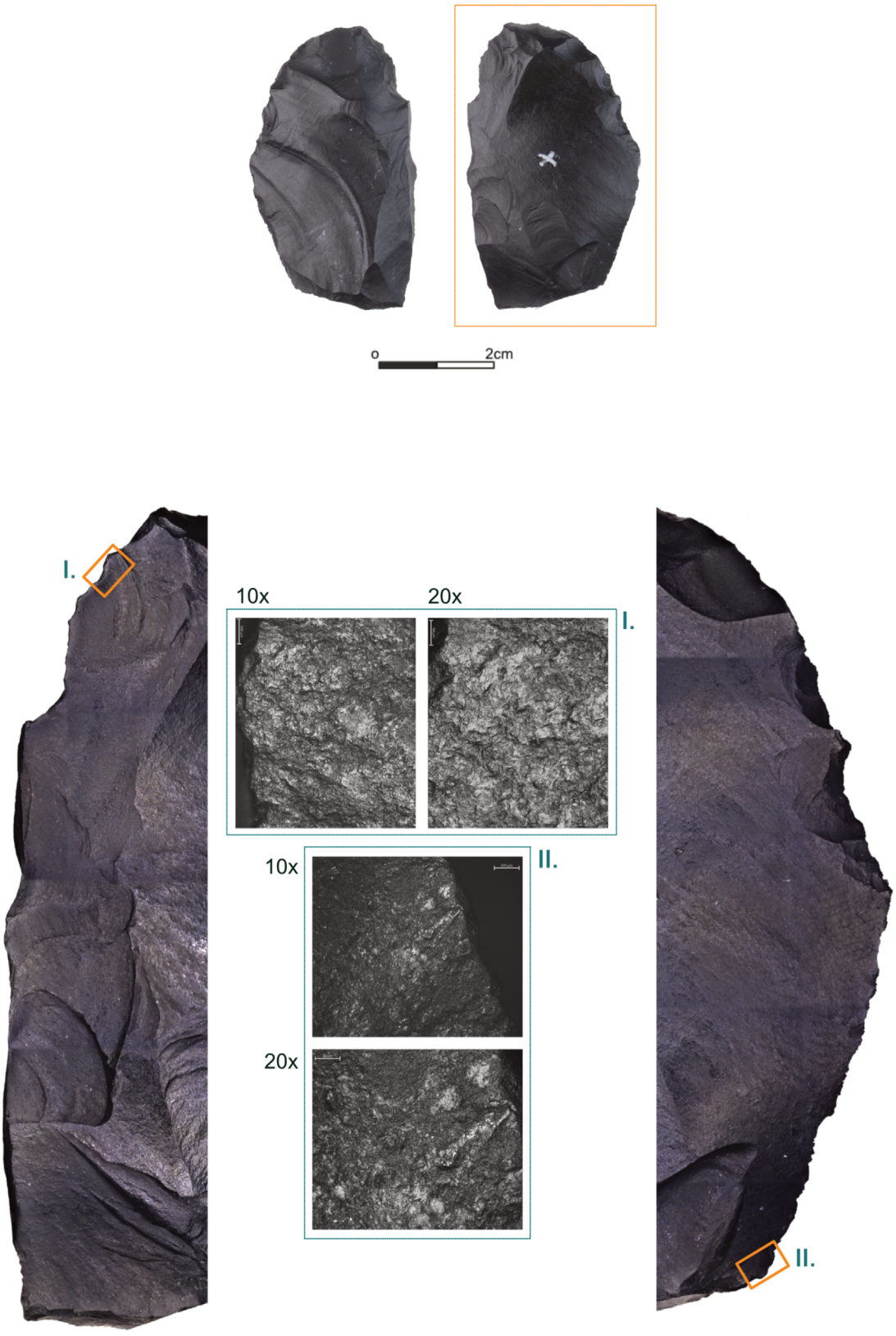

Buhlen, *Prądnik scraper* [ID BU-115; ventral]. The topmost image displays the artefact in original size. The other illustrations are magnifications acquired with a 1.6× objective and a 34-× zoom. The use-wear traces are acquired at magnification of 10× and 20× (I. type V.; II. type V.).

Plate A54

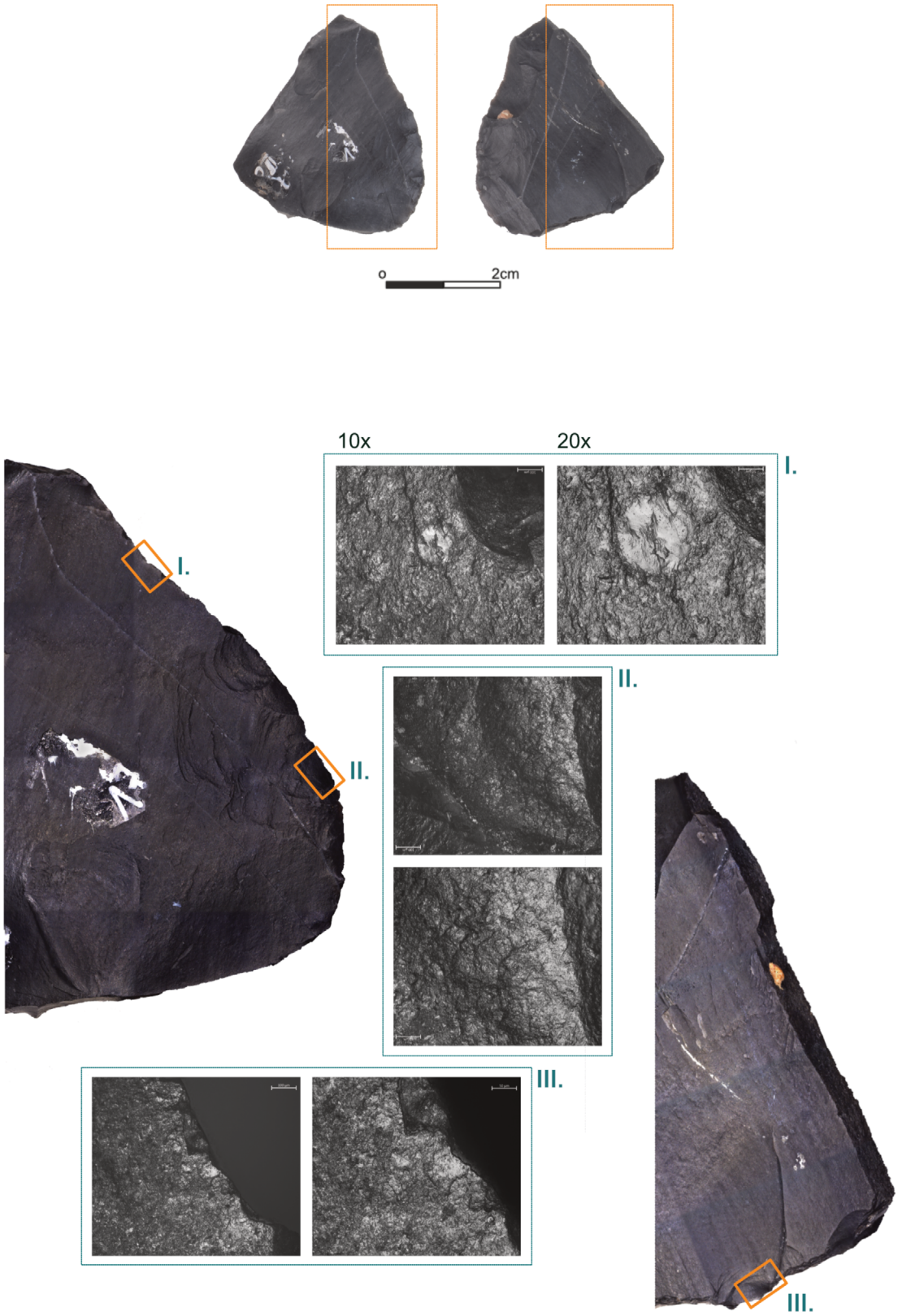

Buhlen, *Prądnik scraper* [ID BU-117]. The topmost image displays the artefact in original size. The other illustrations are magnifications acquired with a 1.6× objective and a 34-× zoom. The use-wear traces are acquired at magnification of 10× and 20× (I. type I.; II. type V.; III. type V.).

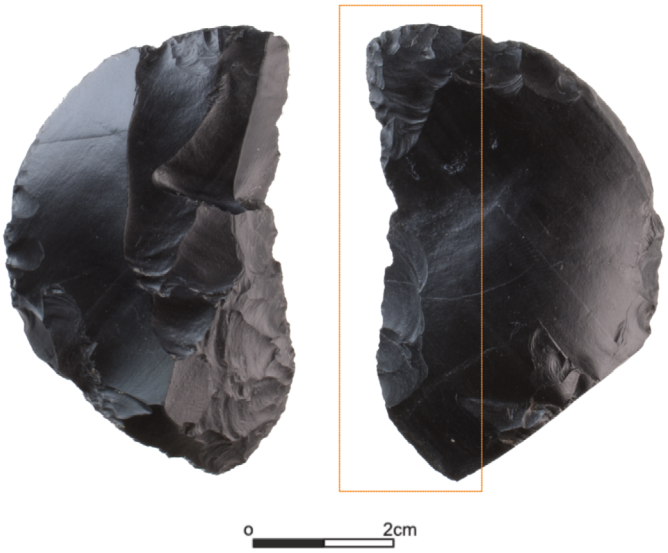

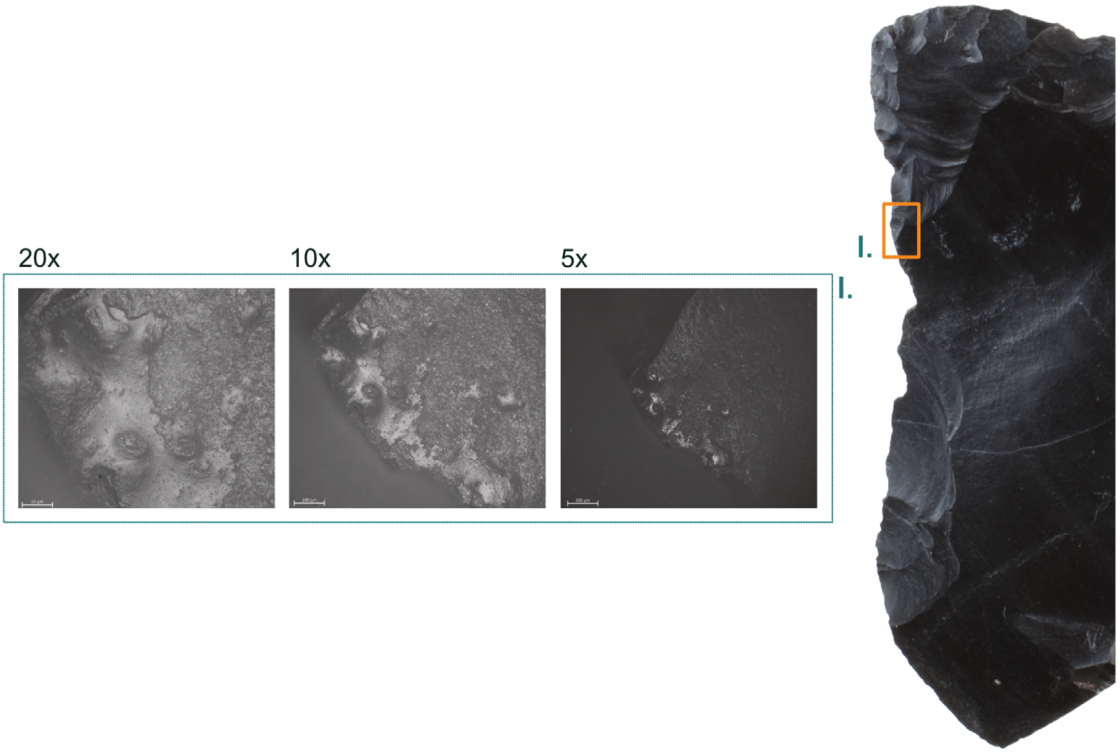

Buhlen, *Prądnik scraper* [ID BU-194]. The topmost image displays the artefact in original size. The other illustrations are magnifications acquired with a 1.6× objective and a 34-× zoom. The use-wear trace is acquired at magnification of 5×, 10× and 20× (I. type VI.).

Plate A56

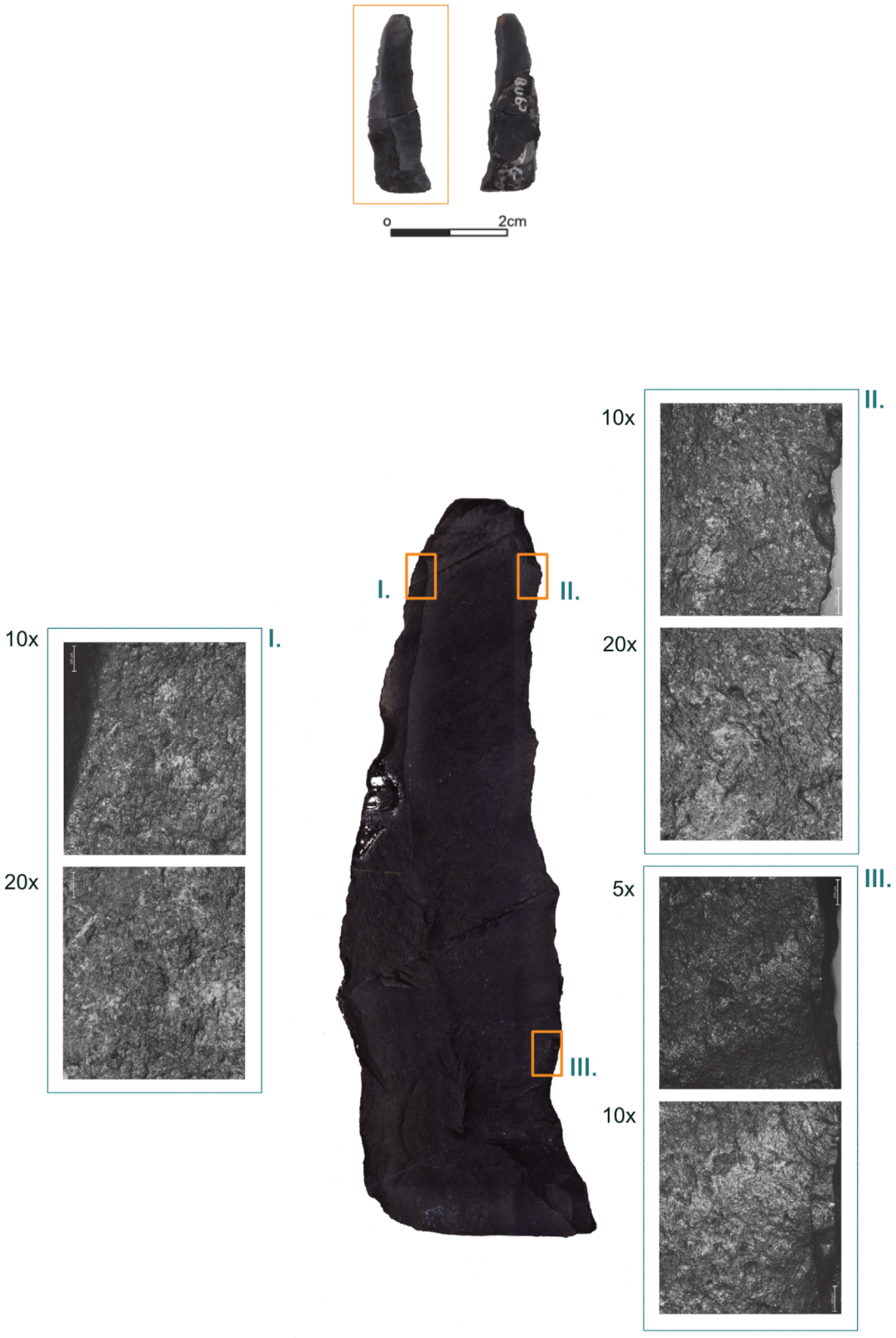

Buhlen, *Prądnik spall* [ID BU-121]. The topmost image displays the artefact in original size. The other illustrations are magnifications acquired with a 1.6× objective and a 34-× zoom. The use-wear traces are acquired at magnification of 5×, 10× and 20× (I. type V.; II. type V.; III. type V.).

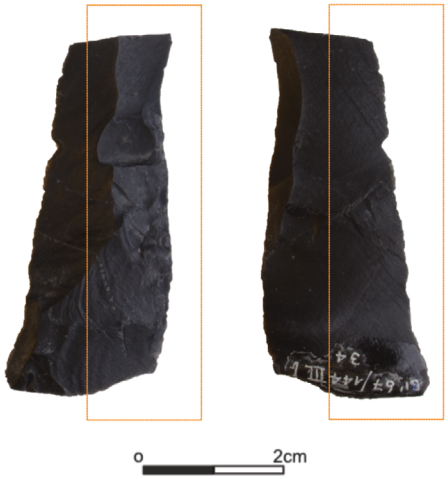

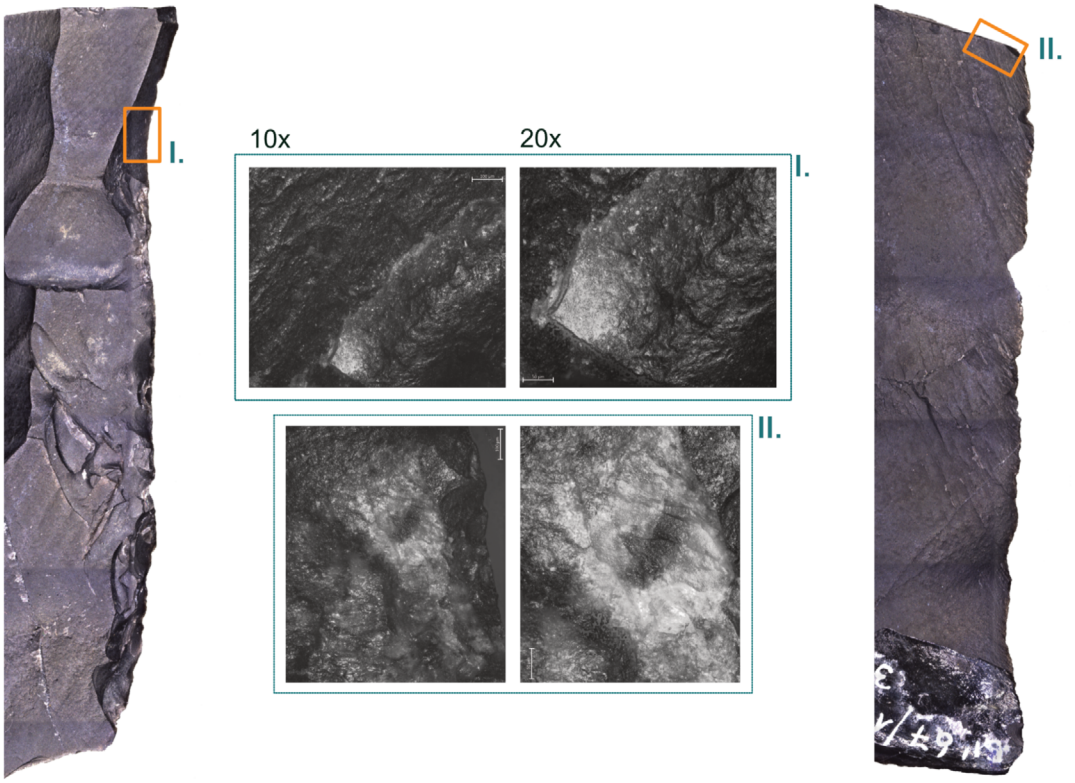

Buhlen, *Prądnik spall* [ID BU-124]. The topmost image displays the artefact in original size. The other illustrations are magnifications acquired with a 1.6× objective and a 34-× zoom. The use-wear traces are acquired at magnification of 10× and 20× (I. type V.; II. type V.).

Plate A58



Buhlen, *Prądnik spall* [ID BU-127]. The topmost image displays the artefact in original size. The other illustrations are magnifications acquired with a 1.6× objective and a 34-× zoom. The use-wear traces are acquired at magnification of 10× and 20× (I. type V.; II. type V.; III. type V.).

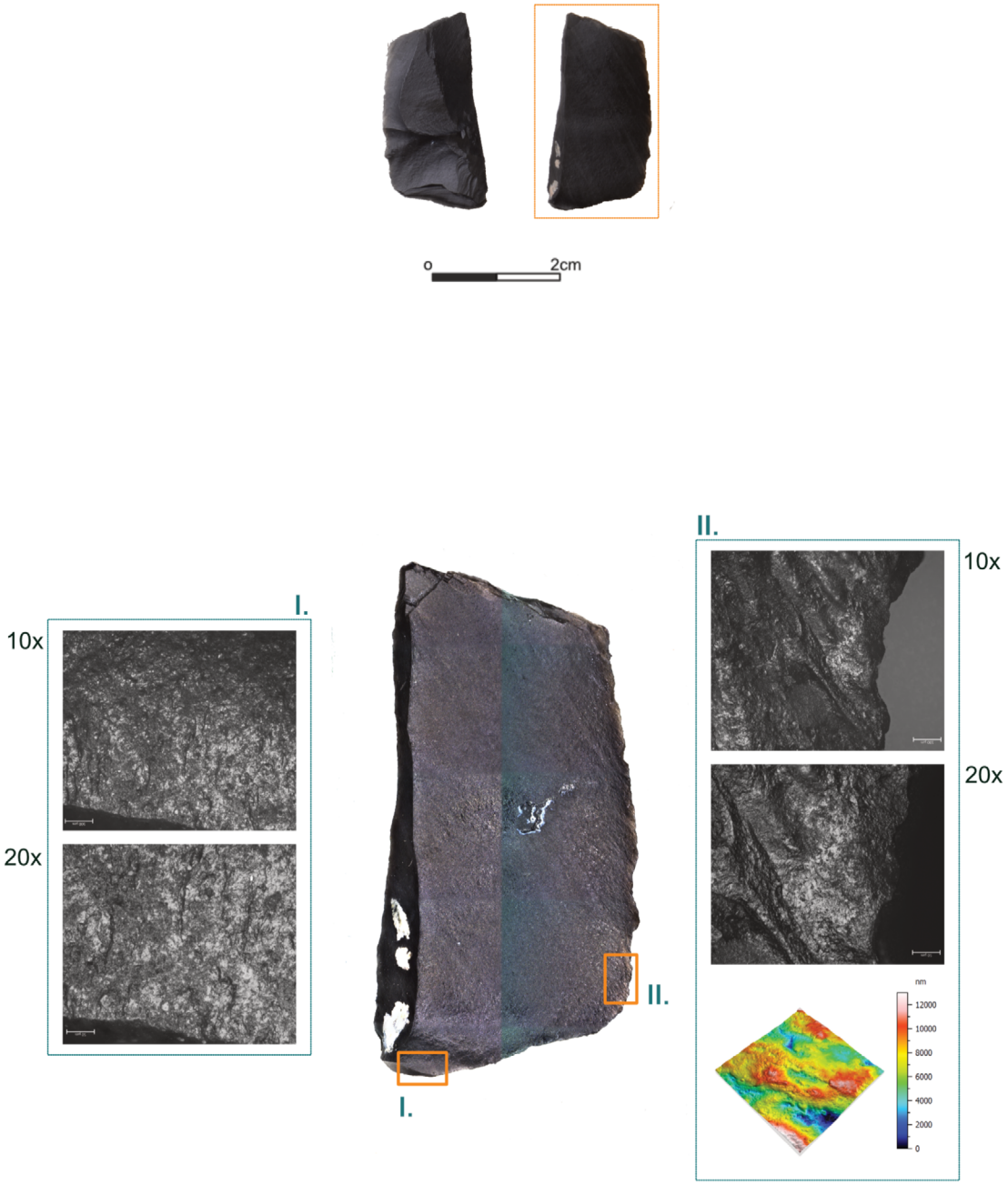

Buhlen, *Prądnik spall* [ID BU-128]. The topmost image displays the artefact in original size. The other illustrations are magnifications acquired with a 1.6× objective and a 34-× zoom. The use-wear traces are acquired at magnification of 10× and 20× (I. type V.; II. type V.).



Buhlen, *Prądnik spall* [ID BU-129]. The topmost image displays the artefact in original size. The other illustrations are magnifications acquired with a 1.6× objective and a 34-× zoom. The use-wear traces are acquired at magnification of 10× and 20× (I. type I.; II. type I.).



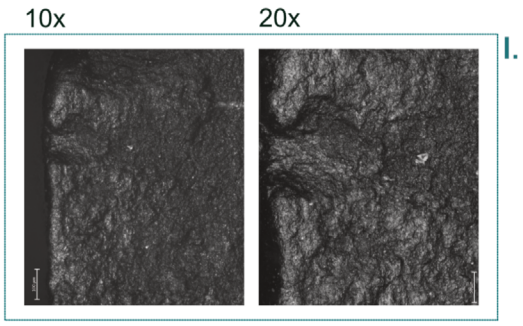



Buhlen, *Prądnik spall* [ID BU-131]. The topmost image displays the artefact in original size. The other illustrations are magnifications acquired with a 1.6× objective and a 34-× zoom. The use-wear trace is acquired at magnification of 10× and 20× (I. type V.).

Plate A62



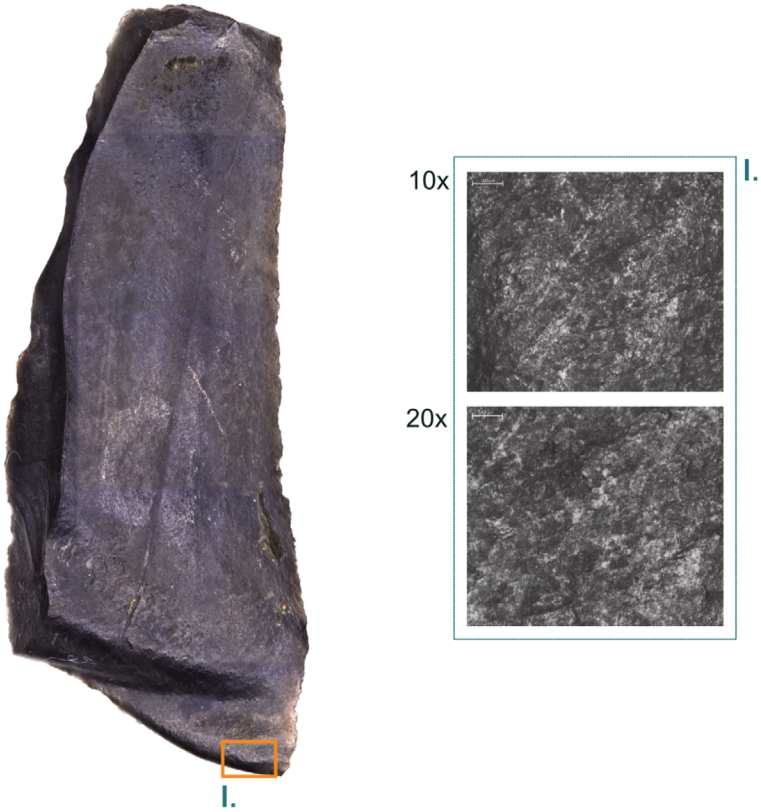

Buhlen, *Prądnik spall* [ID BU-132]. The topmost image displays the artefact in original size. The other illustrations are magnifications acquired with a 1.6× objective and a 34-× zoom. The use-wear trace is acquired at magnification of 10× and 20× (I. type V.).

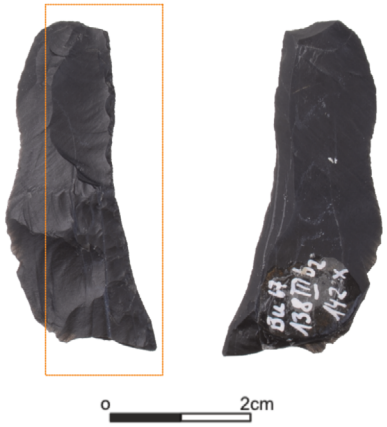

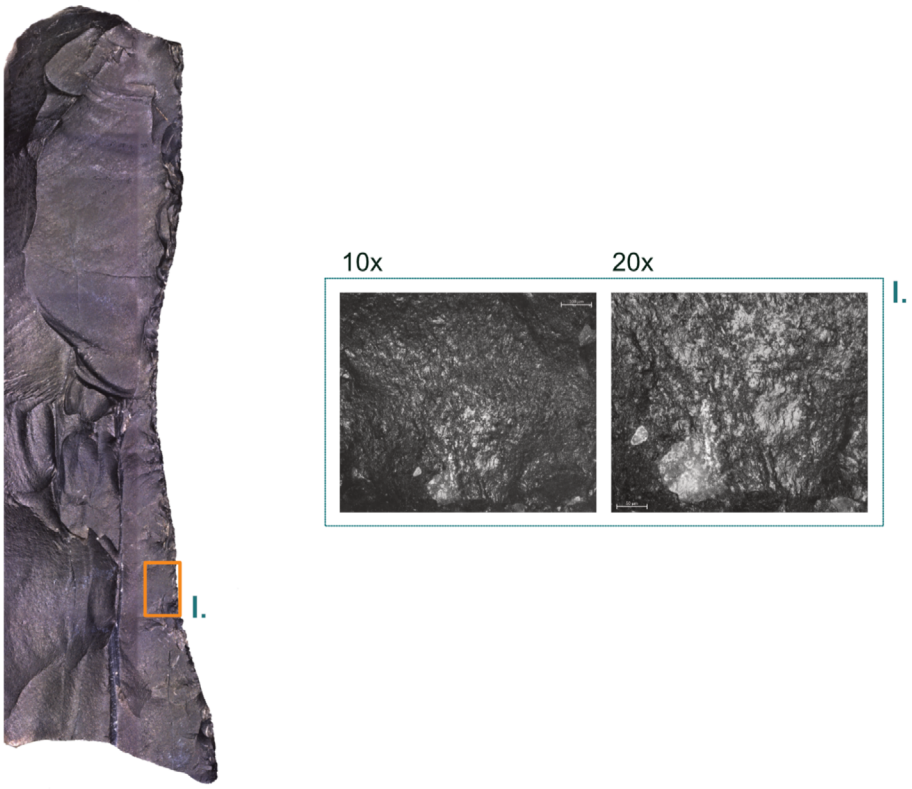

Buhlen, *Prądnik spall* [ID BU-136]. The topmost image displays the artefact in original size. The other illustrations are magnifications acquired with a 1.6× objective and a 34-× zoom. The use-wear trace is acquired at magnification of 10× and 20× (I. type V.).





Buhlen, *Prądnik spall* [ID BU-139]. The topmost image displays the artefact in original size. The other illustrations are magnifications acquired with a 1.6× objective and a 34-× zoom. The use-wear trace is acquired at magnification of 10× (I. type V.).



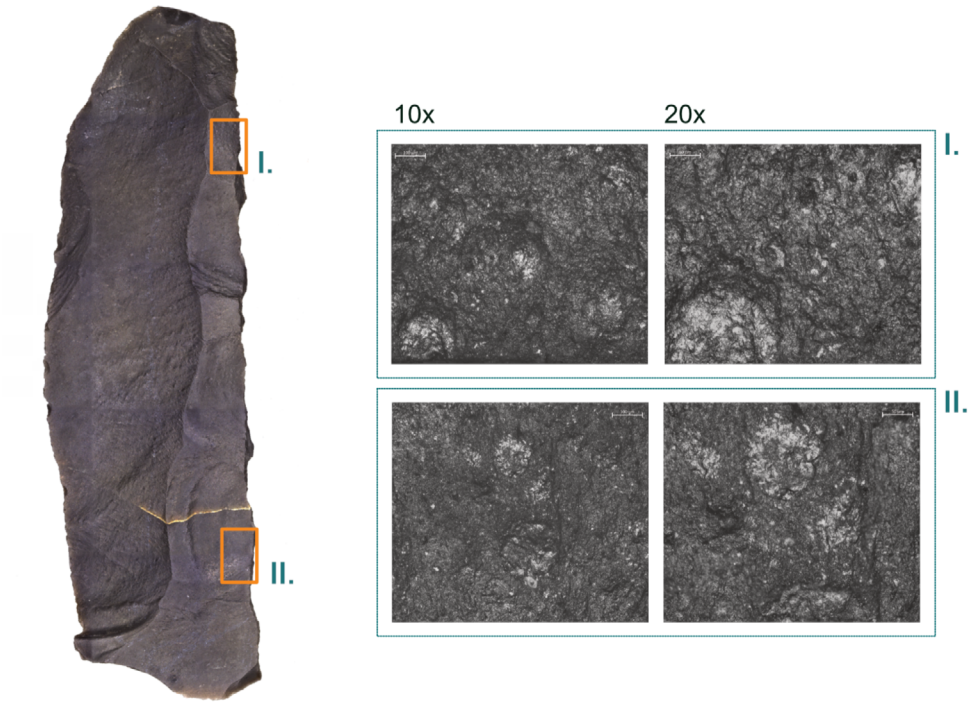

Buhlen, *Prądnik spall* [ID BU-157]. The topmost image displays the artefact in original size. The other illustrations are magnifications acquired with a 1.6× objective and a 34-× zoom. The use-wear traces are acquired at magnification of 10× and 20× (I. type I.; II. type I.).

Plate A66





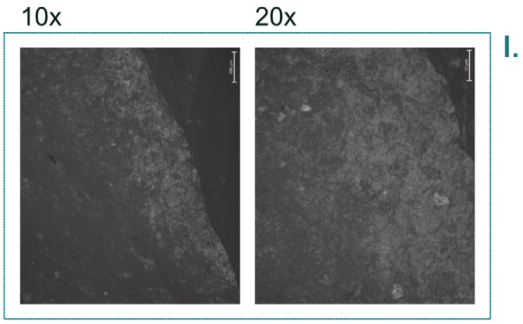

Buhlen, *Prądnik spall* [ID BU-169]. The topmost image displays the artefact in original size. The other illustrations are magnifications acquired with a 1.6× objective and a 34-× zoom. The use-wear trace is acquired at magnification of 10× and 20× (I. type V.).

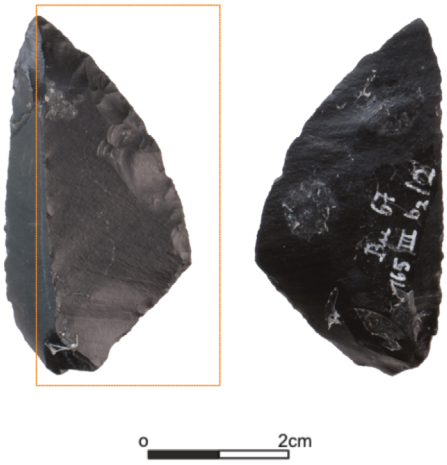

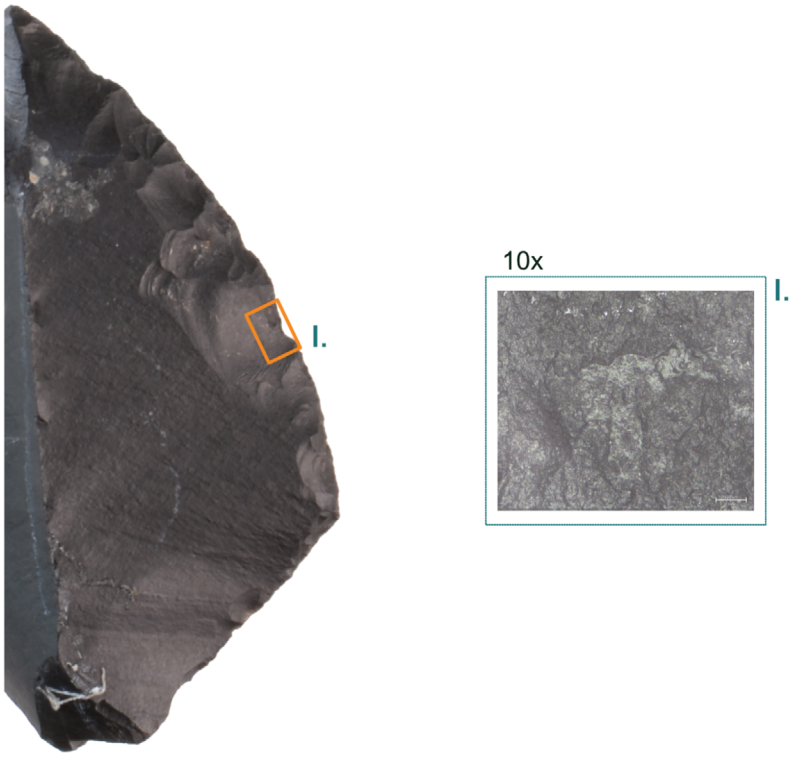

Buhlen, scraper [ID BU-189]. The topmost image displays the artefact in original size. The other illustrations are magnifications acquired with a 1.6× objective and a 34-× zoom. The use-wear trace is acquired at magnification of 10× (I. type V.).

Plate A68

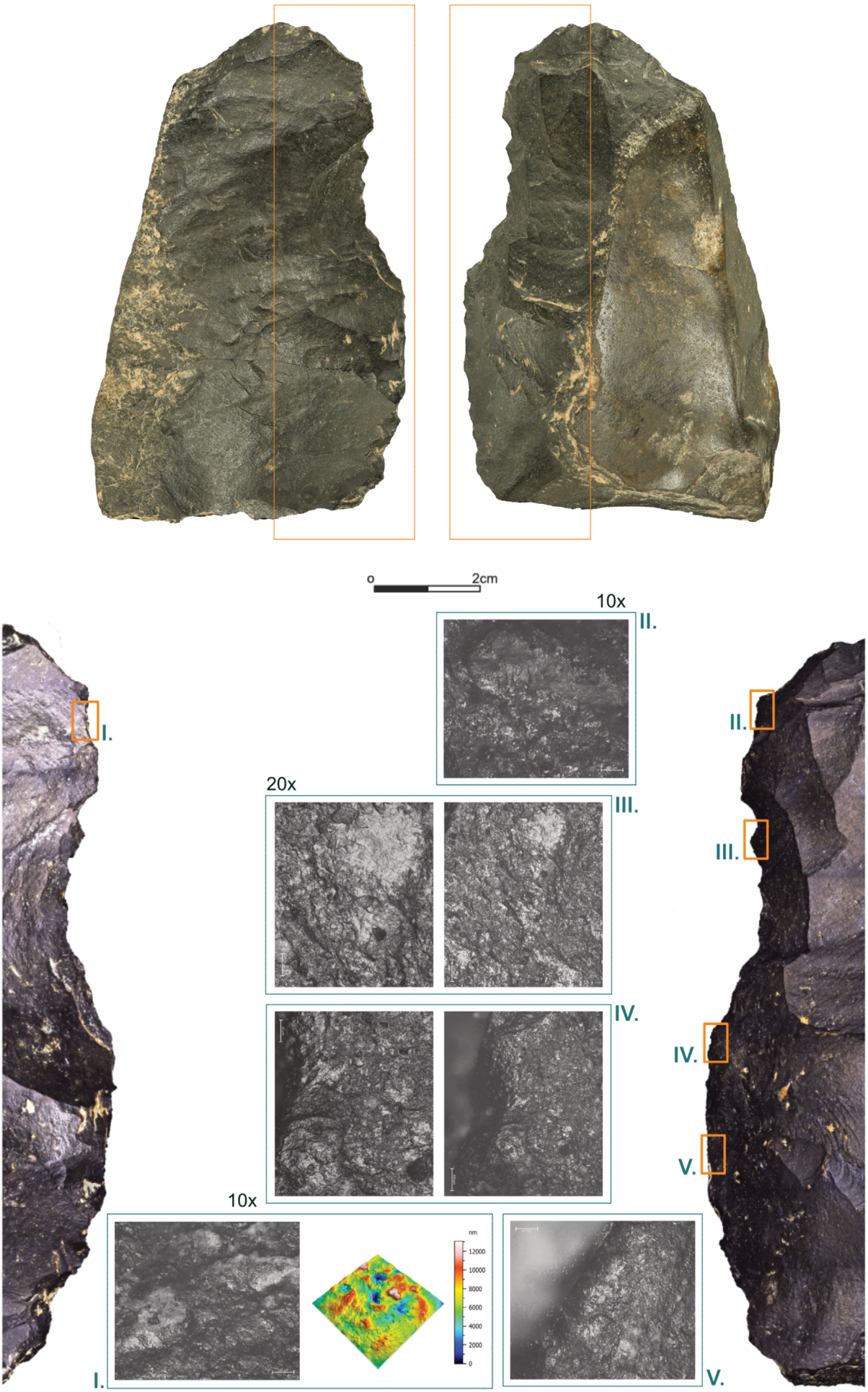
0
2cm
10x
II.
I.
20x
III.
IV.
10x
nm
12000
10000
8000
6000
4000
2000
0
I.
V.
II.
III.
IV.
V.



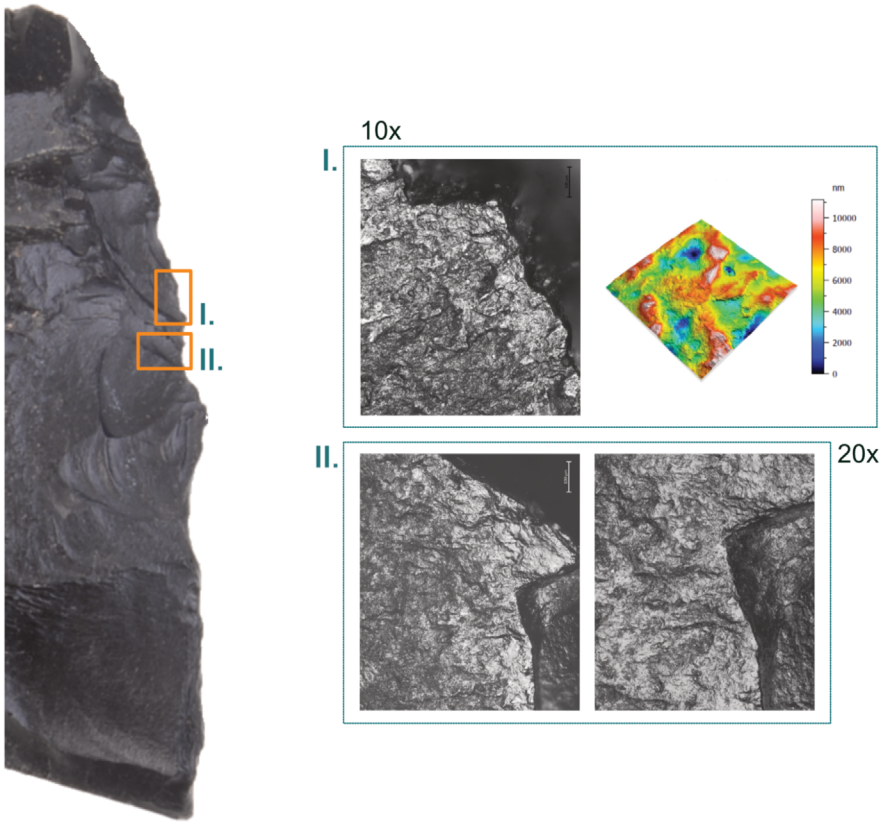

Balver Höhle, *Keilmesser* [ID MU-008]. The topmost image displays the artefact in original size. The other illustrations are magnifications acquired with a 1.6× objective and a 34-× zoom. The use-wear traces are acquired at magnification of 10× and 20× (I. type V.; II. type V.). The micro-surface displays the processed result of the confocal data acquisition with the 50× objective.

Balver Höhle, *Keilmesser* [ID MU-003]. The topmost image displays the artefact in original size. The other illustrations are magnifications acquired with a 1.6× objective and a 34-× zoom. The use-wear traces are acquired at magnification of 10× and 20× (I. type II.; II. type I.; III. type I.; IV. type I.; V. type I.). The micro-surface displays the processed result of the confocal data acquisition with the 50× objective.

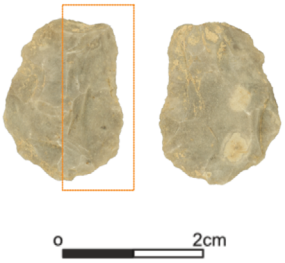



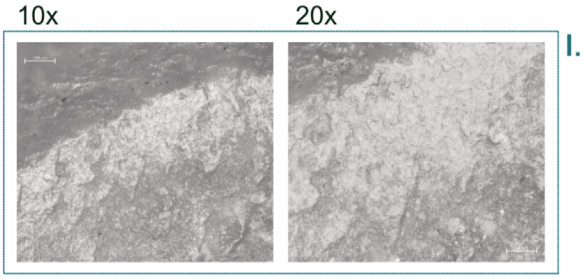

Balver Höhle, *Keilmesser* [ID MU-011]. The topmost image displays the artefact in original size. The other illustrations are magnifications acquired with a 1.6× objective and a 34-× zoom. The use-wear trace is acquired at magnification of 10× and 20× (I. type V.).

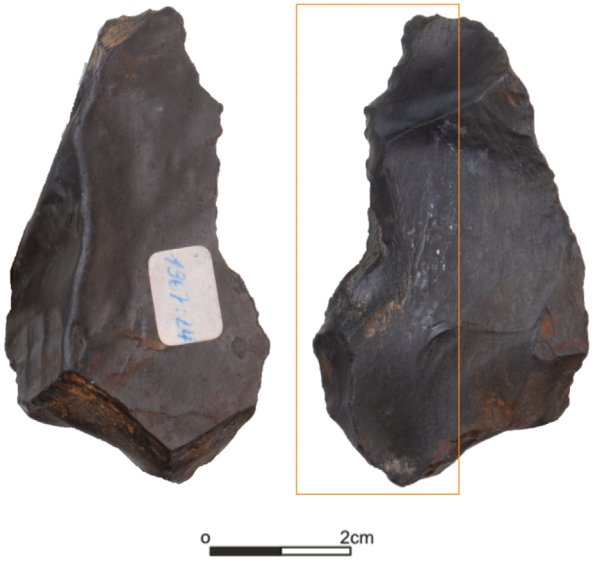

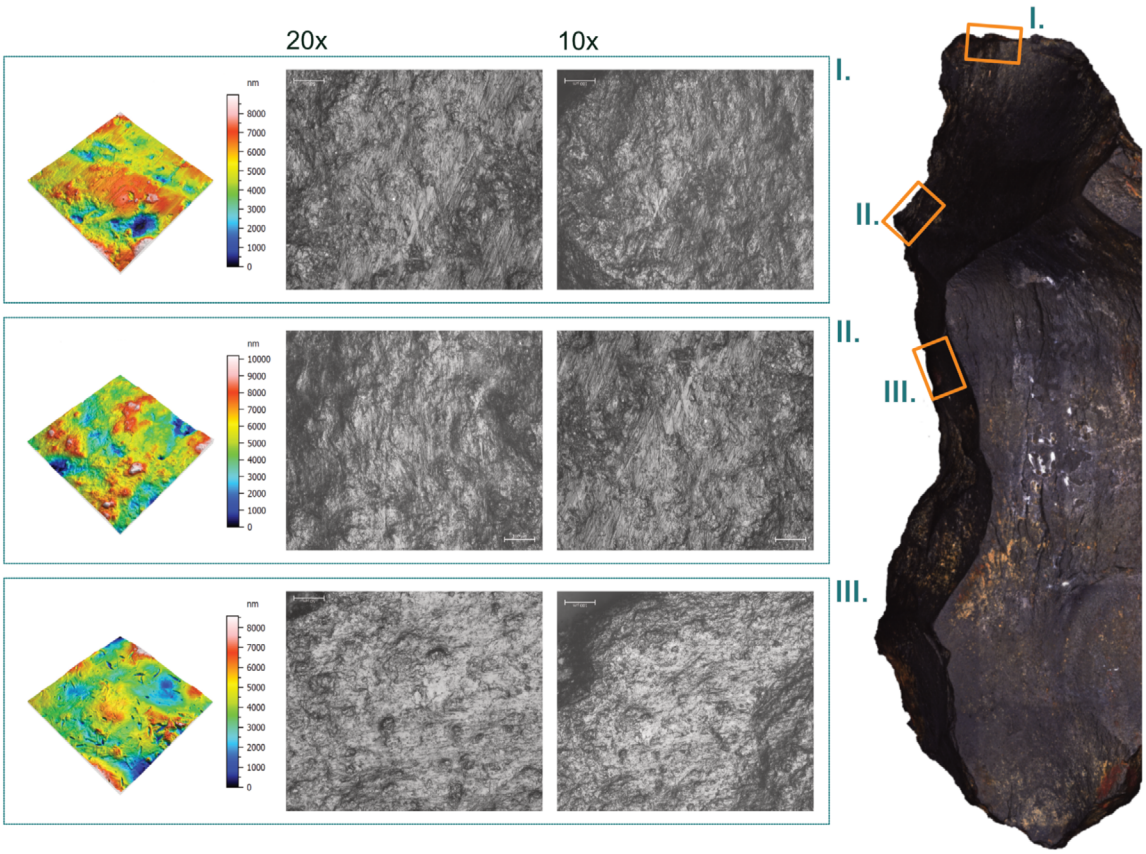

Balver Höhle, *Keilmesser* [ID MU-020]. The topmost image displays the artefact in original size. The other illustrations are magnifications acquired with a 1.6× objective and a 34-× zoom. The use-wear traces are acquired at magnification of 10× and 20× (I. type VI.; II. type VI.; III. type VII.). The micro-surface displays the processed result of the confocal data acquisition with the 50× objective.

Plate A72

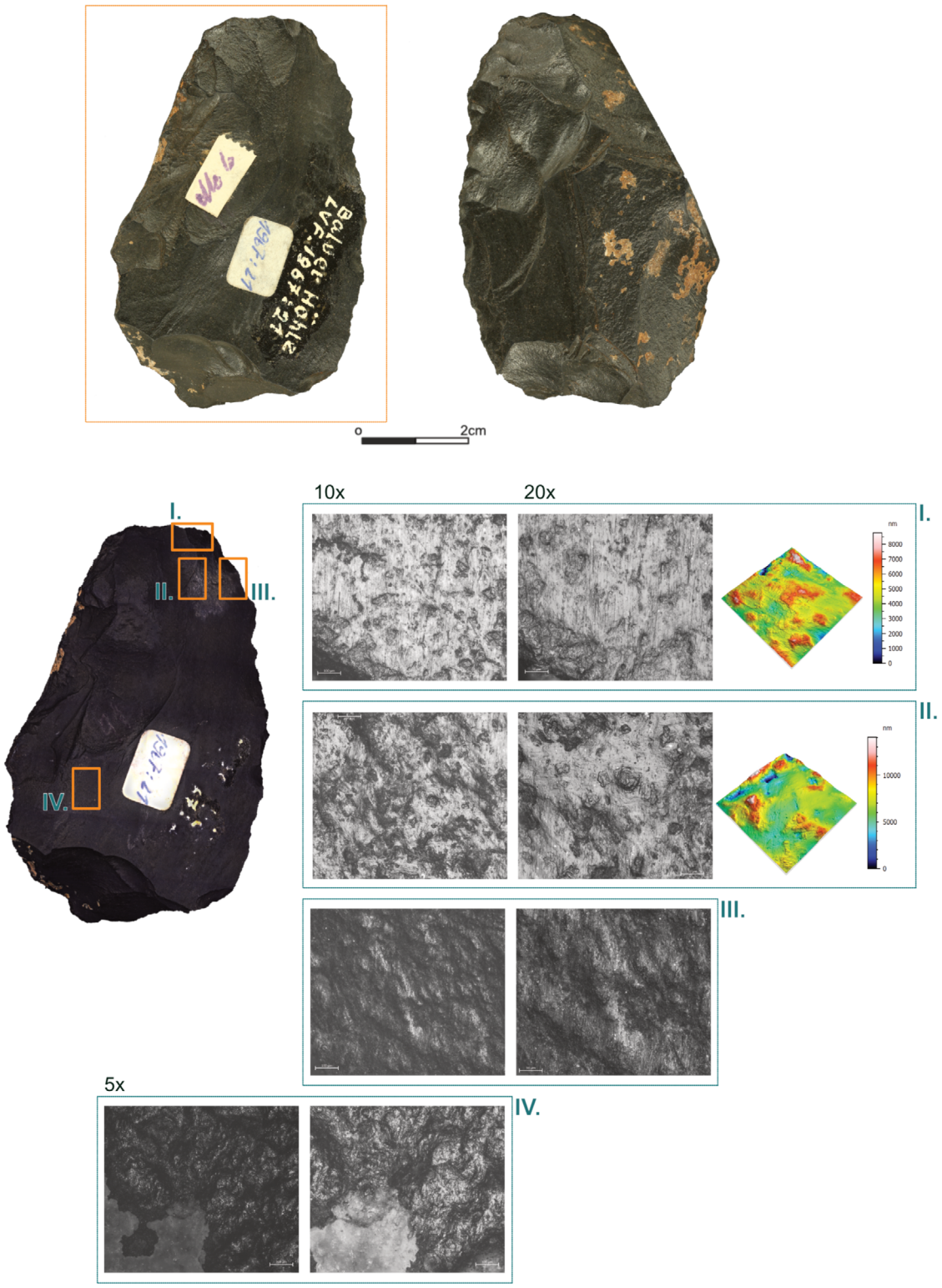

Balver Höhle, *Keilmesser* [ID MU-021]. The topmost image displays the artefact in original size. The other illustrations are magnifications acquired with a 1.6× objective and a 34-× zoom. The use-wear traces are acquired at magnification of 5×, 10× and 20× (I. type VII.; II. type VII.; III. type VII.; IV. type II.). The micro-surface displays the processed result of the confocal data acquisition with the 50× objective.



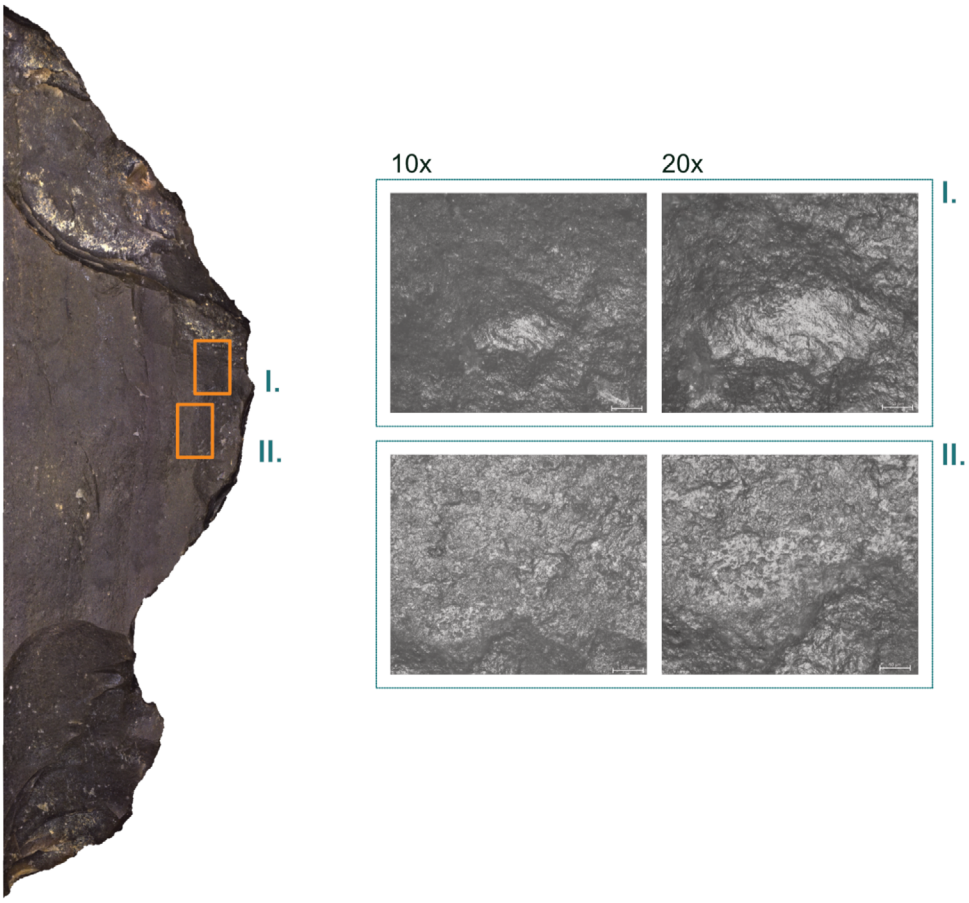

Balver Höhle, *Keilmesser* [ID MU-023]. The topmost image displays the artefact in original size. The other illustrations are magnifications acquired with a 1.6× objective and a 34-× zoom. The use-wear traces are acquired at magnification of 10× and 20× (I. type I.; II. type II.).



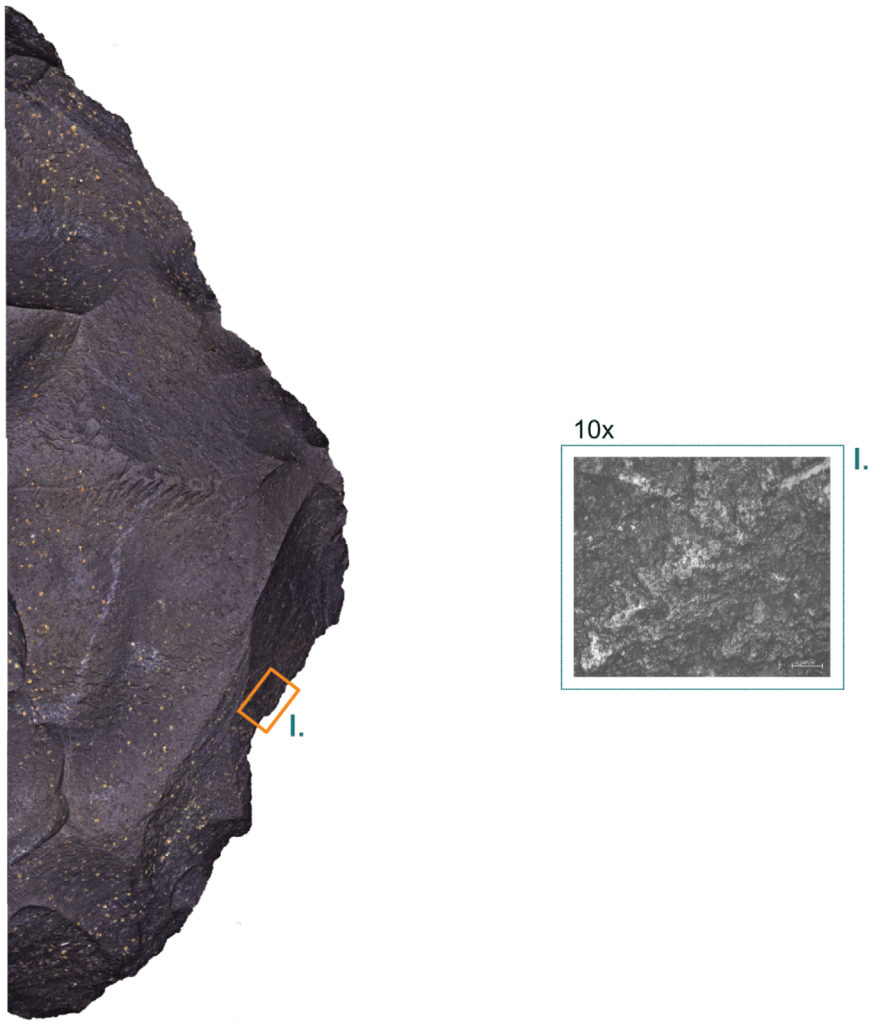

Balver Höhle, *Keilmesser* [ID MU-044]. The topmost image displays the artefact in original size. The other illustrations are magnifications acquired with a 1.6× objective and a 34-× zoom. The use-wear trace is acquired at magnification of 10× (I. type II.).

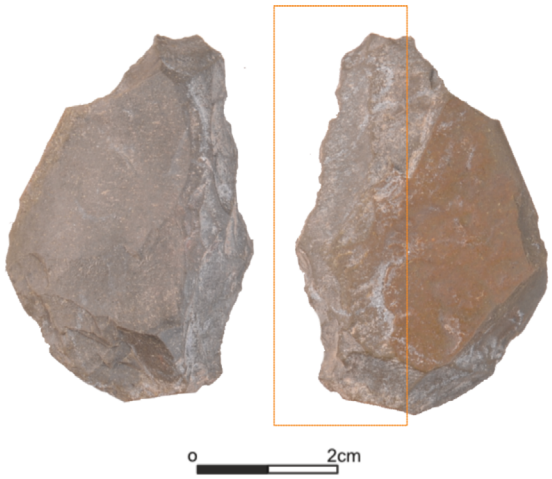

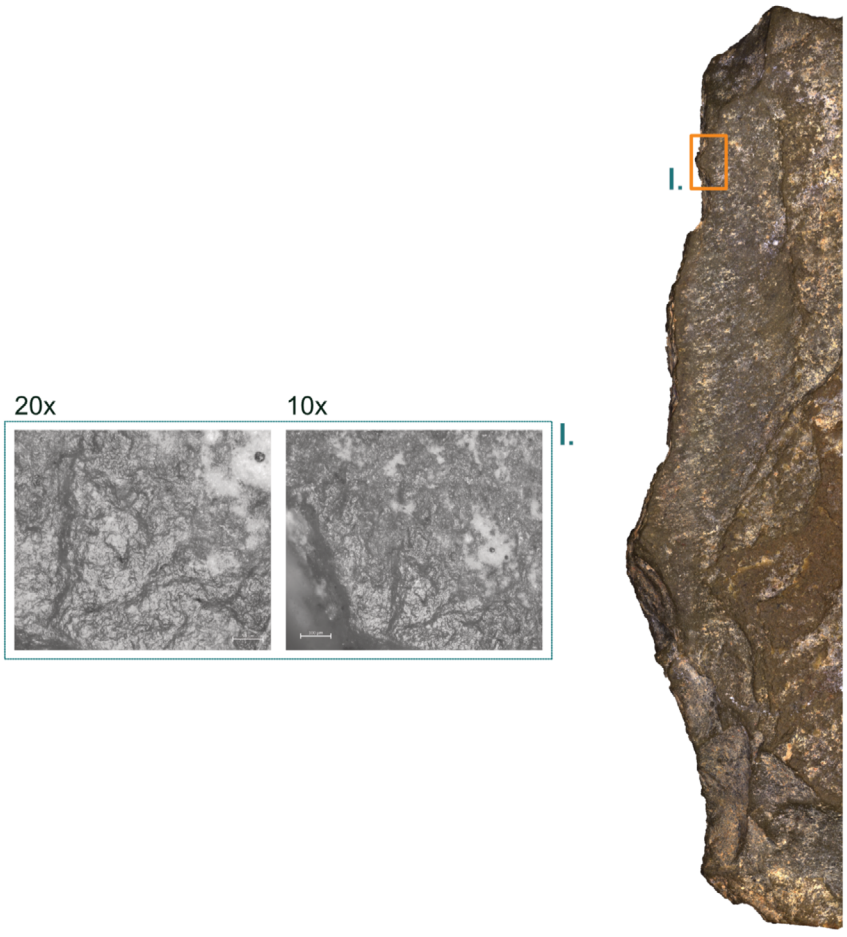

Balver Höhle, *Keilmesser* [ID MU-061]. The topmost image displays the artefact in original size. The other illustrations are magnifications acquired with a 1.6× objective and a 34-× zoom. The use-wear trace is acquired at magnification of 10× and 20× (I. type V.).

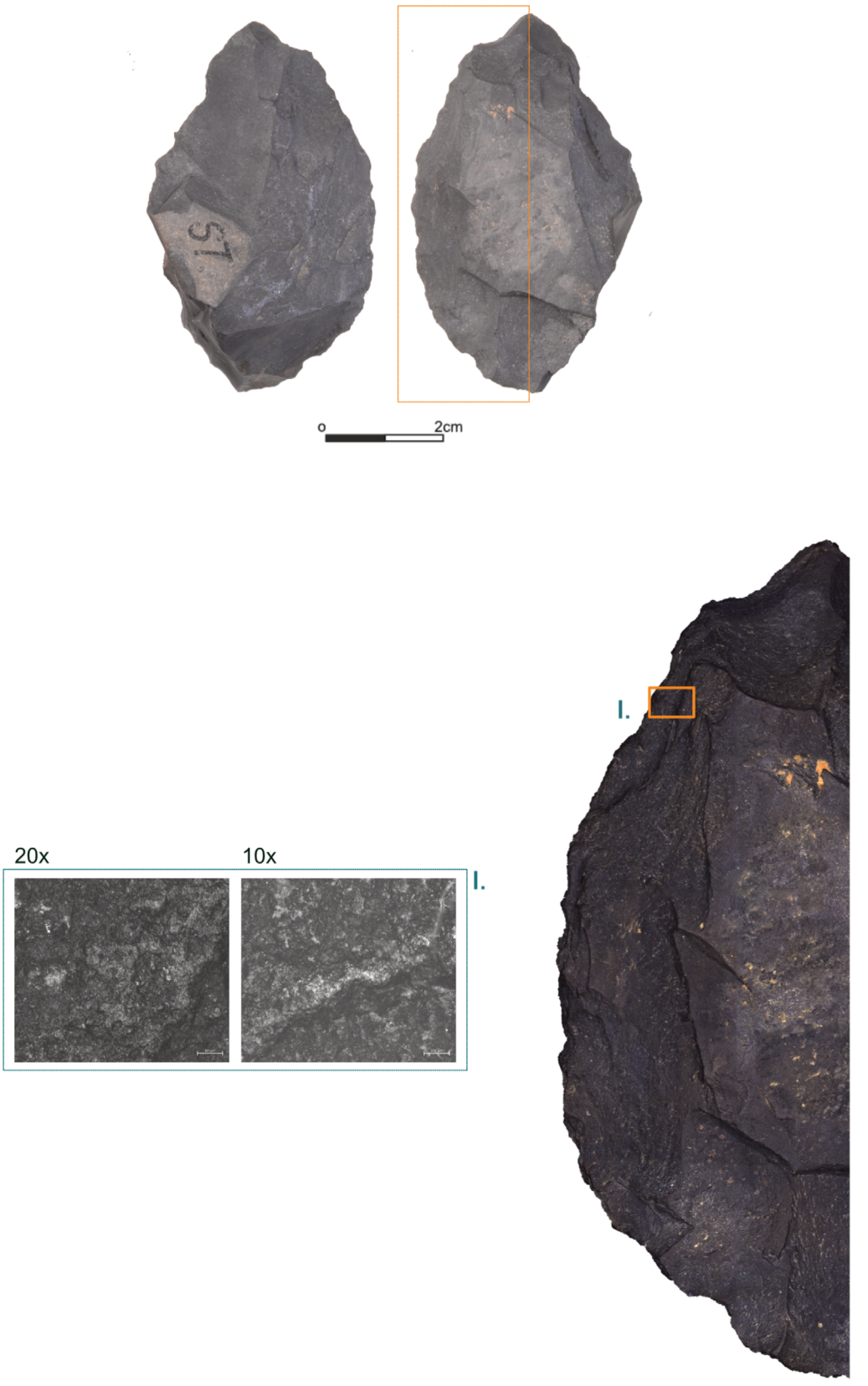

Balver Höhle, *Keilmesser* [ID MU-063]. The topmost image displays the artefact in original size. The other illustrations are magnifications acquired with a 1.6× objective and a 34-× zoom. The use-wear trace is acquired at magnification of 10× and 20× (I. type II.).



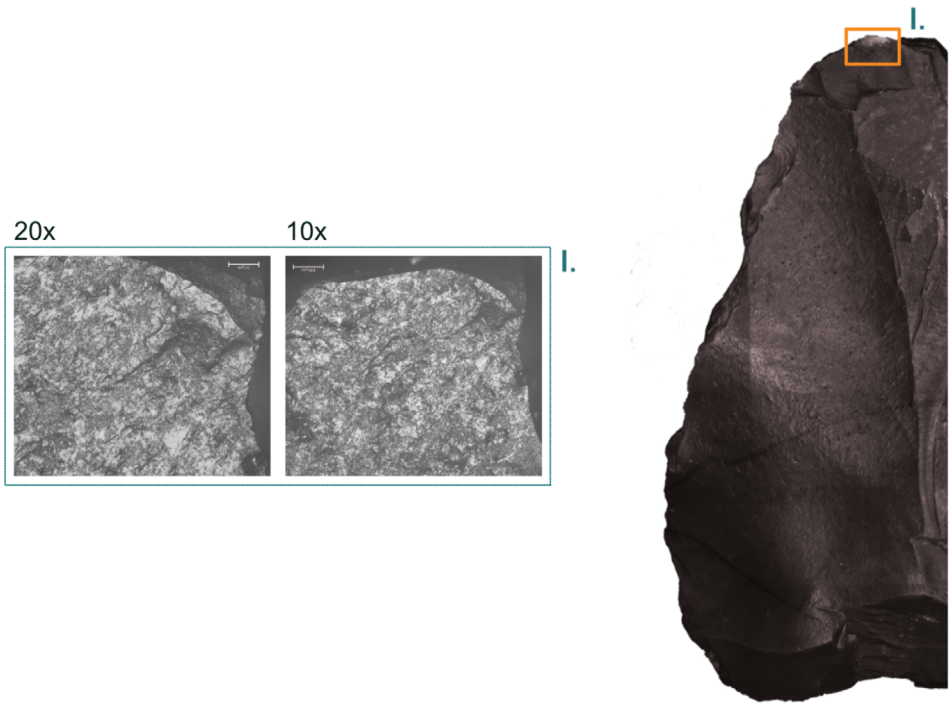

Balver Höhle, *Keilmesser* [ID MU-073]. The topmost image displays the artefact in original size. The other illustrations are magnifications acquired with a 1.6× objective and a 34-× zoom. The use-wear trace is acquired at magnification of 10× and 20× (I. type II.).

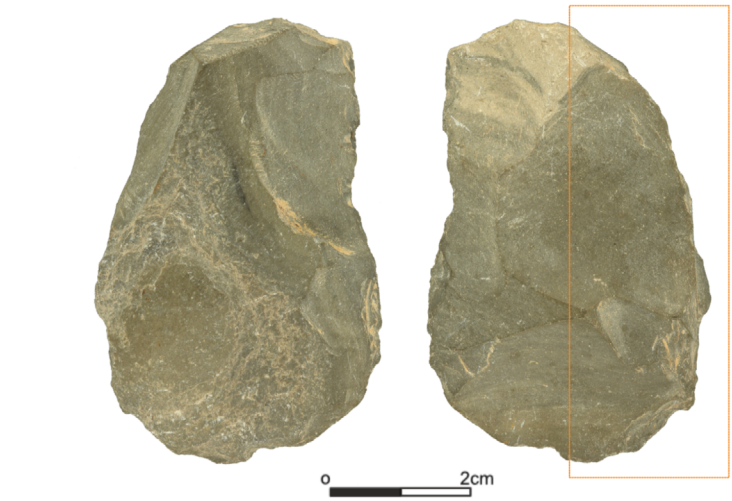

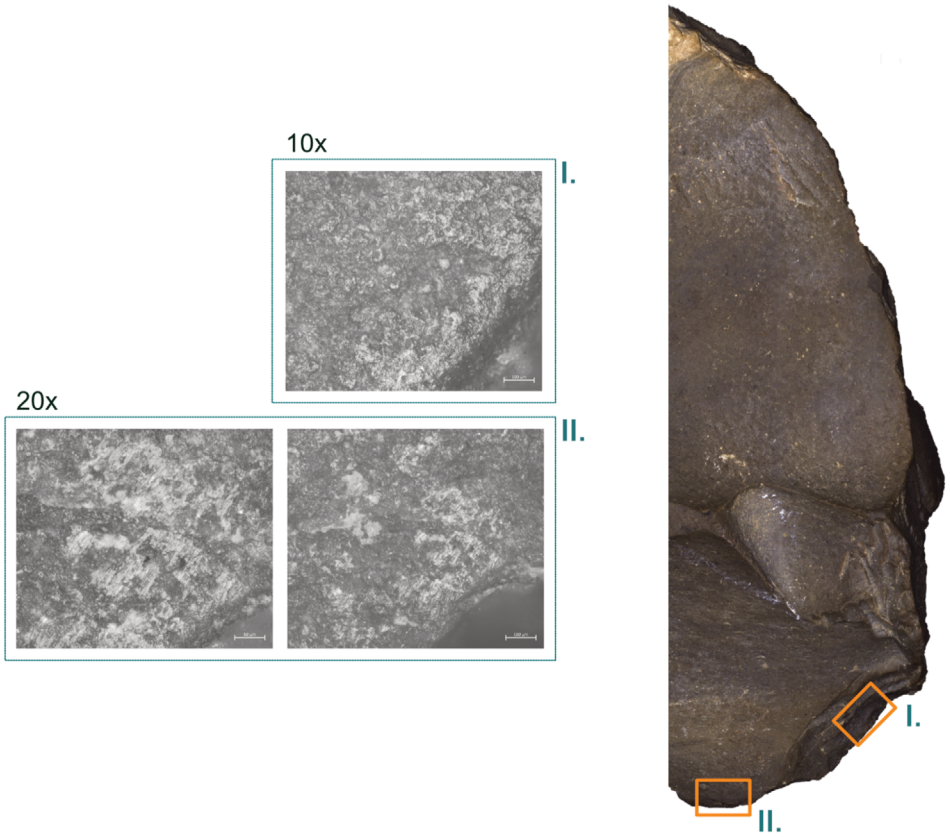

Balver Höhle, *Keilmesser* [ID MU-093]. The topmost image displays the artefact in original size. The other illustrations are magnifications acquired with a 1.6× objective and a 34-× zoom. The use-wear traces are acquired at magnification of 10× and 20× (I. type V.; II. type VII.).

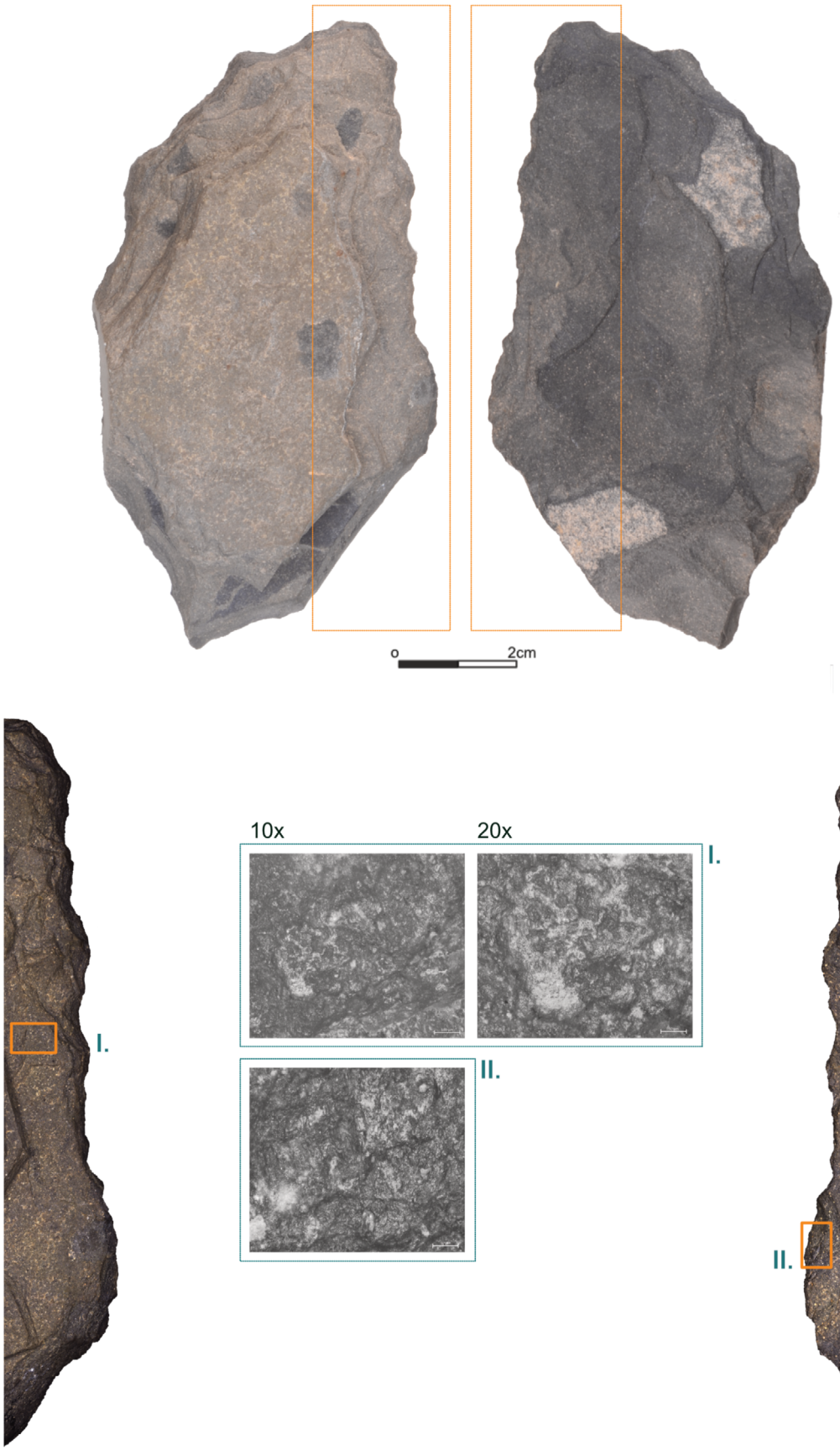

Balver Höhle, *Keilmesser* [ID MU-100]. The topmost image displays the artefact in original size. The other illustrations are magnifications acquired with a 1.6× objective and a 34-× zoom. The use-wear traces are acquired at magnification of 10× and 20× (I. type I.; II. type I.).

Plate A80

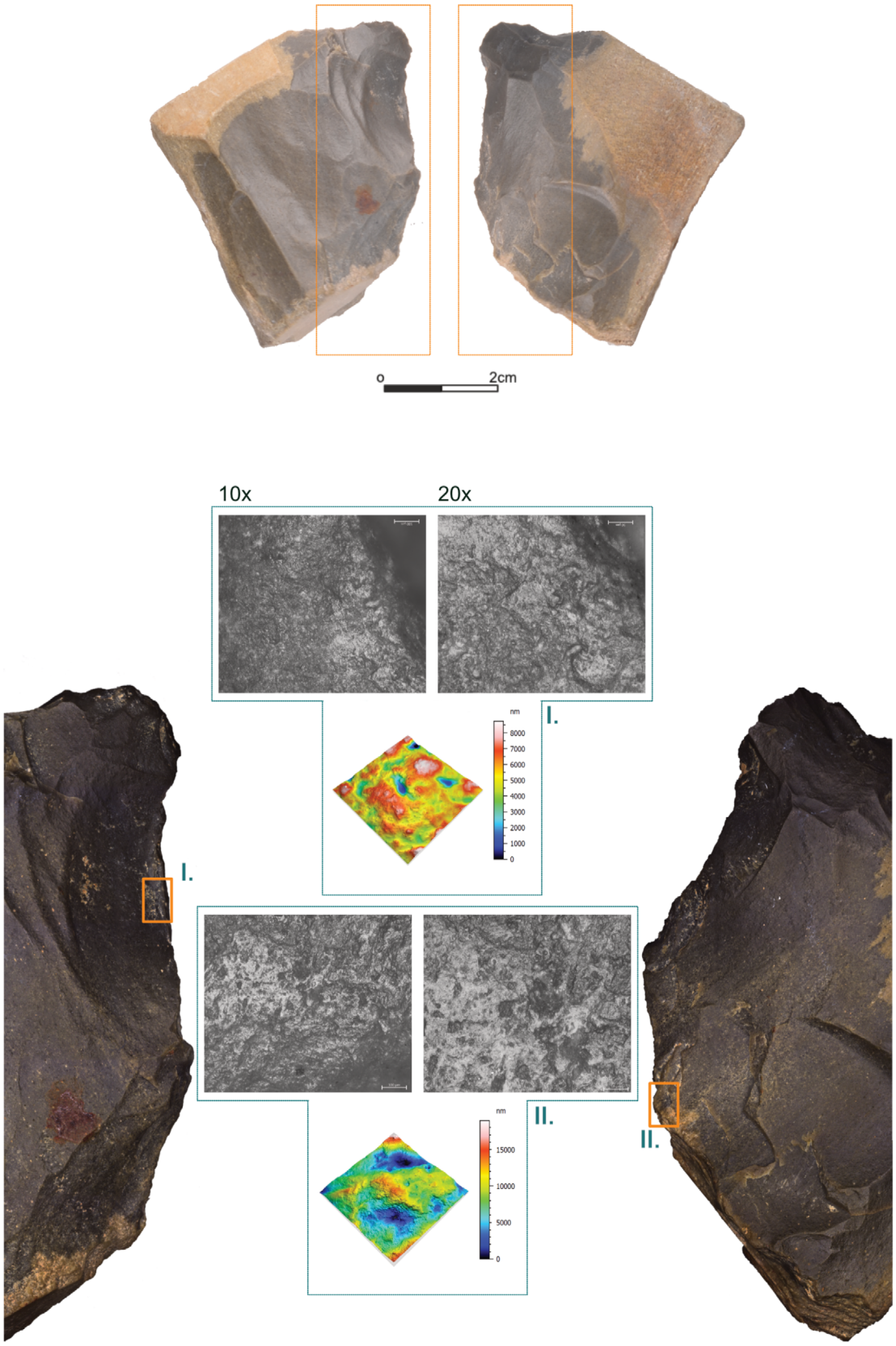

Balver Höhle, *Keilmesser* [ID MU-107]. The topmost image displays the artefact in original size. The other illustrations are magnifications acquired with a 1.6× objective and a 34-× zoom. The use-wear traces are acquired at magnification of 10× and 20× (I. type V.; II. type V.). The micro-surface displays the processed result of the confocal data acquisition with the 50× objective.

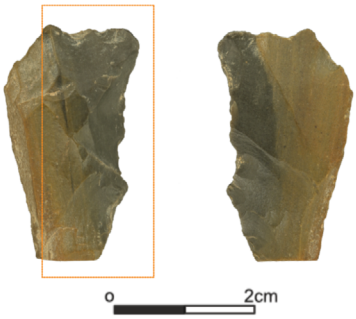

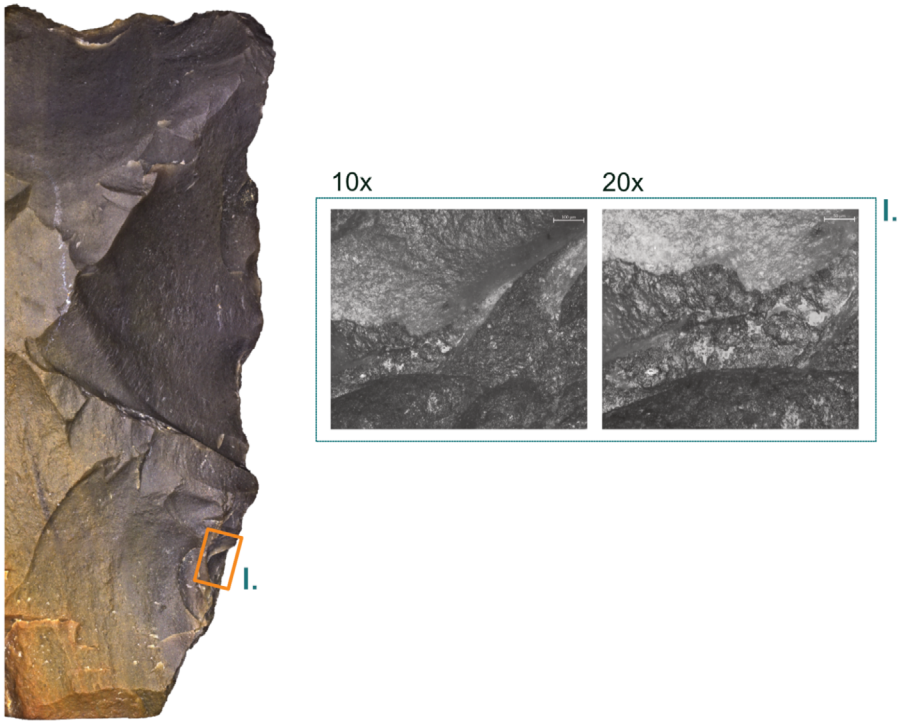

Balver Höhle, *Keilmesser* [ID MU-109]. The topmost image displays the artefact in original size. The other illustrations are magnifications acquired with a 1.6× objective and a 34-× zoom. The use-wear trace is acquired at magnification of 10× and 20× (I. type I.).

Plate A82

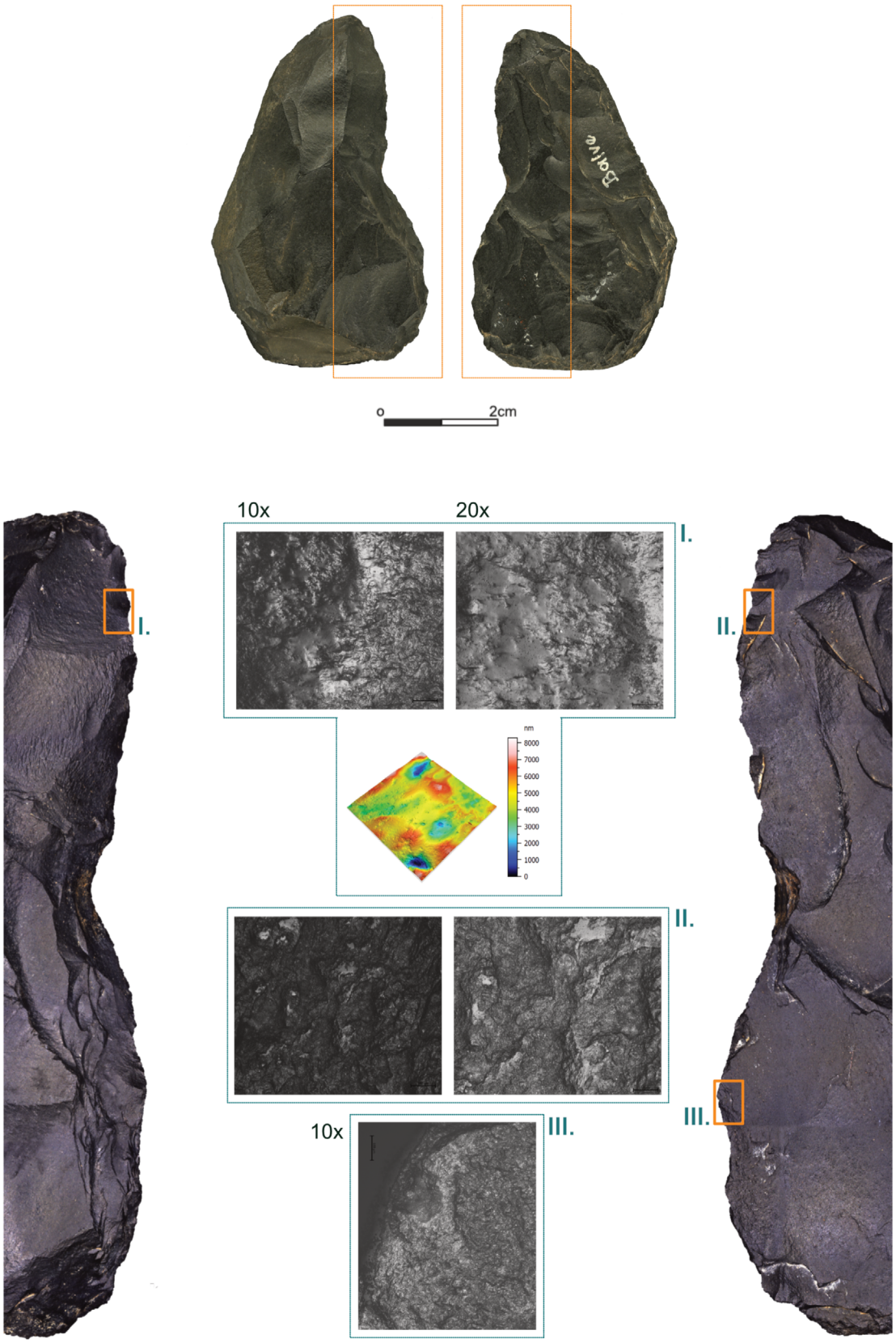

Balver Höhle, *Keilmesser* [ID MU-111]. The topmost image displays the artefact in original size. The other illustrations are magnifications acquired with a 1.6× objective and a 34-× zoom. The use-wear traces are acquired at magnification of 10× and 20× (I. type IV.; II. type IV.; III. type III.). The micro-surface displays the processed result of the confocal data acquisition with the 50× objective.

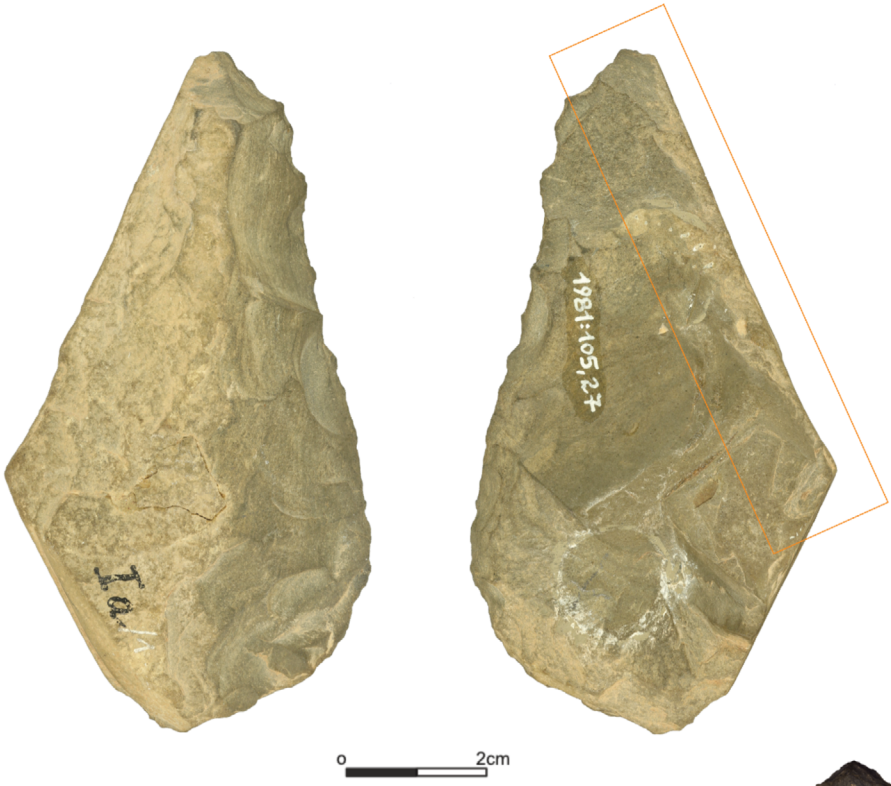

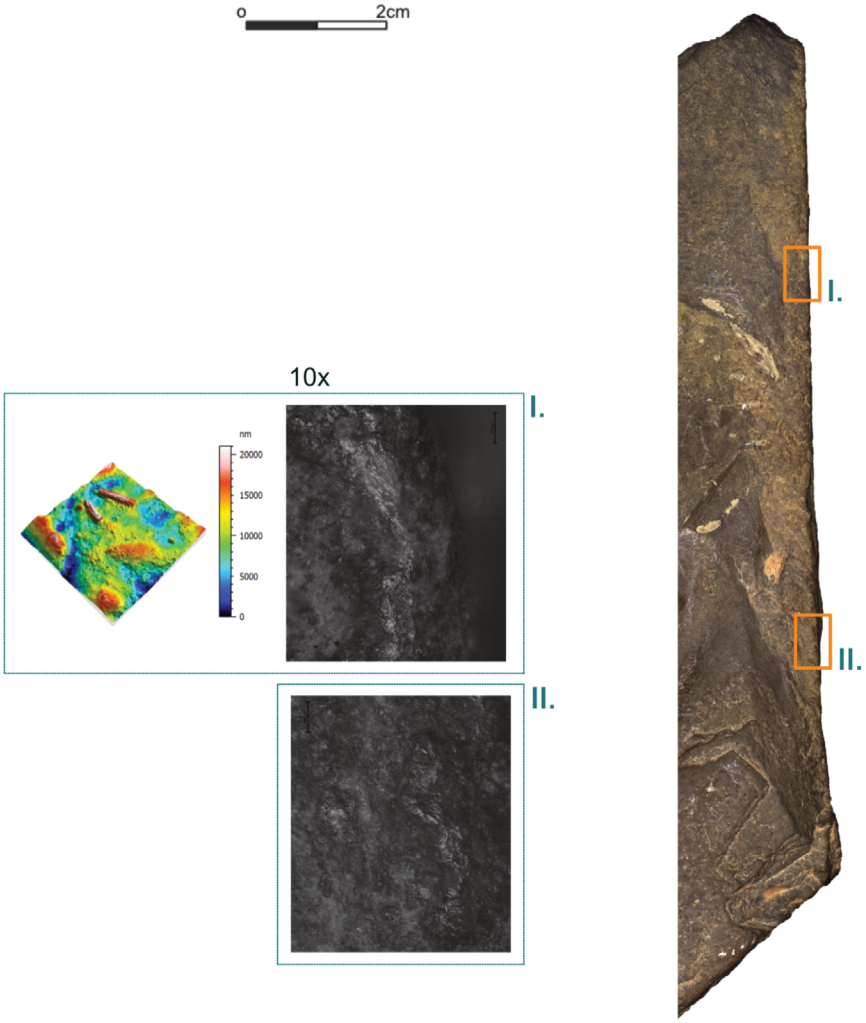

Balver Höhle, *Keilmesser* [ID MU-112]. The topmost image displays the artefact in original size. The other illustrations are magnifications acquired with a 1.6× objective and a 34-× zoom. The use-wear traces are acquired at magnification of 10× (I. type IV.; II. type IV.). The micro-surface displays the processed result of the confocal data acquisition with the 50× objective.

Plate A84

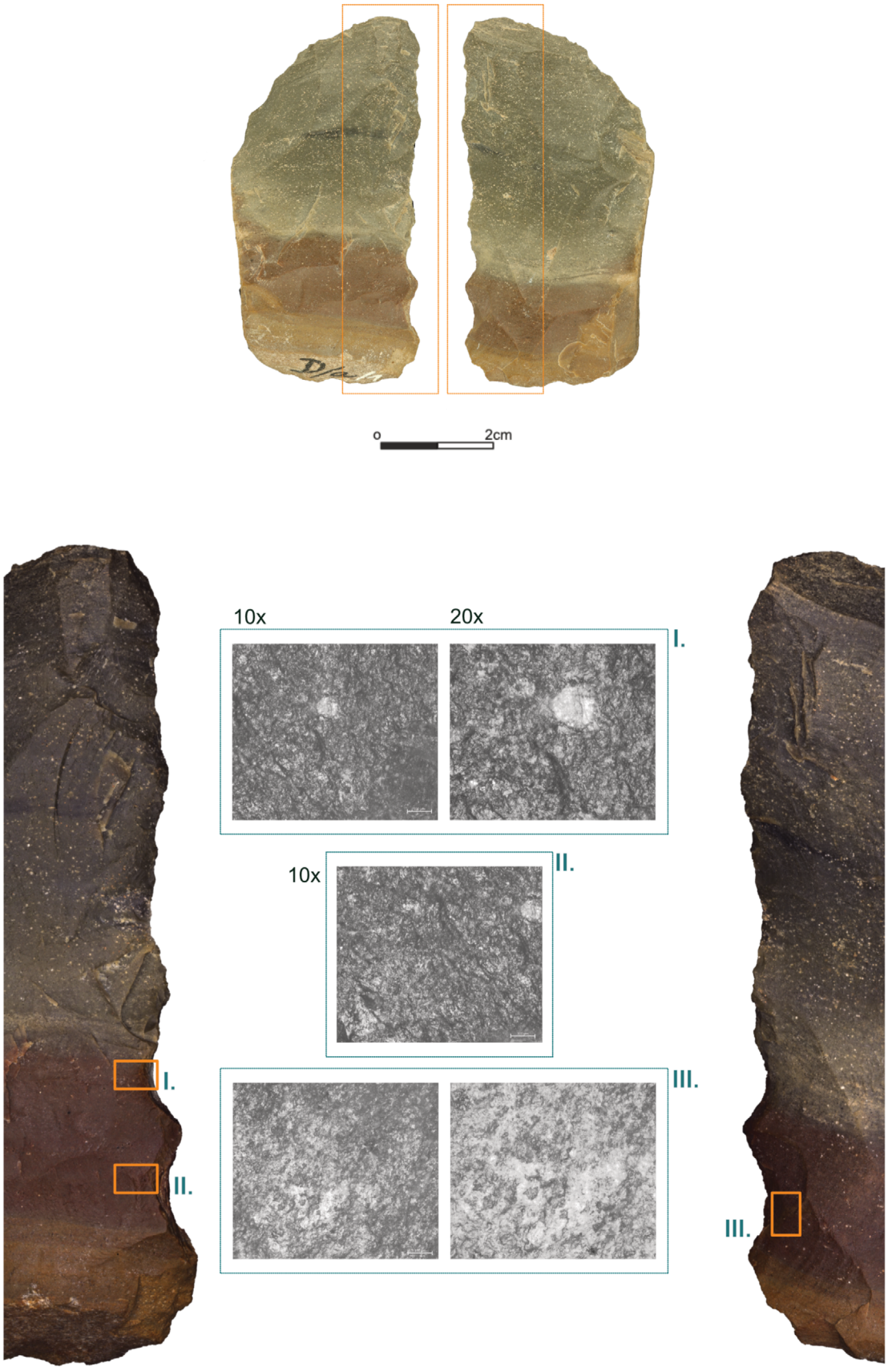

Balver Höhle, *Keilmesser* [ID MU-114]. The topmost image displays the artefact in original size. The other illustrations are magnifications acquired with a 1.6× objective and a 34-× zoom. The use-wear traces are acquired at magnification of 10× and 20× (I. type II.; II. type II.; III. type III.).

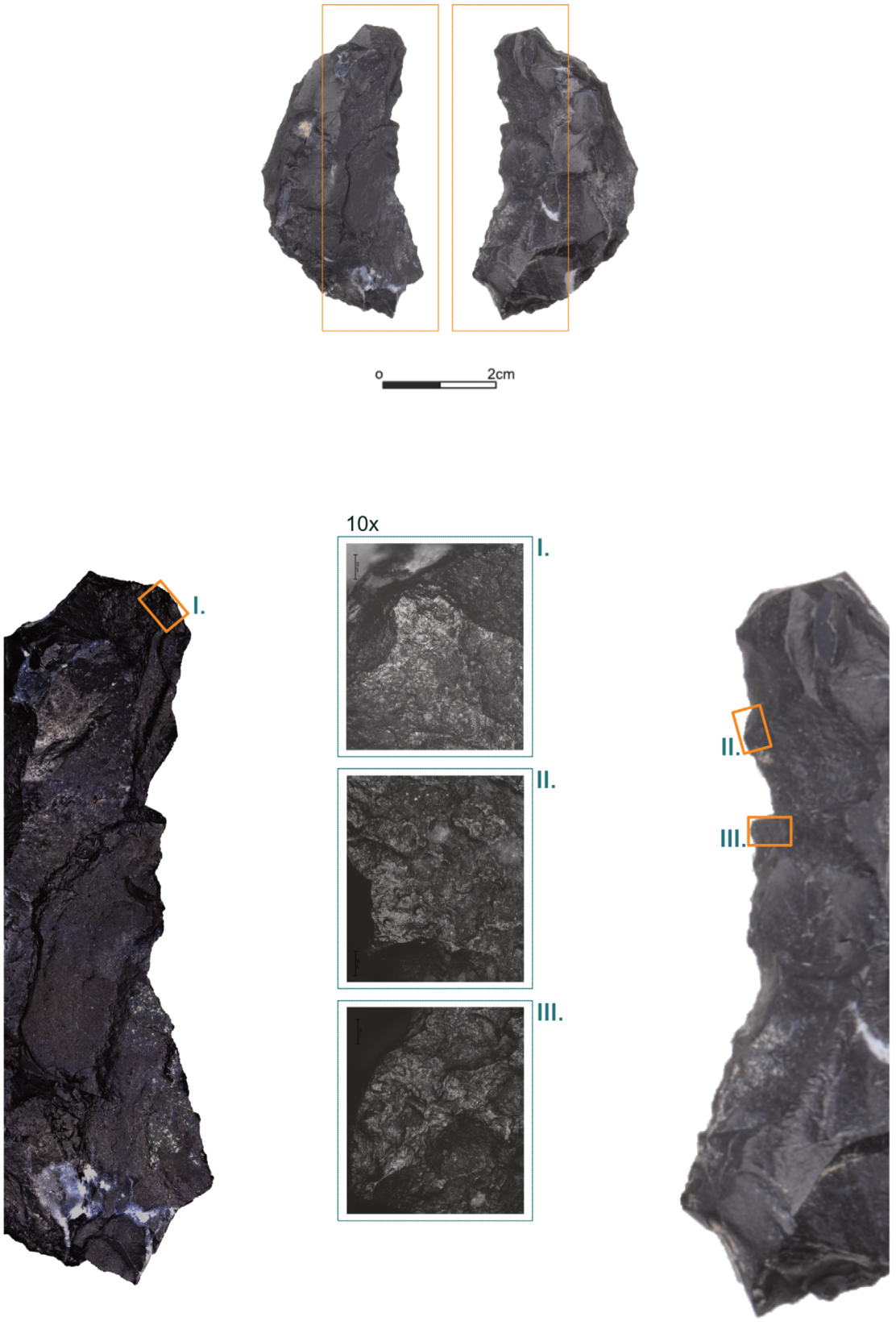

Balver Höhle, *Keilmesser* [ID MU-196]. The topmost image displays the artefact in original size. The other illustrations are magnifications acquired with a 1.6× objective and a 34-× zoom. The use-wear traces are acquired at magnification of 10× (I. type V.; II. type V.; III. type V.).

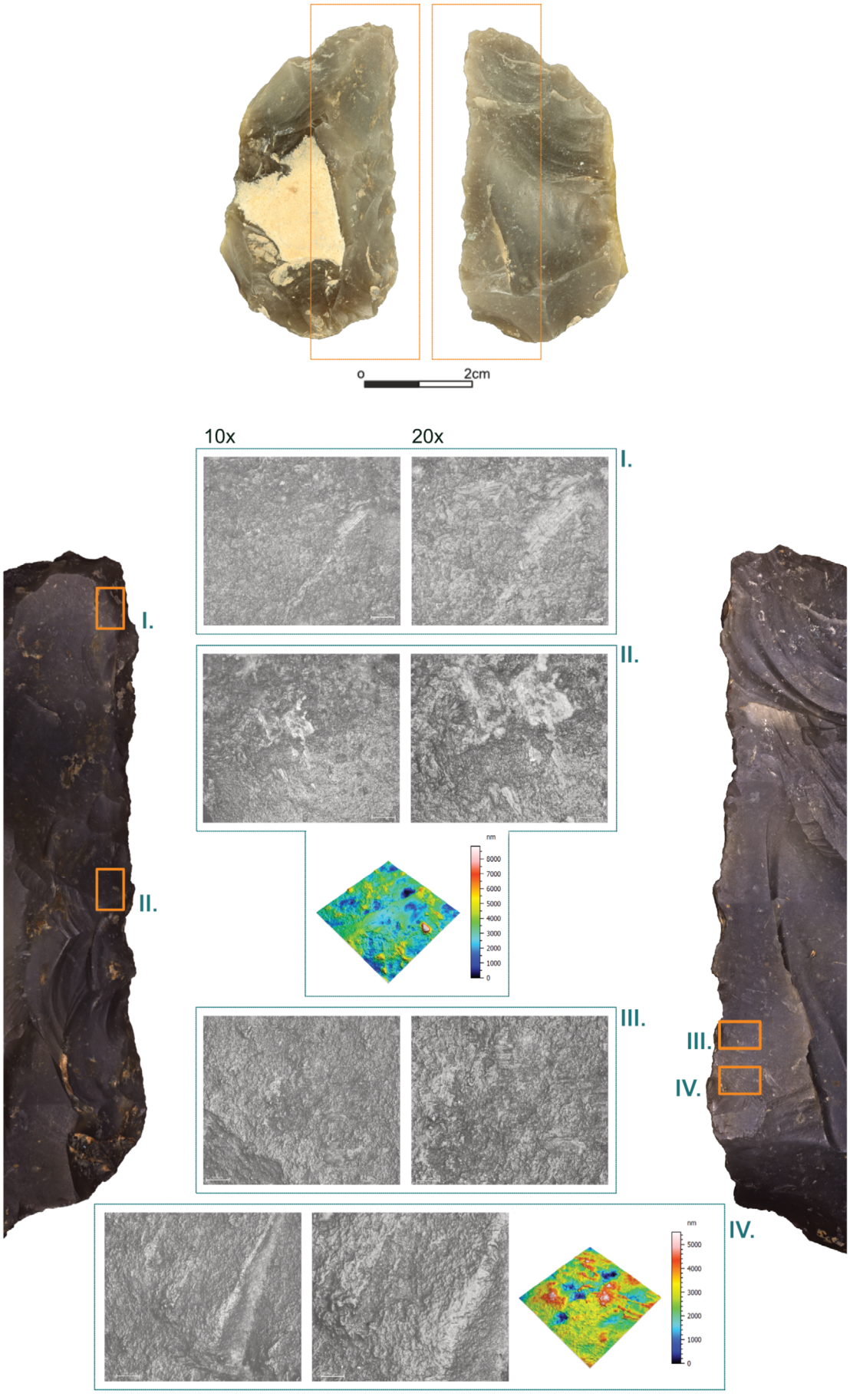

Balver Höhle, *Keilmesser* [ID MU-197]. The topmost image displays the artefact in original size. The other illustrations are magnifications acquired with a 1.6× objective and a 34-× zoom. The use-wear traces are acquired at magnification of 10× and 20× (I. type VIII.; II. type VIII.; III. type V.; IV. type VIII.). The micro-surface displays the processed result of the confocal data acquisition with the 50× objective.

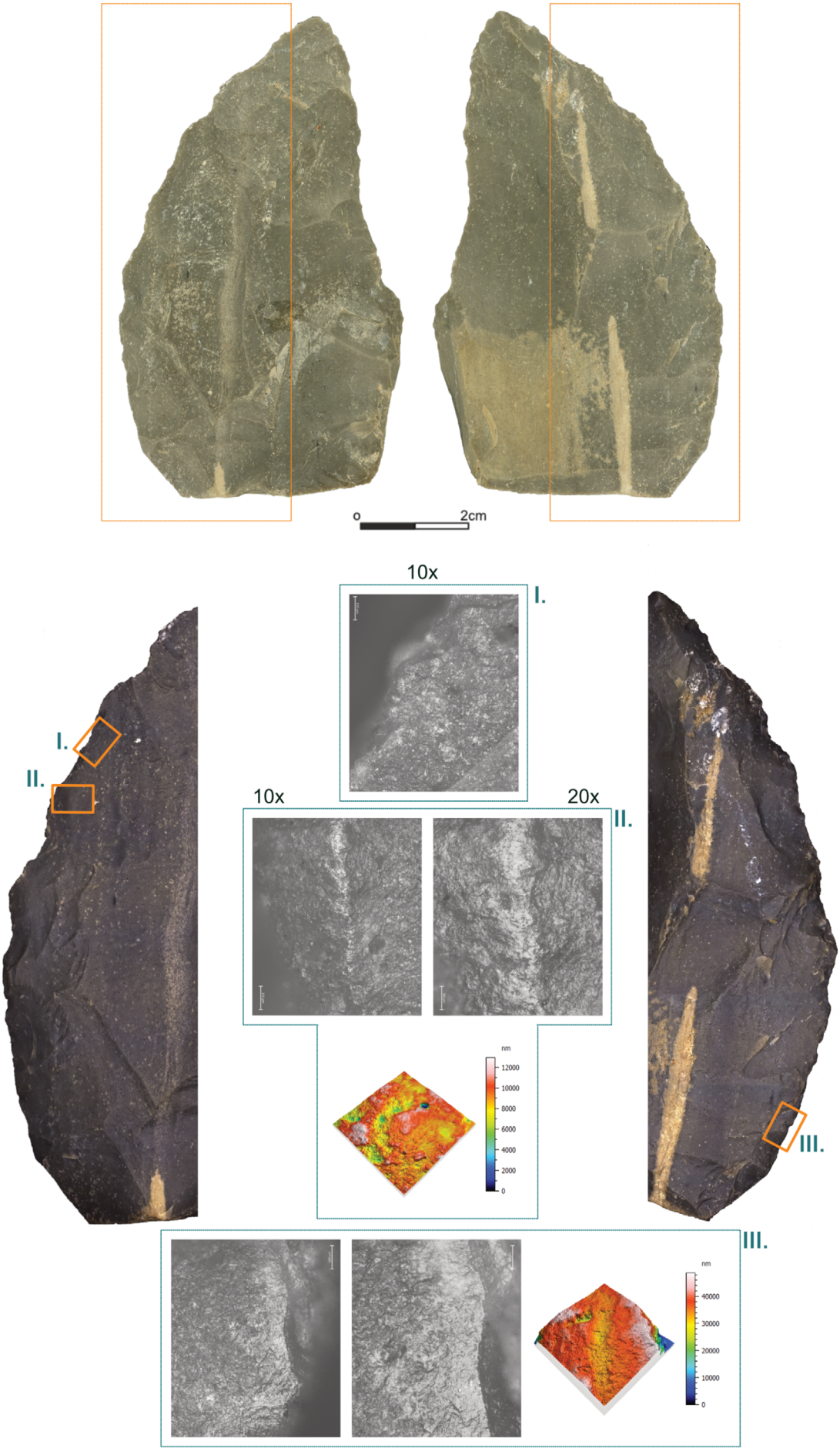

Balver Höhle, *Keilmesser* [ID MU-199]. The topmost image displays the artefact in original size. The other illustrations are magnifications acquired with a 1.6× objective and a 34-× zoom. The use-wear traces are acquired at magnification of 10× and 20× (I. type I.; II. type IV.; III. type V.). The micro-surface displays the processed result of the confocal data acquisition with the 50× objective.

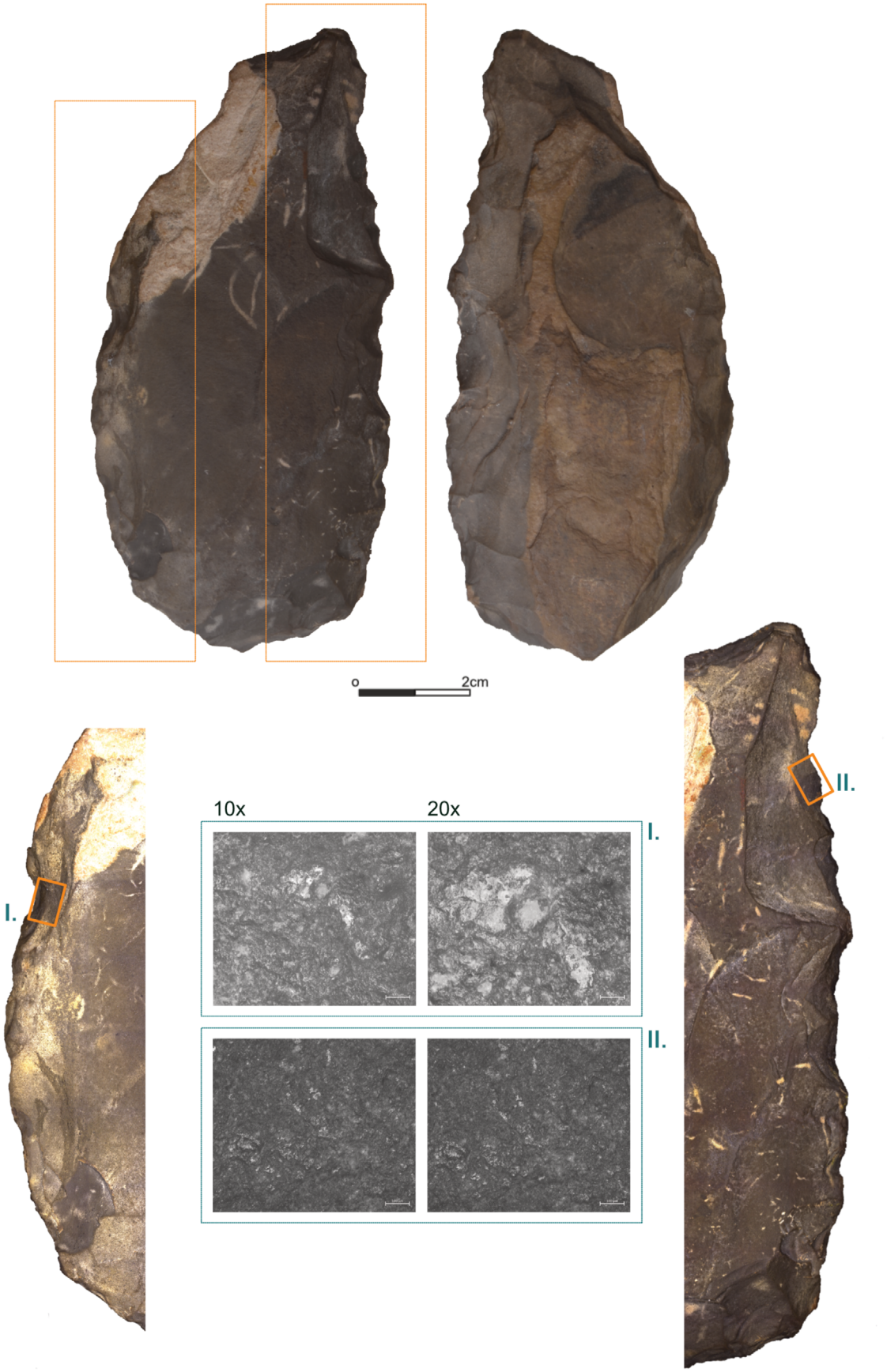

Balver Höhle, *Keilmesser* [ID MU-202; dorsal]. The topmost image displays the artefact in original size. The other illustrations are magnifications acquired with a 1.6× objective and a 34-× zoom. The use-wear traces are acquired at magnification of 10× and 20× (I. type I.; II. type II.).

Balver Höhle, *Keilmesser* [ID MU-202; ventral]. The topmost image displays the artefact in original size. The other illustrations are magnifications acquired with a 1.6× objective and a 34-× zoom. The use-wear traces are acquired at magnification of 10× and 20× (I. type V.; II. type V.; III. type I.). The micro-surface displays the processed result of the confocal data acquisition with the 50× objective.


0
2cm
10x
20x
I.
II.
III.
nm
15000
10000
5000
0
8000
7000
6000
5000
4000
3000
2000
1000
0

Plate A90

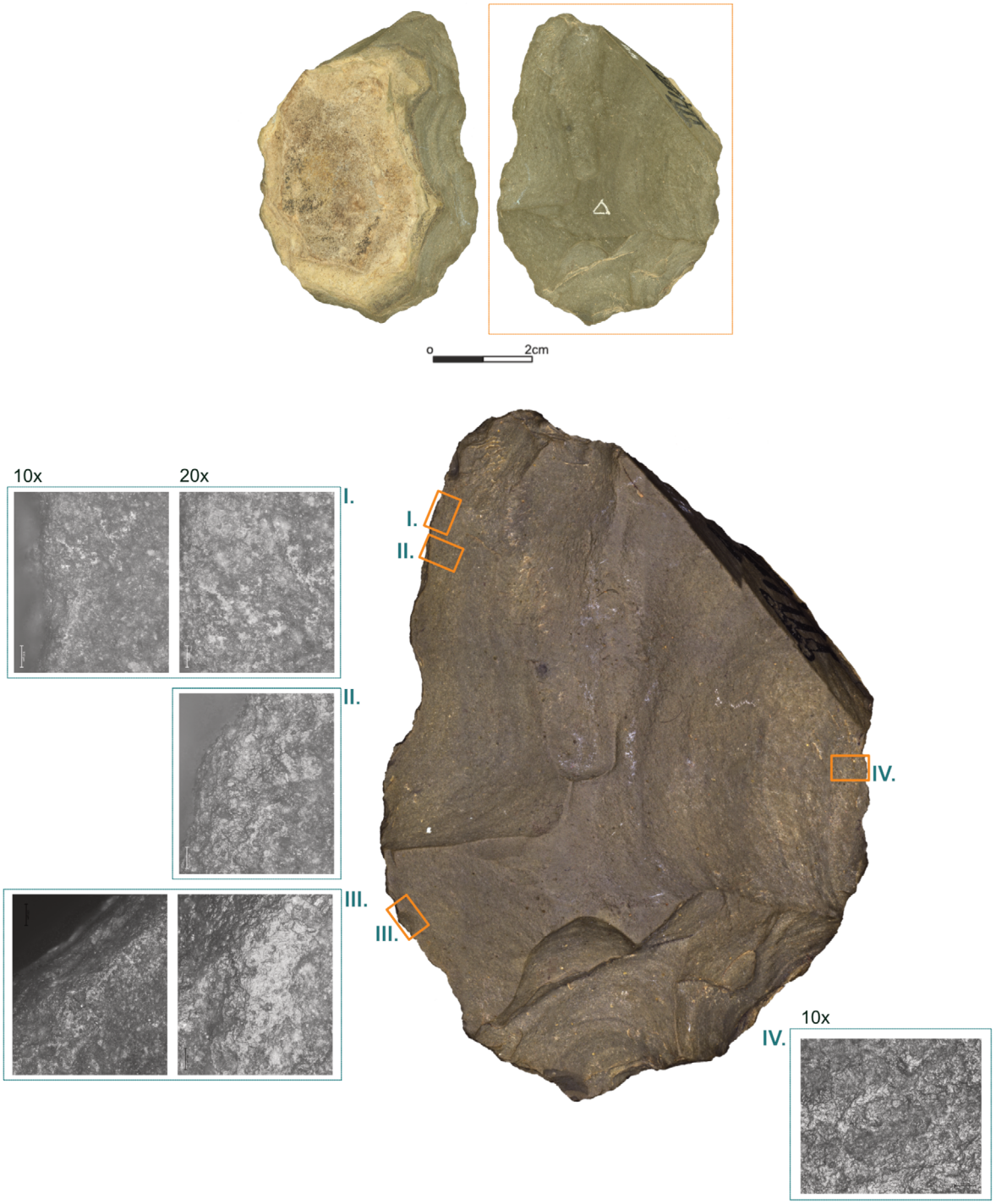

Balver Höhle, *Keilmesser* [ID MU-214]. The topmost image displays the artefact in original size. The other illustrations are magnifications acquired with a 1.6× objective and a 34-× zoom. The use-wear traces are acquired at magnification of 10× and 20× (I. type V.; II. type V.; III. type V.; IV. type V.).

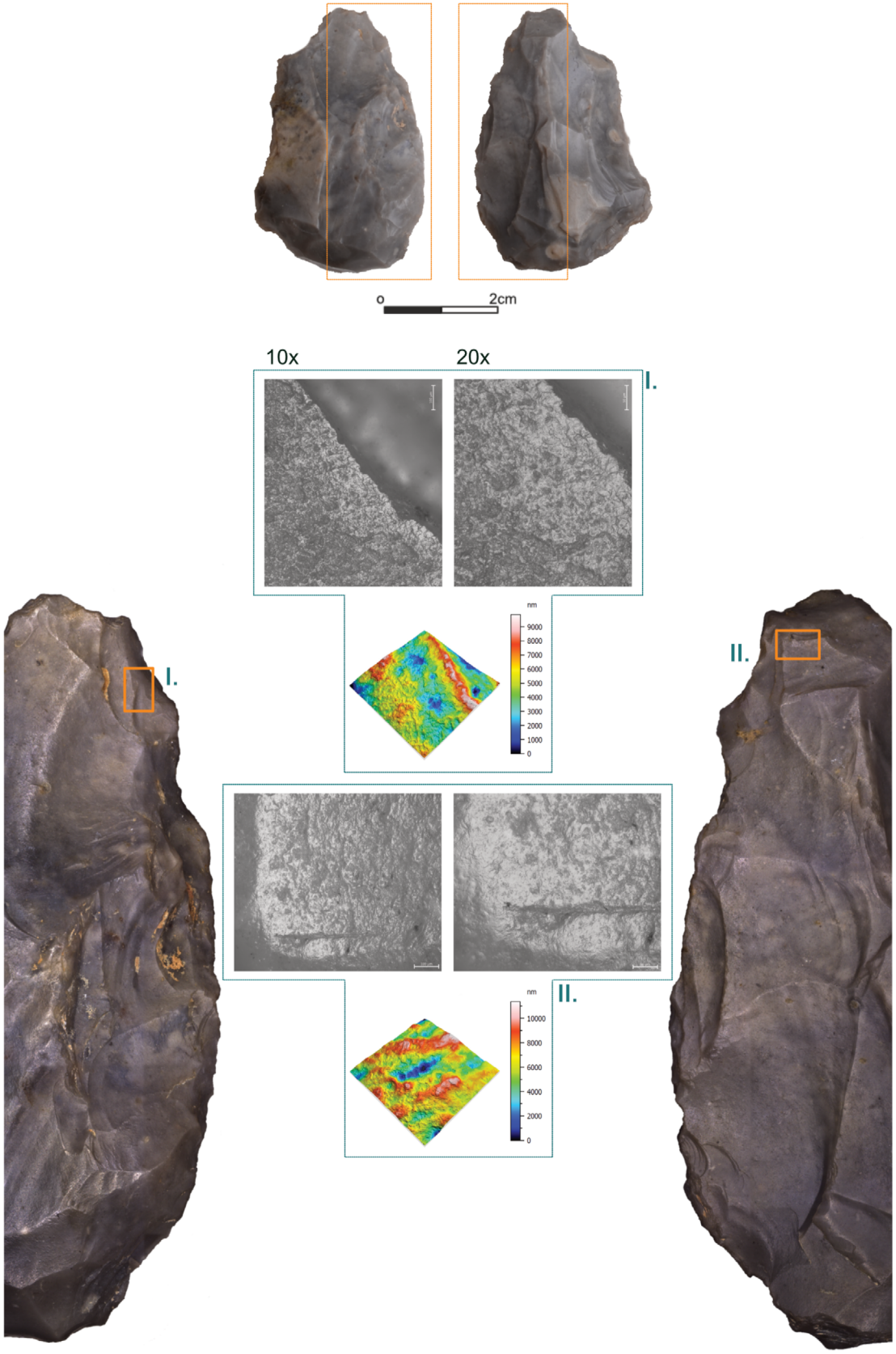

Balver Höhle, *Keilmesser* [ID MU-224]. The topmost image displays the artefact in original size. The other illustrations are magnifications acquired with a 1.6× objective and a 34-× zoom. The use-wear traces are acquired at magnification of 10× and 20× (I. type III.; II. type V.). The micro-surface displays the processed result of the confocal data acquisition with the 50× objective.

Plate A92

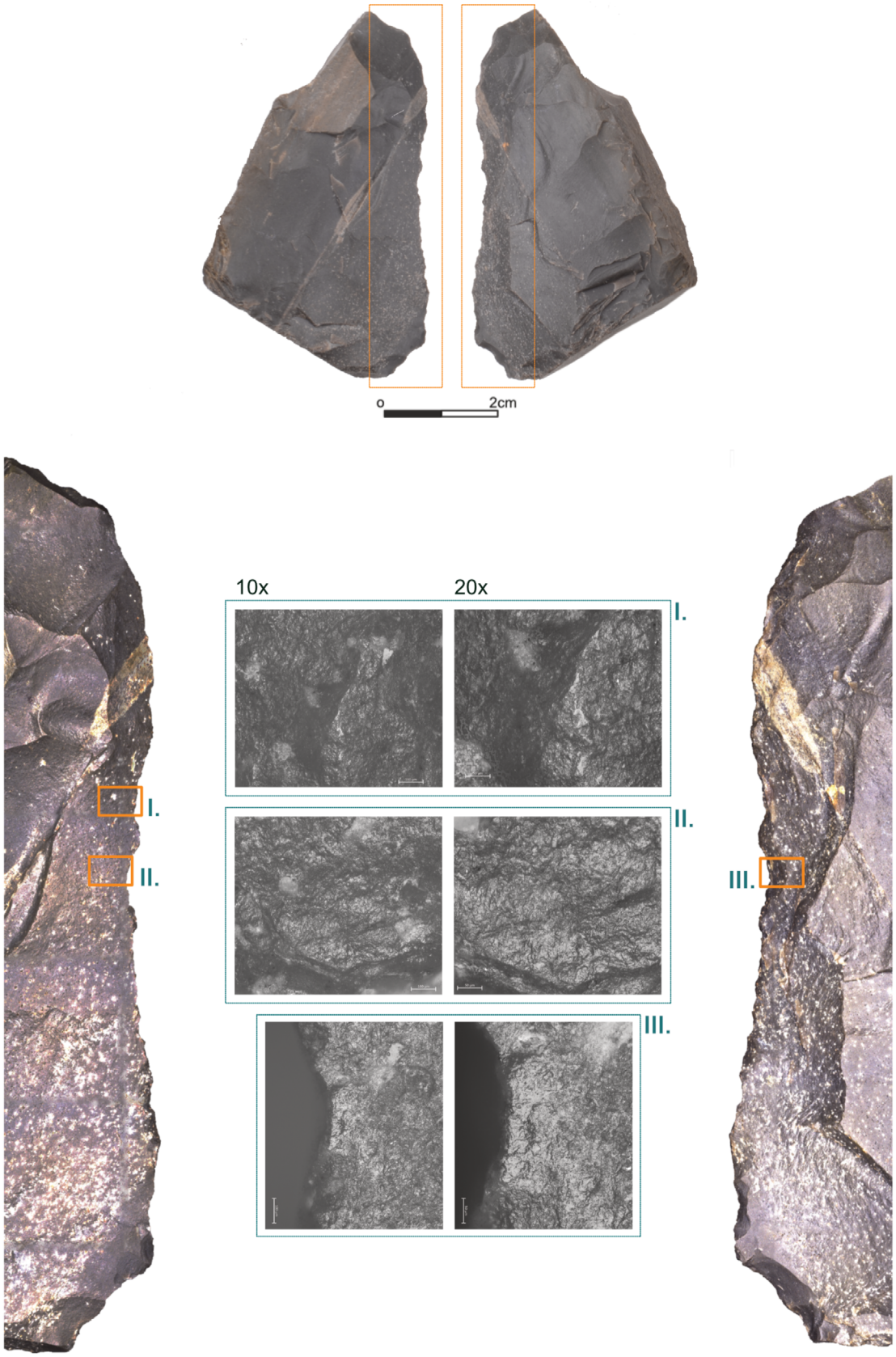

Balver Höhle, *Keilmesser* [ID MU-226]. The topmost image displays the artefact in original size. The other illustrations are magnifications acquired with a 1.6× objective and a 34-× zoom. The use-wear traces are acquired at magnification of 10× and 20× (I. type V.; II. type IV.; III. type V.).

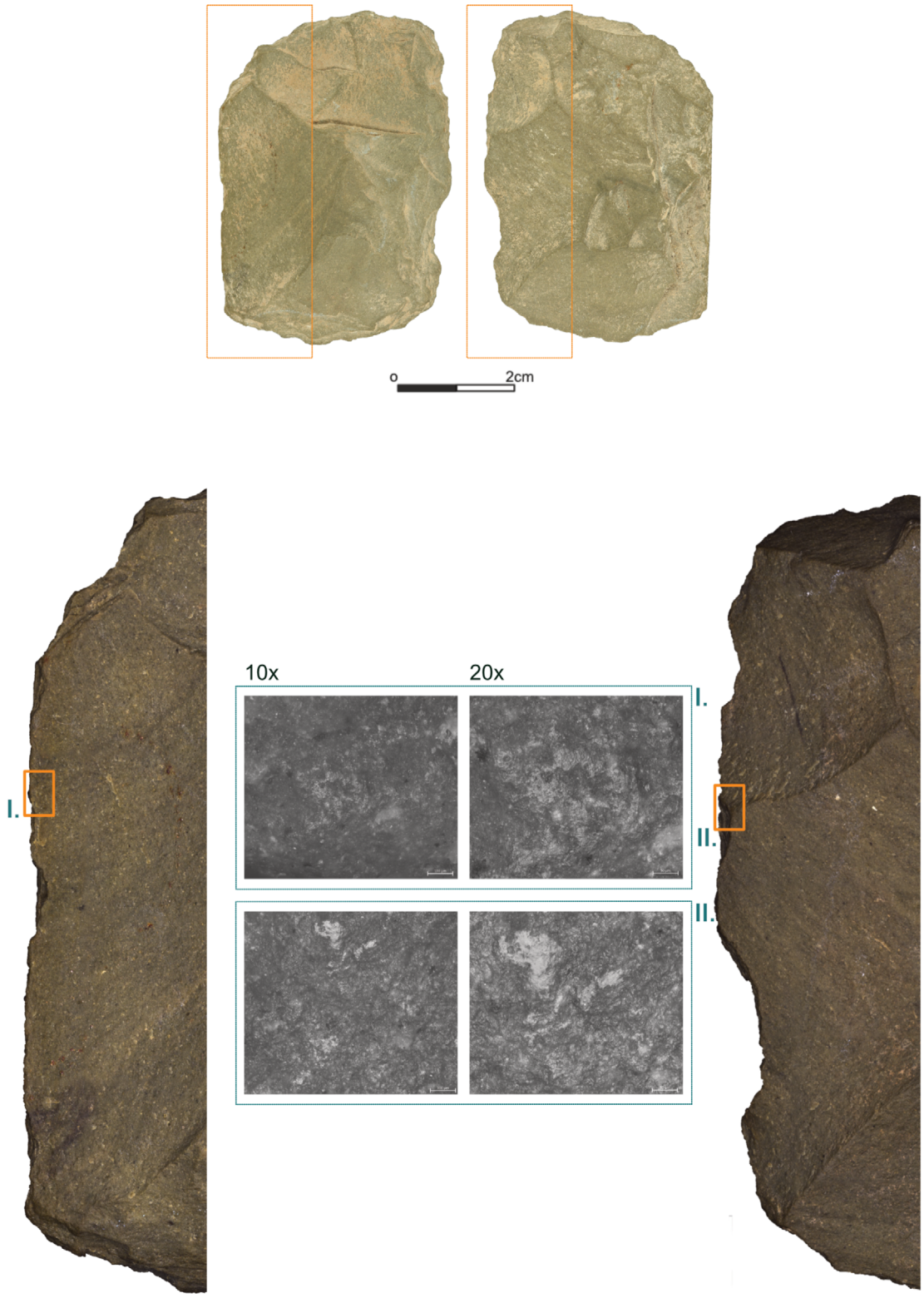

Balver Höhle, *Keilmesser* [ID MU-230]. The topmost image displays the artefact in original size. The other illustrations are magnifications acquired with a 1.6× objective and a 34-× zoom. The use-wear traces are acquired at magnification of 10× and 20× (I. type II.; II. type II.).

Plate A94



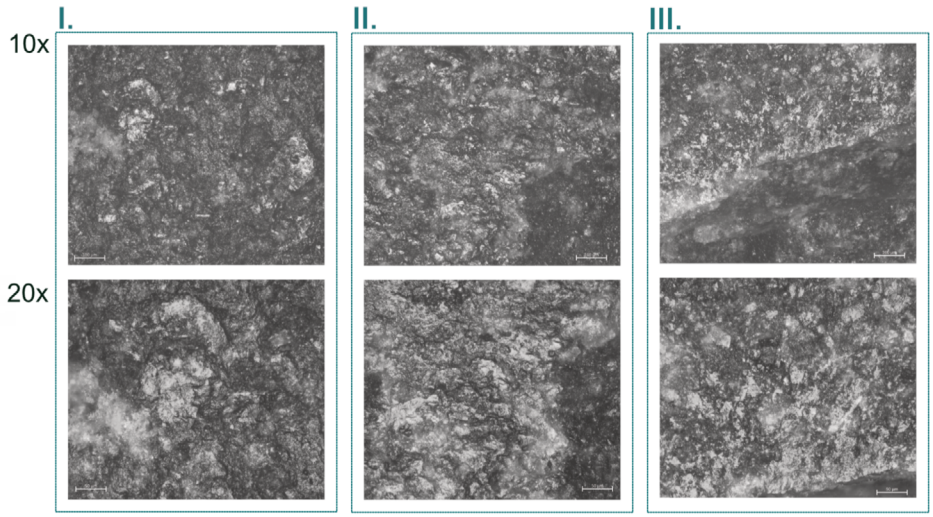

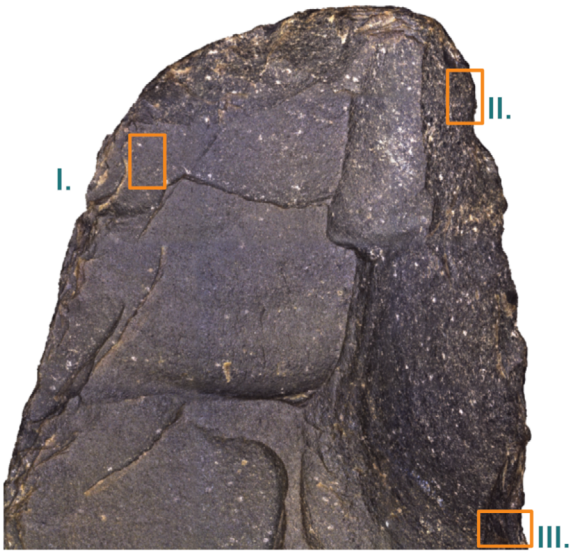

Balver Höhle, *Keilmesser* [ID MU-231]. The topmost image displays the artefact in original size. The other illustrations are magnifications acquired with a 1.6× objective and a 34-× zoom. The use-wear traces are acquired at magnification of 10× and 20× (I. type I.; II. type V.; III. type V.).

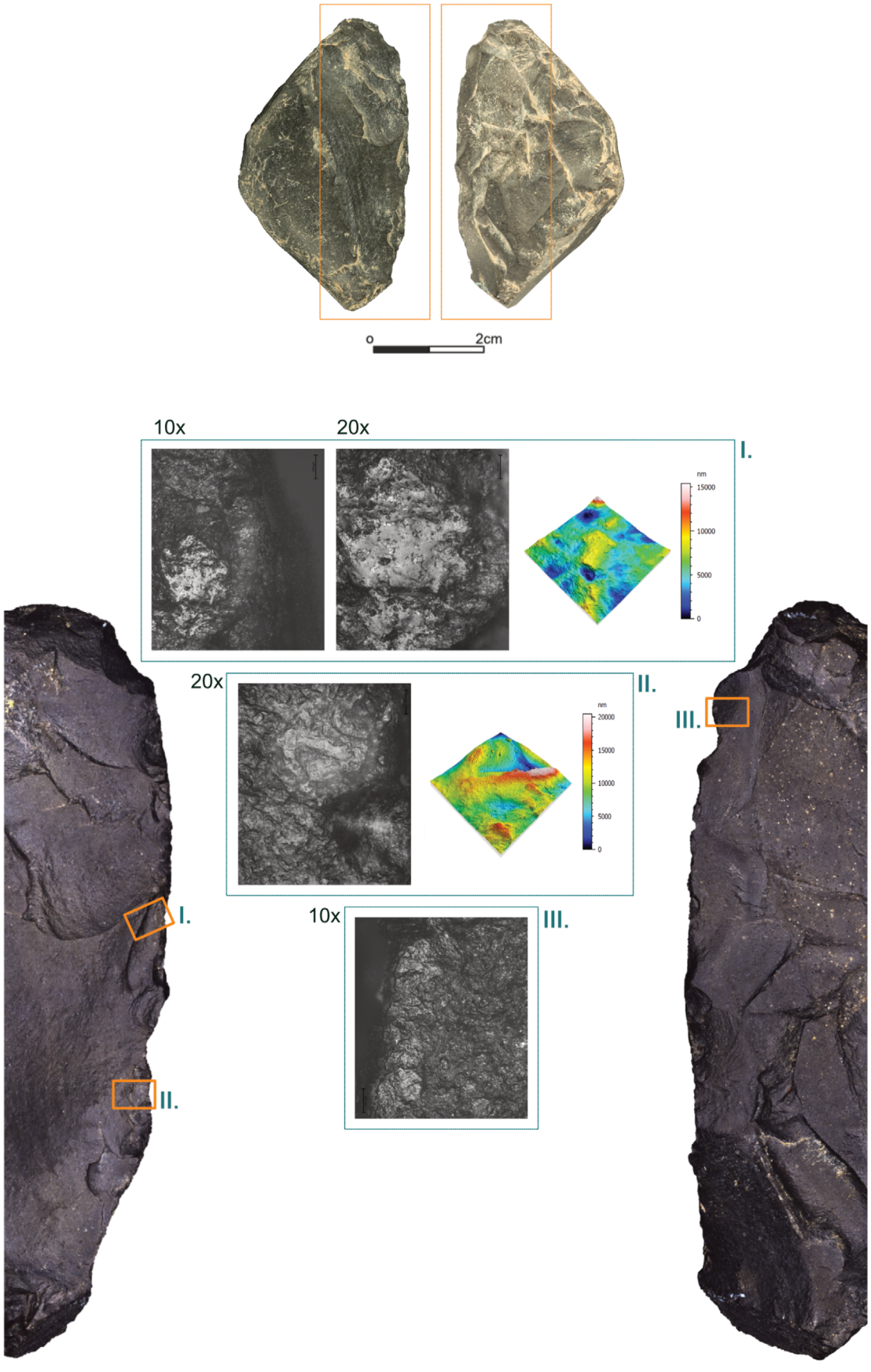

Balver Höhle, *Keilmesser* [ID MU-232]. The topmost image displays the artefact in original size. The other illustrations are magnifications acquired with a 1.6× objective and a 34-× zoom. The use-wear traces are acquired at magnification of 10× and 20× (I. type IV.; II. type I.; III. type V.). The micro-surface displays the processed result of the confocal data acquisition with the 20× and 50× objective.

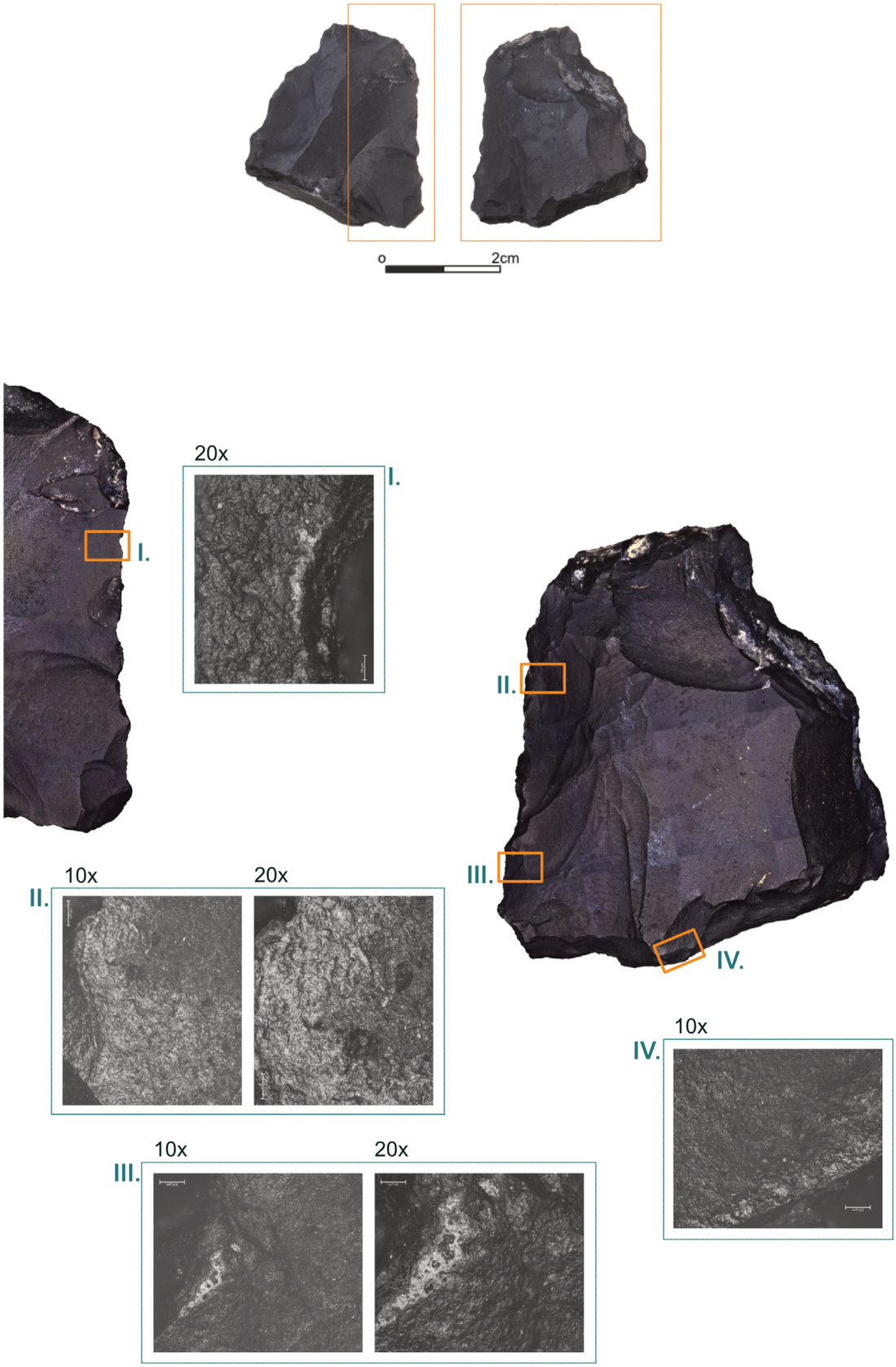

Balver Höhle, *Keilmesser* [ID MU-234]. The topmost image displays the artefact in original size. The other illustrations are magnifications acquired with a 1.6× objective and a 34-× zoom. The use-wear traces are acquired at magnification of 10× and 20× (I. type IV.; II. type V.; III. type III.; IV. type V.).

Balver Höhle, *Keilmesser* [ID MU-240]. The topmost image displays the artefact in original size. The other illustrations are magnifications acquired with a 1.6× objective and a 34-× zoom. The use-wear traces are acquired at magnification of 10× and 20× (I. type V.; II. type VIII.; III. type V. + I.). The micro-surface displays the processed result of the confocal data acquisition with the 50× objective.

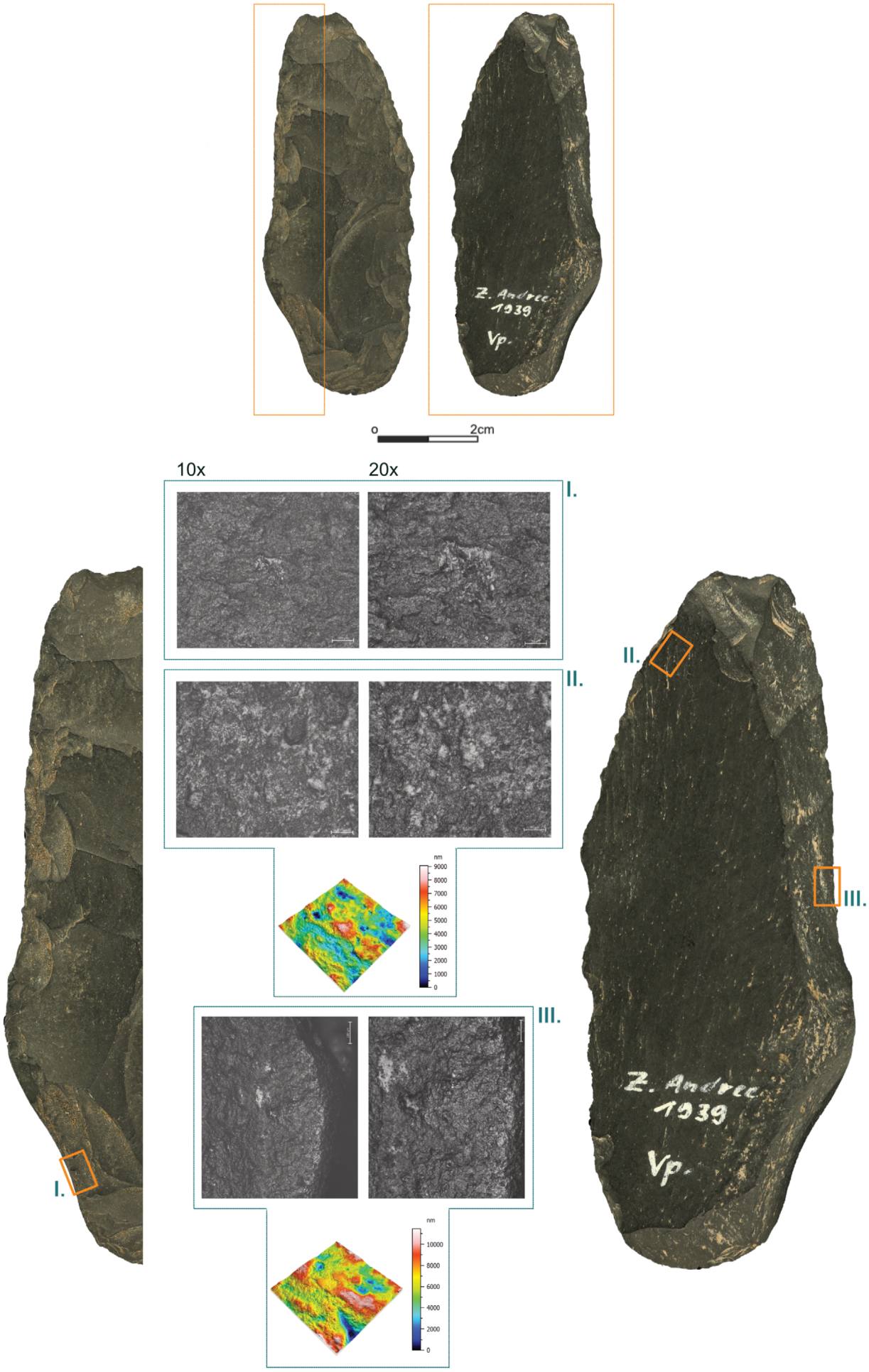
Z. Andrec
1939
Vp.
0
2cm
10x
20x
I.
II.
III.
nm
9000
8000
7000
6000
5000
4000
3000
2000
1000
0
10000
8000
6000
4000
2000
0

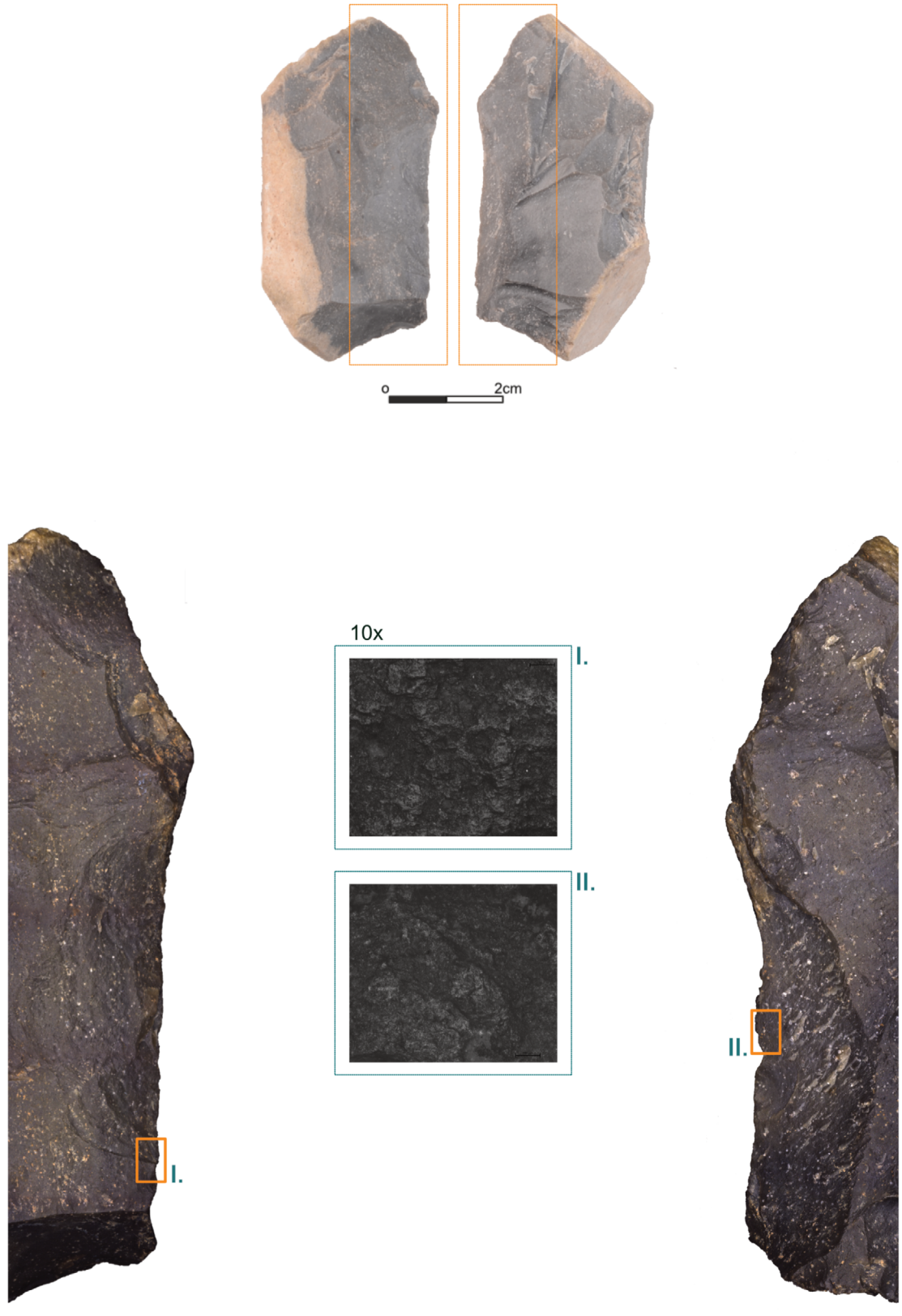

Balver Höhle, *Keilmesser* [ID MU-241]. The topmost image displays the artefact in original size. The other illustrations are magnifications acquired with a 1.6× objective and a 34-× zoom. The use-wear traces are acquired at magnification of 10× (I. type V.; II. type V.).

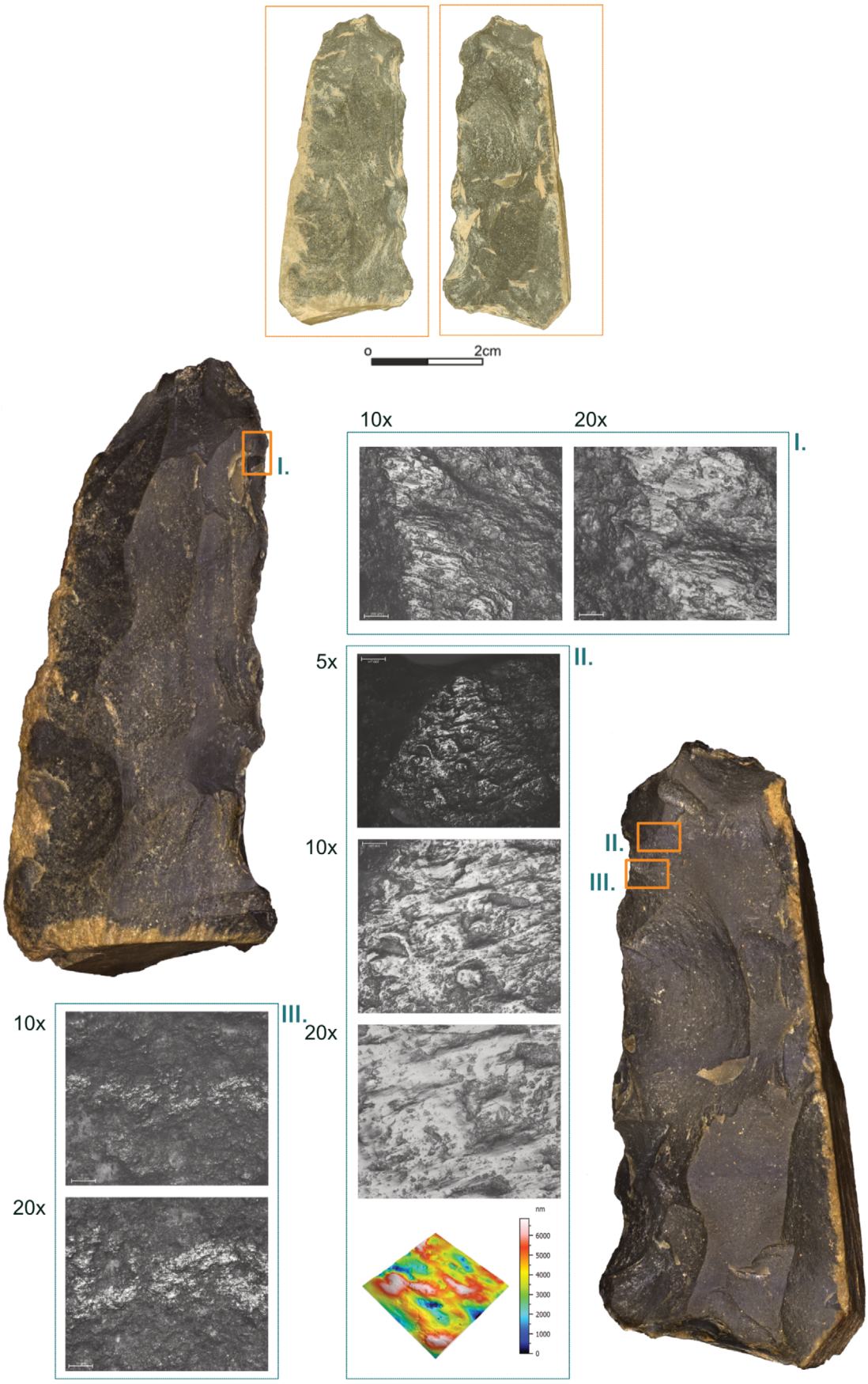

Balver Höhle, *Keilmesser* [ID MU-246]. The topmost image displays the artefact in original size. The other illustrations are magnifications acquired with a 1.6× objective and a 34-× zoom. The use-wear traces are acquired at magnification of 5×, 10× and 20× (I. type V./ IV.; II. type IV.; III. type V. / IV.). The micro-surface displays the processed result of the confocal data acquisition with the 50× objective.

Plate A100



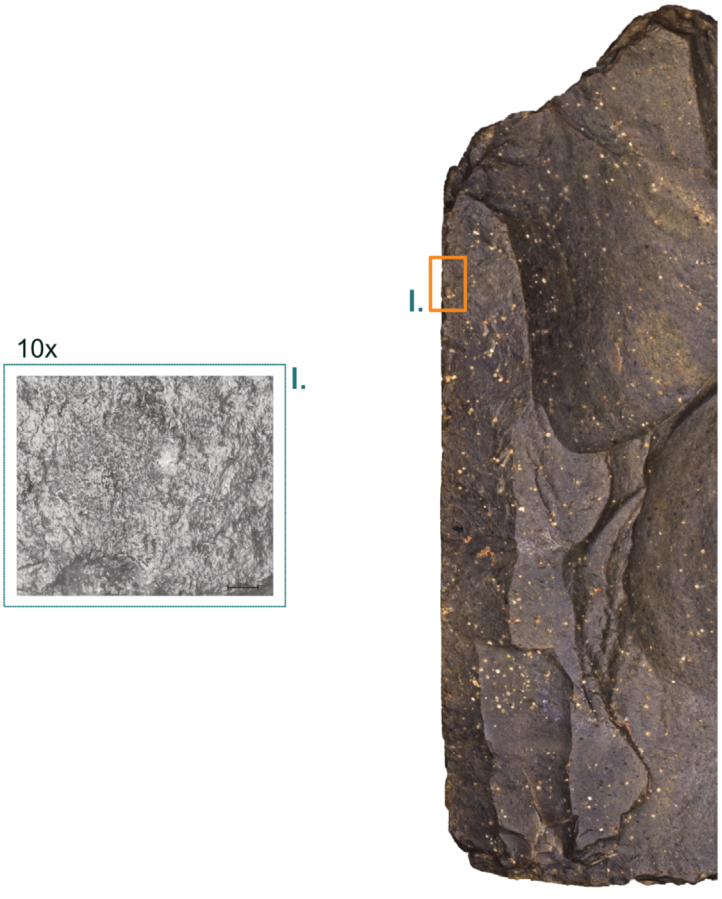

Balver Höhle, *Keilmesser* [ID MU-249]. The topmost image displays the artefact in original size. The other illustrations are magnifications acquired with a 1.6× objective and a 34-× zoom. The use-wear trace is acquired at magnification of 10× (I. type V.).



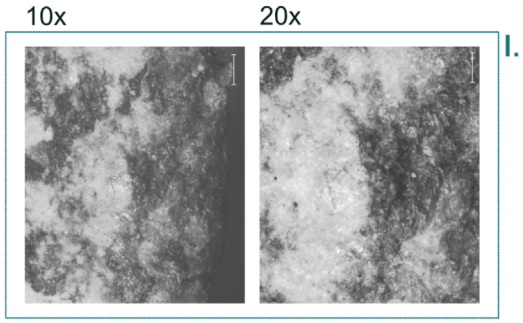



Balver Höhle, *Keilmesser* [ID MU-272]. The topmost image displays the artefact in original size. The other illustrations are magnifications acquired with a 1.6× objective and a 34-× zoom. The use-wear trace is acquired at magnification of 10× and 20× (I. type V. + VIII.).

Plate A102

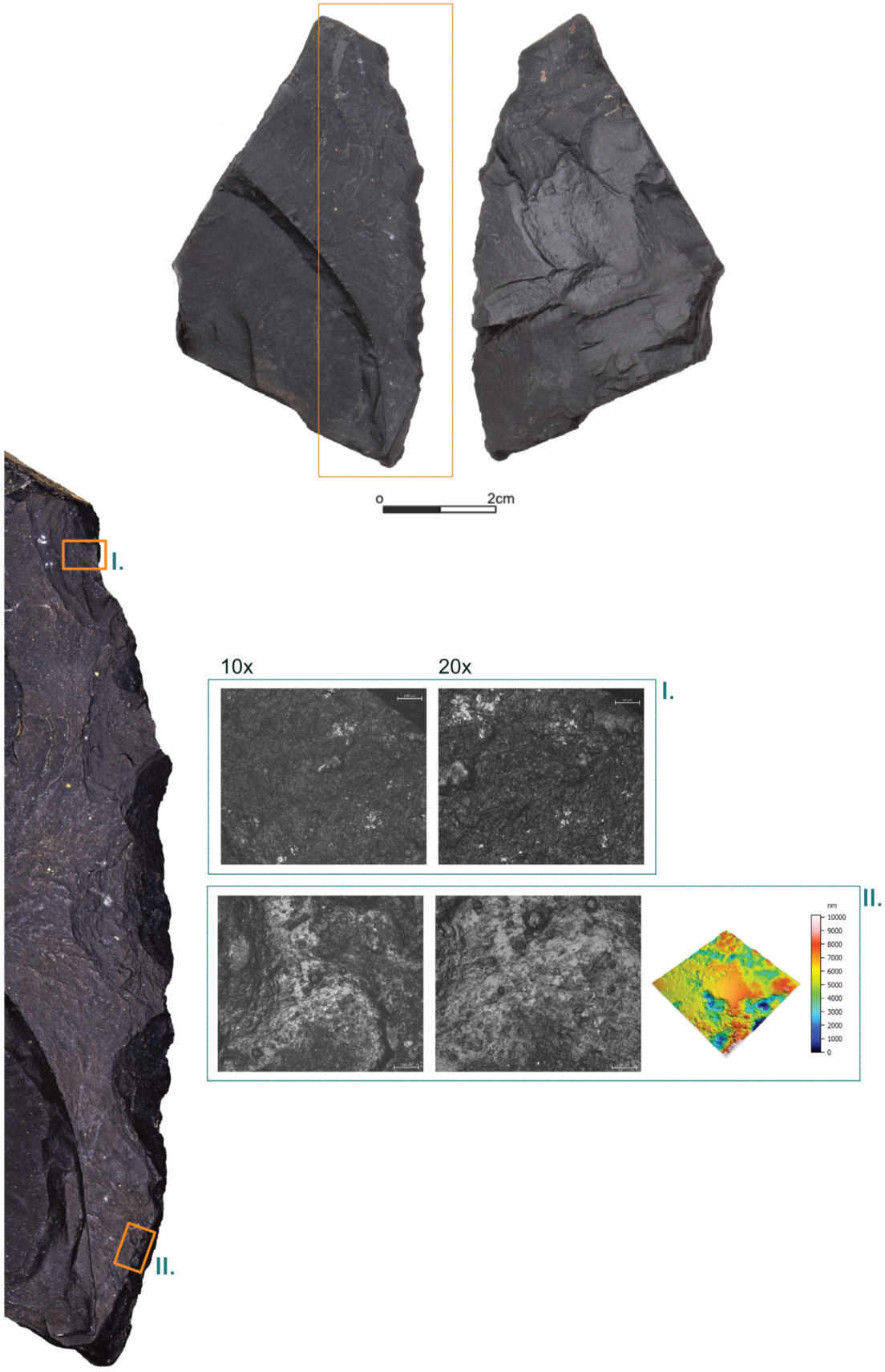

Balver Höhle, *Keilmesser* [ID MU-273]. The topmost image displays the artefact in original size. The other illustrations are magnifications acquired with a 1.6× objective and a 34-× zoom. The use-wear traces are acquired at magnification of 10× and 20× (I. type I.; II. type V. / IV.). The micro-surface displays the processed result of the confocal data acquisition with the 50× objective.

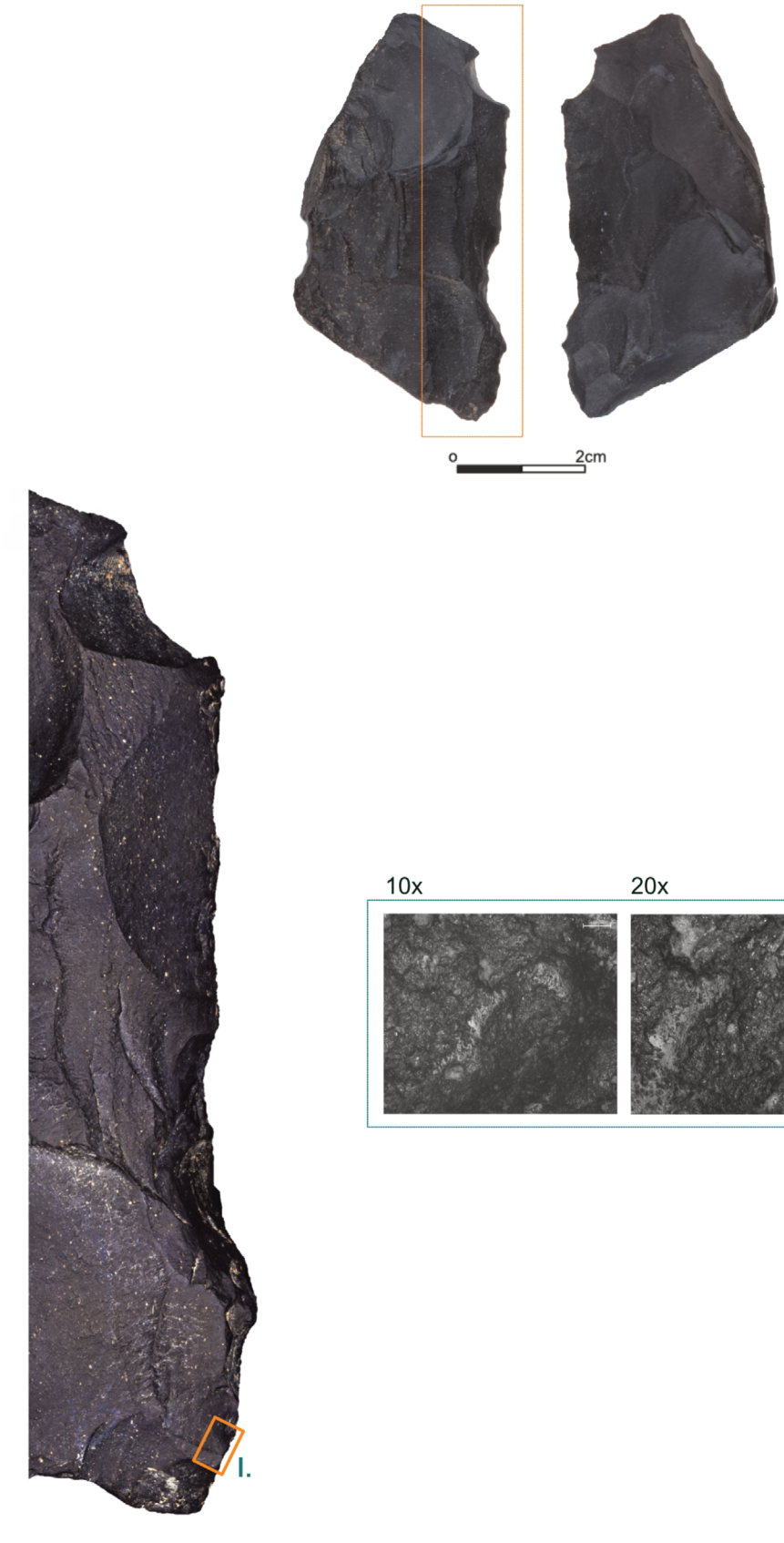

Balver Höhle, *Keilmesser* [ID MU-276]. The topmost image displays the artefact in original size. The other illustrations are magnifications acquired with a 1.6× objective and a 34-× zoom. The use-wear trace is acquired at magnification of 10× and 20× (I. type V. / IV.).

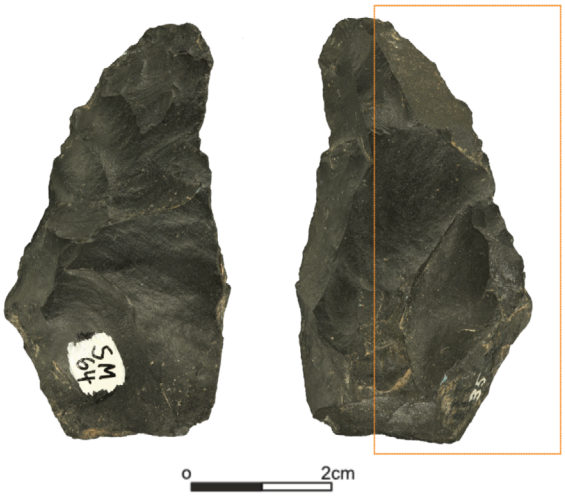

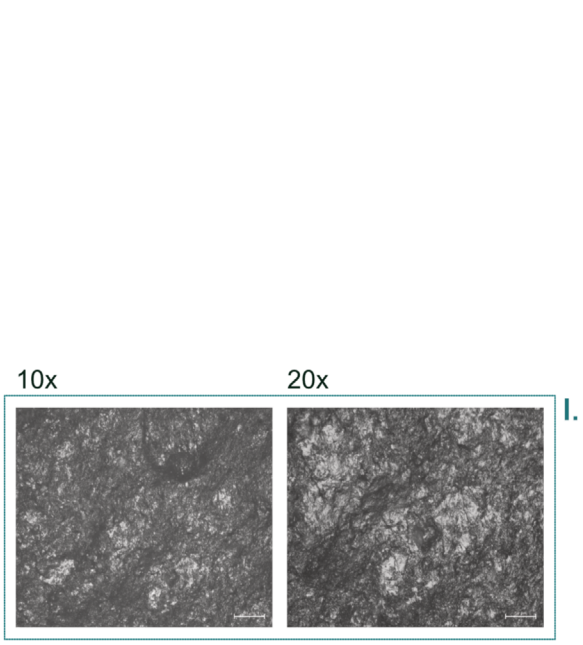



Balver Höhle, *Keilmesser* [ID MU-280]. The topmost image displays the artefact in original size. The other illustrations are magnifications acquired with a 1.6× objective and a 34-× zoom. The use-wear trace is acquired at magnification of 10× and 20× (I. type I.).



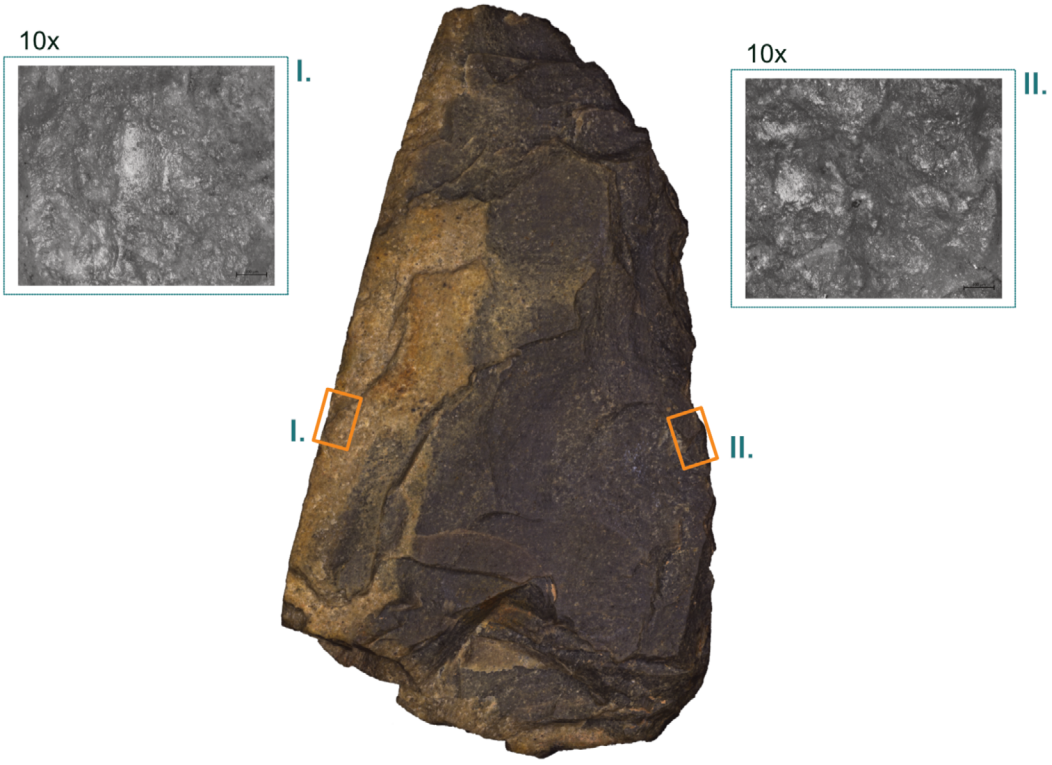

Balver Höhle, *Keilmesser* [ID MU-283]. The topmost image displays the artefact in original size. The other illustrations are magnifications acquired with a 1.6× objective and a 34-× zoom. The use-wear traces are acquired at magnification of 10× and 20× (I. type II.; II. type II.).

Plate A106

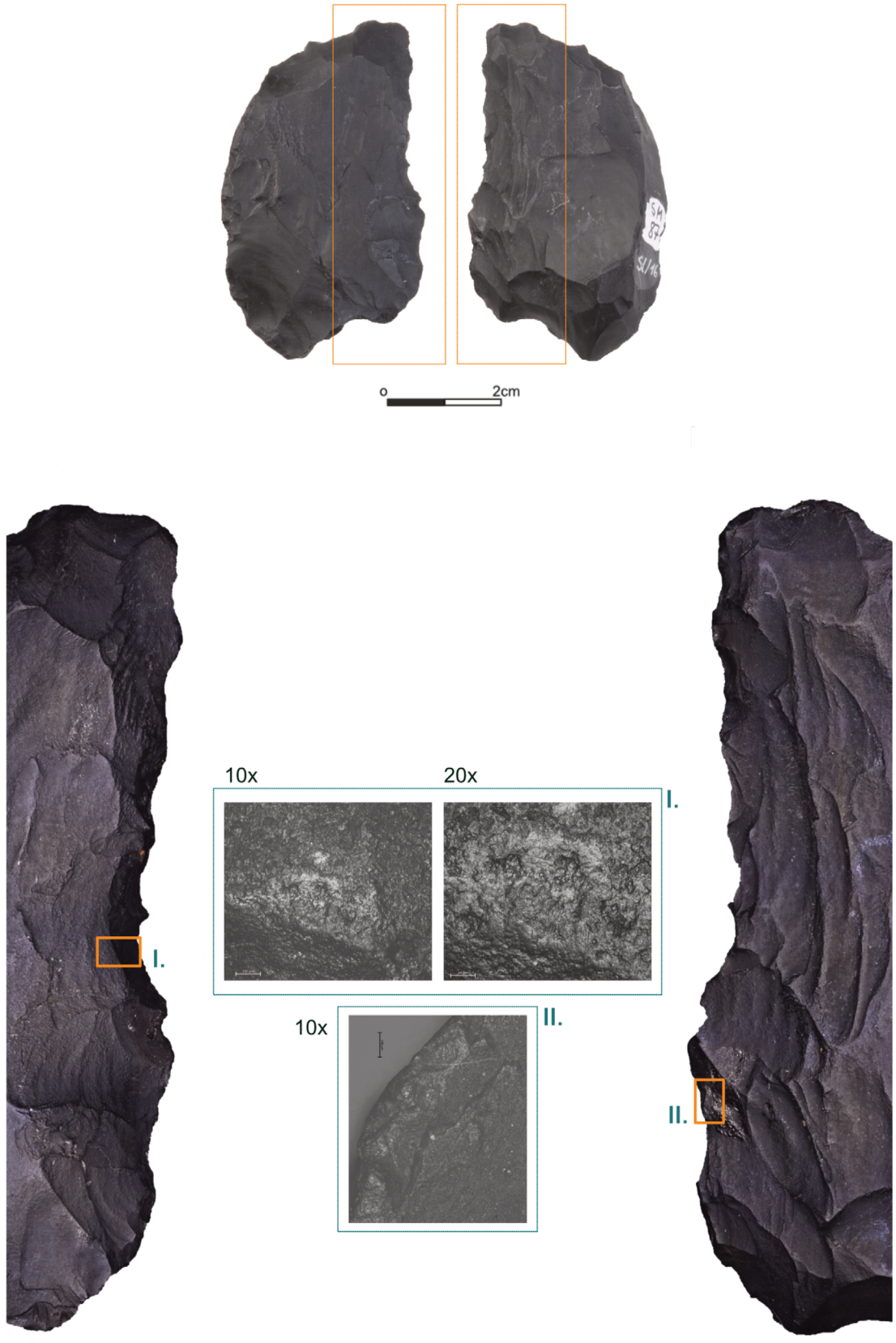

Balver Höhle, *Keilmesser* [ID MU-286]. The topmost image displays the artefact in original size. The other illustrations are magnifications acquired with a 1.6× objective and a 34-× zoom. The use-wear traces are acquired at magnification of 10× and 20× (I. type VII.; II. type V.).

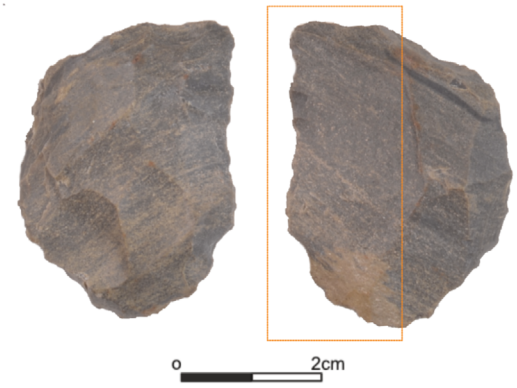

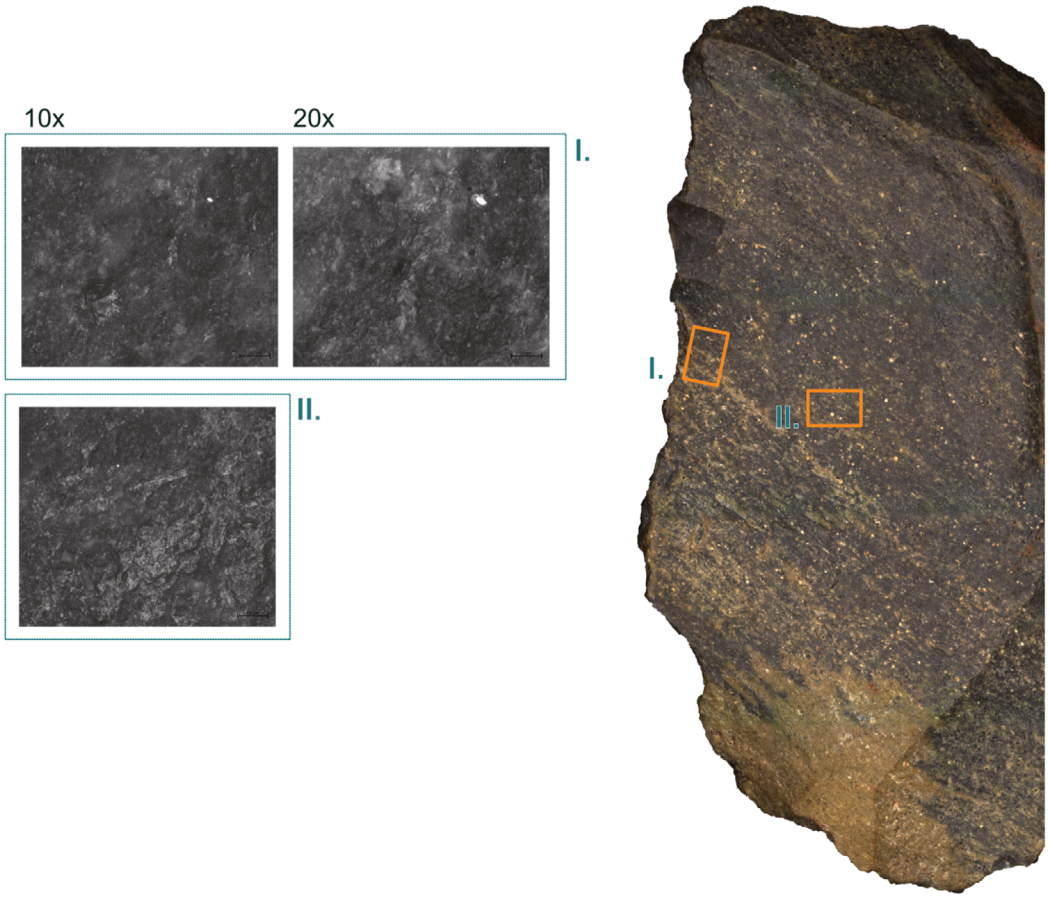

Balver Höhle, *Keilmesser* [ID MU-288]. The topmost image displays the artefact in original size. The other illustrations are magnifications acquired with a 1.6× objective and a 34-× zoom. The use-wear traces are acquired at magnification of 10× and 20× (I. type II.; II. type V.).

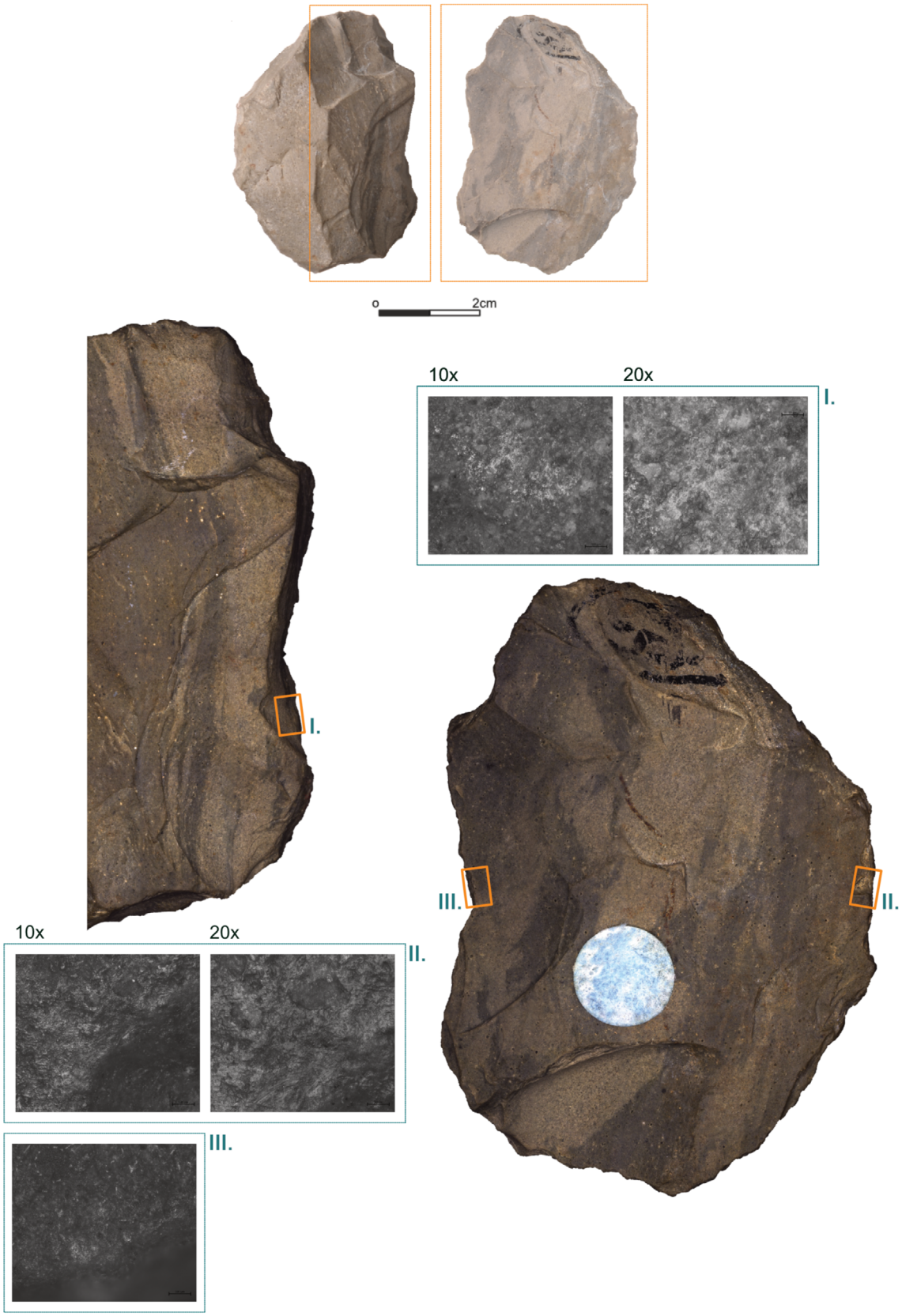

Balver Höhle, *Keilmesser* [ID MU-293]. The topmost image displays the artefact in original size. The other illustrations are magnifications acquired with a 1.6× objective and a 34-× zoom. The use-wear traces are acquired at magnification of 10× and 20× (I. type VII.; II. type I.; III. type VI.).

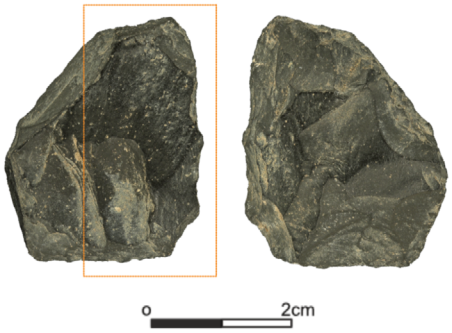

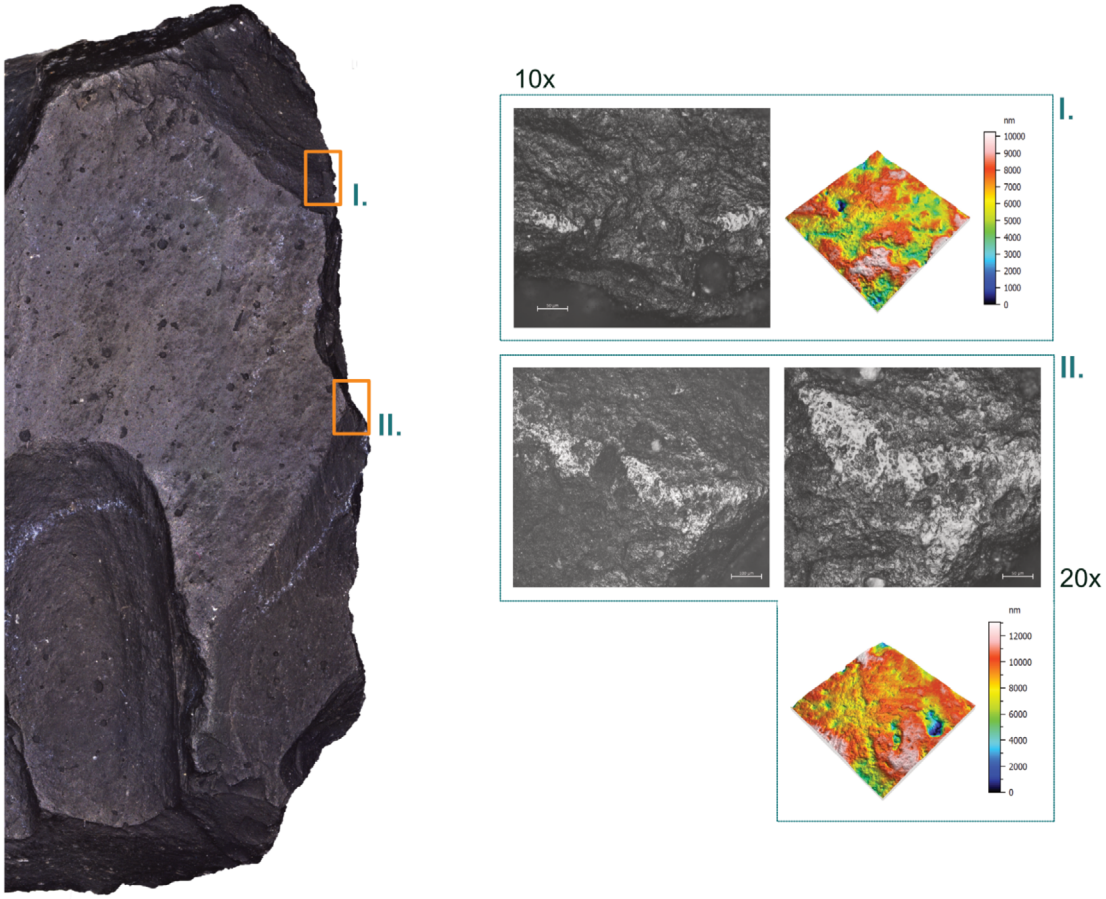

Balver Höhle, *Keilmesser* tip [ID MU-041]. The topmost image displays the artefact in original size. The other illustrations are magnifications acquired with a 1.6× objective and a 34-× zoom. The use-wear traces are acquired at magnification of 10× and 20× (I. type IV.; II. type IV.). The micro-surface displays the processed result of the confocal data acquisition with the 50× objective.

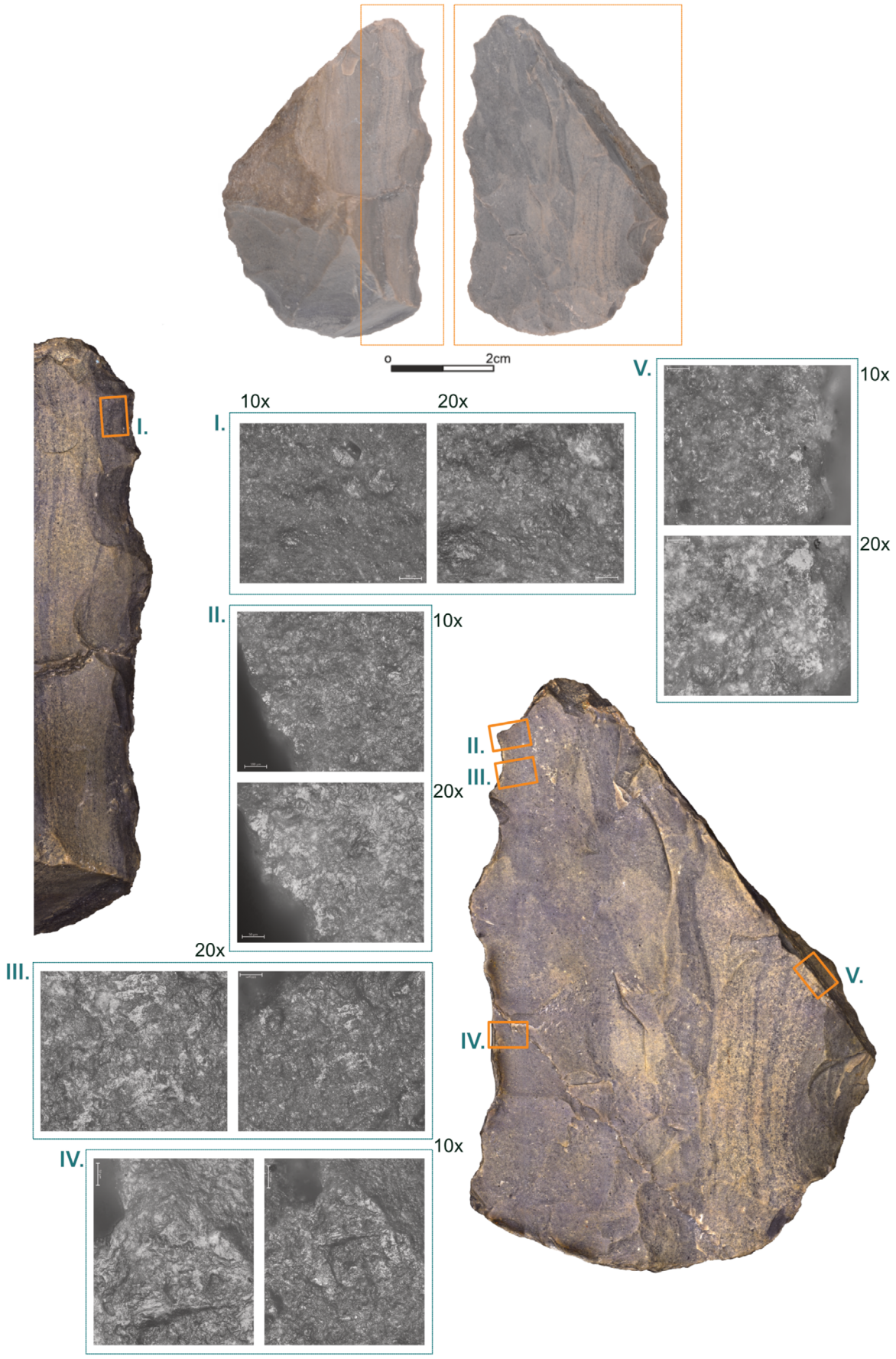

Balver Höhle, *Keilmesser* tip [ID MU-210]. The topmost image displays the artefact in original size. The other illustrations are magnifications acquired with a 1.6× objective and a 34-× zoom. The use-wear traces are acquired at magnification of 10× and 20× (I. type I.; II. type V.; III. type II.; IV. type V.; V. type I.).



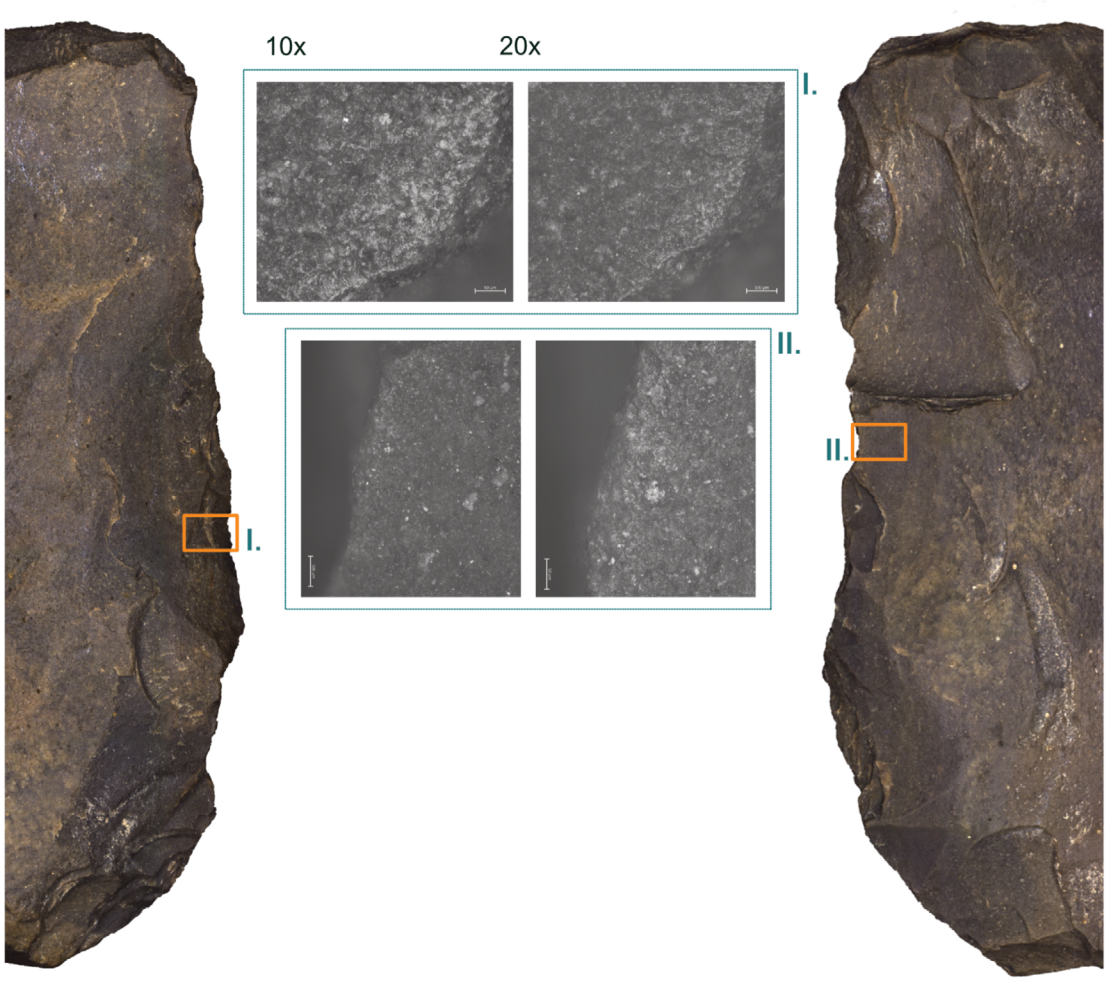

Balver Höhle, *Prądnik scraper* [ID MU-005]. The topmost image displays the artefact in original size. The other illustrations are magnifications acquired with a 1.6× objective and a 34-× zoom. The use-wear traces are acquired at magnification of 10× and 20× (I. type I.; II. type V.).

Plate A112



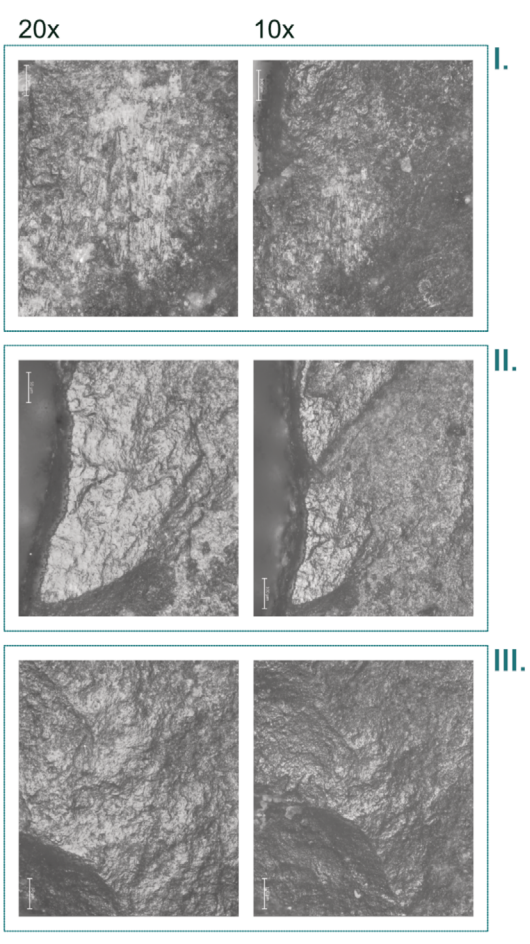



Balver Höhle, *Prądnik scraper* [ID MU-098]. The topmost image displays the artefact in original size. The other illustrations are magnifications acquired with a 1.6× objective and a 34-× zoom. The use-wear traces are acquired at magnification of 10× and 20× (I. type VII.; II. type V.; III. type V.).

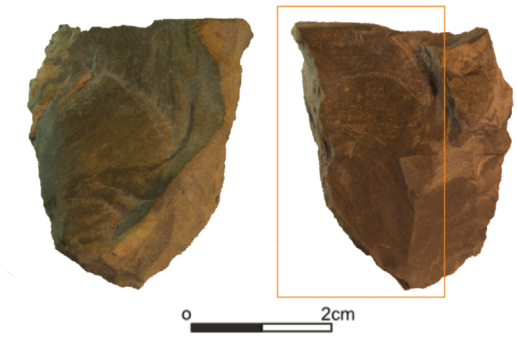

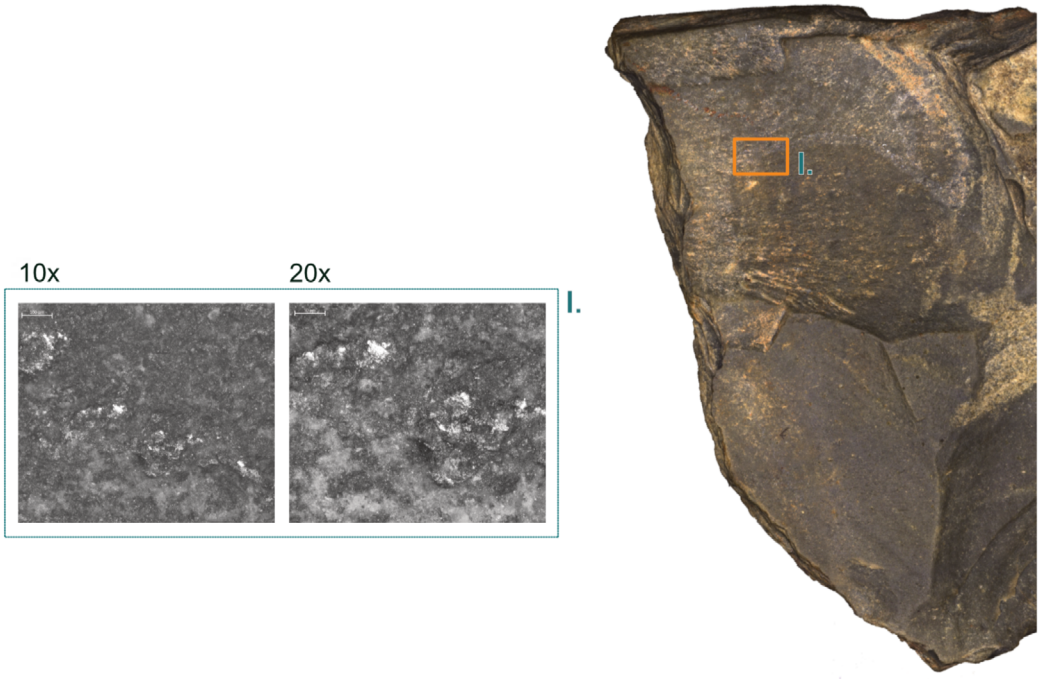

Balver Höhle, *Prądnik spall* [ID MU-095]. The topmost image displays the artefact in original size. The other illustrations are magnifications acquired with a 1.6× objective and a 34-× zoom. The use-wear trace is acquired at magnification of 10× and 20× (I. type II.).

Plate A114

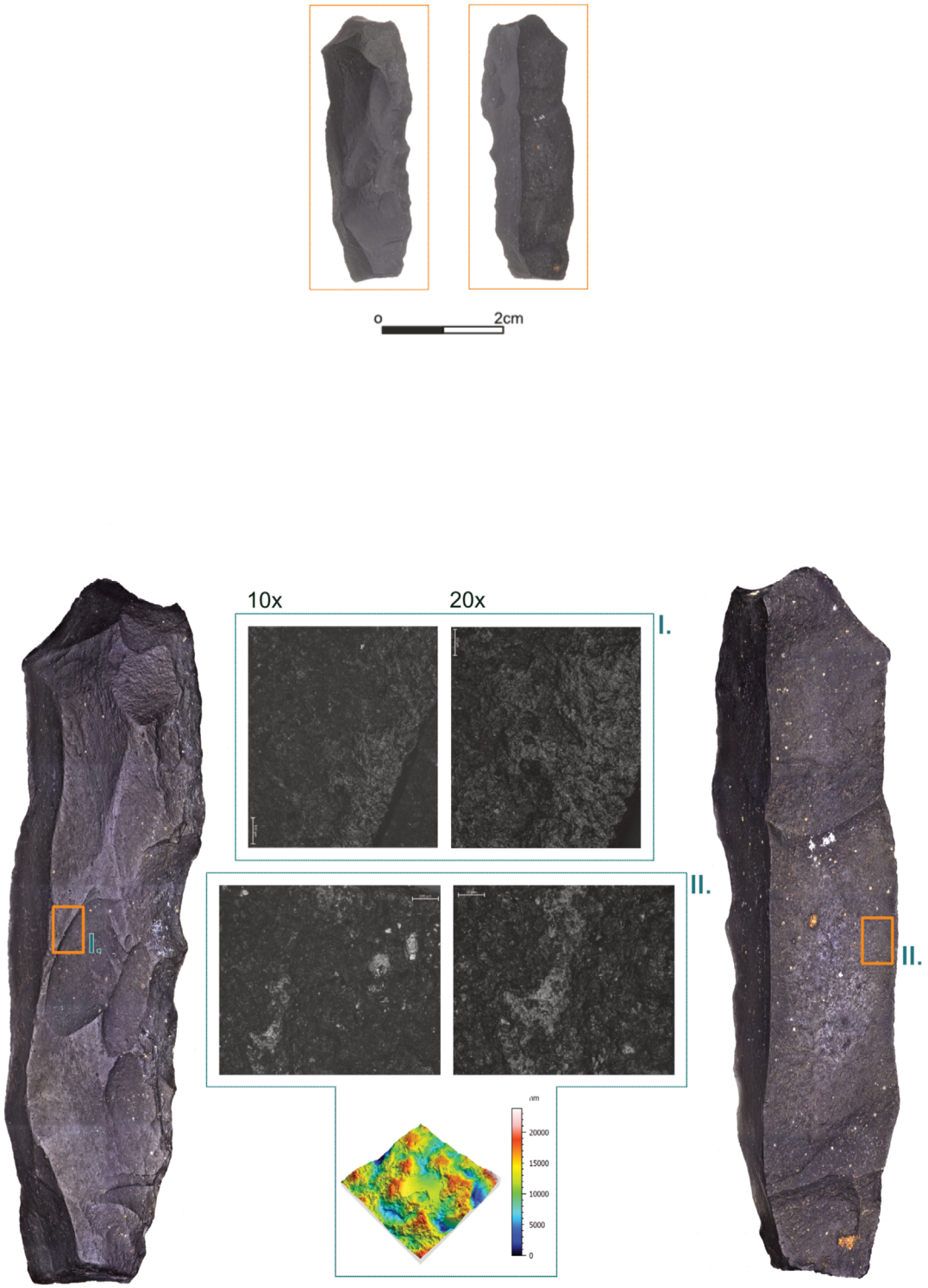

Balver Höhle, *Prądnik spall* [ID MU-104]. The topmost image displays the artefact in original size. The other illustrations are magnifications acquired with a 1.6× objective and a 34-× zoom. The use-wear traces are acquired at magnification of 10× and 20× (I. type V.; II. type V. / IV.). The micro-surface displays the processed result of the confocal data acquisition with the 50× objective.



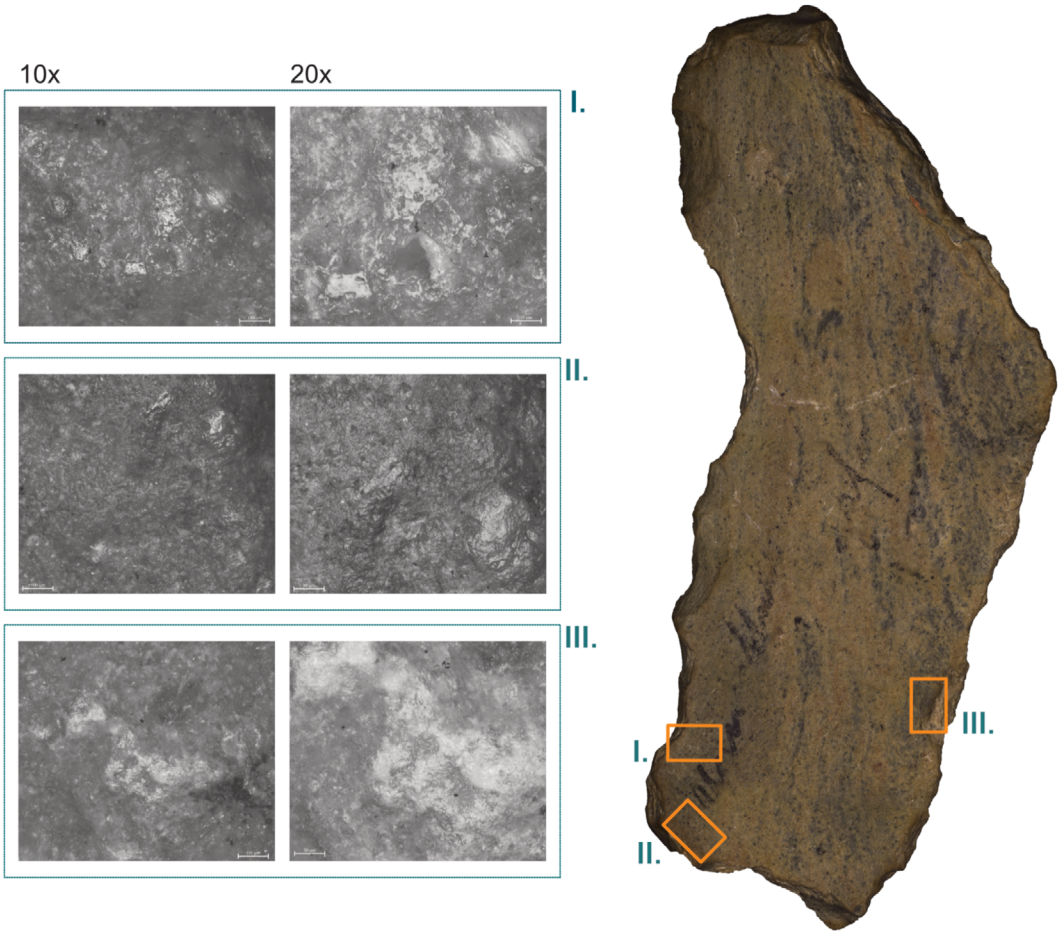

Balver Höhle, *Prądnik spall* [ID MU-118]. The topmost image displays the artefact in original size. The other illustrations are magnifications acquired with a 1.6× objective and a 34-× zoom. The use-wear traces are acquired at magnification of 10× and 20× (I. type V./ IV; II. type II.; III. type V).

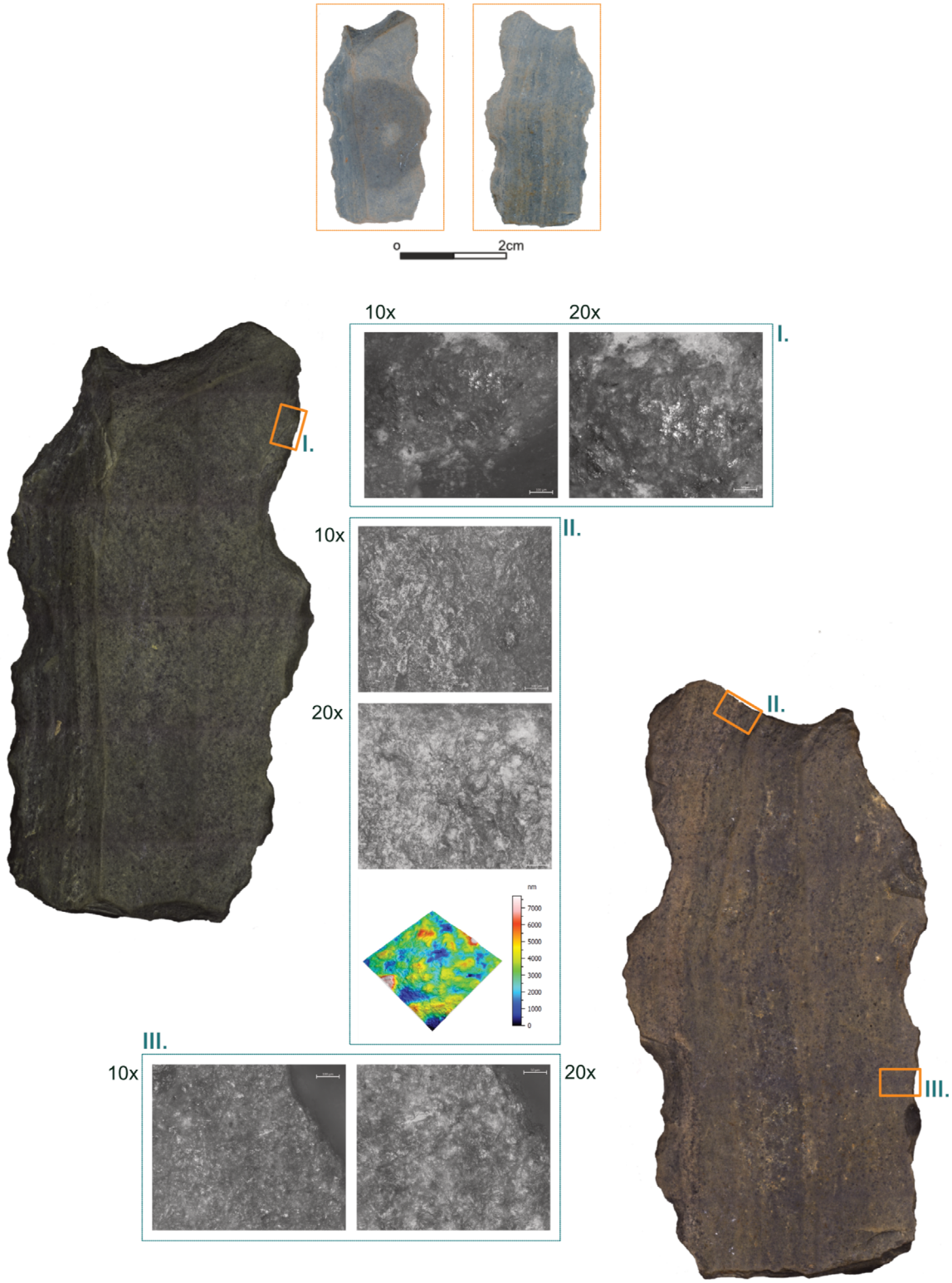

Balver Höhle, *Prądnik spall* [ID MU-119]. The topmost image displays the artefact in original size. The other illustrations are magnifications acquired with a 1.6× objective and a 34-× zoom. The use-wear traces are acquired at magnification of 10× and 20× (I. type I.; II. type V.; III. type I.). The micro-surface displays the processed result of the confocal data acquisition with the 50× objective.



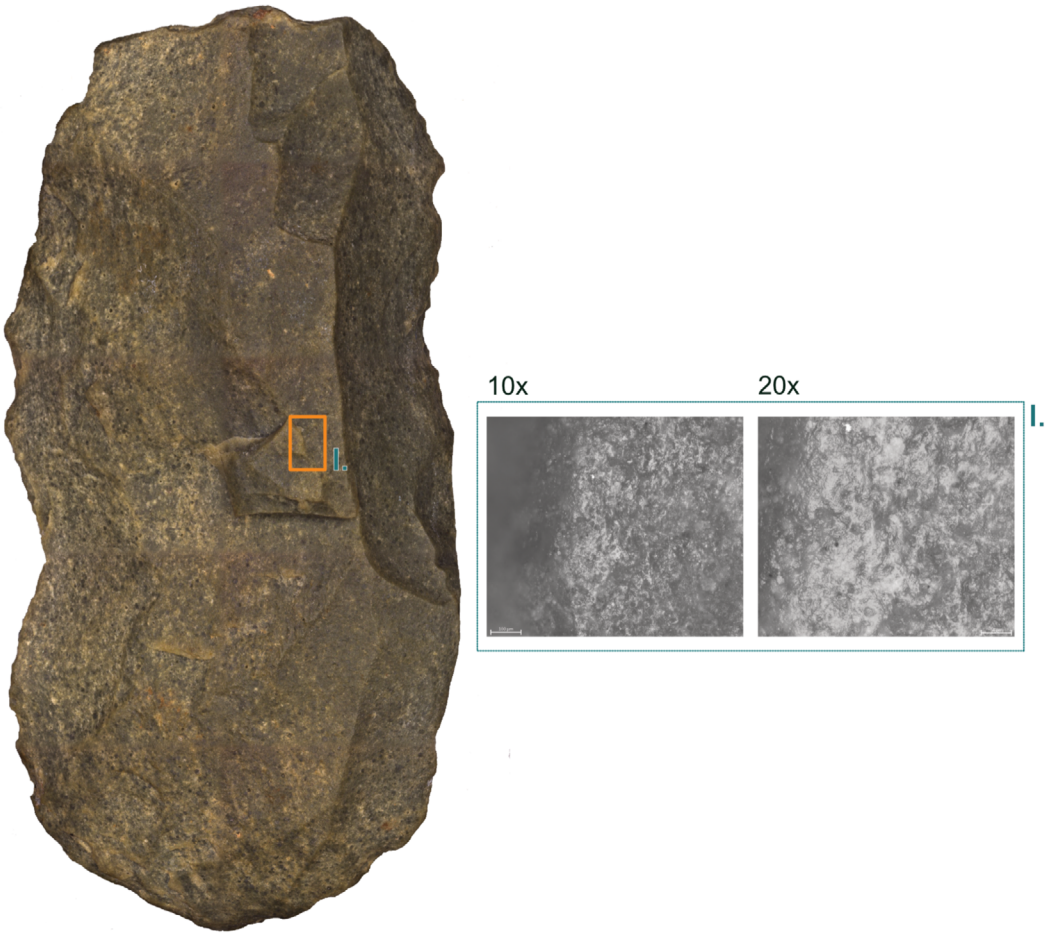

Balver Höhle, *Prądnik spall* [ID MU-153]. The topmost image displays the artefact in original size. The other illustrations are magnifications acquired with a 1.6× objective and a 34-× zoom. The use-wear trace is acquired at magnification of 10× and 20× (I. type V.).

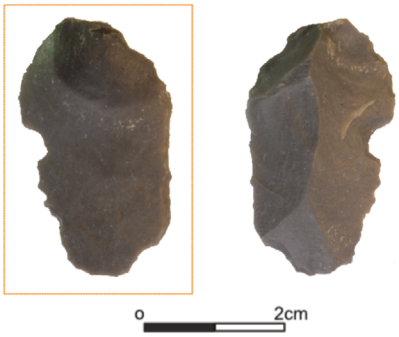

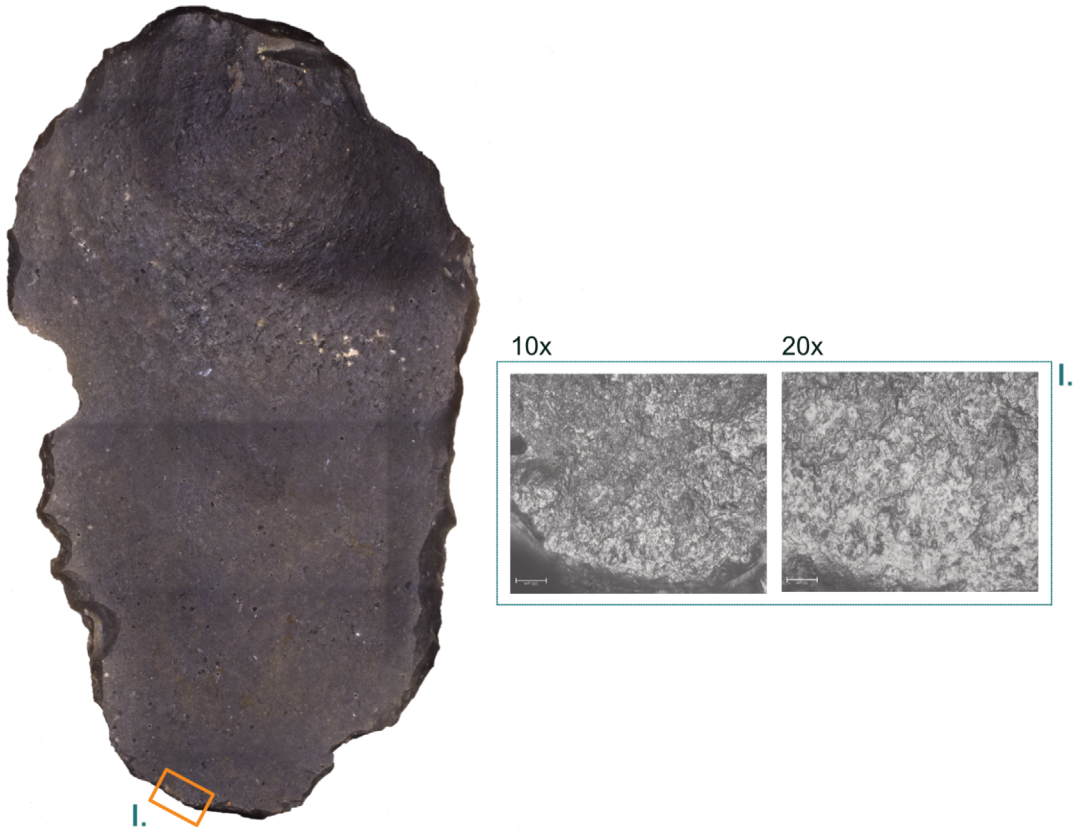

Balver Höhle, *Prądnik spall* [ID MU-161]. The topmost image displays the artefact in original size. The other illustrations are magnifications acquired with a 1.6× objective and a 34-× zoom. The use-wear trace is acquired at magnification of 10× and 20× (I. type V.).



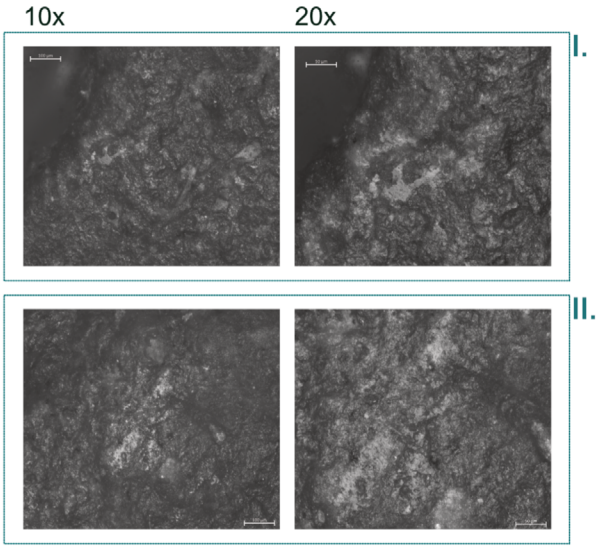



Balver Höhle, *Prądnik spall* [ID MU-164]. The topmost image displays the artefact in original size. The other illustrations are magnifications acquired with a 1.6× objective and a 34-× zoom. The use-wear traces are acquired at magnification of 10× and 20× (I. type II.; II. type II.).

Plate A120

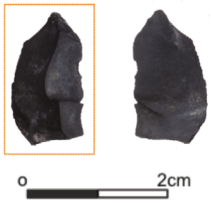

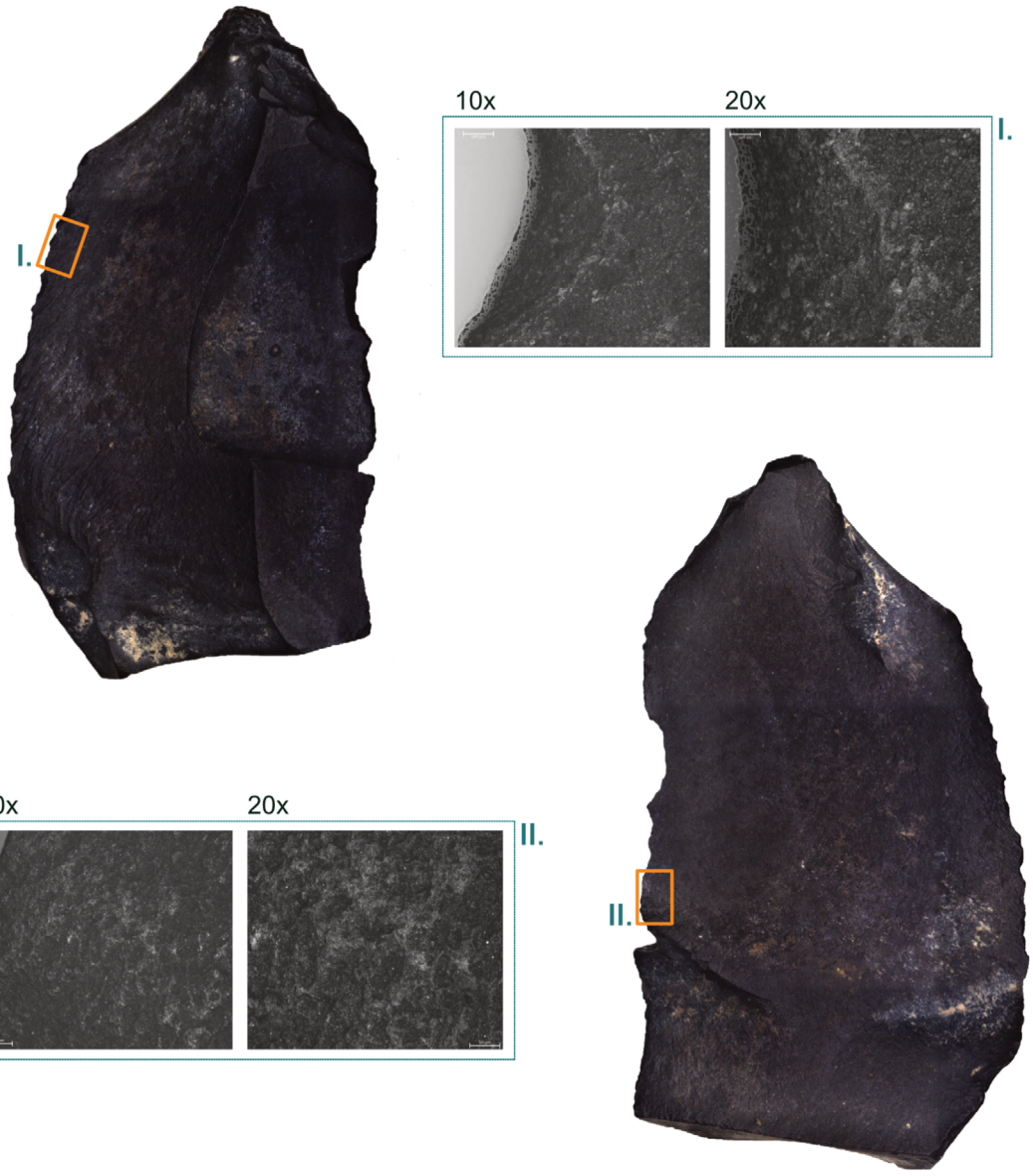

Balver Höhle, *Prądnik spall* [ID MU-173]. The topmost image displays the artefact in original size. The other illustrations are magnifications acquired with a 1.6× objective and a 34-× zoom. The use-wear traces are acquired at magnification of 10× and 20× (I. type V.; II. type V.).



Balver Höhle, *Prądnik spall* [ID MU-180]. The topmost image displays the artefact in original size. The other illustrations are magnifications acquired with a 1.6× objective and a 34-× zoom. The use-wear traces are acquired at magnification of 10× and 20× (I. type V.; II. type V.; III. type VIII.; IV. type V.; V. type V).

Plate A122

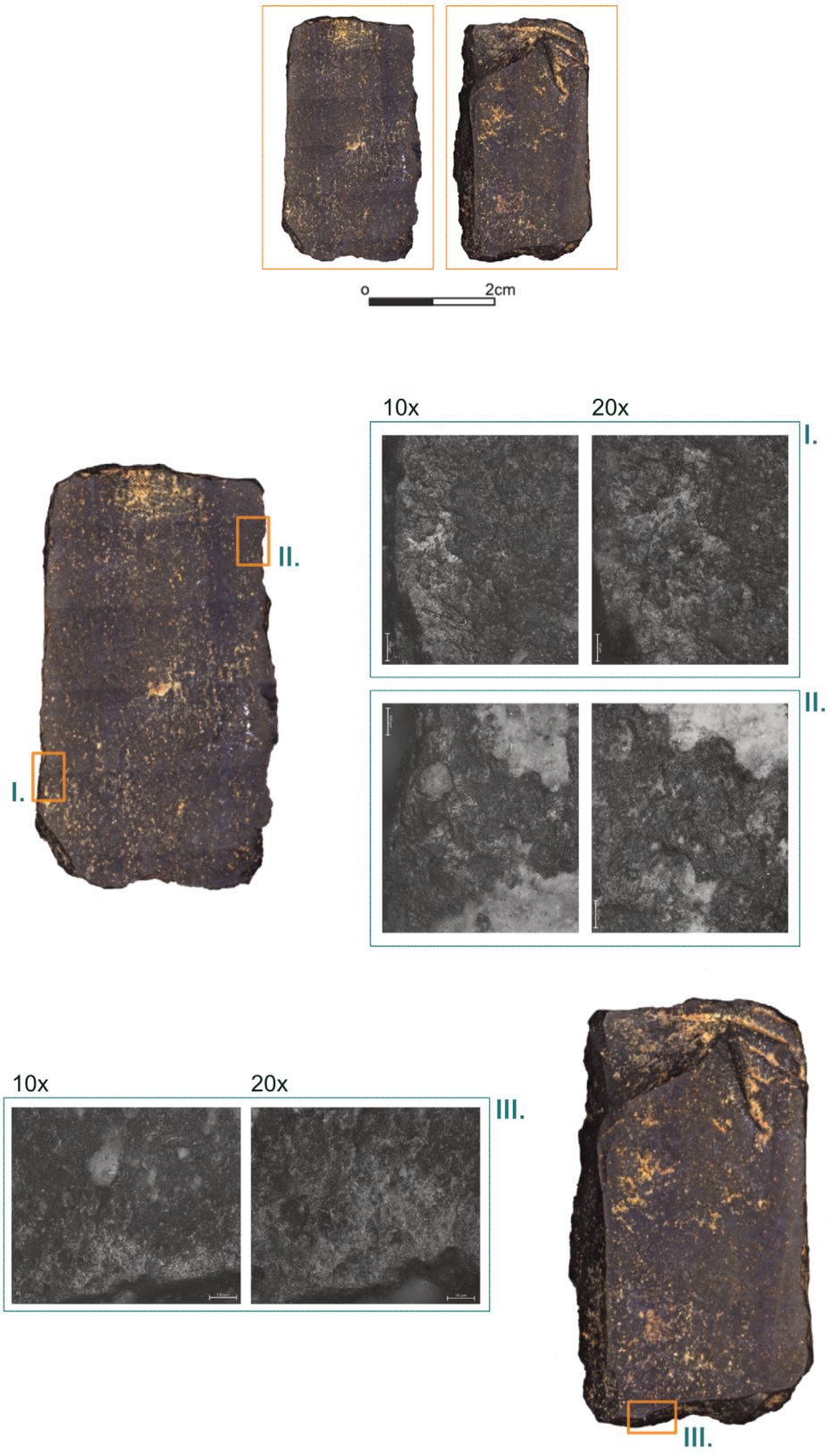

Balver Höhle, *Prądnik spall* [ID MU-186]. The topmost image displays the artefact in original size. The other illustrations are magnifications acquired with a 1.6× objective and a 34-× zoom. The use-wear traces are acquired at magnification of 10× and 20× (I. type VIII.; II. type V./IV.; III. type V).

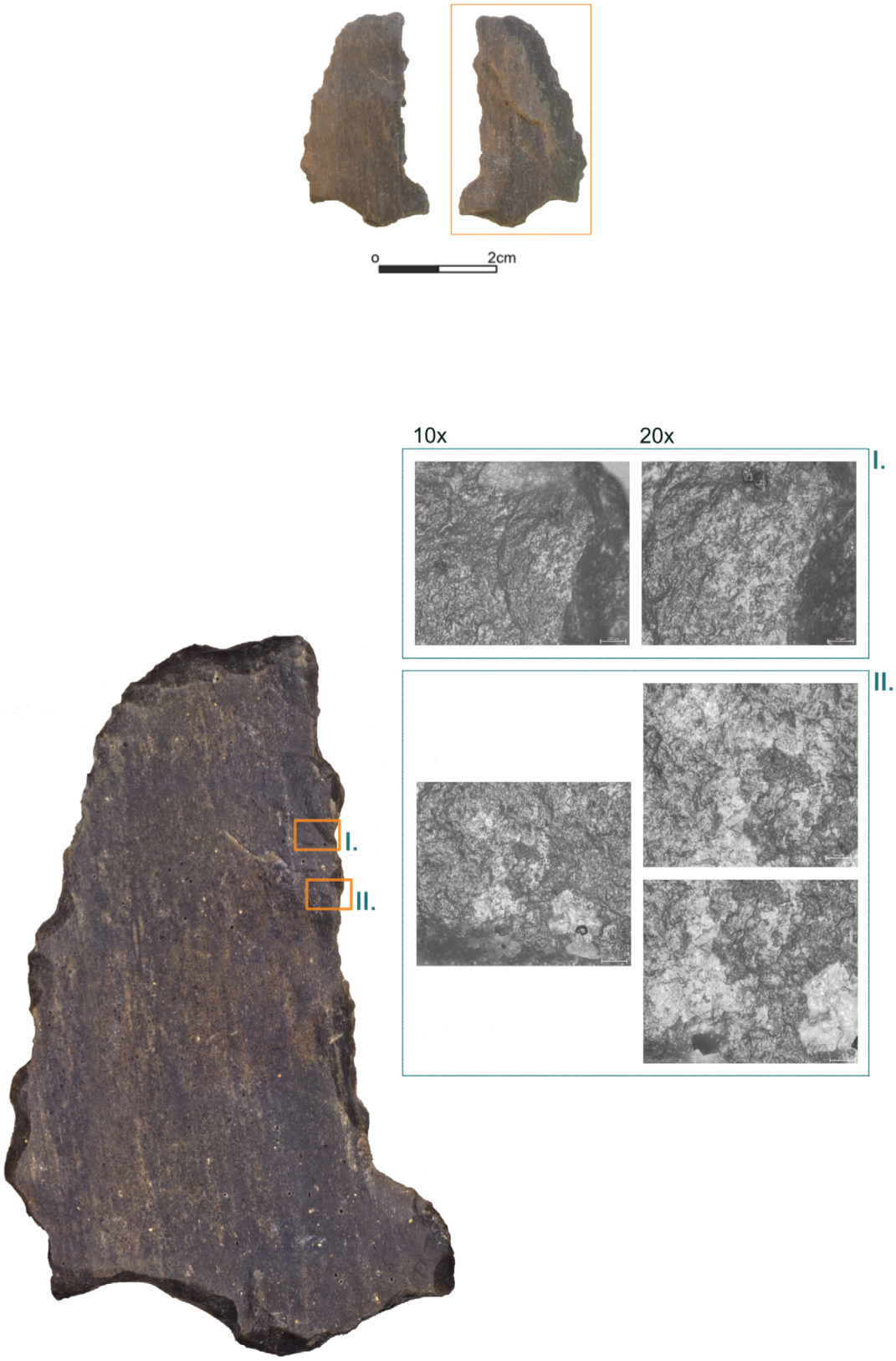

Balver Höhle, *Prądnik spall* [ID MU-190]. The topmost image displays the artefact in original size. The other illustrations are magnifications acquired with a 1.6× objective and a 34-× zoom. The use-wear traces are acquired at magnification of 10× and 20× (I. type V.; II. type VI.).

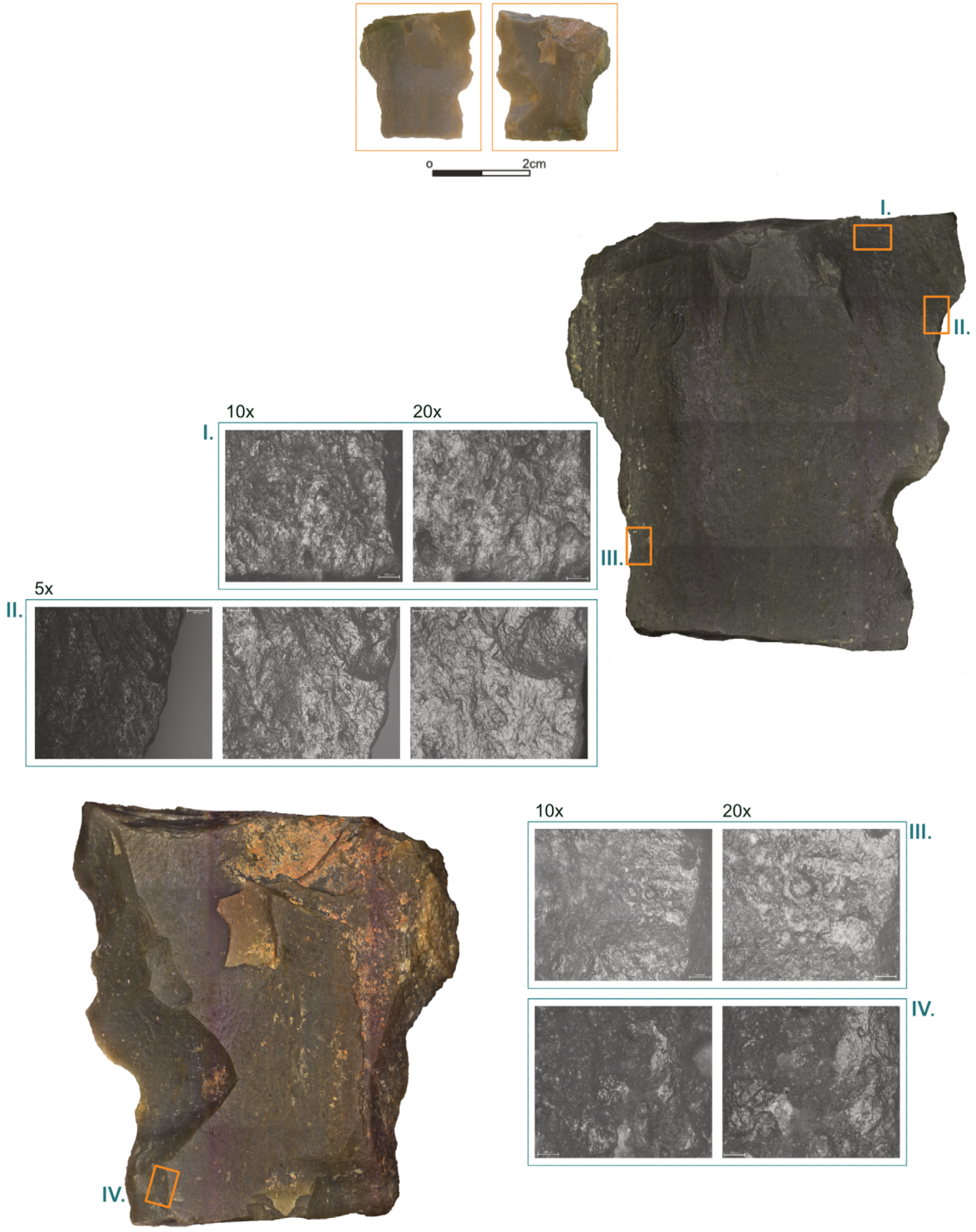

Balver Höhle, *Prądnik spall* [ID MU-194]. The topmost image displays the artefact in original size. The other illustrations are magnifications acquired with a 1.6× objective and a 34-× zoom. The use-wear traces are acquired at magnification of 5×, 10× and 20× (I. type V.; II. type V.; III. type V.; IV. type V.).



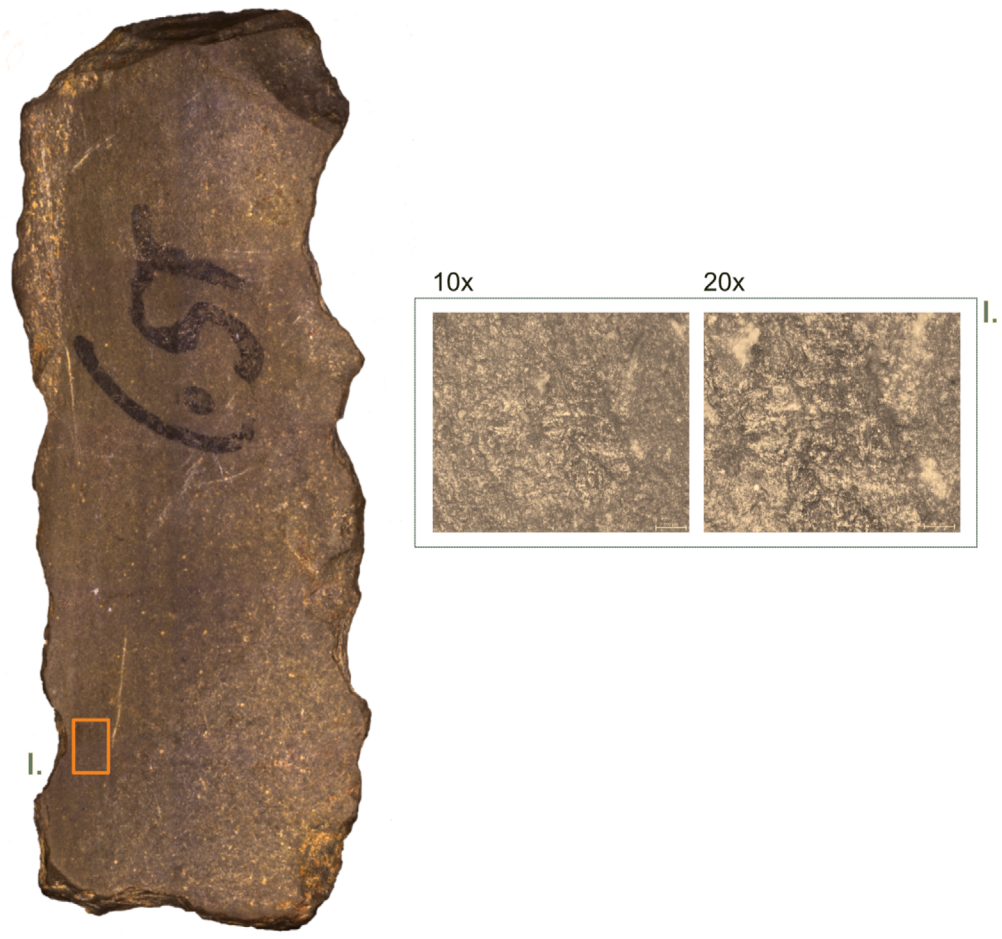

Balver Höhle, *Prądnik spall* [ID MU-203]. The topmost image displays the artefact in original size. The other illustrations are magnifications acquired with a 1.6× objective and a 34-× zoom. The use-wear trace is acquired at magnification of 10× and 20× (I. type VI.).

Plate A126

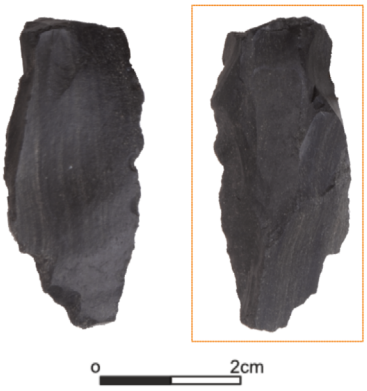

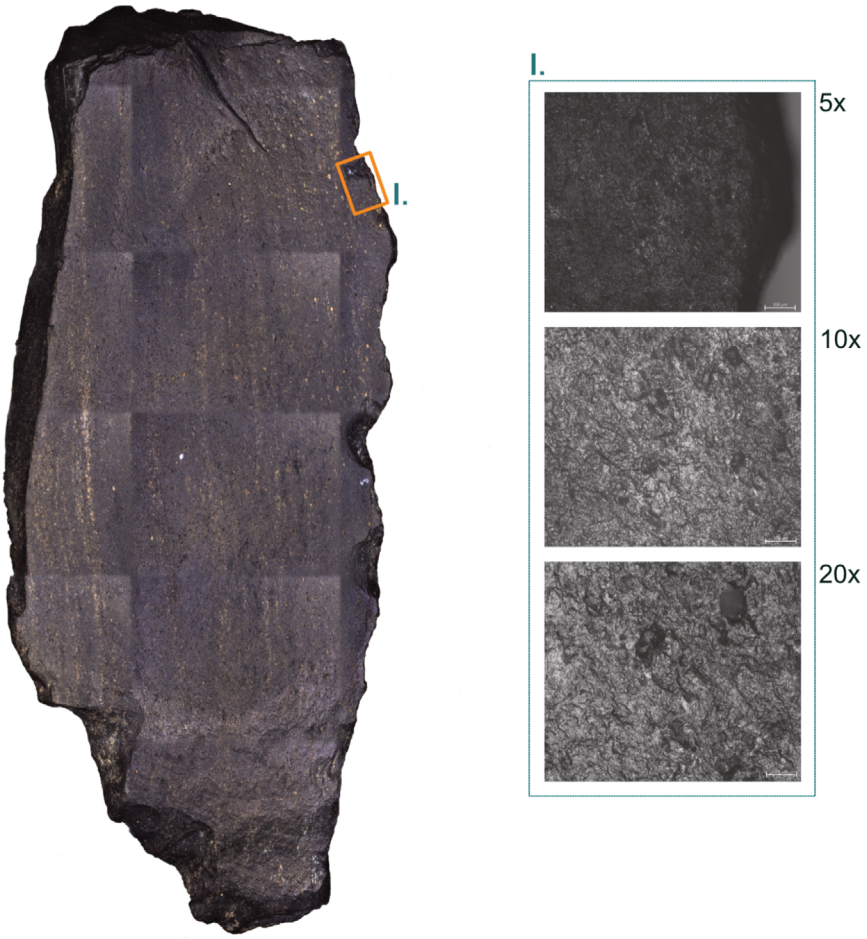

Balver Höhle, *Prądnik spall* [ID MU-204]. The topmost image displays the artefact in original size. The other illustrations are magnifications acquired with a 1.6× objective and a 34-× zoom. The use-wear trace is acquired at magnification of 5×, 10× and 20× (I. type V.).

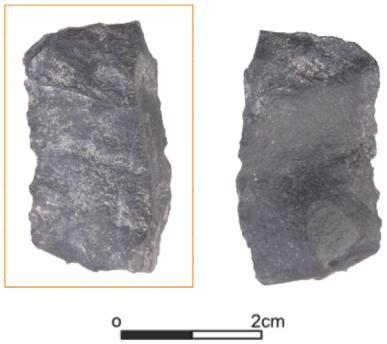

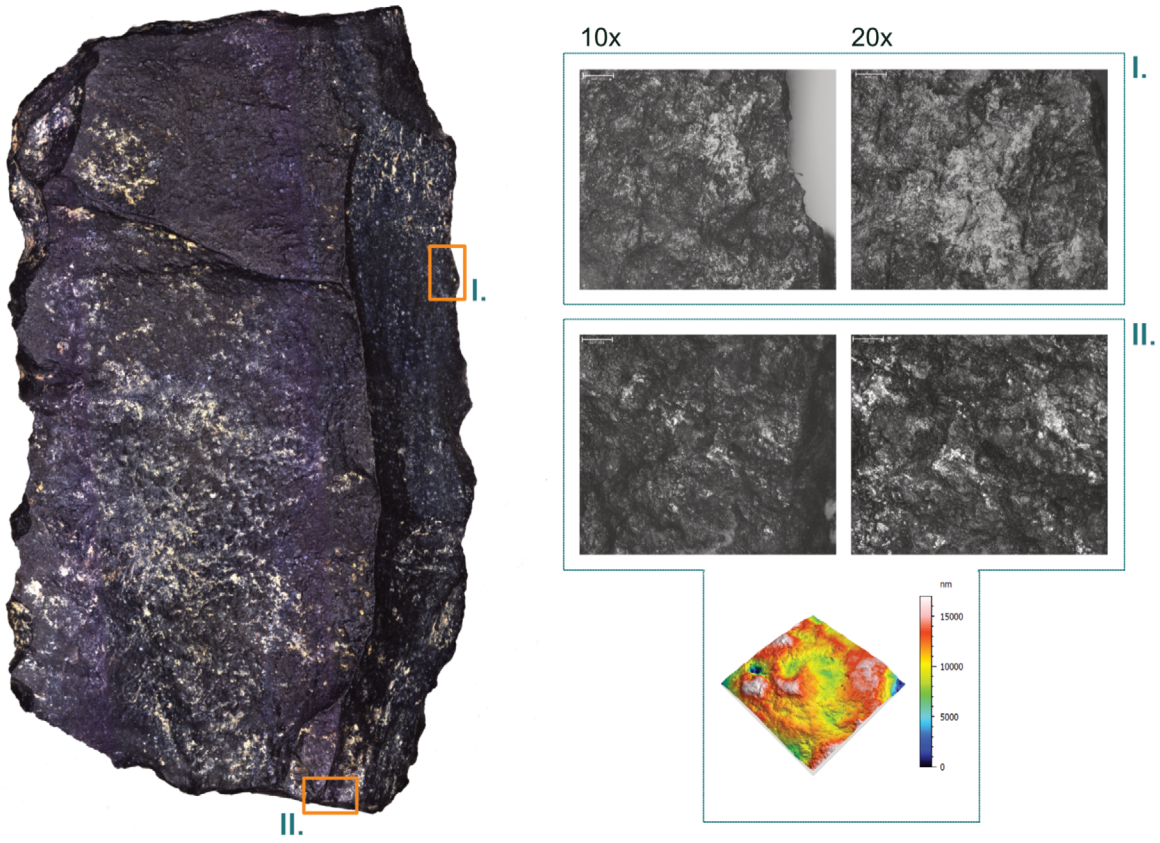

Balver Höhle, *Prądnik spall* [ID MU-217]. The topmost image displays the artefact in original size. The other illustrations are magnifications acquired with a 1.6× objective and a 34-× zoom. The use-wear traces are acquired at magnification of 10× and 20× (I. type V. /IV.; II. type I.). The micro-surface displays the processed result of the confocal data acquisition with the 50× objective.

Plate A128



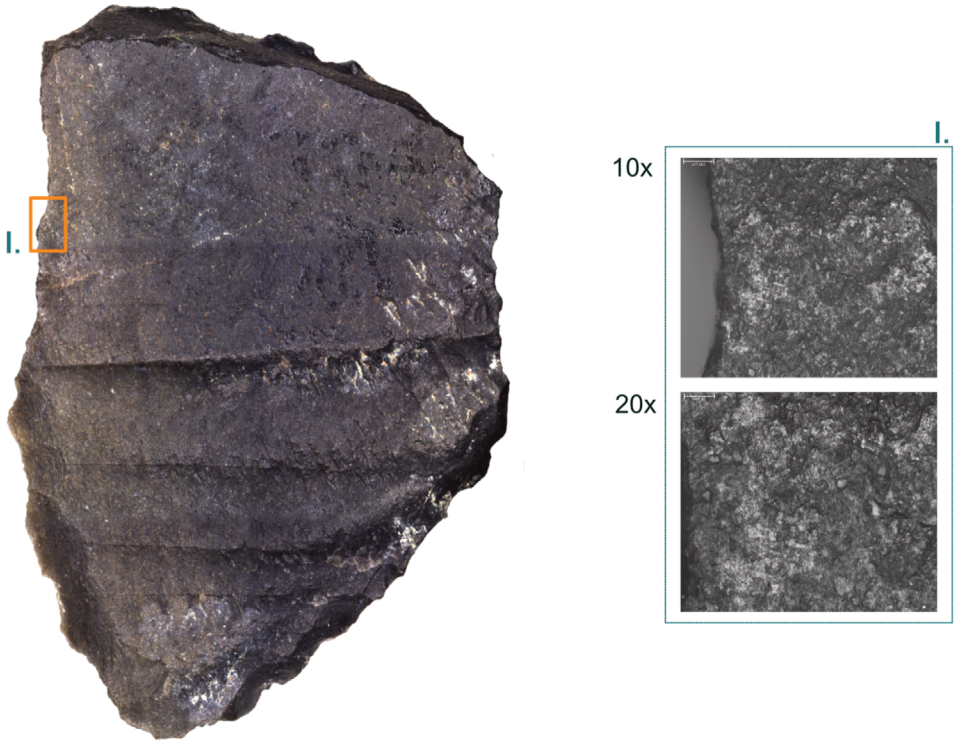

Balver Höhle, *Prądnik spall* [ID MU-301]. The topmost image displays the artefact in original size. The other illustrations are magnifications acquired with a 1.6× objective and a 34-× zoom. The use-wear trace is acquired at magnification of 10× and 20× (I. type V.).

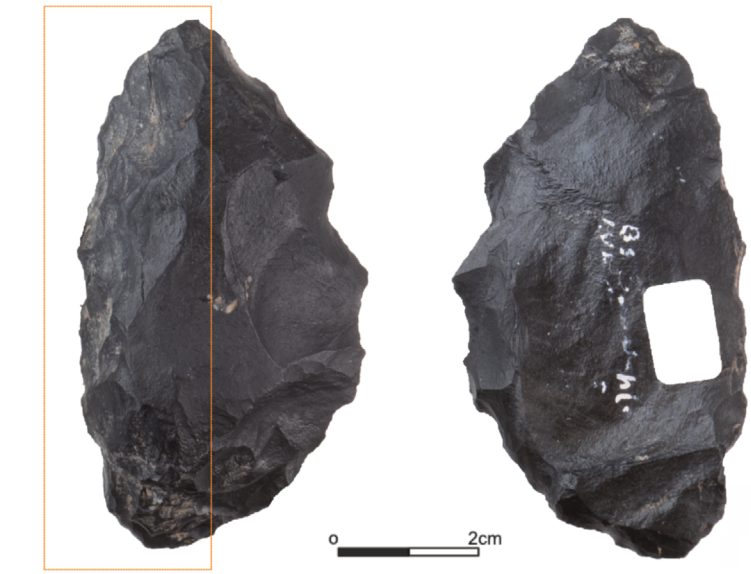

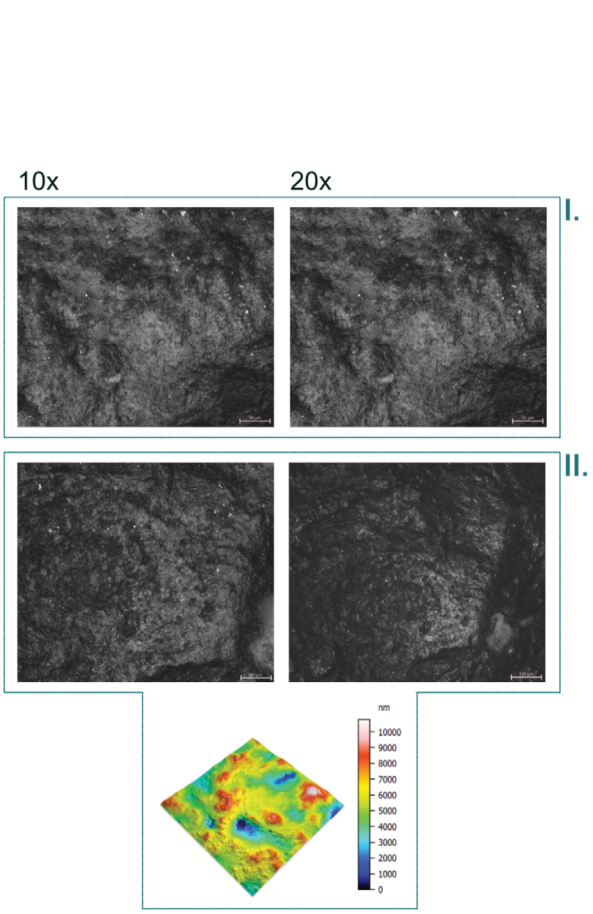

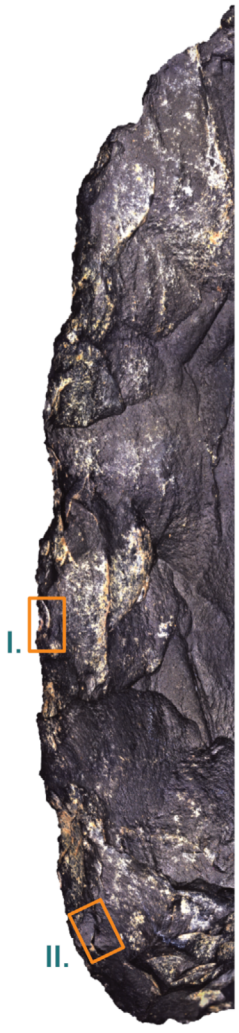

Balver Höhle, scraper [ID MU-019]. The topmost image displays the artefact in original size. The other illustrations are magnifications acquired with a 1.6× objective and a 34-× zoom. The use-wear traces are acquired at magnification of 10× and 20× (I. type VII.; II. type VII.). The micro-surface displays the processed result of the confocal data acquisition with the 50× objective.

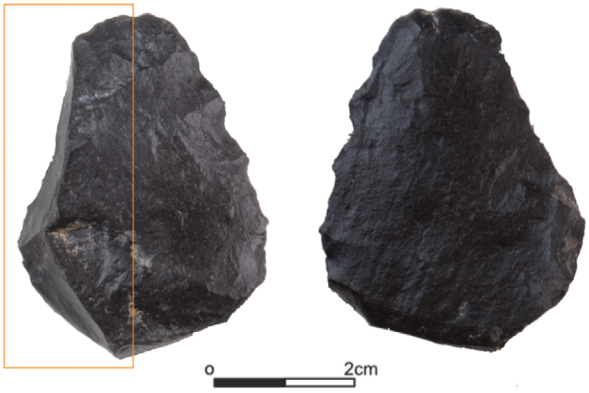

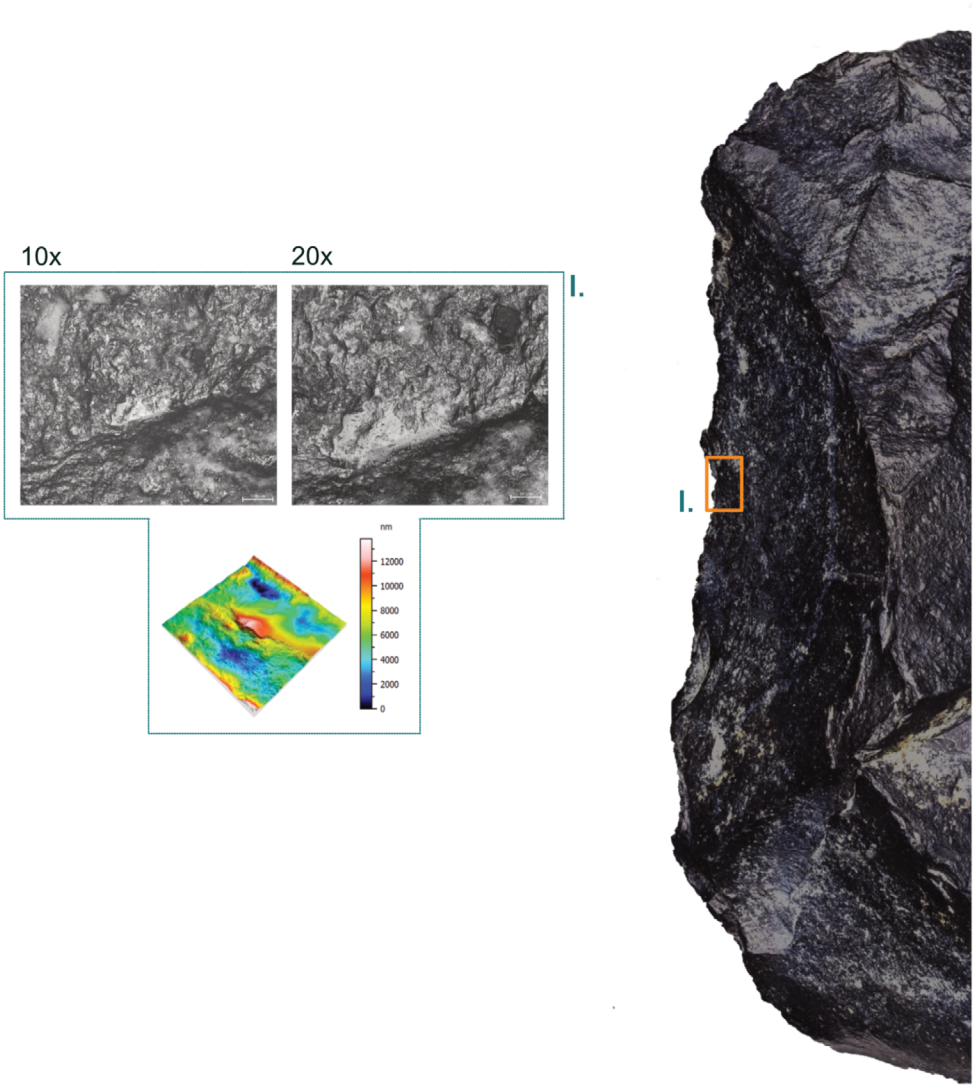

Balver Höhle, scraper [ID MU-025]. The topmost image displays the artefact in original size. The other illustrations are magnifications acquired with a 1.6× objective and a 34-× zoom. The use-wear trace is acquired at magnification of 10× and 20× (I. type II.). The micro-surface displays the processed result of the confocal data acquisition with the 50× objective.

Balver Höhle, scraper [ID MU-030]. The topmost image displays the artefact in original size. The other illustrations are magnifications acquired with a 1.6× objective and a 34-× zoom. The use-wear traces are acquired at magnification of 10× and 20× (I. type IV.; II. type VIII.; III. type I.; IV. type VIII.).


0
2cm

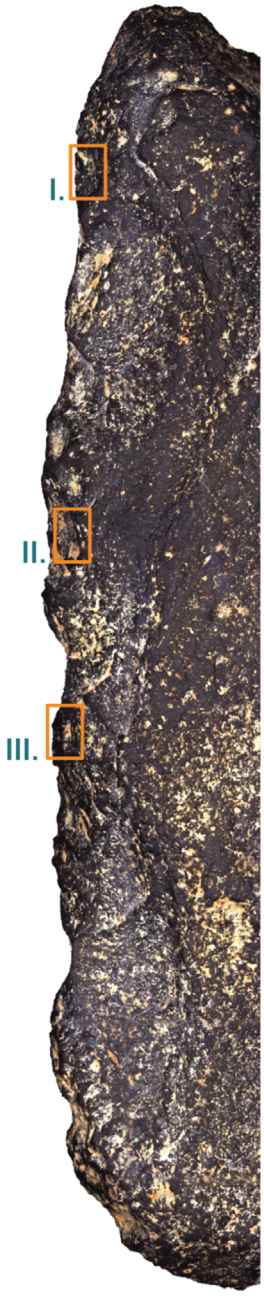
I.
II.
III.

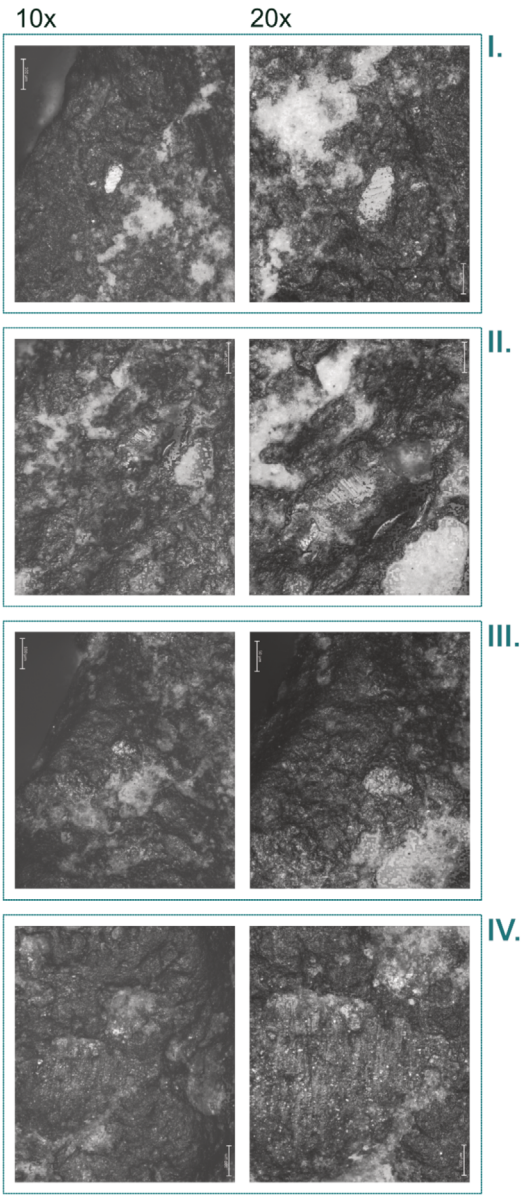
10x
20x
I.
II.
III.
IV.


IV.

Plate A132



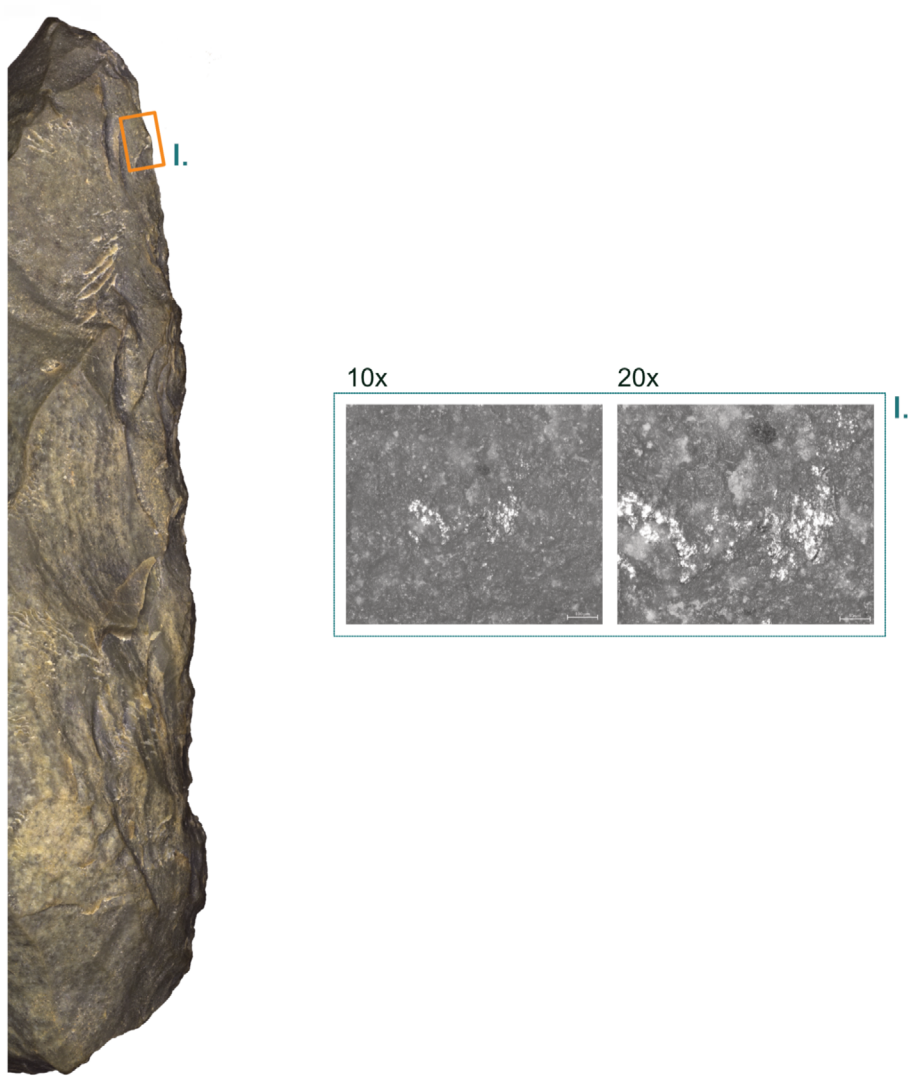

Balver Höhle, scraper [ID MU-201]. The topmost image displays the artefact in original size. The other illustrations are magnifications acquired with a 1.6× objective and a 34-× zoom. The use-wear trace is acquired at magnification of 10× and 20× (I. type I.).

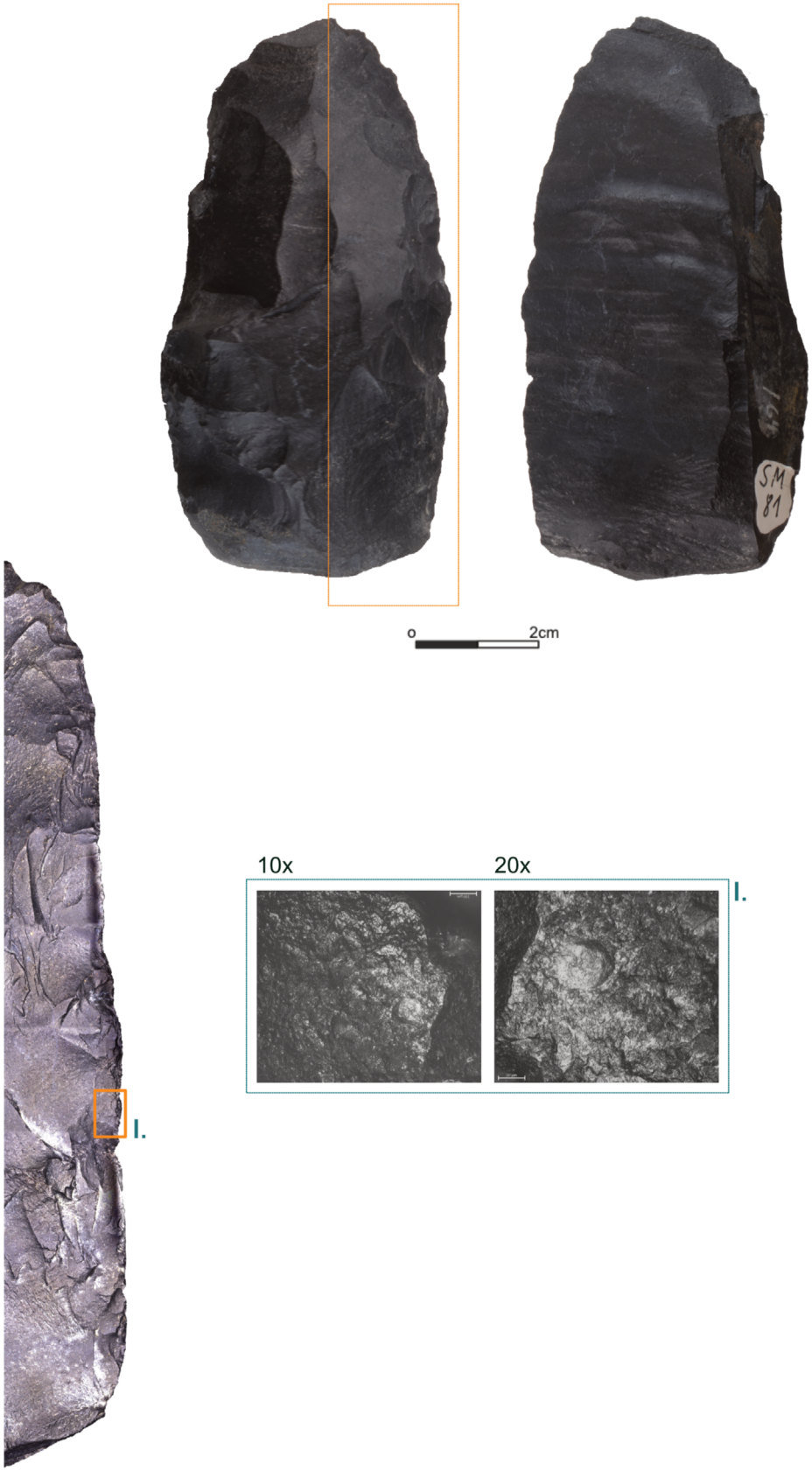

Balver Höhle, scraper [ID MU-274]. The topmost image displays the artefact in original size. The other illustrations are magnifications acquired with a 1.6× objective and a 34-× zoom. The use-wear trace is acquired at magnification of 10× and 20× (I. type V.).

Plate A134

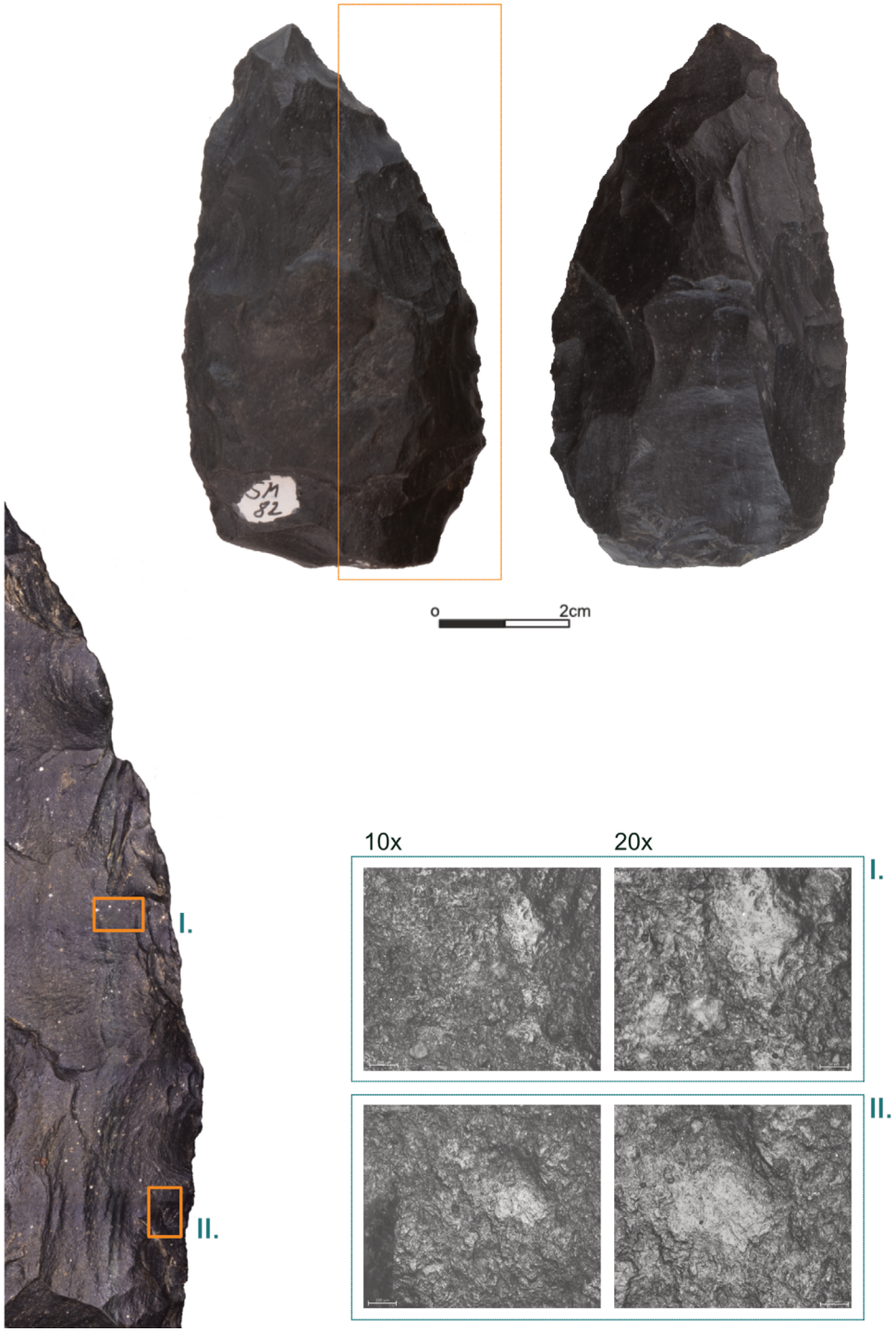

Balver Höhle, scraper [ID MU-278; dorsal]. The topmost image displays the artefact in original size. The other illustrations are magnifications acquired with a 1.6× objective and a 34-× zoom. The use-wear traces are acquired at magnification of 10× and 20× (I. type II.; II. type II.).



Balver Höhle, scraper [ID MU-278; ventral]. The topmost image displays the artefact in original size. The other illustrations are magnifications acquired with a 1.6× objective and a 34-× zoom. The use-wear traces are acquired at magnification of 10× and 20× (I. type V.; II. type V.; III. type V.).

Plate A136

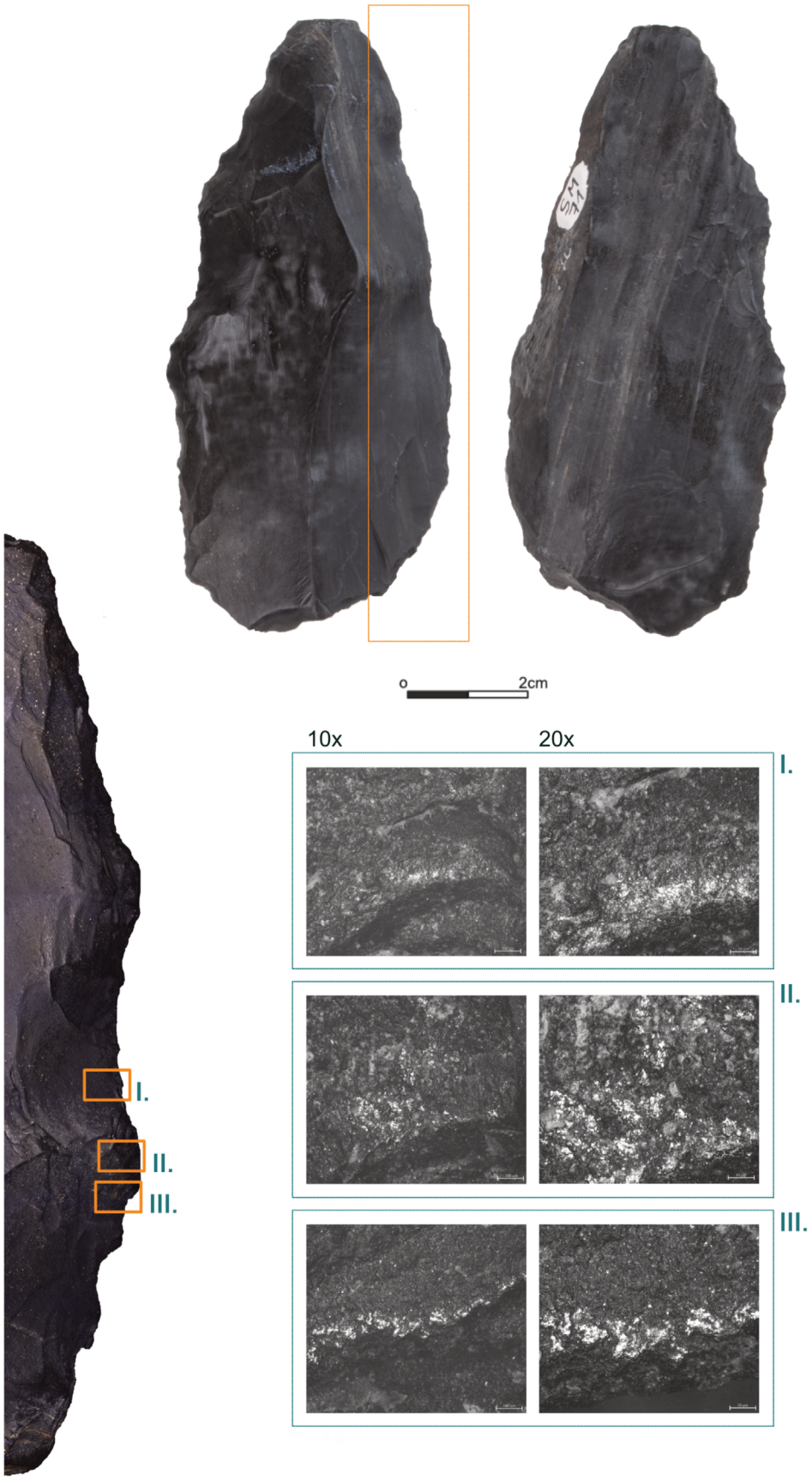

Balver Höhle, scraper [ID MU-279; dorsal]. The topmost image displays the artefact in original size. The other illustrations are magnifications acquired with a 1.6× objective and a 34-× zoom. The use-wear traces are acquired at magnification of 10× and 20× (I. type V.; II. type IV.; III. type IV.).

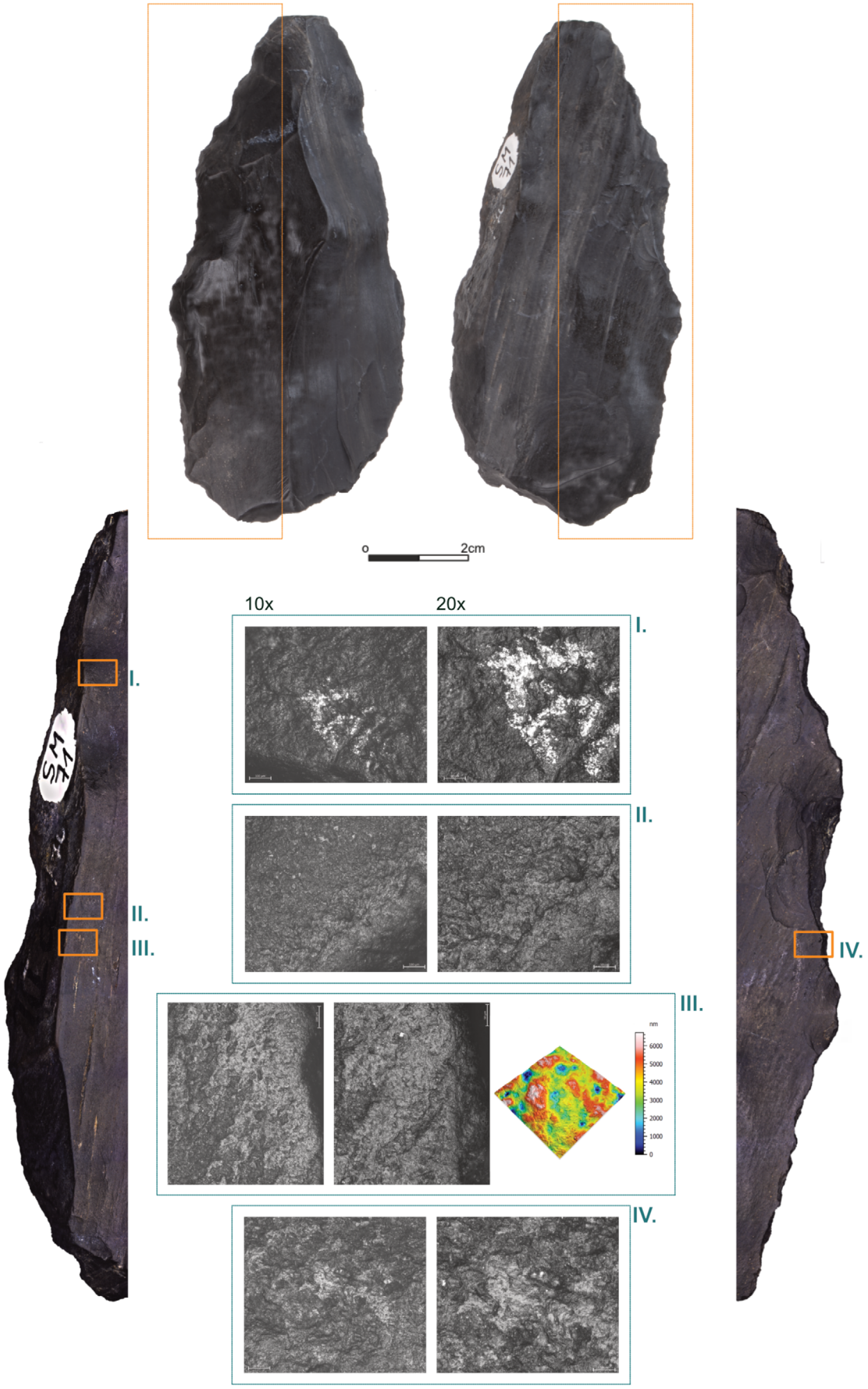

Balver Höhle, scraper [ID MU-279; ventral]. The topmost image displays the artefact in original size. The other illustrations are magnifications acquired with a 1.6× objective and a 34-× zoom. The use-wear traces are acquired at magnification of 10× and 20× (I. type IV.; II. type V.; III. type V.; IV. type V.). The micro-surface displays the processed result of the confocal data acquisition with the 50× objective.

Plate A138

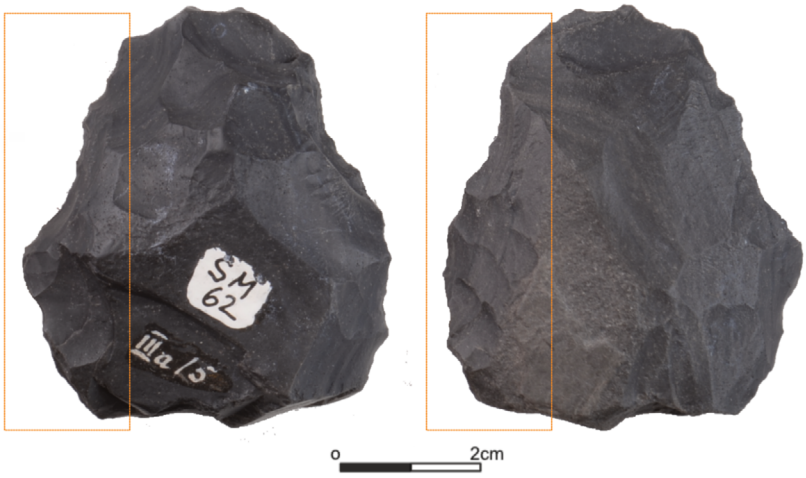

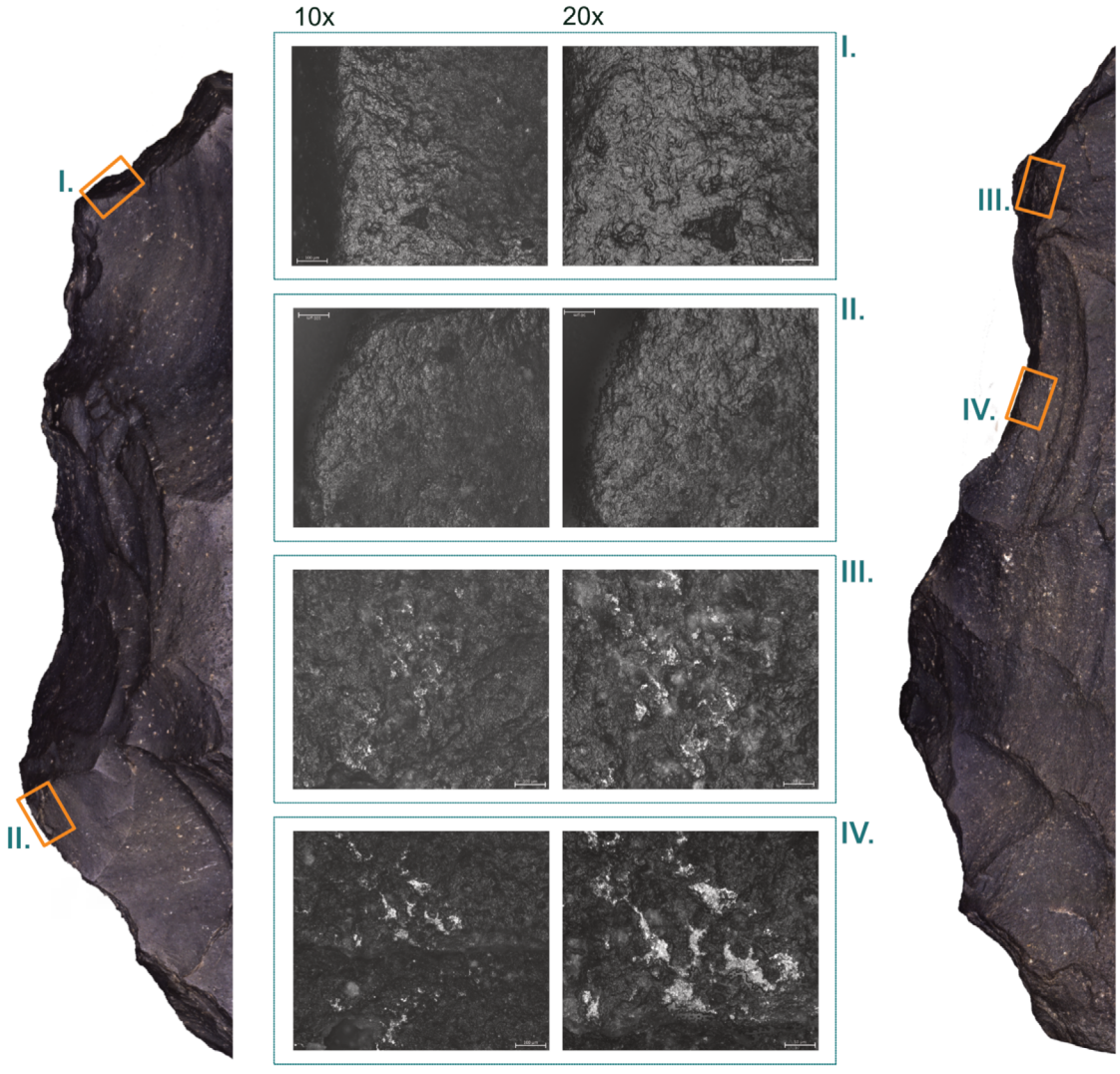

Balver Höhle, scraper [ID MU-285]. The topmost image displays the artefact in original size. The other illustrations are magnifications acquired with a 1.6× objective and a 34-× zoom. The use-wear traces are acquired at magnification of 10× and 20× (I. type V.; II. type V.; III. type I.; IV. type I.).

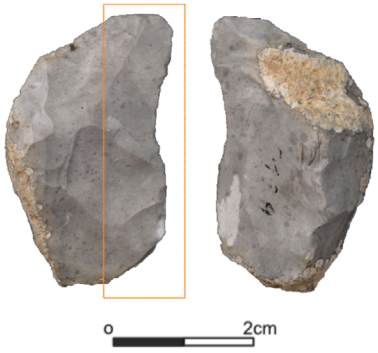

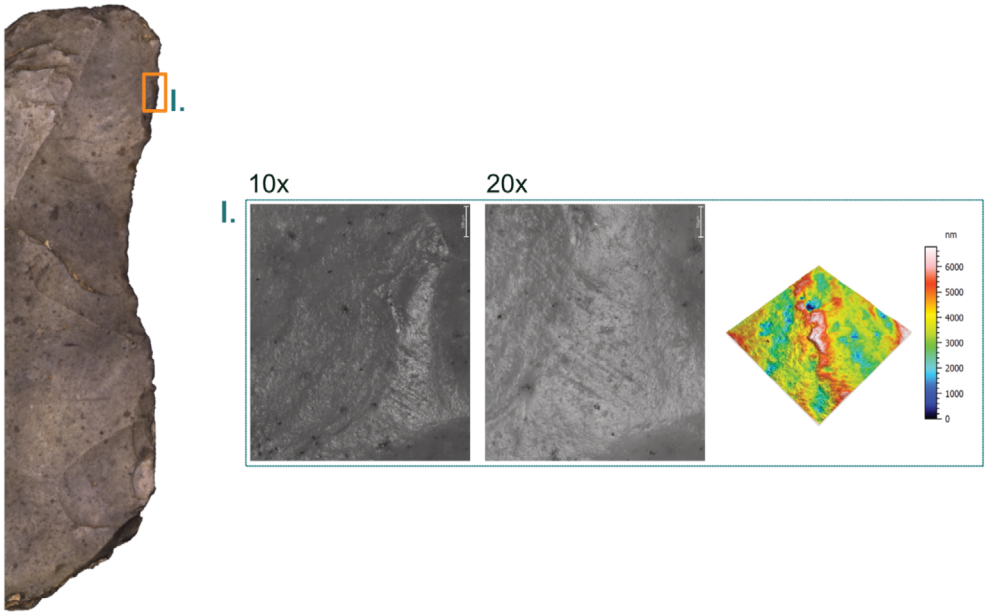

Ramioul, *Keilmesser* [ID R-002]. The topmost image displays the artefact in original size. The other illustrations are magnifications acquired with a 1.6× objective and a 34-× zoom. The use-wear trace is acquired at magnification of 10× and 20× (I. type VI.). The micro-surface displays the processed result of the confocal data acquisition with the 50× objective.

Plate A140

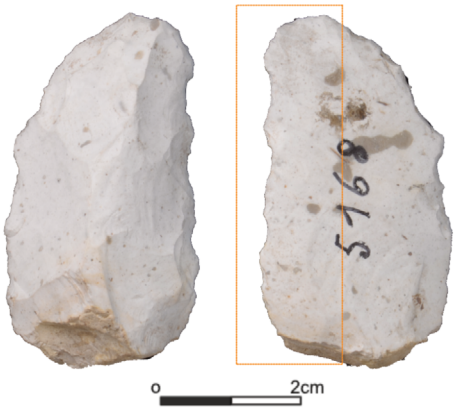

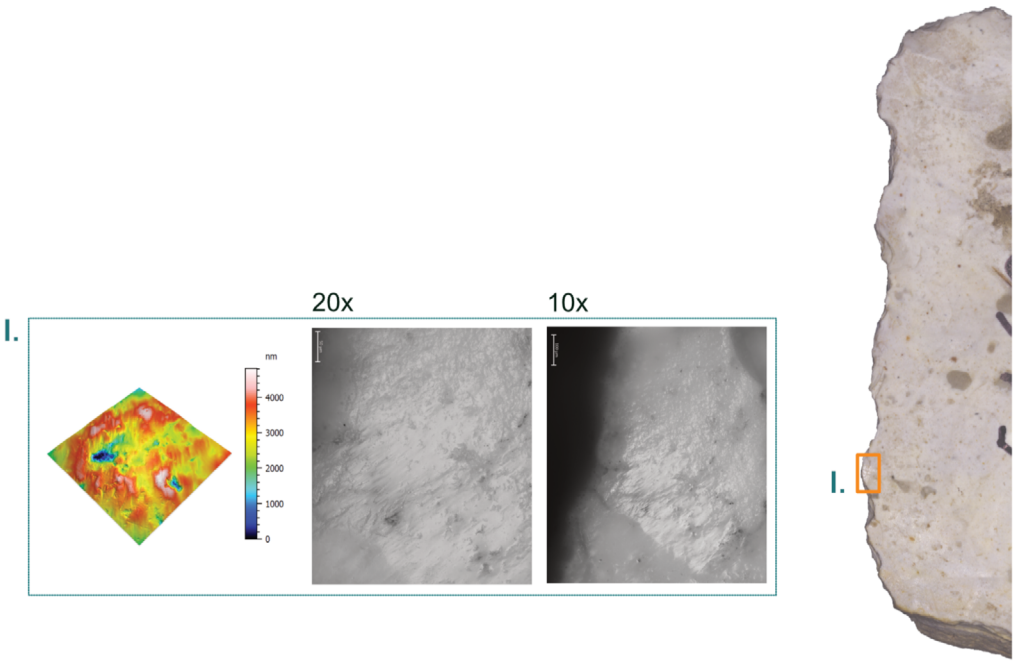

Ramioul, *Keilmesser* [ID R-006]. The topmost image displays the artefact in original size. The other illustrations are magnifications acquired with a 1.6× objective and a 34-× zoom. The use-wear trace is acquired at magnification of 10× and 20× (I. type IV.). The micro-surface displays the processed result of the confocal data acquisition with the 50× objective.

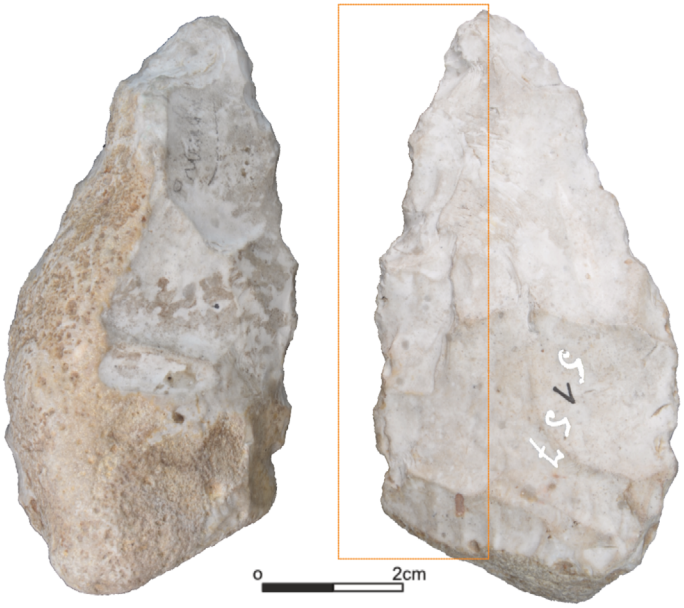

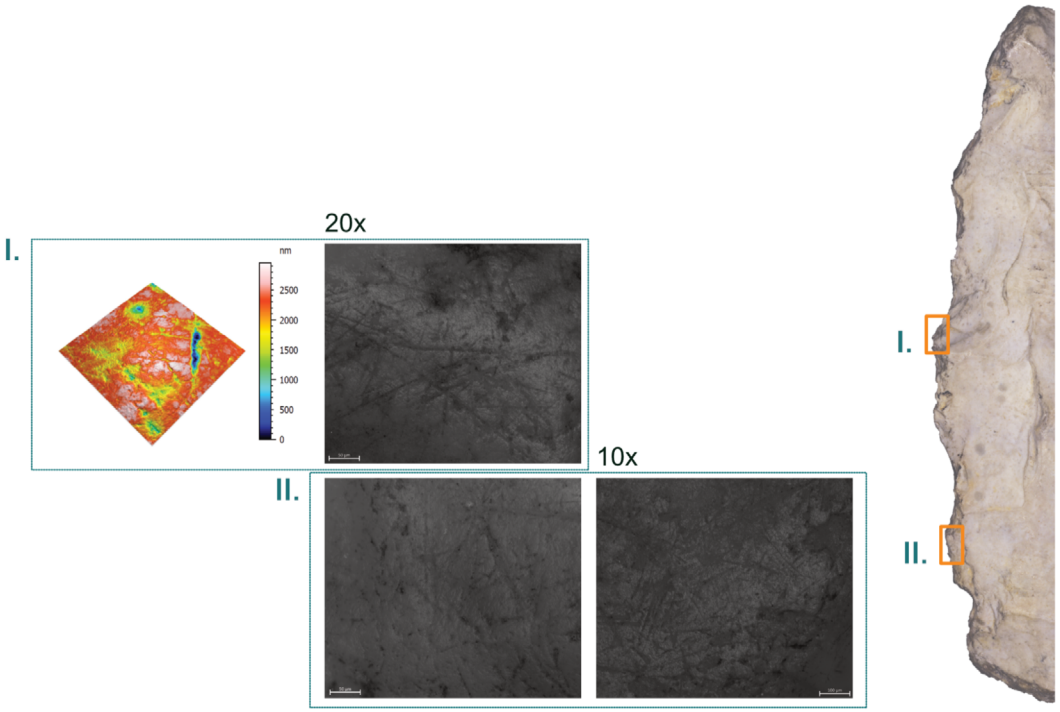

Ramioul, *Keilmesser* [ID R-007]. The topmost image displays the artefact in original size. The other illustrations are magnifications acquired with a 1.6× objective and a 34-× zoom. The use-wear traces are acquired at magnification of 10× and 20× (I. type IX.; II. type IX.). The micro-surface displays the processed result of the confocal data acquisition with the 50× objective.

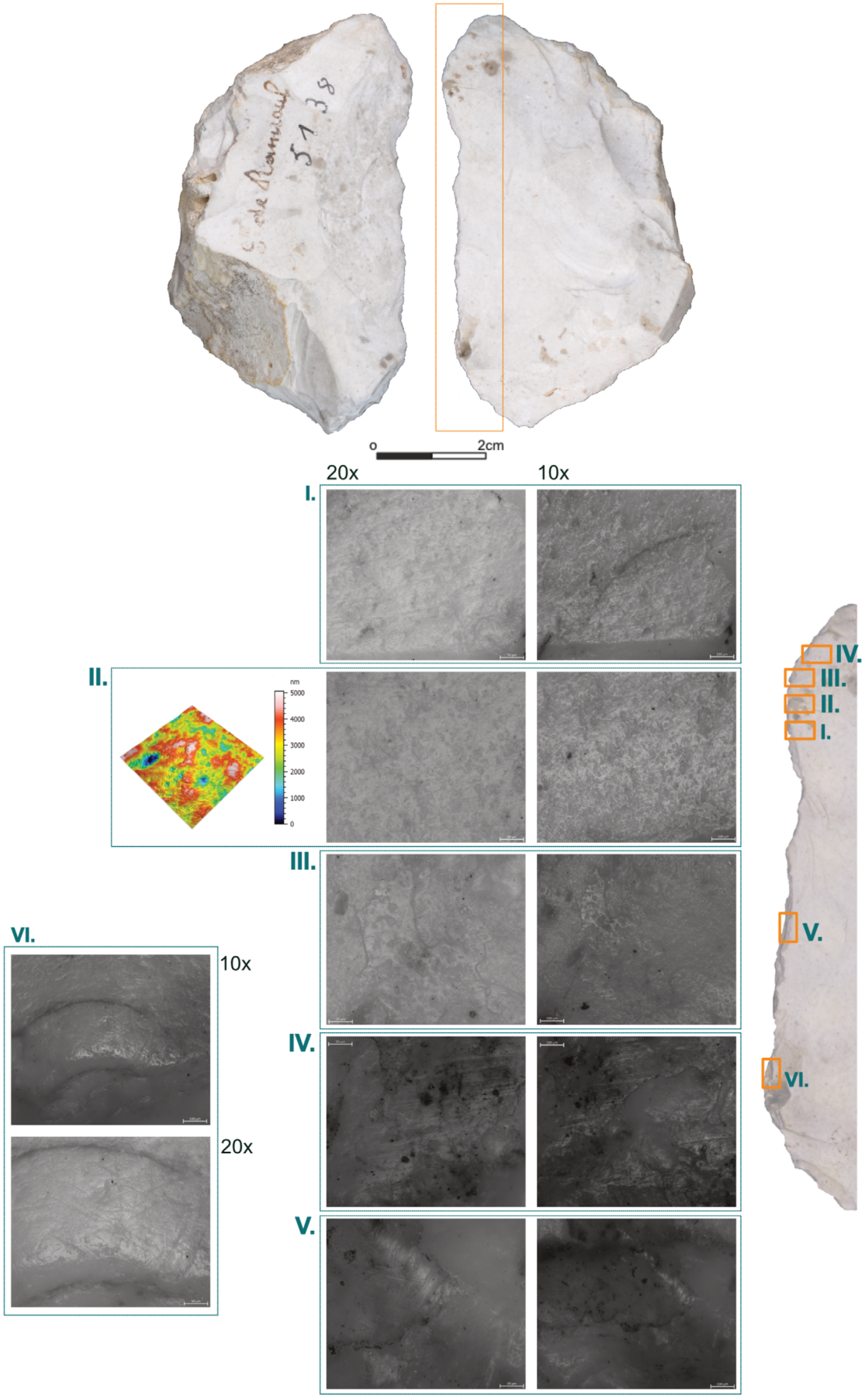

Ramioul, *Keilmesser* [ID R-008]. The topmost image displays the artefact in original size. The other illustrations are magnifications acquired with a 1.6× objective and a 34-× zoom. The use-wear traces are acquired at magnification of 10× and 20× (I. type VI.; II. type VI.; III. type V.; IV. type VI.; V. type VI.; VI. type VI.). The micro-surface displays the processed result of the confocal data acquisition with the 50× objective.

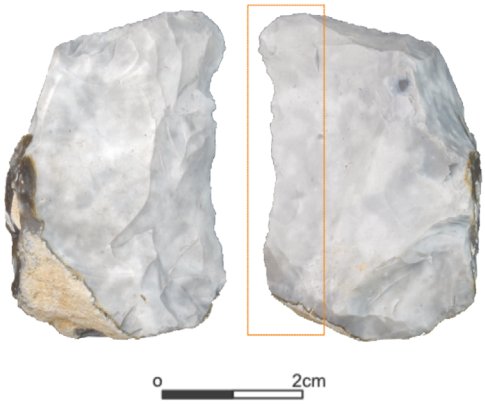

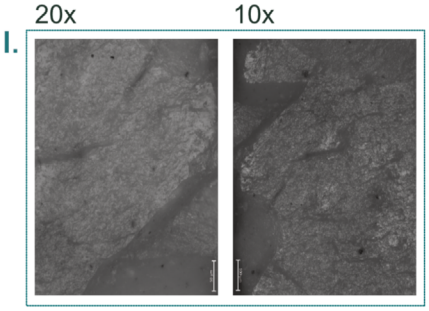

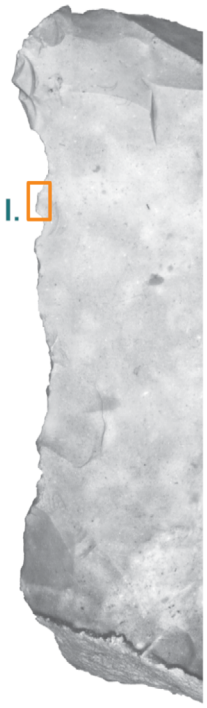

Ramioul, *Keilmesser* [ID R-011]. The topmost image displays the artefact in original size. The other illustrations are magnifications acquired with a 1.6× objective and a 34-× zoom. The use-wear trace is acquired at magnification of 10× and 20× (I. type IV.).



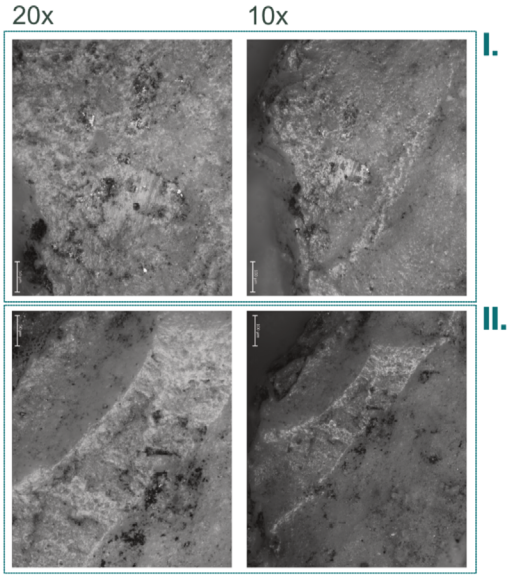



Ramioul, *Keilmesser* [ID R-018]. The topmost image displays the artefact in original size. The other illustrations are magnifications acquired with a 1.6× objective and a 34-× zoom. The use-wear traces are acquired at magnification of 10× and 20× (I. type V. / VI.; II. type V.).

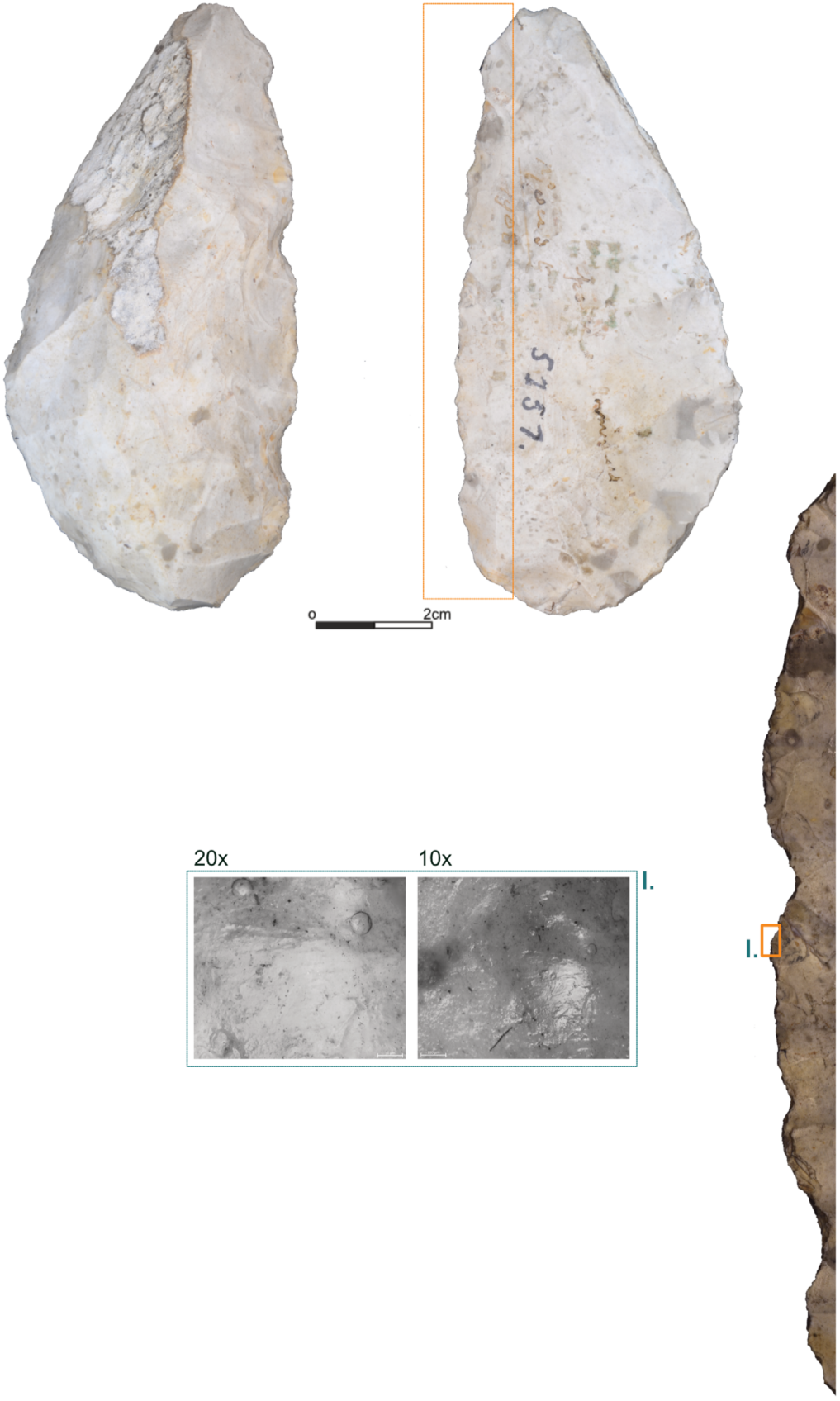

Ramioul, *Keilmesser* [ID R-019]. The topmost image displays the artefact in original size. The other illustrations are magnifications acquired with a 1.6× objective and a 34-× zoom. The use-wear trace is acquired at magnification of 10× and 20× (I. type II.).

Plate A146

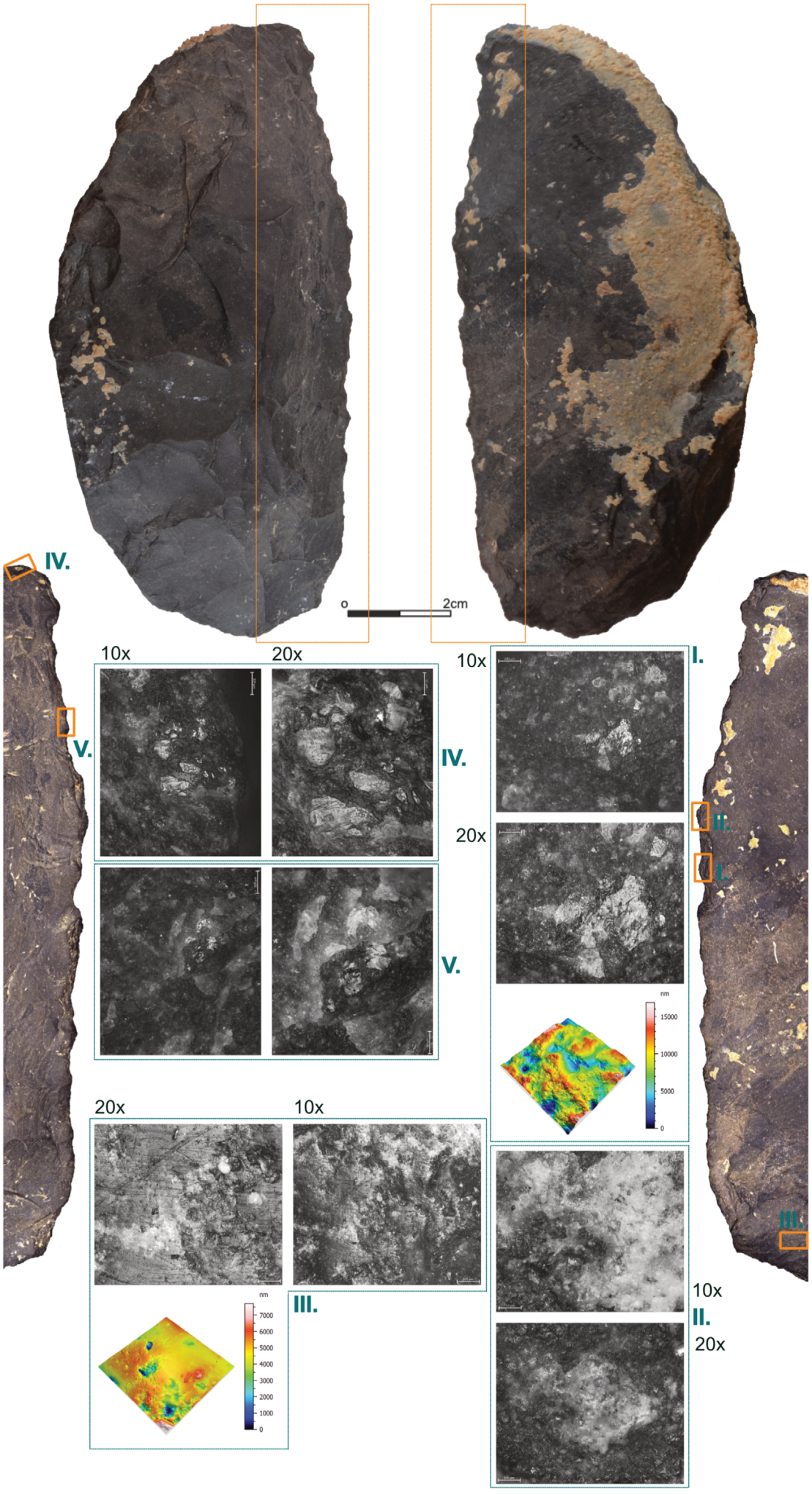
IV.
0
2cm
10x
20x
V.
IV.
V.
10x
I.
20x
II.
I.
III.
20x
10x
III.
nm
15000
10000
5000
0
nm
7000
6000
5000
4000
3000
2000
1000
0
10x
II.
20x

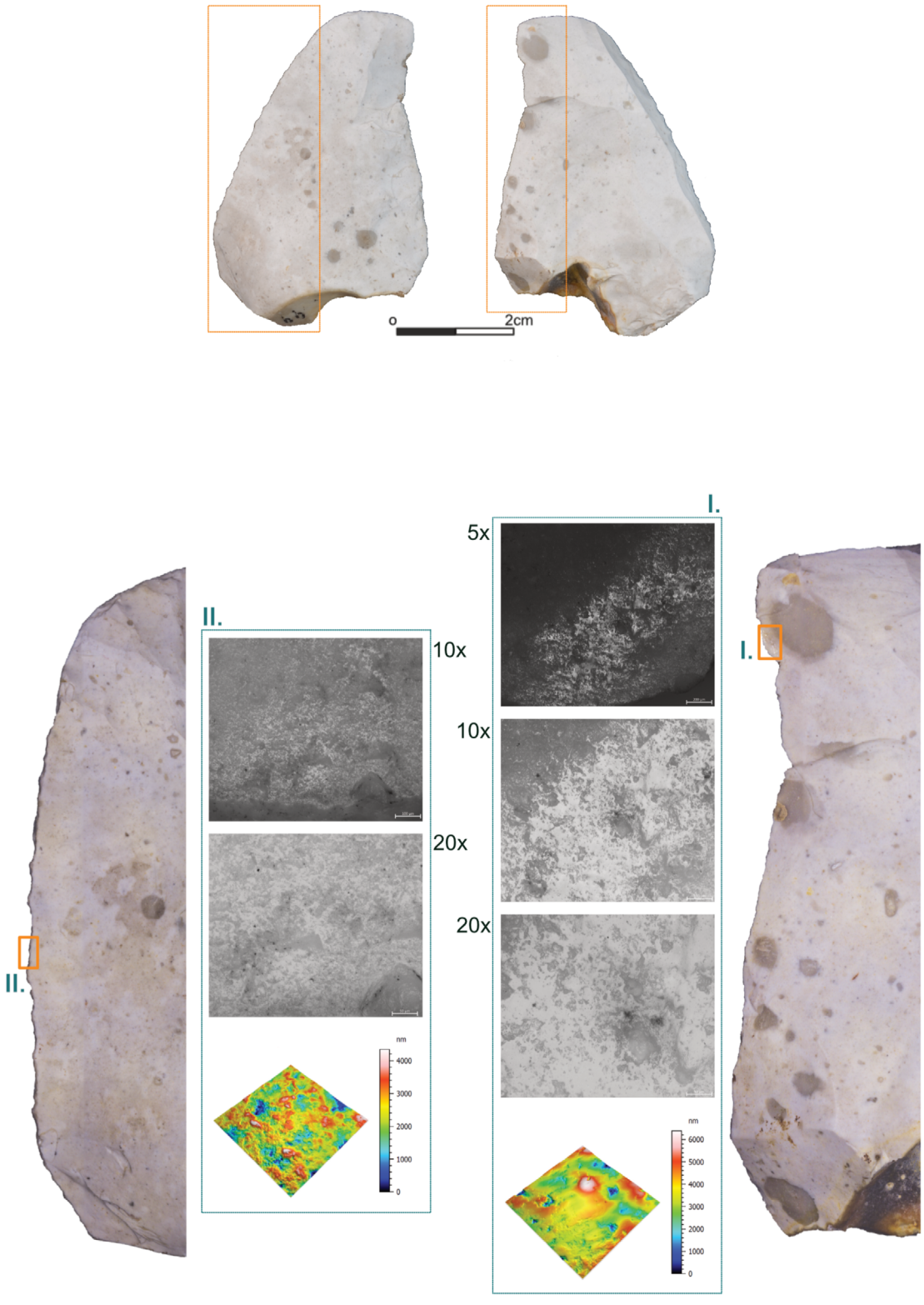

Ramioul, *Keilmesser* [ID R-020]. The topmost image displays the artefact in original size. The other illustrations are magnifications acquired with a 1.6× objective and a 34-× zoom. The use-wear traces are acquired at magnification of 10× and 20× (I. type I.; II. type VIII.; III. type IX.; IV. type II.; V. type II.). The micro-surface displays the processed result of the confocal data acquisition with the 50× objective.

Ramioul, *Prądnik scraper* [ID R-010]. The topmost image displays the artefact in original size. The other illustrations are magnifications acquired with a 1.6× objective and a 34-× zoom. The use-wear traces are acquired at magnification of 5×, 10× and 20× (I. type V. / IV; II. type V.). The micro-surface displays the processed result of the confocal data acquisition with the 50× objective.

Plate A148

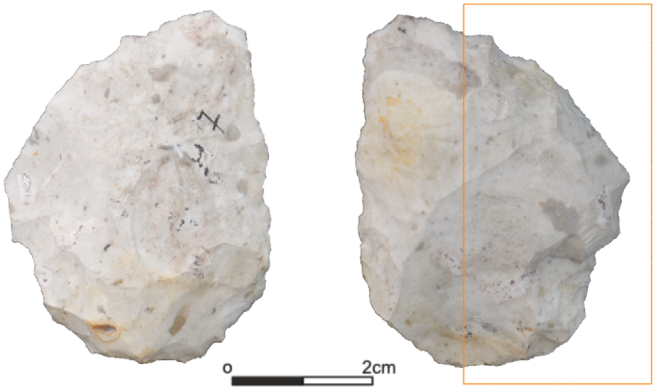

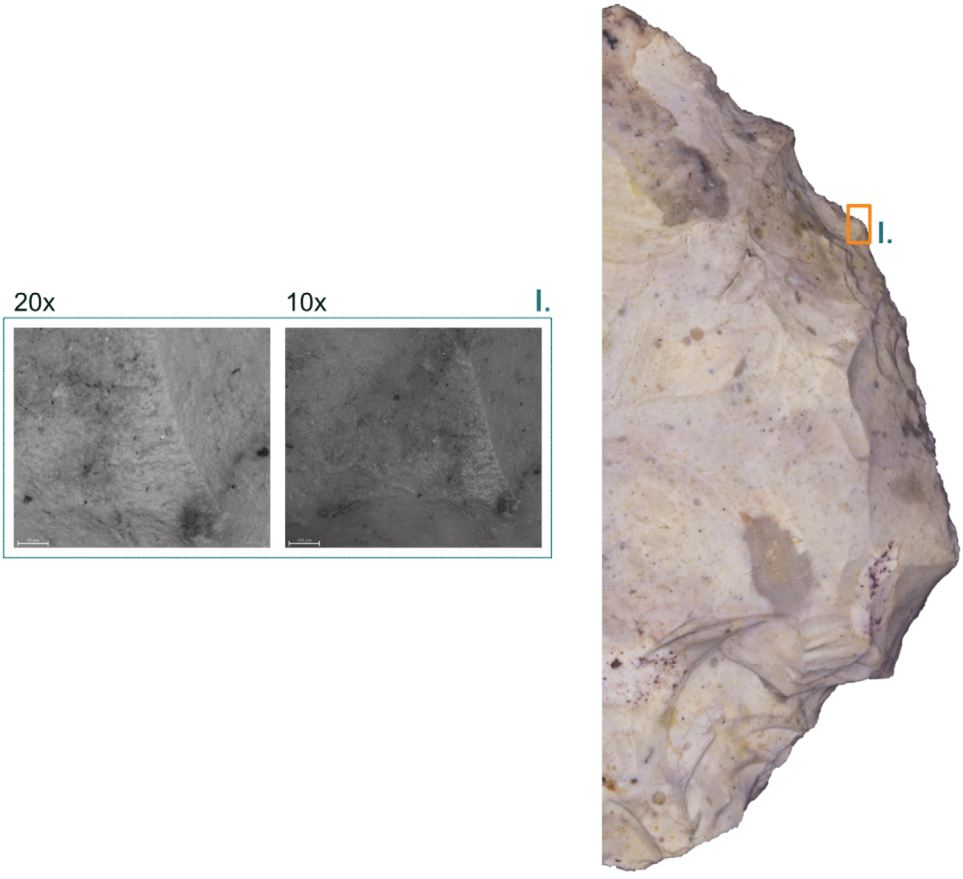

Ramioul, *Prądnik scraper* [ID R-014]. The topmost image displays the artefact in original size. The other illustrations are magnifications acquired with a 1.6× objective and a 34-× zoom. The use-wear trace is acquired at magnification of 10× and 20× (I. type V.).

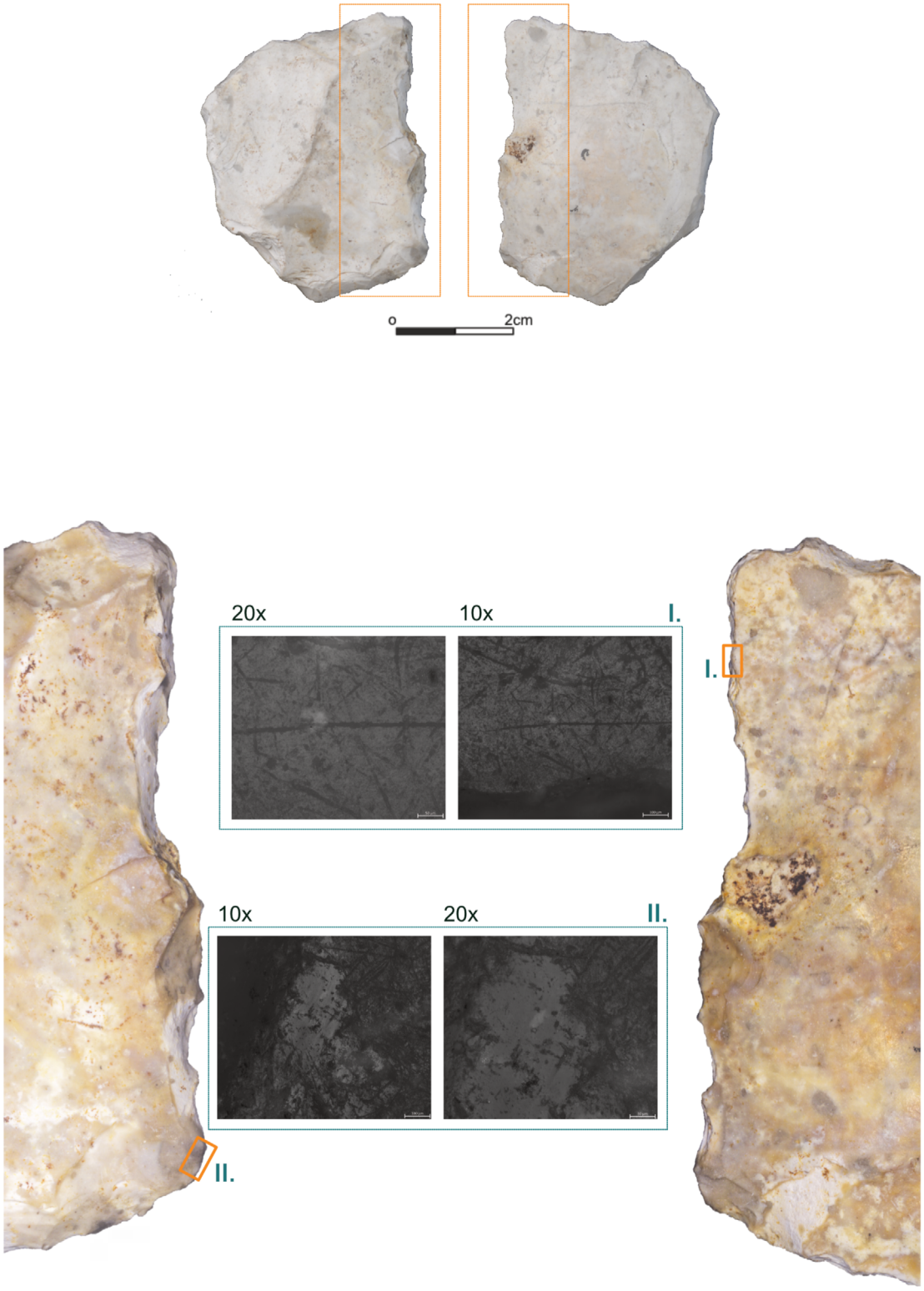

Ramioul, *Prądnik scraper* [ID R-016]. The topmost image displays the artefact in original size. The other illustrations are magnifications acquired with a 1.6× objective and a 34-× zoom. The use-wear traces are acquired at magnification of 10× and 20× (I. type IX.; II. type IX.).

Plate A150

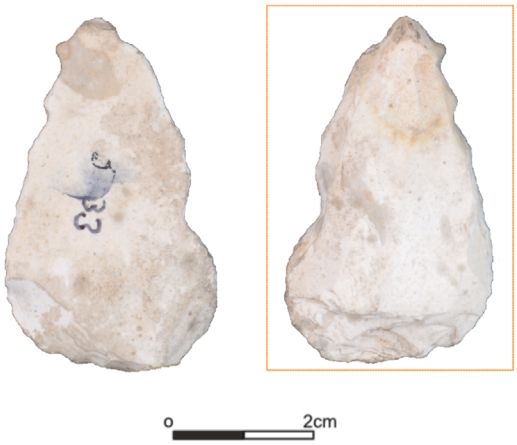

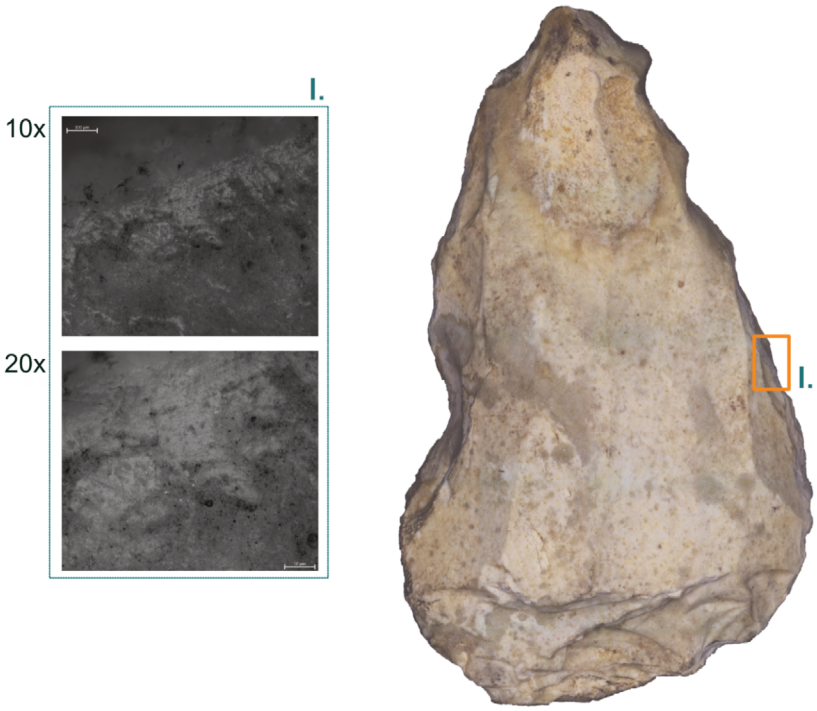

Ramioul, *Prądnik scraper* [ID R-013; dorsal]. The topmost image displays the artefact in original size. The other illustrations are magnifications acquired with a 1.6× objective and a 34-× zoom. The use-wear trace is acquired at magnification of 10× and 20× (I. type IX.).

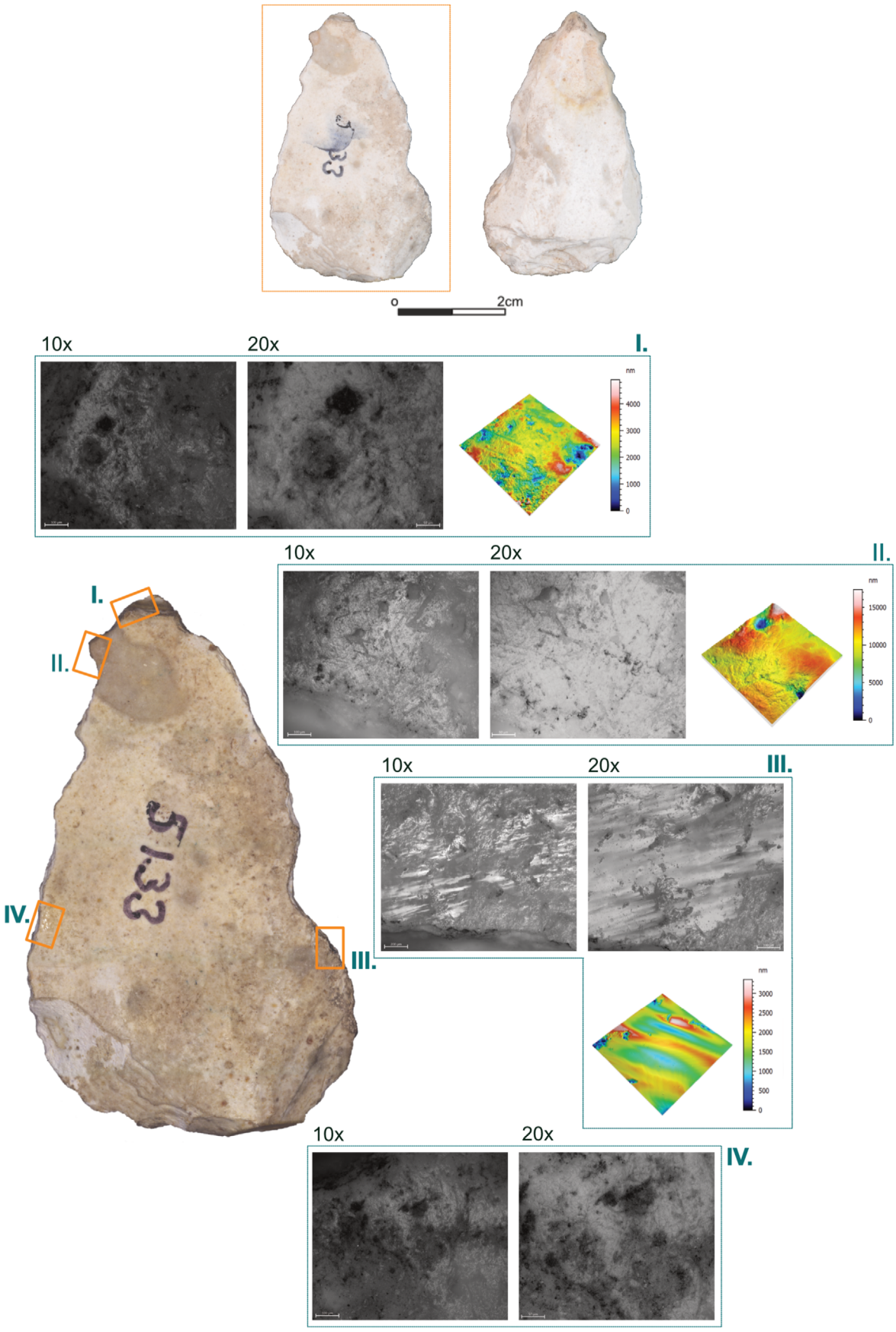

Ramioul, *Prądnik scraper* [ID R-013; ventral]. The topmost image displays the artefact in original size. The other illustrations are magnifications acquired with a 1.6× objective and a 34-× zoom. The use-wear traces are acquired at magnification of 10× and 20× (I. type IX.; II. type IX.; III. type V. / IV.; IV. type VII.). The micro-surface displays the processed result of the confocal data acquisition with the 50× objective.

Plate A152



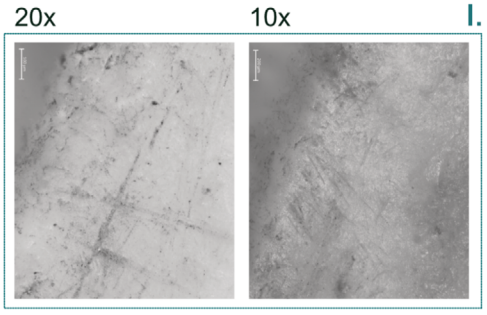



Ramioul, scraper [ID R-015]. The topmost image displays the artefact in original size. The other illustrations are magnifications acquired with a 1.6× objective and a 34-× zoom. The use-wear trace is acquired at magnification of 10× and 20× (I. type IX.).

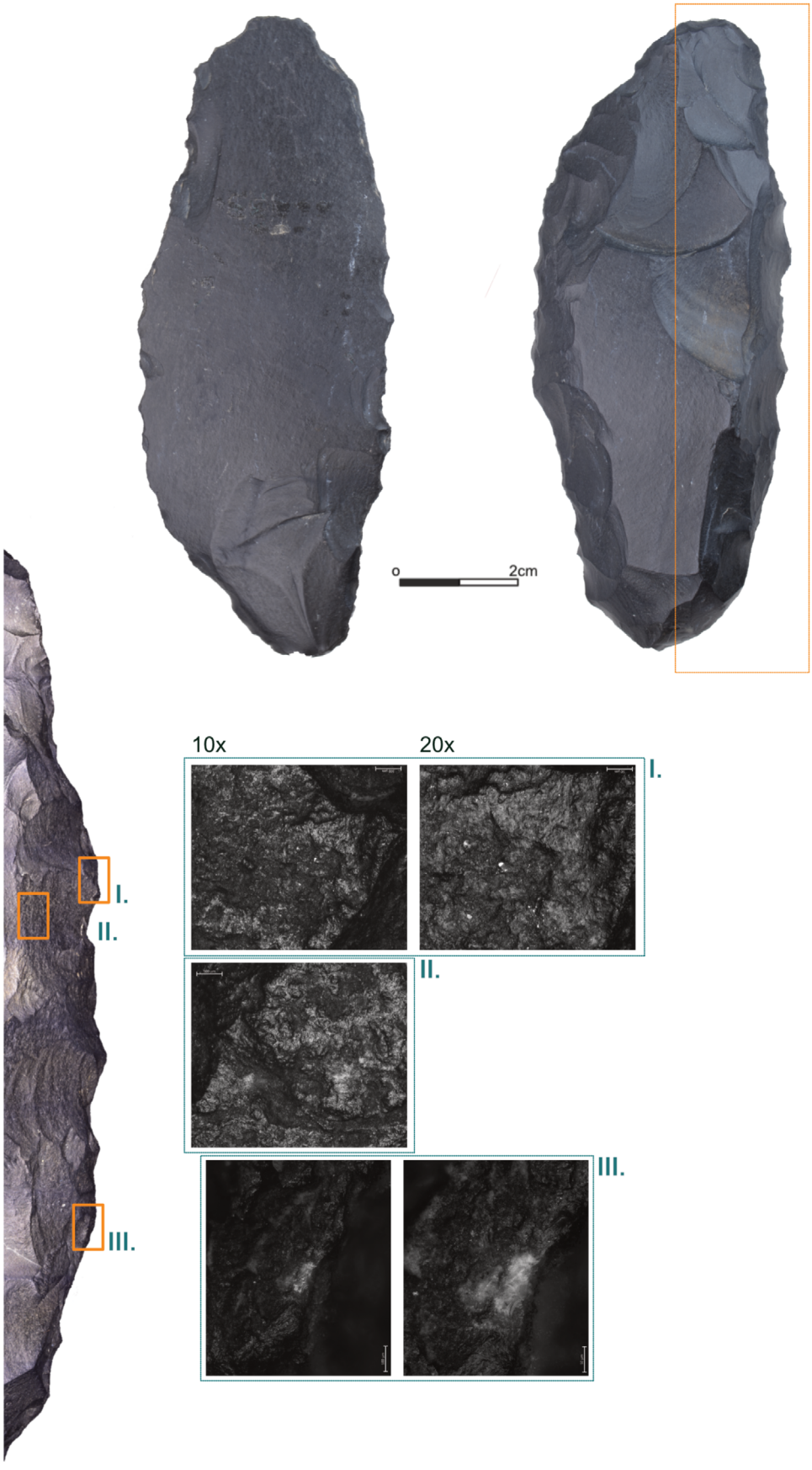

Ramioul, scraper [ID R-017]. The topmost image displays the artefact in original size. The other illustrations are magnifications acquired with a 1.6× objective and a 34-× zoom. The use-wear traces are acquired at magnification of 10× and 20× (I. type V.; II. type V.; III. type IV.).

Plate A154

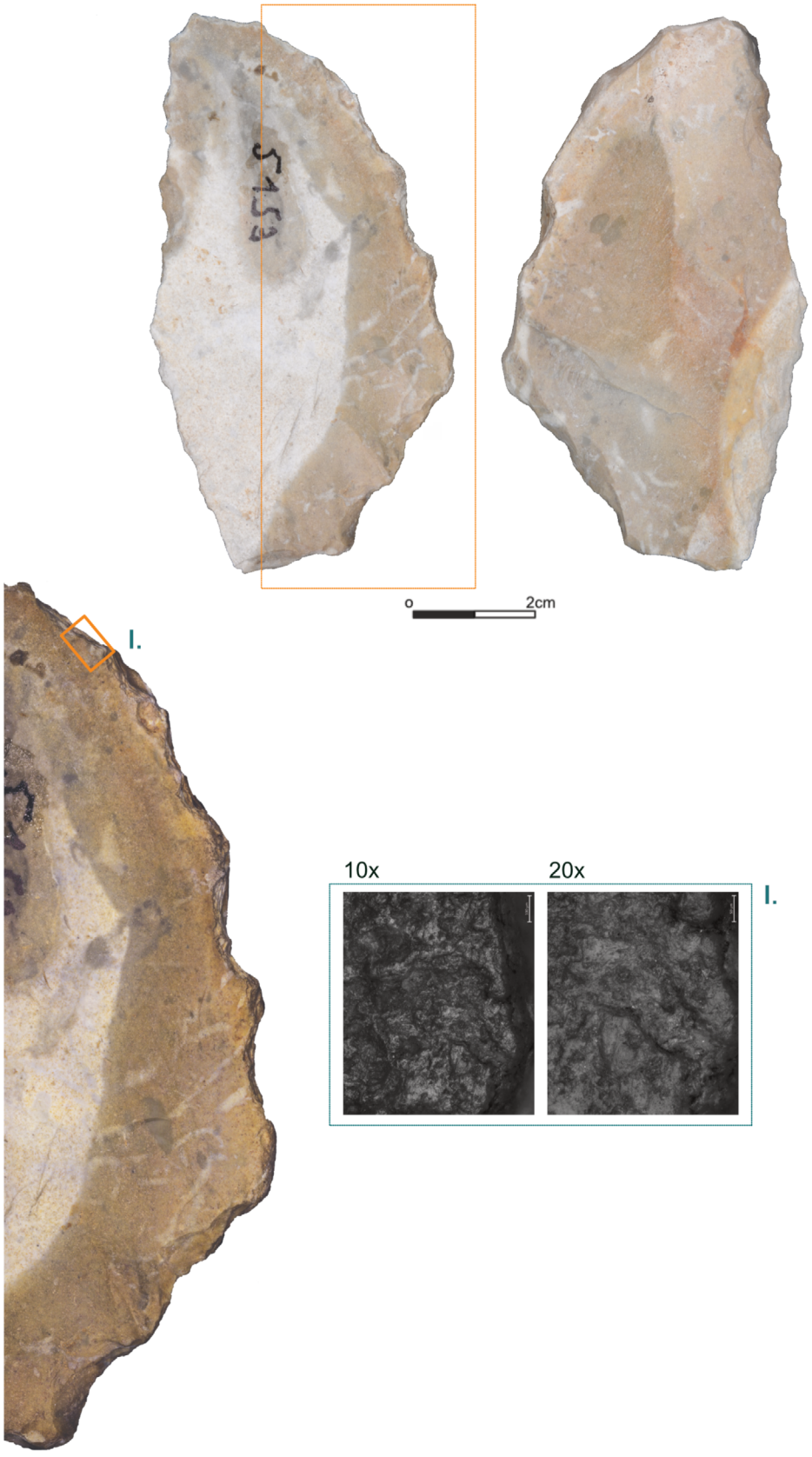

Ramioul, scraper [ID R-012]. The topmost image displays the artefact in original size. The other illustrations are magnifications acquired with a 1.6× objective and a 34-× zoom. The use-wear trace is acquired at magnification of 10× and 20× (I. type V.).

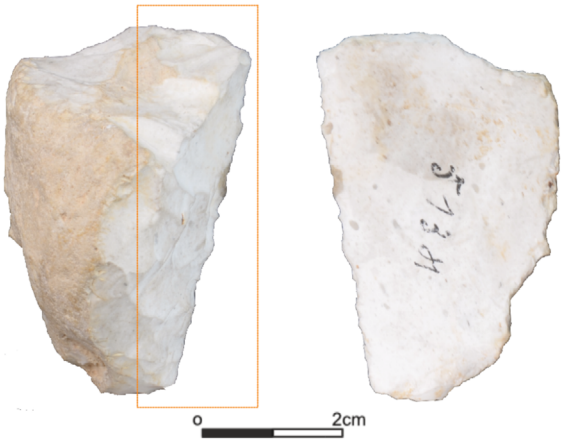

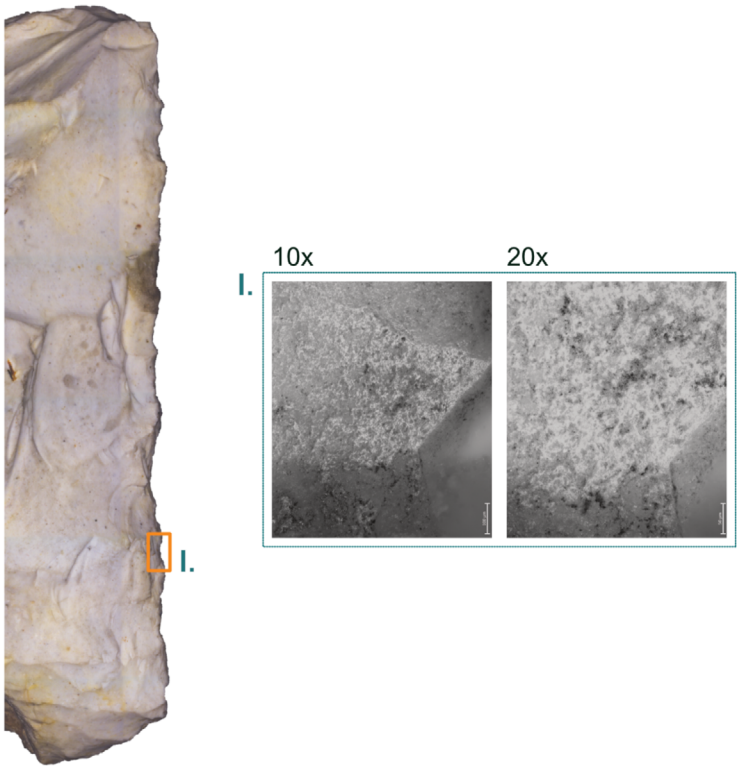

Ramioul, scraper [ID R-003]. The topmost image displays the artefact in original size. The other illustrations are magnifications acquired with a 1.6× objective and a 34-× zoom. The use-wear trace is acquired at magnification of 10× and 20× (I. type V.).

Plate A156

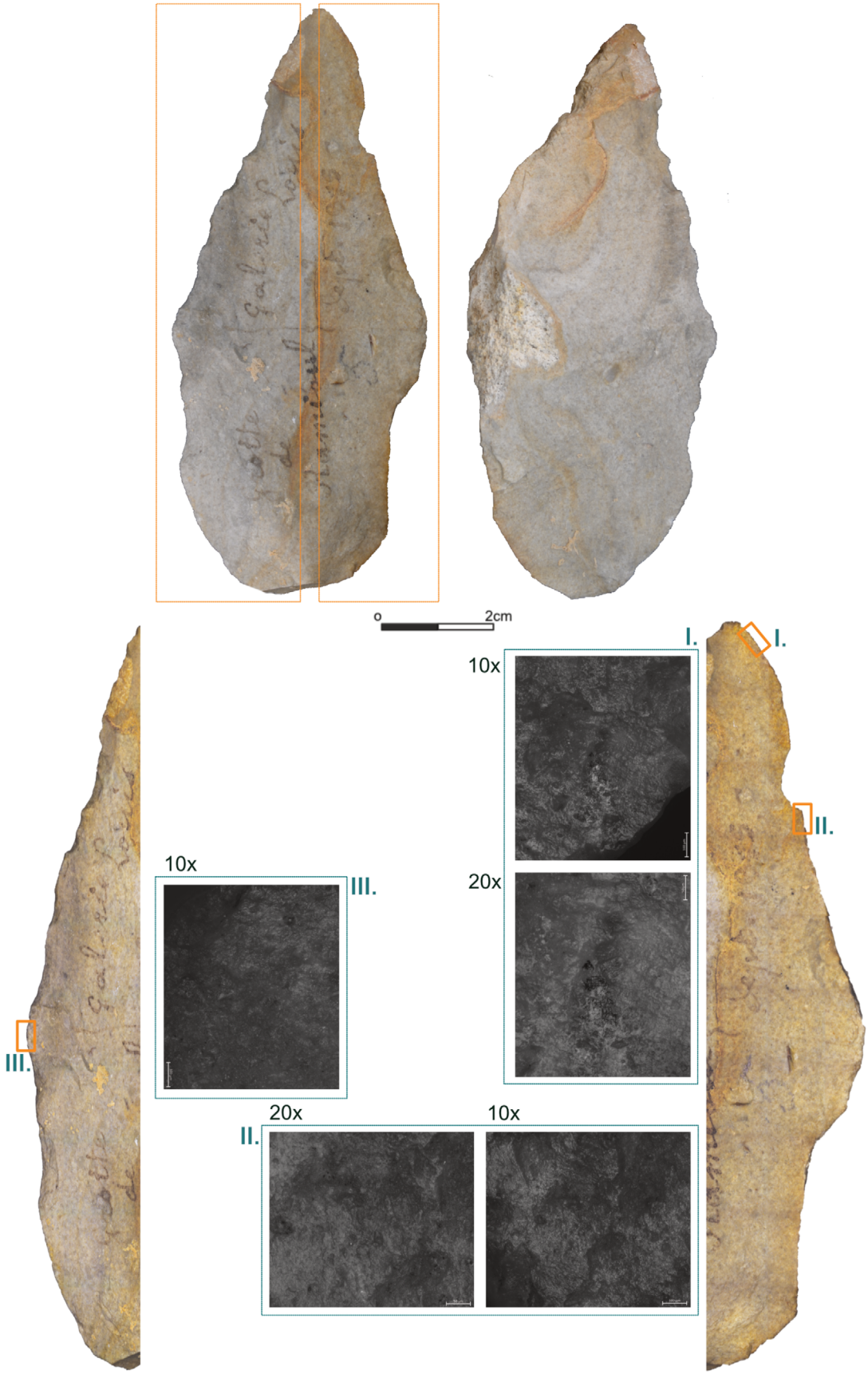

Ramioul, flake [ID R-009]. The topmost image displays the artefact in original size. The other illustrations are magnifications acquired with a 1.6× objective and a 34-× zoom. The use-wear traces are acquired at magnification of 10× and 20× (I. type V.; II. type V.; III. type V.).

APPENDIX II

Results of the qualitative and quantitative use-wear analyses performed on standard samples used during the »artificial VS. natural« experiment and the tool function experiment

PLATES B1-16

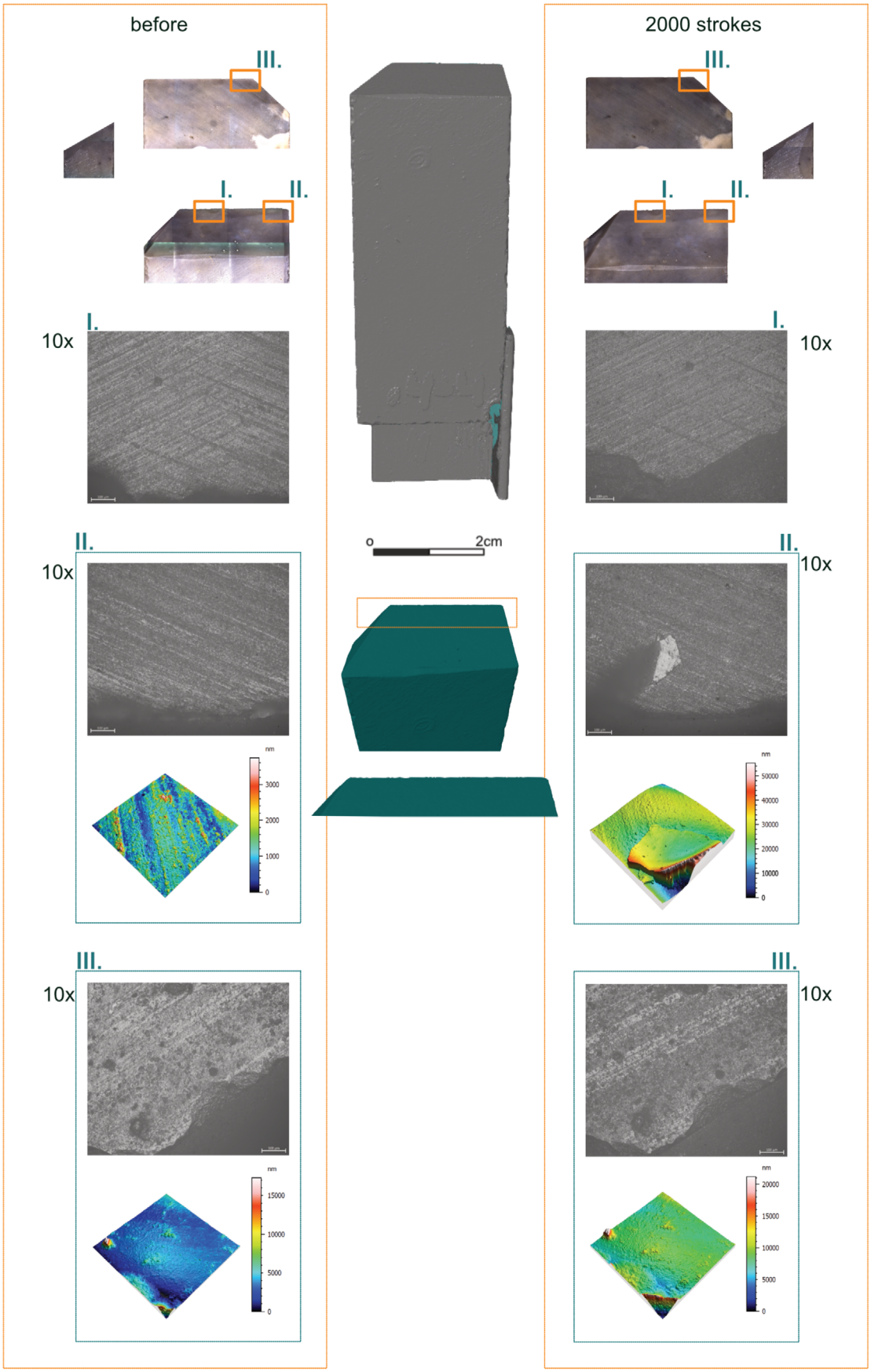

»artificial VS. natural« experiment, flint sample FLT4-4. The topmost image displays the sample in original size before and after 2000 strokes. The 3D model of the sample is shown in the middle (grey) and as a close-up of the edge (turquoise). The other illustrations are magnifications acquired with a 1.6× objective and a 34-× zoom. The use-wear traces are acquired at magnification of 10×. The micro-surface displays the processed result of the confocal data acquisition with the 50× objective.

Plate B2

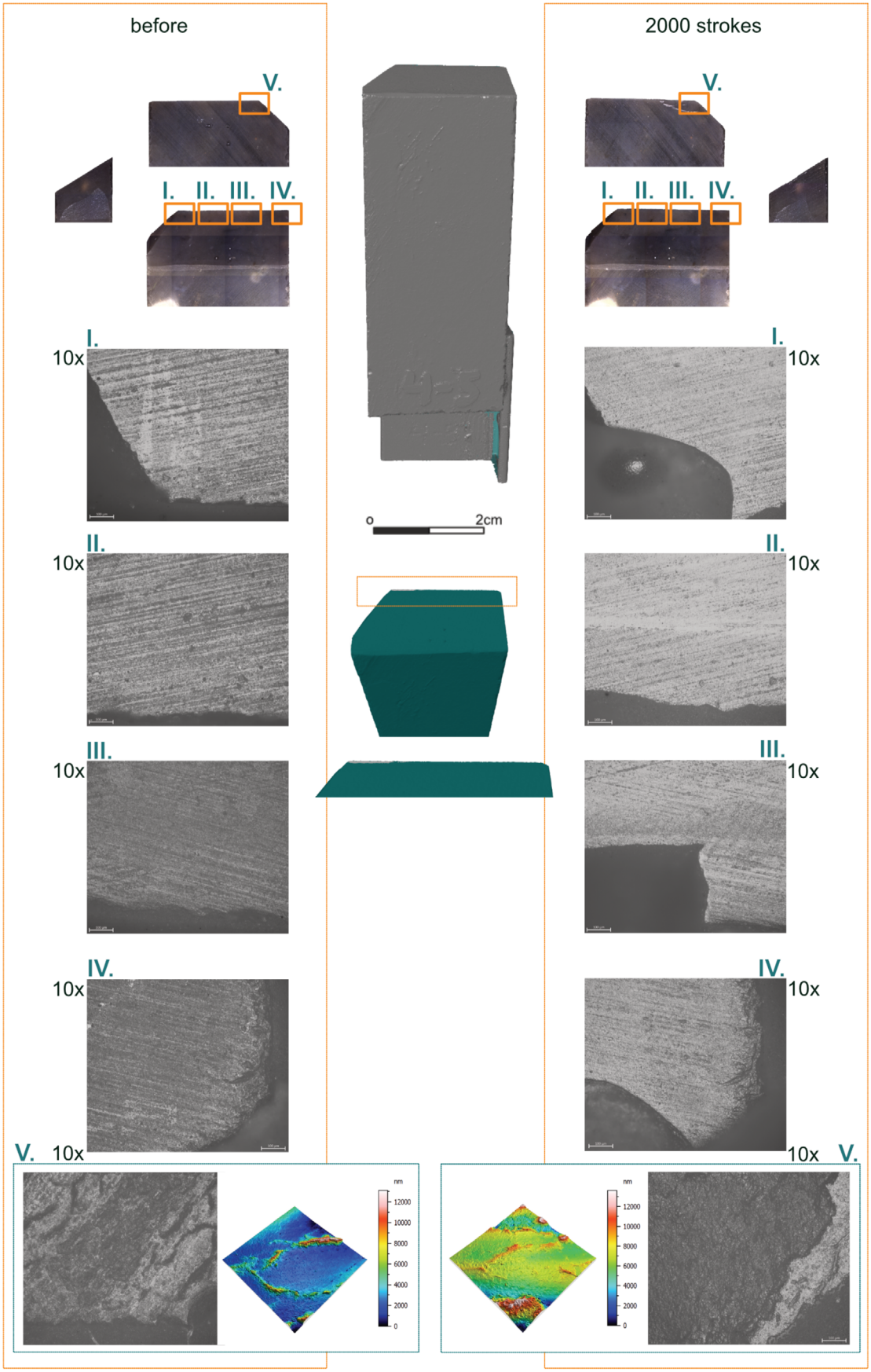

»artificial VS. natural« experiment, flint sample FLT4-5. The topmost image displays the sample in original size before and after 2000 strokes. The 3D model of the sample is shown in the middle (grey) and as a close-up of the edge (turquoise). The other illustrations are magnifications acquired with a 1.6× objective and a 34-× zoom. The use-wear traces are acquired at magnification of 10×. The micro-surface displays the processed result of the confocal data acquisition with the 50× objective.

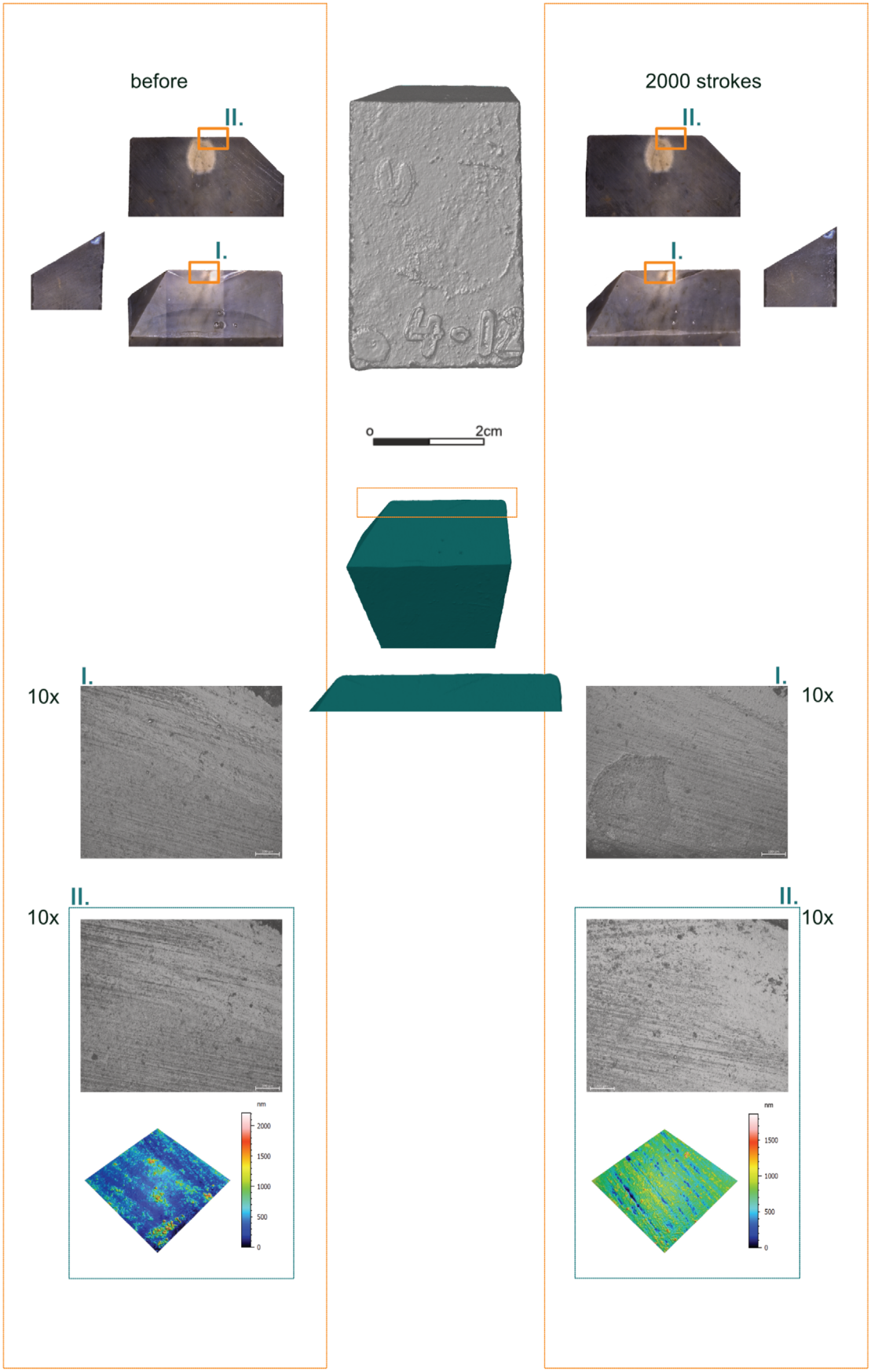

»artificial VS. natural« experiment, flint sample FLT4-12. The topmost image displays the sample in original size before and after 2000 strokes. The 3D model of the sample is shown in the middle (grey) and as a close-up of the edge (turquoise). The other illustrations are magnifications acquired with a 1.6× objective and a 34-× zoom. The use-wear traces are acquired at magnification of 10×. The micro-surface displays the processed result of the confocal data acquisition with the 50× objective.

Plate B4

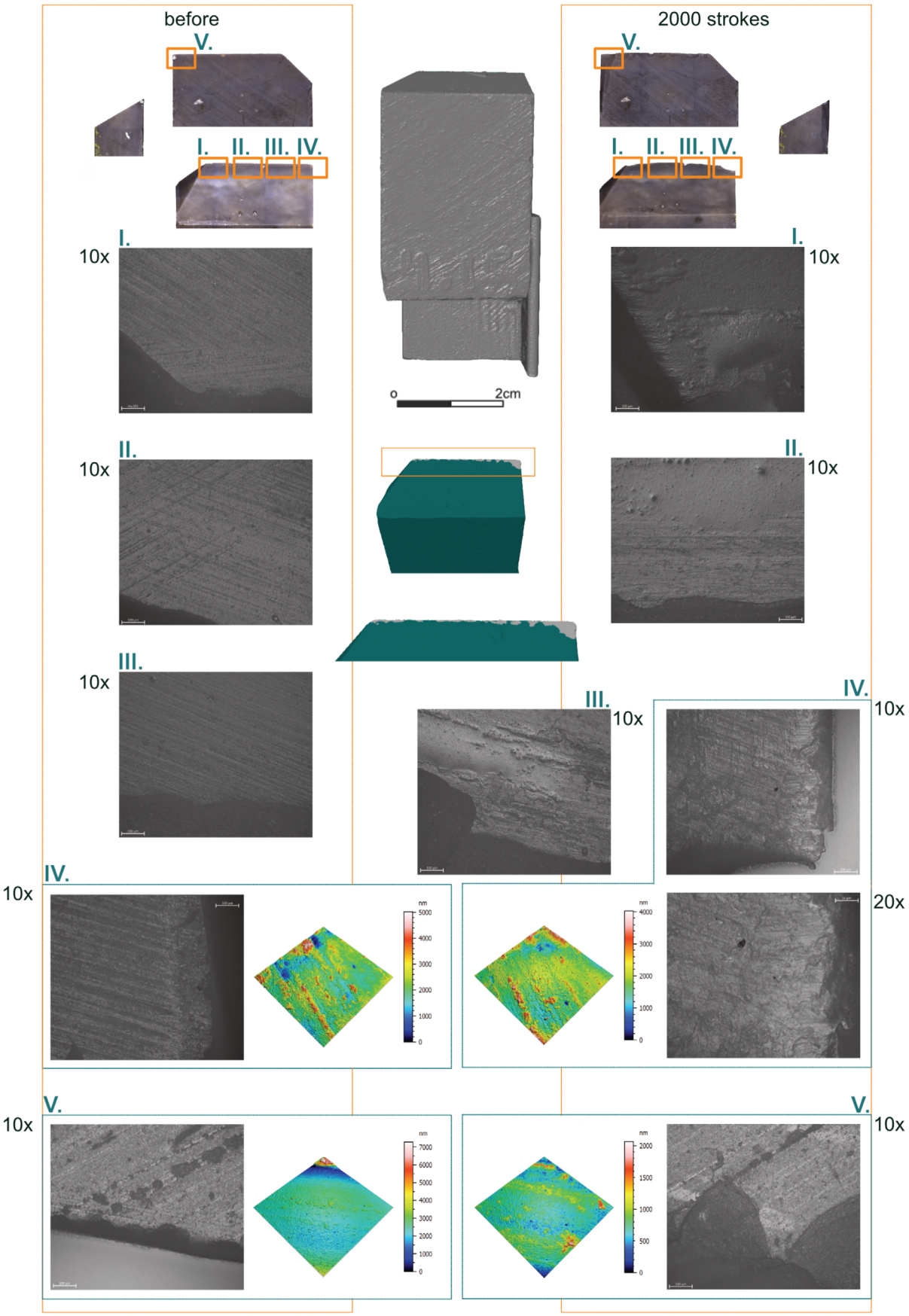

»artificial VS. natural« experiment, flint sample FLT4-15. The topmost image displays the sample in original size before and after 2000 strokes. The 3D model of the sample is shown in the middle (grey) and as a close-up of the edge (turquoise). The other illustrations are magnifications acquired with a 1.6× objective and a 34-× zoom. The use-wear traces are acquired at magnification of 10× and 20×. The micro-surface displays the processed result of the confocal data acquisition with the 50× objective.

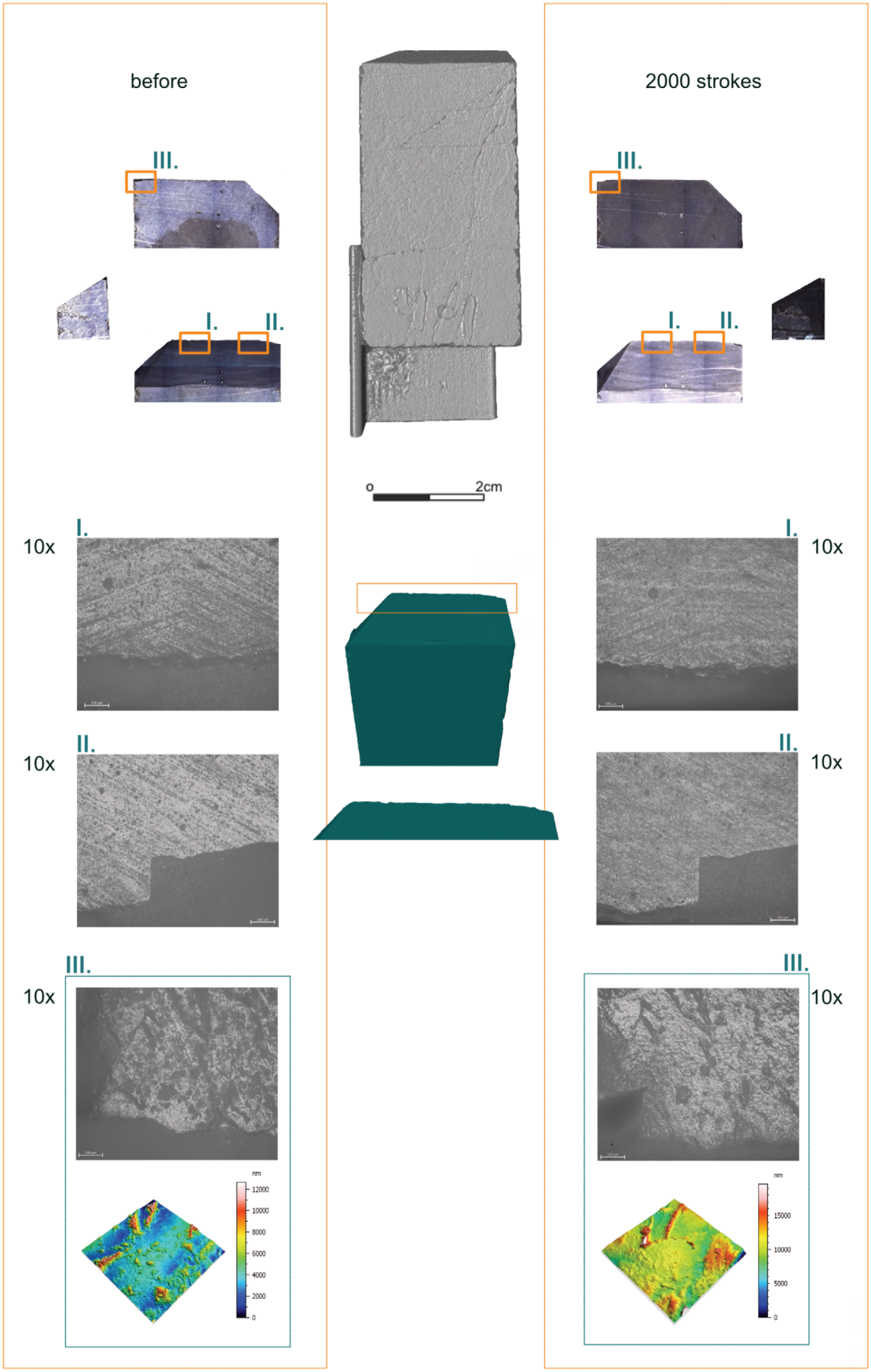

»artificial VS. natural« experiment, lydite sample LYDIT4-1. The topmost image displays the sample in original size before and after 2000 strokes. The 3D model of the sample is shown in the middle (grey) and as a close-up of the edge (turquoise). The other illustrations are magnifications acquired with a 1.6× objective and a 34-× zoom. The use-wear traces are acquired at magnification of 10×. The micro-surface displays the processed result of the confocal data acquisition with the 50× objective.

Plate B6

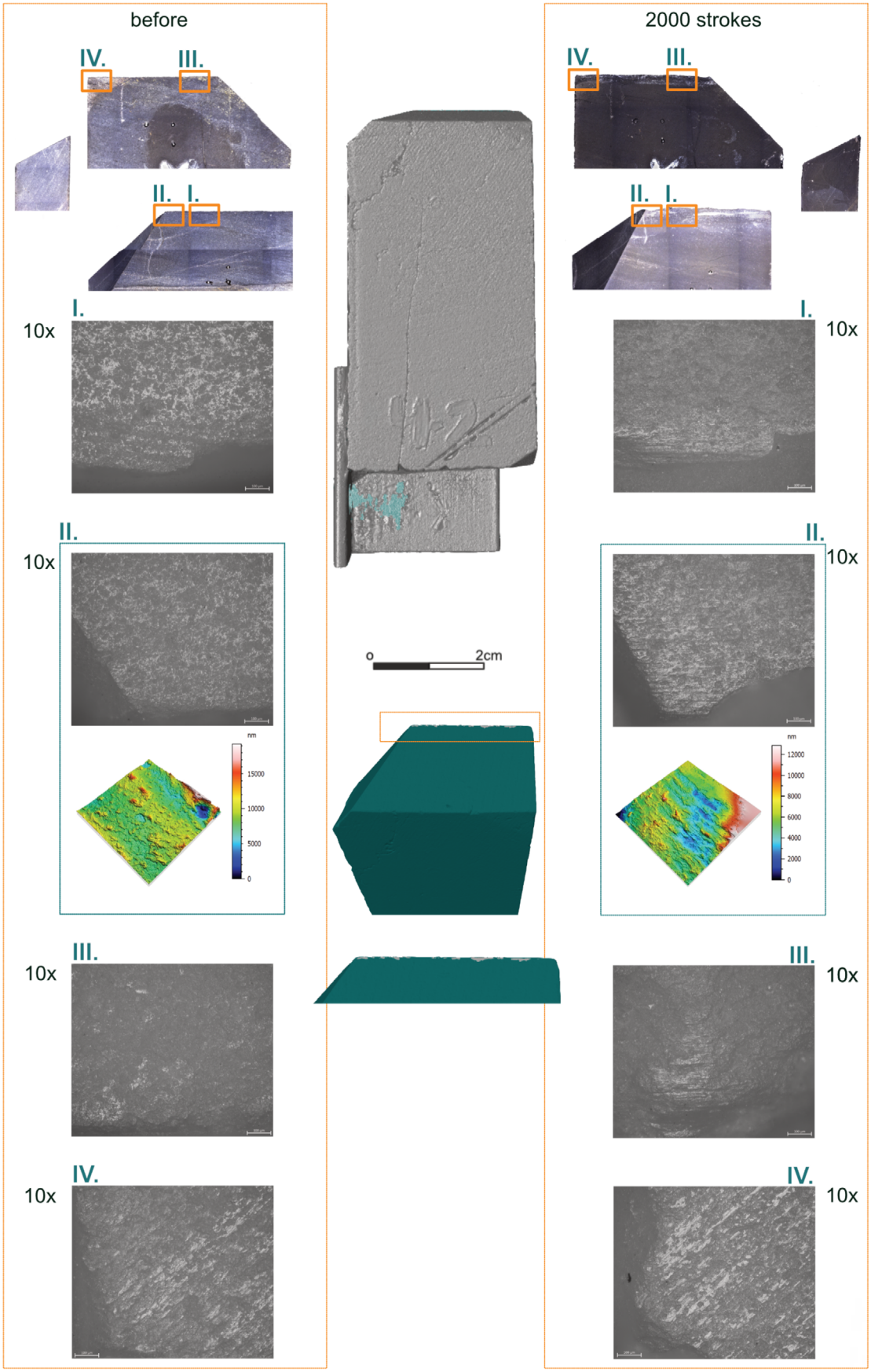

»artificial VS. natural« experiment, lydite sample LYDIT4-2. The topmost image displays the sample in original size before and after 2000 strokes. The 3D model of the sample is shown in the middle (grey) and as a close-up of the edge (turquoise). The other illustrations are magnifications acquired with a 1.6× objective and a 34-× zoom. The use-wear traces are acquired at magnification of 10×. The micro-surface displays the processed result of the confocal data acquisition with the 50× objective.

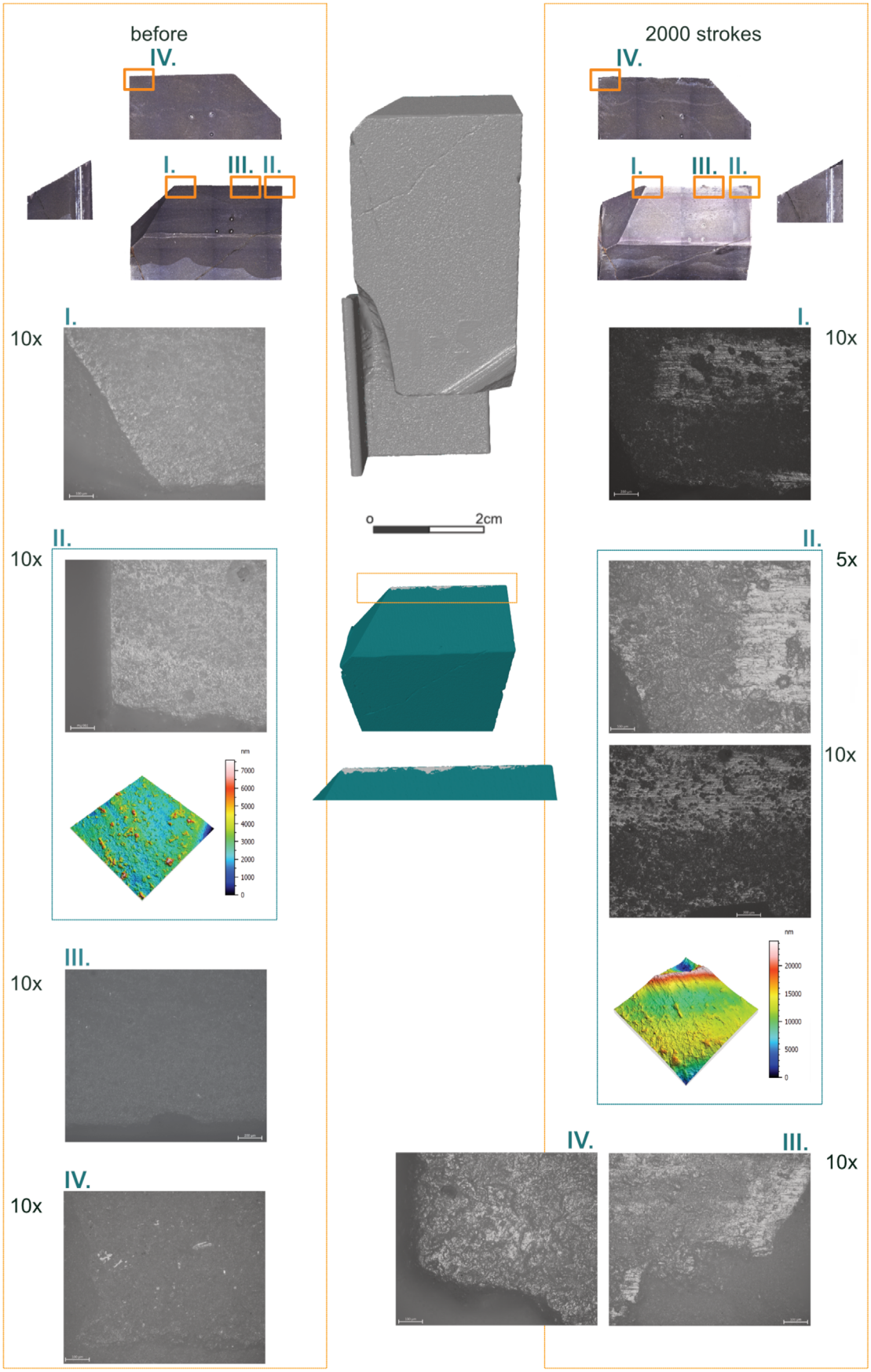

»artificial VS. natural« experiment, lydite sample LYDIT4-5. The topmost image displays the sample in original size before and after 2000 strokes. The 3D model of the sample is shown in the middle (grey) and as a close-up of the edge (turquoise). The other illustrations are magnifications acquired with a 1.6× objective and a 34-× zoom. The use-wear traces are acquired at magnification of 5× and 10×. The micro-surface displays the processed result of the confocal data acquisition with the 50× objective.

Plate B8

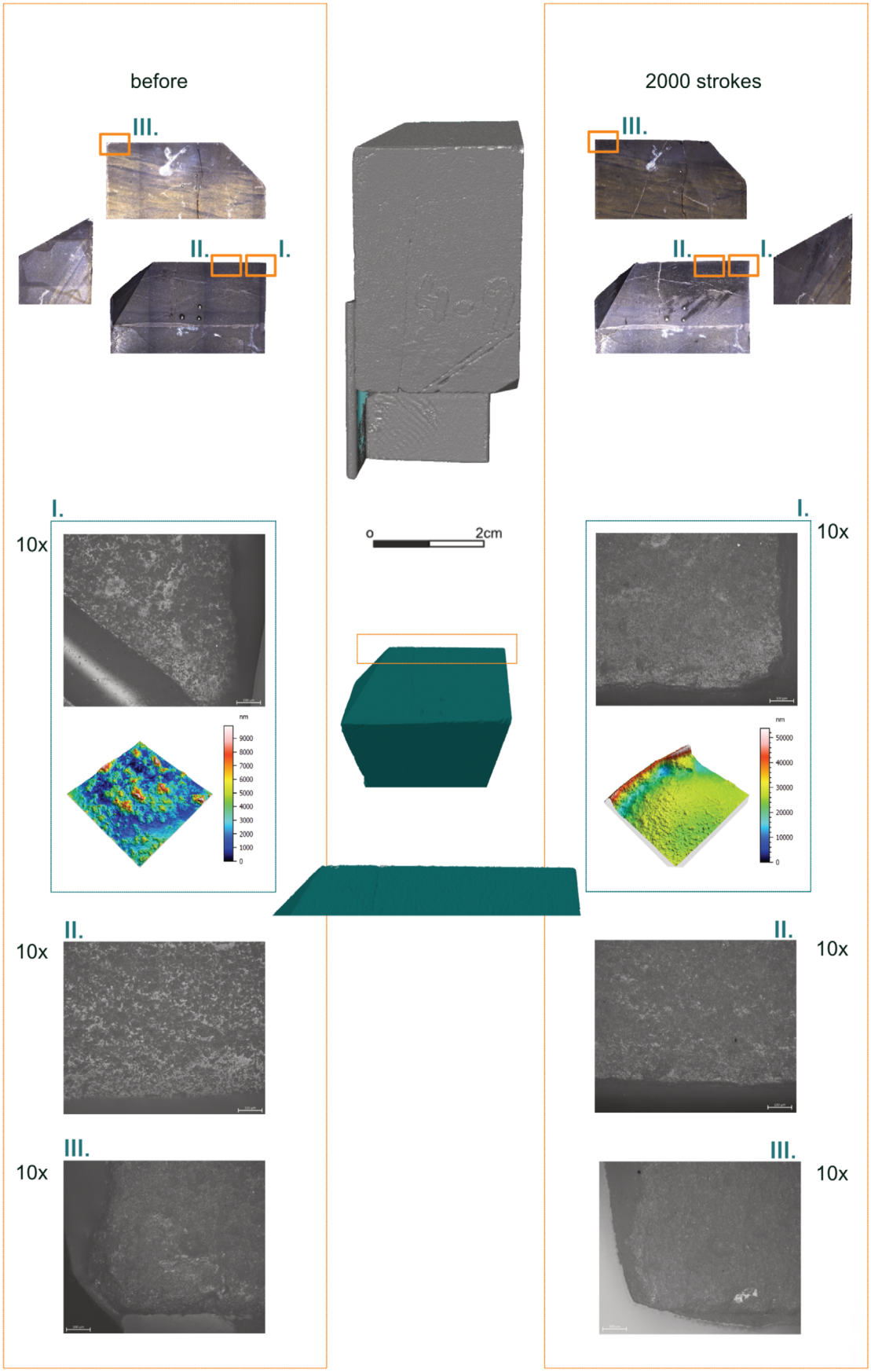

»artificial VS. natural« experiment, lydite sample LYDIT4-9. The topmost image displays the sample in original size before and after 2000 strokes. The 3D model of the sample is shown in the middle (grey) and as a close-up of the edge (turquoise). The other illustrations are magnifications acquired with a 1.6× objective and a 34-× zoom. The use-wear traces are acquired at magnification of 10×. The micro-surface displays the processed result of the confocal data acquisition with the 50× objective.

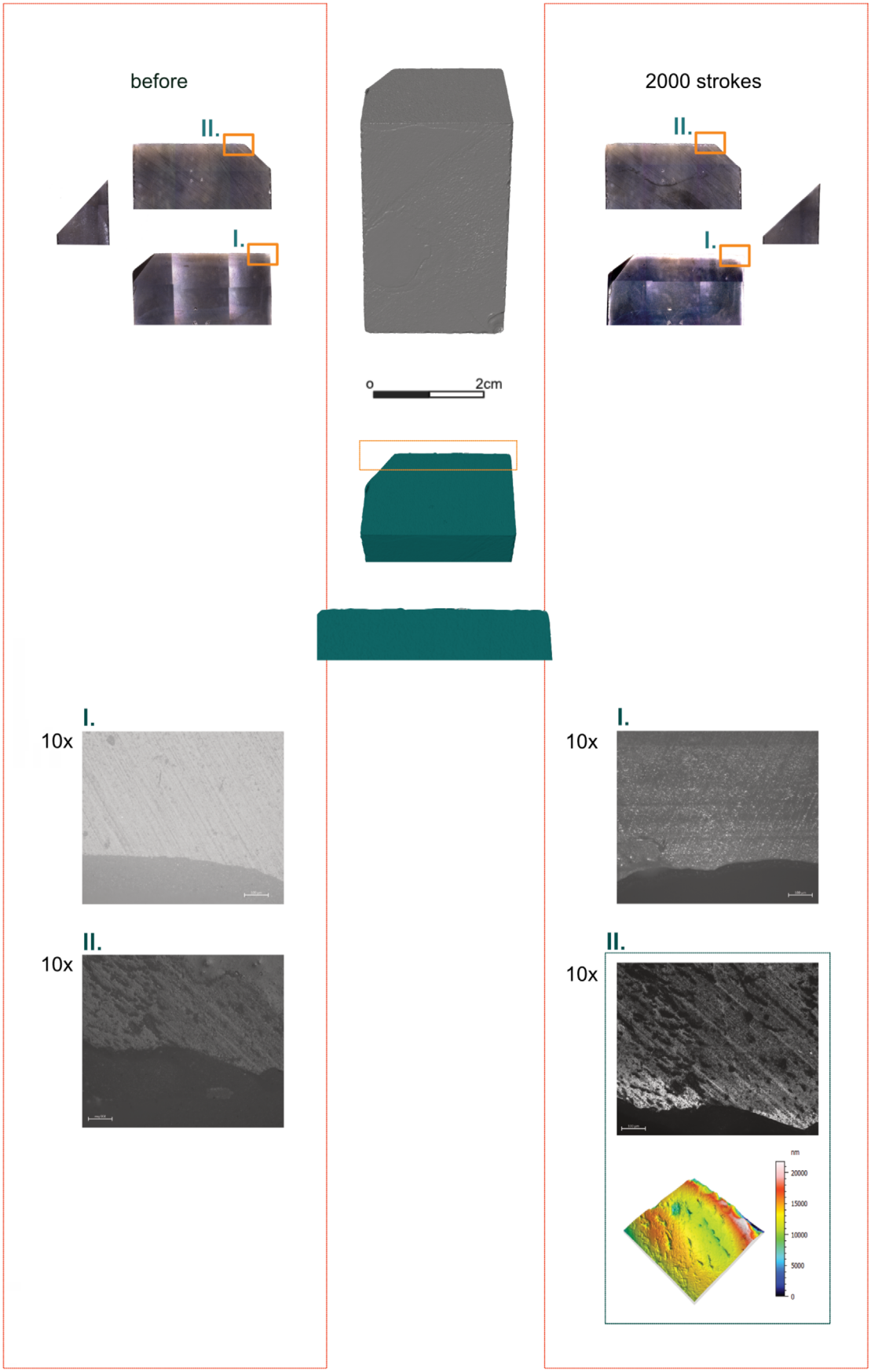

Tool function experiment, flint sample FLT8-2. The topmost image displays the sample in original size before and after 2000 strokes. The 3D model of the sample is shown in the middle (grey) and as a close-up of the edge (turquoise). The other illustrations are magnifications acquired with a 1.6× objective and a 34-× zoom. The use-wear traces are acquired at magnification of 10×. The micro-surface displays the processed result of the confocal data acquisition with the 50× objective.

Plate B10

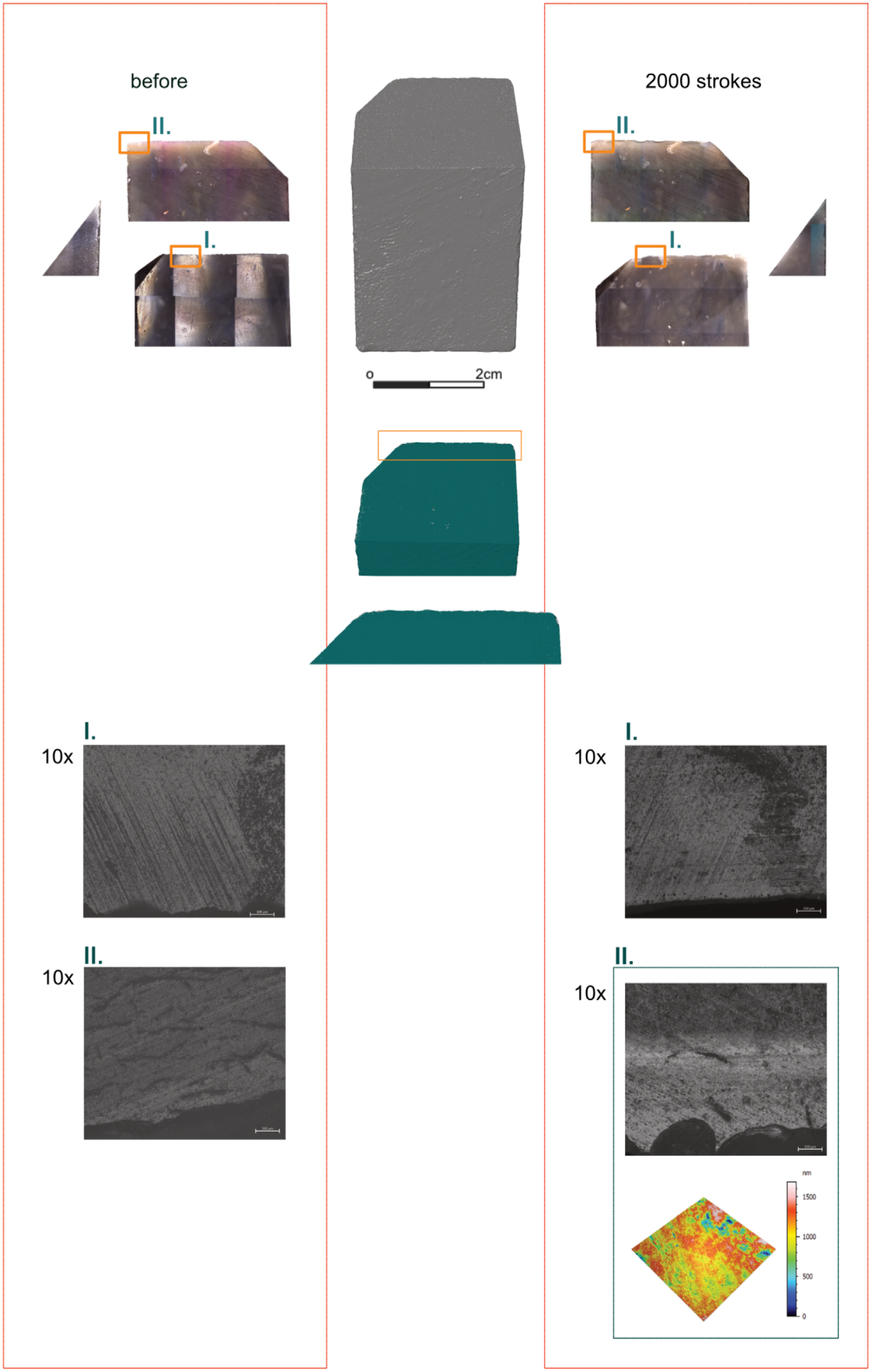

Tool function experiment, flint sample FLT8-5. The topmost image displays the sample in original size before and after 2000 strokes. The 3D model of the sample is shown in the middle (grey) and as a close-up of the edge (turquoise). The other illustrations are magnifications acquired with a 1.6× objective and a 34-× zoom. The use-wear traces are acquired at magnification of 10×. The micro-surface displays the processed result of the confocal data acquisition with the 50× objective.

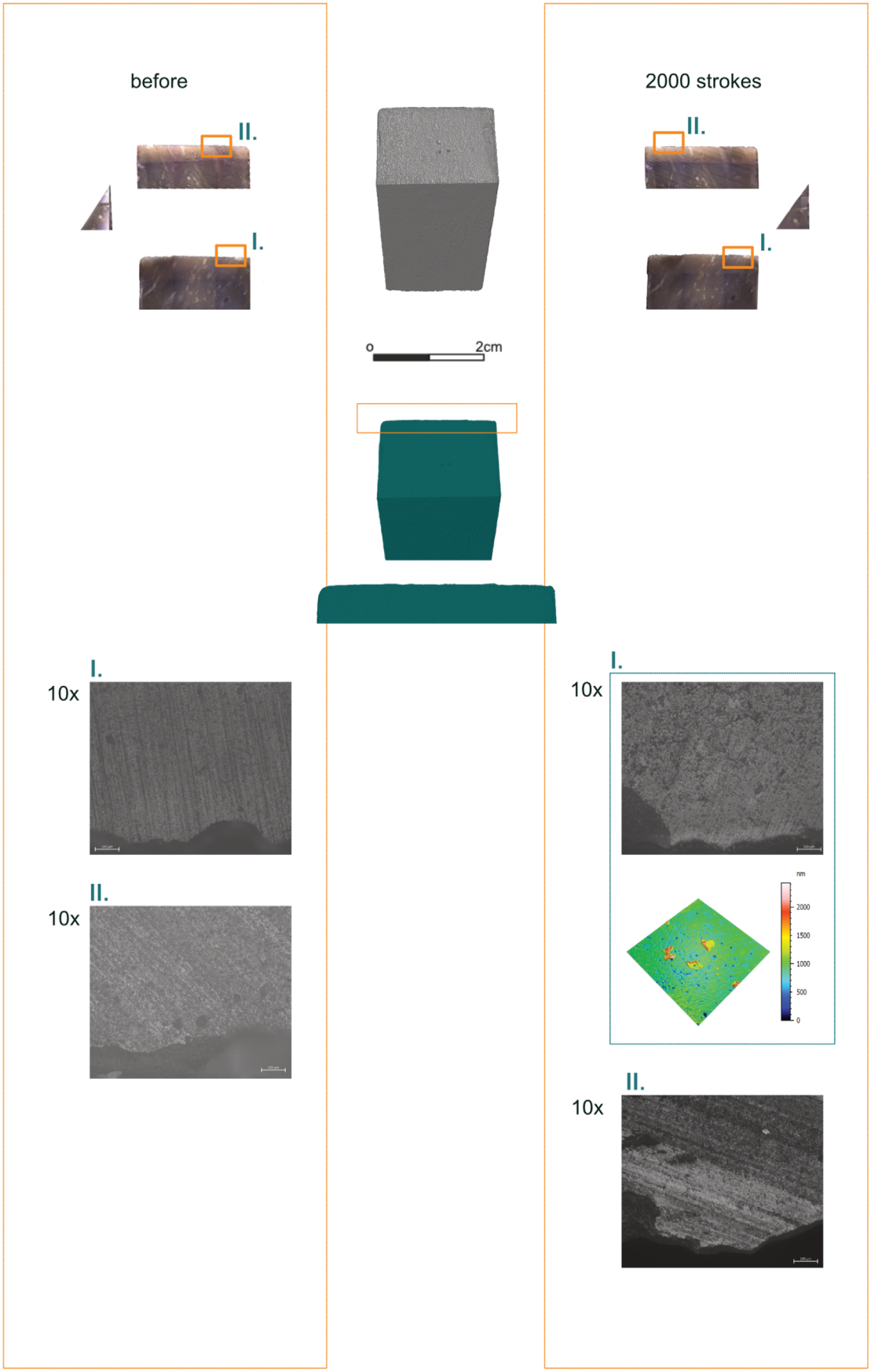

Tool function experiment, flint sample FLT8-9. The topmost image displays the sample in original size before and after 2000 strokes. The 3D model of the sample is shown in the middle (grey) and as a close-up of the edge (turquoise). The other illustrations are magnifications acquired with a 1.6× objective and a 34-× zoom. The use-wear traces are acquired at magnification of 10×. The micro-surface displays the processed result of the confocal data acquisition with the 50× objective.

Plate B12

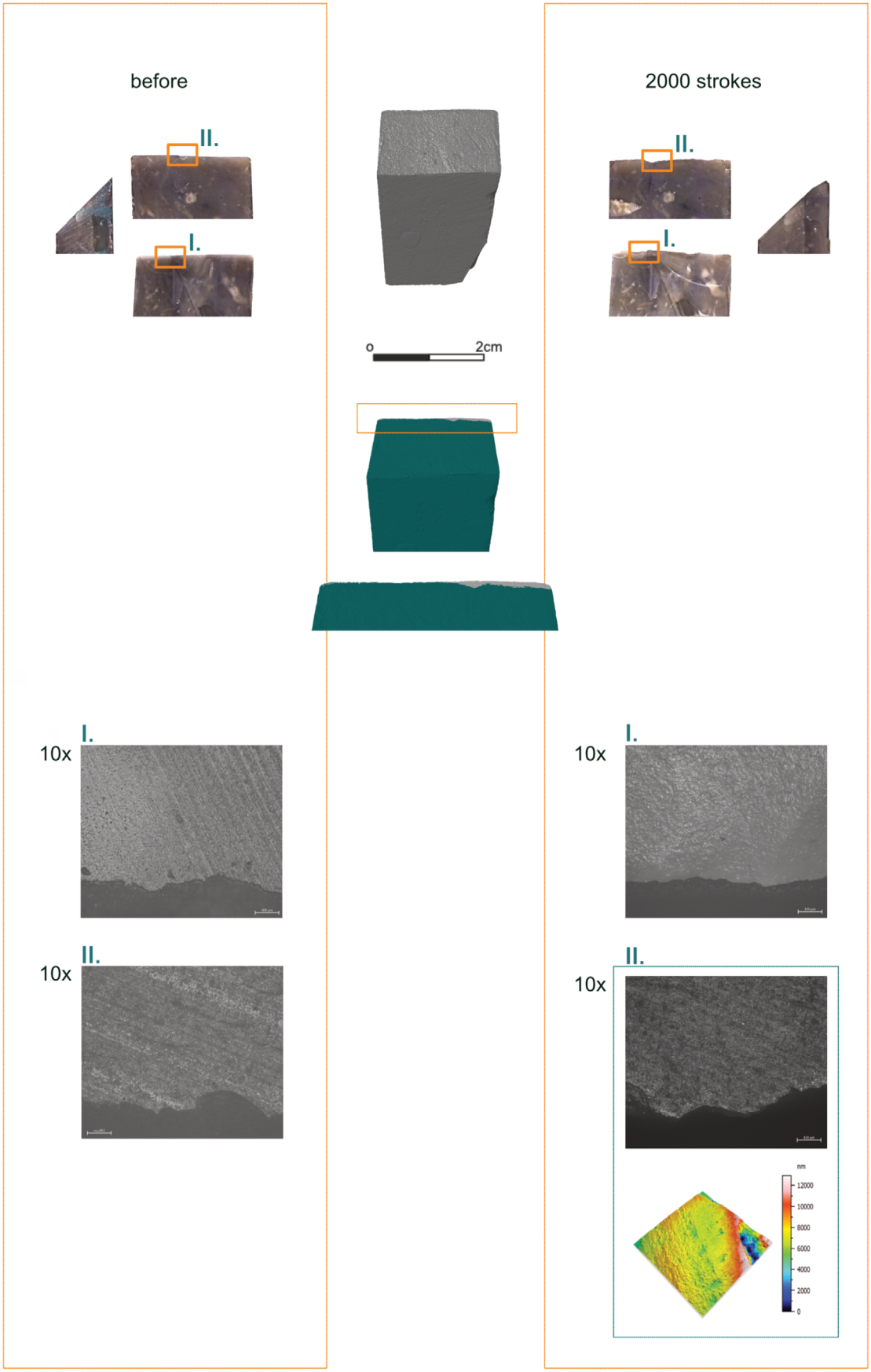

Tool function experiment, flint sample FLT8-10. The topmost image displays the sample in original size before and after 2000 strokes. The 3D model of the sample is shown in the middle (grey) and as a close-up of the edge (turquoise). The other illustrations are magnifications acquired with a 1.6× objective and a 34-× zoom. The use-wear traces are acquired at magnification of 10×. The micro-surface displays the processed result of the confocal data acquisition with the 50× objective.

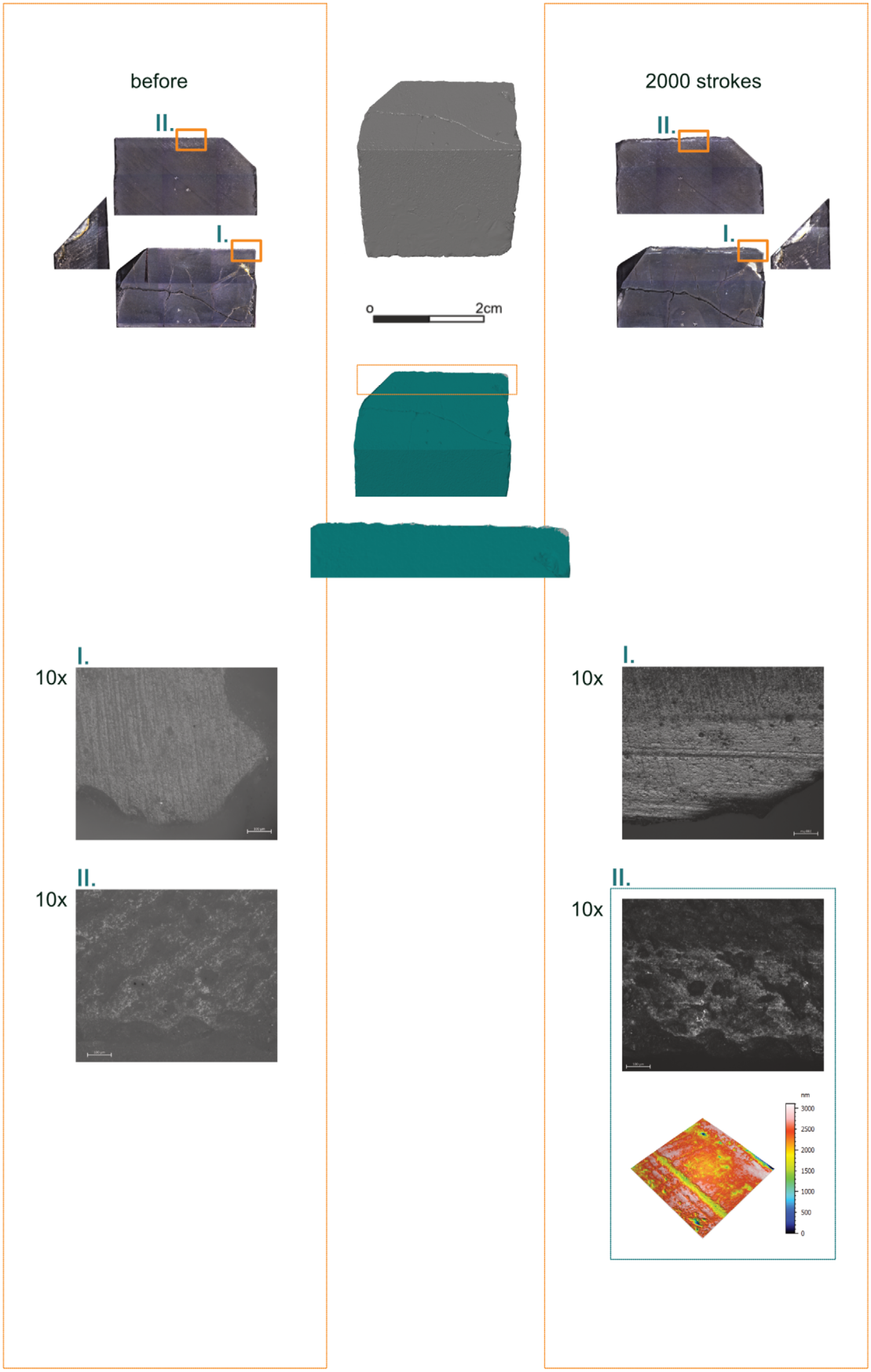

Tool function experiment, lydite sample LYDIT5-2. The topmost image displays the sample in original size before and after 2000 strokes. The 3D model of the sample is shown in the middle (grey) and as a close-up of the edge (turquoise). The other illustrations are magnifications acquired with a 1.6× objective and a 34-× zoom. The use-wear traces are acquired at magnification of 10×. The micro-surface displays the processed result of the confocal data acquisition with the 50× objective.

Plate B14

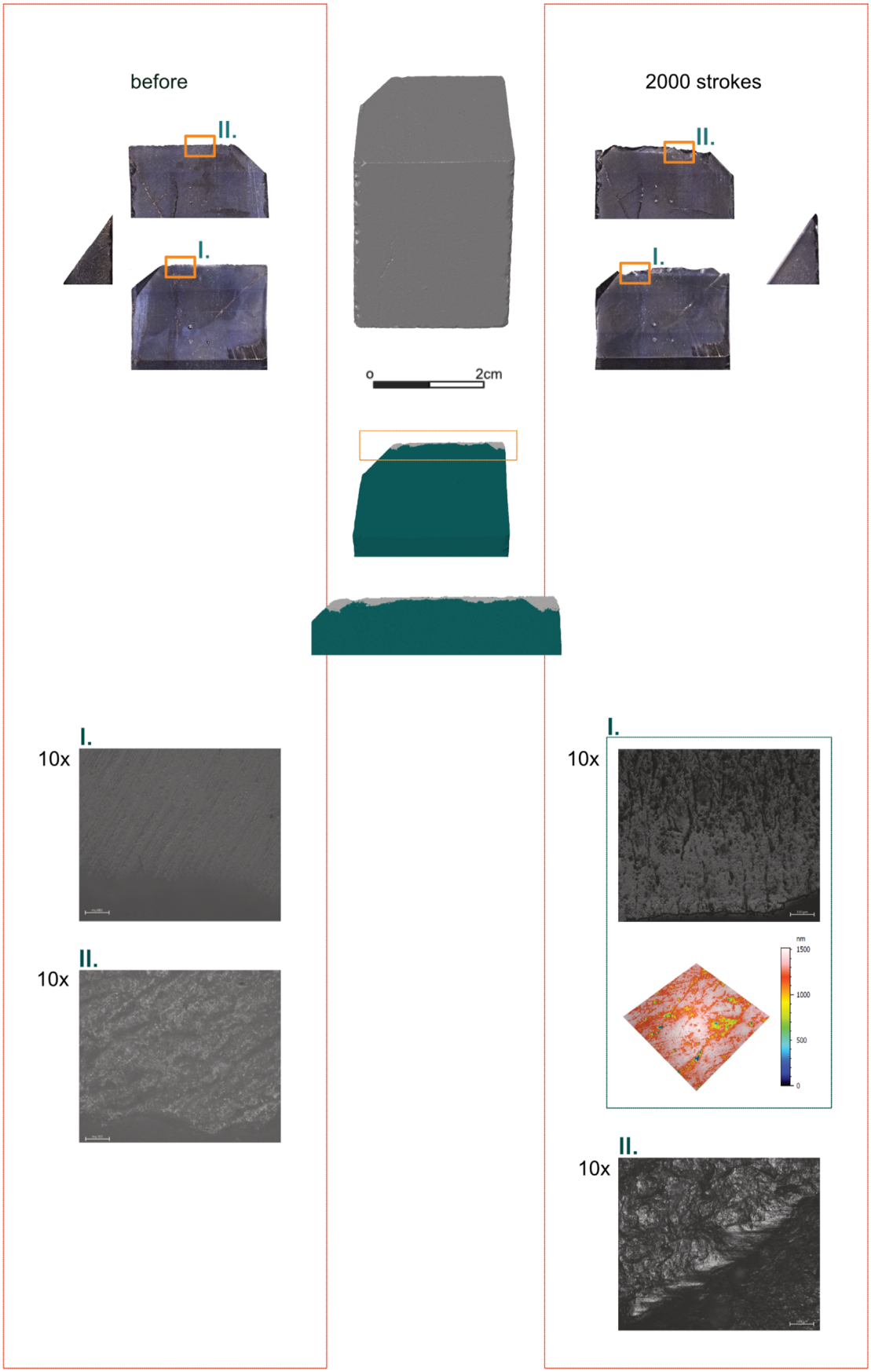

Tool function experiment, lydite sample LYDIT5-7. The topmost image displays the sample in original size before and after 2000 strokes. The 3D model of the sample is shown in the middle (grey) and as a close-up of the edge (turquoise). The other illustrations are magnifications acquired with a 1.6× objective and a 34-× zoom. The use-wear traces are acquired at magnification of 10×. The micro-surface displays the processed result of the confocal data acquisition with the 50× objective.

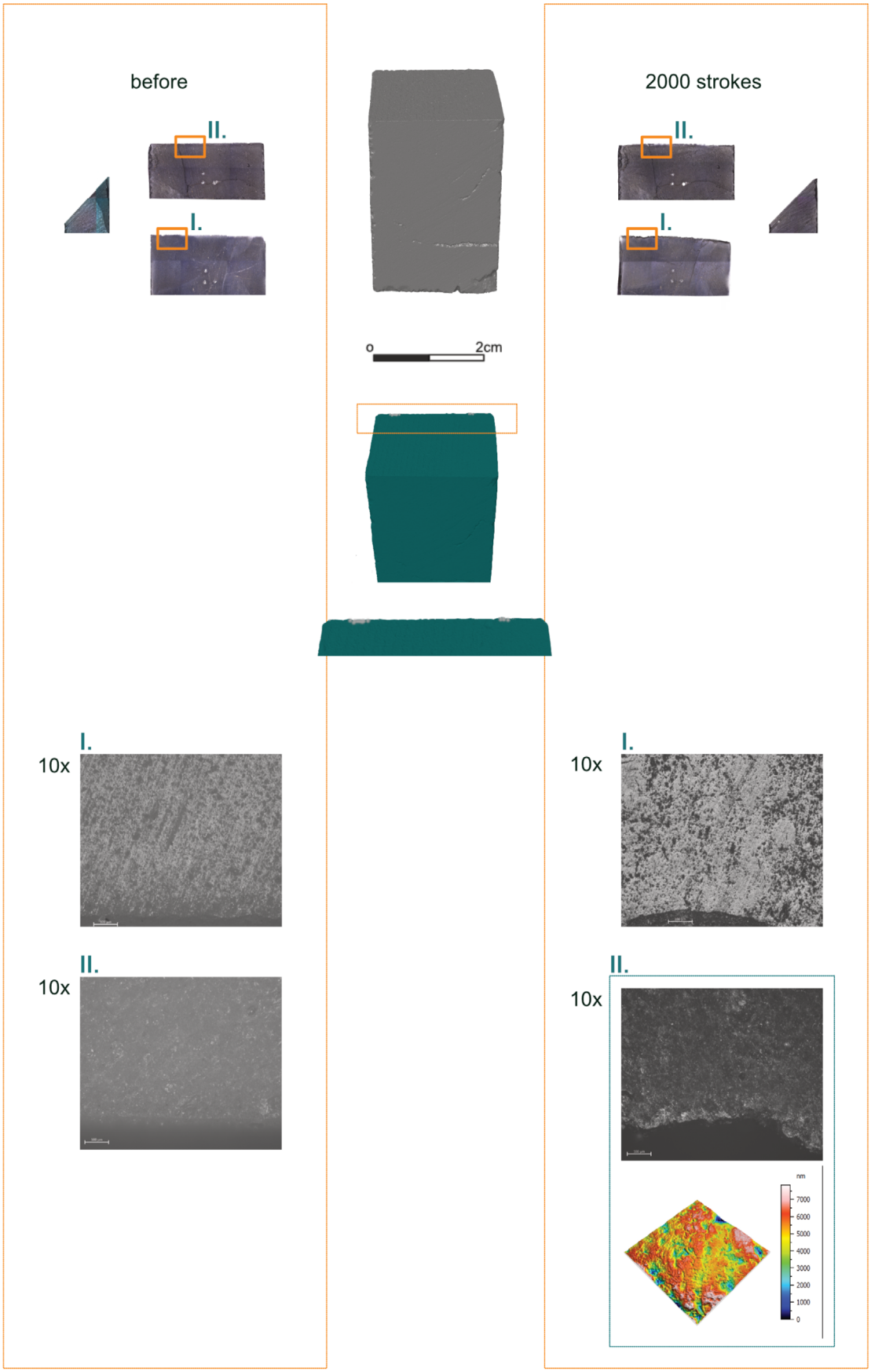

Tool function experiment, lydite sample LYDIT5-8. The topmost image displays the sample in original size before and after 2000 strokes. The 3D model of the sample is shown in the middle (grey) and as a close-up of the edge (turquoise). The other illustrations are magnifications acquired with a 1.6× objective and a 34-× zoom. The use-wear traces are acquired at magnification of 10×. The micro-surface displays the processed result of the confocal data acquisition with the 50× objective.

Plate B16

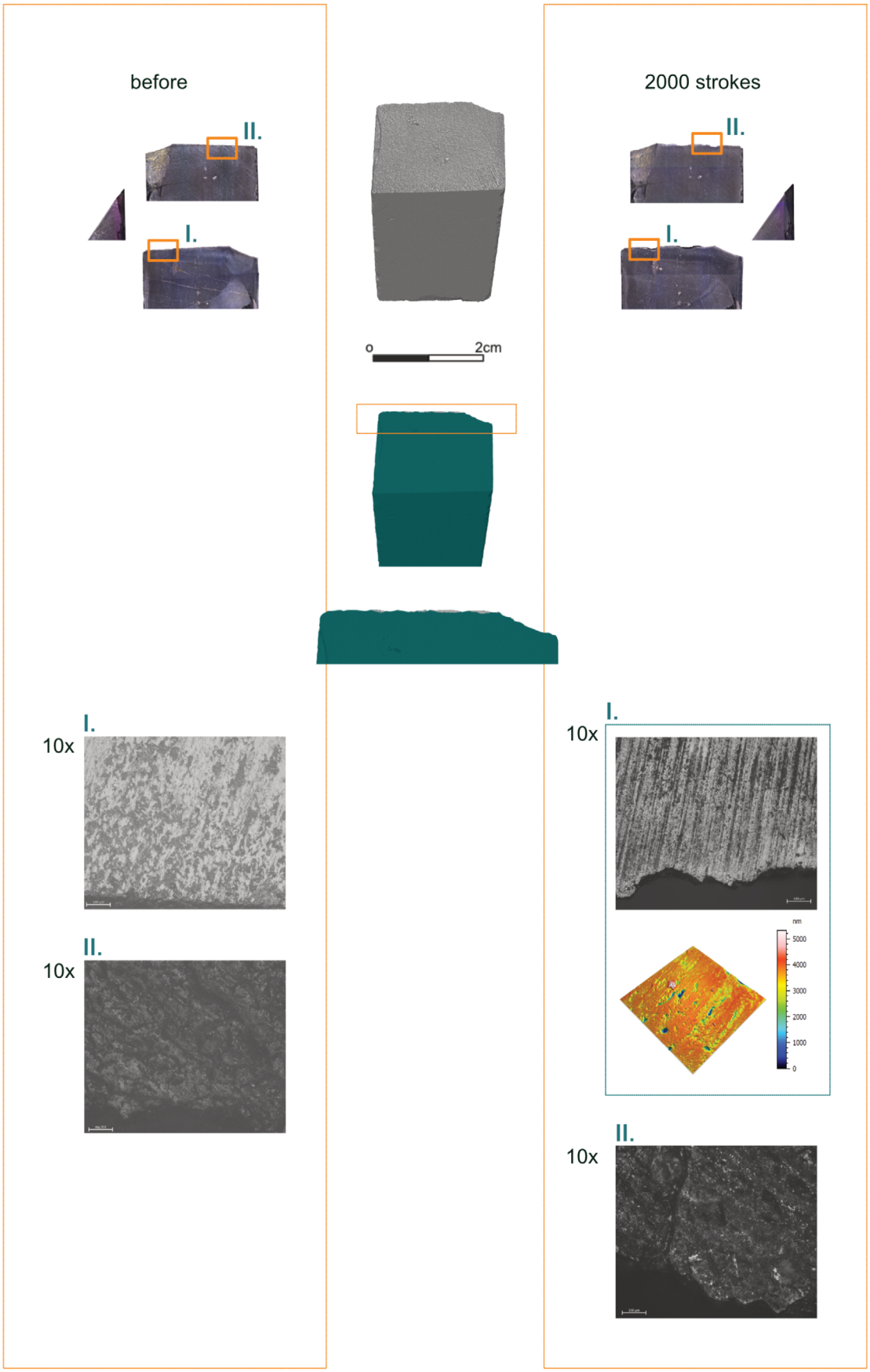

Tool function experiment, lydite sample LYDIT5-12. The topmost image displays the sample in original size before and after 2000 strokes. The 3D model of the sample is shown in the middle (grey) and as a close-up of the edge (turquoise). The other illustrations are magnifications acquired with a 1.6× objective and a 34-× zoom. The use-wear traces are acquired at magnification of 10×. The micro-surface displays the processed result of the confocal data acquisition with the 50× objective.

In the Late Middle Palaeolithic, the variability of Neanderthals' lithic technologies in Central and Eastern Europe was complemented by a specific asymmetric tool type – the so called *Keilmesser*. Due to their morphological characteristics and interpretation as tools in purported long-term use, *Keilmesser* provide a unique archive for tracing late Neanderthal behavioural features. These may range from understanding tool design, production and dedication, to tool function, use and maintenance; along with aspects of technical innovations and transmission of skills and knowledge.

Three *Keilmesser* assemblages from the sites of Buhlen, Balver Höhle (both Germany) and La Grotte de Ramioul (Belgium) were analysed. Applying functional analysis combined with controlled experiments in a multidisciplinary approach, published interpretations were tested and evaluated.

The study presented in this book offers a blueprint to a more holistic approach by systematically employing different methods and scales of analysis. This comprehensive view on *Keilmesser* opens up room for discussions by offering a new perspective on this and, potentially, other specific tool types.

ISBN 978-3-96929-194-8